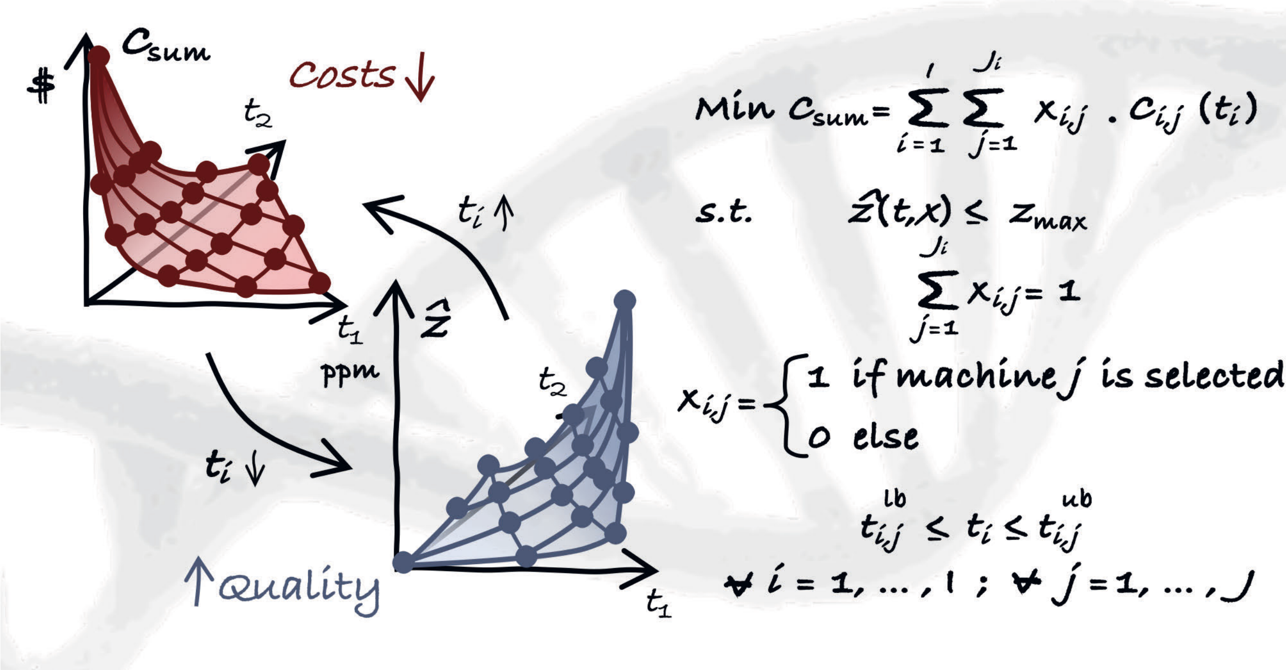

FAU Studien aus dem Maschinenbau 436

Martin Roth

Sampling-based Tolerance-Cost Optimization: The Key to Optimal Tolerance Allocation

FAU University Press

Martin Roth

Sampling-based Tolerance-Cost Optimization: The Key to Optimal Tolerance Allocation

FAU Studien aus dem Maschinenbau

Band 436

Herausgeber/-innen:

Prof. Dr.-Ing. Jörg Franke
Prof. Dr.-Ing. Nico Hanenkamp
Prof. Dr.-Ing. habil. Tino Hausotte
Prof. Dr.-Ing. habil. Marion Merklein
Prof. Dr.-Ing. Sebastian Müller
Prof. Dr.-Ing. Michael Schmidt
Prof. Dr.-Ing. Sandro Wartzack

Martin Roth

Sampling-based Tolerance-Cost Optimization: The Key to Optimal Tolerance Allocation

Dissertation aus dem Lehrstuhl für Konstruktionstechnik (KTmfk)

Prof. Dr.-Ing. Sandro Wartzack

Erlangen
FAU University Press
2024

Bibliografische Information der Deutschen Nationalbibliothek:
Die Deutsche Nationalbibliothek verzeichnet diese Publikation in der Deutschen Nationalbibliografie; detaillierte bibliografische Daten sind im Internet über http://dnb.d-nb.de abrufbar.

Bitte zitieren als
Roth, Martin. 2024. *Sampling-based Tolerance-Cost Optimization: The Key to Optimal Tolerance Allocation.* FAU Studien aus dem Maschinenbau Band 436. Erlangen: FAU University Press. DOI: 10.25593/978-3-96147-720-3.

Der vollständige Inhalt des Buchs ist als PDF über OPEN FAU
der Friedrich-Alexander-Universität Erlangen-Nürnberg abrufbar:
https://open.fau.de/home

Verlag und Auslieferung:
FAU University Press, Universitätsstraße 4, 91054 Erlangen

Druck: docupoint GmbH

ISBN: 978-3-96147-719-7 (Druckausgabe)
eISBN: 978-3-96147-720-3 (Online-Ausgabe)
ISSN: 2625-9974
DOI: 10.25593/978-3-96147-720-3

Sampling-based Tolerance-Cost Optimization: The Key to Optimal Tolerance Allocation

Samplingbasierte Toleranz-Kosten-Optimierung: Der Schlüssel zur optimalen Toleranzallokation

Der Technischen Fakultät
der Friedrich-Alexander-Universität
Erlangen-Nürnberg

zur

Erlangung des Doktorgrades Dr.-Ing.

vorgelegt von

Martin Roth, M.Sc.

Als Dissertation genehmigt
von der Technischen Fakultät
der Friedrich-Alexander-Universität Erlangen-Nürnberg

Tag der mündlichen Prüfung:	21.12.2023
Gutachter:	Prof. Dr.-Ing. Sandro Wartzack Prof. Dr. Kristina Wärmefjord, Chalmers University of Technology, Schweden

Preface

This doctoral thesis evolved during my employment as a research assistant at the Institute of Engineering Design (KTmfk) at the Friedrich-Alexander-Universität (FAU) Erlangen-Nürnberg. Essential parts are based on the scientific findings obtained in the research projects WA 2913/25-1 (TOLerance OPTmization of statically under- and over-constrained assemblies) and WA 2913/25-2 (OptNeTol: Integrated, optimization-based parameter and tolerance design). I gratefully acknowledge the German Research Foundation (DFG) for funding the research activities and making this thesis possible.

With this written work, a long journey and period of my life came to a successful and fantastic end. In the following, I sincerely want to thank every one who has supported me so greatly in the past years. First of all, I would like to thank Prof. Dr.-Ing. Sandro Wartzack, full professor at the Institute of Engineering Design at the FAU Erlangen-Nürnberg, for giving me the chance to start this journey, for the freedom and the trust to shape my research and teaching activities according to my ideas and visions. Dear Sandro, thank you very much for your support as a doctoral supervisor; it was a great time at your institute. Moreover, I would like to thank Prof. Dr. Kristina Wärmefjord, professor at Chalmers University of Technology, for taking over the task of the second referee. I was delighted by your prompt commitment as I have been inspired and educated by the work of your *Geometry Assurance & Robust Design* research group since my first scientific steps. Thank you a lot for the valuable and helpful feedback! Furthermore, I would like to thank Prof. Dr.-Ing. Sebastian Müller for taking over the chair of the examination and ensuring a pleasant atmosphere during the doctoral examination. In addition, the words of gratitude are addressed to Prof. Dr.-Ing. Tobias Günther, professor for Visual Computing at the Department of Computer Science at the FAU Erlangen-Nürnberg, for his interest as the external reviewer and the really smart questions.

The journey was incredible but tedious and, above all, only possible and entertaining with such great companions. First and foremost, this includes the entire dimensional management crew, composed of Benjamin, Björn, Alexander, Stefan, Paul, Michael, Christoph, Dennis, Vincent, and Stephan, with whom the countless working hours did not feel just like a job but rather like a great pleasure. Thank you all for the numerous professional but private conversations, the great support, and the wonderful hours at and after work. Benjamin, Stefan, Michael, and Paul, I want to thank you all, in particular, for your endless support over the last few years. You often untied the knots in my head and helped me to solve the most tricky puzzles. Likewise, the support

of my students Angela, Andreas D., Andreas G., David, Florian, Gabriel, Jennifer, Jonathan, Lukas, Markus, Natalja, Stephan, Sebastian, Vincent, and Yingjie, accompolished this thesis in this form and scope. As your work made a significant contribution to my thesis, I would like to thank you all very much for spending your time and effort. It was fun learning with and from you. Dear Jörg, thank you for creating a vivid and exciting use case with your e-cross skate and providing it for my studies. But not to forget all the great colleagues of the ”KTmfk family”. We have spent lovely years during which so many colleagues have become friends for life.

In addition to all the professional support, I would like to thank my family and friends, who have consciously but also unconsciously supported me significantly over the last few years. Thus, many people have a share in this work. I am sure they know that they can count on me when they need help, just as I could and can rely on them. I especially want to thank my parents for always supporting me and being there for me in word and deed. Mum, Dad, you are the best! My last and deepest gratitude goes to my wonderful wife. Her caring nature, tireless support, and positive attitude are second to none. Dearest Veri, thank you for everything – this thesis is dedicated to you!

Finally, I hope you enjoy flipping through the pages and gaining valuable insight into the exciting field of tolerance-cost optimization.

M. Roth

Erlangen, December 24, 2023 Martin Roth (né Hallmann)

*"Success is 1% inspiration,
98% perspiration, and
2% attention to detail."*

— Phil Dunphy (2012)

Contents

List of Symbols and Abbreviations

Symbol	*Unit*	*Description*
a, b, c, d, f	–	Tolerance-cost coefficients of f_C
$\boldsymbol{A}_{\mathrm{eq}}$	–	Feature equality matrix
$AFESO$	–	Average number of function evaluations
$a_{u,\overline{u}}$	–	Entry of feature equality matrix $\boldsymbol{A}_{\mathrm{eq}}$
b	–	Bias in ANN
$\boldsymbol{B}_{\mathrm{eq}}$	–	Part equality matrix
$b_{l,\overline{l}}$	–	Entry of part equality matrix $\boldsymbol{B}_{\mathrm{eq}}$
$c^{1/0}_{\mathrm{asm},m}$	–	Binary criterion of total assembly (non-)conformance
$C_{\mathrm{fix/var}}$	MU, \$, €, ...	Fixed/variable cost fraction
C_i	MU, \$, €, ...	Manufacturing costs to realize tolerance t_i
$C_{i,j}$	MU, \$, €, ...	Manufacturing costs to realize tolerance t_i with machine/process/supplier j
$\boldsymbol{c}_j$	–	Combination of bins in selective assembly
$c^{1/0}_{k,m}$	–	Binary criterion of single (non-)conformance evaluated for assembly response Y_k
$C^{(\mathrm{opt})}_{l,u,i,j}$	MU, \$, €, ...	(Optimal) tolerance-related manufacturing costs for realizing tolerance $t_{l,u,i}$ with alternative j
$C_{\max}$	MU, \$, €, ...	Maximum of tolerance-related manufacturing costs
C_{pk}	–	Process capability index
$c_{\mathrm{o}}, C_{\mathrm{o}}$	–	Optimization case
C_{relation}	–	Convergence relation
$\overline{C}_{\mathrm{relation}}$	–	Average convergence relation of multiple optimization runs
$c_{\mathrm{s}}, C_{\mathrm{s}}$	–	Sampling case
$C^{\mathrm{opt}}_{\mathrm{sum}}$	MU, \$, €, ...	Optimal cumulated/total tolerance-related manufacturing costs
$C^{\min}_{\mathrm{sum}}$	MU, \$, €, ...	Minimum, total tolerance-related manufacturing costs in current generation g

Symbol	***Unit***	***Description***
$C_{\mathrm{sum}}^{\mathrm{init}}$	MU, \$, €, ...	Total tolerance-related manufacturing costs for initial tolerance allocation
$C_{\mathrm{sum}}^{g=200}$	MU, \$, €, ...	Minimum, total tolerance-related manufacturing costs in current generation $g = 200$
$C_{\mathrm{sum}}^{\mathrm{ref}}$	MU, \$, €, ...	Reference of total tolerance-related manufacturing costs obtained by RSS
d	–	Test data point index in surrogate modeling
D	–	Total amount of test data in surrogate modeling
D'	–	Reduced amount of test data in surrogate modeling
d_{X_i}	mm, ...	Variation from the ideal $X_{i,0}$
dim	–	Dimensions of search space
e	–	Approximation error in surrogate modeling
erf	–	Gauss error function
f_{A}	–	Cost coefficient related to the feature surface area to be machined
f_{act}	–	Activation function of ANN
f_C	–	Tolerance-cost function
f_{F}	–	Cost coefficient related to the type of the feature to be machined
$\hat{f}_h$	–	Probability density function used for kernel density estimation
f_{M}	–	Cost coefficient related to the material and difficulty of the feature to be machined
f_n	–	Adaptive sample size function
f_{net}	–	Input net function of ANN
f_{P}	–	Penalty function
f_Y	–	Assembly response function
F	–	Fitness
$\tilde{f}$	–	Surrogate model of f
$\tilde{f}_{\hat{z}}$	–	Surrogate model to predict $\hat{z}_{\mathrm{asm}}$
$\tilde{f}_{\hat{z}}^{*}$	–	Updated surrogate model to predict $\hat{z}_{\mathrm{asm}}$
FEVs	–	Number of function evaluations

Symbol	***Unit***	***Description***
Flag	–	Criterion for optimization termination
FR	–	Feasibility rate
g	–	Index for generation
G	–	Generation of last adaption of sample size $\tilde{n}$
g_i	–	Inequality constraint i
h_{K}	–	Bandwidth for kernel density estimation
H	–	Peak value of triangular distribution
h_1	–	Function to control the number of individuals to be resampled
h_2	–	Function to control if surrogate model is updated in generation g
h_j	–	Equality constraint j
i	–	Index for tolerance
I	–	Total number of tolerances
idx	–	*idx*-th permutation generated by algorithm
j	–	Index for machine/process/supplier
J_i	–	Total number of available machine/process/supplier alternatives to realize tolerance t_i
$J_{\min}$	–	Minimum number of machines/suppliers
k	–	Cost coefficient
k	–	Index for KCs
K	–	Total number of KCs
$l, \bar{l}$	–	Index for parts
L	–	Total number of parts
L	–	Taguchi's quality loss function
leap	–	Number of points to be ignored in Sobol' sequence generation
Lévy	–	Lévy distribution
Li	–	i-th loop in the presented tolerance allocation framework
LL	mm, ...	Lower limit

Symbol	***Unit***	***Description***
LSL	mm, $\circ$, ...	Lower specification limit
m	$-$	Index of sample
$\overline{m}$	$-$	Mean of the respective outcome for a given population
$\widetilde{m}$	$-$	Median of the respective outcome for a given population
n_{K}	$-$	Number of kernels
n	$-$	Sample size
n_r	$-$	Number of best individuals to be resampled
$n_{\mathrm{min/max}}$	$-$	Minimum/maximum sample size considered in the adaptive sample size strategy
N_c	$-$	Total number of combinations
n_{feas}	$-$	Number of feasible solutions in η_r optimization runs
$n_{i,j}$	$-$	Batch size for machine/supplier j to realize tolerance $t_{i,j}$
$n_{j,\mathrm{min}}$	$-$	Number of achievable assemblies for given combination $\boldsymbol{c}_j$
n_{success}	$-$	Number of successful optimization runs
n_{surplus}	$-$	Total number of surplus, leftover parts
n_{tot}	$-$	Total batch size
$\widetilde{n}$	$-$	Adaptive sample size
$\mathcal{N}$	$-$	Normal distribution
o	$-$	Index for assembly responses
O	$-$	Total number of assembly responses
p	$-$	Process variable
p	$-$	Index for individuals
$p(x)$	$-$	Penalty function used in f_{P} penalizing infeasible solutions
p_{a}	$-$	Probability of discovery in CS
$p_{i,j}$	$-$	Permutation of bins in selective assembly
$\hat{P}, P$	$-$, %	(Estimated) sample proportion of non-conformance

Symbol	***Unit***	***Description***
$q(x)$	$-$	Indicator function
$q_{\hat{z}/z,\alpha/2}$	mm	$\alpha/2$-quantile of $\hat{z}/z$
$q_{\hat{z}/z,1-\alpha/2}$	mm	$(1-\alpha/2)$-quantile of $\hat{z}/z$
$qr_{C,1-\alpha}$	MU	Distance between $q_{\alpha/2}$- and $q_{1-\alpha/2}$-quantiles of C values obtained by simulation
r_p	$-$	Ratio of individuals to be resampled
$r, r_\mathrm{o}, R_\mathrm{o}$	$-$	Index of optimization run/repetition
$r, r_\mathrm{s}, R_\mathrm{s}$	$-$	Index of resampling
R1/2	$-$	Reference points
R^2	$-$	Coefficient of Determination to evaluate the performance of surrogate model
rn	$-$	Random numbers
$RMSE$	mm	Root Mean Square Error to evaluate the performance of surrogate model
s	$-$	Current step in CS
s	$-$	Index for discrete tolerances
S	$-$	Total number of discrete values for tolerance t_i
$skip$	$-$	Shift value in Sobol' sequence generation
SR	$-$	Success rate
T_asm	mm, °, …	Tolerance range of assembly KC to be statistically fulfilled
t_i	mm	Tolerance value i
$t_i^\mathrm{lb/ub}$	mm	Lower/upper bound of tolerance t_i
t_i'	mm	Current tolerance value
t_i^init	mm	Initially allocated tolerance value
t_i^opt	mm	Optimally allocated tolerance value
$t_{l,u,i}$	mm	Tolerance assigned to feature u of part l
$t_{l,u,i}^\mathrm{opt}$	mm	Optimal tolerance value assigned to feature u of part l
T_max	mm, °, …	Maximum tolerance of the assembly KC
$\boldsymbol{t}_p^g$	mm	Tolerance vector in generation g for individual p

Symbol	***Unit***	***Description***
T_{RSS}	mm, ∘, …	Tolerance range of the assembly KC to be statistically fulfilled considering the RSS criteria
T_{Stat}	mm, ∘, …	Tolerance range of the assembly KC to be statistically be fulfilled
T_Y	mm, ∘, …	Resulting tolerance range of the assembly KC under variations
u	−	Multiple of the standard deviation used in six sigma philosophy to express quality requirements
u	−	Index for DOE trial
$u, \overline{u}$	−	Index for the features of part l
U	−	Total number of features per part l
$\mathcal{U}$	−	Uniform distribution
UL	mm	Upper limit
USL	mm, ∘, …	Upper specification limit
$\boldsymbol{v}_p$	−	Design vector with one entry v_{p_i} for each permutation to be chosen by the optimizer
$\boldsymbol{v}_t$	−	Design vector with one entry v_{t_i} for each tolerance to be allocated
$\boldsymbol{v}_w$	−	Design vector with one entry $v_{w_{i,j}}$ for each machine/supplier to be allocated by optimization
$\boldsymbol{v}_x$	−	Design vector with one entry v_{x_i} for each alternative used in mixed-integer optimization
$\boldsymbol{w}$	−	Weighting factors to reduce multiple objectives into one overall single objective
$w_{i,j}$	−, %	Weighting factor of machine j to realize tolerance $t_{i,j}$
$w_{i,j}^{\mathrm{lb/ub}}$	−, %	Lower/Upper capacity limit for machine/supplier j to realize tolerance $t_{i,j}$
$w_{i,j}^{\mathrm{opt}}$	−, %	Optimal weighting factor of machine/supplier j for tolerance $t_{i,j}$
$w_{i,j}'$	−, %	Current weighting factor of machine/supplier j for tolerance $t_{i,j}$
x	−	Input value for training of surrogate model

Symbol	**Unit**	**Description**
$x_{i,j}$	–	Machine/process/alternative selection parameter to realize t_i
$x_{i,j}^{\text{opt}}$	–	Optimal machine/process/alternative selection for tolerance t_i
$x'_{i,j}$	–	Current value of machine/process/alternative selection for tolerance t_i
X_i	mm, ...	Dimension i
$X_{i,\text{o}}$	mm, ...	Nominal dimension of characteristic i
$x_{l,j}$	–	Alternative selection parameter for part l
$x_{l,j}^{\text{opt}}$	–	Optimal alternative selection for part l
X'	–	Uniform random number
Y	mm, ∘, ...	Assembly response
Y_o	mm, ∘, ...	Ideal assembly response
yld_{min}/yld	ppm, %	Minimum yield/ yield
$\hat{y}$	–	Predicted output value via surrogate model $\tilde{f}$
z, NC	ppm, %	Non-conformance (scrap, rejection) rate
z_{max}	ppm, %	Maximum non-conformance rate
$\hat{z}$	ppm, %	Estimated non-conformance rate
$\hat{z}_{(\text{asm})}^{\text{init}}$	ppm %	Estimated (total) non-conformance rate for initially allocated tolerances
$\hat{z}_{(\text{asm})}^{(\text{opt})}$	ppm %	Estimated (total) non-conformance rate for (current) optimally allocated tolerances
$\hat{z}'$	ppm %	Currently estimated non-conformance rate
$\hat{z}_{\tilde{f}_{\hat{z}}}$	ppm %	Estimated total non-conformance rate via surrogate model $\tilde{f}_{\hat{z}}$
$Z_{\alpha/2}$	–	Z-score for $\alpha/2$
α	–	Step length for random walk in CS
α	–	Likelihood to not lie within the confidence interval
β	–	Cost coefficient
$\beta_{1/2}$	–	Parameters of Pearson distribution system
γ, γ_1	–	Skewness
γ_2	–	Excesses kurtosis

Symbol	***Unit***	***Description***
Γ	–	Gamma distribution
δ_{feas}	ppm	Feasibility tolerance
δ_i	mm, …	Process/manufacturing tolerance i
δ_{P_y}	mm	Offset of the virtual axis of steering mechanism in y-direction from the center
$\delta_{\mathrm{success}}$	ppm	Success tolerance
δ_z	ppm	Absolute offset of current $\hat{z}$ to the maximum nc-rate limit z_{max}
$\delta_{\hat{z}^{\mathrm{u/o}}}$	%	Relative deviation between predicted and simulated margin of errors of under-/ overestimation
$\delta_{\hat{z},1-\alpha}$	%	Confidence interval with α of difference between predicted and real value of z
Δ_Y	mm, °, …	Deviation from target value Y_0
$\Delta_{\eta_{\mathrm{F}},\Sigma}$	–	Cumulative difference in function evaluations
ΔC	MU	Difference in cost optima obtained by mixed-integer and minimum-cost curve
Δ_g	–	Distance between two remodeling steps in adaptive surrogate modeling
ΔC_g	MU	Difference between current cost optimum in generation g and previous generation $g-1$
$\Delta\mu_i$	mm, …	Mean shift of X_i
ϵ	mm	Absolute margin of error
$\epsilon_{\%}$	%	Relative margin of error
$\epsilon_{P=0.5}$	mm	Maximum error of nc-evaluation
$\epsilon_{\mathrm{u/o}}$	mm	Margin of error by under-/overestimation
ζ	–	Index for critical assembly configurations
Z	–	Total number of critical assembly configurations
$\eta_{c_{\mathrm{o/s}}}$	–	Total number of optimization/sampling cases
η_F	–	Total number of function evaluations
η_g	–	Total number of generations/iterations
η_g^{opt}	–	Number of generations needed to reach the global optimum

Symbol	***Unit***	***Description***
$\eta_{g,\mathrm{stall}}$	$-$	Total number of stall generations
η_p	$-$	Total number of individuals/Population size
$\eta_{r_{\mathrm{o/s}}}$	$-$	Total number of optimization/sampling repetitions
κ	$-$	Kurtosis
K	$-$	Kernel density function used in kde
λ	$-$	Factor used in GD&T constraints
$\mu, \hat{\mu}$	mm, ...	Mean
$\xi_{1/2}$	$-$	Shape parameter of adaptive sample function f_n
ρ	$-$	Probability distribution/density function (pdf)
$\rho_{i,j}$	$-$	Part tolerance probability distribution resulting for t_i with alternative j
ρ_Y	$-$	Probability density function of assembly response Y
ρ_Y*	$-$	Multivariate probability density function considering multiple assembly responses
σ	mm	Standard deviation
$\sigma^2, \hat{\sigma}^2$	mm²	Variance
τ_{sum}	s,h	Total computing time
$(\overline{\tau}_{\mathrm{feas}}), \tau_{\mathrm{feas}}$	s,h	(Average) computing time for feasible optimization run
$\overline{\tau}_{\mathrm{PreOpt/Opt}}$	s,h	Average computing time for pre-optimization steps (e.g., surrogate modeling)/optimization
$\overline{\tau}_{\mathrm{ReModel}}$	s,h	Average computing time for remodeling
$\overline{\tau}_{\mathrm{ReSamp}}$	s,h	Average computing time for resampling
$\overline{\tau}_{\mathrm{rel}}$	s,h	Average computation time in relation to the minimum
τ_Y	s	Computing time to evaluate all assembly responses $\boldsymbol{Y}$
τ_{samp}	s	Computing time for sampling
$\tau_{\hat{z}}$	s	Computing time for nc-rate estimation
Φ	$-$	Cumulative distribution function (cdf)
Φ^{-1}	$-$	Inverse cumulative distribution function (icdf)

Symbol	*Unit*	*Description*
Ω	–	Manufacturing environment

Abbreviation	*Description*
Alloc	Allocation
Alt sel	Alternative selection
ANN	Artificial Neural Network
ANOVA	Analysis of Variation
AP	Application Protocol
Arith	Arithmetic
ASCII	American Standard Code for Information Interchange
Asm strat	Assembly strategy
ASME	American Society of Mechanical Engineers
CAD	Computer-aided design
CAE	Computer-aided engineering
CAM	Computer-aided manufacturing
CAPP	Computer-aided process planning
CAT	Computer-aided tolerancing
CE	Concurrent Engineering
cdf	Cumulative distribution function
CFD	Computational Fluid Dynamics
Conc	Concurrent tolerance allocation for design and manufacturing
const	constant
CS	Cuckoo Search algorithm
DfX	Design for X
Dim	Dimensional tolerances
DOE	Design of Experiment
E-cross skate	Electrified cross skate
ecdf	Empirical cumulative distribution function
ENG	Engineering

Abbreviation	***Description***
EOL	End of life
FE/FEA	Finite Element/ Finite Element Analysis
Func	Function
GA	Genetic algorithm
Geom	Geometrical
GD&T	Geometric dimensioning and tolerancing
GPS	Geometrical Product Specification
GPU	Graphics Processing Unit
Heur	Heuristic
HLM	High-Low-Median
ISO	International Standardization Organization
icdf	Inverse cumulative distribution function
JT	Jupiter Tessellation™-data format
k-nn	k-nearest neighbor
KC	Key Characteristic
kde	Kernel density estimation
KPI	Key Performance Indicator
LHS	Latin Hypercube Sampling
Manuf	Manufacuturing
MBD	Model-based definition
MCS	Monte Carlo Sampling
MIP	Mixed-integer problem
MU	Monetary unit
nc, NC	Non-conformance
ncdf	Cumulative distribution function of standard normal distribution
nc-est	Non-conformance rate estimation technique
ND	Normal distribution
NP	Non-polynomial
O-1, O-2, O-3	Strategy for handling random numbers in optimization

Abbreviation	***Description***
OEE	Overall equipment efficiency
opt	Optimal
OWL	Web Ontology Language
pdf	Probability density function
ppm	Parts-per-million
Part tol prob distrib	Part tolerance probability distributions
Prod des	Product design
PB	Population-based
PD	Pearson distribution
PDM	Product data management
PDO	Process document
PLM	Product lifecycle management
PMI	Product and manufacturing information
QIF	Quality Information Framework
QL	Quality loss
QMCS	Quasi-Monte Carlo Sampling with low discrepancy Sobol' sequences
Ref/ref	Reference
Req	Requirement
RQ	Research question
RSS	Root sum squares
S-1, S-2, S-3	Strategy for handling random numbers in sampling
Samp	Sampling
Spec	Specification
SQL	Structured Query Language
Stat	Statistical
STEP	STandard for the Exchange of Product model data
SVM	Support Vector Model/Machines
SysML	Systems Modeling Language

Abbreviation	***Description***
TB	Trajectory-based
TCVisVA	Teamcenter® Visualization Variation Analysis
TD	Triangular distribution
Tol	Tolerance
TOPSIS	Technique for Order Preference by Similarity to Ideal Solution
TTRS	Technologically and Topologically Related Surfaces
UD	Uniform distribution
UML	Unified Modeling Language
var	Variable
XML	Extensible Markup Language

List of Figures

List of Tables

1 Introduction

Corporate performance and its directly related profit are highly dependent on the synergy of a variety of activities from all over the entire product development process, "beginning with the perception of a market opportunity and ending in the production, sale, and delivery of a product" [1]. However, thoroughly converting all individual needs, expectations, and information from the different areas into marketable products [2, 3] requires well-founded decisions for the product and all related processes and activities [4, 5]. Product design is, therefore, an essential contributor to corporate success since the resulting product quality and costs are determined to a large extent early in the product design stage [6–8].

Depending on the product lifecycle phase or a particular aspect in focus, the design is primarily aligned to one or several frequently conflicting objectives but simultaneously accompanied by a set of boundary conditions [4, 9]. As a consequence, any decision in product design *for* a particular objective, commonly addressed under the term *Design for X* (DfX) [4, 10], is also a decision *to* meet several requirements forming a dynamically changing set of interdisciplinary objectives and constraints to be complied by the product design.

Although competition has always been fierce [11], the increasingly short product lifecycles and high cost and quality pressure, exacerbated by the demanding international markets, force product development to differentiate itself from competitors more than ever [12–15]. Thus, product development has to be supported continuously by simulation and optimization to find the best, high-quality and cost-aware product design and to survive as one of the fittest on the market with an optimal trade-off between the various objectives and interests.

1.1 Motivation and problem statement

Within this tense, multidimensional field of conflicting objectives and constraints, tolerancing plays a crucial role in the total product development process [16–18]. Its primary aim is to assure a high level of product quality and, thus, customers' satisfaction by limiting the variations of single part features concerning size, location, orientation, and form [19–21]. At the same time, however, the individually assigned part tolerances determine the objectives, requirements, and constraints for the subsequent activities, i.e., manufacturing, assembly, and inspection, while implicitly and unintentionally defining a significant share of the product costs [22–24]. Hence, tolerancing is dominated by a general dichotomy between product and process design leading to severe conflicts of interest [25]. While tight tolerances are needed to guarantee high product quality, loose tolerances should be preferred to save costs by a simplified part manufacturing (see Fig. 1) [26–31]. Although design engineers mostly do not have detailed knowledge about manufacturing costs, available machines, tools, fixtures, etc., they are responsible for allocating suitable tolerance values already in the design stage since they overview the total assembly [32, 33]. The main challenge of tolerance allocation is, thus, to find an answer to the question ”what is [technically] necessary and what is economically possible [or rather reasonable]” [34], enabling a suitable trade-off between the opposite interests of design and manufacturing [25, 35–37].

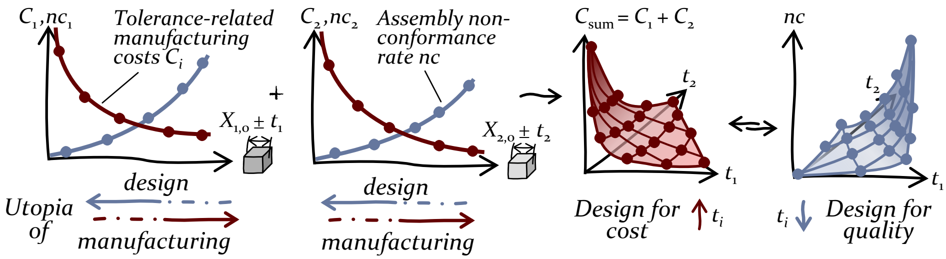

Figure 1: Conflict between total product quality and manufacturing costs as a function of the assigned tolerance values.

Assigning tight tolerances for safety while merely hoping that they are not too expensive [38], rough estimations by general rules-of-thumb and heuristic, (over-)simplified tolerance allocation methods [39–41], as well as the joint iterative application of tolerance and sensitivity analysis [P1], intend to choose a satisfactory solution from the margin of quality between the utopias from design and manufacturing [42] (see Fig. 1). To solve the tolerance-cost conflict more efficiently and find the best solution, tolerance-cost optimization, an optimization-based approach to allocate part tolerance values, was invented in the mid-20th century [P1]. Inspired by its basic idea of an automatic balancing of the individual part tolerances with the aid of optimization, various methods, approaches, and solutions have been presented and improved in literature over the last five decades [P1]. However, in addition to all the advantages of computer-based optimization approaches, there are also significant obstacles to overcome, as their usage requires high-level skills ”to generate, derive, and manipulate complex mathematical models” [43], ”to relate various cost-versus-tolerance functions to a specific problem” [43], and ”to write computer algorithms to perform numerical analysis [and optimization]” [43], which is based not least on a generally high degree of "creative thinking, experience and intuition" [44]. Tolerance allocation and its methods are therefore perceived as broad, (too) complicated, demanding, and tedious [43–47]. As predicted more than 20 years ago, they are therefore only applicable by highly experienced tolerance engineers [P2] and still "a conundrum for many in industry" [43]. Hence, tolerance-cost optimization could not prevail so far and is paid little attention in the industry. As a result, cost potentials and valuable competitive factors through optimal tolerance allocation remain largely unused.

1.2 Methodical approach and general outline of the work

Motivated to overcome these drawbacks, this thesis follows the global aim to *advance the establishment of tolerance-cost optimization enhancing optimal tolerance allocation for assemblies of industrial complexity*. Since its potential is highest in the design phase, as research and surveys prove [48], this thesis focuses on tolerance allocation at the design phase's assembly level. It addresses primarily mechanical products[1] and geometrical part variations.

A systematic approach is required to reach this goal, which is briefly presented in the following. The underlying general outline of this work is illustrated in Fig. 2. A review of the fundamentals of tolerancing, its different activities, and its role in the context of the geometry assurance process in Sec. 2.1 serves as the general basis for the subsequent sections. It is followed by a detailed analysis of the literature in the field of tolerance-cost optimization, where a final retrospect on the last fifty years in Sec. 2.2–2.3 reflects the current state of the art and research. The presented findings help to reveal the general shortcomings of tolerance-cost optimization in Sec. 3.1 restricting its usability in the detail design phase. The subsequent discussion on the combination of sampling-based tolerance analysis and metaheuristic optimization for optimal tolerance allocation in Sec. 3.2 emphasizes its benefits and justifies the research focus of this thesis on sampling-based tolerance-cost optimization, i.e., tolerance-cost optimization with sampling-based tolerance analysis as a subroutine for statistical quality assurance. The discussion on its potentials and shortcomings is used to define the research questions in Sec. 3.3 and the structure of the main part before they are successively answered in Chap. 4–6 focusing on the optimization's accuracy, completeness and efficiency. Chap. 7

[1] Although "the function of mechanical products may depend upon electrical, hydraulic, optical, pneumatic, thermal, or some combinations of these or other physical effects" [49], the expression mechanical assembly/product is suitably used "if [...] parts which comprise the product are primarily mechanical" [49]. The products focused on in this thesis are mechanical assemblies consisting of at least two parts or subassemblies.

summarizes and harmonizes the individual findings and proposes a framework for optimal tolerance allocation based on sampling-based tolerance-cost optimization. Its application and evaluation in Chap. 8 aim to verify the research goals' achievement. Finally, Chap. 9 summarizes this thesis and gives an outlook on further research potentials.

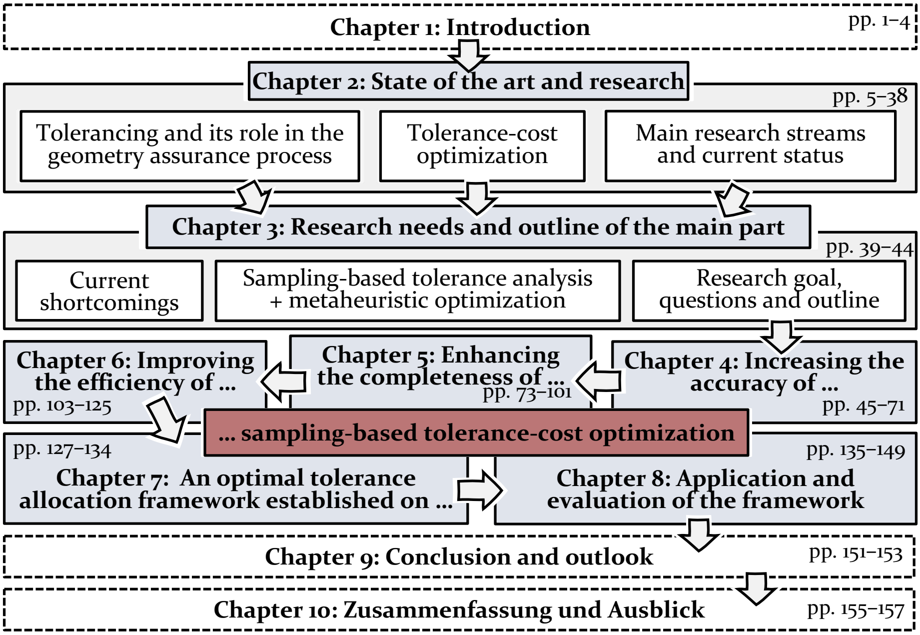

Figure 2: Overview of the outline of the thesis.

2 State of the art and research

The subsequent sections aim to give a holistic overview of the current state of the art and research in the field of tolerancing in general and tolerance-cost optimization in detail.

2.1 Tolerancing, its activities, and its role in the geometry assurance process

Although the demand for individualized and personalized products steadily increases [2], technical products are typically manufactured in high-volume serial or (customized) mass production to ensure profitability. Interchangeability is thereby an essential prerequisite for its successful implementation creating technical products by a pure random assembly of numerous parts originating from different manufacturing machines as well as processes and differing in material and geometry [49]. However, it is significantly complicated by the axiom that all manufacturing and assembly processes are subject to variations from its ideal value[1] [52, 53]. Even if it was possible to reduce manufacturing imprecision to zero and to manufacture all parts *ideally* or *perfectly*, i.e., *identically* and *exactly*, all the time [54–57], which is technically impossible [58], it would be economically not useful [57, 58] (see Fig. 1). As a consequence, variations are compulsorily ubiquitous in all individual processes necessary to realize a product [53, 59] and significantly influence the product's quality, cost, and time for its development and production [60]. For this reason, serious attention has to be paid when claiming to offer ”world-class products” [61]. In contrast to cost and time, product quality is, however, more difficult to first define and second to quantify. Besides numerous other definitions [62], quality can be defined as ”conformance to requirements” [63] and further suitably supplemented by its various dimensions, such as performance, reliability, aesthetics, or perceived quality [64].

Since variations negatively impact the multidimensional quality of a product and cause technical, programmatic, schedule, or cost risks [23, 65], variation has to be verified, reduced, and monitored [66] assuring high product quality and mitigating these variation-dependent risks [67]. As its complete elimination is impossible or often too expensive, product designs and processes are designed to be insensitive or at least less sensitive to variation [68, 69]. Following this general idea, numerous robust design methods have been tailored to the various product development stages [68, 70, 71]. In addition to other

[1] The term *variation* acc. to ASME Y14.5-2018 [50] is preferably used instead of the term *deviation* acc. to the ISO 1101:2017 [51] in this work.

influences and perturbations, many quality problems can be traced back to the geometry of the parts and the associated accumulations of their variations [72]. A holistic geometry assurance process is, thus, indispensable [19, 73]. It comprises a set of activities of product design, pre-production, and production, "contributing to minimizing the effect of geometrical variation in the final product" [19] and "ensur[ing] that all geometrical requirements on the product are fulfilled" [74].

Within this process, both dimensional and geometrical part tolerances, constraining the variation of a part feature in size, location, orientation, and form by defining "the difference between the maximum and minimum limits" [50], are critical design instruments to control the geometrical variations [75].[2] **Tolerancing**, in particular, comprises the set of activities enriched by tools and methods which are linked to tolerance information [78] to "manage [all] **geometrical variations** [...] from preliminary design [and] detailed design [over] process planning [and] manufacturing activities [up to] geometrical inspection" [20]. Hence, they are further addressed under the terms "tolerance management" [34, 79–81] and "dimensional management" [60, 82–84] in both research and industry. Tolerancing contributes to mitigating the individual risks by improving "robustness, reliability, flexibility, evolvability, and interoperability of the final product" [23]. It mainly focuses on variation-dependent aspects of interchangeability, manufacturability, product performance, and customer requirements [23], including not only product functionality but also perceived quality aspects [85–87]. In comparison to methods focusing on robustness and reliability, tolerancing is limited to or concentrates on part manufacturing- and assembly-related variations leading to aleatory uncertainties [23], which are, in contrast to epistemic uncertainties, known and describable via stochastic processes and random variables [88–90]. The original scope of tolerancing with a focus on function and assembly [75, 91] has grown into a comprehensive, holistic framework "to meet [all] predetermined dimensional quality goals" [82]. This includes a variety of issues from the entire product lifecycle and is not limited to the detailed design phase [92, 93] (see Fig. 3).

To strengthen the importance of improving product quality, widely acknowledged in theory [34, 96], but often underestimated in practice [97] leading to daily tolerance-related problems [34], various process models for a step-by-step application of tolerancing tools, methods, and strategies were presented

[2] Depending on the scope of interest and lifecycle phase, there are different views on a feature [76], which lead to different understandings and definitions of the term feature. In this thesis, a *part feature* is seen from a geometrical point of view as "a physical portion of a part" [50], which can be "a point, line, surface, or volume or a set of these elements" [77] and is the result of one or multiple manufacturing processes. Otherwise, it is explicitly stated.

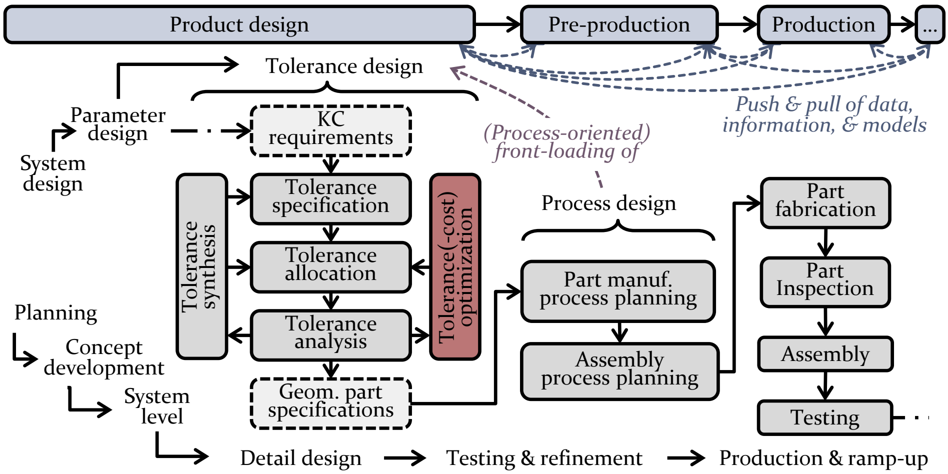

Figure 3: Tolerance-related activities overspread the total product lifecycle leading to a continuous push and pull of data, information, and models, inspired by [1, 73, 94, 95].

in the past, for instance in [98, 99], and have also proven their industrial applicability. Depending on the lifecycle stage in focus, tolerancing activities are driven by the **objectives and viewpoints**, requiring a dynamic change of their role [16]. Accordingly, it is helpful to distinguish whether the methods are applied from the point of view of product design or process design, consisting of part manufacturing, inspection, and assembly process planning [82, 100].

2.1.1 Product design-driven tolerancing activities

The consideration of variations along the product development process can be divided in three main phases acc. to Taguchi [95] (see Fig. 3). While principle solutions and concepts are identified, evaluated, and finally selected in system design, the nominal values for all relevant design parameters are defined in the subsequent parameter design [95, 101]. Efforts in both stages with a focus on product robustness have thereby a positive effect on the subsequent tolerance-related steps [P3] fostering the tackling of tolerance problems early on [7, 20], even if the final geometry is not entirely defined [102]. In **tolerance design**, the last design step and direct link to production planning (see Fig. 3), the focus is on the assignment of the tolerances. Therefore, it covers the following main tolerancing activities [43, 103].

A systematic breakdown of the product quality requirements into smaller geometrical characteristics allows to identify the so-called **Key Characteristics (KC)**, which are sensitive to variations from its nominal, and their variation has a significant influence on the fulfillment of the quality requirements [66]. Although KCs can generally be assigned on the product, (sub-)assembly, or part level [6, 66], the term KC is used in the following for geometrical characteristics on the assembly level. The KCs serve as the basis for the top-down definition of the individual part tolerances flowing from assembly over the part to the feature level [6, 73] making use of tolerance specification, allocation, analysis, and synthesis methods (see Fig. 3).

Tolerance specification is first used to translate the KC requirements into a set of geometrical part specifications for all relevant features by choosing both the types of part tolerances and the datum reference frames in compliance with current tolerancing standards [23, 104]. Further information, e.g., on tolerance zones, material conditions, or filtering operations, complete the specification to compactly and clearly communicate all necessary matters [105]. This leads to *a clear recipe* for part manufacturing and inspection [99], but also already defines the costs to a certain extent [106, 107].[3] With the aim to communicate through an internationally uniformly valid language, tolerance specification is based on international standards for Geometric Dimensioning and Tolerancing (GD&T) [110]. In most cases, either the Geometrical Product Specification (GPS) standards defined by the International Standardization Organization (ISO), which are structured in a comprehensive matrix model [111], or the GD&T guidelines mainly expressed in the ASME Y14.5 by the American Society of Mechanical Engineering (ASME) [50] function as a reference, showing some differences [110], but are both widely applied and accepted in industry. Regardless of the choice of the standard, a comprehensive set of rules with often non-trivial aspects has to be observed but can be supported by computer-aided methods [104]. Examples are rule-based practices, directly integrated into or developed for CAD-systems and stand-alone tools [112–116] as well as enhanced knowledge-based and data-driven approaches [117] based on ontological web language [118–120] and metamodeling [121, 122]. Besides the tolerance types, they partially already propose an initial assignment of tolerance values, e.g., based on general tolerances or previously defined preferred values.

Nonetheless, specific **tolerance allocation** methods are needed to find the values for all specified tolerances more consciously. Rational allocation methods based on heuristics [39–41] have thereby supplemented the pure reliance on standards, textbooks, or guesses keeping general rules-of-thumb such as ”the lower the tolerance, the higher the cost of manufacturing” or ”do not specify higher accuracy than is really needed” in mind [123]. Graphical [124–126],

[3] Depending on the literature referred to, tolerance specification can additionally include the assignment of tolerance values [16, 108, 109].

as well as analytical approaches, distribute the total assembly tolerance on the individual part tolerance values equally and proportionally to part dimensions or process variations [40, 127, 128] – or taking weighted [129], constant precision or complexity factors into account [40, 127]. Optimization-based methods overcome the neglect or predominantly qualitative consideration of cost aspects and their limited applicability. They constitute the group of tolerance-cost optimization approaches, which are discussed in detail in Sec. 2.2.

Tolerance analysis, sometimes named variation analysis/simulation [6, 73, 74, 105], aims to verify if tolerances specified and allocated can fulfill the KC requirements [16]. Arithmetic and statistical methods, harnessed via editable programming codes, spreadsheets, CAD-embedded and stand-alone tools [48, 130, 131], are nowadays state-of-the-art design tools often used daily for analyzing the effects of the accumulation of the individual feature variations [48, 132]. More details on tolerance analysis will be given in Sec. 2.2.2. Systematic methods making adjustments and reassignments, in most cases repetitively, of the GD&T scheme in terms of types or values using the tolerance analysis results can generally be summarized under the term **tolerance synthesis** [78, 133] and include aspects and practices of tolerance allocation, specification, and analysis [78, 134–136]. Consequently, the boundaries between tolerance synthesis and allocation are blurred, definitions for both activities are often quite similar, and no clear distinction is made in literature.

2.1.2 Process design-driven tolerancing activities

The product design stages are followed by a series of planning steps to convert the virtual models into real parts and assemblies in compliance with the specified tolerances and KC requirements (see Fig. 3). In the case of purchased parts, the *point of view changes from assembly to part* regarding part fabrication, whether performed internally or externally [32]. Tolerance allocation, analysis, and synthesis methods, which are similar in their basic idea to the methods in product design, are thereby used with a strong focus on manufacturing-related issues [16]. Their primary goal is to support the transfer of the design tolerances into a process plan [16], which transforms the raw material into the final part while satisfying the design specifications involving several machines, operations, tools, and fixtures [137, 138]. Consequently, if there is more than one manufacturing step needed [139], a design tolerance t_i results from the accumulation of variations from all manufacturing operation steps needed [140]. The assignment of **manufacturing tolerances** δ_i for all intermediate dimensions [139], sometimes called working [141] or process tolerances [140, 142], in combination with a conscious selection of operations and their sequencing [143, 144], i.e., arranging all operations in a logical and chronological sequence [145], datum and machining parameters selection [144, 146], etc., help to meet the design tolerances t_i [140] (see Fig. 4). In this regard, tolerance charts, which graphically represent the dimensions and tolerances for all machining operations as well as the quantity of stock material removed in each manufacturing operation [147, 148], are widely used to analyze and control the workpiece dimensions and their tolerances [16, 148, 149]. By transferring the traditionally manual tolerance charting techniques into computer-aided approaches, research efforts were intensified [28, 147, 150]. This led to an extension of the methods' usability and its instrumentalization using knowledge-based expert systems and tools supporting the individual computer-aided process planning (CAPP) and manufacturing (CAM) tasks [25, 142], including optimization-based tolerance allocation to optimally balance the process tolerance values δ_i (see Fig. 4).

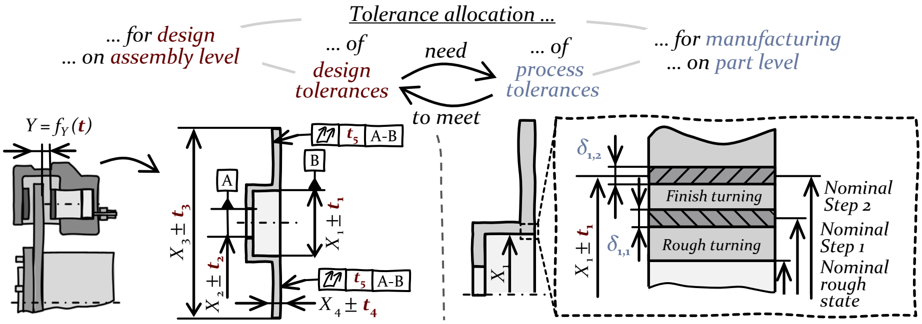

Figure 4: Tolerance allocation for design vs. for manufacturing, freely adopted from [41, P1].

In addition to the part level, numerous tasks have to be tackled during **the planning of the assembly steps**, such as the choice of joining operations, assembly sequences, locating schemes, etc., where attention to variation and tolerances is indispensable [19, 73]. Both product and design process activities are substantially supported by **inspection-driven tolerancing activities**, such as tolerance verification, including planning and metrological procedures to investigate assembly and manufacturing specifications [108], providing a reliable tolerance information basis [151] and to evaluate the assumptions made in the design stage [23, 108, 117].

2.1.3 Influence of Concurrent Engineering

The distinct separation and sequential flow of the presented tolerancing activities were well-established for a long time. However, it complicates internal communication and requires recurring revision loops and design iterations, resulting in time delays, quality degradation, and ultimately high development costs [11, 152, 153]. The philosophy of **Concurrent Engineering** (CE), conceptualized and coined in the 1980s [11, 153], broke these barriers and turned the idea of *throwing the part specifications from design simply over the wall* [11, 82] into a concurrent and joint accomplishment of the interrelated tolerancing tasks [154, 155]. In doing so, the existing barriers are broken by fostering cross-functional cooperation of design and manufacturing with a common, merged knowledge base [11, 152]. As a result, decisions in the design stage are better aligned with manufacturing-related issues. Individual tasks of the process design stage are concurrently finished avoiding tolerance-related problems before they get apparent in prototyping, ramp-up, or series production and, thus, leading to shorter development cycle times with less costs [11, 73, 152, 154].

2.1.4 Computerization and automation of tolerancing

The close interaction of the individual interdisciplinary issues, not at least emphasized by the idea of CE, and the ongoing computerization of the tolerancing methods [75] require an intensive sharing of different information and models from various sources [117]. In contrast to the times where CAD-tools were first widely used (1970s) [8] and CAT was still in its infancy (1990s) [156], simulation and optimization are nowadays everyday tools for tolerance engineers [23, 157], where information from the total lifecycle is needed in addition to the product and part geometry represented by CAD-models [117, 158]. Their enrichment by further **product and manufacturing information (PMI)** using semantic, human-readable, and computer-interpretable annotations supports the idea of a **model-based definition (MBD)** [159, 160], contributing to facilitate and automatize the tolerancing-related downstream activities in a closed loop manner [161, 162, P4]. In addition to direct interfaces, more general solutions are based on neutral, standardized exchange formats [79, 162], primarily STEP (STandard for the Exchange of Product model data) [163], JT (Jupiter Tessellation) [164] and QIF (Quality Information Framework) [165], ensuring general interoperability by lossless and uniform interchangeability and, thus, (re)use of product, manufacturing, and measurement information [166, 167]. Their adaptions or extensions, e.g., by knowledge aspects using Web Ontology Language (OWL) [168–170], allow to enhance their scope to further tolerancing-related purposes. Although MBD mainly supports communication and collaborative work [159, 171], data contextualization and information modeling are complex since it involves "different locations with different people using the data in different ways and in different contexts" [166], causing issues and barriers in its practical use

[172]. Hence, it is still an important research topic with currently unsolved matters, not only in geometrical variation management, where the increasing digitalization of manufacturing in the context of industry 4.0 attracts its attention [117, 158, 162].

To provide the tolerance information unambiguously and without redundancy [25] as well as to support the total workflow of tolerancing more continuously and consciously [108], a variety of specific **tolerance representation models** were proposed in the past [173], which are either based on directly computer-readable languages, e.g., Extensible Markup Language (XML) or OWL, or have to be first translated into a suitable programming language to make them computer-readable, e.g., Technologically and Topologically Related Surfaces (TTRS), Unified Modeling Language (UML), or GeoSpelling model [173]. More detailed information is given in [162, 173].

Intensified research in tolerance information modeling and the ongoing computerization are the basis for the **automation of tolerancing** [174], which is expected to considerably facilitate and accelerate the individual activities [114, 175]. Optimization plays an essential key role in this overall concept, particularly in tolerance allocation [P2] since it allows to automate and expedite the tasks typically solved by trial-and-error [P2, 176].

2.2 Tolerance-cost optimization

As traditional heuristic approaches for tolerance allocation have only limited applicability (see Sec. 2.1), solving more complex problems in the industry by repetitively using a combination of sensitivity and tolerance analysis is often preferred [P1] (see Fig. 5 (a)). Based on an initial guess [P1, 60, 82], experience [35, 60, 144], handbooks, standards, or relying on past and similar product designs [123, 177–180], tolerance analysis is used to check if the KC requirements can be fulfilled or not [P1]. Sensitivity analysis, often named contributor/contribution analysis in tolerance design [60, 181], helps to improve the solution in a structured way. Local methods, widespread in commercial systems for computer-aided tolerancing (CAT), e.g., arithmetical, statistical, and High-Low-Median (HLM)-contributor analysis, as well as more powerful, global, derivative-, variance-, and density-based sensitivity analysis methods are used to identify the contribution of the individual (non-)geometrical variations to the KCs [182, 183]. Small contributor values indicate which tolerances should be widened, as a low leverage on the KCs implicitly consequences a high one on costs. High contributions hint at the tolerances to be tightened, as their adaption will have the largest effect on the resultant KC variation. This more or less endless loop has to be stopped manually by the human-based decision that the current solution is optimal enough [184] or patience has run out [18]. Consequently, optimality cannot be assured [184–186], rather hoped for [187]; it is a time-consuming and tedious approach [188, 189] due to its unsystematic, experience-based procedure [47, 185, 186]. Moreover, it is not based on quantitative cost measures [47, 190].

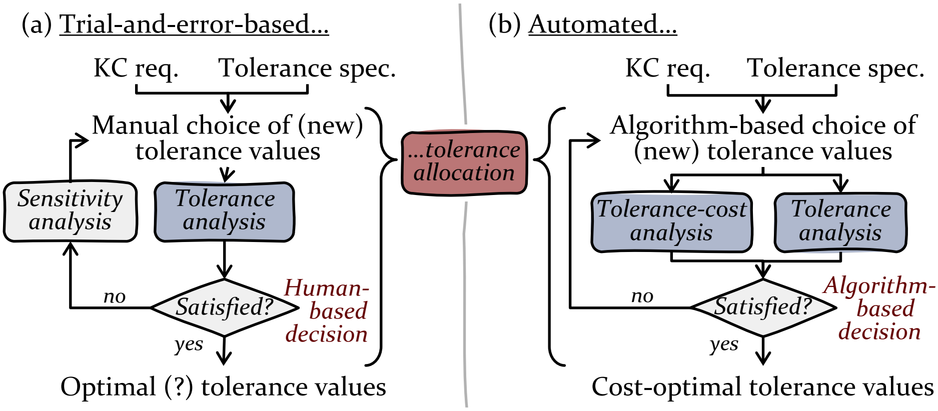

Figure 5: Iterative, trial-and-error-based and automated tolerance allocation in comparison.

To eliminate the iterative adaption of the tolerance values [191], this human trial-and-error-based approach is converted into an optimization problem [192], which is solved in a computer-based and automated way using powerful optimization algorithms [47, 193] (see Fig. 5 (b)). In doing so, tolerances are automatically reallocated using the information of both tolerance-cost and tolerance analysis until the algorithm decides on the basis of quantitative termination criteria that the optimal tolerances must have been found [P5].

Numerous definitions and methods have been presented under different names in literature to describe the optimization-based interpretation of tolerance allocation (see Appx. A.1). The term **tolerance-cost optimization** unifies all presented approaches in one common definition and comprises to **"all methods that aim to identify an optimal set of tolerance [values] with focus on cost and quality using optimization techniques [...] imply[ing] that the cost aspect is covered [(implicitly or explicitly)] by at least one objective or one constraint"** [P1].

Consequently, the representation of the individual pre-production, production, and post-production steps in the lifecycle of a technical product under the perspective from both tolerance-related cost and quality aspects mainly shapes the definition and solution of the optimization problem (see Fig. 6).

From the global perspective of systems thinking, it addresses a whole system covering, in addition to all (pre-)production-related aspects, a variety of further issues, for instance, customer satisfaction, market conditions, ecological aspects, taxes, regulations, etc. [29, 194, 195]. Depending on their scope and level of detail, this requires a more or less intensive front-loading of individual activities from later lifecycle phases and, consequently, always a strong pull of data, information, and models (see Fig. 3). Regardless of differences in detail of the numerous approaches, tolerance-cost optimization is always a combination and harmonization of three main elements, viz. tolerance-cost analysis, tolerance analysis, and the optimization problem (see Fig. 6) [196]. The abstract picture of tolerance-cost optimization, drawn in Fig. 5 (b) and Fig. 6, is gradually detailed in the following.

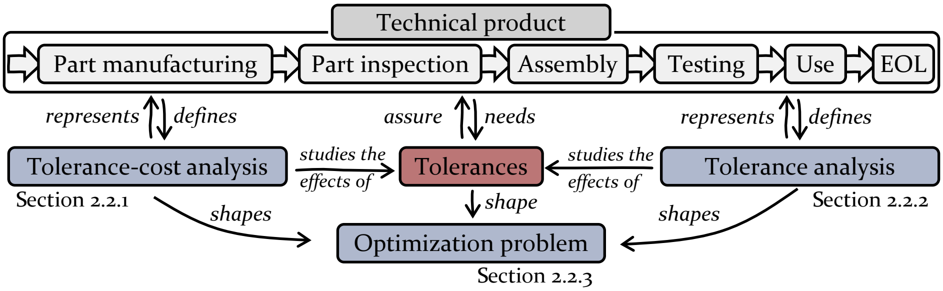

Figure 6: Concept of tolerance-cost optimization with its elements and interrelations.

2.2.1 Tolerance-cost analysis

Tolerance-cost analysis aims at getting insights into the direct and indirect economic impact of the tolerances assigned in product design. In contrast to traditional tolerance allocation, it enables to make quantitative claims about the cost of tolerance, which is defined as the "amount of expenditure needed to achieve certain levels of dimensional and geometrical accuracy" [197]. Hence, its basis, the **tolerance-cost model**, is an important key element [127] and offers decisive competitive advantages [198]. Its definition is, however, challenging and complicated [43, 127, 199, 200], as there is generally a lack [129, 198, 201] and need of a high amount of tolerance-cost data [198, 200]. Moreover, the access to reliable data sets is strongly limited [202] because only little tolerance-cost information is published, presumably mostly for confidential reasons [41, 203, 204]. In any case, their general suitability is questionable, as numerous factors impact the costs, which depend on not only technological aspects but also various external conditions [198], leading to the fact that cost data is always site-, machine-, tool-, operator-, and material-specific [41, 49, 129, 198, 203] and further dependent on the specification, i.e., the type and size, of the tolerated geometrical part feature [190, 200, 203].

Therefore, a systematic procedure for a precise and case-specific quantification of the manufacturing knowledge through a mathematical abstraction of empirical production data is essential [137] since the accuracy of the tolerance-cost model directly influences the reliability of the optimization results [137, 144, 205]. Fig. 7 illustrates the main steps of the tolerance-cost modeling process. The subsequent step-by-step explanation intends to overview the most relevant, interdisciplinary aspects.

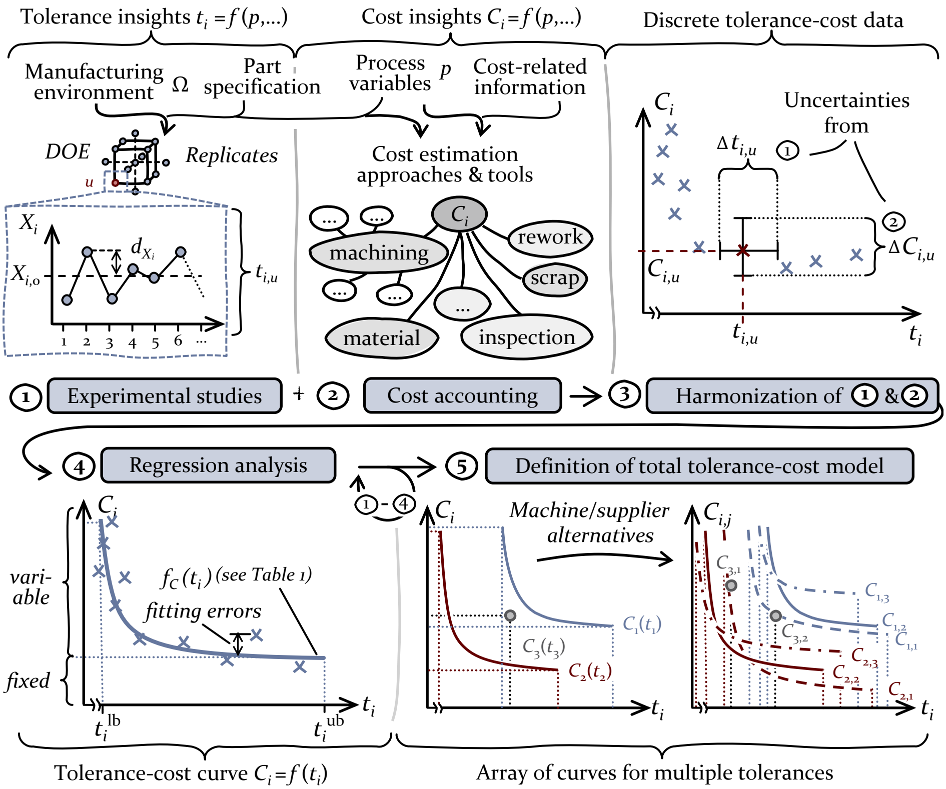

Figure 7: Overview of the main steps for systematically developing tolerance-cost models.

① – Experimental studies The value or magnitude of a tolerance t_i functions as an intrinsic productive factor establishing the link between the part variations and the resulting costs [206, P6]. Therefore, the process knowledge must be acquired and expressed via tolerance values. The unavoidable part variations occur during the single operation steps in the manufacturing process [128] and result in an accumulation of numerous inaccuracies or variations from different internal and external sources, e.g., inaccuracies and deformations of machines, tools, fixtures, and gauges, varying material properties, environmental conditions, etc. [21, 128, 145, 207]. Thus, the total manufacturing environment influences the level of achievable part accuracy. Apart from the machining setup, process parameters are significant control variables to reach a specified tolerance within a given machine/process range $\left[t_i^{\mathrm{lb}}; t_i^{\mathrm{ub}}\right]$ defined by the entirety of all boundary conditions. Experimental studies based on statistical DOE with multiple fabrication repetitions provide a series of measured values deviating with d_{X_i} from the ideal value $X_{i,0}$ [P6]. The tolerance values t_i are derived from the resulting probability of the population using statistical methods and characteristics [206, P6, 208].

Despite the comparatively high efforts in cost and time [P6], the gained knowledge on process variability, expressed through both tolerance values and probability distributions[4], is an essential rational basis for not only a reliable tolerance-cost analysis but also variation simulation in the context of tolerance analysis (see Sec. 2.2.2) [28, 30, 209].

② – **Cost accounting** The consideration of the tolerances' economic impact implies a thorough estimation and mathematical description of all incurred direct and indirect costs [202]. In general, all tolerance-related costs can be broken down into fixed (tolerance-independent) and variable (tolerance-dependent) fractions, while the latter typically decrease with increasing tolerances [200, 203]. Depending on the given application and the individual contribution to the total costs, the different cost fractions are either set as fixed or variable and cannot be classified unambiguously [203]. As tolerance allocation influences the entire product lifecycle (see Sec. 2.2), a variety of individual cost aspects may be of interest, ranging from material [210], machining [127, 210], tooling [211, 212], inspection [37, 210, 213, 214], rework/rejection/scrap [127, 210, 215] over assembly [37, 213, 216], maintenance and service [212] up to ecological [217, 218], and also social costs [217].

③ – **Harmonization of ① & ②** The incorporation of the information $t = f(p, \Omega, \ldots)$, gained in step ①, into the relation $C = f(p, \Omega, \ldots)$, obtained in step ②, is used to establish the relationship between the tolerance t, which serves as the mutual language to communicate the part accuracy requirements defined by design to manufacturing and inspection [219], and the incurred costs C [P6]. The result is a discrete tolerance-cost data set, which is exposed to uncertainties from simplified, approximate cost measures, experimental errors, and measurement uncertainties [203, P6, 220, 221].

④ – **Regression analysis** The empirical data serves as the basis for the subsequent application of regression analysis techniques converting the discrete data into a mathematical relation between cost and tolerance by curve

[4] Manufacturing tolerances are often chosen wider than the experimentally obtained natural tolerances to provide a margin of safety covering further variations such as tool wear [49].

fitting [17, 41, 190], which can indirectly reduce the influence of the uncertainties mentioned above by least square approximation [190]. Various parametric tolerance-cost functions f_C have been presented in literature, meeting the requirements of an ease of use, a sufficient degree of approximation and applicability to given manufacturing situations [202], and are reviewed in detail in [41, 198, 203]. In general, they represent the costs $C_i(t_i)$ as the sum of fixed ($\partial C_{\text{fix}}/\partial t_i = 0$) and variable ($\partial C_{\text{var}}/\partial t_i \neq 0$) cost fractions [123]:

$$C_i(t) = C_{\text{fix}} + C_{\text{var}}(t_i). \tag{1}$$

Except for the direct use of pure discrete data [222], traditional approaches transform the discrete data points into a mathematical expression using (piecewise)-linear [197, 223], exponential, or reciprocal functions with two up to four coefficients [41, 203]. In contrast, non-traditional approaches are either based on higher-order polynomial degrees [224], spline models [137, 225], or combinations of several traditional approaches [P1, 203]. Besides, Artificial Neural Network-based approaches have gained increased attention in literature to enhance the model accuracy of the highly nonlinear tolerance-cost relations [226–231]. Although cost curves are occasionally expressed as functions of process precision [232], variance [232], or process capability [221, 233], the cost-to-design tolerance functions $C(t_i)$ (or cost-to-manufacturing tolerance functions $C(\delta_i)$) have prevailed [P1]. Exponential and reciprocal tolerance-cost functions are preferred in research [198, 203], mostly in combination with fictitious cost data or coefficients relying on largely outdated books and cost charts [39], such as [204, 234–237]. The model type, however, needs to be chosen consciously for the given data minimizing the fitting errors [190, 208] as a sum of model type, term, and coefficient uncertainties [238]. Tab. 1 summarizes the most commonly used functions in literature.

The number, type, and level of detail of the cost aspects considered in step ②, certain industrially relevant elements of series production, e.g., the consideration of part tolerance distributions [198, 239] or cost increases through a 100%-part inspection for too low process capabilities [P7], as well as the deployment of novel manufacturing technologies, e.g., laser technology-based machining [208], manufacturing of composite structures [81, 240], or additive manufacturing [P6, 239, 241], emphasize the need of a continuous improvement of the existing cost accounting approaches. Enhanced approaches using activity-based costing are promising alternatives to cover the wide range of tolerance-related lifecycle activities causing direct and indirect costs [22, 242, 243].

⑤ – Definition of total tolerance-cost model The cost optimum for an assembly can only be achieved by balancing all part tolerances t_i. Thus, a

Table 1: Summary of tolerance-cost functions used and presented in literature [41, 179, 190].

	Cost function type	Mathematical equation f_C
Traditional	Discrete	$C_s(t_s) = c_s \; \forall \; s = 1, \dots, S$
	(Piecewise) linear	$C(t) = a_{(k)} - b_{(k)} \cdot t$
	Reciprocal	$C(t) = a + b \cdot t^{-c}$,
	(Modified) exponential	$C(t) = a + b \cdot e^{-c \; (\cdot d) \cdot t}$
Non-traditional	Hybrid (linear + exponential)	$C(t) = a + b \cdot t + d \cdot e^{-f \cdot t}$
	Hybrid (reciprocal + exponential)	$C(t) = a + b \cdot t^{-c} + d \cdot e^{-f \cdot t}$
	Hybrid (reciprocal · exponential)	$C(t) = a + b \cdot t^{-c} \cdot e^{-d \cdot t}$
	K-th polynomial	$C(t) = \sum_{k=0}^{K} a_k \cdot t^k$
	Spline models	*piecewise curve fitting*
	Artificial Neural Networks (ANN)	*numerical black box*

common tolerance-cost model is to be defined as a set of I several individual tolerance-cost functions predicting the single costs C_i to realize a part tolerance t_i by a predefined process and machine [44, 244]:

$$C_{\text{sum}} = \textstyle\sum_{i=1}^{I} C_i(t_i). \tag{2}$$

If there is more than one machine or process alternative j to realize t_i, each option has to be modeled by an individual cost function $f_{C_{i,j}}$. The resulting total tolerance-cost model, characterized by overlapping machine/process limit ranges [245], makes it possible to analyze the total costs C_{sum} for a given set of tolerances and an individual selection of machines, processes, and suppliers (see Sec. 2.2.4), where the tolerance-independent fixed cost shares play a decisive role. If several production steps are required to achieve a design tolerance t_i, each operation step's tolerance-related process costs must be modeled by an individual cost curve [41, 44].

Besides the presented aspects of tolerance-related single costs $C_i = f_C(t_i)$, a second class of quality-related costs is addressed in tolerance allocation. **Quality loss** costs are based on Taguchi's philosophy of product quality, claiming that any variation Δ_Y from the ideal of a predefined KC with its nominal Y_0, as a result of the assigned part tolerances t_i, leads to a loss of quality QL, customers' dissatisfaction and, thus, indirectly to costs [200, 246] (see Fig. 8 (a) vs. (b)). In contrast, following the traditional quality understanding, quality loss only appears when LSL or USL are exceeded (see Fig. 8 (a)). Loss functions $L(Y)$ are used to convert the expected quality loss into financial figures [247], following three main principles, viz. *nominal/target-the-best*, *smaller-the-better*, and *larger-the-better* [43, 248]. Product degradation occurring over the total product lifetime further amplifies the quality loss [200, 246] and is addressed under the term *present worth of the expected quality loss* [246]. The approximation of the hardly tangible effects of variance and bias of Y on costs and their integration into the optimization problem leads to a conflict since manufacturing costs and quality loss are contradictory [246, 249] (see Fig. 8 (b)).

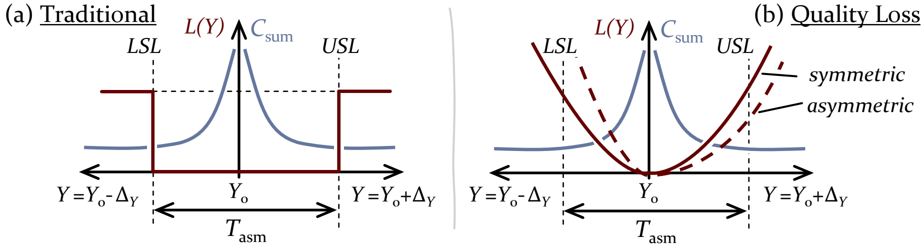

Figure 8: Quality loss $L(Y)$ and manufacturing costs $C(t)$ in conflict, inspired by [43, 250].

As the resulting probability frequency distributions of Y are often non-normal [251], different types of symmetric and asymmetric quality loss functions are needed to represent symmetric and unbalanced tolerances [252, 253], triangular [254, 255], trapezoidal [254], folded normal [256], log-normal [45, 257], and truncated distributions [258] as well as to consider capability indices [233, 258]. To overcome the assumption of non-correlation [259], various approaches have been proposed to describe the interrelations between multiple KCs [17, 260–263].

Although a realistic representation of (non-)tangible costs and quality loss for the whole lifetime of a product is an essential precondition for tolerance allocation, it is complicated by the fact that the necessary cost information is often lacking, the costs are difficult to estimate, or the manufacturing conditions in the design stage are not yet known in detail [264, 265]. *Alternative approaches* aim at facilitating the cost modeling process and enabling tolerance allocation with cost approximations, e.g., utilizing cost sensitivity curves [265, 266] or relative cost factors, taking the general IT-grades into account [203], or estimating the machinability to realize a tolerance [267–270]. In this context, the fuzzy theory is commonly used to represent the tolerance-related importance of the manufacturing cost and quality loss [271, 272], e.g., to consider cost-related aspects of service [273], wear [273, 274], and general usage [274], and to convert linguistic complexity evaluations [271, 275, 276] and expert opinions [272] into figures [277].

2.2.2 Tolerance analysis

Whether tolerance allocation is performed manually or automatically by optimization (see Fig. 5), tolerance analysis is needed to analyze the effect of the allocated part tolerances on the KCs in a repetitive loop [43, 179, 278]. Therefore, the deterministic or statistical **assembly response** Y to the variability of the individual parts can mathematically be described with the aid of an assembly response function f_Y over the stochastic input variables $\boldsymbol{X}$ [16, 57]:

$$Y = f_Y(\boldsymbol{X}). \tag{3}$$

Therefore, the assembly response Y functions as a representative measure to assure the associated KC under uncertainty.[5] The input variables $\boldsymbol{X}$ are not restricted to pure geometrical parameters and their respective tolerances, which are primarily focused on in tolerance design for mechanical assemblies but can be any **internal and external parameter** influencing both geometrical, e.g., gaps and clearances, and non-geometrical KCs, e.g., electrical power or magnetic flux [P1]. Besides the classification of influences into internal and external [285], it is helpful to distinguish them by their nature or how they are represented in optimization (see Fig. 9):

(a) *stochastic* and *deterministic*, if their variance is taken into account or neglected [P1],
(b) *time-variant* and *time-invariant*, if their mean or variance can change or is constant over product lifetime [286, 287],
(c) or *fixed* and *variable*, if their mean, variance, or both are considered as constant or adjustable in optimization [P1, 286].

In context of tolerance-cost optimization, temperature [286–290], mechanical loads through external forces or gravity [286, 287, 291–293] as well as wear [286, 294] are typical examples of additional variables. In contrast to geometrical part tolerances, they are usually set as a priori fixed boundary conditions in tolerance design and, thus, not considered as design variables to be adjusted through optimization (see Sec. 2.2.3).

The analysis results are primarily used to verify if the specified tolerances can assure the predefined KC requirements [16, 112]. Lower and/or upper limits *LSL* and *USL* divide the estimated assembly response distribution into

[5] In literature, numerous terms are used interchangeably for either the assembly response function [279, 280], its output, and its requirements, such as design/stack up function, fundamental equation of the assembly [281] as well as tolerance chain, datum flow chain, dimension loop [282] (according to the model used), critical/functional/assembly/design dimension [280] and assembly function(al) requirements [283, 284]. The terms *assembly response (function)* and *KC (requirements)* are preferably used in this thesis.

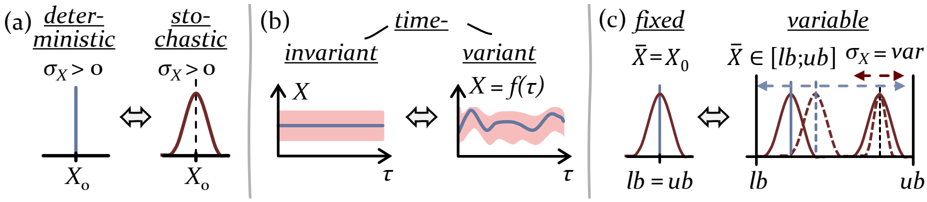

Figure 9: Classification of input variables X in tolerance analysis.

the region of conformance (also named reliability, acceptability [295–297], or yield [298, 299]) and the region of non-conformance/non-conformity (non-acceptance) [300, 301], composed of a lower and upper non-conforming fraction [302]. It is common to generally express these interrelations through probabilities P: [298, 303]

$$1 = \overbrace{P(LSL \le Y \le USL)}^{\text{conforming}} + \overbrace{P(Y < LSL) + P(Y > USL)}^{\text{non-conforming}} \tag{4}$$

or via the integral over the assembly response probability density ρ_Y: [298, 299]

$$\hat{z} = \underbrace{1 - \overbrace{\int_{LSL}^{USL} \rho_Y(\boldsymbol{t}, x)dx}^{\text{yield } yld}}_{\text{non-conformance rate}}. \tag{5}$$

Three interdependent measures are commonly used to evaluate the (non-)conformity of the KCs. The non-conformance rate (nc-rate) z is typically preferred to express the relative frequency of non-conform parts as a percentage or in parts-per-million (ppm) in compliance with the six sigma philosophy [P5].[6] In the case of normality of data, it can directly be converted into unit-less process capability indices, such as the C_{pk}-value [302, 304]. Process capability indices for non-normally distributed and one-sided KCs can be suitably considered by equations and methods developed for on-line process quality control and are internationally standardized by ISO 22514-2 [305]. In doing so, conformance rates and process capability indices are used to describe how many assemblies will probably be within the specified tolerance interval $T_{\text{asm}} = USL - LSL$ and to verify whether they meet the specified minimum conformance rates or process capability values. Besides, the verification can be inverted by checking whether the resulting assembly tolerance interval T_Y, which can be calculated as a multiple of the

[6] Despite their slight differences in meaning, the terms *reject*, *defect*, *failure*, and *scrap rate* are often used synonymously in this context [129, P5, 232, 243]. The term *non-conformance rate* will be used consistently in this thesis to describe the percentage of assemblies which exceed the predefined lower and/or upper limits of a KC.

standard deviation σ_Y for normally distributed Y, is less than or equal to T_{asm} [306].

If there is more than one assembly response function, representing one or **multiple KCs**, and thereby share at least one part tolerance, they are interrelated and correlate [6, 127, 307, 308]. Tolerance compensation methods can help to decouple and transform them into simple, uncoupled functions in advance [181, 309, 310]. However, multiple, often conflicting functions cannot be entirely avoided, leading to challenges in predicting the nc-rate [311, P8] and having to be considered simultaneously in optimization [312, 313].

After having deliberately focused on the result and the objective of tolerance analysis so far, i.e., the assembly response and the parameters for assessing the fulfillment of the KC requirements, the three main preceding steps to get there are now discussed, viz. the representation of geometrical variations on feature level, the modeling of their common influence on the system behavior on assembly level under the presence of variations and their evaluation using arithmetic and statistical tolerance analysis techniques [314].

Geometrical models intend to model and represent the features, primarily computer-aided, with their variations in size, orientation, position, and shape with respect to the specified tolerances, their values, and further process-related information from manufacturing [94, 109, 315, 316]. In this context, different models have been presented and applied in literature and industry, such as variational solid (offset) models [317, 318], tolerance envelopes [319], vector-, matrix-, and small displacement torsor-based models [132, 320–322], and skin model shapes [315, 323].

Behavior models are used for tolerance propagation, representing how the features interact in the presence of variation during assembly and in use [314, 316]. Concerning the geometrical model type serving as input, they can be classified into deviation and tolerance accumulation approaches [314, 316]. Tolerance stacks and vector loop equations [132, 324, 325] as well as matrix models [132, 326] are examples of deviation accumulation, establishing the relation f_Y between t and Y through variations on either analytical or numerical basis [23, 94, 314]. In contrast, approaches based on Tolerance-Maps® [327, 328], polytopes [329, 330] and deviation domains [327, 331], for instance, use certain summation and intersection operations to accumulate the individual tolerance zones directly [94]. Tailored to the individual use case, geometrical and behavior models must be carefully defined and harmonized to establish a realistic expression of the assembly response function f_Y [94] while accepting simplifications at feature, part, and assembly level [323].

Based thereon, the final tolerance evaluation using either **arithmetic** or **statistical methods** follows [314, 332].[7] *Arithmetic* methods [324, 334], mostly named worst-case, rarely sure fit [335] or methods of extremes [244], aim at assuring all possible accumulations of geometrical part variations to provide a 100%-conformance region [324, 336] through absolute interchangeability [336, 337]. Without making any assumptions on part distributions [338], the extreme, worst-case configurations are analyzed, which typically result when the individual input variables are considered at their lower and upper bounds of the assigned tolerance limits [244, 324]. Except for safety-critical applications [337], this approach is too pessimistic for most practical problems [336, 339] where it is statistically unrealistic to realize the worst case configurations very often by random assembly [126]. As a result, tolerances must be chosen extremely tight, which are hard to achieve and control and, thus, cost-intensive [336, 337].

It is far more realistic and cost-effective to choose probabilistic approaches [28], which accept a small fraction of non-conform assemblies giving space to choose wider tolerances [244, 336]. *Statistical* tolerance analysis predicts the assembly probability distribution based on the individual part tolerance distributions, usually expressed by a set of distribution type-dependent parameters and moments, e.g., the mean μ, standard deviation σ, skewness κ, and kurtosis γ [339–341]. The traditional, mostly convolution-based approaches like the root sum squares method (RSS) in modified and generalized versions to cover (estimated) mean shifts and non-normal distributions [40, 179, 180, 342, 343], the Hasofer-Lind reliability index method [186, 344], or first- and second-order reliability methods [303, 345], show their strengths in low computation times for tolerance-cost optimization [41], but generally lack applicability and validity [41, 280].

Sampling-based tolerance analysis, mainly in the form of Monte Carlo Simulation [23, 333], overcomes these limitations [18, 41, 280] and provides the most realistic results [346] since it can handle any distribution [23, 339, 347] and assembly response function, whether it is nonlinear and should not be linearized [282, 339] or it can only be represented implicitly [320, 347]. Random number generators in combination with sampling technique-specific algorithms are first used to derive a set of samples according to a predefined sample size n to represent the stochastic input variables $\boldsymbol{X}$ while taking the part tolerance probability distributions and its assigned tolerances t_i into account (see Fig. 10) [18, 339]. Second, the assembly response Y is

[7] Besides the preferred classification into arithmetic and statistical approaches, different approaches, e.g., based on fuzzy logic and non-probabilistic set theory, are rarely used in literature [78, 333].

repetitively, sample per sample, analyzed, leading to the assembly response distribution [18]. Provided that a sufficiently high sample size n is chosen [18, 328, 348, 349], it serves as a reliable basis for estimating the (non-)conformance rates to statistically evaluate the KC requirement fulfillment [P5]. As predicted early on [350] and in line with uncertainty quantification methods [351], sampling-based tolerance analysis has become the standard in research but also industry [23, 130] due to its simplicity [134, 280, 352], flexibility [280, 347], and broad applicability [130, 280]. It is the basis of most commercial computer-aided tolerance analysis software [333].

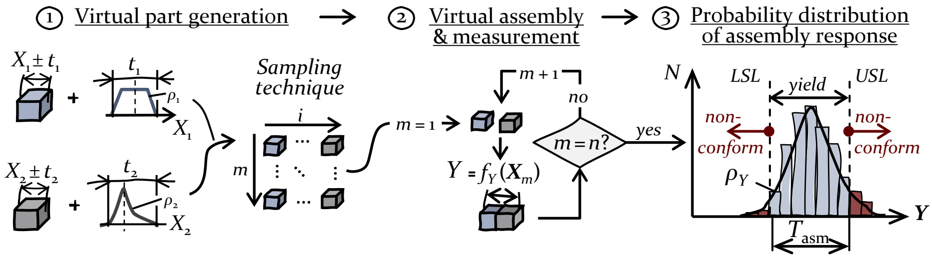

Figure 10: Workflow of sampling-based tolerance analysis adopted from [P9].

Since the choice of the individual models mainly depends on the type and characteristics of the product design and its assembly process [P1, 353], it is helpful to differentiate between two main **assembly types**: part-driven and process-driven assemblies [6]. In **part-driven assemblies**, the positioning of the parts results from joining and constraining them by their prefabricated mating features, so the KCs are primarily influenced by part variations [6, 354]. Compared to isoconstrained, i.e., kinematically/properly constrained, assemblies, gaps are needed to ensure the assembly of overconstrained, part-driven assemblies without mitigating the fulfillment of the KC requirements [6, 314, 355]. The challenge in tolerance allocation is to find a balance between the clearance values and tolerances needed to avoid assembly problems and to assure the KC for all possible gap configurations an assembly can take during assembly or in use, if not all degrees of freedom are finally locked [134, P10]. Besides assuring assembly through clearance, certain degrees of freedom are intentionally left open for mobility in mechanism design[8] [6]. As they are designed to generate a defined movement with a certain accuracy [357, 358], it requires a time-variant evaluation of the KCs, either for the whole movement or predefined, functional-relevant points in time [P1]. As they have traditionally been an integral part of tolerance research, mechanisms

[8] The definition of the term *mechanism* is not consistently used in literature. In this work, it is used to describe all systems in motion as "mechanical portion[s] of a machine that ha[ve] the function of transferring motion and forces from a power source to an output" [356].

with full joints, such as revolute joints, including effects of clearance [358–362] and lubrication [287, 363], and half joints, such as cams [364, 365] and gears [279, 366–368], are in focus of tolerance allocation.

In contrast, **process-driven assemblies** are characterized by the fact that the KCs are influenced mainly by the assembly process [354]. Hence, the process variables serve as essential control variables for the quality assurance of the total assembly [369]. The fixture layout design [55, 370, 371], including the position, type, and number of clamps and locators to lock the open degrees of freedom multiple times [6], its accuracy and further tool variations [369], the sequence of part joining steps of (spot) welding, riveting, clinching, glueing, or clinching [372–374], as well as the assembly sequence order of the individual parts [303, 375] additionally cause part deformations, mechanical stress and spring back-effects [376, P11]. As these assembly-related effects significantly influence the KCs of the overconstrained sheet-metal assemblies, and in contrast to part-driven assemblies to a larger extent than the part fabrication-related part variations, they have to be addressed in detail in variation simulation [369]. To describe the propagation of the numerous variations over the various multi-station assembly steps, specific models have been proposed in literature, e.g., the state space model [377, 378] and the stream-of-variation analysis model [379, 380], and serve as a basis for assembly process-oriented tolerance-cost optimization methods [39, 196, 311, 369, 381]. Consequently, tolerance allocation-related research on process-oriented assemblies differs from part-driven assemblies and forms an own but strongly connected branch [39].

The number and complexity of the different, previously discussed aspects and their interrelations influencing the quality assurance of the KCs make it often difficult or even impossible to express the geometrical and behavior models by mathematical equations and to derive a mathematically closed, explicit definition of the assembly response function [P2]. As a solution, **numerical simulation, optimization, and software tools** are used in the context of tolerance analysis to implicitly support establishing the relationship between tolerances and the KC [314]. While parametric CAD-tools can suffice for simple mechanical assemblies [227, 382], complex contact situations, e.g., in simulations with form defects [383, 384], overconstrained assemblies with gaps [134, 385], or mechanisms with half joints [279, 366, 367] require numerical methods for assembly simulation. Established CAD-integrated software modules, e.g., VSA-3D/Pro [231, 386–388] or Quick-UG stack up module [389], and stand-alone and more detailed CAT-software for tolerance analysis, such as RD&T® [217, P11, 390], 3DCS® [391–393], Cetol6σ® [394, 395], Variation Analysis® [46], eM-TolMate® [193], or Sigmund [396], can be used in tolerance-cost optimization using interfaces and exchange formats. Moreover, FE- and CFD-simulation are helpful tools to consider non-geometrical parameters or effects in more detail, e.g., on both geometrical and non-geometrical KCs, directly or approximated by surrogate models in tolerance analysis [81, 290, 291, 397–399].

With the increasing complexity of the assemblies and the ambition to model them with similar accuracy avoiding to impair the validity by assumption and oversimplification, analyses are not practicable in reasonable computing times [P2] – despite the ongoing increasing computer performance (see Sec. 2.3). Since tolerance analysis is performed repeatedly for a large number of different tolerance combinations within the inner optimization loop [27, 400], the computational and time effort required, which can take up hours or even days [130], has a staggering effect on the efficiency of the entire optimization [296, 401]. The usage of sampling significantly aggravates this dilemma [27, 296, 400, 402], as a large number of random samples are necessary to be able to reliably assure the high industrial requirements in small parts-per-million ranges [18, 40, 339, 352]. Hence, efficient tolerance-cost optimization requires efficient tolerance analysis routines [403]. **Variance reduction methods** help to increase efficiency because they require smaller sample sizes to achieve the same precision as pure Monte Carlo Sampling (MCS) [192, 352]. In the context of tolerance-cost optimization, Latin Hypercube Sampling [192, 392, 404, 405], Hammersley sampling [406], Quasi-Monte Carlo method using Sobol' sequences [392], Number Theoretical Net [311, 400], importance sampling [352, 407], subset sampling [392], antithetic variates [192, 405], correlation functions [352, 407], and polynomial expansion [292, 293] have proven their suitability. Furthermore, an adaptive increase in sample sizes over the optimization iterations can significantly reduce the total number of tolerance analyses required [134, 279, 408].

Besides their intended use in deriving unknown relationships between inputs and experimentally investigated outputs [386], such as in tolerance-cost modeling (see Sec. 2.2.1), surrogate models are used even if these relationships already exist in explicit or implicit form, but their evaluation is computationally time-consuming [409]. Hence, they function as **meta models** making statements about (simulation) models [410, 411]. They mainly aim to speed up the individual tolerance analysis' substeps in tolerance-cost optimization. Different types of regression models, for instance, based on low-order polynomial functions [298, 386, 412, 413], Gaussian and kriging models [81, 311, 402, 413–416], ANNs [398, 399], or support vector machines [P10], are used either as approximate (sub-)models, e.g., to replace computational-intensive FE- and CFD-simulations [81, 240, 398, 399, 414, 415] or as direct surrogates of the total tolerance analysis [298, 311, 386, 402, 412, 413, 417, 418]. In addition to general background information on surrogate modeling and their use in optimization given in the Appx. A.5, a detailed discussion on the different ways of using them in tolerance-cost optimization will follow in Sec. 6.2.

2.2.3 Definition and solution of the optimization problem

Optimization is an automated and, thus, efficient way to solve the tolerance allocation problem [P2] by "obtaining the best result under given circumstances" [419]. For this purpose, it is necessary to express a given problem through the language of optimization, basically consisting of the **objective(s)**, **constraints** and **design variables** [419].

In tolerance allocation, two main strategies can be differed according to their objectives in focus. While **quality-driven** (quality-priority) tolerance-cost optimization aims at optimizing the fulfillment of the quality requirements to obtain the best quality, the aim of **cost-driven** (cost-priority) tolerance-cost optimization is to minimize the total tolerance-related costs necessary for quality assurance [9, 196, 303]. Consequently, objective and constraint(s) are flipped, whether it is designed as *a design for quality to meet cost*-approach or *a design for cost to meet quality*-approach (see Chap. 1)[9], whereas the latter depends on the underlying quality philosophy (see Fig. 8).The main fundamental strategies with their corresponding optimization problems are defined as follows: [192]

$$
\begin{array}{lccccr}
 & & \multicolumn{2}{c}{\textit{b) cost-driven}} & & \\
 & \textit{a) quality-driven} & & \textit{c) robust tolerance design} & & \\
\text{Minimize} & \hat{z} & C_{\text{sum}} & C_{\text{sum}}; L & \textit{objective(s)} & (6) \\
\text{subject to :} & C_{\text{sum}} \le C_{\text{max}} & \hat{z} \le z_{\text{max}} & \hat{z} \le z_{\text{max}} & \textit{constraints} & (7) \\
 & t_i^{\text{lb}} \le \boxed{t_i} \le t_i^{\text{ub}} & t_i^{\text{lb}} \le \boxed{t_i} \le t_i^{\text{ub}} & t_i^{\text{lb}} \le \boxed{t_i} \le t_i^{\text{ub}} & & (8) \\
 & \multicolumn{3}{c}{\textit{design variables}} & &
\end{array}
$$

The objective function(s), the constraints, and the design variables have to be adjusted or extended by additional case-specific elements tailored to the respective field and purpose of application [P12] (see Sec. 2.2.4).[10] This

[9] This distinction is based on the general definition of *design to cost* and *design for cost* acc. to Dean and Unal in [420, 421].

[10] The optimization problem given in Eq. (6)–(8) is restricted to one single KC for reasons of clarity. In case of K multiple KCs, either the number of quality assurance objectives (see Eq. (6) a)) and constraints (see Eq. (7) b)) are extended to K individual equations or an overall quality criterion takes all KCs simultaneously with its correlations into account. In the case of c), the multivariate quality loss is defined by K quality loss objective functions and its correlation terms using covariances.

includes the subroutines of tolerance-cost analysis and tolerance analysis providing the information for both the objective and constraint evaluation.

The **constraints** can be classified according to their purpose into feasibility and acceptability of a design [422]. The tolerance design's feasibility in the context of tolerance allocation means that the obtained solution can be technically realized for a given scenario. Process accuracy/capability constraints defining the lower and upper boundaries t_i^{lb} and t_i^{ub} of the design variables [139, 201, 423] are feasibility constraints ensuring that only tolerances are picked by the optimizer, which a given manufacturing setup can technically realize. Acceptability constraints, in contrast, define if a technically feasible solution also satisfies further constraints, i.e., in case a) an upper-cost limit C_{max} [196] or in case b) a maximum non-conformance limit z_{max} [P5]. The nc-rate $\hat{z}$ acc. to Eq. (5) is exemplarily chosen as a quality measure in Eq. (6) and Eq. (7). In case a), except for the assembly tolerance T_Y, the choice of the process capability C_{pk} and the yield *yld* result in a maximization problem, which, however, is always transformed into a minimization problem by the negative of the objective function value, for example, $\max(C_{pk}) = \min(-C_{pk})$. In case b) and c), the inequality constraints in Eq. (7) are reformulated to $T_Y \leq T_{Y,\mathrm{max}}$, $C_{pk} \geq C_{pk,\mathrm{min}}$, or $yld \geq yld_{\mathrm{min}}$ [41].

The **design variables**, also called decision variables [419], which are "the quantifiable parameters that the algorithm can change" [424], are primarily the magnitude of the design tolerances (or manufacturing tolerances δ_i in process design, see Sec. 2.1.2) [93, 192, 295]. The tolerance types are usually set as fixed [16], with a few exceptions proposed in [192, 405]. The tolerance intervals t_i, defined as the difference between the upper and lower limit $t_i = UL - LL$, are thereby varied by the optimizer. A fixed mean shift is usually used for unbalanced bilateral tolerances (see also Fig. 9 (c)). Considering the nature of the design variables, the tolerance values can either be *continuous*, *discrete*, or *mixed-discrete* as a combination of both types [425]. Besides the choice of any value from the continuous range $\left[t_i^{\mathrm{lb}}; t_i^{\mathrm{ub}}\right]$ with $t_i \in \mathbb{R}^+$, they sometimes have to be selected from a limited, discrete set of predefined options, if either fixed classes in case of external supply or IT standard classes [426] are considered or discrete tolerance-cost functions are used (see Tbl. 1). Moreover, it has to be considered in the design variables and by additional constraints that some of the tolerances may be set as fixed a priori since they should not be optimized and that multiple tolerance values may be set as equal or correlated [427, 428], for instance, if they originate from the same manufacturing process indirectly saving costs through setup reductions or if parts from the same type are used several times in one assembly [96, 127, 307].

In most cases, a least-cost tolerance design b) is prioritized over case a) and defined as a minimization problem of the single tolerance-related costs C_{sum} acc. to Eq. (2) [429], and sometimes supplemented by the assembly-quality related costs due to quality loss in case c).[11] The consideration of quality loss L in case c), which is often addressed under the term **robust tolerance design** in literature [41, 251] (see Sec. 2.2.4), extends the single-objective problem to a *multi-objective problem* with conflicting objectives (see Fig. 8) [432]. The design space is usually limited by the acceptability constraint Eq. (7) c), which is rarely omitted since the quality loss costs can indirectly control the quality assurance. To handle this problem, it can be transformed into a single-objective optimization problem by a weighted summation of the objectives, where the weights w indicate their relative importance [433, 434]:

$$C_{\mathrm{tot}} = w_1 \cdot C_{\mathrm{sum}}(\boldsymbol{t}) + w_2 \cdot L(\sigma_Y) \qquad \text{with: } w_1 + w_2 = 1. \tag{9}$$

Besides an equal weighting [200, 232, 250, 251], individual (normalized) weight factors w_i are chosen based on the designers' prioritization or experience [433, 434]. Avoiding choosing the weights before optimization, multi-objective optimization approaches determine a set of alternative but equivalent best solutions. A certain solution can then be selected from the resulting Pareto set either by a manual prioritizing of the objective functions or supported by decision theory methods such as the TOPSIS method [414, 417, 432].

In the beginnings of tolerance-cost optimization, finding the best solution for the mathematical tolerance allocation problem out of the infinite number of solutions [41, 180, 244] was mostly based on **deterministic optimization techniques** [39]. For simple allocation problems with convolution-based tolerance analysis subroutines, optimal solutions can be found in low computing times [S1]. As they are based on mathematical principles and often need information on gradients or derivatives [39, 352], they mostly impose strict requirements for monotonicity [36, 199, 297], continuity [96, 199, 435], and derivability [96, 435, 436] of the objective and constraint functions [199]. Hence, traditional algorithms, such as linear and nonlinear programming, often reach their limits, not only for industry-relevant problems, like

- non-traditional tolerance-cost functions, process limits, and machine/process alternatives [41, 96, 435] (see Sec. 2.2.4),
- multiple, interrelated KCs [41, 96, 435],
- nonlinear and implicit assembly response functions [41, 368, 437], or

[11] In a few cases, tolerance-related costs are addressed indirectly by a maximum widening of the tolerance values (see, for instance, in [176, 185, 399, 427, 430, 431]).

- sampling-based tolerance analysis techniques [352, 437, 438].

There are numerous strategies and tricks, such as linearization [176], conversion of the probabilistic problem into a deterministic one, for instance, by reliability indices [36, 186, 297, 344], estimation of gradients when using sampling methods [352, 403, 407, 437], or establishing closed-form solutions for quality loss based on Lambert W functions [439–443]. However, their applicability is either limited [44, 435], the tolerance allocation problems are strongly simplified [176], or their implementation requires high mathematical and optimization skills to formulate them correctly.

In line with the general trends for solving real-world, mathematically complex problems, **metaheuristic, stochastic optimization algorithms** are commonly used in tolerance allocation to explore the multimodal, non-convex, partly discrete, and stochastic search spaces efficiently and to find the global optimum [39, 444]. These soft-computing algorithms are mostly population-based and mimic natural processes, usually inspired by biology, physics, and chemistry [445, 446]. As they are global, direct search methods using random principles for exploitation, i.e., local intensification of solutions, and exploration, i.e., global diversification, of the search space, they are not based on gradients or derivatives, their programming and implementation are simple, they solve complex problems while having a higher probability of finding the global optimum, and are resistant to noise [433, 444, 447]. Relying on one of the so-called free lunch theorems [448], claiming that all algorithms perform on average equally well for different values as they all show individual strengths to solve various problems, a wide variety of algorithms have been developed and implemented over the years [445]. Hence, any metaheuristic algorithm[12] can principally be used for tolerance-cost optimization, as long as constraints can be taken into account, and additionally, depending on the problem type, (mixed-)integer or discrete optimization variables as well as multiple objectives can be considered. Thus, not only widely acknowledged algorithms, e.g., simulated annealing [44, 93, 97, 232, 451, 452], genetic algorithm (GA) [21, 96, 290, 291, 303, 431, 432, 434, 447, 453–455], particle swarm optimization [33, 286, 432, 456–462], differential evolution [33, 130, 227, 431, 434, 455, 463], scatter search [464, 465], tabu search [223, 466], and pattern search [467, 468], are studied in literature. But also less established ones, such as ants colony algorithm [469], artificial bee algorithm [470, 471], bat algorithm [472], cuckoo search (CS) [294, 408], whale optimization

[12] Despite the slight difference in the definition of heuristic and metaheuristic optimization that metaheuristic is understood as *higher-level* heuristic approaches, both terms are used interchangeably in literature [445, 449, 450]. Hence, all stochastic algorithms using randomization, local search, and global exploration methods are commonly called metaheuristics [445].

algorithm [473], self-organizing migrating algorithm [474], game theoretic approach algorithms [475–477], seekers algorithm [272], imperialist competitive algorithm [478], teaching-learning-based optimization [479, 480], and intelligent water drops algorithm [14]. Hybrid algorithms, combining the individual strengths of stochastic and deterministic (or several stochastic) algorithms in terms of exploration and exploitation, help to further improve the solution and to increase the probability of finding the global optimum [245, 481–483]. Apart from the substantial benefits of metaheuristic optimization algorithms, they cannot guarantee finding the global optimum [39], they are less efficient as they might need a considerable number of iterations to converge [484], and finding suitable settings for a given problem is crucial, but decisive to identify first a feasible and second a near-optimal solution [485]. In addition to the algorithm itself, the handling of the multiple constraints influences the optimization procedure and its solution. The penalty approach is mostly preferred transforming the problem into an unconstrained one by adding penalty terms to the objective values if constraints are violated [21, 313, 486]. More detailed information on metaheuristic algorithms, in general, is given in Appx. A.3.

Besides the presented strategies using deterministic and stochastic optimization techniques, solution techniques relying on **methods adopted from quality engineering** for off-line-quality control [101, 248] are used, claiming to be more practicable and applicable to complex assemblies [16, 39, 41]. Fractional Factorial DOE, such as orthogonal arrays [266, 487] or Central Composite and Box-Behnken Designs [488, 489], mixture-amount experiments [490, 491] and Monte Carlo Sampling [492], are primarily used in combination with analysis of variance (ANOVA) [39] to explore the design space and to find a suitable solution. However, they represent a comparatively small portion of the tolerance allocation approaches in literature because they cannot be applied universally and do not guarantee optimal solutions [P1].

2.2.4 Optimal tolerance allocation + "X"

Initiated by the stream of CE, various inter- and multidisciplinary aspects from the downstream product development steps have been integrated into the tolerance design phase (see Sec. 2.1). In addition to merely expanding the optimization problem through additional elements such as specific cost details, integrated optimization approaches have prevailed, concurrently addressing one or more activities or problems ("X") from mostly downstream but also upstream product development phases. In doing so, additional or adapted objectives and constraints with shared or additional design variables are considered within one joint, overall optimization problem [216, P12] or by multi-level or -stage optimization strategies [196, 493, 494].

As one of the first, the directly adjacent tasks from tolerance allocation for manufacturing were shifted to the design phase (see Sec. 2.1). The extension of the optimization problem by manufacturing tolerance design variables as well as machining tolerance and stock removal allowance constraints [44, 93, 139, 457, 495] enables a simultaneous consideration of KC requirements on the assembly level and process design-related aspects on the part level. The approaches developed are addressed under the terms **concurrent/simultaneous tolerance design/allocation/synthesis/optimization**. Besides the consideration of dimensional and geometrical tolerances [430, 432, 465, 496], integrated approaches additionally focus on further process design aspects, e.g., optimal machining (cutting) process parameters [211, 497].

Since there is usually more than one predefined machine and/or process alternative to realize an assigned design or manufacturing tolerance t_i or δ_i (see Fig. 7), optimal tolerance allocation is inevitably accompanied by the problem of machine/process selection. As the available options with their process limits dictate the respective achievable tolerance ranges and least-cost combinations, their preselection before optimization cannot lead to the global optimum [498]. Hence, the definition of a concurrent optimization problem inevitably enables a realistic selection of tolerances for the processes and machines used [97, P9]. It further supports make or buy decisions with multiple supplier alternatives [260, 494, 499, 500]. One way to address **alternative selection**[13] in tolerance allocation is to treat it as a nested subproblem to be solved within the inner optimization loop, for instance, using exhaustive or univariate search methods [96, 312, 473, 501–503] or the minimum-cost curve, also called bottom curve follower approach, selecting the least cost-intensive alternatives for the current tolerances t_i [97, 498, 501, 503]. Besides, the idea of simultaneously solving both problems within one global optimization problem, where additional integer design variables take over the selection task, was implemented in different ways, e.g., by means of a multiple-choice knapsack problem [308], pseudo-boolean approach [504], branch-and-bound [186, 312], zero-one integer programming using the Balas' algorithm [38], sequential programming based on Lagrange multipliers [93, 312], and the Box complex method [505]. However, all these methods are mostly too restrictive, inefficient, or cannot find the global optimum for more complex problems, e.g., advanced tolerance-cost functions with process limits or multiple interrelated KCs [38, 41, 312, 501]. They essentially lost their

[13] As machine/process and also supplier selection can be treated equally from the optimization point of view [P9], they are summarized under the term *alternative selection* in this work.

importance as they originate from times with limitations in optimization [P9]. Nowadays, the highly nonlinear, mixed-integer problems are typically solved by metaheuristic optimization [44, 96, 307, 447].

As the selection of machines and processes is strongly connected to **process planning and scheduling**, these methods are often extended by further tolerance-related aspects. Tolerance allocation is, thus, combined with optimal process planning of multi-stage, partially site-distributed production steps [139, 216, 224, 242, 243, 405, 506], partially under a reconciliation of bought-in parts [494], to minimize the overall costs while considering machining, overhead, and idle times, [473, 507], waste [485], resource allocation [215, 508], machine loading capacities [139, 499], product rates and demands [139, 485, 499], and delivery time constraints [509]. The balancing of tolerances and process planning positively impacts the single overall equipment effectiveness (OEE) of the machines involved [349] and, thus, the total manufacturing costs, but also influences the subsequent assembly steps [194, 216].

Consequently, process planning for part fabrication often goes hand in hand with the design of the **assembly process**, significantly influencing the KCs, especially in the case of process-driven assemblies (see Sec. 2.2.2). Therefore, optimization-based fixture layout design and assembly sequence planning, including joining sequences of individual operation steps, e.g., spot welding sequence [372, 510] and part assembly sequences, are acknowledged methods in the industry to assure assembly quality while taking variations from part manufacturing using already fixed tolerances into account [375]. To further exploit its potential, integrated approaches have been developed to align tolerance allocation and assembly process design by embedding fixture layout optimization [196, P11, 493], assembly technique selection [300, 303], or assembly sequence planning [300, 303] into tolerance-cost optimization. Besides the detailed planning of the single process operation steps, this also includes further technical and economic production planning-related decisions and aspects, such as investments, automation, installation, and operation of multi-station assembly lines [216].

In this case, the underlying assembly strategy mainly dictates product and process design. Tolerance allocation is usually based on the concept of interchangeability requiring tight tolerances to fulfill the KC requirements when parts are randomly assembled in mass production [49, 511]. **Selective assembly**, in contrast, compensates the geometrical part variations to a certain degree within the assembly process by a thoughtful pairing of groups of parts of a predefined quality, also called classes, categories, or bins [512, 513], allowing to achieve high precision assemblies with low precision parts [310, 512, 514, 515]. Thus, tolerances can be further widened, leading to a cost benefit [428, 512] while additional costs, e.g., for a 100%-inspection and holding, etc., are amortized [513, 516]. While selective assembly has become well established in the automotive and roller bearing industry over the years [512], it is currently getting more into focus in the context of industry 4.0 and digital twins [514, 517–520]. Optimal selective assembly problems try to find an optimal binning strategy while tolerance values are usually set as fixed [521–525]. In combination with optimal tolerance allocation, tolerance values are considered variable, defining the equal widths or areas of the bins for either a fixed or variable number of bins using the potentials of both subdisciplines [14, 428, 470, 526, 527].

Besides the early consideration of integrated tolerance allocation approaches in the design and pre-production phase, they further offer the potential to be used for real-time optimizations during production taking advantage of adaptive strategies for the design and scheduling of part fabrication and assembly operations [518, 528].

In addition to these streams of front-loading, optimal tolerance allocation is further coupled with parameter design to **concurrently select both nominal and tolerance values**. In addition to costs and quality, the objectives or constraints are commonly supplemented by different measures of robustness [529].[14] The definition of both nominal values and the tolerances of internal and external parameters (see Fig. 9) as variable intends to achieve a global cost and product robustness optimum using different measures, such as the quality loss mentioned before [5, 435, 489, 530, 531], signal-to-noise-ratio [41], sensitivity [41, 461, 469], variability [495], or manufacturing costs' sensitivity [532]. Additional constraints avoid identifying infeasible solutions through invalid parameter combinations [469].

In conclusion, the individual designs and implementations of tolerance allocation, addressing a variety of different lifecycle aspects from design, pre-production, and production in optimization, not only with its primary focus on costs and product quality but also on product robustness as well as risk [533–537], emphasize its vital role in the product development process.

2.3 Main research streams and current status of tolerance-cost optimization

With the first ideas, based on analog and digital computation in the 1950s–'60s [205, 538, 539], the beginnings of optimal tolerance allocation were driven

[14] In this context, the term *robust tolerance design* is commonly used [41], indicating that at least one measure of robustness – in most cases the quality loss (see Eq. (6) c)) – is added to the optimization problem.

by their application to electric circuits [205, 422, 540, 541] and antennas [542]. Since 1970, however, it has increasingly found its way into *classic* tolerancing focusing on mechanical assemblies and has dominated the research on tolerance-cost optimization. Since then, a large number of research papers, approaches, methods, etc., have been developed and implemented, which were initially analyzed in a literature review by the author and the findings were published in [P1].

To create a holistic picture of optimal tolerance allocation and its development, these initial findings are now supplemented by further criteria and current publications.[15] Hence, the following observations are based on an analysis of 399 articles from the period of 1970-2023. Appx. A.2 gives a detailed description of the literature review.

Still severely hampered in its origins by the given constraints in optimization and computer performance (see also Sec. 2.1), tolerance-cost optimization gained momentum especially in the 1990s and developed further in various directions, thus setting the course for the subsequent three decades of intensive research in this field (see Fig. 11 (bottom)). As the tolerances are strongly connected to the machines/processes and suppliers chosen, the idea of **alternative selection** was early formed in the 1960s–'70s [38, 41]. It has mainly drawn attention due to the emergence of metaheuristic algorithms in the following years (see Fig. 11 (a)) and is often chosen as a challenging scenario, e.g., to benchmark optimization algorithms or methods. At the beginning of the 1990s, fostered by the CE movement, the mindset of **concurrent tolerance design** (see Sec. 2.1) was created and since then has represented an important aspect of tolerance-cost optimization. However, most tolerance allocation approaches still focus on the pure design phase and maintain the strict separation of machine and production tolerances. (see Fig. 11 (b)). The elementary equations and interrelationships of tolerances and costs, which laid the foundation for the development of the method in the 1970s [543], were followed by the first concrete approaches to the integration of **quality loss** in the 1990s [200, 249] (see Fig. 11 (c)) after the general introduction of the robust design idea and quality loss in the 1980s [544]. Since then, their consideration has become established in research, is simultaneously considered alongside pure manufacturing costs, and is in the concrete focus of individual research activities [P1].

[15] When analyzing the approaches presented in literature, a distinction must be made between aspects examined in detail and those which are merely a means to an end. Therefore, general statements that individual aspects are less relevant overall cannot be made since the research articles usually focus on selected particular aspects, which means that other aspects are pushed into the background. Nevertheless, the findings indicate the significant trends and the historical development of the method concerning its main research areas.

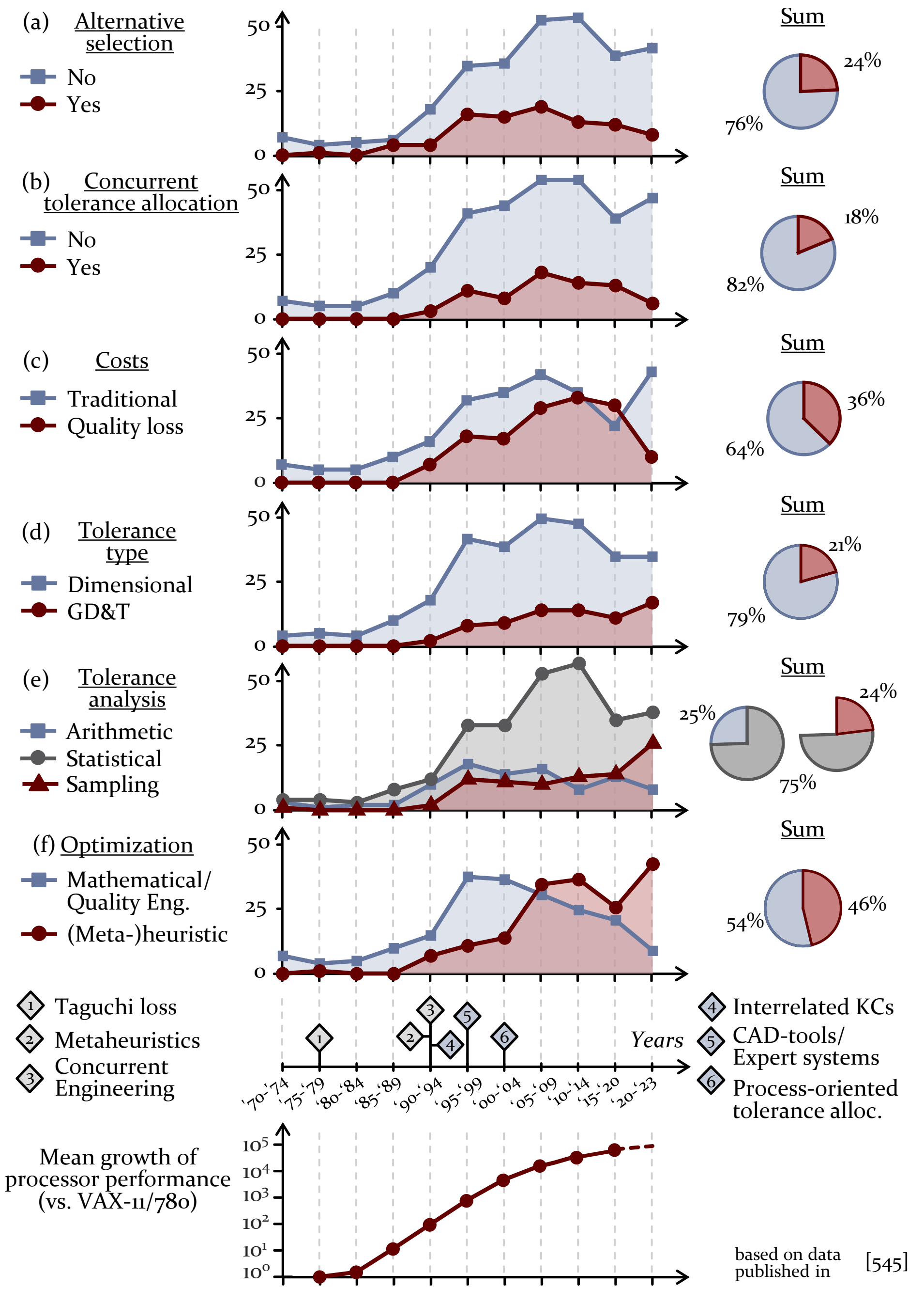

Figure 11: Historical development of tolerance-cost optimization over the last five decades and its main milestones further contrasted to the evolution of computer performance acc. to [545]. The pie plots illustrate the distribution of the approaches used over the entire period (see Appx. A.2 for more details).

Although some approaches have been applied to **dimensional and geometrical tolerances** as the power of the method has increased, the number of methods presented for dimensional tolerances still predominates (see Fig. 11 (d)). This can be mainly attributed to the choice of case studies, which are primarily designed from an academic point of view and are often limited to established one- and two-dimensional standard examples, even if the number of more industry-relevant case studies is slowly increasing. Depending on the purpose of a research article, simple examples are sufficient to study a particular aspect. However, it indirectly leads to the fact that the methods often suffer from an academic character and are perceived by the industry only less suitable for practical use. In contrast, due to their focus on the manufacturing process, the **process-oriented tolerance allocation methods** are far more industry-oriented and practice-driven. Since the first applications at the beginning of the 21st century [376, 381, 546], the shift from product to process has been consistently continued [39] and successively supplemented by various relevant aspects from the downstream process steps (see Sec. 2.2.4).

A closer look at the **tolerance analysis techniques** reveals that simplified arithmetic methods had to give way to statistical evaluation techniques already in the early years. Not least because of tolerance-cost optimization's focus on high quantities and series production (see Fig. 11 (e)). Initially dominated by convolution-based approaches, the methods are increasingly replaced by powerful sampling methods, primarily when external tolerance analysis methods are handled as black boxes by metaheuristic algorithms. Arithmetic approaches are only used if the findings are independent of the chosen tolerance analysis approach.

Shortly after the introduction of the first notable **metaheuristic algorithms**, e.g., genetic algorithms in 1975 [547], scatter search in 1977 [548], simulated annealing in 1983 [549], and particle swarm optimization in 1995 [550], they found their way into tolerance-cost optimization and are mostly preferred nowadays to cope with the increasing complexity of the problems (see Fig. 11 (f)). Thus, among the various aspects already mentioned, **interrelated KCs** increasingly came into focus during this period.

In addition to the individual enhancements of the method, the 1990s were further characterized by the development of **knowledge-based expert systems** for tolerance-cost modeling, tolerance allocation for design, manufacturing, and concurrent tolerance design [137, 152, 225, 267, 551–557]. In contrast to CAT-software for tolerance specification and analysis (see Sec. 2.1), standalone tools for tolerance-cost optimization could, however, not prevail so far [114]. Although several mostly CAD-integrated or CAD-based software prototypes have been presented over the last three decades, such as [155, 242, 452, 558–563], a combination of optimization algorithms and approaches with self-coded or commercial tolerance analysis routines and tolerance-cost analysis software [394, 395, 564] is common [P1].

In summary, tolerance-cost optimization has a long history, is still a current research topic, and has been and will be continuously developed through various research activities strongly shaped by recent global trends.

3 Identification of the need for research and outline of the main part

Based on the state of the art and research presented in Chap. 2, the current shortcomings in the field of optimal tolerance allocation and the need for research are subsequently introduced, followed by the research goal, the research questions, and the outline of the main part.

3.1 Current shortcomings

Optimization-based approaches for tolerance allocation have been intensively studied for over five decades. The individual research activities and the recording of their findings through a remarkable number of articles emphasize the continuous evolution of tolerance allocation in theory (see Sec. 2.3). Despite all scientific efforts, however, it has not yet been able to establish itself in industry. It is still more a scientific *conundrum* than a practical solution for tolerance-cost problems (see Chap. 1). Except for only a few examples of successful implementation in industry, for instance, presented in [P7], manual, iterative approaches are still preferred over automated, optimization-based tolerance allocation while decisive tolerance-cost potentials remain unused.

One reason for the missing acceptance is that the numerous, mostly isolated solutions usually *lack transferability* to other, particularly more complex problems. They are either tailored to specific application cases or limited to simplified, academic case studies with few dimensional tolerances. Correlations of multiple, geometrical tolerances and interrelated KCs for single or multiple assembly configurations are mostly neglected or oversimplified. In addition, they are *insufficiently aligned to industrially relevant aspects*, such as reliable quality measures, mapping of non-normal machine characteristics, or realistic part manufacturing scenarios.

Furthermore, their strong mathematization and scientification constitute a significant obstacle for tolerance engineers without in-depth knowledge of statistics, mathematics, tolerancing, and optimization, further complicating a productive application in practice. Suppose the *ease of use* of a CAT-tool, which is a subjective measure at the end but mainly depends on how fast, easy, and systematically a model can be set up and solved for a wide range of problems, is not given [174]. It is not used, regardless of its potential, alternative workarounds are preferred, or the activity is skipped at all [174]. Consequently, only a few tolerance experts can use these methods insofar as they suit the problem at hand. Even the knowledge-based expert systems presented in literature have not yet been able to change this situation.

Specific detailed research issues, for instance, a sufficient acquisition and processing of data for tolerance-cost modeling in series production, are still open and have to be clarified. However, there is currently *a significant lack of an approach that can serve as the basis for a broadly applicable and powerful tool and convince the industry with its usability*. Otherwise, its potential will still remain unused despite sophisticated details.

3.2 Linking sampling-based tolerance analysis and metaheuristic optimization

The first step to overcome the presented shortcomings is to define the fundament for optimal tolerance allocation. The literature study, summarized in Fig. 11, indicates the trend towards a coupling of sampling-based tolerance analysis methods and metaheuristic optimization algorithms for tolerance allocation. This concept, existing for several years, was coined *sampling-based tolerance-cost optimization* in [P5]. Fig. 12 illustrates its basic idea as an extension of the general workflow given in Fig. 5 (b) for a population-based algorithm. In each optimization iteration (generation) g, a new set of tolerance values, the population p of several individuals, is generated. For the first generation $g = 1$, it is typically based on a random guess. Otherwise, results from the previous generations are considered. The substeps of the inner loops, i.e., the evaluation of both costs and quality using tolerance-cost analysis and sampling-based tolerance analysis acc. to Fig. 10 and its transformation into a fitness F using a suitable penalty function f_P, is repeated for all η_p individuals and all η_g generations until the algorithm meets a termination criterion (see also Appx. A.3 for further information on optimization theory).

At first sight, this idea is reasonable since both methods' broad applicability and general adaptability to arbitrary problems, which both techniques, as so-called "panaceas" [280], inherently bring with them, basically offer an excellent prerequisite to forming a solid basis. A detailed evaluation, however, is needed to contrast the pros and cons. The statements, discussed in the following and summarized in Tbl. 2, are partly based on the results of an initial potential analysis presented in [P2] and [P13].

Sampling-based tolerance analysis is mostly the first choice for analyzing complex problems with 3D and nonlinear effects, making it possible to simulate the impact of geometrical tolerances and complex assembly situations. Thus, sampling-based optimization routines enable a direct integration of standard tolerance analysis software tools preferably used in industry and an

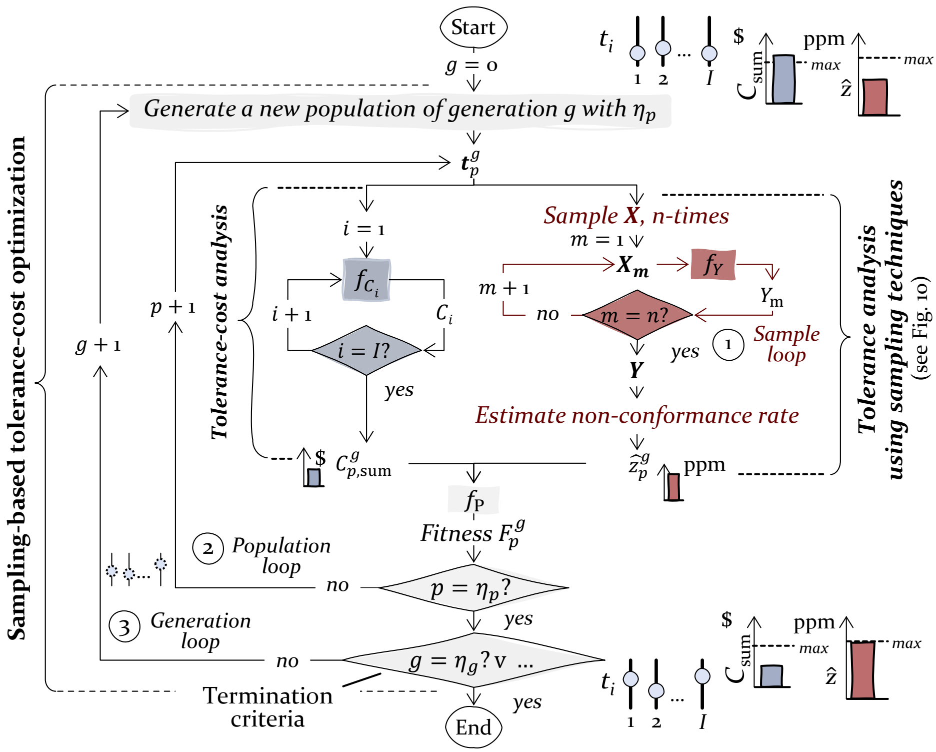

Figure 12: General workflow to solve a sampling-based tolerance-cost optimization problem with population-based metaheuristic optimization algorithms based on [P9].

easy embedding of the method into existing software landscapes. Considering non-normal manufacturing distributions and the freedom to integrate measurement data opens up the possibility of including further manufacturing information in the tolerance allocation for a more realistic representation of relevant industrial scenarios, e.g., for machine and process selection.

Metaheuristics are soft-computing algorithms and therefore do not restrict the choice and setting of tolerance analysis and tolerance-cost models, regardless of the selected optimization case (see Sec. 2.2.3). Nonlinear, discontinuous, and even implicit black box models for tolerance-cost and assembly response functions can be integrated into optimization without adapting the optimization problem and routines. They can deal with the noise from the sampling procedures without further workarounds such as gradient estimation (see Sec. 2.2.3). Similarly flexible, they can solve mixed-integer problems, enabling an extension to discrete decision variables and covering industrial-relevant aspects, such as selective assembly or machine selection. Overall, significantly fewer mathematical foundations for optimization theory to formulate and solve the problems are necessary, facilitating automation and instrumentalization of tolerance allocation by powerful, user-friendly expert tools.

One major drawback, however, is that both methods require significantly more computation time than alternatives, such as statistical, convolution-based tolerance analysis methods and gradient-based algorithms. This dilemma is further aggravated in interaction since the tolerance analysis loop must be solved repetitively for each sample, i.e., n times, within both optimization loops (see Fig. 12). Despite "increased computer power, faster algorithms, and more efficient optimization routines" [157], computationally intensive tolerance simulations are a major challenge for a practical application, even with the use of advanced computer technology such as GPU-computing [130]. Furthermore, both methods are based on the principle of randomness containing statistical and stochastic operators. This leads to uncertainties and, thus, to unreliable, i.e., either invalid or non-optimal, as well as scattering, non-reproducible optimization results. The missing guarantee for optimality and the strong dependence of the results on the chosen optimization algorithm-specific settings make a joint application difficult, particularly for users with less experience.

Table 2: Main benefits and deficits of sampling techniques and metaheuristic optimization algorithms for optimal tolerance allocation.

	Sampling-based tolerance analysis	**Metaheuristic optimization**
Benefits	+ is powerful and highly flexible in handling complex industrial tolerance problems + is able to map individual manufacturing distributions + can directly handle any (implicit and explicit) assembly response function + is mostly used in common tolerance analysis software	+ puts no limits on the use of tolerance-cost and tolerance analysis models + is capable of handling sampling-induced noise + can properly solve mixed-integer problems to address machine-/process selection and selective assembly + requires less mathematical theory
Deficits	– needs high computation times – induces uncertainties leading to invalid or non-optimal optimization results	– needs high computation times – its stochastic operators lead to limited reproducibility and reliability of results – is very sensitive to the settings

3.3 Research goal, questions, delimitation, and outline

A second, more global view on the findings, summarized in Tbl. 2, illustrates that the benefits and deficits have a direct or indirect influence on the usability of the whole tolerance allocation approach. Usability is defined in the ISO 9241-11 as the "extent to which a system, product or service can be used by specified users to achieve specified goals with effectiveness, efficiency, and satisfaction in a specified context of use" [565]. By transferring this general definition to tolerance allocation[1], the *specified user* corresponds to the tolerance engineer, who has basic knowledge of statistical tolerancing and optimization and operates in the *specified context of use*, the tolerance design phase. The significant benefits of harmonizing sampling techniques and metaheuristics for tolerance-cost optimization, identified in the previous Sec. 3.2, lead to the conclusion that sampling-based tolerance-cost optimization as a basis for tolerance allocation offers great potential to close the research gaps given in Sec. 3.1 – provided that its inherent deficiencies in terms of effectiveness, i.e., the "***accuracy** and **completeness** with which users achieve specified goals*" [565], and **efficiency** can be adequately compensated.

Hence, the goal of this thesis is to **enhance the usability of optimal tolerance allocation by sampling-based tolerance-cost optimization fostering its broad applicability in the product development process**.

The research goal is specified by three research questions (RQ) focusing on the three main elements of usability, viz. the accuracy, completeness, and efficiency:

- **RQ1:** How can the **accuracy of sampling-based tolerance-cost optimization** be increased to enable a reliable and realistic consideration of complex assemblies?
- **RQ2:** How can the **completeness of sampling-based tolerance-cost optimization be enhanced** so that industrial-relevant issues are suitably addressed?
- **RQ3:** How can the **efficiency of sampling-based tolerance-cost optimization** be improved to handle complex optimization problems in reasonable computing times?

The relevant aspects are separately investigated in Chap. 4–6 to answer these questions. Novel methods, based on initial findings presented in previous publications by the author as well as students' theses, are proposed for an

[1] The term *usability* and its general definition given in the ISO 9241-11 can further be used to evaluate non-physical products, e.g., software tools [566]. In this work, it is used tailored to tolerance-cost optimization to discuss the developed methods and findings with their primary focus on its effectiveness and efficiency.

accurate, *complete*, and *efficient* solution of the optimal tolerance allocation problem (see Fig. 13). A straightforward but representative case study of a wheel mounting assembly from literature (see Appx. A.8.1) is used in Chap. 4–6 to illustrate and verify the findings. The consolidation and reconciliation of the individual methods serve as the basis for proposing an optimal tolerance allocation approach and its prototypical implementation in Chap. 7. It is applied and evaluated in Chap. 8 for a practical use case of industrial complexity as an example (see Appx. A.8.2) to verify the achievement of the research goals finally. The optimization algorithms GA and CS are exemplarily used to show the benefits of the individual methods. Detailed information on their functionality is given in Appx. A.3. Since the studies primarily address aspects of tolerance analysis and optimization, as well as their interrelations, but are mainly independent of the type and scope of the chosen tolerance-cost model, the work is limited to the most common form of least-cost tolerance allocation, neglecting the idea of quality loss (see Eq. (6)). In addition, the focus is on the allocation of design tolerances concerning geometrical KCs (see Fig. 4). Manufacturing tolerances and concurrent tolerance allocation (see Sec. 2.1.3) are not further discussed, though the findings provide the possibility for transfer.

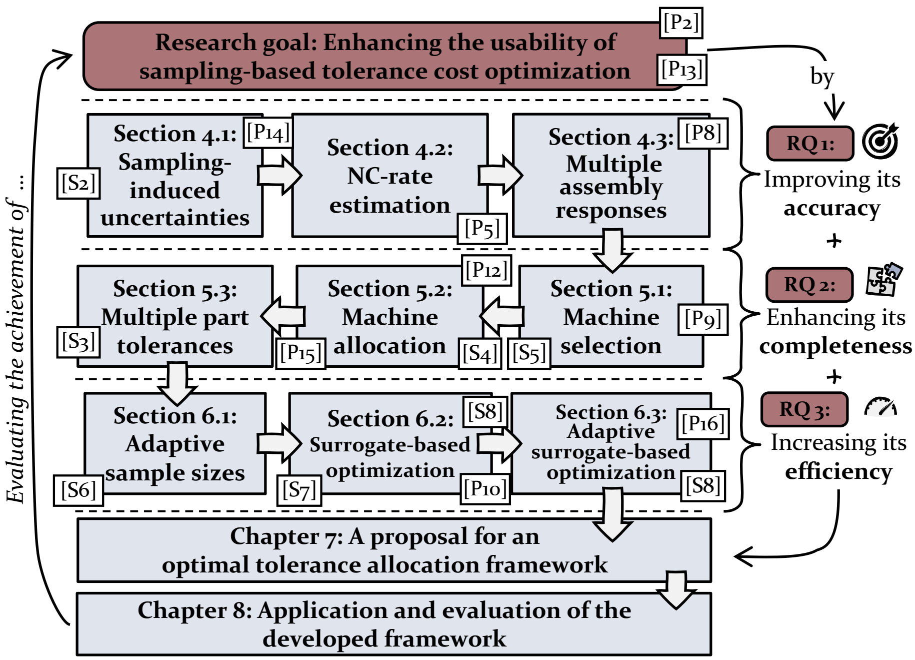

Figure 13: Outline of the main part with the underlying works from the author and students.

4 Increasing the accuracy of sampling-based tolerance-cost optimization

The previous chapters emphasized the elementary role of tolerance analysis in tolerance-cost optimization, simulating part fabrication, assembly, and inspection to assure the resultant quality under variations through a sought cost-optimal set of part tolerances. Fig. 14 takes up the subroutine shown in Fig. 12 and schematically illustrates the steps and their interrelations. The choice of the sampling technique and the sample size n causes aleatory uncertainties propagating through the evaluation of the assembly responses and non-conformance rate (nc-rate) into the quality assurance constraints Eq. (7) b) of the optimization problem [214, 301]. Hence, the sampling and the nc-rate estimation technique influence the **accuracy** of the constraint evaluation and, thus, the optimization history and the results [408] affecting their acceptability and optimality, and, in summary, their reliability.

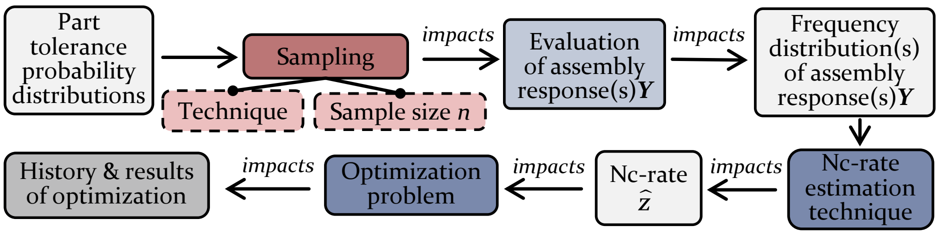

Figure 14: Sampling-based tolerance analysis steps and their effects on optimization.

Besides, the geometrical and behavior models used as the basis for evaluating the assembly responses significantly influence how accurately the tolerance analysis model can represent reality. Questions about representation models are an integral part of decades of research resulting in a large number of different approaches (see Sec. 2.2.2), which always have to be chosen individually by the user as a compromise between accuracy and computing time and, thus, have not to be in the focus of this thesis. Instead, the steps, which are independent of the geometrical and behavior model, are studied with an emphasis on its accuracy in the following – starting with the sampling technique and its uncertainties in Sec. 4.1 and followed by the nc-rate estimation technique of single as well as multiple assembly responses in Sec. 4.2 and Sec. 4.3.

4.1 Managing sampling-induced uncertainties

Sampling methods are used in tolerance analysis to infer the statistical distribution of the assembly response based on representative samples. Their probabilistic behavior consequences that the tolerance analysis results are always subject to sample size-dependent variance and, thus, induce aleatory uncertainties in the optimization problem and its solutions. For this reason, suitable measures to mitigate and control these effects are proposed in the following. The presented aspects are extended from the first concepts introduced in [S2] and [P14].

Problem statement Since the repetition of sampling-based tolerance analysis will result in different probability frequency distributions of $\boldsymbol{Y}$, the derived nc-rates will also differ since $\boldsymbol{Y}$ serves as the data basis for the subsequent nc-rate estimation step.[1] For the moment, however, the conversion of $\boldsymbol{Y}$ into the nc-rate will be put on the background but considered in detail in Sec. 4.2. The focus in the following is on the investigation of the sampling-induced variances of the tolerance analysis results.

The sum of all variances of the estimated nc-rates $\hat{z}$ results in a bilateral margin of error ϵ:

$$\{\hat{z} \in \mathbb{Q}_0^+ \mid z - \epsilon_\mathrm{u} \leq \hat{z} \leq z + \epsilon_\mathrm{o}\}, \tag{10}$$

enveloping the real, but unknown nc-rate value z, as both an over- and underestimation of z can occur. Overestimates of the nc-rate are $\hat{z}$-values estimated to be higher than the real value z. Underestimates mean that z is higher than the predicted value $\hat{z}$ (see Fig. 15 (left)).

Since tolerance analysis is performed for each potential tolerance combination within the optimization, it is exposed to both scattering and discontinuity effects (see Fig. 15 (right)). In this context, scattering effects mean that each combination scatters differently when sampling is repeated during optimization. In contrast, discontinuities describe the deviation of continuity of the total nc-constraint surface and, thus, include the values of the neighboring nc-values. It is well known from the literature that both effects influence the history and results of optimization [27, 349] and negatively impact

- the acceptability, since results are considered acceptable, which are, in fact, not,
- the optimality, since the noise effects complicate the solution of the optimization problem and, thus, the identification of the global optimum,

[1] In this thesis, the primary focus is on the nc-rate as a quality assurance measure, also known as tolerancing KPI [567]. Still, the results are also transferable to yld or C_{pk}.

- and, in summary, the reliability of the results, which is further hampered by the probabilistic behavior of the metaheuristic algorithms.

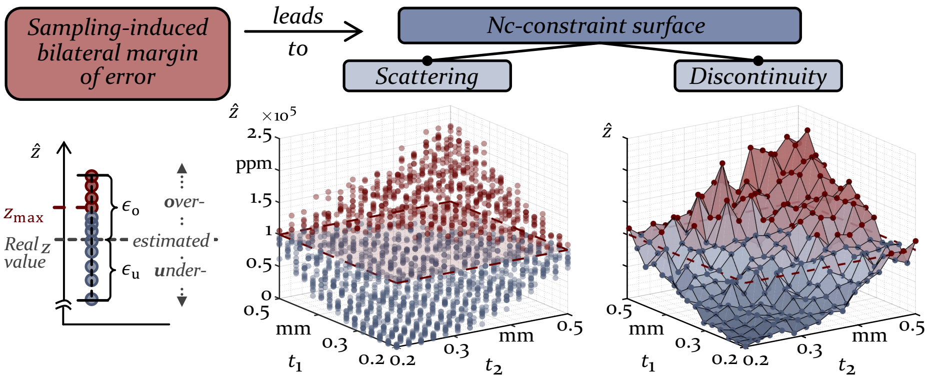

Figure 15: The use of sampling leads to varying analysis results and a bilateral margin of error ϵ resulting in scattering (different results when repeating tolerance analysis with the same tolerance values) and discontinuity effects (non-smooth constraint surfaces) in tolerance-cost optimization.

Estimating the margin of error Confidence intervals of proportions can be used to estimate the accuracy of the estimated nc-rates in ppm based on MCS [336, 348, 568, 569] with $P = z/10^6$ as a function of the sample size n and a chosen confidence level $1 - \alpha$ as follows [570]:

$$\hat{P} - \underbrace{Z_{\alpha/2}\sqrt{\frac{\hat{P}\cdot(1-\hat{P})}{n}}}_{\epsilon/10^6} < P < \hat{P} + \underbrace{Z_{\alpha/2}\sqrt{\frac{\hat{P}\cdot(1-\hat{P})}{n}}}_{\epsilon/10^6}, \tag{11}$$

and, thus, provide a guide to selecting a proper sample size n for tolerance analysis.[2] Fig. 16 (top) emphasizes the benefits and validity of sample size variable confidence intervals for the example of $z = 2{,}700$ ppm, where (a) is approximated via Eq. (11) and (b) is simulated for a 250 times repeated MCS-based tolerance analysis predicting the nc-rate for f_{Y_2} of the wheel mounting assembly (see Sec. A.8.1 and in particular Eq. (84)).[3] With increasing sample size n, the margin of error decreases proportionally to $\sqrt{n}$, whereby the estimated and the predicted margins of error to be faced within optimization show a good agreement (see the relative difference of under-

[2] Eq. (11) is valid, if data is normally distributed, binomial experiment conditions are given and $n \cdot \min\left(P, 1-\hat{P}\right) \geq 5$ [570].

[3] The assembly response in focus is defined by $f_Y = f_{Y_2} = -X_1 - X_2 - X_3 + X_5$ and in detail described in Appx. A.8.1. The specification limits are set acc. to the strategy described in Appx. A.9.

and overestimates $\delta^{\mathrm{u}}_{\hat{z}}$, $\delta^{\mathrm{o}}_{\hat{z}}$ in Fig. 16) and can, thus, be used to estimate ϵ in advance – though the exact location of $\hat{z}$ in this margin is unknown. In addition, ϵ strongly depends on the real value of z. Fig. 16 (bottom) exemplarily illustrates the margin of error ϵ as function over z for $n = 10{,}000$.

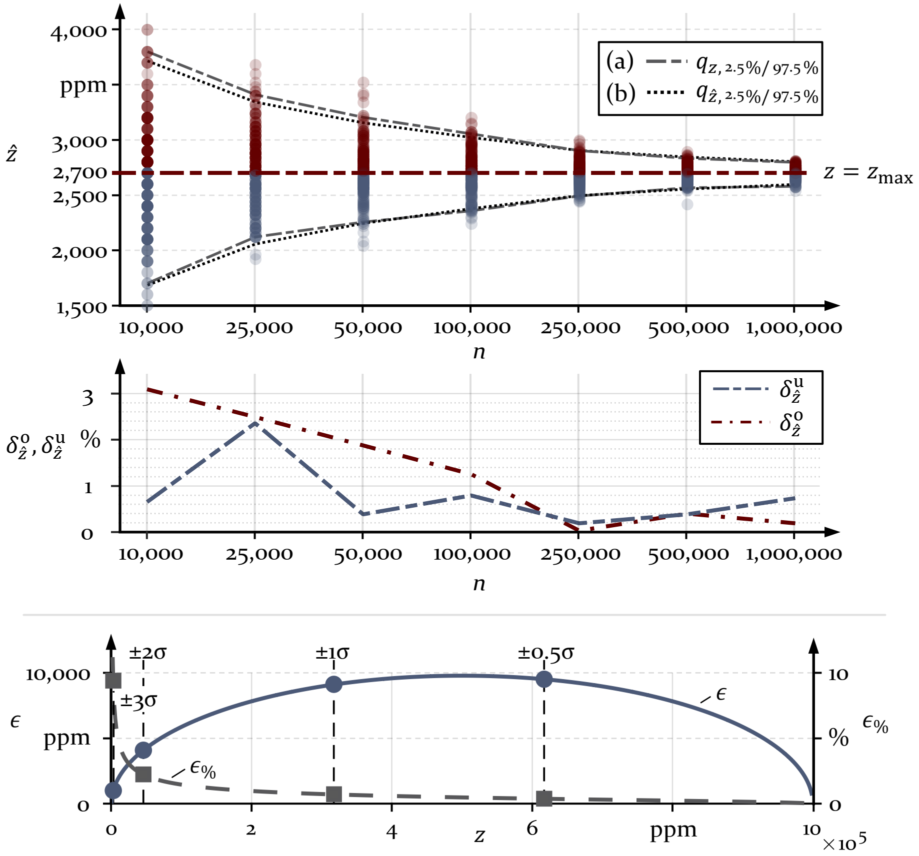

Figure 16: Scattering of nc-rates: lower and upper bounds of confidence interval $q_{z,2.5\%}, q_{z,97.5\%}$ estimated with Eq. (11) with $\alpha = 0.05$ (a) and empirically $q_{\hat{z},2.5\%}, q_{\hat{z},97.5\%}$ as 2.5 %- and 97.5%-quantiles (b) for repeated MCS-based analysis of the wheel mounting assembly problem (top). Relative difference between estimated and predicted confidence interval boundaries $\delta^{\mathrm{u}}_{\hat{z}}$ and $\delta^{\mathrm{o}}_{\hat{z}}$ leading to under- and overestimation in percent (center). Predicted absolute and relative margin of errors $\epsilon, \epsilon_{\%} = f(z)$ for $n = 10{,}000$ (bottom).

Consequently, in tolerance-cost optimization, the predicted nc-rates and the corresponding real values z' vary with the currently chosen tolerance values combination $\boldsymbol{t}'$ during optimization. While under- and overestimation consequently influence the optimization steps, the final results' accuracy is mainly dependent on $z_{\max}$ since the optima are typically near or on the boundaries of the nc-constraint surface. This knowledge offers the potential to incorporate the information on ϵ into the optimization problem by adding them as additional noise terms $\epsilon = f(n, \hat{z}')$ to the nc-rate constraints in either an optimistic or pessimistic manner, as it is for instance introduced in [301]. Going beyond a pure awareness and acceptance of these sampling-induced uncertainties, different methods to mitigate or even eliminate the scattering and discontinuity effects are proposed in the following.

Theoretical solution – Variance reduction in sampling At first, the focus is on the source of the uncertainties, the sampling itself (see Fig. 14). Different ways exist to generate the distribution frequencies for all individual X_i through pseudo-random number generators. The inverse sampling method, which is used in this thesis[4], first generates uniform random numbers between $X_i' \sim \mathcal{U} \in [0, 1]$ and second transforms them into the final variates X_i using the inverse cumulative distribution functions (icdf) for the assumed tolerance part distributions with their density function ρ_i (see Fig. 17).[5] Consequently, the choice of sampling technique and the sample size n affect the first step of the procedure.[6]

It is well known from the central limit theorem that the variance of the tolerance analysis results decreases proportionally to the root of n as n increases in case of normality. This effect can, for example, be seen in Fig. 16. In addition to a conscious choice of high enough sample sizes, variance reduction methods are alternatives to the well-established MCS for tolerance analysis achieving lower variances for the same sample size. These two aspects have already partially been investigated in literature (see Sec. 2.2.2). From theory, it is verified that the scattering of the statistical moments $\hat{\mu}$ and $\hat{\sigma}$ can be reduced, which positively affects the scattering and discontinuity in the constraint evaluation. However, a quantitative discussion on the effects of variance reduction on the nc-rate as a quality measure and its propagation along the entire chain of Fig. 14 on the intermediate and final optimization results is missing so far. For the subsequent studies, *MCS*, *Latin Hypercube Sampling (LHS)*, and *Quasi-Monte Carlo Sampling with low discrepancy Sobol' sequences* (QMCS) are examined in more detail. Their principles and differences are summarized in Appx. A.4.

Practical transfer and findings For investigating the influence of the sampling techniques, the deviation of the determined nc-values from the

[4] The reason for this is given at the end of this section.

[5] More details on sampling techniques are given in Appx. A.4.

[6] In addition, the accuracy of the assumed individual probability density functions (pdf) ρ_i plays an essential role [348]. It is not further studied in detail but finally discussed in Sec. 8.3.

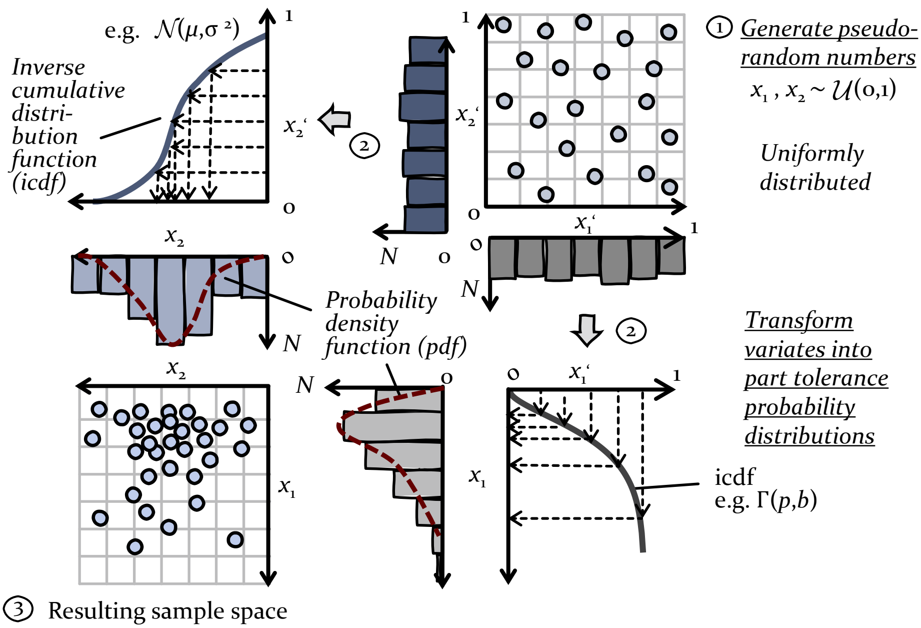

Figure 17: Two-step procedure for sampling continuous probability distributions using the inverse method.

expected value must be known. The linearity of the focused assembly response function of the wheel mounting assembly and the assumption of normality of all contributing individual characteristics $X_i \pm t_i$ allow to directly determine the resulting variance of the assembly response Y as the sum squares of all individual variances $\sigma_i = t_i/6$. This relation can be utilized to inversely define the lower and upper specification limits *LSL*, *USL* so that a given set of tolerances t_i (here $t_i = 0.05$ for all tolerances) yields a predefined nc-rate as the true value. In short, the real values of z_{max} can be determined implicitly via *LSL* and *USL* as a function of the so-called sigma-level u, well known from the six sigma philosophy, where the cumulative distribution function gives the direct relation between nc-rate and sigma level for the standard normal distribution [571].[7] More details on the definition of the specification limits are given at the beginning of Appx. A.9 and its concrete values in Appx. A.9.1. In the subsequent study, the three levels $u = 2, 3, 4$, corresponding to $z_{\text{max}} = 45{,}500; 2{,}700; 63.3$ ppm, serve as a reference, where tolerance analysis using MCS, LHS, and QMCS is repeated 100 times for samples sizes from $n = 10{,}000$ up to 250,000. The results summarized in Tbl. 10 are shown through boxplots in Fig. 18.

[7] The nc-rates for the most commonly used sigma levels u can directly be read from tables [571].

The accuracy of $\hat{z}$ depends mainly on how representative the samples for X_i are to represent, in sum, the tails of the assembly response distribution of $\boldsymbol{Y}$, i.e., the areas below *LSL* and above *USL*, with sufficient probability. Especially for very tight quality criteria, such as $\pm 4\sigma$, these areas are underrepresented at low sample sizes and lead to a strong underestimation of $\hat{z}$.

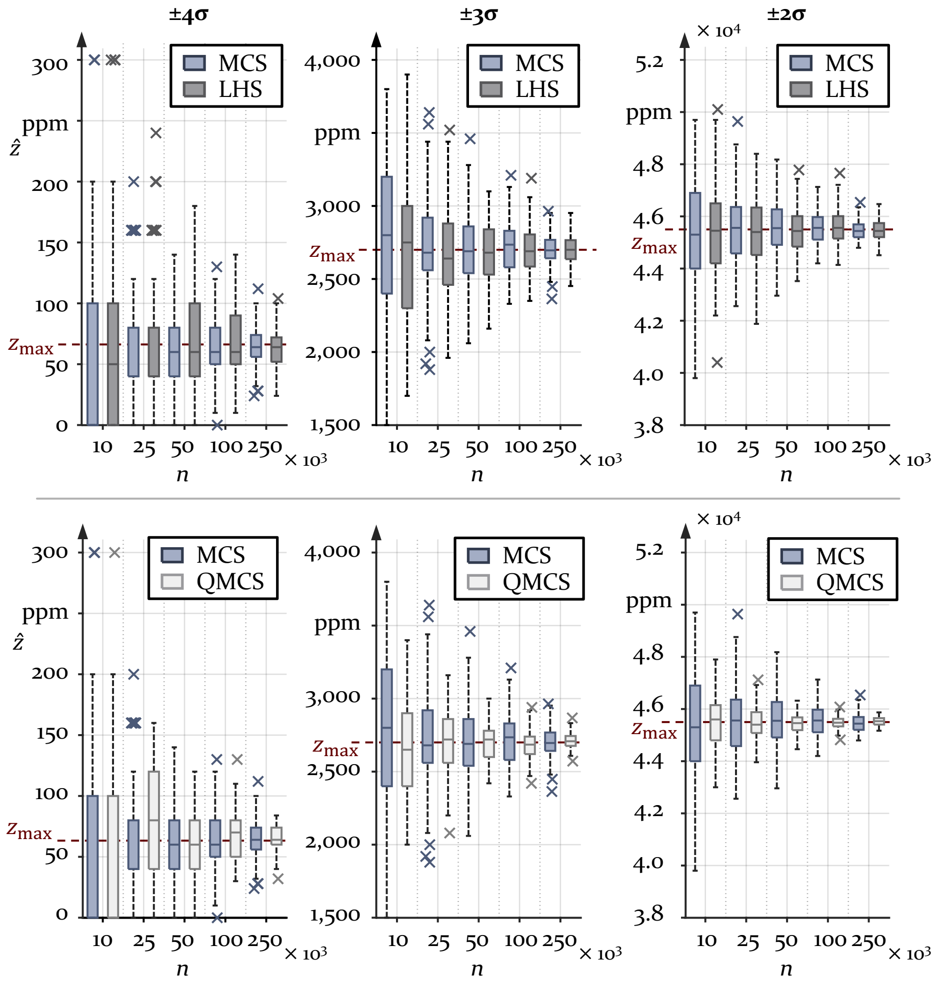

Figure 18: Spread of over- and underestimates of the nc-rate $\hat{z}$, studied for the three sampling strategies (MCS, LHS, QMCS) and sigma levels ($\pm 4\sigma, \pm 3\sigma, \pm 2\sigma$), different sample sizes n and with a 100-fold repetition of each.

As the sample size increases, the samples' density in these areas increases, and the variance of $\hat{z}$ decreases proportionally to $\sqrt{n}$. Its mean values shift to their real values so that the imbalance of the bilateral margin of errors can be equalized with higher sample sizes. While there is no noticeable reduction in variance, the use of QMCS shows a significant reduction in the width of the margin of error.

Fig. 19 takes up the results and sets the 95%-scatter range of the absolute errors $|\hat{z} - z_{\max}|$ in relation to the real value $z_{\max}$, denoted as metric $\delta_{\hat{z},95\%}$. It first emphasizes the comparatively high errors and low accuracy in estimating low ppm rates with low sample sizes. Second, in contrast to the small positive effect for LHS, using QMCS significantly helps to achieve more accurate results with the same sample sizes.

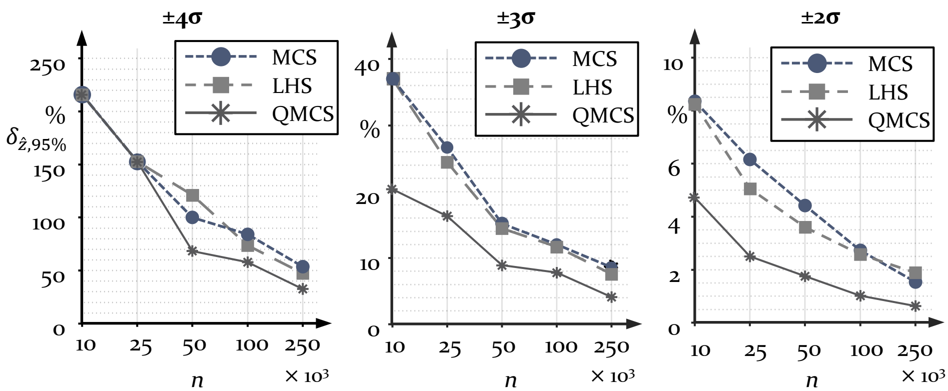

Figure 19: Comparison of the analysis results shown in Fig. 18 making use of the 95%-interval of the absolute error $|\hat{z} - z_{\max|}$ relative to the real value $z_{\max}$, denoted as $\delta_{\hat{z},95\%}$.

Expectedly, the reduction in the variance of the nc-rates, especially evident for QMCS, should have a mitigating effect on the scattering and discontinuity effects in constraint evaluation and, finally, on the scattering of the optimization results. Besides the summary in Tbl. 11, Fig. 20 illustrates the results of a 50-fold repeated tolerance-cost optimization for the selected example of the wheel mounting assembly using the CS algorithm with $n = 10{,}000$ and $z_{\max} = 2{,}700$ ppm. Under the condition that each part tolerance t_i has the same contribution to both nc-rate and costs, the global cost optimum $C_{\text{sum}}^{\text{ref}}$, serving as reference, can analytically be determined for $t_i = t^{\text{opt}}$, where the maximum limit of $z_{\max}$ is fully exploited. The latter is ensured using the same tolerance-cost functions for all tolerances (see Tbl. 8).

While MCS and LHS show comparable results, the variance reduction by QMCS leads to a noticeable variance reduction of the obtained optima $C_{\text{sum}}^{\text{opt}}$. This is reflected in the smaller range between the 2.5%- and 97.5%-quantile $qr_{C,95\%}$, covering 95% of all cost optima since the constraint evaluations during optimization are subject to minor variance for the same sample size n (see Fig. 20 (left)). Besides the impact of sampling-induced uncertainties on the evaluation of the fitness of the solutions during optimization, the resulting margin of errors or confidence intervals with the finally determined tolerance values are, in particular, critical to the reliability and acceptability of the results. Fig. 20 (right) shows the superposition of the margins of error for $\hat{z}_{\mathrm{opt}}$, which result from a 100-fold evaluation of the nc-rates for the 50 feasible, optimally identified tolerance combinations after optimization. As expected, the margins of error for the QMCS are significantly lower than for MCS and LHS. The reasons for the significantly more frequent exceeding of $\hat{z}_{\max}$ for all sampling strategies and the corresponding shift from the global cost optimum $C_{\mathrm{sum}}^{\mathrm{ref}}$ results from the imbalance mentioned above of the margin of error and tendency to underestimation for low sample sizes.

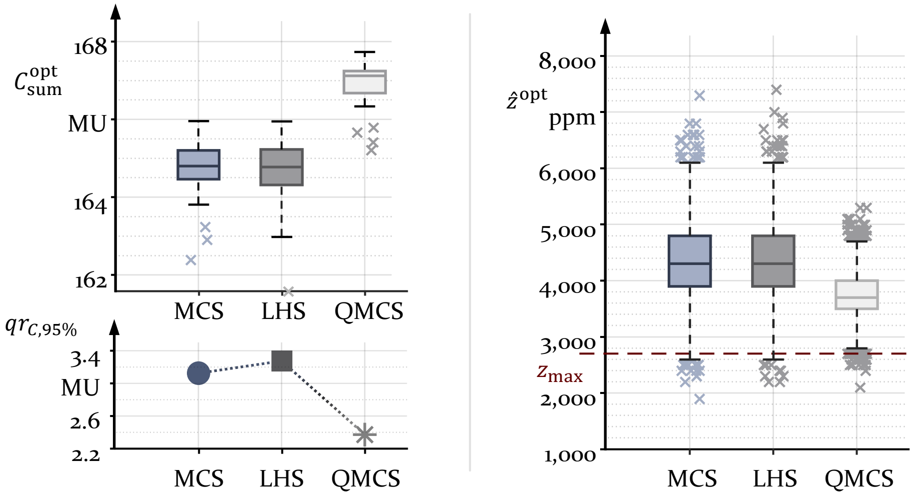

Figure 20: Scatter of optima $C_{\mathrm{sum}}^{\mathrm{opt}}$, its resulting 95%-quantile range $qr_{C,95\%}$ obtained for a 50-fold repetition of solving the wheel mounting assembly problem taking the three sampling strategies into account (left). Scatter of nc-rates $\hat{z}^{\mathrm{opt}}$ for a 100 times resampling and tolerance analysis using the identified optimal tolerances (right).

Theoretical solution – Scattering and discontinuity elimination The above results show that variance reduction methods can reduce scattering and discontinuities, but also that these can never be avoided entirely, mainly for computational time reasons. Since the scattering results from the repetitive execution of the tolerance analysis, it is purposeful to mitigate these effects to a minimum or even to eliminate them.

Following this idea, it is useful if the scattering in two succeeding optimization steps can be avoided for the elitist solutions, i.e., the best solutions of the current generation g and included in the population in the next generation $g+1$. By skipping the step to analyze them again with newly generated random numbers, solutions that were valid beforehand are not evaluated as invalid in the subsequent generation lying in the upper part of the margins of error, i.e., in the region of underestimation. This will lead to less perturbation in the intensification steps, which, in addition to diversification, are crucial for achieving the global optimum (see Appx. A.3). Fig. 21 exemplarily contrasts two optimization runs for the wheel mounting assembly allocation problem, whereas in strategy (a), the whole population, including the elitists from the previous generation, and in (b) only the new individuals are evaluated. Additional background information on the study is given in Tbl. 12.

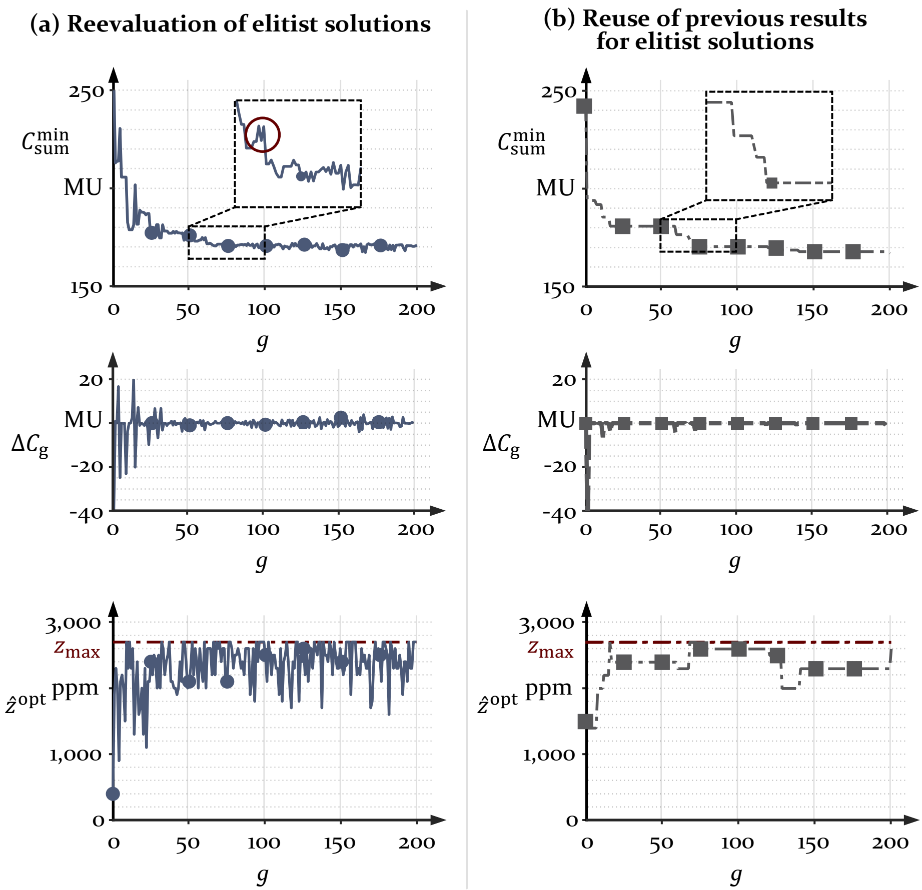

Figure 21: Optimization history for the optimal costs C_{sum}^{min} and its related nc-rates $\hat{z}^{opt}$ over the generations g and the change in two succeeding generations ΔC_g for strategy (a), reevaluating the elitist solutions, and strategy (b), reusing of previous results for elitist solutions, in comparison.

Having a look at the optimization history for strategy (a), there is a noisy course of $\hat{z}$ and $C_{\mathrm{sum}}^{\mathrm{min}}$ over g, leading to erratic changes in the current optimal cost $C_{\mathrm{sum}}^{\mathrm{min}}$ in two successive generations ΔC_g. Besides stagnation $\Delta C_g = 0$ or improvement $\Delta C_g < 0$, the results can also deteriorate $\Delta C_g > 0$ because the previously elite solutions are now classified as invalid and another individual with higher costs and mostly lower nc-rate is identified as the best solution. Strategy (b) eliminates this effect, resulting in a less scattered and noisy optimization. Most of the implementations of metaheuristic algorithms already consider this aspect, as it not only reduces scattering in stochastic optimization algorithms but also has the advantage of shorter computation times in deterministic problems. Theoretically, if all intermediate results are remembered and not repeated, the scattering could be eliminated entirely. Nevertheless, the calculated nc-rates for all potential tolerance combinations are subject to aleatory uncertainties. Hence, the position in the margin of error is purely random and discontinuous response surfaces result, where the chosen sampling procedure and the sample size n define the extent of discontinuity.

Motivated by the proven positive effect of eliminating scattering results from repeated tolerance analysis, the idea is now expanded to *completely avoid both scattering and discontinuity effects in optimization*. The variance of the results originates from the generation of the uniformly distributed random numbers in the first sampling step of Fig. 17. However, this first step is identical in all optimization steps. Only the second step, the transformation of the uniform variates into the current characteristics X_i, is different in each optimization step since the currently allocated tolerances t_i serve as the input for the icdfs. Instead of repeating the random number generation step for each individual p in each generation g, it makes sense to perform it only once at the beginning and to reuse the generated uniform numbers for all tolerance analyses performed during the optimization, turning the stochastic problem into a deterministic one. Fig. 22 depicts the idea of reusing initially generated uniform pseudo-random numbers (b) compared to the standard method of iterative resampling (a).

Practical transfer and findings Using the wheel mounting assembly as a case study with the same settings for CS again, both strategies (a) and (b) are studied in the following. Fig. 23 summarizes the results, given in detail in Tbl. 13, the achieved cost optima $C_{\mathrm{sum}}^{\mathrm{opt}}$ for z_{max} as well as the margin of error when repeating the optimization 50 times with MCS and a sample size $n = 10{,}000; 50{,}000; 100{,}000$. First, it can be seen that the variance of the optima and its mean shift from the real optimum is decreasing with increasing sample size n, whereas the proportionality to $\sqrt{n}$ is recognizable. The optima $C_{\mathrm{sum}}^{\mathrm{opt}}$ obtained by strategy (a) are, however, significantly lower

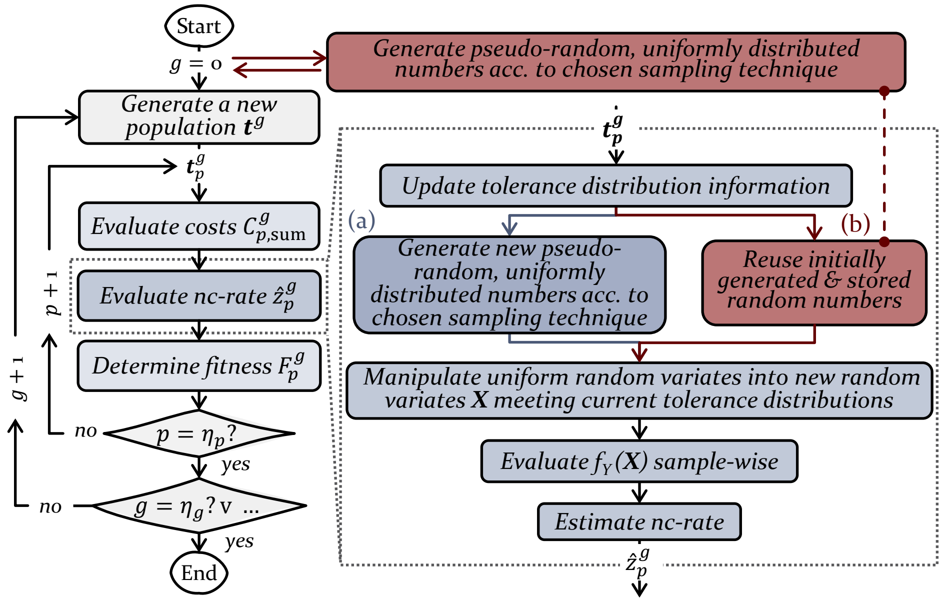

Figure 22: Random numbers used in sampling-based tolerance-cost optimization: iterative resampling (a) vs. reuse of initially generated uniform random numbers (b).

than the reference value $C_{\mathrm{sum}}^{\mathrm{ref}}$, which can be explained by the high frequency of underestimation of the nc-rates $\hat{z}^{\mathrm{opt}}$. In comparison, using the same random numbers (strategy (b)), $C_{\mathrm{sum}}^{\mathrm{opt}}$ leads to significantly higher variance, but the mean shift to the reference values is smaller.

The obtained differences in the results can be suitably explained by taking a closer look at the optimization history. Therefore, Fig. 24 visualizes two exemplary optimization runs utilizing its intermediate optima $C_{\mathrm{sum}}^{\mathrm{min}}$ and corresponding nc-rates with $n = 10{,}000$, where the results of a 100 times repeated tolerance analysis for each best intermediate solution are visualized as a scatter plot. For strategy (a), the optimizer tries to improve the current solution by widening the tolerances as far as possible whenever it finds a set of random numbers that yield lower cost values by underestimating the nc-rate. Thus, by giving the optimizer a sufficiently large number of trials, i.e., by high numbers of generations η_g, the probability of finding a sample that gives larger underestimates of the nc-rate increases. The acceptability constraints hold for the current sample set and, thus, further improvement of the objective function and a new cost optimum is achieved. In contrast, the initial chosen set of random numbers in strategy (b) defines the constant shift from the real value. When repeating the optimization, the distribution of the location in the margin of error is symmetrical, having both under- and overestimation of z represented in the final solutions. This effect leads in

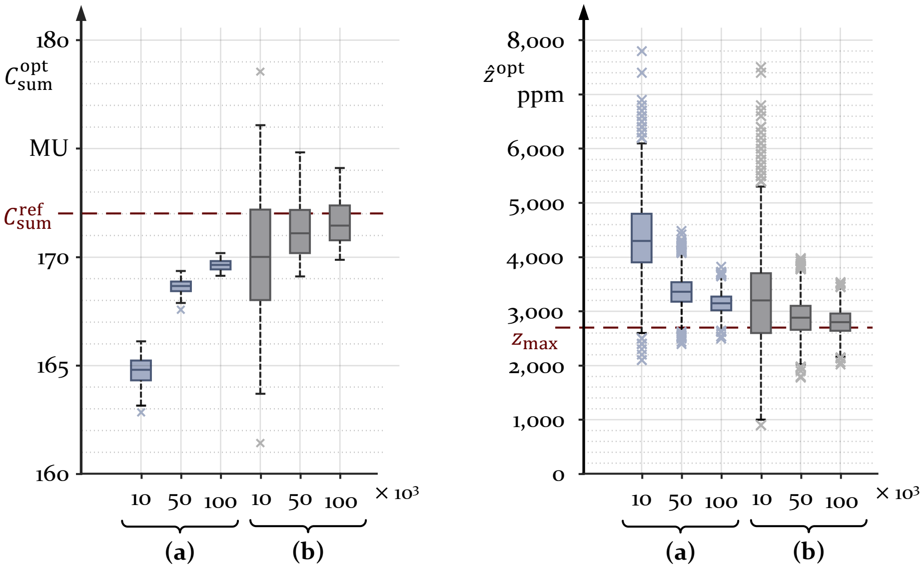

Figure 23: The scatter of the obtained optima C_{sum}^{opt} and their corresponding nc-rates $\hat{z}^{opt}$ results for a 50-fold repetition of sampling-based tolerance-cost optimization of the wheel mounting assembly using strategy (a), iterative resampling, and (b), reuse of same random numbers.

sum to the higher variances in C_{sum}^{opt} and $\hat{z}^{opt}$ but lower mean shifts to their real values in Fig. 23.

Although strategy (a) generally tends to underestimate, it cannot be claimed if and where exactly the algorithm converges in the region of underestimation. It always depends on the problem's complexity, structure, and chosen settings for optimization. However, the results obtained by strategy (b) are not more reliable per se since they are always subject to a constant shift from the real value during optimization. In contrast, the exact value of the shift is purely random and depends on the chosen sampling. The confidence intervals proposed help to estimate the total margin of error, providing information about the range of potential variance in advance. The deterministic nature of strategy (b) helps to ensure the comparability of different optimization algorithms or strategies. Therefore, Appx. A.7 overviews different strategies to handle random numbers in optimization and sampling, serving as reference in this thesis. In addition to the reduced noisiness in the optimization, the overall optimization time is reduced, which has a positive effect, especially when using time-consuming sampling techniques such as the LHS. For these reasons, the proposed inverse sampling method with the same random numbers is recommended for sampling-based tolerance-cost optimization.

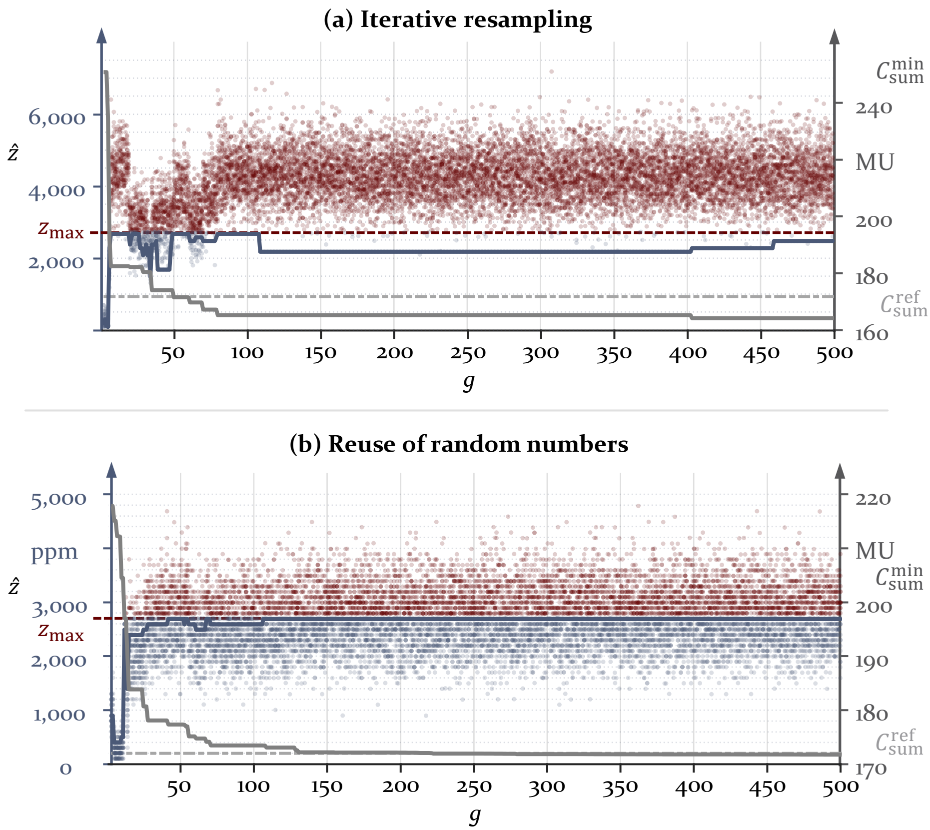

Figure 24: Optimization history expressed by the objective values $C_{\text{sum}}^{\text{min}}$, the respective nc-rates $\hat{z}$, and its scatter for a 100 times repetition in comparison: (a) iterative resampling vs. (b) using the same, initially generated random numbers for repetitive tolerance analysis acc. to Fig. 22.

In conclusion, variance reduction in combination with the reuse of random numbers constitutes an effective method for increasing the accuracy of tolerance-cost optimization. At the same time, the latter ensures the comparability of optimization results since the randomness of the results from the sampling is eliminated and these are only subject to the randomness from the metaheuristics. Nevertheless, its potential is limited when using commercial tolerance analysis software. Since they often exclude a modification of the sampling routines, the sample size remains the only countermeasure.

> *Sampling-based tolerance analysis induces aleatory uncertainty in tolerance-cost optimization and negatively influences its accuracy. High sample sizes, variance reduction techniques, and the reuse of previous results and random numbers within optimization help to reduce and*

eliminate scattering and discontinuity effects on the constraint surface, improving the results' reliability.

4.2 Estimation of product (non-)conformance

The second main contributor to the accuracy of tolerance analysis and optimization results is the nc-rate estimation method (see Fig. 14). The different nc-rate estimation methods presented in [P5] are discussed in more detail below, incorporating the findings from Sec. 4.1.

Problem statement It is already known from Sec. 2.2.2 that the specification limits LSL and USL divide the solution space of Y into a conformance and non-conformance region. Hence, the yld or conformance corresponds to the probability that the critical assembly response Y will fall in this region of conformance, which can be mathematically expressed as an integration of the multivariate probability distribution of all characteristics X_i with their lower and upper boundaries $X_i^{\text{lb}}, X_i^{\text{ub}}$ involved [27]:

$$z = 1 - yld = 1 - \int_{X_1^{\text{lb}}}^{X_1^{\text{ub}}} \dots \int_{X_n^{\text{lb}}}^{X_n^{\text{ub}}} q\left(X_1, \dots, X_n\right) \rho\left(X_1, \dots, X_n\right) \mathrm{d}\chi_1 \dots \mathrm{d}\chi_n, \tag{12}$$

where $q(X_1, \dots, X_n)$ represents a binary indicator evaluating if the condition $LSL \leq f_Y(\boldsymbol{X}_m) \leq USL$ is met ($q(\boldsymbol{X}_m) = 1$) or not ($q(\boldsymbol{X}_m) = 0$).

In sampling-based tolerance analysis, the integral of Eq. (12) is not solved explicitly but approximated by numerical integration. In the first step, n samples for the characteristics X_i are drawn from the part tolerance probability distributions ρ_i, purely randomly or more systematically depending on the sampling procedure chosen (see also Sec. 4.1 and Appx. A.4), and the respective Y values are calculated via $f_Y(\boldsymbol{X}_m)$. The result is a frequency distribution of Y for which a statistical conclusion about the conformance of the population is to be made in the second step. Mathematically, this second step, i.e., the nc-rate estimation, can be expressed as an integral over the resulting probability density function ρ_Y or consequently with the associated cumulative frequency distribution Φ_Y (see Fig. 25):

$$\hat{z}(t) = 1 - \int_{LSL}^{USL} \rho_Y(\boldsymbol{t}, \chi) \mathrm{d}\chi = 1 - (\Phi_Y(USL) - \Phi_Y(LSL)), \tag{13}$$

where one-sided, only lower- or upper-bounded assembly response functions are represented by $USL = \infty$ or $LSL = -\infty$. Consequently, the accuracy of the nc-rate estimation depends primarily on the "fit of [the] statistical distribution [ρ_Y] to the resultant assembly data [$\boldsymbol{Y}$]" [348], besides the quality of the input data, i.e., the sampled data $\boldsymbol{Y}$ based on the assumed probability distributions ρ_i [348].

Theoretical solution Therefore, the main question in nc-rate estimation is *how the cumulative distribution function (cdf)* Φ_Y *can be obtained*. The answer differs if the assumption of the distribution of Y can be confirmed or if it must be dealt with an unknown distribution of Y. Suppose the assumption of normality or non-normal distributions, such as the log-normal or beta distribution, can be verified with the help of suitable statistical tests, such as the *Kolmogorov-Smirnov-test* [572] or the *Anderson-Darling-test* [573]. It is then possible to predict $\hat{z}$ numerically (with the aid of known, formulaic relationships for the cumulative frequency distribution and the statistical moments determined from Y, e.g., $\hat{\mu}$ and $\hat{\sigma}$) or practically (via tabulated z-values [574]). For the assumption of normality and based on the underlying statistical principles [575, 576], Eq. (13) can be transformed into:[8]

$$\hat{z} = 1 - \left(\Phi_{\hat{\mu},\hat{\sigma}}(USL) - \Phi_{\hat{\mu},\hat{\sigma}}(LSL)\right) \tag{14}$$

$$\text{with:} \quad \Phi_{\hat{\mu},\hat{\sigma}}(x) = \frac{1}{\sqrt{2\pi}\hat{\sigma}} \int_{-\infty}^{x} \exp\left(-\frac{(\chi - \hat{\mu})^2}{2\hat{\sigma}^2}\right) \mathrm{d}\chi, \tag{15}$$

$$\text{where} \quad x = LSL \text{ or } x = USL. \tag{16}$$

Consequently, the accuracy of the nc-rate estimation (ncdf) acc. to Eq. (14)–(16) depends on the deviation of the true and estimated value of the statistical moments $\mu - \hat{\mu}$ and $\sigma^2 - \hat{\sigma}^2$.

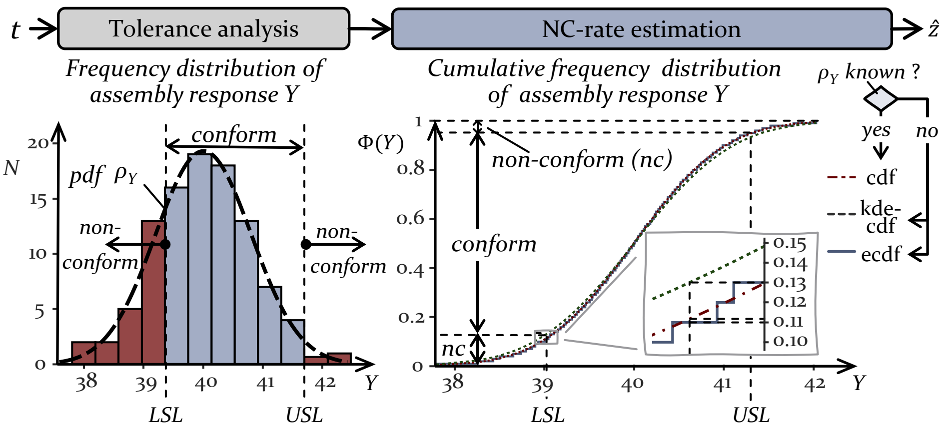

Figure 25: Principle of cdf-based nc-rate estimation for known and unknown assembly response distributions ρ_Y.

[8] An alternative expression of Eq. (14)–(16) results with the error function erf known and used in literature: $\Phi(x, \mu, \sigma) = 0.5 \cdot \left(1 + \operatorname{erf}\left(\frac{x-\mu}{\sigma\sqrt{2}}\right)\right)$ [576].

However, if the distribution type of ρ_Y is unknown, the cdf must be approximated using non-parametric procedures [577]. The *kernel density estimation* (kde) is one possible way to estimate Φ_Y over a sequence of densities of selected kernels K with a defined bandwidth h_{K} [578]. Here, the estimation quality depends on the fit of the chosen kernel K, i.e., the selected single density function, and its bandwidth h_{K} to $\boldsymbol{Y}$. More details on kde are given in Appx. A.4.

In comparison, it is mathematically less complex to describe the cdf with an *empirically approximated cdf* (ecdf) as follows:

$$\hat{z} = 1 - \frac{\sum_{m=1}^{n} q(Y_m)}{n}, \tag{17}$$

$$\text{with:} \quad q\left(Y_m\right) = \begin{cases} 1 & \text{if } LSL \leq Y_m \leq USL, \\ 0 & \text{otherwise,} \end{cases} \tag{18}$$

$$Y_m = f_Y(\boldsymbol{X}_m), \tag{19}$$

where $q(Y_m)$ is an indicator function for product conformance. In words, it means that all the samples $\boldsymbol{Y}$, which are smaller and larger than LSL and USL, respectively, are counted and then put in ratio to the total number of samples n. Consequently, the estimator depends on the sample size n and the sampled data $\boldsymbol{Y}$.

Practical transfer and findings The subsequent investigations aim to study the difference between the proposed parametric and non-parametric nc-rate estimation methods. The wheel mounting assembly from the previous section with the same assumptions is used again as a case study. MCS, QMCS, and LHS is repeated 100-fold for different sample sizes n from 10,000 up to 250,000. In line with Sec. 4.1, the influence of the three proposed nc-rate techniques ncdf, kde-cdf, and ecdf is studied for $z_{\max} = 63; 2{,}700; 45{,}500$ ppm ($\pm 4\sigma$; $\pm 3\sigma$; $\pm 2\sigma$). Because of the linearity of f_Y and the normally distributed input variables X_i, normality for Y is given and the parametric estimation follows Eq. (14)–(16). A Cauchy kernel K is chosen for kde-based nc-rate estimation, where the bandwidth is individually selected to optimally estimate normal density acc. to [579] (see Appx. A.4 and Appx. A.9.1).

Fig. 26 gives an overview of the predicted nc-rate values $\hat{z}$ for MCS. The estimates using ecdf and kde-cdf yield comparable wide margins of error, which decrease successively over n as expected. In particular, ecdf shows a strong underestimation of the nc-rate, especially when n is too small.

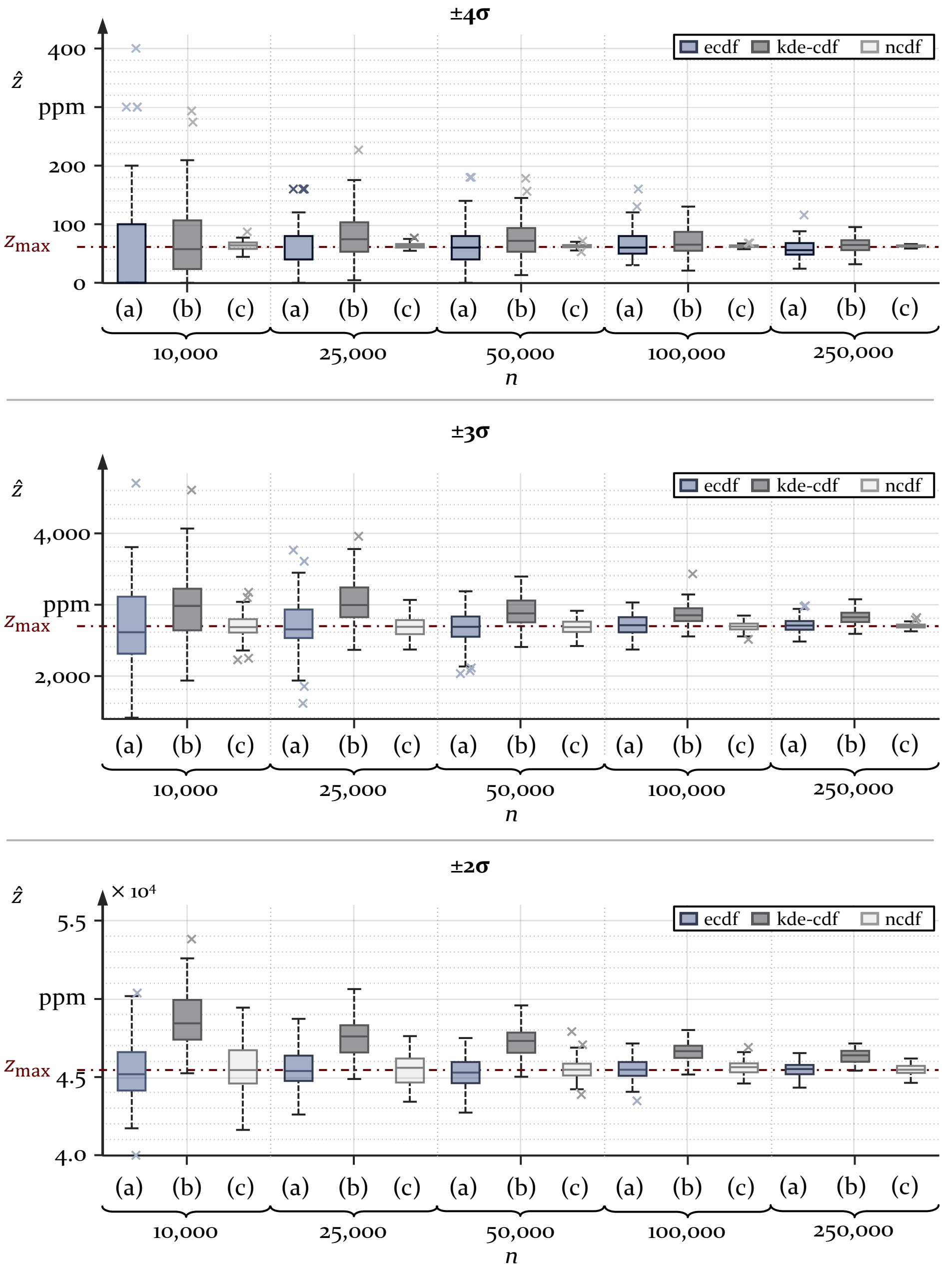

Figure 26: Overview of tolerance analysis results for MCS, different sample sizes, and nc-rate estimation techniques: empirically estimated cdf (ecdf) (a), cdf based on kernel density estimation (kde-cdf) (b), cdf for normal distribution $\mathcal{N}(\hat{\mu}, \hat{\sigma}^2)$ (ncdf) (c).

This effect is particularly evident in the case of very low expected nc-rates. The reason for this is the determination of the nc-rates by the discrete, piecewise-linearly defined cdf, which results in a strong discretization of the nc-rates in dependence of n. For example, considering $n = 10{,}000$, a sample more or less in the tails of ρ_Y outside LSL or USL leads to a difference/change of $(1 : 10{,}000) \cdot 1 \cdot 10^6$ ppm $= 100$ ppm.

In comparison, the estimates using kde-cdf and ncdf lead to more symmetric error margins. The continuous cdfs determined via kde or given directly for standard distributions, such as normal distribution in the case of ncdf, result in a more balanced ratio of underestimates and overestimates. At this point, it must be said retroactively that all studies in the previous section are based on an ecdf-based nc-rate estimation acc. to Eq. (17)–(19), further explaining the results in Fig. 18 et seq. Particularly striking are the narrow margins of error resulting through the robust estimation of the statistical moments of $\hat{\mu}$ and $\hat{\sigma}$ for cdf. The use of variance-reducing sampling methods further enhances this effect. Fig. 27, contrasting the results obtained with MCS and QMCS for $z_{\text{max}} = 2{,}700$ ppm, emphasizes the positive effect of variance reduction for all estimation methods, but especially significant for ncdf.

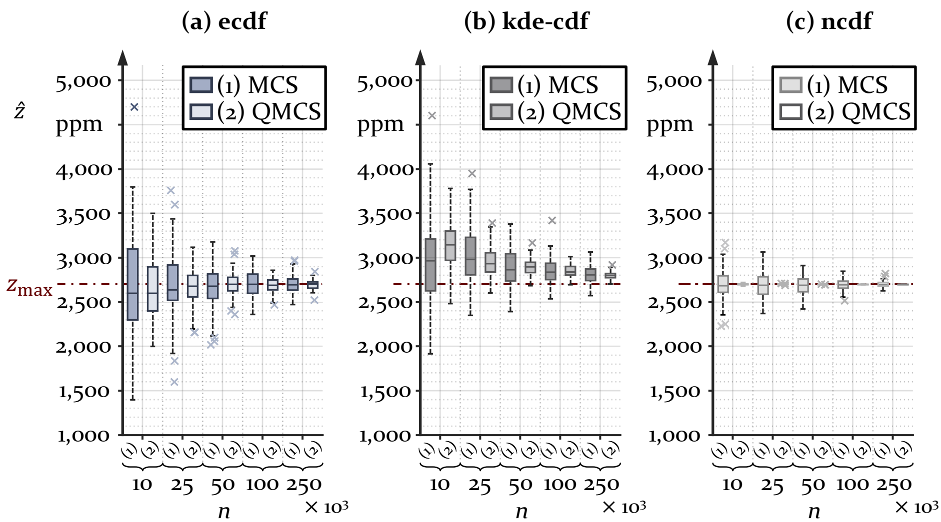

Figure 27: Comparison of the results obtained for a 100 times repeated tolerance analysis based on MCS and QMCS and the presented nc-rate estimation techniques ecdf (a), kde-cdf (b), and ncdf (c).

Besides, it illustrates the tendency of ecdf to underestimation and kde-cdf to overestimation, which can be seen in the shift of the scatter boxes and the median from the true value z_{max}. In contrast, the margins of error for ncdf are centered around z_{max}. In line with the findings from Sec. 4.1, the results for LHS are comparable to those for MCS, whereby the previously made findings, specific for the respective nc-rate estimation techniques, are confirmed. Thus, no detailed discussion of these results is given at this point. The complete set of results is summarized in Tbl. 14–16 and additionally visualized in Fig. 97.

To further study the effects on optimization, the tolerance allocation problem from Sec. 4.1 is now solved 50 times following the strategy of same random numbers from Sec. 4.1. MCS is chosen as tolerance analysis technique and optimization is performed for the different nc-rate estimation techniques, each for $n = 10{,}000; 50{,}000; 100{,}000$. CS is used for optimization (for the settings, see Appx. A.9.1). Fig. 28 illustrates the results, summarized in Tbl. 17, by means of the achieved cost optima C_{sum}^{opt} for z_{max} (left).

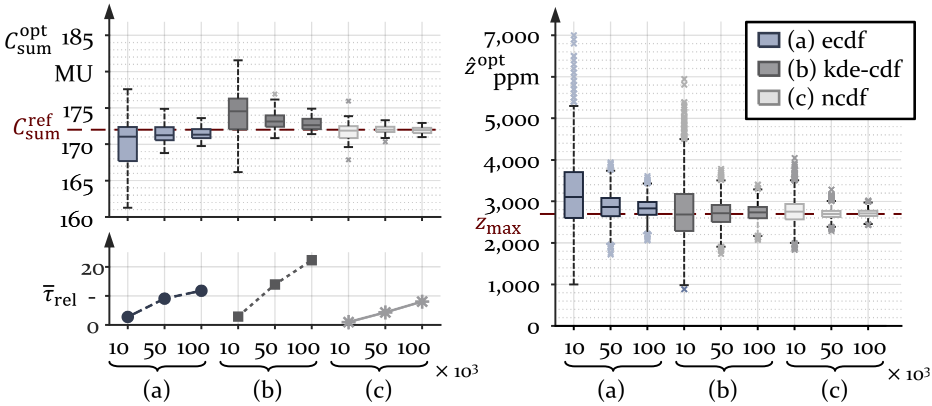

Figure 28: Overview of the obtained optima C_{sum}^{opt}, the average computation times in relation to the minimum one $\overline{\tau}_{rel}$, and the scatter of final nc-rates $\hat{z}^{opt}$ for a 50-fold repetition of optimization making use of the proposed nc-rate estimation techniques ecdf (a), kde-cdf (b), and ncdf (c).

Similar to Fig. 23, it shows the variance of $\hat{z}$ when repeating tolerance analysis and nc-rate estimation 100 times after optimization taking the optimally allocated tolerance values into account (right). The ncdf-specific effects of lower variances and more centered error margins of $\hat{z}$, already observed in the analysis studies, have a direct impact on lower variances as well as the centrality of C_{sum}^{opt} (see Fig. 28 (c)). Given that this study uses the same sampling within the optimization (as proposed in Sec. 4.1), the values below C_{sum}^{ref} obtained for ecdf are observed much more frequently due to the higher probability of underestimation of $\hat{z}$ (see Fig. 28 (a)). In comparison, the tendential overestimation of the kde-cdf, additionally influenced by the stochastic approach of the optimizer, which does not exclude an early convergence outside the global optimum, leads in total to higher optima $C_{\text{sum}}^{\text{opt}}$ (see Fig. 28 (b)). In terms of computational efficiency, kde is inferior to ncdf and ecdf, which is reflected in the comparison of the relative average optimization times $\overline{\tau}_{\text{rel}}$ in Fig. 28.

In summary, the estimation of nc-rates using ncdf provided the best results. At the same time, the variance reduction method QMCS is suitable to further improve the accuracy of sampling-based tolerance-cost optimization. However, parametric estimators are only applicable if a predefined assumption of the distribution is proven to be true for at least the optimal solution. But, for all intermediate tolerance value sets (which might be numerically cost-intensive), the distribution type of Y may also change during the optimization, for example, since the contributors of tolerances t_i vary with their currently allocated values or the input distributions ρ_i of the single features X_i dynamically alter, as it is the case in machine selection/allocation (see Sec. 5.1–5.2).

> *Provided that the distribution of the assembly response is known and passes a statistical test, the use of its cumulative distribution function for parametric nc-rate estimation leads to a tighter margin of error and more accurate optimization results at the same sample size. Otherwise, non-parametric nc-rate estimation based on ecdf is superior to kde.*

4.3 Non-conformance rate estimation for multiple assembly responses

The reflections so far restrict that the total assembly quality is expressed by only one KC and represented in tolerance analysis by a single assembly response function. However, it is common in practical applications that a set of multiple KCs contribute to total product quality, which first impacts the nc-rate estimation and second the definition and solution of the tolerance-cost optimization problem. The findings below summarize and extend the research presented in [P8, P10] introducing a solution to handle multiple assembly responses and their correlations accurately in tolerance-cost optimization.

Problem statement At first, the difference between KC and assembly response, as understood in this thesis, should be emphasized. A KC is a characteristic on the assembly level critical for the overall product quality, e.g., a gap or an angle. In comparison, assembly responses Y act as virtual metrics, which represent the KCs in simulation alone or in part and can be determined via implicit and explicit functions f_Y (see Sec. 2.2.2). Fig. 29 follows this distinction and overviews different cases where multiple assembly responses Y are needed for product quality assurance by simulation, where either one or multiple KCs are of interest.

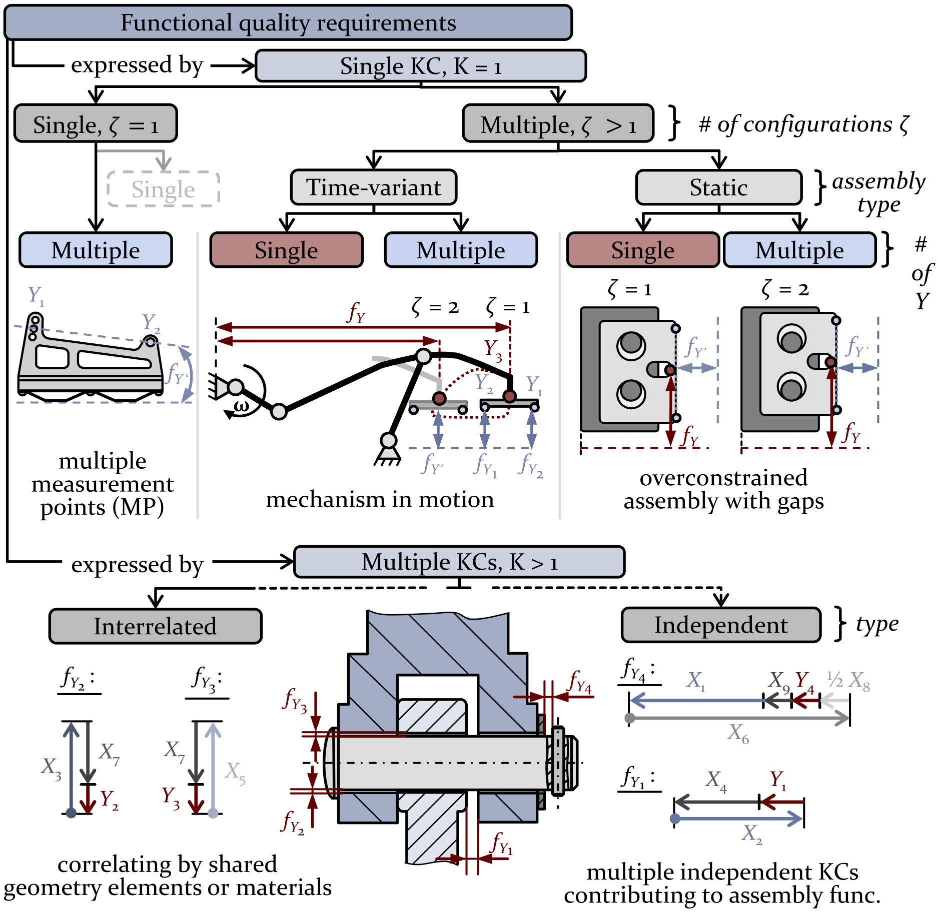

Figure 29: Multiple assembly responses to be handled in nc-rate estimation. Functional requirements expressed by one KC ($K = 1$) (top) and multiple KCs ($K > 1$) (bottom). The examples are freely adopted from [183, 203, 287].

Depending on the assembly and KC type and their modeling, several assembly responses Y are often necessary to represent **one single KC**. In this respect, the definition of the assembly response function f_Y, including the selected geometrical and behavior model, plays an essential role. If, for example, a minimum distance in 2D is defined as KC and shape variations are neglected, it can, for instance, be represented by two virtual measurements. Either the separately determined Y measures are transferred into a substitute response value Y' (here $f_{Y'} = \min(Y_1, Y_2)$) or they are checked each individually via respective specification limits. In comparison, an angularity requirement can only be evaluated through Y' because the KC limits are defined by both assembly response information (see Fig. 29 (top)).

Besides, multiple assembly responses occur if a KC must be assured for different assembly configurations ζ. Typical examples are time-variant mechanisms, for which certain positions or the entire motion, e.g., to evaluate its motion accuracy, are considered to be critical. Similarly, different configurations may occur in static assemblies during the assembly process, either randomly or intentionally, e.g., due to gravity or external forces for alignment. In the case of overconstrained assemblies with gaps, for example, all admissible gap configurations must be considered (see Fig. 29 (top)). They originate from the degrees of freedom intentionally left open by clearance [134, 355] and are finally locked by subsequent joining or assembly operations, i.e., by additional elements for part-driven assemblies or by joining operations for process-driven assemblies (see Sec. 2.2.2).

Moreover, even for simple assemblies, **multiple KCs** ($K > 1$) may be relevant, although axiomatic design pretends that these situations should be avoided in advance [580]. For instance, multiple critical gaps must be within predefined specification limits to ensure assembly functionality (see Fig. 29 (bottom)). If the KCs do not share any common elements, they are independent of each other and variations of characteristics $\boldsymbol{X}$ always affect only one KC [6]. Otherwise, they are interrelated via common geometrical features or non-geometrical characteristics. Typical examples are dimensional and geometrical variations or variable material properties, e.g., the temperature expansion coefficient. Interrelated KCs are correlating, but some KCs may play a minor role in comparison [6] because the contributors of the common characteristics $\boldsymbol{X}$ to them are significantly smaller and/or the boundaries and/or the specification limits are wider and, thus, less critical. In contrast, if the variations of $\boldsymbol{X}$ contribute in a contradictory way in their algebraic sign (e.g., $X_i \uparrow \rightarrow\ Y_1 \uparrow\ \&\ Y_2 \downarrow$), the KCs conflict and some KCs will degrade the others [6, 580].

A review of the approaches from the literature shows that, especially when several KCs are taken into account, they are usually assessed separately and checked with K individual constraints following Eq. (4). However, the small example in Fig. 30 illustrates that the correlations of several assembly responses impacting the higher-level assembly quality are neglected in nc-rate estimation. While the isolated evaluation of Y_1 and Y_2 indicates two and four non-conform assemblies, the sample-per-sample assessment of all criteria leads to five non-conform assemblies. Approaches using QL-functions capture these effects appropriately by additional covariance terms. These effects are, however, neglected when estimating the nc-rate (or the directly related

C_{pk}-values) by sampling methods or T_Y by convolution-based approaches, for instance, by the RSS or estimated mean shift method (see Sec. 2.2.3). Consequently, this shortcoming negatively affects the constraint evaluation's accuracy and, thus, the optimization results' acceptability.

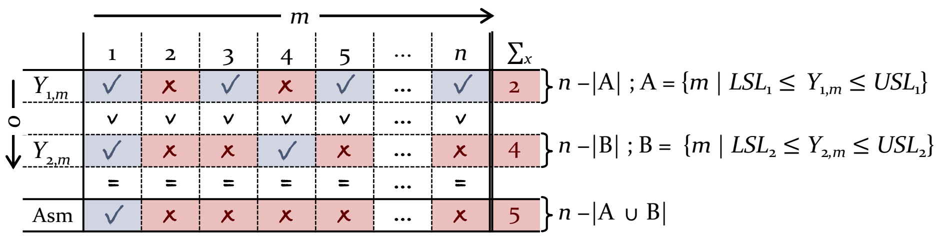

Figure 30: Illustration of the effect of multiple assembly responses on nc-rate estimation.

Instead of an independent consideration of a set of single nc-rates according to Eq. (5) with the aid of a univariate pdf ρ_{Y_o}, a multiple integral over one common multivariate pdf ρ_Y^* can handle this problem properly:

$$\hat{z}(\boldsymbol{t}) = 1 - \int_{LSL_{o=1}}^{USL_{o=1}} \cdots \int_{LSL_O}^{USL_O} \rho_Y^*(\boldsymbol{t}, \chi_1, \dots, \chi_O) d\chi_1 \dots d\chi_O. \tag{20}$$

Theoretical solution Since ρ_Y^* cannot be easily described mathematically so that it can be integrated or transformed into a multivariate cdf, it is reasonable to solve this problem by an ecdf-based nc-rate estimation method. Therefore, Eq. (17) is extended to a multivariate ecdf covering multiple assembly responses Y by a set of test functions q, covering the cases shown in Fig. 29.

The functions $q(\boldsymbol{X}_m)$ check if the k-th KC is fulfilled for $\boldsymbol{X}_m$:

$$q_k(\boldsymbol{X}_m) = \begin{cases} 1 & \text{if} \quad LSL_k \leq f_{Y_k}(\boldsymbol{X}_m) \leq USL_k, \\ 0 & \text{otherwise.} \end{cases} \tag{21}$$

If there are multiple configurations, $q_{k,\zeta}(\boldsymbol{X}_m)$ is used to check if the k-th KC is fulfilled for the ζ-th assembly configuration:

$$q_{k,\zeta}(\boldsymbol{X}_m) = \begin{cases} 1 & \text{if} \quad LSL_k \leq f_{Y_k}(\boldsymbol{X}_m) \leq USL_k, \\ 0 & \text{otherwise.} \end{cases} \tag{22}$$

Eq. (22) could further be extended to multiple assembly responses separately evaluated for the k-th KC. However, it makes no difference in the result if they are first reduced to a critical response Y' and then assessed or evaluated for all configurations. For clarity, this case is not further mathematically specified in Eq. (22).

Aggregating the developed test functions for all K KCs with Z configurations in one overall nc-rate estimation equation, Eq. (17) expands to:

$$\hat{z}_{\text{asm}} = 1 - \frac{\sum_{m=1}^{n} q_{\text{asm}}(\boldsymbol{X}_m) \cdot \prod_{k=1}^{K} \prod_{\zeta=1}^{Z} q_{k,\zeta}\left(Y_{k,\zeta,m}\right)}{n}, \tag{23}$$

$$\text{with:} \quad q_{\text{asm}}(\boldsymbol{X}_m) = \begin{cases} 1 & \text{if asm. reqs. are fulfilled for } \boldsymbol{X}_m, \\ 0 & \text{otherwise,} \end{cases} \tag{24}$$

$$q_{k,\zeta}\left(Y_{m,k,\zeta}\right) = \begin{cases} 1 & \text{if } LSL_k \leq Y_{m,k,\zeta} \leq USL_k, \\ 0 & \text{otherwise ,} \end{cases} \tag{25}$$

$$Y_{m,k,\zeta} = f_{Y_k,\zeta}(\boldsymbol{X}_m, \zeta), \tag{26}$$

where q_{asm} is a test function to evaluate whether the parts with the current variations $\boldsymbol{X}_m$ can be assembled at all. Again, the modeling decides whether the assemblability criterion has to be mapped explicitly or is already implicitly contained in f_Y. Part non-interference equations, for instance, have to be satisfied while finding the worst-case configurations by optimization [134] or the solution of mechanisms are not allowed to be complex so that the Y-values can be determined either at all or correctly [581]. In contrast, using vector models, for example, the assemblability can be considered directly via f_Y with reasonable specification limits discarding part interference.

Practical transfer and findings The effects of the correlations between multiple assembly responses on the optimization results for least-cost tolerance allocation are the focus of the subsequent studies. Therefore, two optimization strategies are compared, viz. quality assurance with an individual nc-constraint for each assembly response (a) and with one overall nc-rate constraint (b) according to Eq. (23)–(26). The maximum nc-rate is set for all K constraints as well as for the total nc-rate to $z_{k,\max} = z_{\max} = 2{,}700$ ppm. A second KC supplements the wheel mounting assembly from the previous example, so two KCs ($K = 2$) are functional-critical for one assembly configuration Z = 1 (see Fig. 90). As the geometrical and behavior model are based on a vector model, the assemblability condition q_{asm} is implicitly considered in the specification limits and must not be evaluated separately. All K lower specification limits $LSL_k > 0$, so negative gaps and part intersections are excluded via the nc-rate estimation. Each characteristic is still assumed to be normally distributed. As in the previous sections, this allows to define the specification limits LSL and USL inversely as a multiple of the root sum squares of the sum of all individual part tolerances $t_i = 0.5 \cdot \left(t_i^{\text{ub}} - t_i^{\text{lb}}\right)$ leading to a balanced solution space with 50% feasible and 50% non-feasible solutions (see Appx. A.9.1). This implies that the boundaries and the tolerance-cost parameters are equal for all tolerances. For optimization, the CS algorithm is used with $\eta_p = 25, \eta_g = 200$, $\eta_{g,\text{stall}} = 50$. The same MCS with $n = 100{,}000$ is used for the individual repetitions for both strategies (a) and (b) ($\eta_r = 10$), ensuring the comparability of the results while following strategy O-2/S-3 acc. to Tbl. 6. Further details on the study are given in Tbl. 7 and Appx. A.9.1. The main optimization results are visualized in Fig. 31. All details are given in Tbl. 18–20.

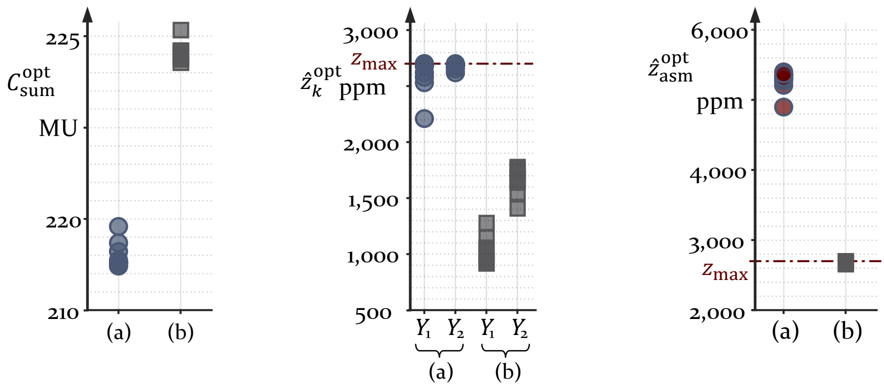

Figure 31: Tolerance-cost optimization results with multiple assembly responses handled by (a) K nc-constraints and (b) one overall total nc-constraint.

It is evident that the obtained cost minima $C_{\text{sum}}^{\text{opt}}$ are lower for case (a) (see Fig. 31 (left)). For case (b), tighter tolerances are needed not to exceed the maximum limit of the total nc-rate. This finally leads to higher manufacturing costs since $\hat{z}_{\text{asm}}^{\text{opt}}$ is always higher due to its correlation terms than the dominant, most critical k-th nc-rate and thus the acceptability constraints are more restrictive in case (b) (see Fig. 31 (center)). On the one hand, these interrelations can be observed in comparing the optimal tolerance values for the respective best runs in Fig. 32. On the other hand, the comparison of the total nc-rates in Fig. 31 (right), where these are calculated for strategy (a) after optimization for the obtained best tolerance values, indicates that they are much higher than the nc-rates obtained by strategy (b). Hence, the study exemplarily proves the theoretical considerations discussed above.

Consequently, if the focus is ultimately on the overall assembly quality, only the ecdf-based nc-rate estimation according to Eq. (23)–(26) can represent it accurately. Further transferring the findings on best-quality tolerance allocation (see Eq. (6) a)), the number of K objectives for the K single nc-rates is reduced to one objective for the total nc-rate, whereby the multi-objective optimization can be turned into a single-objective optimization. Finally, it is essential to note that the level in the KC flow-down is decisive. In the above considerations, quality was only considered at the functionality level. In the example, both KCs define function fulfillment, so it is reasonable that the conformity requirements for the functionality must be fulfilled in total. If further criteria, such as aesthetics, are considered for quality assurance, an individual assessment and prioritization or weighting of the requirements can make sense.

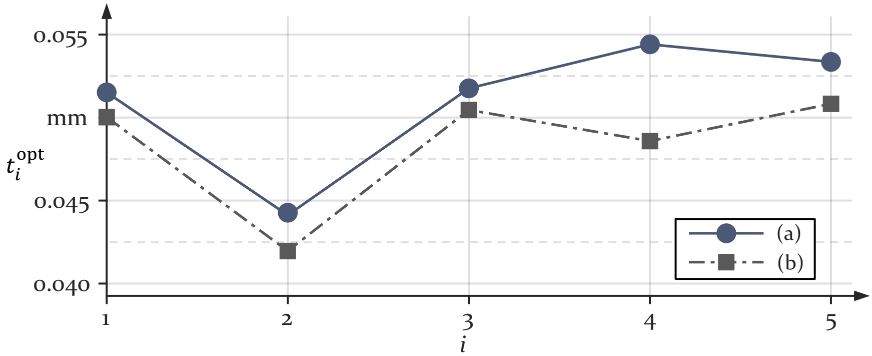

Figure 32: Obtained optimal tolerance values for the best runs from Fig. 31.

> *If multiple KCs or measurements are required to virtually assure the total product quality, their correlations can adequately be considered through an overall empirical cdf-based nc-rate estimation. Their consideration acc. to Eq. (23)–(26) and in optimization by one acceptability constraint leads to tighter tolerances and higher costs, but it can assure the total product quality more accurately.*

5 Enhancing the completeness of sampling-based tolerance-cost optimization

In academia and industry, it is agreed that tolerance-cost optimization should be performed as one of the last product design steps [48]. Its inclusion in the product-driven tolerance design phase is reasonable since it is the only phase where the tolerance expert can overview the entire assembly and balance the individual design tolerances across the parts. After that, their interrelations over the KCs are generally lost in the subsequent part manufacturing process planning steps acting on the part level. Consequently, the main *context of use* of tolerance-cost optimization is specified for product design, in which the answering of product design relevant questions are put in the spotlight, e.g., the representation of the assembly behavior in use. Although the manufacturing and assembly processes are to be simulated virtually in tolerance analysis (Fig. 10), process design aspects are represented in a simplified way or neglected, which can partly be explained by the lack of information on the machines, processes, and suppliers to be used, which are not yet defined. Extensions of optimization-based tolerance allocation methods to early consider issues from process planning, such as machine selection and process scheduling, intend to counteract the lack of manufacturing orientation but are partly hampered when using convolution-based tolerance analysis techniques due to the abstraction of information by one single tolerance value and relying on often freely chosen or estimated standard part tolerance probability distributions. Sampling techniques, in contrast, are generally capable of answering these questions more realistically through machine-specific manufacturing distributions, but the current scope of sampling-based tolerance-cost optimization limits its potential.

Hence, the subsequent sections focus on the shortcomings mentioned above in its **completeness**, the second important aspect of effectiveness (see Sec. 3.3). Novel machine/supplier selection and allocation methods with multiple, geometrical tolerances are introduced to cover more practical industrial fabrication scenarios. An early consideration of relevant process design aspects and tasks helps to better link and tailor the adjacent tolerance allocation and process planning phases and to represent the tolerance allocation problem more completely. As in the previous section, the wheel mounting assembly example, described in detail in Appx. A.8.1, accompanies the presentation of the methods as the use case with different scenarios.

5.1 Alternative machine and supplier selection

In the previous chapters, the part tolerance probability distributions were set fixed before optimization and assumed to follow normality. In practice, it is instead the case that the selection of tolerance values also requires choosing a suitable machine for a manufacturing process or a supplier, which differs not only in its tolerance-related costs but also in the resulting geometrical part quality (see Fig. 33). The subsequent discussion is limited to the decision on machines for single-stage processing and suppliers without considering additional process selection. However, process selection can be regarded as an additional task to machine selection in the same manner since the general problem to be solved in optimal tolerance allocation stays the same [P9]. The subsequent findings are based on initial studies presented in [S5] and published in [P9].

Problem statement Sampling provides the advantage that machines/suppliers-dependent frequency distributions can be considered within tolerance analysis. As literature has already proven, a preselection of machines/processes or suppliers before optimization cannot lead to the cost minimum. Instead, they must always be selected together with the tolerances during optimization (see Sec. 2.2.4). It is assumed, for the moment, that there is only one tolerance i per part. Fig. 33 visualizes the concurrent tolerance allocation and machine/supplier selection problem for two tolerances ($I = 2$) with three machine alternatives ($J_i = 3$) each with randomly selected values t_i'. Depending on the currently chosen tolerance value t_i', a decision has to be made which machine firstly can and secondly should be chosen to realize t_i. In this example, t_2' could be realized by all alternatives while t_1' is too tight for alternative $j = 2$.

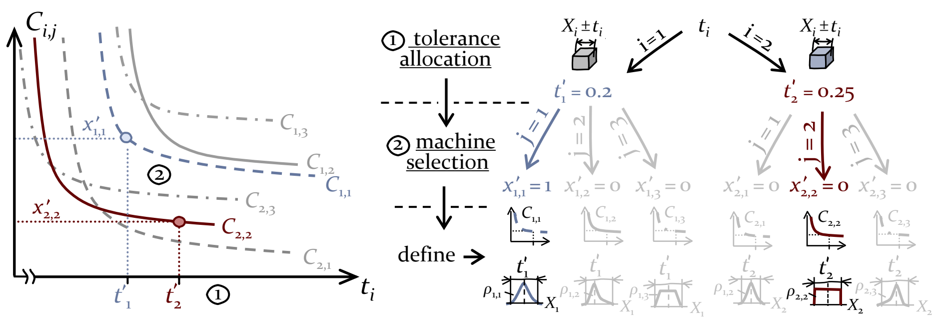

Figure 33: General idea of machine selection in sampling-based tolerance-cost optimization.

Adopting the mathematical notation from [38, 44], the optimization problem from Eq. (6)–(8) b) expands to:

$$\text{Minimize} \quad C_{\text{sum}}(\boldsymbol{t}, \boldsymbol{x}) = \textstyle\sum_{i=1}^{I} \sum_{j=1}^{J_i} x_{i,j} \cdot C_{i,j}(t_i), \tag{27}$$

$$\text{subject to:} \quad \hat{z}(\boldsymbol{t}, \boldsymbol{x}) = 1 - yld(\boldsymbol{t}, \boldsymbol{x}, \boldsymbol{USL}, \boldsymbol{LSL}) \leq z_{\max}, \tag{28}$$

$$\textstyle\sum_{j=1}^{J_i} x_{i,j} = 1 \qquad \forall\ i = 1, \dots, I \tag{29}$$

$$x_{i,j} = \begin{cases} 1 & \text{if machine } j \text{ is selected for } t_i, \\ 0 & \text{otherwise,} \end{cases} \tag{30}$$

$$t_{i,j}^{\text{lb}} \leq t_i \leq t_{i,j}^{\text{ub}} \quad \forall\ i = 1, \dots I \wedge x_{i,j} = 1, \tag{31}$$

where the binary, zero-one selection parameter $x_{i,j}$ selects one alternative with its costs $C_{i,j}$ and part tolerance distribution $\rho_{i,j}$ out of all available J_i options for each tolerance t_i [307, 495]. Whether a tolerance value can be achieved, depends on the process range of the selected machine (see Eq. (31)). $t_{i,j}$ and $x_{i,j}$ are then defined by:

$$\{x_{i,j} \in \mathbb{N}_0 \mid x_{i,j} \in [0;1]\}, \tag{32}$$

$$\left\{t_{i,j} \in \mathbb{R}^{>0} \mid t_{i,j} \in [t_{i,j}^{\text{lb}}; t_{i,j}^{\text{ub}}]\right\} \text{ or } \left\{t_{i,j} \in \mathbb{R}^{>0} \mid t_{i,j} \in \{t_{i,1}; \dots; t_{i,S}\}\right\}, \tag{33}$$

where Eq. (33) (left) is valid for continuous tolerance values. In the case of discrete tolerance values, which result from a limited freedom of choice, e.g., in the case of defined supplier classes with S fixed values specified by the supplier, the domain is limited by Eq. (33) (right). They can be represented in optimization by discrete or integer variables but require capable algorithms [P17].[1]

Theoretical solution Since both costs C_{sum} and the nc-rate $\hat{z}$ are functions of $\boldsymbol{t}$ and $\boldsymbol{x}$ (see Eq. (27) and Eq. (28)), both design variables must not only be mapped in tolerance-cost and tolerance analysis in each optimization step, i.e., for each individual p in each generation g (see also Fig. 12), but also be balanced optimally by a suitable routine. For this reason, two approaches, viz. the *minimum-cost curve approach* (a) and *mixed-integer optimization* (b), are studied in the following. Both approaches have proven to be more efficient in solving problems by parallel consideration than additional search algorithms nested in the optimization to identify the best combination of machines for

[1] It is also possible to consider all tolerances as discrete values with a certain accuracy, in µm, for example [P17]. Optimization problems with discrete optimization variables are usually more difficult to solve but can be handled by metaheuristic optimization algorithms. For clarity, tolerances are considered continuous in this thesis, except fixed tolerance classes for external supply.

each intermediate value set (see Sec. 2.2.4). Fig. 34 compares both methods for the example of Fig. 33.

When applying the so-called minimum-cost approach (a), the parallel branches of tolerance-cost and tolerance analysis (see Fig. 12) are serial. Before tolerance analysis can be performed, tolerance-cost analysis has to be completed since the results indicate the machine/supplier characteristics for realizing t_i'. In line with the global aim, viz. cost minimization, the lowest-cost alternative is always chosen, resulting in a piecewise total minimum-cost curve, which gives the approach its name (see Fig. 34 (left)). In case (b), the choice is left to the optimizer by an additional set of integer design variables $\boldsymbol{v}_x$, including one variable v_{x_i} for each tolerance t_i, $\{\, v_{x_i} \in \mathbb{N} \mid v_{x_i} \in [1; J_i] \,\}$ (see Fig. 34 (right)). Together with the design vector $\boldsymbol{v}_t$ for tolerance allocation, they form a mixed-integer problem. For $x_{i,j}$, the respective pre-specified pdf $\rho_{i,j}$ and its parameters, or rather by the corresponding inverse cumulative distribution function (see Fig. 17), are picked and used for sampling to generate the geometrical part variations. Except for this additional selection step, the tolerance analysis routine remains the same as shown in Fig. 10.

The selection parameter $x_{i,j}$ for (a) and (b) is defined as follows:

$$\underbrace{x_{i,j} = \begin{cases} 1 \text{ if} & C_{i,j}(t_i) < C_{i,k}(t_i),\ k \neq j, \\ & t_{i,j}^{\text{lb}} \leq t_i \leq t_{i,j}^{\text{ub}} \\ 0 \text{ else.} & \end{cases}}_{\text{(a) minimum-cost curve}} \quad \underbrace{x_{i,j} = \begin{cases} 1 \text{ if} & v_{x_i} = j, \\ 0 \text{ else.} & \end{cases}}_{\text{(b) mixed-integer optimization}} \tag{34}$$

The design vector $\boldsymbol{v}_t$, comprising I entries v_{t_i} for the choice of t_i, is the same for both cases. The lower and upper boundaries t_i^{lb}, t_i^{ub} result from the process limits of all alternatives (see Fig. 34):

$$t_i^{\text{lb}} = \min\left(t_{i,j}^{\text{lb}}\right) \quad \wedge \quad t_i^{\text{ub}} = \max\left(t_{i,j}^{\text{ub}}\right) \quad \forall j = 1, \dots, J_i. \tag{35}$$

The minimum-cost curve approach (a) only takes machines/suppliers feasible for t_i' into account (see Eq. (34)). Hence, Eq. (31) is always implicitly fulfilled. However, in the case of mixed-integer optimization (b), the information about the capability to realize t_i' is lost by splitting the choice of machine/supplier and tolerances over the two independent decision variable vectors $\boldsymbol{v}_t$ and $\boldsymbol{v}_x$. As a result, tolerance and machines/suppliers may be chosen although they are not defined for them (see t_2^* in Fig. 34).

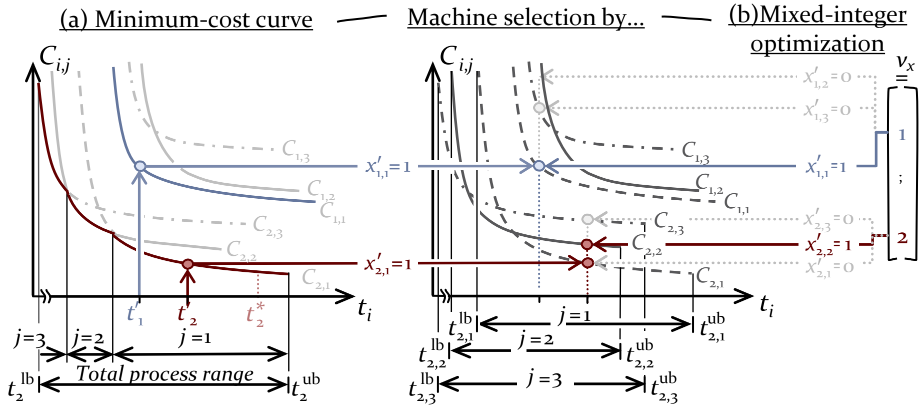

Figure 34: Machine selection based on (a) minimum-cost curves vs. (b) by mixed-integer optimization.

Explicitly defined linear inequality constraints following Eq. (31) exclude this issue for each part i:

$$\underbrace{\begin{bmatrix} t_{i,1}^{\text{lb}} \\ \vdots \\ t_{i,J_i}^{\text{lb}} \end{bmatrix}}_{\boldsymbol{t}_i^{\text{lb}}} \odot \underbrace{\begin{bmatrix} x_{i,1} \\ \vdots \\ x_{i,J_i} \end{bmatrix}}_{\boldsymbol{x}_i} \leq \underbrace{\begin{bmatrix} t_i & \cdots & 0 \\ \vdots & \ddots & \vdots \\ 0 & \cdots & t_i \end{bmatrix}}_{\boldsymbol{I}_{J_i \times J_i} \cdot t_i} \cdot \underbrace{\begin{bmatrix} x_{i,1} \\ \vdots \\ x_{i,J_i} \end{bmatrix}}_{\boldsymbol{x}_i} \leq \underbrace{\begin{bmatrix} t_{i,1}^{\text{ub}} \\ \vdots \\ t_{i,J_i}^{\text{ub}} \end{bmatrix}}_{\boldsymbol{t}_i^{\text{ub}}} \odot \underbrace{\begin{bmatrix} x_{i,1} \\ \vdots \\ x_{i,J_i} \end{bmatrix}}_{\boldsymbol{x}_i}, \tag{36}$$

where the constraints for the currently selected alternative j are enabled through $x_{i,j}$.

Any section in the entire process range where no alternative can realize the chosen tolerance with process reliability must be represented in both cases via additional constraints or directly via high penalty costs so that the optimizer avoids these regions. Fortunately, metaheuristic algorithms tackle the occurring discontinuities and non-convex problems well.

Practical transfer and findings The proposed approaches for concurrent machine/supplier and tolerance selection are now applied to the wheel mounting assembly with its two critical KCs (see Fig. 90) using the ecdf-based nc-rate estimation technique from Sec. 4.3. Except for tolerance t_4 ($J_i = 2$), $J_i = 4$ alternatives with individual costs and limits are considered for all tolerances. The first study (1) assumes that all machines have standard normally distributed characteristics. The data is summarized in Tbl. 21. For optimization, a GA is used with continuous design variables for the minimum-cost curve approach (a) and mixed-integer ones for the optimization-based alternative selection (b). The algorithm settings were chosen based on preliminary studies and are summarized in Appx. A.9.2. To evaluate the influence of the number of individuals on the results and its scattering, two population sizes $\eta_p \in \{50; 100\}$ are studied in a tenfold repetition ($\eta_r = 10$). The same MCS with equal random numbers, $n = 100{,}000$, excluding sampling-induced scattering effects (see Sec. 4.1), are used (O-2/S-3 acc. to Tbl. 6). Fig. 35 contrasts the optimization results for (a) and (b) at a glance, more details are given in Appx. A.9.2, Tbl. 22.

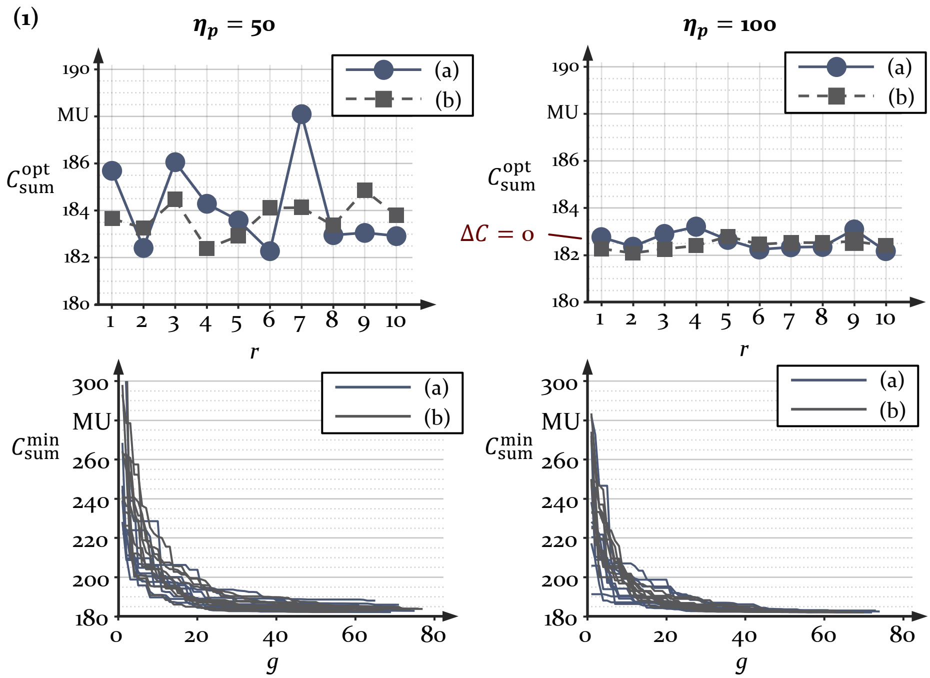

Figure 35: Optimization results for concurrent machine/supplier selection using (a) minimum-cost curve approach vs. (b) mixed-integer optimization: study (1) $\rho_{i,j} = \rho_i$, normally distributed.

Both approaches lead to the same cost optima for the different runs, apart from minor differences resulting from the stochastic approach of the optimizer. As expected and at the expense of the computation time, the duplication of the population size has a positive effect on finding the global optimum. The differences in the optima significantly decrease and the rate of successful runs increases (see Tbl. 23). The chosen alternatives for both best runs are identical, so the choice by the optimizer in case (b) leads to the same decision as based on least costs using the minimum-cost approach (a) (see Tbl. 24).

For the second study (2), the normality assumption is discarded and individual machine-specific part tolerance distributions are now defined. Tbl. 25 summarizes the alternatives with their individual part tolerance distributions and statistical moments. Besides normal and uniform distributions, the Pearson system can represent different machine-dependent probability distributions (see Appx. A.4). In addition, part 2 with t_2 is now considered as a purchased part and has to be chosen cost-optimally from the choice of four options with discrete tolerances and costs. All optimization settings, etc. are identical to the study (1).

Comparing the results given in Fig. 36 with the ones from the previous study in Fig. 35, it can be seen that the mixed-integer optimization (b) now achieves lower costs than the minimum-cost curve approach (a). Since all the predicted nc-rates $\hat{z}_{\text{asm}}$ are slightly below or equal to $z_{\text{max}} = 2{,}700$ ppm for both approaches and the chosen tolerances are within the defined limits, the obtained solutions are all feasible and acceptable (see Tbl. 26–27).

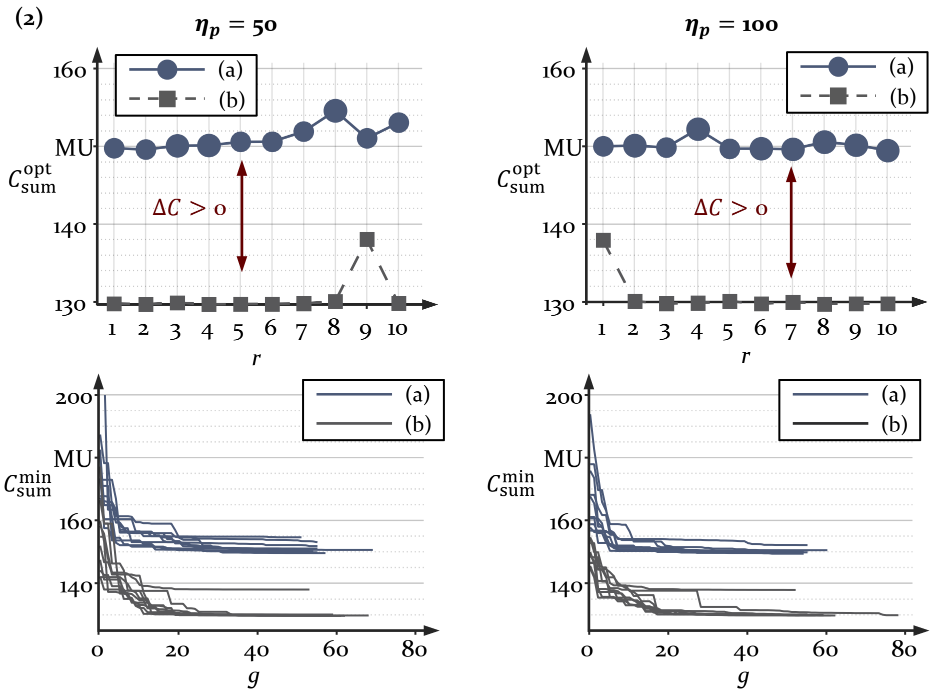

Figure 36: Optimization results for concurrent machine/supplier selection using (a) minimum-cost curve approach vs. (b) mixed-integer optimization: study (2) $\rho_{i,j} = var$.

To explain the difference in optima, Fig. 37 picks out the best results for both approaches and breaks down the total costs $C_{\text{sum}}^{\text{opt}}$ into its individual cost shares $C_{i,j}$ for the optimally selected alternatives $x_{i,j}^{\text{opt}}$. It reveals that the optimizer has preferred supplier 3 with higher costs $C_{2,3}$ to realize part 2 over $C_{2,4}$, but the additional costs are amortized by lower costs for all other parts achieved by wider tolerances. Hence, it can be useful to admit higher single costs for one tolerance, as the better, more problem-tailored part quality resulting from both the optimally chosen tolerance value and the part tolerance probability offers freedom to widen the other tolerances (and/or select other machine/supplier combinations). Using the minimum-cost curve approach (a), the selection is, however, always made part-wise in a least-cost manner, so some sections of the cost curves are always discarded and not considered at all (see Fig. 34). In this example, $C_{2,4}$ is, thus, always preferred over $C_{2,3}$ acc. to Eq. (34) since $C_{2,4} < C_{2,3}$. However, it consequences tighter tolerances for the other parts and, thus, higher individual and total costs (see Tbl. 24 and Tbl. 28). Although the complexity of the optimization problem increases by the higher dimensions of the search space (in this case $\dim_{(a)} = 5$ and $\dim_{(b)} = 10$), mixed-integer variables and the additional set of constraints (see Eq. (36)), alternative selection by optimization (b) leads to the global cost optimum. If the alternatives only differ in their costs, as it is considered for study (1) and typically done for more approximate approaches such as RSS, a choice on minimum costs separate for each part or in sum leads to the same results, so both approaches lead to the global optimum.

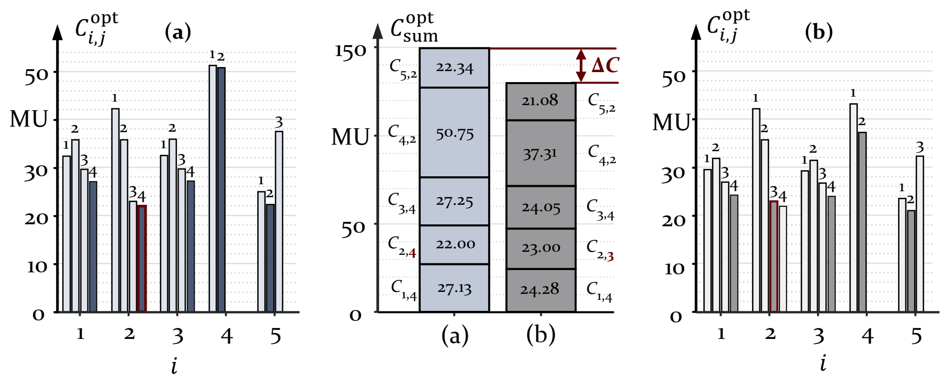

Figure 37: Comparison of the costs for the best runs of machine/supplier selection using (a) minimum-cost curve approach vs. (b) mixed-integer optimization: study (2) $\rho_{i,j} = var$.

The proposed extension of sampling-based tolerance-cost optimization to machine/supplier selection offers the possibility to consider given manufacturing conditions through part tolerance distributions. If the alternatives differ in their achievable distributions, mixed-integer optimization *should be preferred over the minimum-cost curve approach to find the global cost optima. However, it leads to higher search space dimensions, additional constraints, and mixed-integer variables.*

5.2 Multiple machine/supplier selection

In addition to the primary task of finding the least-cost tolerance values, the extensions for sampling-based tolerance-cost optimization introduced in Sec. 5.1 enable the concurrent selection of machines and suppliers. However, as mathematically defined in Eq. (30) and Eq. (34), only one single machine/supplier is allowed to be chosen to produce the entire batch. Although this simplification may often be satisfactory in the tolerance design phase, the probability distribution-based mapping of the individual machine/supplier characteristics also entails the potential to further expand the alternative selection to multiple machines with distributed manufacturing and suppliers. Sec. 5.2.1 introduces the idea and implementation of concurrent tolerance and machine allocation for random assembly.[2] Afterwards, Sec. 5.2.2 expands it on aspects for selective assembly. As in Sec. 5.1, each part is assumed to contribute only with one tolerance value to the assembly response and the associated total product quality.

5.2.1 Machine/supplier allocation and random assembly

Problem statement In the context of series production, which is characterized by vast quantities and makes tolerance-cost optimization profitable through economies of scale, a distribution of the entire production volume over several machines is quite common. If it can be assumed that the part tolerance distributions are equal for the respective machines or suppliers, the previously proposed method can be suitably extended by aspects of process scheduling. This includes additional objectives and constraints, for instance, to address machine capacities, overhead, machining and idle times, product demands, and delivery times during optimization (see Sec. 2.2.4). Integrating these aspects would affect the definition and solution of the optimization problem presented in Eq. (27)–(31). The subroutine of tolerance analysis, however, stays the same. An allocation of an entire batch on alternatives considering same part tolerance values $t_{i,j} = t_i$ or distributions $\rho_{i,j} = \rho_i \; \forall \, j = 1, \cdots, J_i$ does, from the simulation point of view, not influence the virtual manufacturing and assembly steps within tolerance analysis.

[2] The term *machine allocation* is used in this thesis to allocate an entire manufacturing batch on multiple machines/suppliers with individual machine loads or batch sizes by optimization.

However, suppose the various selected machines/suppliers differ significantly in their part tolerance distributions (a), their allocated tolerance values, or both (b). In that case, it must be appropriately represented in optimization and tolerance analysis. The subsequent detailed investigations of the problem and its methodical solution continue the thoughts presented in [P15]. For this purpose, Fig. 38 picks up the example from Fig. 33 and extends it to the outlined problem for case (b).

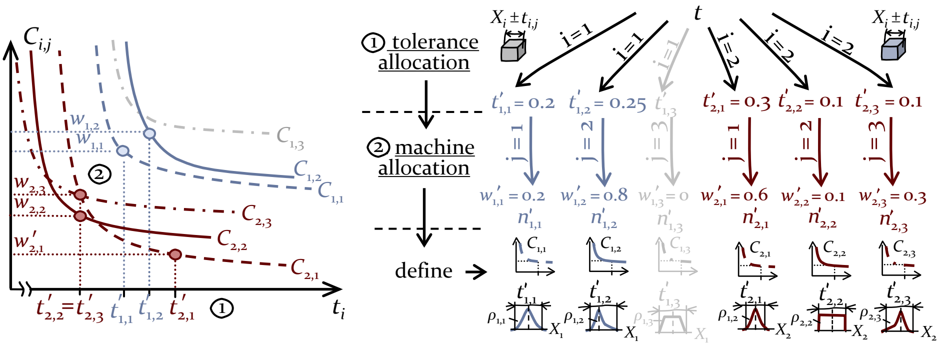

Figure 38: General idea of machine allocation with variable machine loads $w_{i,j}$.

Compared to machine selection, a weight factor $w_{i,j}$ replaces the selection parameter $x_{i,j}$. It indicates the percentage of the entire batch to be realized by machine j with $t_{i,j}$ and $\rho_{i,j}$. Hence, the optimization problem of Eq. (27)–(31) expands to a concurrent allocation problem for both tolerances and machines:

$$\text{Min} \quad C_{\text{sum}}(\boldsymbol{t},\boldsymbol{w}) = \textstyle\sum_{i=1}^{I}\sum_{j=1}^{J_i} w_{i,j}\cdot C_{i,j}\left(t_{i,j},w_{i,j}\right), \tag{37}$$

$$\text{s. t.:} \quad \hat{z}(\boldsymbol{t},\boldsymbol{w}) = 1 - yld(\boldsymbol{t},\boldsymbol{w},\boldsymbol{USL},\boldsymbol{LSL}) \leq z_{\max}, \tag{38}$$

$$\textstyle\sum_{j=1}^{J_i} w_{i,j} = 1, \tag{39}$$

$$w_{i,j}\begin{cases} > 0 & \text{if machine is allocated with } n_{i,j}, \\ = 0 & \text{if machine is not allocated,} \end{cases} \tag{40}$$

$$w_{i,j}^{\text{lb}} \leq w_{i,j} \leq w_{i,j}^{\text{ub}} \quad \forall i = 1,\ldots,I;\ \forall j = 1,\ldots,J_i \ \wedge\ \forall\, w_{i,j} \neq 0, \tag{41}$$

$$t_{ij}^{\text{lb}} \leq t_{i,j} \leq t_{i,j}^{\text{ub}} \quad \forall i = 1,\ldots,I;\ \forall j = 1,\ldots,J_i \ \wedge\ \forall\, w_{i,j} \neq 0, \tag{42}$$

where Eq. (39)–(40) denotes the allocation of at least one up to J_i machines. The case $w_{i,j} = 0$ leaves the option open to omitting a machine or supplier, whereby the chosen tolerance $t_{i,j}$ becomes irrelevant for both tolerance-cost and tolerance analysis (see, for instance, machine $j = 3$ for part $i = 1$ in Fig. 38). Therefore, the batch sizes $n_{i,j}$, varying over the optimization process, are given by $n_{i,j} = w_{i,j}\cdot n_{\text{tot}}$, $n_{i,j} \in \mathbb{N}_0$. The total batch size n_{tot} is equal to the sample size n in tolerance analysis and results in $n_{\text{tot}} = \sum_{j=1}^{J_i} n_{i,j}$. Optional capacity constraints in Eq. (41) can further ensure that alternatives from and only up to a certain threshold $w_{i,j}^{\text{lb}}$ and $w_{i,j}^{\text{ub}}$ may be selected. On the one hand, this facilitates the mapping of manufacturing process-relevant aspects and opens up possibilities for process scheduling. On the other hand, it avoids that low values that are not economically viable due to high shortage surcharges or setup costs are assigned for a machine or supplier. The cumulative tolerance-related costs C_{sum} in Eq. (37) can be approximated by the sum of the individual costs $C_{i,j}$, where $C_{i,j}$ could further be a function over $w_{i,j}$ to represent costs arising from distributed manufacturing/supply. However, following the general focus of the thesis, the tolerance-cost modeling for machine allocation is not investigated in more detail. $C_{i,j}$ is thus considered only as a function of $t_{i,j}$ and constant over $w_{i,j}$.

Theoretical solution For the same reasons that apply to single machine/supplier selection, it is reasonable to prefer a concurrent overall optimization approach over nesting a second, search- or optimization-based subroutine into the tolerance-cost optimization workflow. The tolerance allocation task is now changing since each alternative can be allocated by an individual value (see Fig. 38) in case (b). Hence, the design vector $\boldsymbol{v}_t$ needs to be extended to J_i entries, where the lower and upper bounds for the design variables correspond to the process limits $t_{i,j}^{\text{lb}}$,$t_{i,j}^{\text{ub}}$, directly satisfying Eq. (42). For case (a) with $t_{i,j} = t_i$, $\boldsymbol{v}_t$ remains the same. The boundaries are defined by Eq. (35) and additional constraints similar to Eq. (36) are required since the relations between the allocated machine/suppliers and their capabilities get lost.

The design variables for machine/supplier allocation $\boldsymbol{v}_w$ include an entry $v_{w_{i,j}}$ for each part i and each machine/supplier option j, $\{ v_{w_{i,j}} \in \mathbb{R}_0 \mid v_{w_{i,j}} \in [0;1] \}$, so that $v_{w_{i,j}}$ can be chosen continuously between 0 and 1 and a mixed-integer problem arises only when discrete tolerance values are considered. Since the weights $w_{i,j}$ are interrelated (see Eq. (40)) but have to be chosen independently by the optimizer, the values for machine/supplier allocation variable $w_{i,j}$ have to be calculated by weighting $v_{w_{i,j}}$ over all J_i entries in $\boldsymbol{v}_{w_i}$ for part i:

$$w_{i,j} = \frac{v_{w_{i,j}}}{\sum_{j=1}^{J_i} v_{w_{i,j}}}. \tag{43}$$

Additional linear inequality constraints $\sum_{j=1}^{J_i} v_{w_{i,j}} > 0$ assure that at least one machine is allocated (see Eq. (39)) and avoids a dividing by zero in Eq. (43). The capacity constraints from Eq. (41) for each part i are transformed into linear inequality constraints completing the required set of constraints:

$$\underbrace{\begin{bmatrix} w_{i,1}^{\text{lb}} \\ \vdots \\ w_{i,J_i}^{\text{lb}} \end{bmatrix}}_{\boldsymbol{w}_i^{\text{lb}}} \odot \underbrace{\begin{bmatrix} \text{sgn}(w_{i,j}) \\ \vdots \\ \text{sgn}(w_{i,J_i}) \end{bmatrix}}_{\text{sgn}(\boldsymbol{w}_i)} \leq \underbrace{\begin{bmatrix} w_{i,1} \\ \vdots \\ w_{i,J_i} \end{bmatrix}}_{\boldsymbol{w}_i} \odot \underbrace{\begin{bmatrix} \text{sgn}(w_{i,j}) \\ \vdots \\ \text{sgn}(w_{i,J_i}) \end{bmatrix}}_{\text{sgn}(\boldsymbol{w}_i)} \leq \underbrace{\begin{bmatrix} w_{i,1}^{\text{ub}} \\ \vdots \\ w_{i,J_i}^{\text{ub}} \end{bmatrix}}_{\boldsymbol{w}_i^{\text{ub}}} \odot \underbrace{\begin{bmatrix} \text{sgn}(w_{i,j}) \\ \vdots \\ \text{sgn}(w_{i,J_i}) \end{bmatrix}}_{\text{sgn}(\boldsymbol{w}_i)}, \quad (44)$$

where $\text{sgn}(w_{i,j})$ serves as activation function for all constraints with $w_{i,j} \neq 0$.

Besides the suggested extensions in optimization, tolerance analysis must allow for the total sample set to consist of the subsets of the allocated machine/suppliers with its current batch size $n_{i,j}$. Fig. 39 exemplifies that $n_{i,j}$ virtual parts are first generated batch-wise for the respective pdfs $\rho_{i,j}$, and $t'_{i,j}$, second merged into an entire batch, and third shuffled to preserve randomness. This excludes the use of a LHS or QMCS and requires an MCS since allocating the individual samples to each other is not purely random. Hence, it must be evaluated first completely and second in the same association (see Appx. A.4 for more information). The subsequent tolerance evaluation and nc-rate estimation steps stay the same.

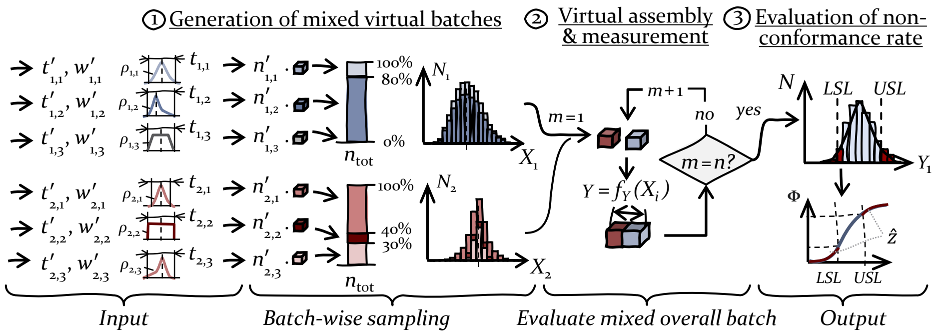

Figure 39: Subroutine of tolerance analysis with individual batch sizes $n_{i,j}$ and part tolerance distributions $\rho_{i,j}$ illustrated for the example shown in Fig. 38 and a single assembly response Y.

Practical transfer and findings To study its applicability, the proposed method is now applied to the use case of the wheel mounting assembly from the previous section. Therefore, the example is transferred to an illustrative scenario where an optimal allocation of multiple machines constrained by individual upper machine-specific capacity limits $w_{i,j}^{\text{ub}}$ is searched for. All tolerance-cost and further information is summarized in Tbl. 29. An equal MCS with $n = 100{,}000$ is used for all $\eta_r = 10$ repetitions (O-2/S-3 acc. to Tbl. 6) and both studied cases, viz. (a) $t_{i,j} = t_i$ and (b) $t_{i,j} = var$. Not only due to address both assembly responses properly, ecdf acc. to Eq. (23)–(26)

is chosen for nc-rate estimation. But also, because the variable weights $w_{i,j}$ and the tolerance values $t_{i,j}$ in combination with the alternative-specific distributions $\rho_{i,j}$ may lead to a dynamic change in the distribution type of the mixed batches X_i and consequently of Y within the optimization process, making a parametric nc-rate estimation complicated. While the settings chosen for optimization with GA are given in Appx. A.9.2, Tbl. 30–32 contain all information on the optimization results. Fig. 40 (top) overviews the obtained cost optima $C_{\text{sum}}^{\text{opt}}$ with its nc-rates $\hat{z}_{\text{asm}}^{\text{opt}}$ for all optimization runs.

It can be seen that all runs lead to feasible and acceptable results, satisfying the defined maximum nc-rate of z_{max} as well as the defined machine process and capacity limits. The latter can be seen in Fig. 40 (bottom), where the optimal values for the tolerances $t_{i,j}^{\text{opt}}$ and weights $w_{i,j}^{\text{opt}}$ are shown for the best runs. All tolerance values are within the predefined lower and upper boundaries $t_{i,j}^{\text{lb}}$ and $t_{i,j}^{\text{ub}}$ and the chosen machine loads do not exceed the individual limits $w_{i,j}^{\text{ub}}$ (see settings given in Tbl. 29). The more extensive scattering of the cost optima compared to the previous studies indicate that the complexity of the optimization problem has increased due to the higher number of variables and constraints. The additional consideration of an individual tolerance per machine in case (b) further leads to a higher dimensionality of the problem, increased by $J_i - 1$ per part i, which is reflected in the larger spread of the results in comparison to (a). Adapting the algorithm-specific optimization settings to the complexity of the problem, which increases with the number of tolerances, machines/suppliers, and their restrictions in capacity and capabilities, can reduce the scatter of the different results and increase the probability of finding the global optimum.

Apart from the effect on the performance of the optimization, the results show that the allocation of an individual tolerance $t_{i,j} = var$ for each machine enables an individual widening to exploit the nc-rate limit fully and consequently leads to lower overall costs in case (b). However, it has to be mentioned that the solutions found by optimization must also be technically implementable in series production. Nonetheless, the proposed method offers a methodical basis for representing multiple machine selection in tolerance-cost optimization using the sampling-based tolerance analysis. The results prove its applicability and offer the potential for extension by further aspects from process planning and to be examined for its application in an industrial context. Finally, to clarify the idea of mixed batches simplified sketched in Fig. 39, Fig. 41 shows an enhanced version of the $w_{i,j}$-heatmap for the best run of case (b) with the individual sampled frequency distributions and the resulting mixed overall batches.

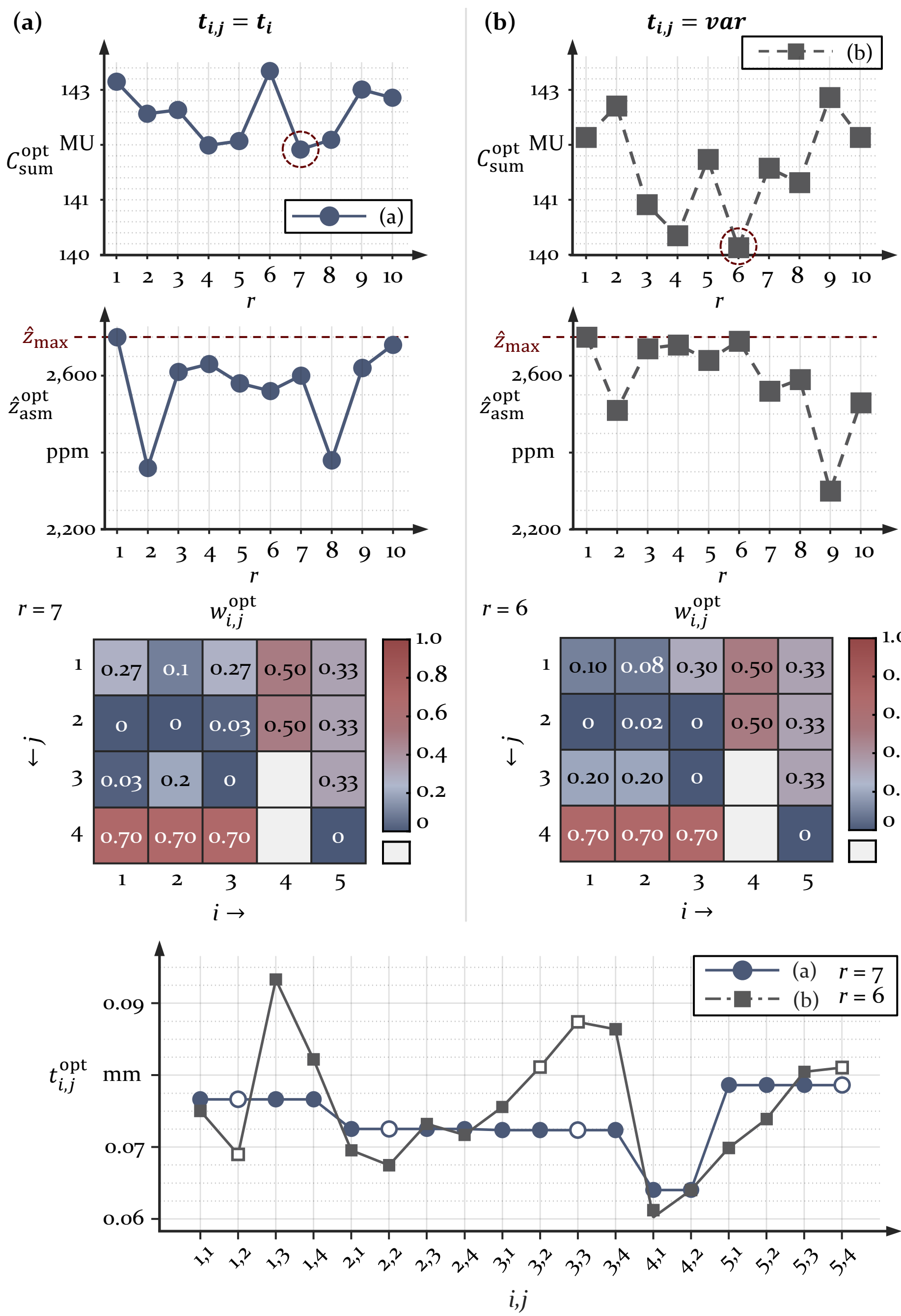

Figure 40: Overview of obtained cost optima $C_{\text{sum}}^{\text{opt}}$, corresponding nc-rates $\hat{z}_{\text{asm}}^{\text{opt}}$ for concurrent tolerance and machine/supplier allocation with variables batch sizes and random assembly (top) and details on the final weights $w_{i,j}^{\text{opt}}$ and tolerances $t_{i,j}^{\text{opt}}$ of the best runs (bottom). (a) same tolerance value for all machines vs. (b) individual tolerance values for each machine.

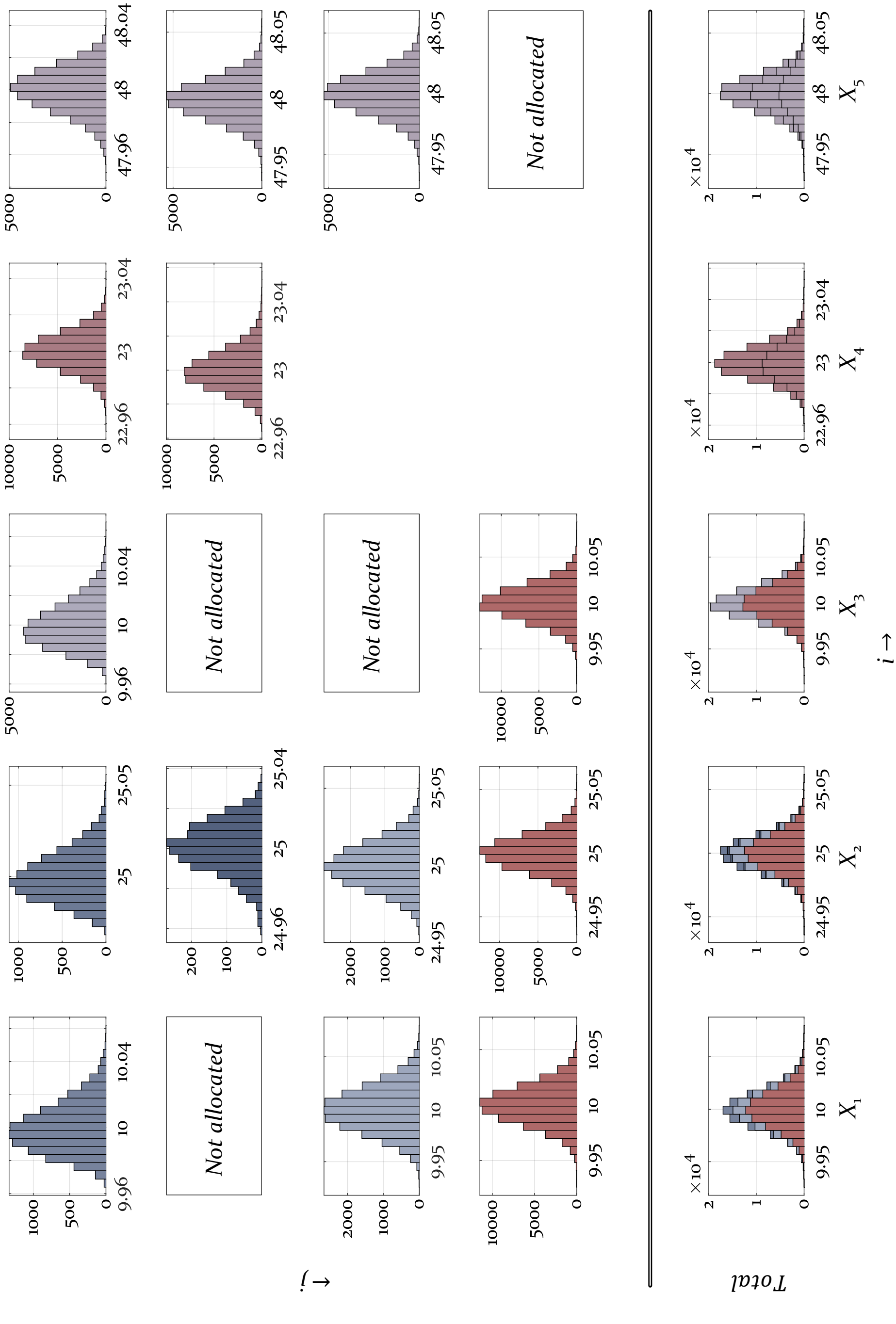

Figure 41: Visualization of the optimal batch sizes and tolerance values for the best run of case (b) through individual part characteristic histograms and resultant mixed batches.

5.2.2 Machine/supplier allocation and selective assembly

In the previous section, the primary focus was on representing distributed part fabrication in sampling-based tolerance-cost optimization. For this purpose, random assembly, which is predominant in practical use, was represented by forming a randomly shuffled entire batch from the virtually generated individual batches and randomly selecting the parts for assembly (see Fig. 39). However, the potentials of the proposed machine/supplier allocation method with variable batch sizes can further be exploited for selective assembly, first studied in [S4], second published in [P12], and presented in the following.

Problem statement Due to the different weights of the individual machines, the entire sample set is already divided into several classes, which correspond to the respective assumed distribution $\rho_{i,j}$ and the current tolerance values $t_{i,j}$ (see Fig. 39). Instead of discarding this pre-classification by forming an entire mixed batch, the resulting classes are now used for selective assembly. In contrast to traditional selective assembly applications, in which all components are measured in advance and then divided into their classes by distinct strategies (see 2.2.4), the binning step has already been done by machine/supplier allocation. A subsequent optimal assignment of the individual bins, which are then interchangeably assembled, aims to reduce the nc-rate $\hat{z}$ compared to a pure random assembly. In tolerance-cost optimization, this gives additional room to widen the individual tolerance values and/or adjust the machine/supplier allocation, further reducing the tolerance-related costs C_{sum}. However, the resulting cost savings must amortize additional costs caused by the additional selective assembly steps, such as warehousing or logistics. In the following, they are assumed to be constant over the tolerances, machine weights, and sorting. Therefore, they are not represented in the tolerance-cost model but must always be set in relation to the optimal costs for random assembly.

To represent the selective assembly by simulation, the subroutine of tolerance analysis from Fig. 39 has to be adapted. The individual batches are now paired with each other concerning a selected combination $\boldsymbol{c}_j$, and the individual assembly response functions Y_{k,c_j} are then determined by random assembly within their combination (see Fig. 42).

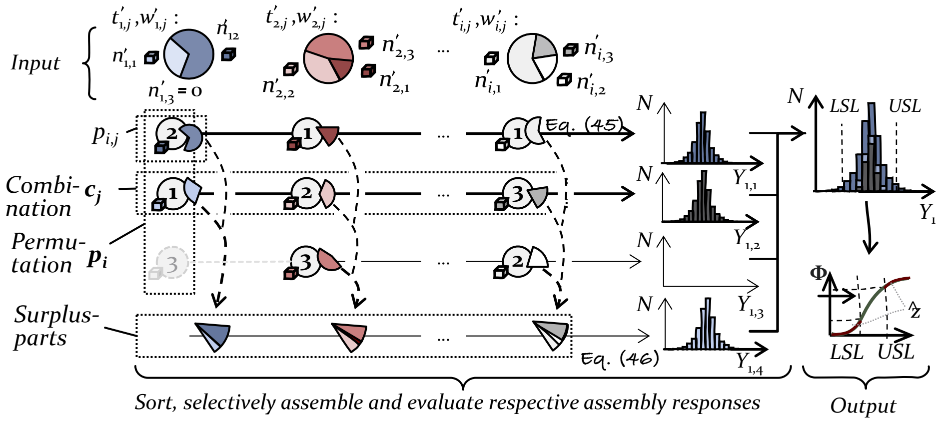

Figure 42: Subroutine of tolerance analysis with individual batch sizes $n_{i,j}$ and selective assembly illustrated for one single assembly response Y_1.

The bin with the smallest number of parts in each combination $\boldsymbol{c}_j$ dominates the number of achievable assemblies:

$$n_{j,\min} = \min\left(n_{1,p_{1,j}}, \ldots, n_{I-1,p_{I-1,j}}, n_{I,p_{I,j}}\right). \tag{45}$$

Since the bins are typically unequal in size due to the varying machine/supplier weights above optimization, so-called surplus parts are left over in each combination $\boldsymbol{c}_j$:

$$n_{\text{surplus}} = \sum_{j=1}^{J_i} n_{j,\text{surplus}} = \sum_{j=1}^{J_i}\left(n_{i,p_{i,j}} - n_{j,\min}\right), \tag{46}$$

whereby the different number of machines/suppliers will lead to comparatively large imbalances. Usually, a smart binning strategy minimizes the surplus parts and, thus, avoids unpaired parts and rejects. This approach randomly assembles all leftover parts at the end (see Fig. 42). This completes the total batch size n_{tot} and the sample size n in simulation:

$$n = n_{\text{tot}} = \sum_{j=1}^{J_i} n_{j,\min} + n_{\text{surplus}}, \tag{47}$$

resulting in the frequency distribution for Y_k from the individual assembly responses Y_{k,c_j} and $Y_{k,\text{surplus}}$.

The minimum number of machines $J_{\min} = \min(J_1, \ldots, J_{I-1}, J_I)$ dictates the number N_c of different combinations $\boldsymbol{c}$:

$$N_c = \underbrace{\frac{1}{J_{\min}!}}_{\text{(III)}} \cdot \underbrace{\prod_{i=1}^{I} \frac{J_i!}{\underbrace{(J_i - J_{\min})!}_{\text{(II)}}}}_{\text{(I)}}. \tag{48}$$

Fig. 43 illustrates Eq. (48) using a simple example. The number of all possible combinations is the full factorial permutation of all single permutations $\boldsymbol{p}_i$, which results from swapping single elements $p_{i,j}$ within a part-column (I) corresponding to a J_i-permutation without repetition. However, the different number of bins results in identical solutions (II), since all combinations above $c_{j>J_{\min}}$ are treated as surplus parts (see also Fig. 42). This reduces the number from $J_i!$- to $J_i^{J_{\min}}$ -permutations $\boldsymbol{p}_i$. Likewise, the sequence of the combinations c_j is irrelevant in the total (III), reducing the total number by $J_{\min}!$ to N_c.

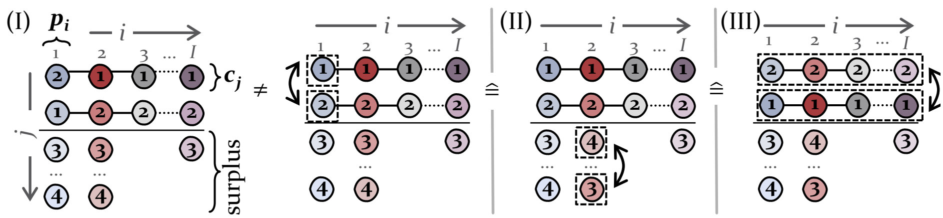

Figure 43: Simple example illustrating identical selective assembly solutions for different combinations of permutations.

Theoretical solution The concurrent optimization problem from Eq. (37)–(42) is now extended to additionally find the optimal combination among the N_c combinations. The expression of $\boldsymbol{c}$ as a combination of permutations $\boldsymbol{p}_i$ is suitable for this purpose. Common algorithms can be used to generate the $J_i^{J_{\min}}$-permutations, whereby an associated index *idx* indicates the particular permutation $\boldsymbol{p}_i$. For instance, the *idx*-th permutation of part 1 shown in Fig. 43 is given as follows:

$idx \rightarrow$	1	2	3	4	5	6	7	8	9	10	11	12
j	1 2	1 3	1 4	2 1	2 3	2 4	3 1	3 2	3 4	4 1	4 2	4 3

Thus, an additional design vector $\boldsymbol{v}_p$ can be defined with a set of integer design variables $\left\{v_{p_i} \in \mathbb{N} \mid v_{p_i} \in \left[1; J_i^{J_{\min}}\right]\right\}$ to represent the respective index *idx*, which leads in combination with $\boldsymbol{v}_t$ and $\boldsymbol{v}_w$ to a mixed-integer optimization problem.[3] The nc-constraint in Eq. (38) is, thus, additionally a function of the permutations $\boldsymbol{p}$.

Practical transfer and findings In line with the previous chapters, the developed method is once again applied to the example of the wheel mounting assembly. The tolerance-cost data and part tolerance distributions are listed in Tbl. 33. To evaluate the proposed method, two different scenarios are considered, viz. study (1) with predefined weights $w_{i,j} = 1/J_i$, equally distributed among all available machines, and study (2) with variable weights, where optimal binning is done indirectly by machine/supplier allocation. For comparison, both studies are performed for random assembly (a) and selective assembly (b). GA is used again for mixed-integer optimization; the settings are given in Appx. A.9.2. Fig. 44 (top) shows the optimization results of the 10-fold repeated optimization runs ($\eta_r = 10$) based on the same MCS with $n = 10{,}000$ (O-2/S-3 acc. to Tbl. 6). Fig. 44 (bottom) illustrates the optimally identified combinations out of $N_C = 1296$ options by the optimizer for the best runs.

All optimization runs have succeeded in satisfying all acceptability and feasibility constraints (see also Tbl. 34–35, Tbl. 37–38). In line with the previous section's findings, adding the design vector $\boldsymbol{v}_p$ to identify the best combinations for selective assembly further complicates the optimization problem. This leads to the scattering of the optimization optima $C_{\text{sum}}^{\text{opt}}$, which is higher for case (2) due to the additional task of finding optimal weights for all machines (see Fig. 44 (top)). It is apparent that the random assembly approach (a) leads to higher manufacturing costs than the proposed selective assembly approach (b) for both studies, while the resultant nc-rates $\hat{z}_{\text{asm}}^{\text{opt}}$ reach the acceptable nc-rate thresholds of $z_{\max} = 2{,}700$ ppm. The difference in optima can be explained by having a look at the nc-rates $\hat{z}_{\text{asm}}^{\text{opt}}$ (b*) when the tolerance values optimally obtained for selective assembly (b) are repeated for random assembly after optimization. It illustrates that the total non-conformance rates are significantly lower through selective assembly without tightening the tolerances. Hence, this leads to the aforementioned additional room for the optimization algorithm to further widen the individual part tolerances (see Tbl. 36, Tbl. 39).

---

[3] Using the proposed approach, each combination in the real also has only one parameter combination assigned to in optimization. If evolutionary algorithms are used, this is referred to as phenotype-genotype mapping, which has already shown its potential for optimal selective assembly in [582].

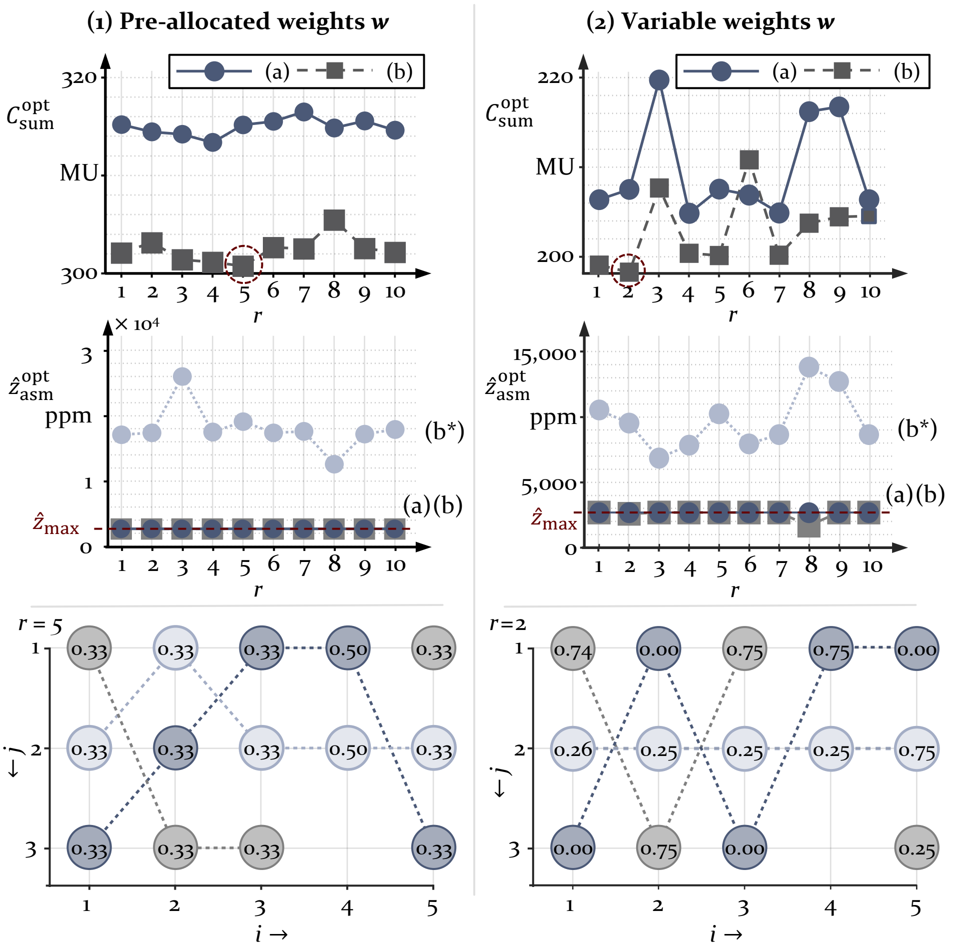

Figure 44: Results for concurrent tolerance and machine/supplier allocation with selective assembly: cost optima $C_{\text{sum}}^{\text{opt}}$, corresponding nc-rates $\hat{z}_{\text{asm}}^{\text{opt}}$ (top) and details on the final batch combinations of the best runs (bottom); (a): random assembly, (b): selective assembly.

The studies exemplify its applicability with pre-allocated machines/suppliers and as an overall optimization of the machine loads and their batch-wise pairing. Different routines such as an additional splitting of the individual machine batches can help to increase assembly efficiency. At this point, it becomes apparent that the method has been able to demonstrate its general potential, but at the same time offers a variety of possible applications as well as a need for further scientific investigations and answers to questions about technical feasibility and profitability in practice. Hence, it provides a methodological basis for extending sampling-based tolerance-cost optimization from series production with interchangeability to batch production with selective assembly. It can also be useful for dynamic tolerance allocation approaches applied in ramp-up or production phases.

> *Sampling-based tolerance analysis enables the extension of single machine/supplier selection to multiple machine/supplier selection with individual batch sizes. The proposed methods are helpful for a concurrent consideration of optimal tolerance and machine allocation for random and selective assembly revealing hidden cost potentials and serving as a general basis that can be tailored to given manufacturing situations.*

5.3 Coping with multiple part tolerances in optimization

So far, the proposed methods are limited to assemblies consisting of parts with just one tolerance each. In the following, they are extended to multiple, geometrical part tolerances based on the first findings reported in [S3].

Problem statement In practice, multiple part features and their variations determine the probabilistic assembly behavior. Hence, a set of geometrical tolerances are needed to limit them for all functional relevant features, influencing the optimal tolerance allocation procedure on different levels (see Fig. 45):

- **At feature level**, it is common to specify multiple tolerances for one feature u to control its size, location, orientation, and form (a). The conformance of the tolerance specification to the referenced tolerancing standards, either the ASME-Y14.5 or the GPS-ISO standards, is already assured in the tolerance specification. Nonetheless, suppose the envelope principle is applied (either as default by rule #1 in the ASME-Y14.5 [50] or by specifying the relevant features by the Envelope Requirement Symbol Ⓔ acc. to the ISO 8015 [583]). In that case, the independency of the multiple tolerance values is repealed and has to be represented properly in the optimization problem.
- **At part level**, identical features are used in part design when intended to have the same function (b). Same tolerances with the same tolerance values are, thus, helpful to reduce the tolerance-related costs by holding the setup costs for fabrication and inspection low [127].
- **At assembly level**, the multiple use of parts of the same quality is a common practice to reduce product complexity and costs (c). In doing so, an identical tolerance specification for all multiple parts is reasonable.

Besides the influence of the effects on the tolerance allocation itself, it also affects the tasks of machine/process selection and allocation and their implementation in optimization. In tolerance allocation for manufacturing as

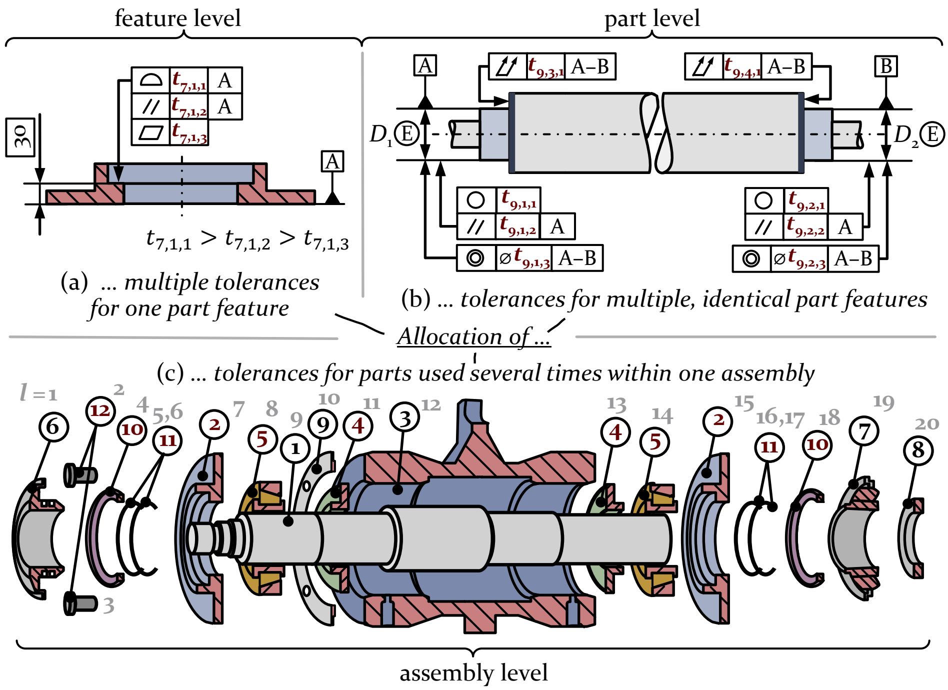

Figure 45: Multiple tolerances per part and feature influencing the definition and solution of the tolerance allocation optimization problem.

well as concurrent tolerance allocation (see Sec. 2.2.4), the individual manufacturing operations, including the definition of the manufacturing datums, selection of tools, process parameters to reach the individual manufacturing tolerances for each process step, are defined and tailored to each other in detail. In sum, this leads to the part features with their assigned design tolerances. A thorough modeling of numerous correlations and interrelations is inevitable [584, 585]. Its complexity, scope, and lack of information in the design stage make a detailed and complete process design extremely difficult. Thus, these aspects are often considered in a highly simplified manner, in which design tolerances are defined from the assembly functionality point of view as requirements for the subsequent part fabrication, and just a preselection of machine or supplier alternatives is made. As a compromise, alternative selection can be approximated as the selection of one predefined total set of manufacturing process combination alternatives with a set of part tolerance probabilities $\boldsymbol{\rho}$ for the final design tolerances $\boldsymbol{t}$. Therefore, the focus of the selection parameter $x_{i,j}$ changes from tolerance to part level $x_{l,i}$ to select an alternative j from J_l alternatives for each part l. Consequently, the objective function from Eq. (27) modifies to:

$$C_{\text{sum}}(\boldsymbol{t}, \boldsymbol{x}) = \sum_{l=1}^{L} \sum_{j=1}^{J_l} \sum_{u=1}^{U_l} \sum_{i=1}^{I_{u_l}} C_{l,u,i,j}\left(t_{l,u,i}\right) \cdot x_{l,j}, \tag{49}$$

with the individual tolerance-related manufacturing costs $C_{l,u,i,j}$ for realizing the tolerance $t_{l,u,i}$ assigned to the i-th tolerance of the u-th feature of the l-th part realized by the j-th machine/supplier alternatives combination.

From a pure methodological point of view, the methods for machine/supplier allocation from Sec. 5.2 can also be extended in the same way to multiple and geometrical tolerances. From a practical point of view, however, a strong simplification of the various manufacturing aspects does not allow a meaningful, comparatively detailed specification of part manufacturing and assembly aspects, such as the scheduling or allocation of machines. Although the methods from Sec. 5.2 offer potential for dynamic tolerance allocation in ramp-up or serial production and can also be extended in a process-oriented manner, the subsequent discussion is limited to tolerance allocation with alternative selection based on mixed-integer optimization in the design phase (see Sec. 5.1).

Theoretical solution – feature level (a) Assigning multiple tolerances to one feature u is to individually refine the tolerances by additional location, orientation, or form tolerances [50]. For instance, the profile tolerance $t_{7,1,1}$, assigned to part $l = 7$ shown in Fig. 45 (a), limits the location primarily but encloses the restriction of parallelism and flatness of the planar feature $u = 1$ of the cover. Since the control of the form of a feature might already be established through an orientation, runout, or profile tolerance [50], the value of the form tolerance cannot be freely chosen. Otherwise, it violates the virtual condition as a collective effect of all variations at their maximum limits [50]. For instance, the additional parallelism $t_{7,1,2}$ and flatness tolerance $t_{7,1,3}$ impose tighter requirements on the orientation and form. Their values must be chosen smaller than the profile tolerance value (and also the parallelism tolerance): $t_{7,1,1} > t_{7,1,2} > t_{7,1,3}$. Consequently, the tolerance values are dependent and cannot be chosen freely by the optimizer. Complying with the GD&T rules and the envelope principle for size tolerances within tolerance-cost optimization, an additional set of linear inequality constraints must be added for each feature u if multiple tolerances $I_{u_l} > 1$ are assigned to it.

For a correlated tolerance tuple $\langle t_{l,u,\bar{i}}, t_{l,u,i}\rangle$, it applies:

$$t_{l,u,\bar{i}} < \lambda \cdot t_{l,u,i}, \quad i \neq \bar{i}, \tag{50}$$

$$\lambda = \begin{cases} 0.5 & \text{if } t_{l,u,i} \text{ is a size tolerance,} \\ 1 & \text{otherwise.} \end{cases} \tag{51}$$

The number of tuples and required constraints depend on the number and type of tolerances specified.

Theoretical solution – part level (b) To treat all identical part features equally in optimization, all tuples of identical features have first to be identified and second be consolidated in a quadratic feature equality matrix $\boldsymbol{A}_{\text{eq}}$ for each part:

$$\boldsymbol{A}_{\text{eq}} = \begin{bmatrix} a_{1,1} & a_{1,2} & \cdots & a_{1,U} \\ a_{2,1} & a_{2,2} & \cdots & a_{2,U} \\ \vdots & \vdots & \ddots & \dots \\ a_{U,1} & a_{U,2} & \cdots & a_{U,U} \end{bmatrix} = \left(a_{u,\overline{u}}\right)_{u=1,\cdots,U;\overline{u}=1,\cdots U} \tag{52}$$

$$\text{where } a_{u,\overline{u}} = a_{\overline{u},u} = \begin{cases} 1 & \text{if feature } u \text{ and } \overline{u} \text{ are identical,} \\ 0 & \text{otherwise.} \end{cases} \tag{53}$$

Using this information, the tolerance values for identical features of one part can then mathematically be defined as follows:

$$t_{\overline{u},i} = t_{u,i} \quad \text{if} \quad a_{u,\overline{u}} = 1 \quad \forall\, u, \overline{u} = 1, \dots, U; \forall i = 1, \dots, I_{u_l}; u \neq \overline{u}. \tag{54}$$

To handle this case for all considered parts in optimization, additional linear equality constraints could be added for all tolerances. However, due to lower dimensions and less constrained design spaces, a **design dimension reduction** method is preferred in this thesis. In doing so, the design variables are reduced to a minimum before the optimization, where some of them are used as shared variables for all identical feature tolerances. Its basic principle is shown in Fig. 46 (left) for the shaft $l = 9$ using a gene string representation. Four design variables are sufficient to define all eight tolerances. Therefore, $\boldsymbol{A}_{\text{eq}}$ is used in each iteration to expand the reduced design vector to the total number of tolerances as an inverse operation of the dimension reduction. In general (and at least approximately in this thesis), it can then be assumed that, besides the equal costs, the variations of the same features with the same setup result in similar frequency distributions. Hence, the same part tolerance probability distributions can be considered for tolerance analysis. For the sampling, different uniform random numbers X' for all characteristics (see Sec. 4.1) have to be generated to avoid unrealistic correlations of the simulated variations.

Theoretical solution – assembly level (c) Similar to the idea of the feature equality matrix acc. to Eq. (52)–(53) in case (b), the definition of a part equality matrix $\boldsymbol{B}_{\text{eq}} = \left(b_{l,\bar{l}}\right)_{l=1,\cdots,L;\bar{l}=1,\cdots L}$ can be used to mathematically describe case (c) allocating equal tolerances for all multiple used parts:

$$t_{\bar{l},u,i} = t_{l,u,i} \text{ if } \quad b_{l,\bar{l}} = 1 \forall\ l,\bar{l} = 1,\cdots,L;\ u_l = 1\ldots,U_l; i = 1,\ldots,I_{u_l}; l \neq \bar{l}, \tag{55}$$

$$\text{with } b_{l,\bar{l}} = b_{\bar{l},l} = \begin{cases} 1 & \text{if part } l \text{ and } \bar{l} \text{ are identical,} \\ 0 & \text{otherwise.} \end{cases} \tag{56}$$

From a cost point of view, it is further reasonable to choose the same alternatives for all identical parts:

$$x_{\bar{l},j} = x_{l,j} \quad \text{if } b_{l,\bar{l}} = 1 \forall\ \bar{l} = 1,\cdots,L; j = 1\ldots,J_l; \quad l \neq \bar{l}, \tag{57}$$

which further leads to the same tolerance-related costs per part. In line with case (b), the same part tolerance distributions can be assumed for the identical parts. By transferring the idea of dimension reduction from part to assembly level with $\boldsymbol{B}_{\text{eq}}$, a minimum design vector $\boldsymbol{v}$ uniquely describes the tolerance and alternative selection for identical parts. Fig. 46 (right) illustrates an intermediate solution for the covers $l = 7, 15$.

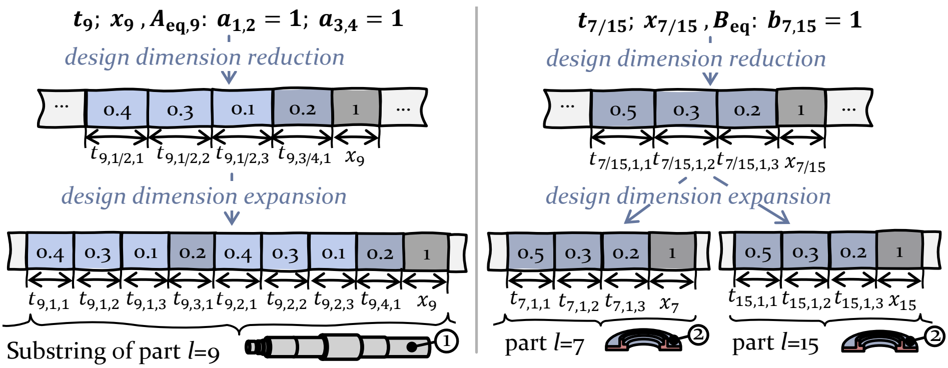

Figure 46: Handling tolerance allocation and alternative selection with multiple identical part features (left) and parts in an assembly (right) by design dimension reduction illustrated by the examples from Fig. 45.

Practical transfer and findings The proposed method is now exemplarily applied to the wheel mounting assembly example from the previous sections (see Fig. 47). It is extended to a 3D problem with multiple geometrical tolerances, including several correlated tolerances to be allocated. Both supports, part 1 and 3, are considered as equal parts $b_{1,3} = 1$ (see Eq. (85)).

Multiple feature tolerances are specified for all parts requiring additional linear inequality constraints following Eq. (50)–(51). For instance, the cylindrical feature $u = 3$ of the shaft $l = 5$ is covered by two GD&T constraints:

$$t_{5,3,2} < 0.5 \cdot t_{5,3,3}, \tag{58}$$

$$t_{5,3,2} < t_{5,3,1}. \tag{59}$$

In total, eight constraints are needed, which are summarized in Eq. (86). For the parts $l = 1, 3, 5$ two alternatives $J_l = 2$ are considered to realize them.

Moreover, the size tolerances $t_{1,3,2}, t_{3,3,2}, t_{4,4,1}, t_{5,3,3}$ and $t_{5,4,1}$ are prefixed before optimization forming the respective clearance between the shafts and holes. This leads to a reduction from 27 tolerances to 18 – decreased by four prefixed size tolerances and five equally defined tolerances for part $l = 1, 3$ by the proposed dimension reduction method. Besides, the design vector $\boldsymbol{v}$ for optimization includes two entries for the alternative selection for parts $l = 1, 3$ and $l = 5$. All information on the tolerance-cost model, its freely chosen cost coefficients, tolerance boundaries, and the individual part tolerance probability distributions are summarized in Tbl. 40. The example is described in more detail in Appx. A.8.1.

TCVisVA is used as an MCS-based tolerance analysis tool and embedded as a black box into the optimization workflow for iterative nc-rate evaluation. In case of a violation of the feasibility constraints on feature level case (a), tolerance analysis is skipped and the solution is directly penalized. More details on using TCVisVA as tolerance analysis subroutine in batch mode for optimization, including optimal alternative selection, are given in Appx. A.6. The optimization is repeated $\eta_r = 10$ times. Using the same random seed when recalling TCVisVA with $n = 10{,}000$ inside the optimization loop enables the realization of the equal random numbers strategy presented in Sec. 4.1 (O-2/S-3 acc. to Tbl. 6).

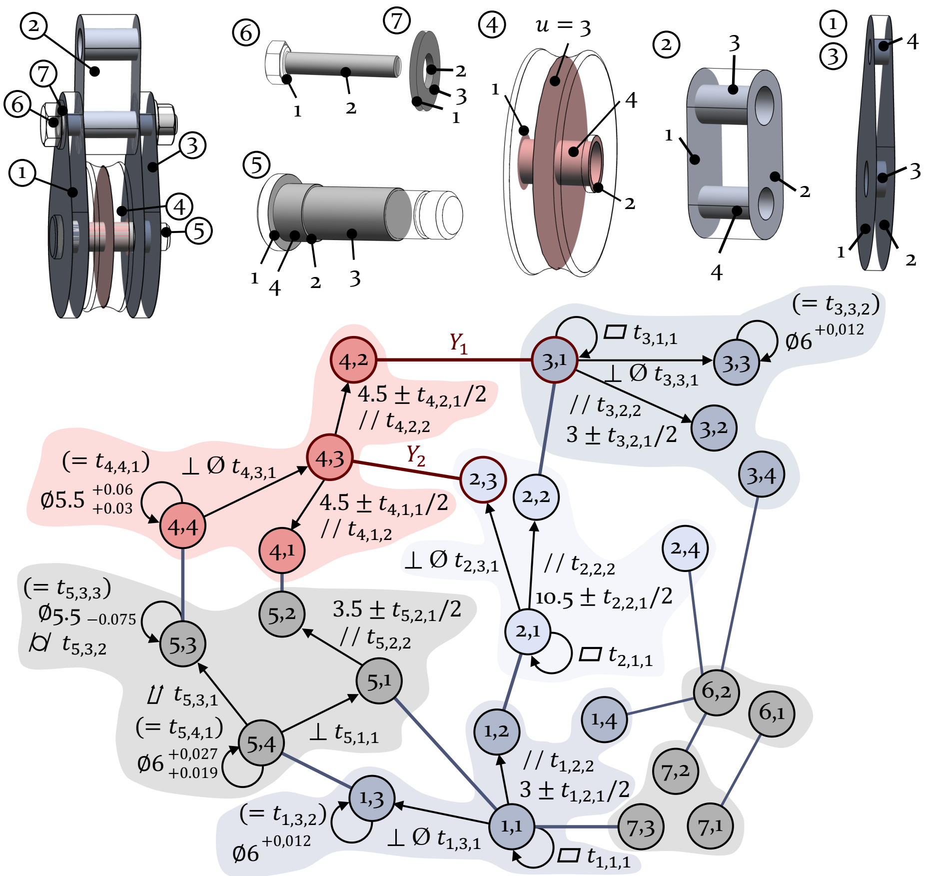

Figure 47: Overview of the extended wheel mounting assembly example in 3D: parts with its features (top), assembly structure, and tolerance specification visualized as graph (bottom). The part tolerance specifications are further detailed in Fig. 91. Explanations on the graph notation are given in Fig. 96.

The optimization results using mixed-integer GA (all settings are given in Sec. A.9.2) are presented in Fig. 48. The details are summarized in Tbl. 41–43.

Seven of the ten optimization runs were successful in satisfying all constraints, viz. the nc-rate limits (see Fig. 48 (right)), the individual part tolerance limits for each tolerance as well as the additional constraints to represent the GD&T rules. The validity of the results is exemplarily illustrated for the best run in Fig. 49. The dimension reduction assures that all tolerances and alternatives were chosen equally for part $l = 1, 3$, which can directly be seen when comparing the individual values for $t_{l,u,i}^{\text{opt}}$ as well as $x_{l,j}^{\text{opt}}$ given in Tbl. 43. As a result, this leads to the same cost shares $C_{l,u,i}^{\text{opt}}$ for $l = 1, 3$. To

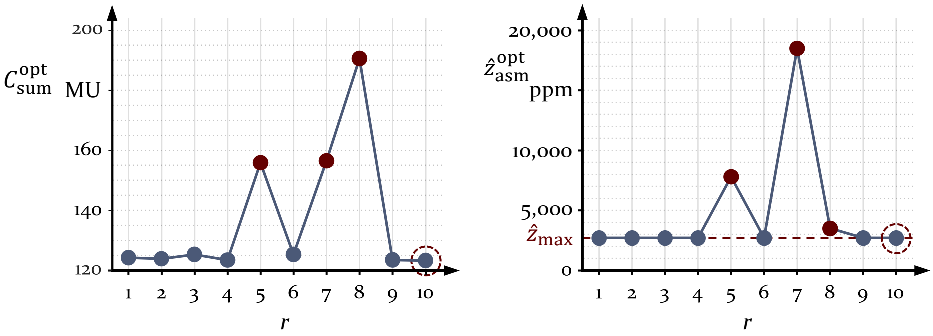

Figure 48: Overview of the optimization results for the wheel mounting assembly example with multiple geometrical tolerances.

sum it up, the example emphasized that the proposed method first helps to systematically structure the optimization problem by breaking it down into assembly, part, and feature levels. Second, using equality matrices and inequality constraints is helpful to directly integrate the tolerancing knowledge and logic in the optimization problem. In combination with metaheuristic optimization, standard proprietary tolerance analysis software tools can directly be embedded as black boxes. However, this is at the expense of the efficiency of the optimization. The average computing time for all feasible solutions $\overline{\tau}_{\text{feas}}$ is mainly dominated by the time effort necessary for the iterative call of TCVisVA with the updated tolerance values and the import of the resultant quality information Y serving as the basis for the subsequent nc-rate evaluation. For the comparatively low sample size of $n = 10{,}000$, one feasible optimization run already took 16.5 h on average (Tbl. 42).

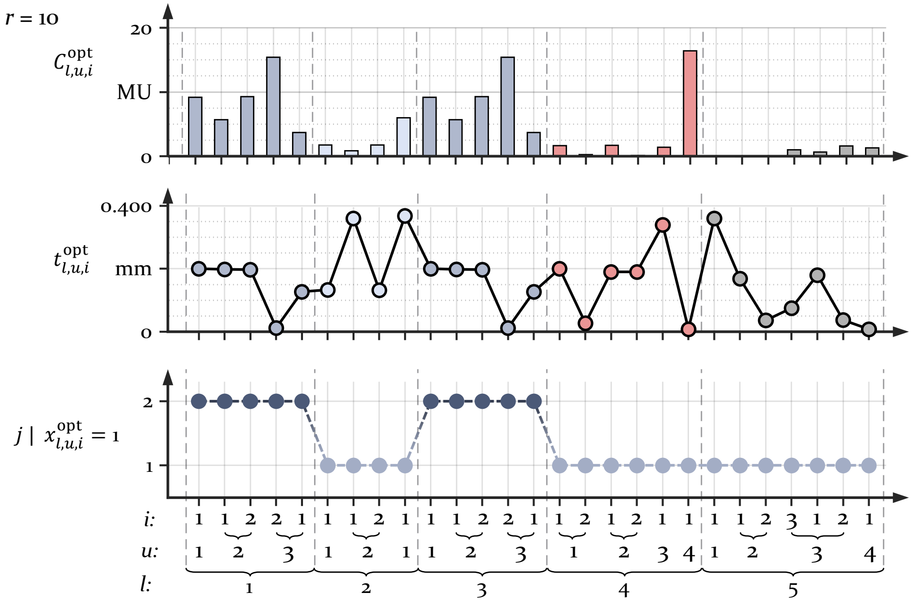

Figure 49: Details on the best run with achieving minimum cost $C^{\text{opt}}_{\text{sum}}$: individual cost shares $C^{\text{opt}}_{l,u,i}$, optimally allocated tolerances $t^{\text{opt}}_{l,u,i}$ for the wheel mounting assembly example.

> *Multiple tolerances per feature and part lead to correlated design variables. Additional inequality constraints and design dimension reduction methods help to assure reliable and technical proper tolerance allocation and alternative selection results. In addition, it enables the direct embedding of proprietary tolerance analysis software in the optimization workflow such as TCVisVA.*

6 Improving the efficiency of sampling-based tolerance-cost optimization

In general, product development has benefited significantly from the steady increase in computing performance (see Fig. 11 (bottom)), which gave the efficiency of simulation- and optimization-based methods a massive boost. In compliance with the ISO 9241-11, the efficiency is defined as the "*sources expended in relation to the accuracy and completeness in which users achieve goals*" [565] and also referred to as an essential measure to evaluate the optimization performance [586]. In the following, it is studied as the third key element of the usability of tolerance-cost optimization.

The fundament of an efficient optimization routine is a thoughtful choice of programming language and code implementation in combination with high computing performances and advanced programming subroutines, such as parallel and GPU-computing [130, S2]. Besides, however, the time effort to repetitively evaluate the constraints and objective functions until the algorithm converges mainly influences the **efficiency** and, thus, the final calculation time required. As [P2, P10] conclude, the computation time for one feasible tolerance-cost optimization run τ_{feas} mainly depends on the repetitive application of tolerance analysis within the optimization loops (see Fig. 12). In contrast, the computation time for the tolerance-cost analysis is negligible. In simplified terms, the tolerance analysis-related share of the total optimization time τ_{sum} can be estimated by

$$\tau_{\text{sum}} \approx \overbrace{\eta_p \cdot \eta_g}^{\text{optimization}} \cdot \overbrace{(\tau_{\text{samp}} + n \cdot \tau_Y + \tau_{\hat{z}})}^{\text{tolerance analysis}}, \tag{60}$$

with the population size η_p, number of generations η_g, the time for the sampling τ_{samp}, the time for the evaluation of all assembly response functions τ_Y and the time for the nc-rate estimation $\tau_{\hat{z}}$.[1] Fig. 50 visualizes the interrelations given in Eq. (60) using a small optimization study as an example (see Appx. A.9.3 for more details). The chance to find the global optimum can be increased with high numbers of generations η_g and sample size n (see Fig. 50 (left)). It gives the optimizer more trials to explore the whole design and intensify the best solutions while avoiding large margins of error and scattering effects in the acceptability constraints (see Sec. 4.1). However, the

[1] Eq. (60) assumes an iterative resampling in each optimization step, under the assumption of one tolerance analysis per individual per optimization step. In the case of reusing the same set of random numbers, the time for the sampling has only to be invested once before optimization (see Sec. 4.1).

optimization time needed increases significantly. The share of the subroutine of sampling-based tolerance analysis in the average total computing time confirms its main contribution (see Fig. 50 (right)).

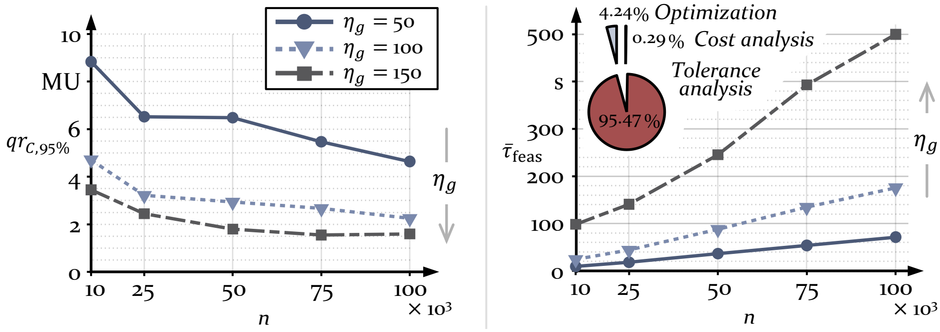

Figure 50: Illustration of the main contributors to the scattering of cost optima expressed by the 95%-quantile range $qr_{C,95\%}$ and average total computation time $\bar{\tau}_{\text{feas}}$ of sampling-based tolerance-cost optimization illustrated for an exemplary study of the wheel mounting assembly.

Following Eq. (60), τ_{sum} can, on the one hand, be decreased by **scaling the total number of optimization iterations down** through a robust optimization problem definition, efficient algorithms, thoughtfully chosen settings for the population size η_p as well as the settings and termination criteria influencing the total number of generations η_g finally needed.[2] On the other hand, it is purposeful to **reduce the total time effort for the sampling-based tolerance-analysis** through fast sampling techniques and nc-rate estimation techniques, low sample sizes n, and time-efficient models for evaluating the multiple assembly responses f_{Y_k}.[3]

The choice of sampling technique and the nc-rate estimation have already been examined in Chap. 4, with a primary focus on their effectiveness, but it secondary included the aspect of computation times due to their direct interdependence. The following sections will present advanced sampling methods and surrogate model-assisted optimization routines to increase the efficiency of sampling-based tolerance-cost optimization.

[2] Finding an optimal set of algorithm-specific tuning parameters is critical in metaheuristic optimization. General rules and results from prior, similar optimizations are a useful starting point for a manual adaption or optimization of the hyperparameters. Despite its importance, this thesis does not study the influence of optimization settings in detail since it is always specific for a given optimization problem.

[3] In the given study, the time effort to evaluate the explicitly defined assembly response functions is comparatively low. Besides the findings from literature (see Sec. 2.2.2), the examples shown in [P11, P14, S9] and in Sec. 5.3 emphasize that the computational effort and the computation times can significantly increase up to several days for one optimization run.

6.1 Adaptive sample sizes

Motivated by the proof of benefits in literature [134, 408] and an initial implementation in [S6], the subsequent discussion focuses on the concept of adaptive, over the optimization variable sample sizes. It studies their potential for increasing the efficiency of sampling-based tolerance-cost optimization by scaling down the sample size n (see Fig. 50).

Problem statement One of the main subjects of the studies in Chap. 4 is the correlation of the accuracy of tolerance analysis and, thus, of tolerance-cost optimization, and the sample size n. Aiming to assure the accuracy of the final nc-rate predicted for the optimal tolerance values, the number of samples n must be consciously chosen with respect to the achievable accuracy before optimization. Consequently, it is used for each repetitive tolerance analysis step. For the general case of an optimization iteration with one tolerance analysis per individual, the total number of function evaluations for each assembly response function then approximately corresponds to:

$$\eta_F = \eta_p \cdot \eta_g \cdot n. \tag{61}$$

A constantly high number of function evaluations is needed in each generation, significantly slowing down the optimization and being a major limiting factor for its efficiency.

Theoretical solution Although the sample size n for the generation g in which the optimization converges must be fixed for achieving reliable results, not all the numerous nc-constraint evaluations must necessarily be performed with the same accuracy while searching for the optimum. The basic idea of adaptive sample sizes is to start with a smaller sample size $n_{\min}$ and to successively increase it over the optimization up to the last generation G to $n_{\max}$. The increase of $\tilde{n}$ over the generations g, $\{\tilde{n} \in \mathbb{N} \mid n_{\min} \leq \tilde{n} \leq n_{\max}\}$ can be defined by the fitting function f_n, for example a tanh-function with two free shape parameters ξ_1 and ξ_2, as presented in [134], as follows:

$$\tilde{n} = f_n(g) = n_{\min} + (n_{\max} - n_{\min}) \cdot 0.5 \cdot \{1 + \tanh\left[\xi_1 \cdot (g/G - \xi_2)\right]\}. \tag{62}$$

When applying Eq. (62), however, it must be ensured that $n_{\max}$ is reached at the end and prevented that the algorithm terminates already prematurely after $n(g) < n_{\max}$ generations. This can be the case if a termination criterion, besides the maximum number of generations η_g, is assigned and reached, for example, if no improvement could be found in $\eta_{g,\text{stall}}$ generations, the so-called stall generations. A suitable remedy is to extend Eq. (62) to a piecewise function:

$$\tilde{n} = \begin{cases} f_n(g) & \text{for } g \in \left[1; \eta_{g,\text{stall}}\right], \\ n_{\max} & \text{for } g > \eta_{g,\text{stall}}, \end{cases} \tag{63}$$

where $G = \eta_{g,\text{stall}}$ is defined in $f_n(g)$ acc. to Eq. (62). The interrelations of Eq. (63) are shown for three sample size curves in Fig. 51 (left).

In doing so, the iterative improvement of the solutions by trial-and-error mechanisms of metaheuristic optimization algorithms is exploited. In early generations, a lower "precision of the fitness" [134] is sufficient to identify promising hot spots by predominant exploration steps since, despite larger uncertainty, it allows for evaluating poor solutions as not being nearly in the region of optimum or not being acceptable exceeding the nc-rate by far. In later stages, the algorithm has already been able to identify the potential areas with the aid of information from the previous generations. When intensifying the current best solutions through exploitation becomes more in focus and convergence approaches, higher sample sizes are required to exclude a negative impact on the optimization process through large sampling-induced uncertainties. Fig. 51 (right) exemplarily illustrates the decrease of the margin of error $\epsilon_{P=0.5}$ with gradually increasing sample size $\tilde{n}$.

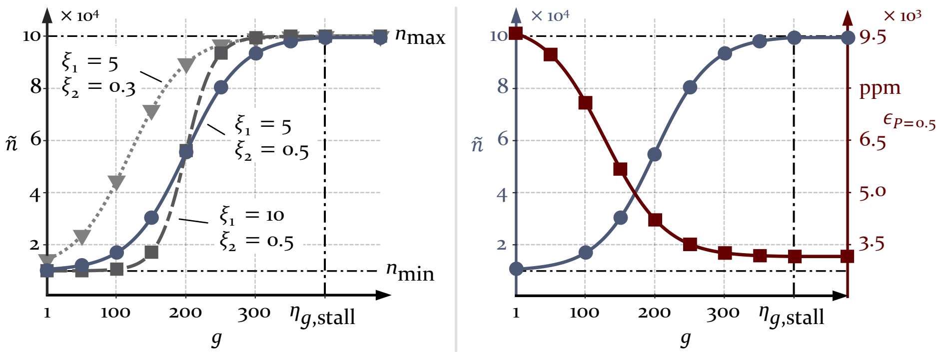

Figure 51: General idea of adaptive sample sizes for tolerance-cost optimization: three examples of adaptive sample curves following Eq. (62) (left). Decrease of the margin of error of nc-evaluation $\epsilon_{P=0.5}$ (i.e., $z = 5 \cdot 10^5$ ppm) over g estimated by Eq. (11) for $\alpha = 0.05$ (right).

The tuning of ξ_1, ξ_2 and $n_{\min}$ to the algorithm-specific optimization settings, chosen with respect to the given problem complexity, is decisive for optimization success with a significantly lower number of function evaluations. While a too-early increase of n leaves efficiency potential unused, a too-late increase can cause the total optimization to take longer in total since it gets lost in the search space due to over-and underestimations of the constraints.

To mitigate the latter effect, it might also be helpful to **recalculate a number of the most promising solutions** of the current generation $\{n_r \in \mathbb{N}_0 \mid n_r \in [0; \eta_p]\}$. Hence, r_p is defined as the ratio of recalculations $r_p = \frac{n_r}{\eta_p}$. Since the optima typically lie near or on the nc-rate constraint surface due to the trade-off between cost and quality, the n_r individuals with a minimum absolute offset to the maximum nc-limit $\delta_z = |\hat{z} - z_{\text{max}}|$ are the most relevant ones, influencing the ranking of the elitist solutions surviving and shaping the next generation. The recalculation of these solutions with n_{max} aims to avoid under- and overestimates, leading to solutions being incorrectly evaluated as acceptable or unacceptable. The general idea of this extension is shown in Fig. 52 (left).

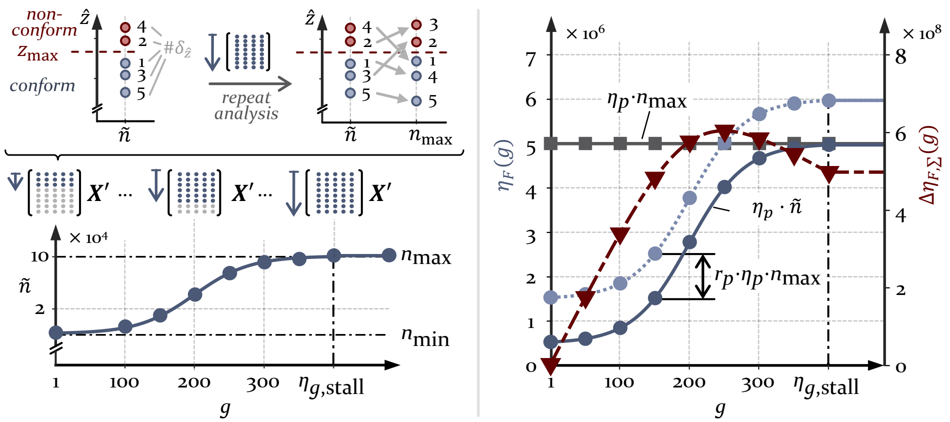

Figure 52: Basic principle of adaptive sample sizes with recalculation of most promising solutions and equal random numbers (left). Number of function evaluations $\eta_F(g)$ illustrated for a constant sample size $\eta_p \cdot n_{\text{max}}$, an adaptive sample size $\eta_p \cdot \tilde{n}$, and its raise by additional recalculations $r_p \cdot \eta_p \cdot n_{\text{max}}$ and cumulated difference $\Delta\eta_{F,\Sigma}$ acc. to Eq. (64) (right).

Lastly, it makes sense to include the strategy of equal random numbers presented in Sec. 4.1 to mitigate the scattering of the intermediate nc-estimation results due to different samplings. MCS is valid for this purpose, as it offers the possibility for only a partial evaluation or the addition of new random numbers. As exemplified in Fig. 52 (left), an initially generated set of n_{max} uniform random variates $\boldsymbol{X}'$ can serve as an overall set to be evaluated only for the first $\tilde{n}$ random numbers in the respective generation g. In contrast, the individual samples within LHS and QMCS are aligned with each other, requiring the evaluation of all samples and complicating subsequent expansion without sophisticated methods and effort. In contrast to these variance reduction methods from Sec. 4.1, the method of adaptive sample sizes is more universally applicable for non-code-based tolerance analysis software. The sample size can usually be controlled externally via commands in addition to the current tolerance values and part tolerance probability distributions. Using TCVisVA, for instance, an identical random seed, as already proposed in Sec. 5.3, used in all optimization steps further supports the elimination of the sampling-induced scattering and discontinuity effects (see Appx. A.6).

Finally, the cumulative difference in function evaluations in the range of $[1; \eta_{g,\text{stall}}]$ can be roughly estimated as follows:

$$\Delta\eta_{F,\Sigma} = \sum_{g=1}^{\eta_{g,\text{stall}}} \left\{n_{\max} - \left[\left(\tilde{n}(g) + r_p(g) \cdot n_{\max}\right]\right\} \cdot \eta_p \quad (64)$$

and multiplies for multiple, separately evaluated assembly response functions (see Fig. 52 (right)). However, the exact number of function evaluations depends on the geometrical behavior model and the structure of the optimization algorithm used.

Practical transfer and findings To prove the theoretically discussed potential of adaptive sample sizes for sampling-based tolerance-cost optimization, the method is exemplarily applied to the 3D wheel mounting assembly example presented in Sec. 5.3. For simplicity, alternative selection is neglected in the following and all tolerances are considered normally distributed (see the summary of tolerance-cost data in Tbl. 45). The CS algorithm, in its basic form described in Appx. A.3.2, is adapted for handling the variable input of adaptive sample sizes as a function of the current generation g and to repeat the n_r promising individuals in each iteration.

The subsequent studies aim to:

1. study the influence of the shape parameters of f_n on the results,
2. investigate the benefit/impact of recalculating the n_r relevant individuals by comparing the results to the ones gained by adaptive sample sizes without repeated analysis.

Therefore, in study (1), the tolerance-cost optimization for $n_{\min} = 5{,}000$ and $n_{\max} = 10{,}000$ is performed for $\xi_1 = 7$ and the three levels $\xi_2 = [0.3, 0.5, 0.7]$. Each of them is performed without ($r_p = 0$) and with the proposed repetition of tolerance analysis with final sample size $n = 10{,}000$ ($r_p = 0.2$, $n_r = 5$ for $\eta_p = 25$) and compared to the traditional approach with a fixed sample size. The different optimizations are repeated five times $\eta_r = 5$ with the same random numbers used for tolerance analysis in TCVisVA (O-2/S-3 acc. to Tbl. 6). Avoiding an early convergence of the optimization algorithm, the stall generation limit is set to $\eta_{g,\text{stall}} = 200$ and the maximum number of generations to $\eta_g = 250$. Consequently, there is no adaptive sample size adjustment from generation $g = 201$ on. The step to recalculate the best solutions is omitted since the final sample size $n = n_{\max}$ is reached in generation $g = \eta_{g,\text{stall}} = 200$ (see Eq. (63)). In addition to Tbl. 46–47 in the appendix, Fig. 53 and Fig. 54 contrast the main results of study (1) for the different settings. The results are sorted by ascending average computation time $\bar{\tau}_{\text{feas}}$, with all optimization runs satisfying the feasibility and acceptability constraints.

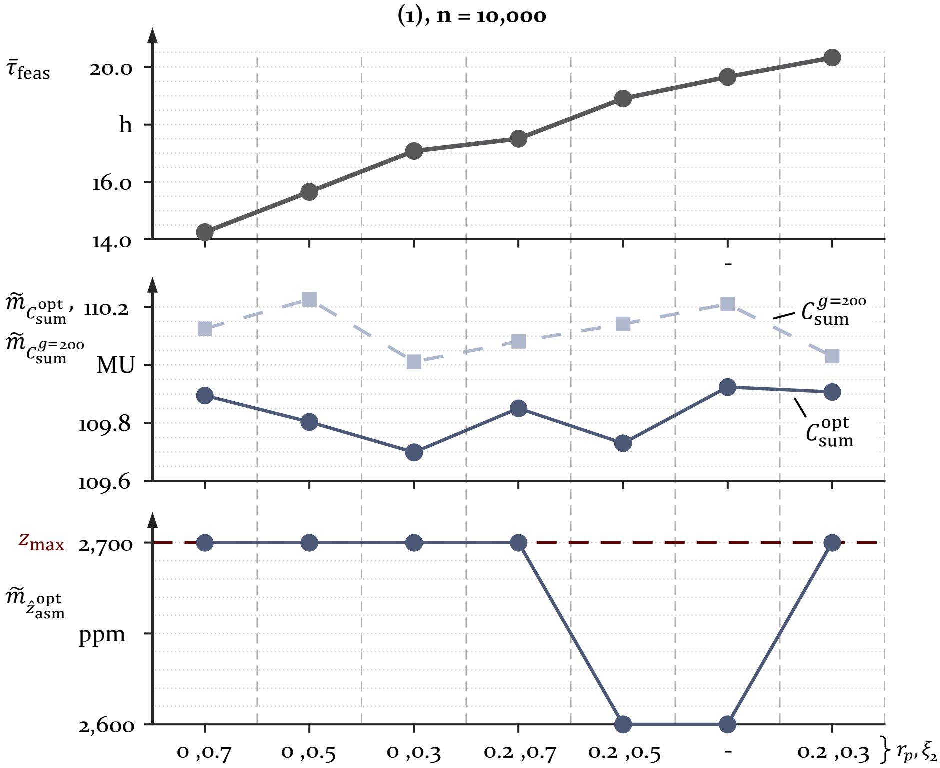

Figure 53: Optimization results with adaptive sample sizes in comparison: average computing time $\bar{\tau}_{\text{feas}}$ (top), median of the obtained intermediate and final cost optima $\tilde{m}_{C_{\text{sum}}^{g=200}}$ and $\tilde{m}_{C_{\text{sum}}^{\text{opt}}}$ (center), median of the nc-values for the obtained optima $\tilde{m}_{\hat{z}_{\text{asm}}^{\text{opt}}}$ (bottom) for study (1) with $n = n_{\max} = 10{,}000$ and different settings of ξ_2 and r_p for a dynamic sample size adaption.

All optimization runs terminated in the maximum generation $g = 250$, whereas the nc-limits were mostly fully pushed to their maximum limit of $z_{\max} = 2{,}700$ ppm (see for instance the median of the nc-rate values of all five runs for the obtained optima $\tilde{m}_{\hat{z}_{\text{asm}}^{\text{opt}}}$ in Fig. 53 (bottom)). As expected, lower

ξ_2 values, leading to a faster increase in $\tilde{n}$ (see Fig. 51), consequently lead to higher optimization times $\overline{\tau}_{\text{feas}}$. Moreover, an additional recalculation further increases the required time effort (see Fig. 53 (top)). The medians of the obtained cost optima $\tilde{m}_{C_{\text{sum}}^{\text{opt}}}$ in Fig. 53 (center) illustrate that the optima found are lower than the ones for the fixed sample size. The scattering of the results, explicitly shown in the scatter plot in Fig. 54, originates from the stochastic optimization operations since sampling-induced uncertainties were omitted beforehand by using the same random numbers. While a general trend of lower values for $r_p = 0$ with lower ξ_2 values is apparent, better results are only partly and not directly visible for all settings using the strategy of repeating the $n_r = 5$ best individuals.

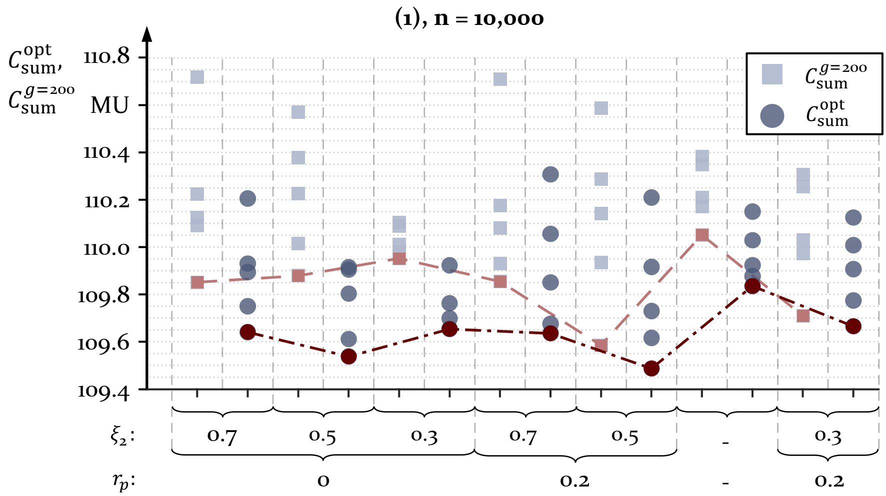

Figure 54: Optimization results with adaptive sample sizes in comparison: scattering of intermediate and final cost optima $C_{\text{sum}}^{\text{opt}}$ and $C_{\text{sum}}^{g=200}$ for study (1).

Supplementary, study (1) is now repeated in study (2) for the same settings but with $n_{\min} = 10{,}000$ and $n_{\max} = 100{,}000$. Due to the higher sample sizes, the total computation time significantly increases. For this reason, the optimization procedures are not repeated ($\eta_r = 1$). The results of all feasible runs, additionally summarized in Tbl. 48, are shown in Fig. 55. In line with study (1), the runs of the adaptive sample sizes performed at least as well as the run with the fixed sample size (see $C_{\text{sum}}^{\text{opt}}$), whereas the effect on the required computation times are strongly amplified (see τ_{feas}).

At this point, at the latest, it must be claimed that the derivation of general statements is not possible or reasonable for several reasons. First, both studies are only investigated for one set of random numbers used in tolerance

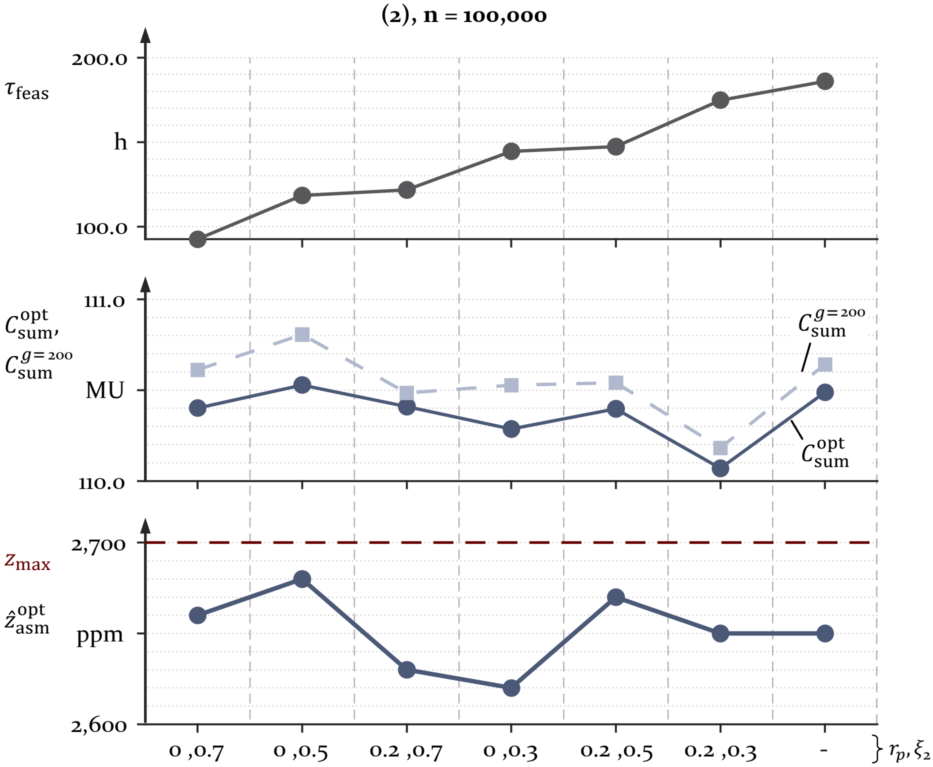

Figure 55: Optimization results with adaptive sample sizes in comparison: computing time τ_{feas} (top), intermediate and obtained cost optima $C_{\text{sum}}^{\text{opt}}$ and $C_{\text{sum}}^{g=200}$ (center), nc-values for the obtained optima $\hat{z}_{\text{asm}}^{\text{opt}}$ (bottom) for study (2) with $n = n_{\max} = 100{,}000$ and different settings of ξ_2 and r_p for dynamic sample size adaption.

analysis. Second, the chosen settings might not be valid for reaching the global optimum. On the one hand, this can be seen when comparing the optimal values with the optimal intermediate results $C_{\text{sum}}^{g=200}$ in the last generation of adaption, revealing that in the last 50 generations further improvement is made for all variants. On the other hand, the nc-rates $\hat{z}_{\text{asm}}^{\text{opt}}$ for the optima obtained in study (2) (see Fig. 55) show that there might still be some room for improvement left since the maximum limit $z_{\max}$ is not reached. Third, the comparatively low number of repetitions further makes quantitative statements difficult. At the same time, the results strongly depend on the chosen settings, the optimization problem's complexity, and the studied parameter.

Nonetheless, the studies demonstrate the benefits of the proposed method for significantly lowering the necessary computation times (up to ≈ -5 h/by $\approx -26\%$ in study (1), up to ≈ -93 h/by $\approx -50\%$ in study (2)) while achieving similar or partly better results. A fine-tuning of the parameters of f_n to the respective tolerance allocation problems can help to further exploit its potential. Moreover, an additional adaption of the ratio of recalculations r_p dynamically during optimization might be profitable and is worth to be examined, where in-depth studies on different use cases with different complexity are needed to derive general statements on the harmonization of the settings for adaptive sample sizes and algorithm-specific stochastic operations.

> *Adaptive sample sizes combined with equal random numbers can reduce the total amount of function evaluations while assuring the same accuracy of the final optimization results. The alignment of the adaptive function and the number of recalculations of the best intermediate solutions with the problem and the optimization settings is decisive to increase the chance of achieving the global optimum efficiently.*

6.2 Surrogate model-based optimization

Supporting optimization through surrogate models has gained its attention in the last years [587, 588]. In the context of optimal tolerance allocation, they primarily aim to accelerate the tolerance analysis subroutine and to overcome the deficiencies in efficiency [P16]. In the following, different strategies for using surrogate-assisted sampling-based tolerance-cost optimization, in excerpts presented in [P10, S7, S8, P18], are introduced and discussed.

Problem statement Jointly with the sample size n, the substeps for the statistical evaluation of the assembly responses, including part variations modeling and their propagation on the assembly level through the behavior model, significantly influence the total computation time (see Fig. 50). While, for instance, vector or torsor models are far less computationally demanding and optimizations can be solved in a few minutes or hours, depending on the optimization problem complexity, the previous sections illustrated that the direct integration of numerical software tools into the optimization workflow could usually only be realized with a high investment of resources or not at all in reasonable computation times.Which model fits best to represent the respective assembly behavior under variations mainly depends on the tolerance engineers' expertise. A substitution or approximation of higher-level geometrical and behavior models by lower ones can significantly reduce the required computing time τ_Y to evaluate all assembly response functions f_{Y_k} (see Eq. (60)). However, the resulting accuracy and completeness suffer simulteanously from a strong (over-)simplification of reality.

Theoretical solution Instead, **surrogate model-based optimization** approaches approximate the sufficiently accurately represented and not necessarily explicitly known models in objective and constraints [588] utilizing a "cheap-to-run" model $\tilde{f}$ [587]. An increase in efficiency is expected, as the design space can be searched and the optimum can be found much faster, "at the expense of a (hopefully slight) loss of accuracy" [589]. Traditionally, surrogate modeling and optimization are two sequential activities and fully decoupled. The substeps of data generation, fitting of a selected model to these data, and its validation are preceded by optimization [587, 588]. Besides the choice of the level at which approximation takes place in the sampling-based tolerance analysis, tailoring these pre-processing steps to the different tolerance allocation problems plays an essential role in minimizing the influence of the approximate estimates in the acceptability constraints in the optimization.

Fig. 56 supplements the branch of the sampling-based tolerance analysis from Fig. 12 by the findings on alternative selection (see Sec. 5.1) and multiple assembly response functions (see Sec. 4.3) and illustrates different possible levels of approximation.[4]

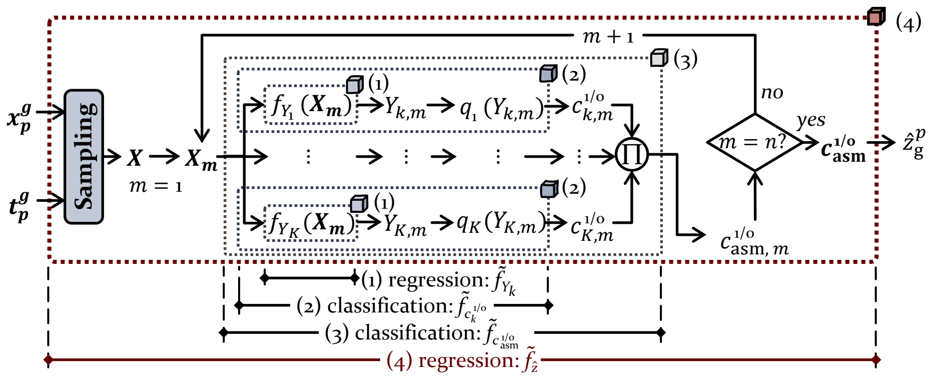

Figure 56: Different strategies of the usage of surrogate models as black box models in sampling-based tolerance-cost optimization.

Aiming to accelerate the evaluation of the nc-rate constraints, the subsequent black-boxing strategies are generally conceivable:

(1) regression model $\tilde{f}_{Y_k}$ for the k-th assembly response function f_{Y_k} to predict the assembly response $\tilde{Y}_k$ ($\widehat{=}\ \hat{y}$) for the characteristics $\boldsymbol{X}_m$ ($\widehat{=}\ x$),

[4] In addition, [P10] introduces the idea of classification surrogates to quickly predict if an assembly with the current part characteristics $\boldsymbol{X}$ can be assembled or not. For clarity, however, an additional evaluation of the assemblability by additional criteria, as formalized in Eq. (23)–(24), is neglected in the following. In line with Sec. 5.3, the subsequent discussion focuses on alternative selection, but the methods offer the possibility of extending to machine allocation.

(2) classification model $\tilde{f}_{c_k^{1/0}}$ to check the single conformance $c_k^{1/0}$ ($\widehat{=}\ \hat{y}$) of the k-th assembly response function with $\boldsymbol{X}_m$ ($\widehat{=}\ x$).
(3) classification model $\tilde{f}_{c_{\text{asm}}^{1/0}}$ to check the total conformance $c_{\text{asm}}^{1/0}$ ($\widehat{=}\ \hat{y}$) for all assembly response functions acc. to Eq. (23) with $\boldsymbol{X}_m$ ($\widehat{=}\ x$),
(4) regression model $\tilde{f}_{\hat{z}}$ ($\widehat{=}\ \hat{y}$) to substitute the total tolerance analysis and nc-rate evaluation to directly predict $\hat{z}_{\text{asm}}$ for a current set of tolerance values $\boldsymbol{t}$ and set of chosen alternatives $\boldsymbol{x}$ ($\widehat{=}\ x$),

where x and $\hat{y}$ indicate the in- and outputs and $\tilde{f}$ the surrogate model, following the fundamental equation of surrogate modeling with the approximation error e: [589]

$$\hat{y} = \tilde{f}(x) \quad \text{with} \quad y = \hat{y} + e. \tag{65}$$

Depending on the sub-steps to be substituted, the type of output differs between continuous values (1,4) and categories (2,3) and requires methods for regression (1,4) or classification (2,3). As both methods are decoupled, the data set must be created in advance, a regression model selected, its parameters chosen, and their predictive quality evaluated (see also Fig. 88 (left) in Appx. A.5). Literature (see Sec. 2.2.2) and the findings made in [P10, P18] confirm the positive effect of substituting assembly response functions or additionally the nc-rate estimation (1) and (3) on the total optimization efficiency.[5]

However, in case proprietary tolerance analysis software tools are used, the applicability of the proposed strategies is limited by the insights into the sampling routines and the outputs provided by the software [P19]. Using TCVisVA, for instance, the assembly response values $\boldsymbol{Y}$ can be exported and used for subsequent evaluation steps, but the user lacks the information about the sampled characteristics $\boldsymbol{X}_m$ values [P19]. For this reason, only strategy (4) is applicable and studied in detail in the following. The general workflow is shown in Fig. 57.

The inputs x, also called predictors, are the tolerance values and the alternatives, making the factors and boundaries for the DOE equal to those of the design variables $\boldsymbol{v}_t$ and $\boldsymbol{v}_x$ for optimization. Therefore, limiting the input variables x to the set of minimum tolerance variables resulting from the design dimension reduction method proposed in Sec. 5.3 is useful. The choice of the DOE and the number of sample points in the first step is always subject to a conflict of initial computation time to invest and the resulting prediction quality mitigated by the approximation error e. Efficient sampling

[5] Strategy (2) and (3) are only applicable for the nc-rate estimation with ecdf acc. to Eq. (17) or Eq. (23), due to its sample-wise evaluation of the (non)-conformance.

of the total design space considered in optimization is decisive. It can be achieved systematically, e.g., by (full)-factorial DOE, or randomly, e.g., by LHS, varying the individual input parameters between their lower and upper boundaries at equal intervals [589]. According to the chosen DOE, the search space of the optimization is screened and for each test point d, a tolerance analysis is performed with n samples taking the current tolerance values and the probability density functions for the current alternatives into account. The respective single nc-rate $\hat{z}$ (for $K = 1$) or more generally the total nc-rate $\hat{z}_{\text{asm}}$ (for $K > 1$) serves as output y (see Fig. 57). The data set should cover the total design space in optimization. However, when multiple tolerances are assigned to one geometrical part feature, it can include combinations of tolerances that do not conform to the GD&T inequality constraints of Eq. (50)–(51). A subsequent data cleaning step becomes necessary. While they are directly discarded and penalized by high nc-rates in optimization, as the definition is not valid and tolerance analysis does and can not be performed, these combinations are excluded from the data set. As a result, the initial data with D samples is reduced to the feasible ones D' before the step of surrogate model fitting.

Although general guidelines and metrics help to select a model type with its parameters, the final assessment of their suitability, similar to metaheuristic optimization algorithms, remains an individual decision. More simplistic regression models can further enable the use of traditional optimization algorithms, e.g., sequential quadratic programming [298]. However, they may not be sufficient to model the highly nonlinear relations between the individual in- and outputs implicitly drawn by numerical simulation. Hence, it corresponds to an iterative process to fit and validate several models preselected from the various surrogate modeling techniques developed over the last years. The model with the best fitness is chosen as the final surrogate, based on established metrics, such as *RMSE* or R^2 (see Appx. A.5).

The efficiency of the whole approach depends on the time effort for the pre-optimization steps for surrogate modeling τ_{PreOpt} and the actual optimization steps. τ_{PreOpt} depends significantly on the number of points D and, depending on the case, the downstream steps necessary to generate the required outputs y, in addition to the time to create the DOE once and the time to train the surrogate models. Due to the approximation of the total tolerance analysis routine in case (4), τ_{PreOpt} is significantly dominated by the D times repeated tolerance analysis with n samples for data generation. The nc-rate evaluation within each optimization iteration reduces to just one function evaluation with $\tilde{f}_{\hat{z}}$.

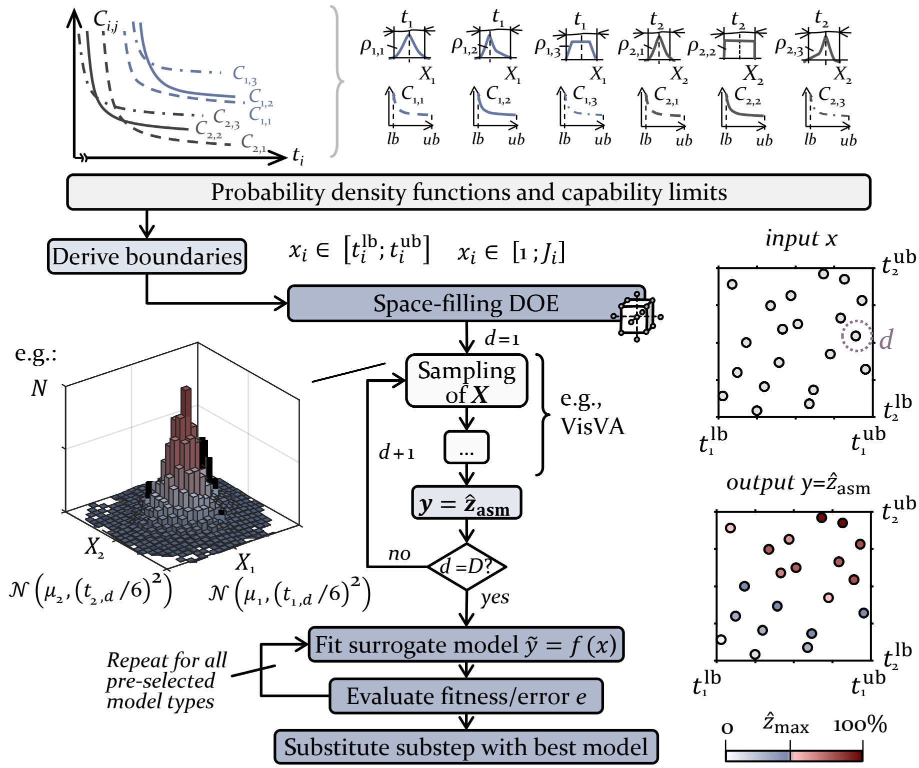

Figure 57: Workflow to generate the database for regression model as surrogate for the overall tolerance analysis (4) in line with Fig. 56.

Practical transfer and findings The average time $\overline{\tau}_{\text{feas}} \approx 19.5$ h spent on solving the wheel mounting assembly problem with $n = 10{,}000$ in Sec. 6.1 emphasized the conflict in time using TCVisVA. The same allocation problem is now used to study the potential of surrogate model-assisted tolerance-cost optimization. In doing so, five different sample sizes for data generation using LHS are studied. Since all tolerances are considered normally distributed, and alternative selection is not considered, the lower and upper tolerance boundaries define the space for the surrogate model to be covered. In line with Sec. 5.3, the minimum number of 18 decision variables define the predictors, while the corresponding nc-rates evaluated based on TCVisVA are the responses for the surrogate model training. Approximately 1/3 of the sampled tolerance combinations fulfill the GD&T constraints, leading to the reduced amount of data D' after data cleaning. For surrogate modeling, Artificial Neural Networks (ANN) are taken into account based on their best fit. A wide, single-layered ANN with rectified linear unit activation function is chosen based on the best *RMSE*-values for a 20%-hold out for splitting the data set into training and test data.[6] For all surrogate models for the five data set sizes, optimization using CS algorithm is repeated five times (O-2/S-3 acc. to Tbl. 6), where the final tolerance values are reevaluated with the real model, i.e., by using TCVisVA. The optimization results are illustrated in Fig. 58 and summarized in Tbl. 49, supplemented with more details on the study.

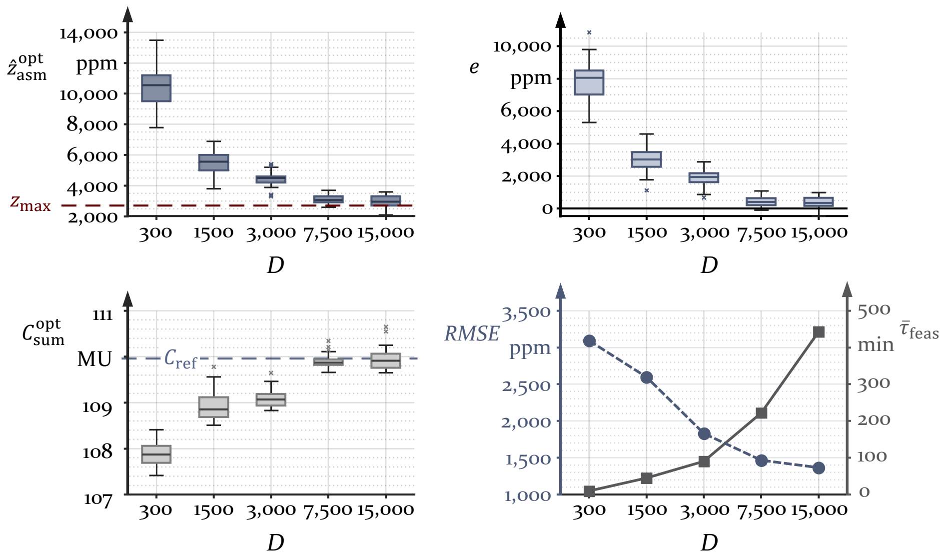

Figure 58: Optimization results for the 3D wheel mounting assembly problem using surrogate model-based tolerance-cost optimization for five different data set sizes D. Nc-rates $\hat{z}_{\mathrm{asm}}^{\mathrm{opt}}$ based on TCVisVA for optimally identified tolerances, prediction error $e = \hat{z}_{\mathrm{asm}}^{\mathrm{opt}} - \hat{z}_{\tilde{f}_{\hat{z}}}$, cost optima $C_{\mathrm{sum}}^{\mathrm{opt}}$, and prediction accuracy through *RMSE* vs. average time effort $\overline{\tau}_{\mathrm{feas}}$.

At first glance, the strong correlation between the data size for surrogate modeling and the optimization results is striking. With increasing D, the prediction error e between the real value $\hat{z}_{\mathrm{asm}}^{\mathrm{opt}}$, reevaluated for the optimally identified tolerances with TCVisVA, and $\hat{z}_{\tilde{f}_{\hat{z}}}$, obtained by the respective surrogate model, is decreasing. In line with the global aim of the optimization to identify the least-cost tolerances, the optimizer tries to find the combinations where the tolerances can be widened the most, which typically lie in regions where the surrogate model is characterized by underestimations of the nc-rate $e > 0$. This effect can be seen in the shift of $\hat{z}_{\mathrm{asm}}^{\mathrm{opt}}$ from the nc-rate limit $\hat{z}_{\max}$ and is comparable to the tendency to underestimation due to sampling-induced uncertainties, e.g., illustrated in Fig. 23, with the difference that the inaccuracy, which the optimizer specifically exploits, originates from the

[6] Refer to Appx. A.5 for more background information on surrogate modeling theory.

surrogate model. As a result, the obtained cost optima $C_{\mathrm{sum}}^{\mathrm{opt}}$ converge from below to the reference value C_{ref}, which in this case is defined as the mean of five optimization runs with TCVisVA. The curves are directly related to the surrogate model accuracy, indicated by the corresponding *RMSE*-values. A suitable trade-off between the size of the data set and the computation time for its generation is decisive for achieving a beneficial increase in efficiency with acceptable losses in results reliability. While doubling D from 7,500 to 15,000 in this example has minimal impact on e, this results in a doubling of computation time since the time effort for optimization is negligible compared to data generation (see Tbl. 49).

Consequently, the main challenge in the design of the surrogate modeling process is that it is unknown a priori where the surrogate model must be accurate or is allowed to be inaccurate. Thus, while surrogate model decisions based on a global metric such as the *RMSE* are suitable to evaluate the entire optimization design space's accuracy, it does not necessarily mean that the chosen model must also have the highest accuracy in regions of optimality.

> *Regression models as surrogates are profitable tools to speed up sampling-based tolerance-cost optimization significantly under the provision of a use case-customized definition of the design space, the distribution and amount of training data, surrogate model types, and their hyperparameters. Even though prediction errors can be reduced, they cannot be entirely avoided and mitigate the reliability of the optimization results.*

6.3 Adaptive surrogate model-based optimization

The previous section emphasizes that surrogate models, replacing the computationally intensive steps of tolerance analysis, are profitable measures to enhance the efficiency of tolerance-cost optimization. However, the final results are always subject to prediction errors mitigating their reliability. Inspired by successful applications in other disciplines [588], the idea of adaptive surrogate model-based optimization is transferred on sampling-based tolerance-cost optimization in [S8], further extended for its publication in [P16], and in detail presented in the following.

Problem statement Harmonizing the design of experiment for data generation and choice of model type while approximating a usually unknown relationship is crucial but decisive to obtain accurate enough nc-rate estimates with the lowest possible amount of the representative samples (see Sec. 6.2). By decoupling surrogate modeling and optimization and using a static sampling [351], the prediction accuracy or error e, varying over the total design space considered in optimization, is prefixed. Consequently, models are chosen by their global best fit but can be unacceptable and inaccurate in regions of optimality. The theory of adaptive sequential sampling tries to reduce the prediction errors of an initially generated model by selective resampling in areas of lower accuracy and, thus, improve the overall quality of prognosis [590]. Although this approach is quite promising, the entire design space is regarded as equally interesting. Similar in its fundamental idea, the strategy of adaptive sample sizes from Sec. 6.1 reveals that an intentional acceptance of larger prediction errors in areas of non-feasible or non-optimal regions and the reduction of prediction errors in those near-optimal ones is more beneficial. However, *the regions worth to be resampled are usually unknown* before optimization. Otherwise, the optimal set of tolerances and alternatives would already be known, making a cumbersome identification by numerical optimization needless.

Theoretical solution Though at the beginning there is little or no detailed information about the near-optima as interference of objective and constraints, this situation changes by the gradual improvement of the solution while progressing through the design space by trial-and-error. To avoid the decisions made based on results influenced by the prediction errors, it may be worth repeating the evaluation of the most promising individuals with the real model and substituting the approximated ones. The idea is similar to the one for adaptive sample sizes presented in Sec. 6.1, except that the higher accuracy is achieved using the real model instead of higher sample sizes. On the one hand, this excludes taking non-acceptable solutions as elitist solutions. On the other hand, it offers further potential to improve the surrogate models' accuracy. If not only approximate solutions are generated in each generation by surrogate models, new information about the constraint surface and near-optimal solutions is available. However, the indirectly gained knowledge can only be used when optimization and surrogate modeling are not decoupled.

Adaptive surrogate model-based optimization overcomes this limitation and updates the surrogate models [591, 592] with the newly gained information by resampling during optimization "on the fly" in each generation [593]. In doing so, it is possible "to quickly find the local or global optima" [594] while mitigating the impact of uncertain surrogate estimates on the optimization process and results. The "zoom[ing] in the regions of interest" [592] takes over the task of resampling, which forms the basis for the subsequent remodeling step [587]. To use its general potential in the context of optimal tolerance allocation, Fig. 59 introduces the concept of adaptive surrogate models to further enhance the efficiency of sampling-based tolerance-cost optimization. For the sake of clarity, the following discussion is limited to case (4) (see Fig. 56), replacing the total tolerance analysis with one surrogate model (see Sec. 6.2).

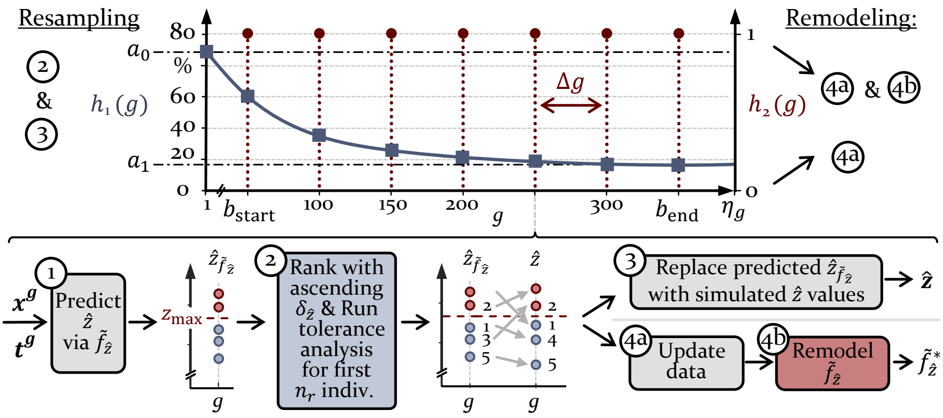

Figure 59: General principle of adaptive surrogate model-based tolerance-cost optimization with the substeps of resampling and remodeling. Examples of resampling and remodeling functions $h_1(g)$ and $h_2(g)$ (top). Procedure of selective resampling of the best solutions and remodeling of the surrogate model $\tilde{f}_{\hat{z}}$ serving as new surrogate model $\tilde{f}^*_{\hat{z}}$ for the next Δg generations (bottom).

At the top of Fig. 59, the implementation of the two main mechanisms of resampling and remodeling in the optimization process is illustrated. While the function $h_1(g)$ controls the proportion of recalculations $r_p(g) \in [0;1]$ over the generation g, $h_2(g)$ serves as activation function with its image $\{0;1\}$ deciding if a remodeling of $f_{\hat{z}}$ in generation g takes place ($h_2(g) = 1$) or not ($h_2(g) = 0$). As shown at the bottom of Fig. 59 for one selected generation, the results from the preceding resampling step ② of $n_r = r_p \cdot \eta_p$ identified individuals are used to augment the database and to remodel the surrogate model within the optimization loop in step ④. The resulting surrogate model $\tilde{f}^*_{\hat{z}}$ replaces the previous model $\tilde{f}_{\hat{z}}$ and is used for the next $g + \Delta_g$ generations until it is replaced again. As indicated in step ③, the real values $\hat{z}$ replace the nc-rates $\hat{z}_{\tilde{f}_{\hat{z}}}$ estimated by the surrogate model. In addition to the computational effort for resampling, the iterative remodeling operations lead to an additional time effort. The distance between two remodeling iterations Δ_g is a suitable parameter to control this time effort. Furthermore, to preserve the overall efficiency of the method, the parameters of h_1 are worth to be studied and to be selected consciously. r_p is defined as constant, but an adaption over h_1 over the optimization history, similar to the idea of adaptive sample sizes, might be useful. The exponential function in Fig. 59 serves only as an illustration. In addition to the shape of the function, the initial sampling generating the database for the first surrogate model $\tilde{f}_{\hat{z}}$ is essential. Besides a systematic space-filling sampling before optimization (as illustrated in Fig. 57), it is also conceivable to start with an initial random sampling in generation $g = 0$, defined by the optimizer, and use it as a database for the first surrogate model $\hat{f}_{\hat{z}}$.

Practical transfer and findings For studying its benefits, the proposed adaptive surrogate model strategy is applied to the wheel mounting example and compared to the results from the previous section. In doing so, case (a) without surrogate modeling and case (b) with fixed ANN are supplemented by case (c) with additional resampling and case (d) with additional resampling and retraining. A modified version of the CS algorithm is used to integrate the steps of surrogate modeling into the optimization workflow. The pseudo-code is given in [P16]. Using a fixed number of resampled individuals with $h1(g) = 0.2$, a retraining of the surrogate model with a decreasing frequency over the optimization process is selected as follows:

$$h_2(g) = \begin{cases} 1 & \text{if} \quad g \bmod 1 = 0, g \leq 3, \\ 1 & \text{if} \quad g \bmod 5 = 0, g \leq 25, \\ 1 & \text{if} \quad g \bmod 10 = 0, g \leq \eta_g, \\ 0 & \text{otherwise.} \end{cases} \tag{66}$$

The same settings used in Sec. 6.2 for optimization, tolerance analysis, and layout of the ANN are applied to ensure comparability between the different approaches. The same random numbers (O-2/S-3 acc. to Tbl. 6) for the $\eta_r = 5$ times repeated optimization runs provide comparability of the results. The proposed approaches are studied for three different sizes of training data sets $D = 300, 750, 1{,}500$.

To begin with, Fig. 60 illustrates the effect of refining the accuracy of the surrogate models in the regions of interest by contrasting the optimization histories for one exemplary run ($D = 300$). In line with the findings from the previous section, it can be seen that the use of the surrogate model without taking the information on the real value by TCVisVA into account (b) leads to huge underestimations of the nc-rate and, thus, high errors $e = \hat{z} - \hat{z}_{\tilde{f}_{\hat{z}}}$. At the same time, the difference between the real nc-rate values $\hat{z}$ and the ones obtained by $\tilde{f}_{\hat{z}}$ for the intermediate best results continuously increases over the optimization progress. In comparison, resampling the n_r nearest solutions to the constraint surface with $z_{\max} = 2{,}700$ in each optimization iteration eliminates the prediction errors e. Case (c) avoids erroneously taking unacceptable solutions as elitist solutions for the next generation. Additionally, by taking the minimum distance $\hat{z}_{\tilde{f}_{\hat{z}}} - z_{\max}$ as a criterion for the selection of the n_r individuals to be resampled, tolerance combinations, which are evaluated as infeasible by the surrogate model, but actually conform with $z_{\max}$ ($e < 0$), are considered within optimization.

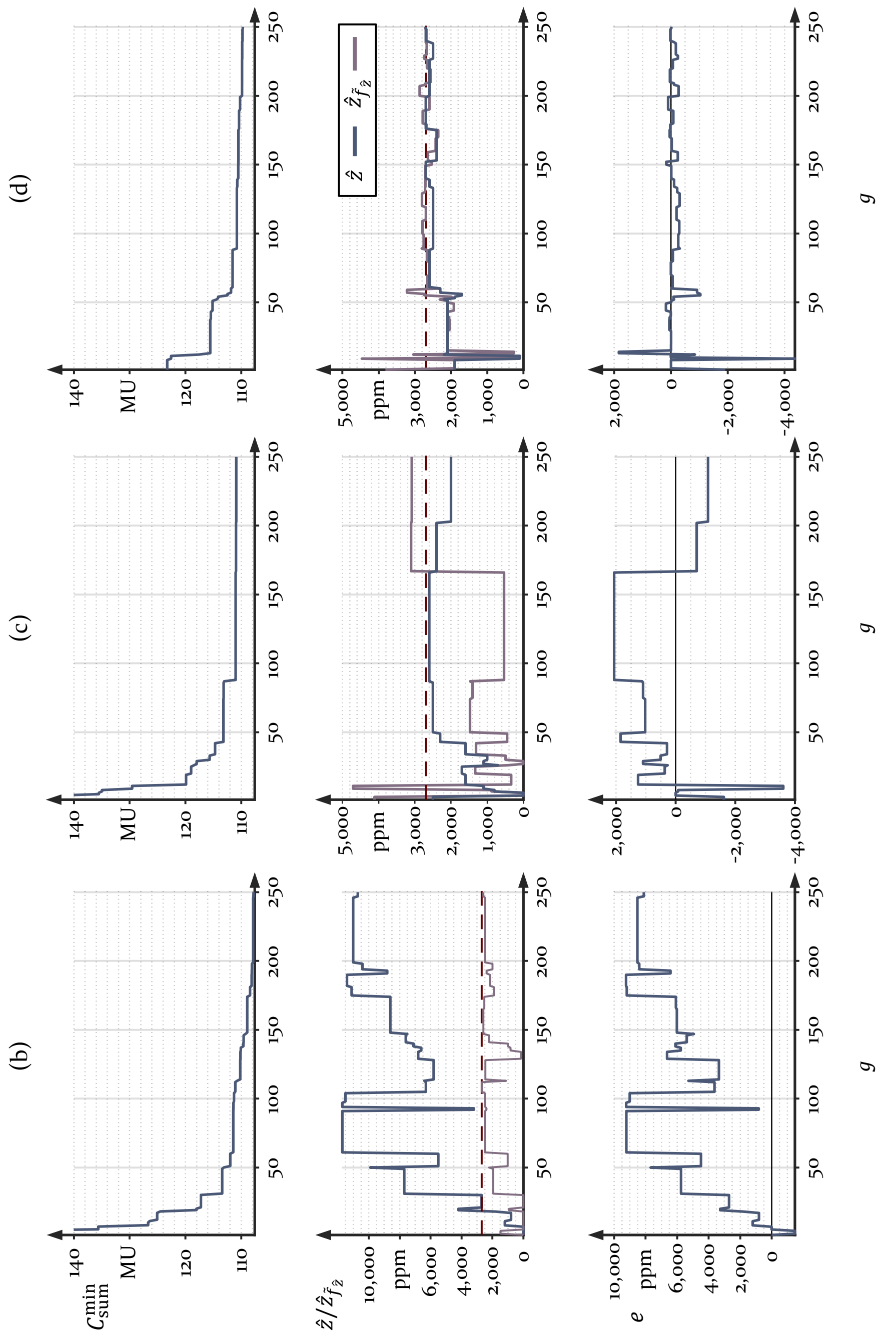

Figure 60: Illustration of optimization runs to solve the wheel mounting assembly allocation problem in comparison: minimum costs $C_{\text{sum}}^{\text{min}}$, corresponding nc-rates $\hat{z}$ estimated using TCVisVA and ANN $\hat{z}_{\tilde{f}_{\hat{z}}}$, and prediction error e for (b) surrogate-model based, (c) surrogate model-based with resampling, (d) adaptive surrogate model-based optimization ($D = 300$).

As a result, the error e is significantly lower, z_{max} can be ensured by the optimally allocated tolerances. The additional remodeling step for case (d) can be noticed by the small error e, resulting from the increased prediction accuracy in the regions of optimality. The exemplarily discussed effects are reflected in the final optimization results, which are summarized in Tbl. 50 and visualized in Fig. 61.

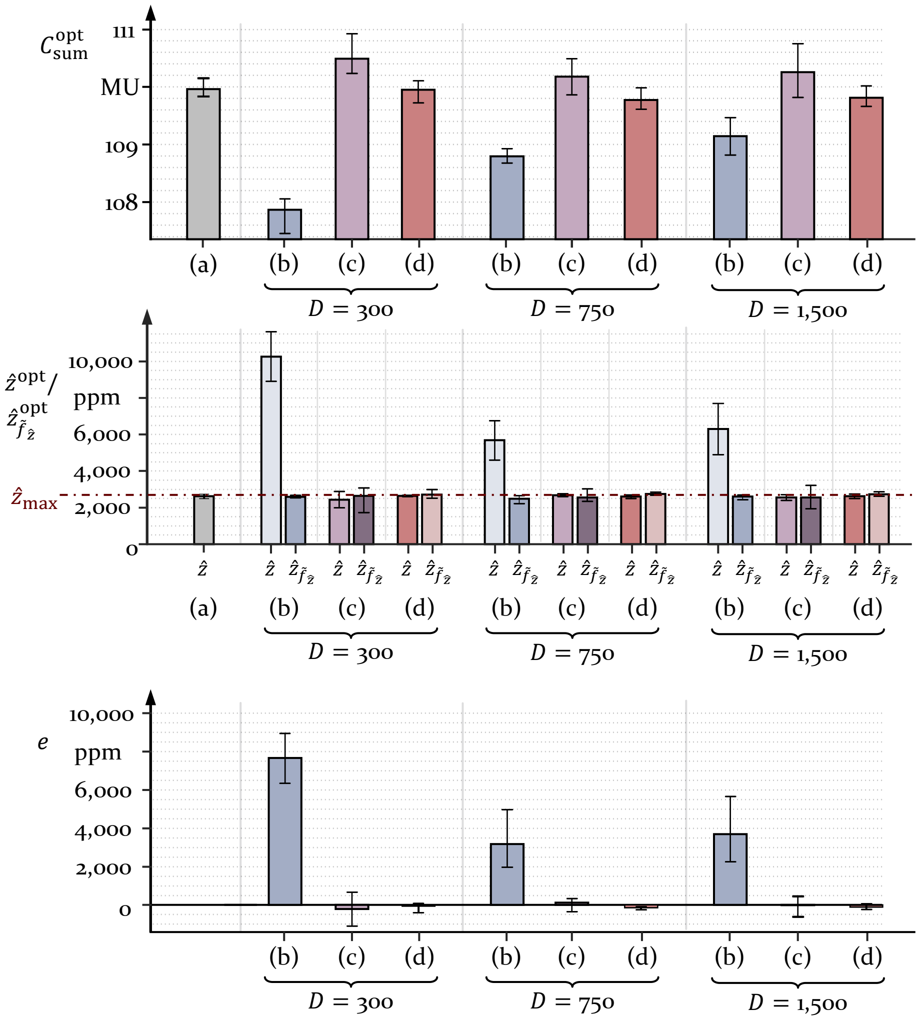

Figure 61: Cost optima $C_{\mathrm{sum}}^{\mathrm{opt}}$, surrogate estimates $\hat{z}_{\tilde{f}_{\hat{z}}}^{\mathrm{opt}}$ and real values $\hat{z}^{\mathrm{opt}}$ for optimally allocated tolerances, and errors of prediction e defined as the difference between $\hat{z}_{\tilde{f}_{\hat{z}}}^{\mathrm{opt}}$ and $\hat{z}^{\mathrm{opt}}$ for three sizes of training data D for surrogate modeling in comparison: (a) direct embedding of TCVisVA, (b) surrogate-model based, (c) surrogate model-based with resampling, (d) adaptive surrogate-model based. The errorbars indicate the range of the obtained solutions.

The differences in the nc-rate evaluation are directly reflected in the obtained optima: The comparatively high underestimates for (b) give additional space to widen the tolerances and, thus, lead to the lowest costs, but obviously non-reliable results. By remodeling the surrogate model in case (d), lower cost optima than for case (c) can be achieved through lower errors. The positive effect on the accuracy of the results for case (c) and (d) is at the expense of the total optimization time.[7] As Fig. 62 exemplarily illustrates for $D = 300$, the average optimization time $\overline{\tau}_{\text{feas}}$ mainly increases by the additional time effort for the resampling $\overline{\tau}_{\text{ReSamp}}$ primarily defined by the expenses for running TCVisVA, whereas the time for remodeling $\overline{\tau}_{\text{ReModel}}$ is negligible. Despite higher computation times compared to (b), the presented method can contribute to a significant increase in efficiency compared to the direct embedding of the tolerance analysis (a) while ensuring reliability. The influence of the initial data set's size, the chosen surrogate model, and its hyperparameters on the optimization process and the final results remains. However, adaptive remodeling can mitigate their influence by successively augmenting the data set and refining the surrogate model.

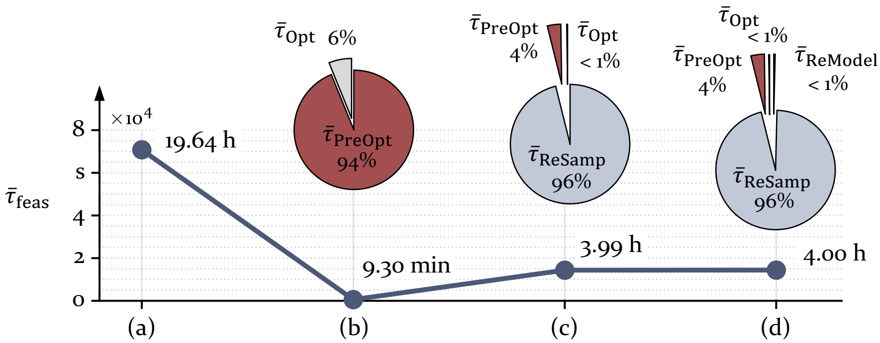

Figure 62: Average total optimization time $\overline{\tau}_{\text{feas}}$ of sampling-based tolerance-cost optimization without surrogate model (a), based on a fixed ANN (b), with additional resampling of best elitist solutions (c), and additional remodeling of the surrogate model (d) to solve the wheel mounting assembly allocation problem, data set size: $D = 300$.

Based on this first proof of benefits, further studies are helpful to provide interesting insights into a clever definition of the resampling and remodeling functions h_1 and h_2 with their individual parameters to further increase the overall efficiency. Switching the model type during optimization or using several surrogate models for different sections of the design space bears research potential.

[7] Detailed information on the efficiency of the different approaches can be found in Tbl. 51.

Updating surrogate models with data resampled during optimization mitigates the influence of prediction errors and speeds up the search for the global optimum. The accuracy of the surrogate models is improved selectively and sequentially at points of potential optima, enabling reliable and near-optimal tolerance allocation results in significantly lower computation times.

7 An optimal tolerance allocation framework established on sampling-based tolerance-cost optimization

So far, different aspects regarding the *effectiveness*, in terms of *accuracy and completeness*, and the *efficiency* of sampling-based tolerance-cost optimization were examined and the developed methods were proposed partly separated from one another in the respective sections. In the following, it is now the aim to unite and align them in a structured **framework for optimal tolerance allocation** while considering the individual findings obtained. The term framework refers to aligning all essential activities with their underlying methods for optimal tolerance allocation using sampling-based tolerance-cost optimization in one workflow. Fig. 63 illustrates the chronological sequence of eleven main steps, whose style is adopted from the SysML syntax and its usage proposed in [595] to formalize variation management processes.[1] In addition to the main activities presented and the three key main elements, viz. tolerance-cost analysis, tolerance analysis, and the definition of the optimization problem (see also Fig. 6), it illustrates the individual flows of information. For clarity, they are limited to the main information classes specified and explained in more detail below. Further direct, partially manual inputs are neglected.

As emphasized at the beginning of this thesis by Fig. 3, tolerance-cost optimization is usually applied in the last steps of tolerance design and, thus, in product design, building the bridge to the subsequent process design phases. Consequently, the given workflow presumes that the system and parameter design phases are already completed, though they indirectly influence the optimization and its results.[2] Findings obtained by the author in [P3] thereby prove that a robust product concept, which can be achieved, for example, with the aid of the Axiomatic Design principles acc. to Suh [596], help to avoid interrelated KCs and lead to less and wider tolerance values and, thus, lower tolerance-related manufacturing costs.

[1] Not only due to reasons for visualization but also to present a workflow independent from the used software with its specific data in- and outputs, the activity diagram in Fig. 63 slightly differs from the proposed approach given in [595]. Thus, the respective sources of information are not explicitly named. Still, they are summarized under the term *process design/product design information models* following the term used in the context of tolerancing in [173].

[2] An additional harmonization of nominal values and tolerances in the sense of concurrent parameter and tolerance design is proven in literature to be beneficial (see Sec. 2.2.4). However, it goes beyond the scope of this thesis.

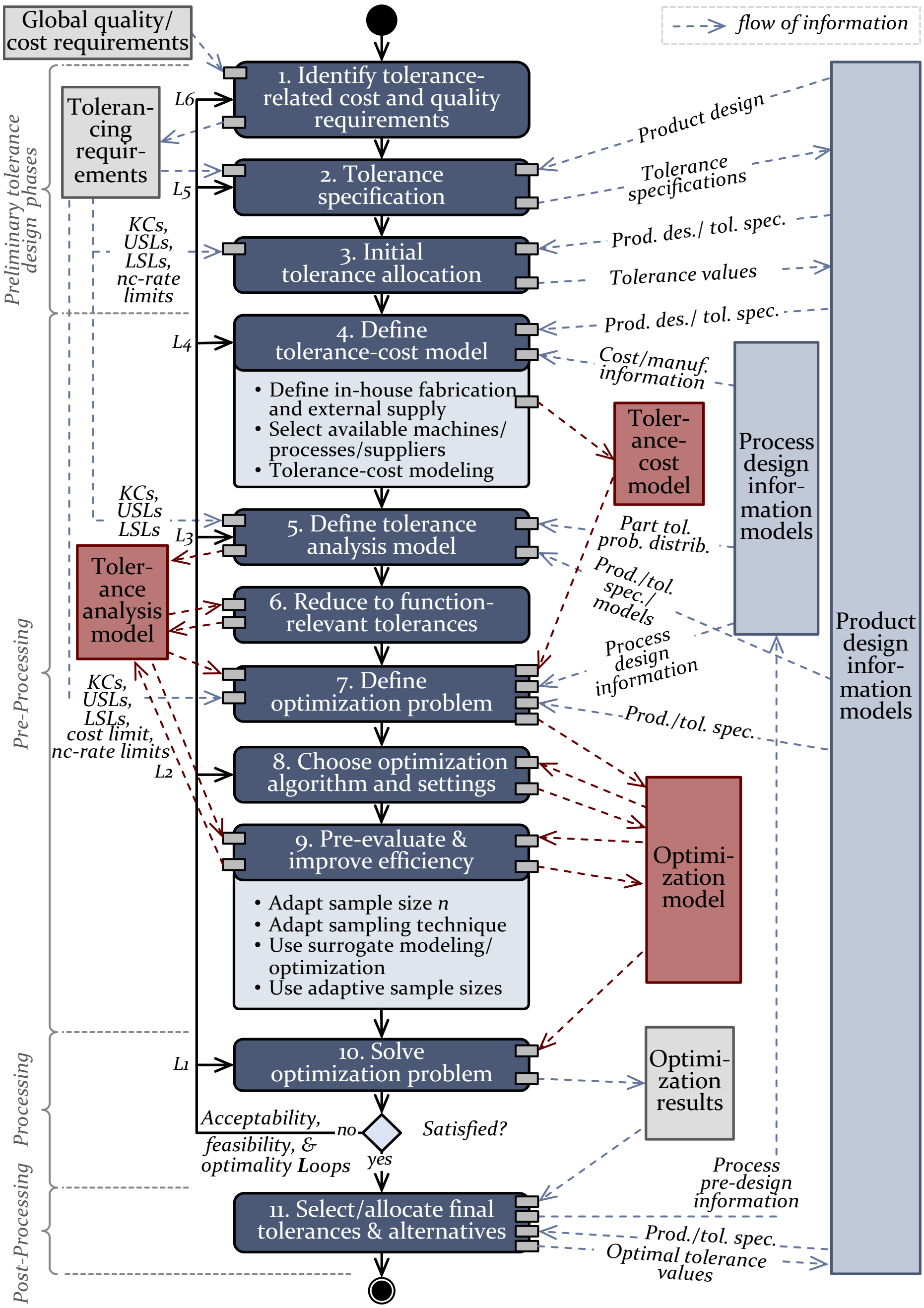

Figure 63: Overview of the developed framework for optimal tolerance allocation based on sampling-based tolerance-cost optimization.

At this point, it has to be emphasized that tolerance allocation is not limited to a specific point in product development and can be applied in the late design phases but also in process planning steps and even when production is already in progress. The allocation problems' variety is discussed in more detail in Sec. 8.3. Nonetheless, the proposed framework is generally valid.

Based on the product design, Fig. 63 starts with the identification of the tolerance-related cost and quality requirements in *step 1*, represented by a set of relevant KCs with their critical limits and acceptable nc-rates as well as a tolerance-related cost limit, starting from the global quality and cost requirements on the final product.

In line with Fig. 3, the succeeding **tolerance specification** in *step 2* aims at defining standards-compliant tolerance schemes for the individual parts covering all critical product geometry elements. These primarily consist of information on tolerance types and datums but are expected to include all necessary information for a complete and unambiguous geometry product specification (see Sec. 2.1.1). This requires detailed information on the product design, including the assembly structure and sequence, part geometry features with their nominal values, material properties, etc.

The tolerance specification activity is followed in *step 3* by a **first, but optional tolerance allocation** step, where initial tolerance values are identified, whether purely intuitive or using workarounds and methods far from optimal tolerance allocation (see Sec. 2.1.1) and can, thus, not lead to cost-optimal results. In addition to the product design information, a strong pull of process design information is required for the **definition of the tolerance-cost model** in *step 4*, depending on the scope and area of application of tolerance allocation. When taking the process detailed into account, this presupposes that the available machine/process/supplier alternatives for realizing all tolerances to be allocated are known. The tolerance-cost relations, as well as the machine- or supplier-specific capability and capacity ranges, must be available in quantitative form (see also Eq. (31), Eq. (41)–(42)). Moreover, feature and part equality information is necessary to set up the equality matrices acc. to Eq. (52)–(56) for the proposed design dimension reduction method in Sec. 5.3.

Afterward, the **tolerance analysis model**, with its submodels and methods, i.e., the geometrical model, the behavior model, and the techniques for tolerance evaluation, has to be defined in *step 5*. It strongly depends on the technical product in focus, the specified tolerances, its assembly type, and its behavior in use in combination with the nature of the KCs (see also Sec. 2.2.2). Consequently, besides the pure information about the product design itself, primarily represented by CAD-models, product data sheets, and technical drawings, further information and models are needed, e.g., to describe compliant or time-variant assembly behavior in fabrication and/or use. Depending on the existing manufacturing strategy and available machine/process/supplier alternatives, the methods of batch-wise sampling presented in Sec. 5.2 are required for the virtual generation of the geometrical parts and their random or selective assembly. An essential input for the sampling is the part tolerance probability distributions, fully specified by its type and a set of distribution-dependent parameters, which are known or estimated based on real measurement data or virtual data from manufacturing simulations. Besides the sampling, tolerance evaluation modules include the techniques for the nc-rate estimation presented in Sec. 4.2–4.3.

The succeeding *step 6* aims at **identifying the tolerances that contribute to the predefined KCs**, or rather do not, using sensitivity analysis methods established in tolerancing. A helpful instrument when using sampling is the density-based sensitivity analysis presented in [597]. It offers the possibility to determine the contributors directly via the distributions of the individual characteristics $\boldsymbol{X}$ and the distribution of the assembly responses $\boldsymbol{Y}$ by using the kernel density estimation technique, independent of the used sampling procedure and part tolerance probability distributions.[3] In doing so, the search space dimensions can be reduced in advance by restricting the optimization variables to only the function-relevant tolerance values. This becomes further useful when using surrogate models to increase the efficiency of tolerance-cost optimization.

In *step 7*, the tolerance-cost and tolerance analysis models are integrated into the **mathematical definition of the optimization problem** employing the objective function and inequality condition, which mainly depends on the global optimization goal (cost-driven vs. quality-driven tolerance-cost optimization) as well as the chosen alternative selection or allocation strategies (see Chap. 5). This further includes defining the design variables with their lower and upper boundaries and the capacity/feasibility constraints. Moreover, incorporating general tolerancing knowledge through a set of inequality constraints for all correlated tolerances on feature level acc. to Eq. (50)–(51) assures the compliance of the allocated tolerances with the GD&T rules defined in the respective ASME/ISO standards. Based thereon, *step 8* serves to choose an **optimization algorithm and its settings**, which is capable of handling the type of variables needed, i.e., either continuous variables for

[3] Proprietary tolerance analysis software tools partially preclude the application of density-based tolerance analysis due to the missing information on the sampled inputs but generally provide in-built methods for contributor analysis.

problems without alternative selection or equal machine characteristics (see Sec. 5.1) or mixed-integer variables as discussed in Sec. 5.2.

Before starting to solve the optimization problem in *step 10*, it is beneficial to first **evaluate in advance and, if necessary, to improve the efficiency** in *step 9*. Depending on the given optimization problem, the techniques presented in Chap. 6 support the user to make improvements in the efficiency and effectiveness. The obtained optimization results always have to be critically evaluated [286], particularly concerning the technical feasibility, acceptability, and optimality criteria presented in Sec. 2.2.3. To improve the results, one or multiple manual iterations loops *L*, such as

- *L1:* repeating the optimization to increase the probability of finding a technically feasible, acceptable, and finally optimal solution,
- *L2:* adjusting the settings or choosing another optimization algorithm with better fitness to the given optimization problem,
- *L3:* reshaping the tolerance analysis model and its submodels as well as the sampling and nc-rate estimation techniques used for tolerance evaluation,
- *L4:* adapting the tolerance-cost model considering additional machines and suppliers with lower costs and/or better capabilities,
- *L5:* revising the tolerance specification in the sense of manual tolerance synthesis,
- *L6:* verifying the cost and quality requirements, and, if possible, their relaxation,

are needed until a satisfactory result is achieved.

The workflow ends with *step 11*, where, based on satisfactory optimization results, **the final tolerances and alternatives are selected/allocated**, communicating the part quality requirements from the perspective of design with first process design information for the subsequent downstream activities of process planning, e.g., the considered machine characteristics and weights (see Sec. 5.1–5.2).

The framework of Fig. 63 can serve as the basis for its **technical implementation** in the form of a software system. The actual realization depends on the available, preferred, and necessary tools to solve the optimization problems and, secondarily, perform the tolerance-cost and tolerance analysis as realistically as needed. For the final application and evaluation of the proposed framework, following in Chap. 8, it is exemplarily implemented in MATLAB®[4], whereas the structure of the software prototype into its single

[4] The file extensions .m, .mat, and .fig are MATLAB®-specific files for scripts/functions, formatted data, and graphic objects (see Fig. 64).

modules for the proposed methods in Chap. 4–6 aims to assure its adaptability and extensibility. An overview of the implementation is given in Fig. 64, while Appx. A.10 provides detailed information on the workstation and software versions used.

To guarantee its interoperability, the optimization tool is not directly integrated into a CAD-system but takes advantage of the idea of model-based definition to partially automate the workflow, as already illustrated, for instance, in [394, 395] and verified in [S10], by using appropriate interfaces and the neutral exchange formats *STEP AP 242* and *JT*.

The CAD-software Siemens NX, as an example, supporting the model-based tolerance specification and allocation in *step 2,3 & 11* allows the semantic mapping of the tolerance information as PMIs, which can be reused in the subsequent steps, in particular in the definition of the tolerance-cost model and the tolerance analysis module. Besides additionally annotated manufacturing information, they carry the information on the feature geometry and type and the assembly structure of the total product. For a software-neutral product design information exchange, the use of *STEP*-file interpreters, as presented by the author in extracts in [P4], is beneficial.

Depending on the approach followed, different tolerance analysis routines are helpful. Besides the purely programming code-based tolerance analysis method, the previous chapters emphasized the benefits of using the commercial CAT-software TCVisVA combined with the developed methods for nc-rate estimation in MATLAB. This allows a partially automated generation of tolerance analysis models using the information from the product data model in *JT*-format and saved in the TCVisVA-specific data format *PDO*. For details on the batch command usage of TCVisVA based on the exchange format *TXT*, please refer to its initial presentation in [P19] and its more detailed presentation in Appx. A.6. Beyond this, the benefits of embedding CAT-tools into the tolerance-cost optimization workflow such as RD&T for the tolerance analysis of process-driven assemblies, are, for instance, emphasized in [P11].

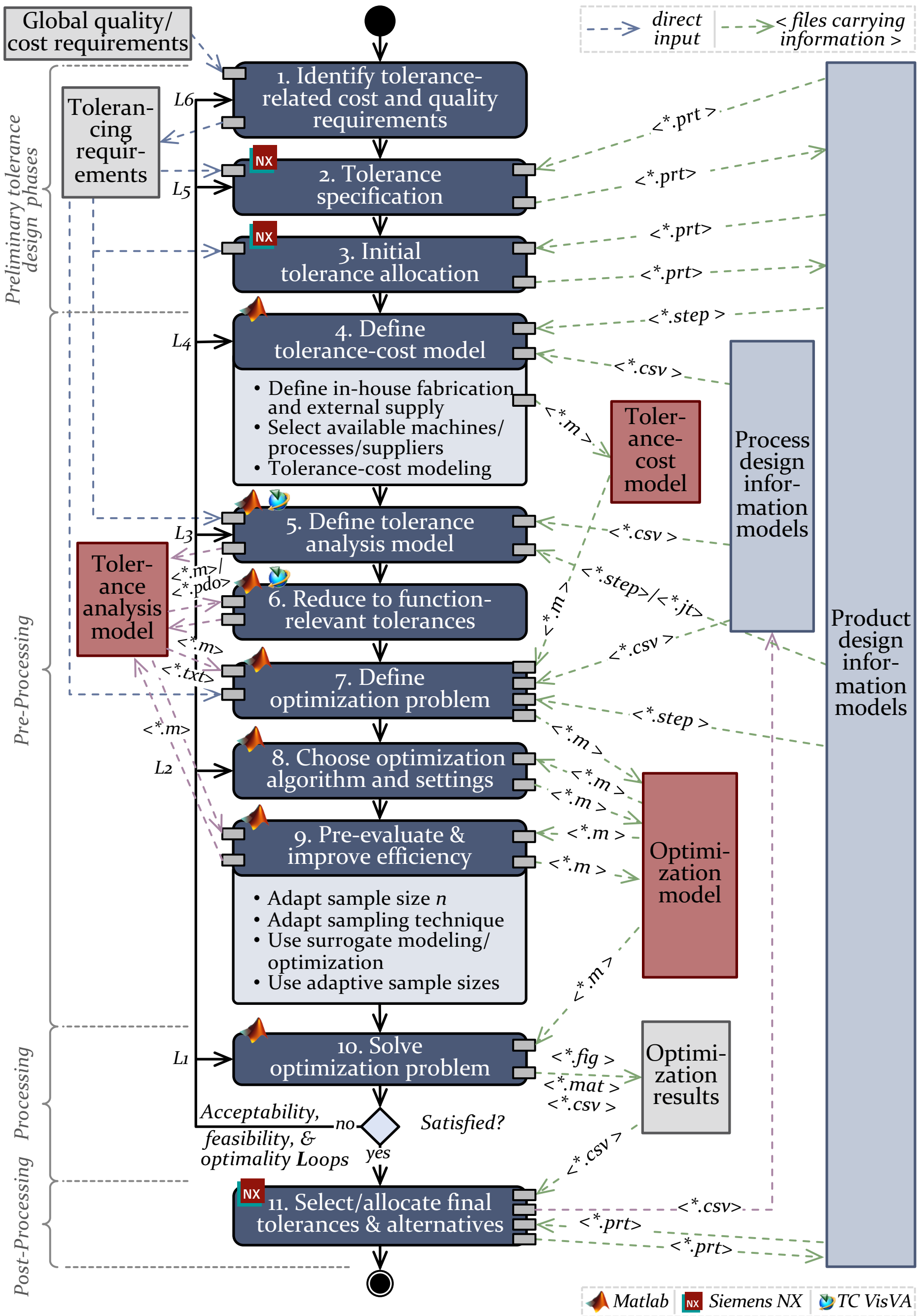

Figure 64: Exemplary implementation of the framework of Fig. 63 with the used software systems and the main data files.

The exchange of the necessary manufacturing process-related data can, for instance, be simplified via textual input files or manual inputs.[5] In line with the previous sections, GA and CS are exemplarily used as optimization algorithms covering the range of the tolerance-cost optimization problems focused on in this thesis.

> *The previously presented methods are closely linked and directly or indirectly embedded in the tolerance-cost optimization problem. The proposed framework arranges them in a coherent workflow illustrating all necessary activities while considering the individual interrelations. Combined with the illustration of the main information flows, it serves as a guideline for a software implementation for optimal tolerance allocation using sampling-based tolerance-cost optimization.*

[5] A direct coupling with PDM-/PLM-systems as well as the use of other exchange formats might be beneficial for its practical application, but at the same time raises further and currently open research questions on the structured acquisition, storage, and provision of tolerancing information (see for instance [117, 158, 598]). In [S11], a SQL-based proposal for tolerance-cost data was developed and applied. However, the representation of the process-related information is not the focus of this thesis. It is not further discussed, despite the importance for its final implementation in a practical tolerance allocation tool.

8 Application and evaluation of the developed optimal tolerance allocation framework

To finally evaluate the presented approach and summarize the findings made so far, the proposed tolerance allocation framework from Chap. 7 is now applied to a case study of industrial complexity. In addition, a final discussion on achieving the underlying research goals and potential for future research is given.

8.1 Allocation of least-cost tolerances for an electrified cross skate

Fostered by the increasing awareness of sustainability, the way people move has changed in the last few years. Micro-mobility devices, for instance, electrified scooters, bicycles, or skates, are widely accepted solutions for personal transportation. Electrified cross (e-cross) skates are a newly developed solution, where a pair of single-row cross skates are electrically driven and the skating speed is controlled via inclination sensors by the rider's weight shifting. To shorten the curve radius and enable a cornering without lifting and replacing the skates, the front wheel axle system can be turned by a novel, patented steering system [599] (see Fig. 65). More details on the e-cross skate system are given in Appx. A.8.2 and Fig. 92.

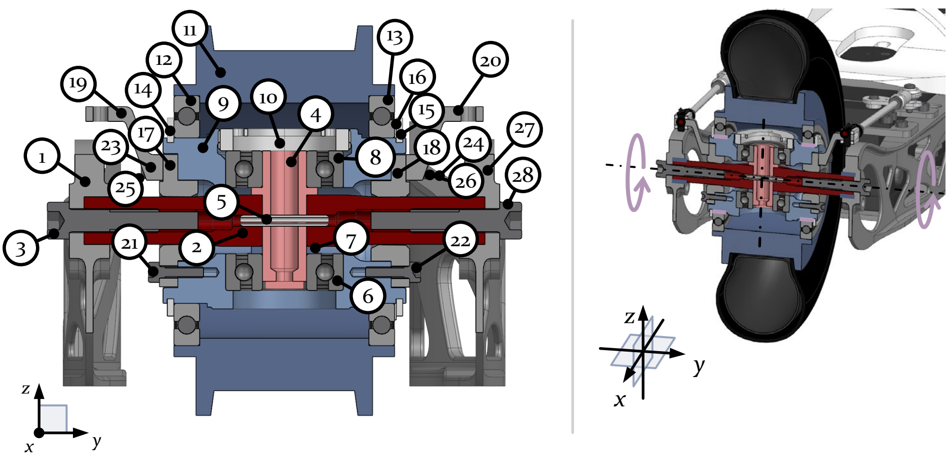

Figure 65: Overview (right) and cross section (left) of the e-cross skate's front wheel assembly.

Assuring the e-cross skate's functionality, three KCs are considered for optimal tolerance allocation in the following (see Fig. 66). First, the angle Y_1 between the wheel and the frame should be between 88.5° and 91.5° to ensure the inclination sensors' functionality and not mitigate the driving performance. Second, the tilting angle Y_2 and the eccentricity of the effective axis Y_3, resulting from the reference points R1 and R2 where the steering mechanism assembly is mounted, are specified to conform within $[-1.5°; 1.5°]$ and $[-1.0\ \text{mm}; 1.0\ \text{mm}]$ (see Fig. 66). The front wheel assembly is analyzed in the neutral wheel position, i.e., driving in a straight line, in the following. A maximum nc-rate of $z_{\text{max}} = 2{,}700$ ppm must be complied with.

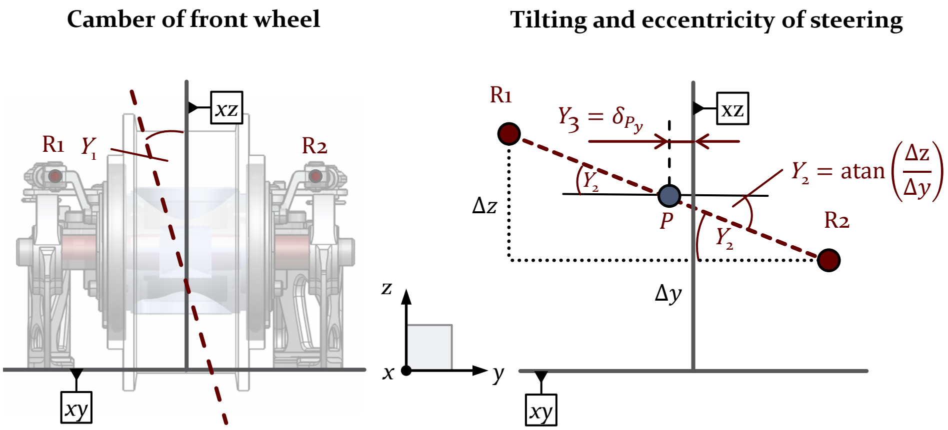

Figure 66: KCs considered as functionally relevant for the e-cross skate front wheel assembly. Y_1: camber of the front wheel, Y_2: tilting angle between the points of reference R1, R2 of the front steering mechanism, Y_3: eccentricity of the steering.

Based on these tolerance requirements, all relevant part tolerances are specified. The result of the manual, function-oriented tolerance specification for all parts contributing to the three KCs are summarized in Fig. 67 and Fig. 68.[1] In addition, rough tolerance values are allocated as a first guess. The direct assignment of the tolerance callouts through PMIs first supports checking the conformity with the ASME standards and second facilitates the subsequent steps of tolerance analysis and cost modeling. By picking up the idea of relative tolerance-related costs, as proposed in [203, 600], the semantic feature and tolerance information in the form of PMIs can be directly used to define the tolerance-cost model serving as the objective function.

In doing so, the reciprocal tolerance-cost relations are approximated by the features' size, type, and machinability and do not take more specific machine

[1] Fig. 93 in the appendix gives a more detailed overview of the individual part features.

or process information into account. The individual lower and upper tolerance limits are defined following general tolerance and reasonable experience values. For reasons of clarity, machine selection and allocation are not included in this example. All tolerances are assumed to be normally distributed. The tolerance-cost data is summarized in Tbl. 52.

Based on the 3D model in JT-format, the feature-based TCVisVA-model for tolerance analysis is defined. Using the feature information, it is possible to represent the variations on the feature level, propagate the variations through the assembly using virtual assembly operations, and finally evaluate their accumulated effects on the KCs using virtual measurement operations predicting the assembly responses (see the assembly and tolerance graph in Fig. 94–95.) In line with the previous sections, the TCVisVA-model is embedded in the acceptability constraint directly or indirectly through surrogate models. Due to multiple assembly responses, ecdf-based nc-rate estimation acc. to Eq. (23)–(26) is applied.

Completing the optimization problem, all dimensional tolerances are first set as fixed tolerances. In addition, the frame parts ($l = 1, 27$), the bearings ($l = 6, 8, 12, 13$), and additional elements, viz. the screws, shims, and circlips, are supplier parts and not considered as variables within the tolerance allocation problem. The front axle's symmetrical assembly structure further simplifies the optimization problem in advance by equating tolerance values for the functional identical parts and features. With the help of the design dimension reduction method presented in Sec. 5.3, the initial problem of 80 tolerance values is reduced to a minimum of 28 tolerances to be represented as design variables.[2] The correlations are highlighted in Fig. 67–68, the corresponding feature and equality matrices are given in Appx. A.8.2. The objective and nc-constraint are supplemented by eleven GD&T constraints, conforming to the ASME Y14.5-standard, and are listed in detail in Eq. (87).

For optimization, the CS algorithm is used with a population size of $\eta_p = 25$ and a maximum number of generations of $\eta_g = 250$ as a compromise of computation time and achievable results' optimality. Optimization is repeated five times with the same random numbers for the sampling within TCVisVA with a sample size of $n = 10{,}000$ (O-2/S-3 acc. to Tbl. 6), eliminating the scattering and discontinuity effects in optimization (see Sec. 4.1).

[2] The 80 tolerances are reduced by 52, the union of 35 fixed tolerances and 30 tolerances affected by dimension reduction. Fixed tolerances can also be affected by design dimension reduction leading to intersections in both sets.

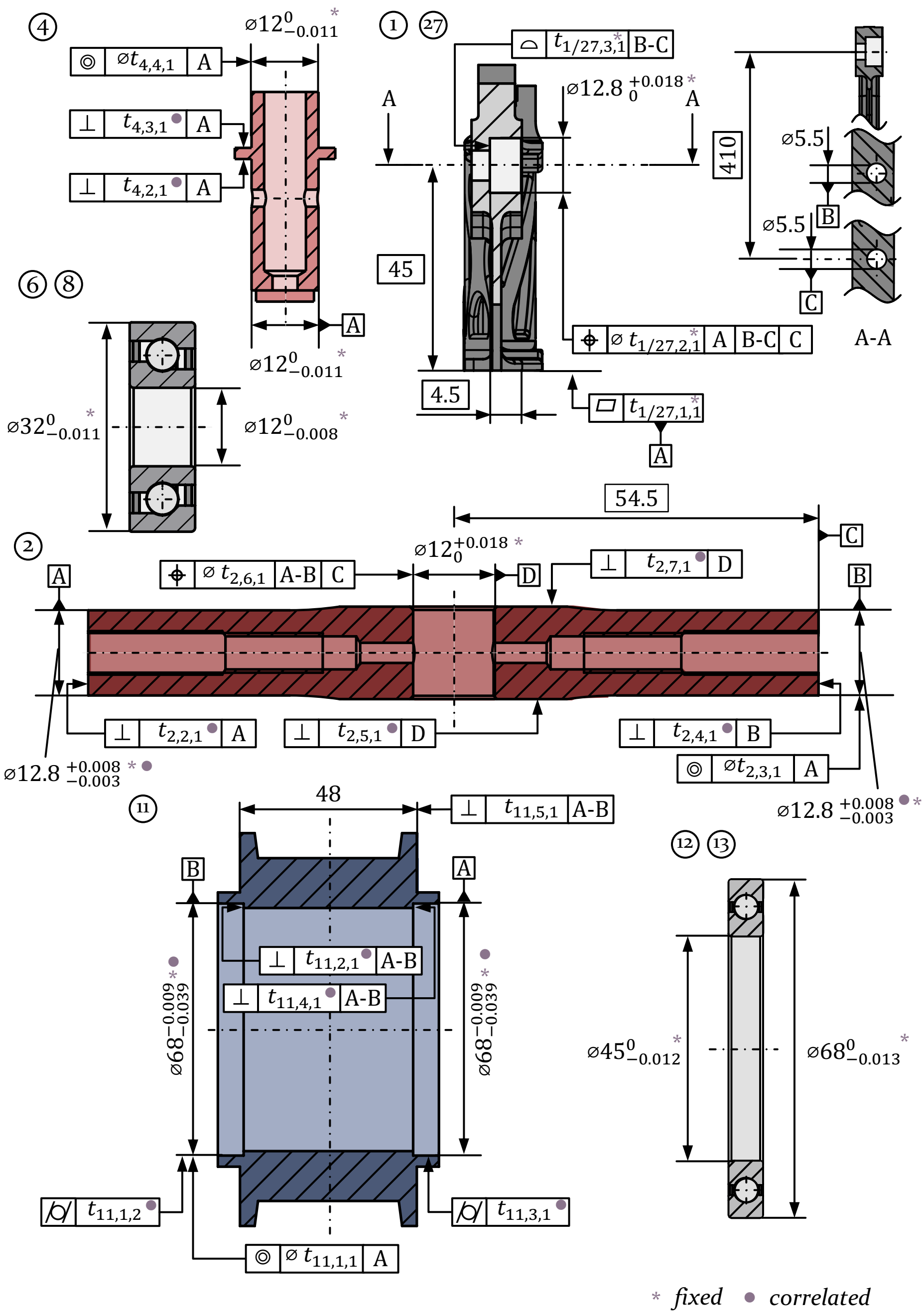

Figure 67: Overview of the part tolerance specifications of the e-cross skate example – I.

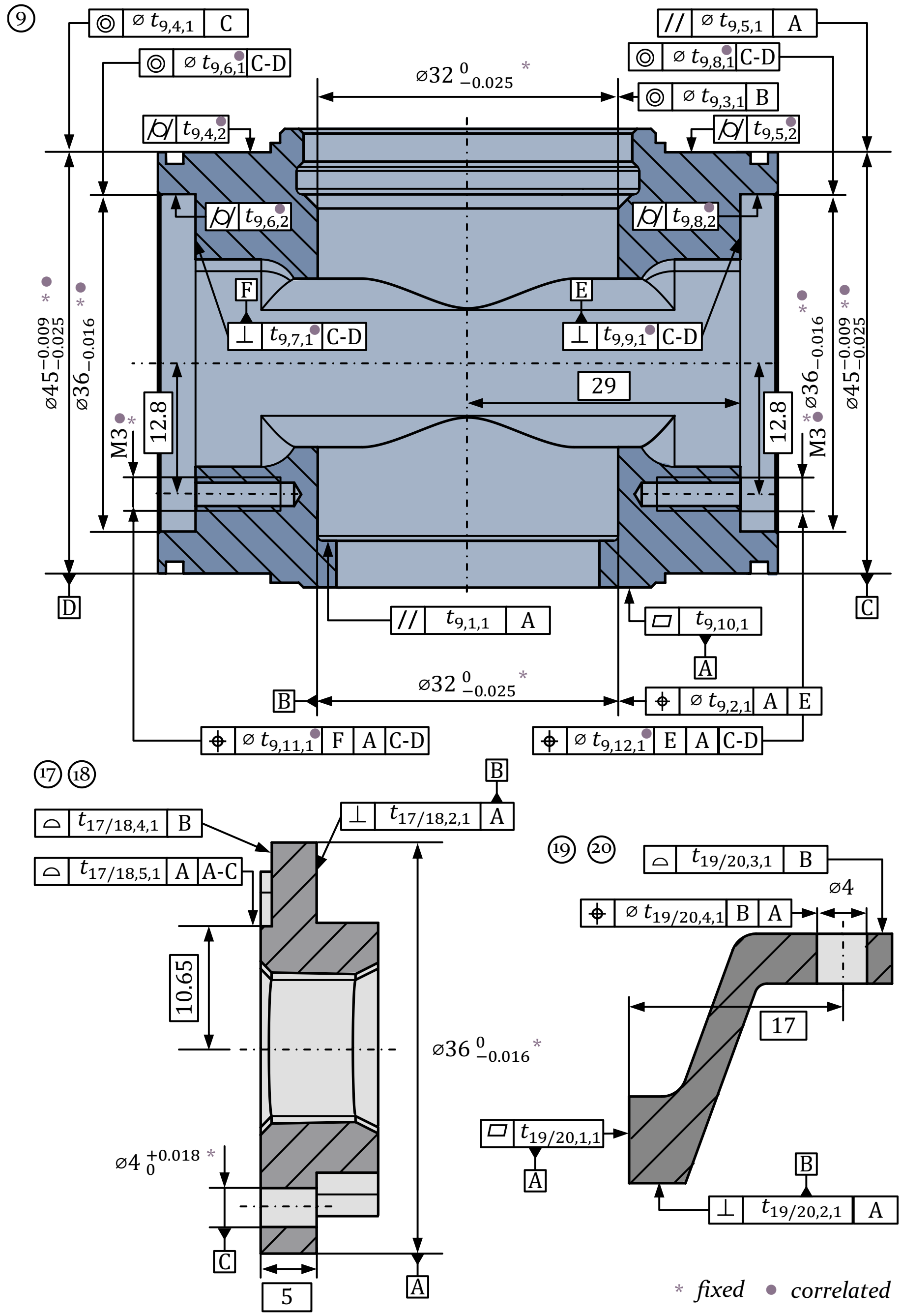

Figure 68: Overview of the part tolerance specifications of the e-cross skate example – II.

8.2 Discussion of the results

An overview of the obtained cost optima $C_{\text{sum}}^{\text{opt}}$, the final nc-rates $\hat{z}_{\text{asm}}^{\text{opt}}$, and the average computation times $\bar{\tau}_{\text{feas}}$ are given in Fig. 69. Besides the direct integration of TCVisVA (a), which on average took approximately two days per run, the adaptive sample sizes strategy (b) from Sec. 6.1 and adaptive surrogate model-based optimization (c) from Sec. 6.3 are applied to accelerate the sampling-based tolerance-cost optimization. All optimization runs are valid as they meet the GD&T constraints and the nc-constraint $z_{\text{max}} = 2{,}700$ ppm. The use of adaptive sample sizes (b), here with $\xi_1 = 7, \xi_2 = 0.5, n_{\text{min}} = 5{,}000$ and a recalculation rate of $r_p = 0.2$, reduced the computation times by ≈ 4 h on average while ensuring compliance with the nc-rate. Still, it does not achieve the optima from (a).

In comparison, the adaptive surrogate model-based optimization in this example is superior in efficiency improvement. In line with the previous chapters, using a wide, single-layered feed-forward ANN to substitute the time-intensive TCVisVA simulation by adaptive surrogate models helped to roughly shorten the computation time in quarters. The results for the two data set sizes of $D = 500$ ($RMSE = 5{,}341$ ppm) (c1) and $D = 1{,}000$ ($RMSE = 3{,}900$ ppm) (c2) with a 20%-resampling rate for dynamic retraining of the surrogate models indicate that higher initial data set sizes lead to optima nearer to the optimal values obtained for the direct embedding of TCVisVA (a). Likewise the adaptive sample sizes, the increased efficiency is at the expense of the optimality of the results, characterized by higher difference in the optimal results with an acceptable deviation from the final optima of the best results of 0.82 MU ($\widehat{=}$ 0.13%) (c1) and 0.04 MU ($\widehat{=}$ 0.06%)(c2) compared to the best results of (a). In addition, the time saving allows the optimization to be performed several times while still taking less time than (a), and is, thus, more likely to find the optimum.

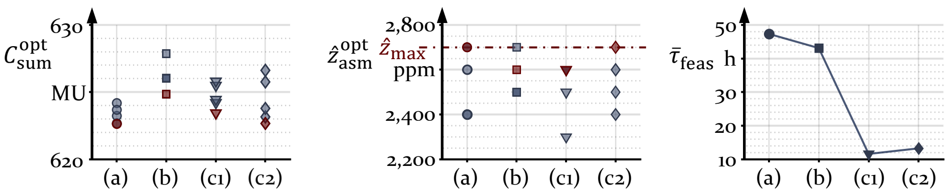

Figure 69: Overview of the optimization results for the e-cross skate example obtained through sampling-based tolerance-cost optimization (a), with adaptive sample sizes (b) acc. to Sec. 6.1, and adaptive surrogate models with two different data set sizes (c1) & (c2) acc. to Sec. 6.3.

The final costs $C_{\text{sum}}^{\text{opt}}$ for the best run obtained in (a) are compared to the initial expenses $C_{\text{sum}}^{\text{init}}$ in Fig. 70. The latter result for the initial tolerances more or less randomly chosen primarily on the middle of the tolerance ranges.

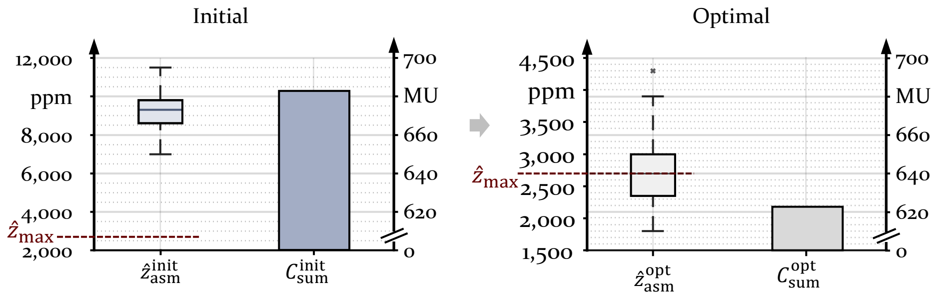

Figure 70: Nc-rates $\hat{z}_{\text{asm}}^{\text{init/opt}}$ and total costs $C_{\text{sum}}^{\text{init/opt}}$ before and after tolerance-cost optimization exemplarily illustrated for the best optimization results (see Tbl. 55). The variances of $\hat{z}_{\text{asm}}^{\text{init/opt}}$ resulting from a 100-fold repetition of tolerance analysis with the initial and optimal tolerances illustrate the sampling-induced margins of error of the final nc-rates.

Using the proposed sampling-based tolerance-cost optimization approach, the costs are reduced by 61.10 MU ($\widehat{=}$ 8.94%). Besides cost reduction, the nc-rate ranging between 7,000 and 11,500 ppm is additionally lowered to 2,700 ppm on average for the final tolerances. A 100-fold repetition of tolerance analysis aims to illustrate the scattering of the nc-rates for the initial and final tolerances with different random numbers to illustrate the margins of errors due to sampling-induced uncertainties. In this example, the approach helped in automatically finding a tolerance design that is first possible to fulfill the nc-requirements and second more cost-efficient than the initial tolerance design. For comparison, the costs and nc-rates range between $C_{\text{sum}}^{\text{max}} = 1{,}499.66$ MU and $\hat{z}_{\text{asm}}^{\text{max}} = 0$ ppm for all tolerances maximal tightened and $C_{\text{sum}}^{\text{min}} = 601.40$ MU and $\hat{z}_{\text{asm}}^{\text{min}} = 324{,}480$ ppm for the maximal widened ones.

The frequency distributions of the three KCs before and after optimization for the random numbers taken into account in optimization are illustrated in Fig. 71. The optimal balancing of the part tolerances narrows the distributions so that in sum a nc-rate of 2,700 ppm can be guaranteed. The interrelations of the three KCs can be seen in the size of the final single nc-rates $\hat{z}_1 = 1{,}500$ ppm, $\hat{z}_2 = 600$ ppm, $\hat{z}_3 = 1{,}100$ ppm, which on their own are lower than the maximum but in sum meet the maximum threshold of $\hat{z}_{\text{asm}}^{\text{opt}} = 2{,}700 \text{ ppm} \leq \hat{z}_{\text{max}}$ (see Tbl. 55).

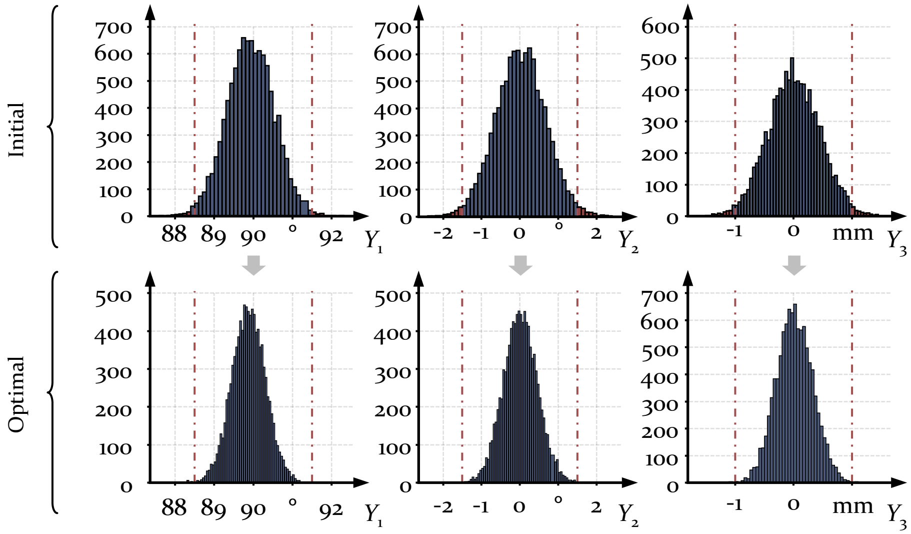

Figure 71: Frequency distributions of the e-cross skate's KCs Y_1,Y_2, Y_3 before and after tolerance-cost optimization obtained with a direct embedding of TCVisVA (a) for the best result.

Fig. 72 contrasts the initially chosen tolerances and the final, optimally chosen tolerances. At first sight, it is apparent that the optimizer selectively widened the major part of the tolerances, which have a minor influence on product functionality and, thus, offer the potential to reduce costs by higher tolerance values. The tightening of some tolerances with high impact on the functionality, e.g., $t_{9,7,1} = t_{9,9,1}$ of the housing $l = 9$, helps to significantly decrease the nc-rate while having a comparatively minor effect on costs worth to be invested to reach the global cost optimum. Fig. 72 is further helpful to check the tolerance values, which should be equated via the design dimension reduction method. For instance, the final tolerances for the housing covers ($l = 17, 18$) and the steering connectors ($l = 19, 30$) share the same tolerance values. In addition, the fixed tolerances can be easily identified by the identical tolerance values for initial and optimal status.

> *In summary, the example underlines the potential of the proposed sampling-based tolerance-cost optimization approach to find an optimal balance between costs and quality for industrial complex assemblies with multiple KCs and geometrical tolerances.*

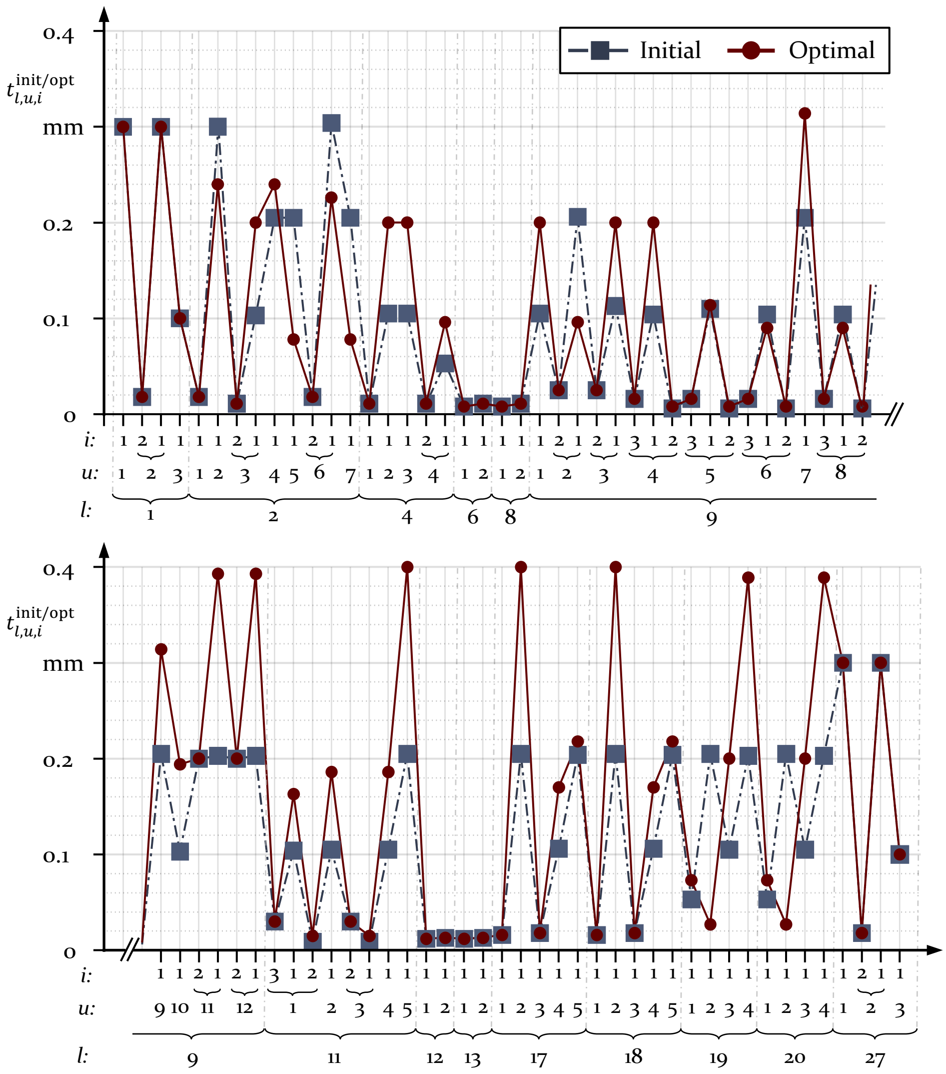

Figure 72: Initial and optimal dimensional and geometrical part tolerances $t_{l,u,i}^{\mathrm{init/opt}}$ for the e-cross skate example obtained with a direct embedding of TCVisVA (a) in comparison (for more details, refer to Tbl. 56).

8.3 Potentials and limits

Based on the benefits and weaknesses reflected in Chap. 3, the combination of sampling-based tolerance analysis and metaheuristic optimization was identified at the beginning of this thesis as the basis to enhance optimal tolerance allocation. So far, the positive impact of the proposed methods on certain usability's aspects of optimal tolerance allocation could be outlined. The final evaluation in the following aims to evaluate the success of answering the research questions and their impact on the overall research goal.

RQ1: How can the accuracy of sampling-based tolerance-cost optimization be increased to enable a reliable and realistic consideration of complex assemblies?

The problem-independent applicability of sampling methods enables the analysis of complex systems under variations, typically characterized by highly nonlinear assembly functions, which can only implicitly be represented via numerical simulation. By predicting the statistical assembly responses' distribution through a number of representative samples, it is possible to evaluate the product functionality through the widely accepted and illustrative nc-rate in parts-per-million for both one- and two-sided KCs. However, sampling-based tolerance analysis induces aleatory uncertainties into the optimization problem, leading to noise and scattering effects. In combination with the stochastic approach of the metaheuristic algorithms, the reliability of the results is significantly mitigated. If they are not considered during optimization or when interpreting the results, the tolerances finally determined can fall short of the required nc-rates many times over, despite adding the nc-limits as hard acceptability constraints.

This thesis has shown that, besides the well-known suggestion to use high sample sizes, *variance reduction methods*, particularly the Quasi-Monte Carlo Sampling based on Sobol' sequences, can significantly mitigate these effects. Even though commercial CAT-tools are mainly based on crude Monte Carlo Sampling procedures, it is a good alternative in code-based tolerance analysis routines. Besides, the resulting margin of error depends on how the selected nc-rate is derived from the resultant frequency distribution of the function-relevant KCs. While the literature has mainly preferred non-parametric methods, the proposed mathematical description of the estimation via the cumulative frequency distribution of the assembly responses provides parametric alternatives for estimating the nc-rates. If the distribution follows a verifiable distribution, *parametric cumulative distribution function-based nc-rate estimation* leads to significantly more accurate results with the same number of samples. However, their use only accurately applies to assemblies with a single KC. If several KCs are function-relevant, the occurring correlations can only be represented by the proposed non-parametric nc-rate estimation. Not only the last example of the e-cross skate has shown exemplarily that *the incorporation of one overall nc-rate in the optimization problem has a positive effect on its accuracy and avoids the disadvantages of the common separate consideration via multiple constraints*. Although the methods above can reduce the noise in the optimization and, thus, the final scatter in the optimization results, certain randomness remains due to the repetitive execution of the sampling-based tolerance analysis. The proposed *idea of using the same random numbers for the inverse sampling* transforms the probabilistic problem into a deterministic one and eliminates these effects within the optimization. As quantified, it contributes to accuracy and stability in solving the optimization problem and to avoid a dominant underestimation of the nc-rates.

Besides these concrete countermeasures, however, *increased awareness of the impact of sampling on the obtained cost optima and final nc-rates is essential*. Low maximum nc-rate limits require significantly higher sample sizes to make reliable statements. Initial estimates using proportion confidence intervals and repetition of the analysis with different random numbers can be used to estimate the error before or after optimization and to draw the appropriate conclusions.

RQ2: How can the completeness of sampling-based tolerance-cost optimization be enhanced so that industrial-relevant issues are suitably addressed?

A further essential benefit of sampling-based tolerance analysis is that any distribution type can be virtually mimicked for the geometrical part characteristics. This advantage can be exploited in sampling-based tolerance-cost optimization to address *optimal machine/supplier selection simultaneously with tolerance allocation*. The proposed mixed-integer optimization method allows for cost-optimal decisions to be made already in the design phase at the assembly level by mapping machine- and supplier-specific part tolerance distributions while considering alternatives for realizing the individual parts with their optimally allocated tolerances. Based on this, the proposed method extension solves the previously existing limitation to a single choice selection by enabling the virtual mapping of *distributed manufacturing to several suppliers or machines per tolerance*. The sampling-based representation of the individual batches significantly contributes to ensuring that these can be appropriately addressed in the optimization and determined in a least-cost manner. In addition to pure random assembly, the novel idea also *offers opportunities for sophisticated assembly strategies such as selective assembly*. An approach for concurrent tolerance allocation and selective assembly has been developed and applied in this thesis. The results indicate that they foster the already initiated shift to a process-oriented design of tolerance allocation by representing practical part manufacturing scenarios more realistically.

One crucial shortcoming hindering its application in industry is the lack of focus of the methods on geometrical tolerances. A systematic structuring of geometrical tolerances on feature, part, and assembly level is helpful to identify occurring correlations between several components and features. The advantages are particularly evident in larger assemblies such as the final e-cross skate example making the problem's complexity manageable. The introduced method of *design dimension reduction based on equality matrices and adding further constraints to conform with the GD&T rules* allow the derivation of valid and industrially applicable tolerance values. Thus, the presented enhancements close open gaps regarding the completeness and, thus, increase the applicability of tolerance-cost optimization.

RQ3: How can the efficiency of sampling-based tolerance-cost optimization be improved to handle complex optimization problems in reasonable computing times?

While statistical approaches based on convolution or reliability methods require only one function evaluation and, thus, a fraction of the computation time, several hours are standard for one single optimization run using sampling-based tolerance analysis, significantly depending on the sample size, as the different case studies in this thesis have shown. The presented methods for increasing the efficiency with *adaptive sample sizes* and *adaptive surrogate models* can demonstrably provide a remedy. A harmonized increase of the sample size over optimization with simultaneously recalculating the relevant solutions with the final sample size ensures the validity of the solutions in lower computation times. Replacing the entire tolerance analysis with surrogate models and continuously retraining them with the real values of promising intermediate results can counteract the computational disadvantage of a repetitive evaluation of the real assembly response functions. Consequently, adaptive surrogate model-based optimization can drastically reduce computation times, so advanced tolerance analysis software can be incorporated into the optimization problem. Though the concrete impact of the method always depends on the choice of algorithms, their settings, as well as the optimization problem's nature and complexity, it can nevertheless be stated that the optimization times can be reduced to an acceptable level while simultaneously ensuring the optimality and feasibility of the results.

Impact of the scientific findings on this thesis' global research goal

Tolerance allocation, as one of the main activities in tolerance design, can be performed at different stages with different objectives, boundaries, and groups of interests. Fig. 73 emphasizes that it can be applied in early tolerance design stages where only little data, information, and knowledge is available but also in the late design stages, pre-production stages, or even in production with a strong focus on the manufacturing and assembly process when in-depth data and information is usable. For this reason, the development of a *modular framework adaptable to the users' needs* (see Fig. 63) was preferred over a direct implementation into a specific CAT-tool or CAD-environment. Using sampling methods for tolerance analysis in combination with metaheuristics provides a profound basis for its implementation as a broadly applicable and ease of use tool for designers – although algorithms and optimization-based workarounds "do not completely exclude the expertise of a tolerance designer" [192].

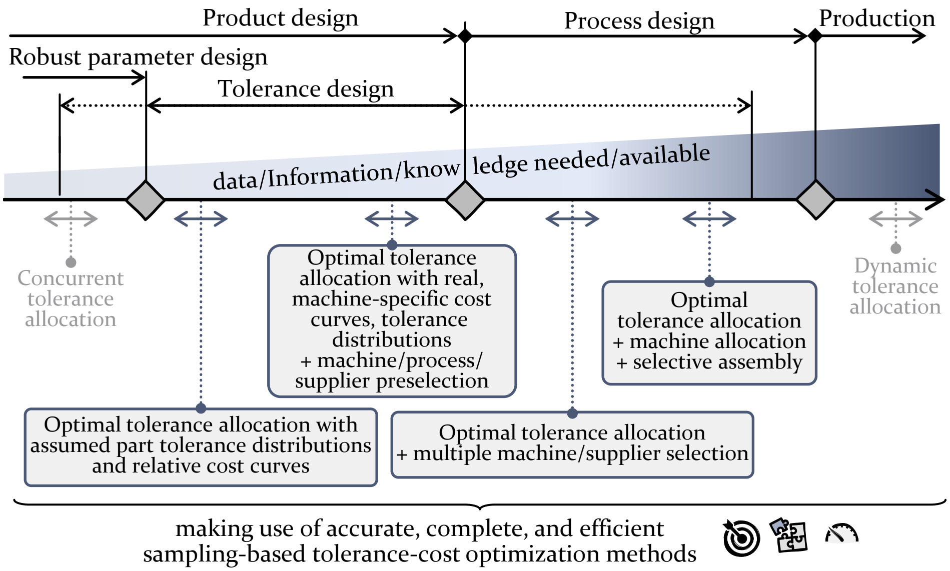

Figure 73: Different stages in the product development process to perform optimal tolerance allocation with different objectives.

Open issues and future challenges

The later sampling-based tolerance-cost optimization is applied in the product development process, the more crucial it is that it is based on meaningful tolerance-cost information, process limits, and part tolerance distributions. Numerous scientific approaches already exist for systematically acquiring tolerance-cost curves, but these mostly provide for extensive preliminary studies on suitable test specimens [P6, P7, S12]. However, initially derived machine-specific distributions do not remain constant over lifetime but are subject to variations. Furthermore, the simplified assumption that they are the same for all selectable tolerance values may not reflect reality.

Instead, for reliable conclusions and approaches such as machine selection and allocation, a large amount of up-to-date data is necessary to map the respective manufacturing situations accurately. Otherwise, insufficient sample sizes, unavoidable measurement uncertainties, and fitting errors of the part tolerance probabilities [601] result in misleading optimization results. The potential of directly using inspection data in tolerance design is well known [198, 598]. Innovative approaches based on digital twins are getting attention for tolerance allocation to gather the knowledge on part tolerance probability distributions in production and have to be continued to obtain and provide the necessary information "on the fly". From a methodological point of view, tolerance allocation is ready for practical application. However, the general lack of tolerance-cost information and the effort to gain it is still a significant obstacle to its profitable application in the industry, which must finally be tackled in future research works.

The presented methods for increasing its efficiency have proven their potential. Further research, e.g., on the *selection of hyperparameters in surrogate modeling and optimization* or *the choice of the adaptive function, its parameters, and surrogate model types for adaptive surrogate model-based optimization*, may provide essential findings to further accelerate tolerance-cost optimization. Moreover, the developed methods for machine selection and allocation enable their extension by aspects of process scheduling, thus further expanding the current context of use to the manufacturing pre-processing and processing phases. This allows, for instance, a dynamic tolerance allocation in ramp-up or series production to respond to variations such as suppliers or machine capacities and availability.

The focus of this thesis was primarily on increasing the accuracy, completeness, and efficiency of defining the tolerance-cost optimization problem and solving it by metaheuristic algorithms using sampling-based tolerance analysis techniques to statistically assure product quality. However, the applicability of optimal tolerance allocation is also largely dictated by the effectiveness and efficiency of all activities, particularly the preliminary pre-processing ones, comprising the tolerance specification and the definition of the tolerance analysis and tolerance-cost model. Although the proposed framework can serve as an initial basis for the practical implementation of a structured optimal tolerance allocation process, *detailed studies are still* *required to assess its suitability for its application to the problems and scenarios faced in the industry*. Findings from prototypical benchmark tests in real product development processes are vital to turn the methods, which have already been thoroughly elaborated in academic research, into a practicable tool for cost-optimal tolerance allocation and establish it as an essential part of the product development process. Since the ease of use and users' satisfaction are essential for its usability, but highly subjective [174], representative user studies are required to identify the need for improvement and further research.

> *To conclude, the developed methods combined with the scientific knowledge gained help to take a further step towards a severe, practical solution for optimal tolerance allocation capable of addressing the problems faced in the industry. Despite its major but manageable challenge in computational efficiency, sampling-based tolerance-cost optimization bears the potential to be the key to exploiting the largely unused cost potentials in tolerance design while finding an optimal trade-off between the various objectives and interests.*

9 Summary and Outlook

The challenge in tolerance allocation is to bring the tolerance values of all individual parts into line with each other and specify them *only as tight as necessary, but as wide as possible* to meet the high quality and cost requirements. The method of tolerance-cost optimization picks up this merely qualitative principle and transforms it into a mathematical optimization problem, whereby the manual search for the quality-cost optimum can be automated and accelerated with powerful algorithms.

Although the scientific achievements of the last five decades have continuously increased the scope and performance of this optimization-based method for tolerance allocation, it still needs to meet the requirements for solving practical problems of industrial complexity. The synergy effects of combining sampling methods for statistical tolerance analysis and metaheuristic algorithms for optimization have been recognized early in research and practice. Promising approaches for sampling-based tolerance-cost optimization are already available. However, despite their potential, they currently still show major weaknesses in effectiveness and efficiency, making a productive use difficult.

Following the global aim of improving the **usability of optimization-based tolerance allocation**, this thesis emphasized the development of appropriate methods to increase the **accuracy, completeness, and efficiency of sampling-based tolerance-cost optimization** and their alignment in a coherent framework (see Fig. 74).

The first part of this work has indicated that the sampling technique, the sample size, and the method for non-conformance rate estimation significantly influence the **accuracy of the tolerance analysis** and, thus, the optimization. On the one hand, the developed methods help to reduce sampling-induced uncertainties. On the other hand, they enable a sufficiently accurate estimation of the nc-rate for single and multiple interrelated assembly response functions. The studies have proven that these countermeasures can ensure the validity, optimality, and, thus, the reliability of the optimization results.

The second part of this work has made use of the description of geometrical variations via probability distributions and supplemented tolerance allocation by a realistic selection and allocation of manufacturing machines and suppliers. The expansion of the search space to include design variables for machine selection and allocation and the definition of linear and nonlinear constraints offer the possibility to map the manufacturing process and capacity limits as well as geometrical tolerances being correlated through shared geometrical features and multiple used parts. The preceding representation of elements from manufacturing process planning not only contributes to the **completeness of sampling-based tolerance-cost optimization for its application in the design phase** but also provides opportunities for its use in further product development phases, such as in the fabrication and assembly process planning phase and production phases.

Aiming to reduce the high computational effort, which results from the iterative procedure of the optimization algorithms and which is mainly dominated by the sampling-caused repetition of the prediction of the accumulated part variations in the assembly, the third part of this work dealt with the development of methods to **increase the efficiency of sampling-based tolerance-cost optimization**. It has been shown that variable sample sizes increasing over the optimization history and the approximation of tolerance analysis steps through surrogate models can substantially reduce the computation time. Refining surrogate models during optimization with selectively recalculated intermediate results – also known in literature under the term *adaptive surrogate models* – is proven to further enhance the efficiency of tolerance-cost optimization without the need to oversimplify the tolerance allocation problem.

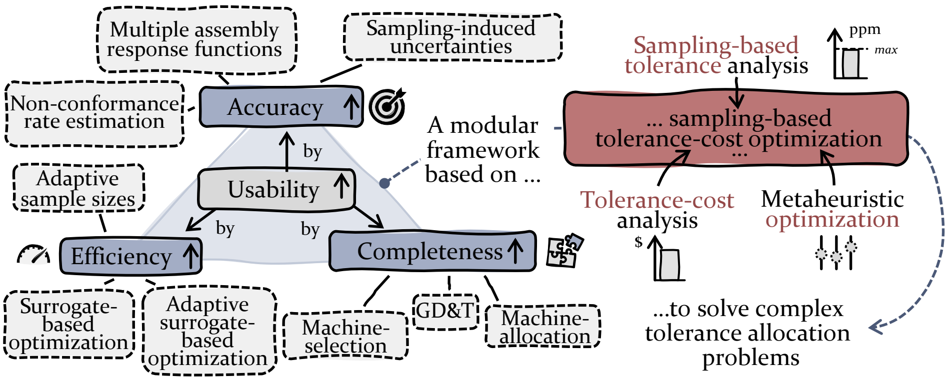

Figure 74: Main contents of the work and developed methods increasing the accuracy, completeness, and efficiency of sampling-based tolerance-cost optimization at a glance.

The application and evaluation of the developed and prototypically implemented framework for optimal tolerance allocation based on sampling-based tolerance-cost optimization in the fourth part have shown that it allows for a cost-optimal tolerance allocation for complex assemblies. The example of a front wheel axle assembly of an electrified cross skate showed its potential to cope with nonlinear assemblies with several interrelated assembly response functions and correlated geometrical tolerances. It can be performed in reasonable computing times but without having to restrict the accuracy and completeness of the problem too much in support of efficiency.

Nevertheless, the final evaluation of its strengths and weaknesses revealed that there is a need for further research that goes beyond the scope of this thesis. In addition to the enhancement of the methods for machine/supplier allocation and selection and for increasing efficiency, there is a need for further research in the implementation and testing of the proposed tolerance allocation workflow in practical product development processes gaining insights on further shortcomings in the accuracy, completeness, and also satisfaction. In doing so, a prerequisite for its application is the availability of up-to-date tolerance-cost data. The manufacturing probability distributions modeled in the sampling require comparatively large amounts of data to provide an accurate prognosis. Therefore, their systematic acquisition, processing, and provision must be studied in detail in further research activities.

In conclusion, the methods and findings presented in this thesis can make an important contribution to the evolution of tolerance-cost optimization as the key to optimal tolerance allocation, which has grown over the past half-century. Nevertheless, further years of intensive research will still be necessary to exploit its full potential in industrial practice.

10 Zusammenfassung und Ausblick

Die Herausforderung in der Toleranzallokation besteht darin, die Toleranzwerte aller Einzelbauteile aufeinander abzustimmen und *lediglich so eng wie nötig, jedoch so weit wie möglich* festzulegen, um so den hohen Qualitäts- und Kostenanforderungen gerecht zu werden. Die Methode der Toleranz-Kosten-Optimierung greift diesen rein qualitativen Grundgedanken auf und überführt ihn in ein mathematisches Optimierungsproblem, wodurch sich die manuelle Suche nach dem Qualitäts-Kosten-Optimum mithilfe von Algorithmen automatisieren und beschleunigen lässt.

Obgleich sich diese optimierungsbasierte Variante der Toleranzallokation durch die wissenschaftlichen Errungenschaften der letzten fünf Jahrzehnte kontinuierlich in Umfang und Leistungsfähigkeit steigern konnte, kann sie den Ansprüchen zur Lösung praktischer Problemstellungen von industrieller Komplexität derzeit noch nicht gerecht werden. Die Synergieeffekte, welche sich aus der Kombination von Samplingverfahren für die statistische Toleranzanalyse und metaheuristischen Algorithmen zur Optimierung ergeben, wurden in der Literatur und Praxis schon sehr früh erkannt. So liegen bereits vielversprechende Ansätze für die samplingbasierte Toleranz-Kosten-Optimierung vor. Trotz ihres Potentials zeigen diese derzeit jedoch noch große Schwächen in Effektivität und Effizienz und erschweren dadurch einen produktiven Einsatz.

Unter der globalen Zielsetzung, die **allgemeine Anwendbarkeit der optimierungsbasierten Toleranzallokation** zu verbessern, legte die vorliegende wissenschaftliche Arbeit den Schwerpunkt auf die Entwicklung geeigneter Methoden zur Steigerung der **Genauigkeit, Vollständigkeit und Effizienz der samplingbasierten Toleranz-Kosten-Optimierung** sowie deren Abstimmung in einem Rahmenwerk (siehe Fig. 75).

Der erste Teil dieser Arbeit hat dabei gezeigt, dass das Samplingverfahren, die Stichprobengröße und die Methode zur Ausschussratenschätzung die **Genauigkeit der Toleranzanalyse** und dadurch auch der Optimierung wesentlich beeinflussen. Die entwickelten Methoden tragen einerseits zur Reduktion der samplinginduzierten Unsicherheiten bei, anderseits erlauben diese eine hinreichend genaue Schätzung der Konformitätsrate für eine sowie mehrere verknüpfte Baugruppenantwortfunktionen. Die Untersuchungen haben unter Beweis gestellt, dass dadurch die Gültigkeit und Optimalität der Optimierungsergebnisse sichergestellt werden kann.

Der zweite Teil dieser Arbeit hat sich die Beschreibung von Geometrieabweichungen über Häufigkeitsverteilungen zu Nutze gemacht und die

Toleranzallokation um eine realitätsnahe Vorauswahl und -allokation von Fertigungsmaschinen bzw. Zulieferern vervollständigt. Die Ausweitung des Suchraums auf Designvariablen zur Maschinenselektion und -allokation sowie die Definition von linearen und nichtlinearen Nebenbedingungen erlauben die Abbildung von Fertigungsprozess- und -kapazitätsgrenzen sowie geometrische, über gemeinsame Fertigungsschritte und Geometrieelemente korrelierte Toleranzen. Die vorgelagerte Abbildung von Elementen aus der Fertigungsprozessplanung trägt hierbei nicht nur zur **Vollständigkeit der Methode für ihre Anwendung in der Designphase** bei, sondern eröffnet darüber hinaus auch Möglichkeiten zur Nutzung in weiteren Produktentstehungsphasen, wie z. B. in Planungsphasen von Einzelteilfertigungs- und Montageprozessen und während der Produktion.

Um den hohen Rechenaufwand zu reduzieren, welcher sich durch das iterative Vorgehen der Optimierungsalgorithmen ergibt und dabei wesentlich durch die samplingbedingte Wiederholung der Simulation der abweichungsbehafteten Baugruppenzustände bestimmt wird, widmete sich der dritte Teil dieser Arbeit der Entwicklung von Methoden zur **Steigerung der Effizienz der samplingbasierten Toleranz-Kosten-Optimierung**. Es hat sich gezeigt, dass variable, über dem Optimierungsverlauf zunehmende Stichprobengrößen sowie die Approximation von Toleranzanalyseschritten durch Ersatzmodelle die Rechenzeiten wesentlich reduzieren können. Eine Verfeinerung der Metamodelle während der Optimierung mit gezielt nachgerechneten Zwischenergebnissen – in der Literatur auch unter dem Namen *adaptive surrogate models* bekannt – trägt nachweislich zur weiteren Verbesserung der Effizienz der Toleranz-Kosten-Optimierung bei, ohne dabei das Toleranzallokationsproblem zu sehr vereinfachen zu müssen.

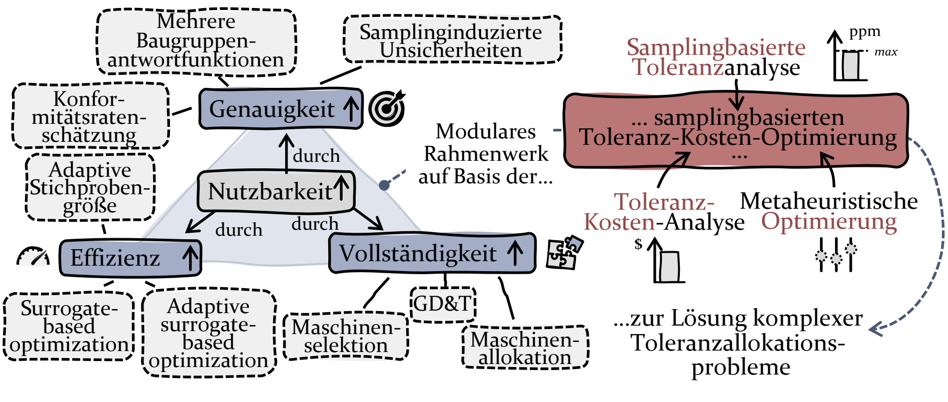

Figure 75: Wesentliche Inhalte der vorliegenden Arbeit und entwickelte Methoden zur Steigerung der Genauigkeit, Vollständigkeit und Effizienz der samplingbasierten Toleranz-Kosten-Optimierung im Überblick.

Die finale Anwendung und Evaluierung des im vierten Teil entwickelten und prototypenhaft implementierten Ansatzes hat exemplarisch am Beispiel einer Vorderachsbaugruppe eines elektrifizierten Cross Skates gezeigt, dass die aufeinander abgestimmten Einzelmethoden gewährleisten, dass eine kostenoptimale Toleranzallokation für komplexe, nichtlineare Baugruppen mit mehreren verknüpften Baugruppenantwortfunktionen sowie voneinander abhängigen Form-und Lagetoleranzen in vertretbaren Rechenzeiten durchgeführt werden kann, ohne dabei die Genauigkeit und Vollständigkeit der Problemstellung zugunsten der Effizienz zu stark einschränken zu müssen.

Nichtsdestotrotz hat die abschließende Beurteilung der Stärken und Schwächen ergeben, dass es über diese Arbeit hinaus noch Forschungsbedarf gibt. Neben der Weiterentwicklung der Methoden zur Maschinen-/Zuliefererselektion und -allokation sowie zur Effizienzsteigerung gilt es, das vorgeschlagene Rahmenwerk zur Toleranzallokation in praktische Produktentwicklungsprozesse zu implementieren und zu erproben, um Erkenntnisse über mögliche Defizite in der Genauigkeit, Vollständigkeit und Benutzungszufriedenheit zu gewinnen. Voraussetzung, dass die Toleranz-Kosten-Optimierung jedoch überhaupt angewandt werden kann, ist die Verfügbarkeit aktueller Toleranz-Kosten-Daten. Dabei erfordern die im Sampling abbildbaren Fertigungshäufigkeitsverteilungen vergleichsweise große Datenmengen, um eine valide Prognose liefern zu können. Deren systematische Erfassung, Verarbeitung und Bereitstellung muss daher in weiteren Forschungsaktivitäten gezielt untersucht werden.

Abschließend lässt sich festhalten, dass die in dieser Arbeit vorgestellten Methoden und Erkenntnisse einen wichtigen Beitrag zur Weiterentwicklung der über des letzten halben Jahrhunderts gereiften Methode zur Toleranz-Kosten-Optimierung als Schlüssel für die optimale Toleranzallokation liefern können. Dennoch sind weitere Jahre an intensiver Forschung nötig, um ihr Potential in der industriellen Anwendung vollständig ausschöpfen zu können.

Appendix

A.1 Terminology in the field of tolerance-cost optimization

Several terms are used in literature presenting methods that aim to find an optimal set of tolerance values [P1]. In this regard, they are composed mainly of a suitable noun and one or more additional adjectives. Fig. 76 gives an overview of the used terms, identified by a screening of the database presented in the subsequent Appx. A.2.

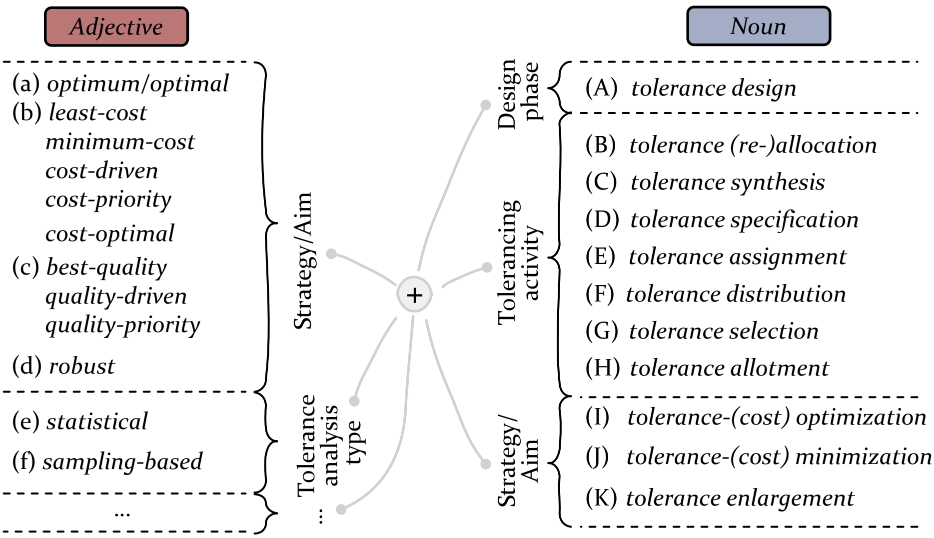

Figure 76: Terms often used in literature for methods aiming to find optimal tolerance values.

Besides the product development phase in focus, the *tolerance design* (A), different names of tolerancing activities (B)-(H), which are not consequently differed in literature, are often used interchangeably (see Sec. 2.1) to introduce or apply optimization-based tolerance allocation techniques. The adjectives (a)–(d) indicate the strategy or concrete aim. In addition to adjectives, which are used to emphasize the usage of *statistical* (e) or *sampling* techniques (f) for tolerance analysis, other words may be prefixed, for instance, *dimensional* or *geometrical* to indicate the tolerance types in focus, the problem type, such as *non-linearity*, or optimization-specific details, e.g., regarding the number of objectives, the existence of constraints or the nature of the equations and design variables and their permissible values [419]. Moreover, the terms *tolerance(-cost) optimization* (I), *minimization* (J), and *enlargement* (K) can be used to emphasize the aim or strategy of the method directly.

As a consequence, numerous definitions were presented in literature over the years to characterize the methods aiming to find the optimal tolerance values as a compromise between cost and quality. Tab. 3 gives an overview of different definitions and their references. In this thesis, the term tolerance-cost optimization and its definition, given in Sec. 2.2, are preferred. In addition, it can suitably be extended by the adjective *sampling-based*, thus leading to the detailed definition for the methods focused in this thesis given in Sec. 2.2.

Table 3: Featured definitions and descriptions of methods to identify feasible and optimal part tolerance values.

Definition	**Ref.**
"[Tolerance allocation is to be] asked to specify the individual components dimensional tolerances to satisfy the total assembly tolerance which is dictated by functionality and quality requirements."	[179]
"Tolerance allocation involves the assignment and the distribution of the values of tolerances and therefore is the inverse problem of tolerance analysis."	[23]
"Tolerance allocation asks the question, given the system tolerances what should the component tolerances be?"	[264]
"Tolerance allocation is the process to distribute or to assign proper tolerance specifications to a part or to an assembly. The distribution criteria are often based on manufacturing costs."	[602]
"Tolerance allocation [aims at] determining how to distribute the allowable variation on the dimension of interest amongst all the independent contributors."	[282]
"[Optimal tolerance selection] is a method for specifying independent functional tolerances in an optimal least-cost manner."	[38]
"[T]olerance allocation uses optimization techniques to assign component tolerances such that the cost of production of an assembly is minimized."	[129]
"Tolerance synthesis is formulated [...] as an optimization problem by treating cost minimization as the objective function and the stack-up conditions as the constraints."	[297]
"[T]olerance allotment becomes an optimization problem to determine the optimal allotment of the tolerances under the constraints of the function requirements and acceptance probability."	[27]
"[T]olerance allocation is to distribute tolerances among relevant design constraints to achieve the lowest overall manufacturing costs."	[603]
"Tolerance allocation uses overall assembly tolerances and allocates component tolerances based on relative contributions to the assembly and production costs."	[604]
"Tolerance allocation [...] is concerned with allocating component tolerances while observing the total assembly tolerance in a way to minimize total manufacturing cost."	[498]

– Continued from Tbl. 3 –

Definition	Ref.
"Tolerance selection is a simultaneous design activity that involves the analysis of all factors that affect product variability, over the life cycle of the product and of the process, and their associated costs."	[346]
"[T]olerance allocation: the values of all specified tolerances are determined by either refining empirical tentative values or optimizing them according to cost–tolerance functions."	[104]
"Optimal tolerance design aims at assigning tolerances such that the functionality requirements are achieved with minimum cost."	[605]
"The objective of tolerance design is to determine the component tolerances such that the requirement of assembly tolerance can be met and the assembly cost may be minimized."	[606]
"Tolerance allocation is closely related to the quality and cost of a product, in that the lowest possible manufacturing cost is sought while satisfying certain quality requirements."	[299]

A.2 Literature review

The underlying literature review of this thesis, presented in Sec. 2.3, is an update of the findings published in 2020 by the author in [P1], and extended by additional categories and aspects. The general aims of the literature review are in correspondence to [607]; first, to illustrate the general trends of research and the historical development of tolerance-cost optimization from 1970–2023; second, to summarize and classify the individual findings; and, third, to reveal the current gaps based on this information. As various terms for tolerance-cost optimization have been used interchangeably in the past (see Appx. A.1), the research databases and engines *Google Scholar*, *Scopus*, *ResearchGate* and *Semantic Scholar* were used for a first systematic screening using the terms given in Appx. A.1 as search strings. The number of identified papers was manually reduced to the relevant ones by studying their abstracts and full texts. In a second step, the remaining articles were screened manually for appropriate cross-references to identify the articles which were missed out in the first run. As a result, an initial topic-related database was created and served as the basis in [P1, P2]. To keep the database up-to-date, it was further extended by recent publications[1]. As a result, a total

[1] The literature study considers all articles published and accessible to the author until the cut-off date of 05/01/2023 related to tolerance-cost optimization. Thus, it does and cannot claim to be fully complete. Nonetheless, it covers the most relevant, officially published research works.

amount of 399 relevant papers was finally identified, mainly contributing to the research field of tolerance-cost optimization (see Fig. 77).

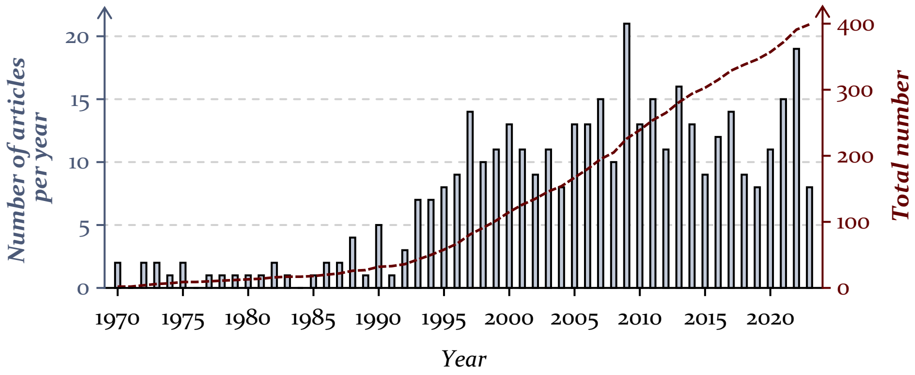

Figure 77: Number of articles published between 1970-2023 considered in the literature review.

In a further step, they were classified by the author concerning the following aspects:

1. Type of costs: either only the manufacturing costs C or additional costs due to quality losses QL are defined as objective(s) and/or constraint(s) (*Cost type*: $C/C + QL$).
2. Alternative selection: if an optimal selection of either machines and/or processes and/or suppliers to realize a part tolerance value are considered in addition to tolerance allocation or not (*Alt. sel.*: *No*/*Yes*).
3. Concurrent tolerance allocation: either only design tolerances or additional machine tolerances form the design variables (*Conc.*: *No*/*Yes*).
4. Type of tolerance: classifies if the values of dimensional or geometrical and dimensional tolerances are allocated by the optimization algorithm (*Tol. type*: *Dim*/*GD&T*).
5. Type of tolerance analysis method: the tolerance analysis methods used in the optimization are classified in arithmetic, worst case, and statistical, while statistical approaches are further classified if they are sampling-based or not (*Tol. analysis type*: *Arith.*/*Stat.*/*Samp.*).
6. Type of solution procedure: the presented approaches are classified into non-metaheuristic, i.e., mathematical optimization algorithms, search algorithms or methods adopted from quality engineering, e.g., DOE- and ANOVA-based approaches, and (meta-)heuristic optimization algorithms (*(Meta-)heur.*: *No*/*Yes*).

The results, visualized in Fig. 11 and discussed in detail in Sec. 2.3, are summarized in Tbl. 4.

Table 4: List of classified references as the basis for the literature review presented in Sec. 2.3.

Ref.	Year	Cost type		Alt. sel.		Conc.		Tol. type		Tol. analysis type			(Meta-)heur.	
		C	$C+QL$	*No*	*Yes*	*No*	*Yes*	*Dim*	*GD&T*	*Arith*	*Stat*	*Samp*	*No*	*Yes*
[244, 608]	1970	x		x		x		x		x			x	
[126]	1970	x		x		x		x			x		x	
[541]	1972	x		x		x				x			x	
[306]	1972	x		x		x		x			x		x	
[609]	1973	x		x		x		x			x		x	
[610]	1973	x		x		x					x	x	x	
[422]	1974	x		x		x				x			x	
[357]	1975	x		x		x		x			x		x	
[611]	1975	x		x		x		x		x			x	
[38]	1977	x			x	x		x			x		x	
[127]	1978	x		x		x		x			x		x	
[358]	1979	x		x		x		x			x			x
[540]	1980	x		x		x					x		x	
[295]	1981	x		x		x		x		x			x	
[296]	1982	x		x		x		x			x		x	
[360]	1982	x		x		x		x			x		x	
[191]	1983	x		x		x		x		x			x	
[535]	1985	x		x		x		x			x		x	
[176]	1986	x		x		x		x		x			x	
[278]	1986	x		x		x		x			x		x	
[184]	1987	x			x	x		x			x		x	
[501]	1987	x			x	x		x			x		x	
[40]	1988	x		x		x		x			x		x	
[504]	1988	x			x	x		x			x		x	
[359]	1988	x		x		x		x			x		x	
[179]	1988	x		x		x		x		x			x	
[186]	1989	x			x	x		x			x		x	
[180]	1990	x		x		x		x			x		x	
[312]	1990	x			x	x		x			x		x	
[249]	1990		x	x		x		x			x			
[297]	1990	x		x		x		x			x		x	
[123]	1990	x		x			x	x		x			x	
[97]	1991	x		x		x		x		x				x
[438]	1992	x				x		x			x	x		x
[451]	1992		x	x		x		x			x			x
[44]	1992	x			x		x	x		x				x
[266]	1993	x		x		x					x		x	
[27]	1993	x		x		x		x			x	x		x
[36]	1993	x		x		x		x			x		x	
[200]	1993		x	x		x		x			x		x	
[364]	1993	x		x		x			x	x			x	
[93]	1993	x		x			x	x		x				x
[177]	1993	x			x	x		x			x			x
[612]	1994		x	x		x		x		x			x	
[190]	1994	x		x		x			x	x			x	
[613]	1994	x			x	x		x		x			x	
[264]	1994	x		x		x					x		x	
[614]	1994		x	x		x							x	
[615]	1994		x	x		x		x		x			x	
[558]	1994		x	x		x		x		x			x	
[250]	1995		x	x		x		x			x		x	
[26]	1995		x	x		x		x			x		x	
[616]	1995	x		x		x		x			x			x
[136]	1995	x			x	x		x		x			x	
[498]	1995	x			x	x		x			x		x	
[199]	1995	x		x		x		x		x			x	

– Continued from Tbl. 4 –

Ref.	Year	Cost type		Alt. sel.		Conc.		Tol. type		Tol. analysis type			(Meta-)heur.	
		C	*C + QL*	*No*	*Yes*	*No*	*Yes*	*Dim*	*GD&T*	*Arith*	*Stat*	*Samp*	*No*	*Yes*
[617]	1995		x	x		x		x		x			x	
[9]	1995	x				x		x		x			x	
[428]	1996	x		x		x		x			x		x	
[271]	1996	x		x			x	x		x				x
[46]	1996	x		x		x			x		x	x		x
[436]	1996		x	x		x		x			x		x	
[37]	1996	x		x		x			x	x				x
[618]	1996	x			x	x		x			x	x	x	
[192]	1996	x			x	x			x		x	x		x
[403]	1996		x	x		x		x			x	x	x	
[32]	1996	x			x		x	x			x		x	
[154]	1997	x		x			x	x		x				x
[133]	1997	x		x		x		x		x				x
[603]	1997	x			x		x	x		x			x	
[47]	1997	x		x			x	x		x				
[251]	1997		x	x		x		x			x		x	
[258]	1997		x	x		x					x		x	
[135]	1997	x		x		x		x			x	x	x	
[221]	1997	x			x		x	x			x			x
[405]	1997	x			x	x			x		x	x		x
[619]	1997	x		x			x	x		x			x	
[620]	1997	x			x		x	x		x			x	
[352]	1997		x	x		x		x			x	x	x	
[232]	1997		x		x	x		x			x			x
[621]	1997		x	x		x		x			x		x	
[452]	1998	x		x		x		x			x			x
[406]	1998		x	x		x					x	x	x	
[363]	1998	x		x		x		x			x		x	
[551]	1998	x			x		x	x		x				
[222]	1998	x			x		x	x		x				
[622]	1998	x			x	x		x		x			x	
[487]	1998		x	x		x		x					x	
[532]	1998	x		x		x		x			x	x	x	
[259]	1998		x	x		x		x			x		x	
[623]	1998		x	x		x		x			x		x	
[204]	1999	x			x	x		x			x		x	
[129]	1999	x			x	x		x			x		x	
[624]	1999	x		x		x			x		x		x	
[265]	1999	x		x		x			x		x		x	
[488]	1999		x	x		x		x		x			x	
[387]	1999		x	x		x			x		x	x	x	
[386]	1999		x	x		x			x		x	x	x	
[625]	1999	x			x	x		x		x			x	
[626]	1999		x	x		x		x			x	x	x	
[185]	1999	x		x			x	x		x			x	
[627]	1999	x		x		x		x			x		x	
[447]	2000	x			x	x		x			x			x
[628]	2000		x	x		x					x		x	
[505]	2000		x		x	x		x			x		x	
[606]	2000		x	x		x		x			x		x	
[629]	2000		x	x			x	x		x			x	
[630]	2000	x			x	x		x			x	x	x	
[631]	2000	x			x	x		x			x		x	
[632]	2000	x			x	x			x		x		x	
[633]	2000	x		x		x			x		x		x	
[634]	2000	x		x		x		x		x				x
[277]	2000	x		x		x		x			x			x
[299]	2000	x		x		x		x			x	x	x	

– Continued from Tbl. 4 –

Ref.	Year	Cost type		Alt. sel.		Conc.		Tol. type		Tol. analysis type			(Meta-)heur.	
		C	$C+QL$	*No*	*Yes*	*No*	*Yes*	*Dim*	*GD&T*	*Arith*	*Stat*	*Samp*	*No*	*Yes*
[17]	2000		x	x		x		x					x	
[231]	2001		x	x		x			x		x	x		x
[247]	2001		x	x		x		x			x		x	
[144]	2001	x			x		x	x			x			
[260]	2001		x		x	x		x			x		x	
[635]	2001	x			x	x		x			x		x	
[412]	2001		x	x		x			x		x	x	x	
[335]	2001		x	x		x		x			x		x	
[636]	2001	x		x		x		x		x			x	
[139]	2001	x			x		x	x		x				x
[187]	2001	x		x		x		x			x		x	
[400]	2001	x		x		x		x			x	x	x	
[365]	2002	x		x		x					x		x	
[344]	2002	x		x		x		x			x		x	
[54]	2002	x		x		x		x		x				x
[5]	2002		x	x		x		x			x	x	x	
[489]	2002		x	x		x		x			x	x	x	
[288]	2002		x	x		x		x			x	x	x	
[298]	2002	x		x		x		x			x	x	x	
[223]	2002	x		x		x			x		x		x	
[637]	2002		x		x	x		x		x			x	
[342]	2003	x		x		x		x			x		x	
[638]	2003	x		x		x			x	x			x	
[213]	2003	x		x		x			x	x			x	
[21]	2003	x		x		x			x		x	x		x
[546]	2003	x		x		x		x			x		x	
[281]	2003	x		x			x	x			x			x
[639]	2003	x		x		x				x				x
[640]	2003	x		x		x		x		x			x	
[641]	2003	x				x		x		x			x	
[201]	2003		x	x			x	x			x		x	
[424]	2004	x		x		x			x		x		x	
[381]	2004	x		x		x					x		x	
[189]	2004	x		x		x		x			x			x
[56]	2004		x		x		x	x			x		x	
[307]	2004	x			x		x	x			x			x
[642]	2004	x			x	x		x		x				x
[96]	2004	x			x	x		x		x				x
[643]	2004	x		x		x		x			x	x	x	
[369]	2005	x		x		x					x		x	
[453]	2005		x	x		x		x			x			x
[283]	2005	x		x		x			x		x			x
[644]	2005	x		x		x			x		x			x
[263]	2005		x	x			x	x		x				
[645]	2005		x		x	x		x			x		x	
[469]	2005	x		x		x		x		x				x
[646]	2005	x		x		x			x	x			x	
[361]	2005	x		x		x		x			x		x	
[647]	2005	x			x		x	x			x			x
[313]	2005	x			x	x		x		x				x
[497]	2005		x		x		x	x			x		x	
[345]	2005	x		x		x		x			x		x	
[648]	2006		x	x		x		x			x			
[649]	2006	x			x	x		x			x			x
[212]	2006		x	x		x					x		x	
[233]	2006		x	x		x		x			x		x	
[45]	2006		x	x		x		x			x		x	
[464]	2006	x		x			x	x			x			x

– Continued from Tbl. 4 –

Ref.	Year	Cost type		Alt. sel.		Conc.		Tol. type		Tol. analysis type			(Meta-)heur.	
		C	$C+QL$	*No*	*Yes*	*No*	*Yes*	*Dim*	*GD&T*	*Arith*	*Stat*	*Samp*	*No*	*Yes*
[493]	2006	x		x		x								x
[398]	2006	x		x		x		x			x	x		x
[456]	2006		x	x		x		x		x				x
[650]	2006		x	x		x					x		x	
[495]	2006	x			x		x	x			x			x
[481]	2006	x			x		x	x		x				x
[457]	2006	x		x			x	x			x			x
[279]	2007	x		x		x			x		x	x		x
[389]	2007	x		x		x			x	x				x
[103]	2007	x		x		x			x		x	x		x
[563]	2007	x		x		x		x			x		x	
[242]	2007	x			x		x		x		x			x
[284]	2007	x		x		x			x		x			x
[527]	2007	x		x		x		x			x			x
[390]	2007		x		x	x					x	x	x	
[425]	2007		x		x	x					x	x	x	
[465]	2007		x	x			x		x		x			x
[651]	2007	x		x		x		x		x			x	
[275]	2007	x		x		x		x						
[652]	2007	x		x		x		x			x		x	
[276]	2007	x		x		x		x						
[274]	2007		x	x		x		x			x		x	
[362]	2008	x		x		x		x			x			
[368]	2008	x		x		x			x		x	x		x
[604]	2008		x		x		x		x		x	x		x
[496]	2008	x			x		x		x	x			x	
[653]	2008		x	x		x		x			x		x	
[196]	2008	x		x		x					x		x	
[261]	2008		x	x			x	x			x		x	
[654]	2008		x	x		x		x		x			x	
[490]	2008	x		x		x		x		x			x	
[245]	2008	x			x		x	x			x			x
[437]	2009	x		x		x		x			x	x	x	
[655]	2009		x	x		x		x			x			
[656]	2009	x		x			x	x			x		x	
[474]	2009		x	x		x		x			x			x
[461]	2009	x		x		x		x			x			x
[605]	2009	x		x		x		x			x		x	
[311]	2009	x		x		x					x	x	x	
[503]	2009	x			x	x		x		x			x	
[466]	2009				x	x		x		x				x
[657]	2009		x	x		x		x			x			x
[658]	2009		x	x			x	x			x			x
[218]	2009	x		x		x		x			x		x	
[257]	2009		x	x		x		x			x		x	
[659]	2009		x	x		x		x			x			x
[458]	2009		x		x	x		x			x			x
[467]	2009		x	x			x	x			x			x
[502]	2009	x			x	x		x		x			x	
[432]	2009		x		x		x		x		x			x
[506]	2009		x		x		x	x		x			x	
[134]	2009	x		x		x			x		x	x		x
[483]	2009		x	x		x		x		x				x
[660]	2010		x	x		x					x		x	
[661]	2010	x			x	x			x		x	x	x	
[211]	2010		x	x			x	x						x
[291]	2010		x	x		x			x		x			x
[227]	2010		x	x		x			x		x			x

– Continued from Tbl. 4 –

Ref.	Year	Cost type		Alt. sel.		Conc.		Tol. type		Tol. analysis type			(Meta-)heur.	
		C	$C + QL$	*No*	*Yes*	*No*	*Yes*	*Dim*	*GD&T*	*Arith*	*Stat*	*Samp*	*No*	*Yes*
[475]	2010	x		x		x								x
[509]	2010		x		x	x		x			x		x	
[463]	2010	x		x		x		x			x		x	
[662]	2010		x	x			x	x			x			x
[468]	2010		x	x			x	x			x			x
[455]	2010		x	x		x		x			x			x
[663]	2010	x		x		x			x		x			
[272]	2010		x	x		x		x		x				x
[664]	2011	x		x		x		x			x		x	
[59]	2011	x		x		x		x			x		x	
[665]	2011	x		x		x		x			x		x	
[290]	2011		x	x		x		x			x			x
[404]	2011	x		x		x		x			x	x	x	
[270]	2011	x		x		x		x		x				
[454]	2011		x	x			x	x			x			x
[330]	2011	x		x		x			x	x			x	
[462]	2011		x	x		x		x			x			x
[33]	2011		x	x			x	x			x			x
[500]	2011		x		x	x		x			x			
[434]	2011		x		x		x	x			x			x
[433]	2011		x		x		x	x		x				x
[435]	2011		x		x		x	x			x			x
[666]	2011		x	x		x		x			x			x
[667]	2012	x		x		x		x		x				x
[193]	2012	x		x		x			x		x	x		x
[397]	2012		x	x		x		x		x				x
[668]	2012	x		x		x		x		x			x	
[669]	2012		x	x		x		x			x	x		x
[670]	2012	x			x	x					x	x	x	
[477]	2012	x		x			x		x	x				x
[262]	2012		x		x	x		x			x		x	
[671]	2012	x		x		x		x			x		x	
[672]	2012		x	x			x	x			x		x	
[431]	2012		x		x		x		x		x			x
[300]	2013	x		x		x					x	x		x
[673]	2013	x		x		x		x			x		x	
[507]	2003		x		x		x	x		x				x
[427]	2013	x		x		x		x			x		x	
[674]	2013	x		x		x		x			x			x
[217]	2013	x		x		x		x			x	x		
[675]	2013	x		x		x		x			x	x		x
[676]	2013	x				x			x		x	x		x
[677]	2013	x		x		x			x		x	x		x
[678]	2013		x		x	x		x			x		x	
[441]	2013		x	x		x		x			x		x	
[491]	2013		x	x		x		x			x		x	
[479]	2013	x		x			x	x			x			x
[679]	2013		x	x		x					x	x		x
[482]	2013	x		x			x	x			x			x
[478]	2013		x	x		x		x						x
[680]	2013	x		x		x		x			x	x		
[303]	2014	x		x		x					x			x
[602]	2014	x		x		x		x			x		x	
[681]	2014	x		x		x		x			x		x	
[382]	2014		x	x		x			x		x			x
[682]	2014		x		x	x		x			x		x	
[293]	2014	x		x		x			x		x			x
[499]	2014		x		x	x		x			x		x	

– Continued from Tbl. 4 –

Ref.	Year	Cost type		Alt. sel.		Conc.		Tol. type		Tol. analysis type			(Meta-)heur.	
		C	$C + QL$	*No*	*Yes*	*No*	*Yes*	*Dim*	*GD&T*	*Arith*	*Stat*	*Samp*	*No*	*Yes*
[31]	2014	x		x		x		x			x			x
[480]	2014		x		x		x	x			x			x
[683]	2014	x		x		x		x			x		x	
[684]	2014	x		x		x			x		x			x
[289]	2014	x		x		x		x			x	x		
[685]	2014		x	x		x			x		x		x	
[686]	2015		x	x		x			x		x	x	x	
[687]	2015		x	x			x	x		x				x
[254]	2015		x	x			x	x		x			x	
[688]	2015		x		x	x		x		x			x	
[689]	2015	x		x		x		x			x			x
[396]	2015	x				x			x		x	x	x	
[286]	2015	x			x	x		x			x	x		x
[690]	2015		x		x		x	x			x			
[691]	2015		x	x		x		x		x				
[416]	2016		x	x		x		x			x		x	
[459]	2016	x			x	x		x			x	x		x
[472]	2016		x		x		x	x			x			x
[12]	2016	x		x		x			x					x
[692]	2016		x		x	x		x			x		x	
[693]	2016		x	x		x		x		x				x
[198]	2016	x		x		x		x			x		x	
[694]	2016	x			x	x		x		x				x
[695]	2016	x		x		x		x		x				x
[287]	2016	x		x		x			x		x	x		x
[255]	2016		x	x		x		x			x			
[273]	2016		x	x		x		x			x		x	
[430]	2017		x		x		x		x	x				x
[243]	2017	x		x			x		x		x	x		x
[269]	2017		x	x			x	x			x		x	
[696]	2017		x	x			x	x			x		x	
[697]	2017		x	x		x		x		x				x
[402]	2017		x	x		x					x	x	x	
[698]	2017		x	x		x		x					x	
[699]	2017		x	x		x		x			x		x	
[700]	2017		x	x		x		x					x	
[423]	2017		x	x		x		x			x		x	
[701]	2017	x		x		x					x	x		
[702]	2017		x		x	x		x			x			
[703]	2017	x		x		x					x			x
[408]	2017	x		x		x			y		x	x		x
[704]	2018		x	x			x	x		x			x	
[367]	2018	x		x		x			x		x	x		x
[415]	2018	x		x		x		x			x	x		x
[492]	2018		x	x			x	x		x			x	
[705]	2018		x		x	x			x		x			x
[494]	2018		x		x		x	x			x			x
[706]	2018		x	x			x			x			x	
[426]	2018	x		x		x		x			x		x	
[366]	2018	x		x		x			x		x	x		x
[239]	2019	x		x		x		x			x		x	
[460]	2019		x	x		x		x			x			x
[707]	2019	x		x		x			x		x			x
[708]	2019	x		x		x			x					x
[414]	2019	x		x		x					x	x		x
[559]	2019		x	x			x	x			x		x	
[471]	2019	x		x		x		x		x				x
[709]	2019		x		x	x		x			x	x		x

– Continued from Tbl. 4 –

Ref.	Year	Cost type		Alt. sel.		Conc.		Tol. type		Tol. analysis type			(Meta-)heur.	
		C	*C + QL*	*No*	*Yes*	*No*	*Yes*	*Dim*	*GD&T*	*Arith*	*Stat*	*Samp*	*No*	*Yes*
[710]	2020	x		x		x		x			x		x	
[203]	2020	x		x		x		x			x		x	
[711]	2020	x		x		x			x		x	x	x	
[564]	2020	x		x		x		x		x				x
[P8]	2020	x			x	x		x			x	x		x
[418]	2020		x	x		x		x			x	x		x
[712]	2020	x		x		x			x		x			x
[713]	2020		x	x		x		x			x	x		x
[14]	2020	x		x		x		x			x	x		x
[229]	2020	x		x		x		x						x
[216]	2020	x		x		x		x		x				x
[301]	2021	x				x			x		x	x		x
[81]	2021	x		x		x			x		x	x		x
[417]	2021		x	x		x			x		x			x
[P3]	2021	x		x		x		x			x	x		x
[130]	2021	x				x		x			x	x		x
[P9]	2021	x			x		x	x			x	x		x
[P2]	2021	x		x		x		x			x	x		x
[476]	2021	x		x		x		x		x				x
[473]	2021	x		x			x	x		x				x
[P11]	2021	x			x	x			x		x	x		x
[714]	2021	x		x		x		x						x
[485]	2021	x		x		x		x			x		x	
[715]	2021		x	x		x					x	x		x
[442]	2021		x	x		x			x		x		x	
[399]	2021	x		x		x			x		x	x		x
[716]	2022	x		x			x	x			x		x	
[394]	2022	x		x		x			x		x	x		x
[P15]	2022	x			x	x		x			x	x		x
[P14]	2022	x		x		x		x			x	x		x
[717]	2022	x			x	x		x		x				x
[P12]	2022	x			x	x		x			x	x		x
[718]	2022	x		x		x		x						
[508]	2022	x		x		x		x			x			x
[214]	2022	x		x			x		x					x
[395]	2022	x		x		x			x		x	x		x
[600]	2022	x		x		x			x		x		x	
[719]	2022	x		x		x		x					x	
[215]	2022	x		x		x		x			x			x
[537]	2022	x		x		x		x			x		x	
[720]	2022		x	x		x		x						x
[721]	2022		x	x			x	x		x				x
[294]	2022	x		x		x			x		x	x		x
[240]	2022	x		x		x		x			x	x		x
[722]	2022	x		x		x		x		x				x
[723]	2023		x	x		x			x		x			x
[724]	2023	x		x		x		x			x	x		x
[725]	2023		x	x			x	x			x			x
[726]	2023	x			x	x		x			x	x		x
[727]	2023	x			x	x			x		x	x		x
[728]	2023	x		x		x		x			x	x		x
[729]	2023	x				x			x		x	x		x
[730]	2023		x	x		x			x	x				x
	Σ =	**252**	**144**	**299**	**92**	**326**	**73**	**290**	**75**	**95**	**281**	**89**	**202**	**174**

The following criteria and aspects were further considered in the classification: In case multiple categories fit to one article, e.g., it considers both worst-case and statistical tolerance analysis as constraints, the more advanced category is chosen. However, suppose techniques are only used as a reference, such as to benchmark a closed-form solution with Lagrange multipliers with (meta-)heuristic optimization algorithms. In that case, the solution proposed and focused in the article is considered. Blank spaces for single criteria indicate that the information is not given in the paper or only incompletely, which did not lead to a clear classification. Thus, non-mechanical products, e.g., electronic circuits or antennas, were not considered in the category *Tol. type*, as only non-geometrical tolerances are being focused on. Following the definition in Sec. 2.2, all proposed approaches that address the costs in the objective(s) or constraints are considered, even if the cost aspect is only indirectly addressed. The main focus is put on tolerance allocation for multiple-part assemblies. However, if methods are applied to single parts and do not address tolerance charting, they are also considered. Assembly technique selection, most relevant in process-driven tolerance allocation, is not included in the criterion *Alt. sel.* as it does not influence the achievement of an allocated part tolerance. Besides metaheuristic optimization algorithms, ANNs and reinforcement learning-based approaches were also classified as (meta-)heuristic.

A.3 Background information on metaheuristic optimization algorithms

Practical, real-world, technical, and scientific optimization problems are mostly mathematically complex since the search spaces are multidimensional and large, they are characterized by multimodal and complex mathematical or numerical, implicit objective functions and are often strongly constrained [444, 484]. Most of these problems are so-called non-polynomial (NP)-hard problems, where the problem's complexity hinders finding a solution in polynomial time [444, 446, 731].

Since resources in time and money are often critical [450], the need for computational resources and times have to be significantly reduced [449] excluding the usage of exact methods [444, 731, 732]. Instead, *high quality, but only near-optimal solutions* to be found in reasonable computing times are considered a sufficient compromise [449]. Stochastic, mostly metaheuristic optimization algorithms have proven their suitability to solve NP-hard problems for various applications in the past [444, 445, 449] and are, thus, often preferred over traditional, mostly deterministic, mathematically programming-based optimization algorithms [445, 446], which show severe deficits in computational efficiency [444, 732], general applicability [446, 449], and are challenging to implement [449].

Based on the general principle of trial-and-error [445, 450], the group of stochastic algorithms comprises practical, efficient, and general-purpose soft-computing optimization techniques [444, 445, 450, 484], which are not based on mathematical theory rather than on heuristics and experience [733]. In this context, the term *metaheuristic* is used to indicate that these algorithms are higher-level heuristic methods, better performing than heuristics [445, 446, 450], which are tailored to specific problem types and, thus, can not easily be applied to others [449, 731].

Since both a purely random, blind-fold search and an exhaustive search are not useful enough on their own [449, 450], metaheuristic algorithms combine the ideas of both local and random search, also called random walks [450]. While the latter helps to exploit a current, promising solution in its neighborhood, randomization helps to explore the total search space and to avoid getting stuck in local minima (see Fig. 78) [444–446, 450]. A thoughtful harmonization of **exploitation**, i.e., **intensification**, and **exploration**, i.e., **diversification**, helps to find the global optimum for multimodal optimization problems [449, 450, 586]. Otherwise, either the algorithm does converge very slowly or not at all, or the global cannot be reached [445, 449].

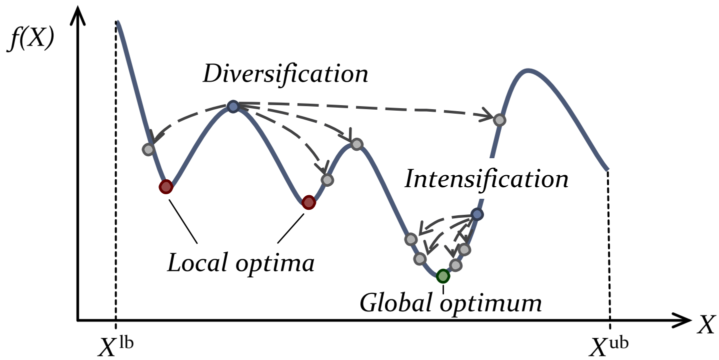

Figure 78: Principle of diversification and intensification illustrated for a multimodal function with local and global minima.

In contrast to deterministic algorithms, metaheuristic algorithms

- do not put any requirements on the type and complexity of objective function [449],
- thus, fit a huge range of problems as black box algorithms [444, 731], even without having to know exactly how the algorithms work [450],
- tolerate uncertain, imprecision or approximate data and functions [444],

- and additionally show their strengths in their simple implementation and potential to be parallelized [449, 731].

However,

- they are highly sensitive to the choice of the algorithm-specific parameters controlling extrapolation and exploitation [484], which are a priori unknown, experience-based and have to be individually defined and tailored to the given problem by the user [449],
- the results are non-deterministic and scatter in different trials caused by random elements [446, 450, 586], and
- they cannot guarantee feasibility, a certain quality, or optimality in advance [445, 449, 450].

Among the different taxonomies [445, 450], for example according to the source of inspiration (see [731, 732]), it is useful to classify them into **trajectory-based** (TB) and **population-based** (PB) algorithms [446, 731]. While the first group is based on a gradual improvement of one single solution, the second one uses a set, the so-called population, of multiple solutions, which is partly or totally replaced by new solutions in each iteration [444, 731]. Despite their lack in efficiency [444], PB optimizers show their strengths in exploration [444] and are, thus, preferably used for more complex problems with numerous local minima.

Regardless of the nature and implementation of the algorithm, the main steps of metaheuristic algorithms can be described in general by the pseudocode illustrated in Algorithm 1. Initially, randomly chosen or based on problem-specific knowledge predefined solutions serve as the starting points where the algorithm improves the solution by algorithm-specific exploitation and exploration operations step by step [444]. This implies selecting the current best [445] and combining and/or modifying the previous solutions [444] based on the fitness values obtained by the objective function while taking the constraints into account by suitable constraint handling methods [450]. The penalty approach is widely used to transform the problem into an unconstrained one by adding a penalty term, typically through a simple sum, to the fitness [21, 734, 735]:

$$f_\mathrm{P}(\boldsymbol{x}) = f(\boldsymbol{x}) + p(\boldsymbol{x}) \qquad (67)$$
$$\text{with: } \begin{cases} p(\boldsymbol{x}) = 0 \text{ if } \boldsymbol{x} \text{ is feasible} \\ p(\boldsymbol{x}) > 0 \text{ otherwise,} \end{cases}$$

where the penalty function $p(\boldsymbol{x})$ can be constant or variable [735]. In doing so, the population moves from neighborhood to neighborhood while intensifying potential optimal solutions [444, 449] until a predefined termination criterion is met, such as a limit of total time or a number of evaluations, etc. [444, 449].

Create one (TB) or more (PB) initial solutions;
while *termination criterion is not met* **do**
  if *exploit* **then**
    Create new solution(s) by exploitation step;
  else
    Create new solution(s) by exploration step;
  end
  Update best-found solution;
end

Algorithm 1: Basic workflow of metaheuristic optimization acc. to [731].

Although there is nowadays a wide variety of different algorithms [731–733], they are similar in their structure and principles [444, 445] and often only variants of already existing metaheuristics imitating successful mechanisms from nature under a new, appealing name [444, 732]. Though it is difficult to assure solution quality through a proper selection, implementation, and application of an algorithm [445], there is a general lack of clear guidelines [445]. Users often pay less attention to evaluating its suitability for the given problem type and its performance [445, 484], which is complicated by their stochastic behavior in any case [449].

Nonetheless, different efficiency and effectiveness measures, sometimes also called robustness [444], help to analyze the performance and interpret the optimization results [586]. This thesis uses the subsequently presented measures to evaluate and compare the obtained optimization results. The formulas are aligned to the notation given in the review in [586]. However, the notation and symbols are slightly adapted for clarification and to fit the symbols already introduced and used in this work. In addition, suitable references where the metrics are used or defined are given respectively.

Feasibility rate FR: Ratio of n_{feas} feasible runs to total number of runs η_r [736]:

$$FR = \frac{n_{\text{feas}}}{\eta_r} = \frac{\sum_{r=1}^{\eta_r} q_{\text{feas}}(\boldsymbol{x_r})}{\eta_r}, \tag{68}$$

where q_{feas} serves as an indicator function to assess the feasibility of the optimization results of run r, which is given when all inequality and equality constraints $g_i(\boldsymbol{x_r})$ and $h_j(\boldsymbol{x_r})$ are satisfied within a tolerance δ_{feas}:

$$q_{\text{feas}}(\boldsymbol{x_r}) = \begin{cases} 1 & \text{if} \quad g_i(\boldsymbol{x_r}) \leq 0 + \delta_{\text{feas}};\ i = 1, \dots, I, \\ & \quad\ \ h_j(\boldsymbol{x_r}) = 0 + \delta_{\text{feas}};\ j = 1, \dots, J. \\ 0 & \text{otherwise.} \end{cases} \tag{69}$$

Success rate *SR*: Ratio of n_{success} successful runs to total number of runs η_r [736, 737]:

$$SR = \frac{n_{\text{success}}}{\eta_r} = \frac{\sum_{r=1}^{\eta_r} q_{\text{feas}}(\boldsymbol{x_r}) \cdot q_{\text{success}}(\boldsymbol{x_r})}{\eta_r}, \tag{70}$$

where q_{success} serves as an indicator function to assess the success of optimization run r, which is given when optimality is reached within the tolerance δ_{success}:

$$q_{\text{success}}(\boldsymbol{x_r}) = \begin{cases} 1 & \text{if} \quad f(\boldsymbol{x_r}) \leq f(\boldsymbol{x}_{\text{opt}}) + \delta_{\text{success}}, \\ 0 & \text{otherwise.} \end{cases} \tag{71}$$

Convergence relation: Ratio of η_g^{opt} generations needed to reach the global optimum (with a predefined tolerance) to the total number of generations η_g [738]:

$$C_{\text{relation}} = \frac{\eta_g^{\text{opt}}}{\eta_g}. \tag{72}$$

Average number of function evaluations *AFESO* taking the number of function evaluations *FEVs* of all n_{success} successful optimization runs acc. to Eq. (71) into account [739]:

$$AFESO = \frac{1}{n_{\text{success}}} \sum_{i=1}^{n_{\text{success}}} FEVs_i. \tag{73}$$

Average computing time $\overline{\tau}_{\text{feas}}$ of all n_{feas} feasible optimization runs with optimization time τ_i:

$$\overline{\tau}_{\text{feas}} = \frac{\sum_{i=1}^{n_{\text{feas}}} \tau_i}{n_{\text{feas}}}. \tag{74}$$

A.3.1 Genetic algorithm (GA)

Evolutionary computation includes numerous search and optimization algorithms based on general evolutionary principles, such as Darwin's theory on the survival of the fittest and natural selection [734, 740]. Well-known examples are evolutionary strategies, evolutionary programming, genetic programming, and genetic algorithms (GA) [734, 735, 741], which show similarities in structure and function, but differences in details, e.g., in the way to represent the decision variables[2] or the used stochastic operators [734, 741]. After its introduction by Holland in 1975 [547] and its first successful applications, GA has become the most popular evolutionary PB algorithm [450, 734, 735, 740, 741] and has proven its strengths to solve a wide range of applications, not only in the field of mechanical engineering [450]. It mimics the biological evolution following the theory of natural selection and genetics [741, 742]. A dynamic population of individuals evolves over the iterations through a set of genetic reproduction/variation operations [21, 740, 743]. Inspired by its biological example, a population consists of a group of **chromosomes** (individual solutions) [731, 743], each characterized by a sequence of **genes** as basic elements [734, 743] representing a single value, also named allele [740], of a design variable [734] (see Fig. 79). New individuals, generated as children from their parents for the next generation, are called the offspring [735, 743]. A portion of both parents and children form the mating pool for the next generation [740]. Furthermore, theory differs between the **genotype**, which is the pure genetic information in the form of chromosomes, and the **phenotype**, which is the expression or trait of the genotype as a result of its interaction with its environment [734, 740, 743].

The main steps of a GA, viz. **recombination**, **mutation** and **selection**[3] [741], are repeated for each generation until a predefined termination criterion is met (see Fig. 79). Since the genetic operators are applied on the genotypes, i.e., on the coded parameter set [734, 735, 742], and selection is performed with respect to the phenotypes [735], the representation of the genotype as well as strategies for mapping the phenotype space to the genotype space (**encoding**) and vice versa (**decoding**) have to be defined first [21, 740]. In literature, various strategies were presented, such as binary, octal, hexadecimal, real number, value, and tree encoding [734].

In alignment with Appx. A.3, the GA starts with an initial, in most cases randomly generated, population with individual chromosomes and the evaluation of its fitness [740], which is "the value of an objective function for its phenotype" [734] (see Fig. 79). In this regard, different techniques to handle constrained optimization problems by GA have been proposed in literature. Although strategies that either directly reject all infeasible solutions, try to repair infeasible ones to become feasible, or modify genetic operators assure that no infeasible individuals are part of the surviving population, it is useful,

[2] Representation describes the way data is structured in the genotype space. However, the word can also be used as the synonym for the encoding process itself. [740]

[3] As emphasized in Appx. A.3, exploration and exploitation have to be balanced within a metaheuristic optimization procedure. In GA, random search is mainly performed by the two genetic operators for reproduction, viz. recombination (crossover) and mutation, while the local search and its exploitation are realized by selection. [735]

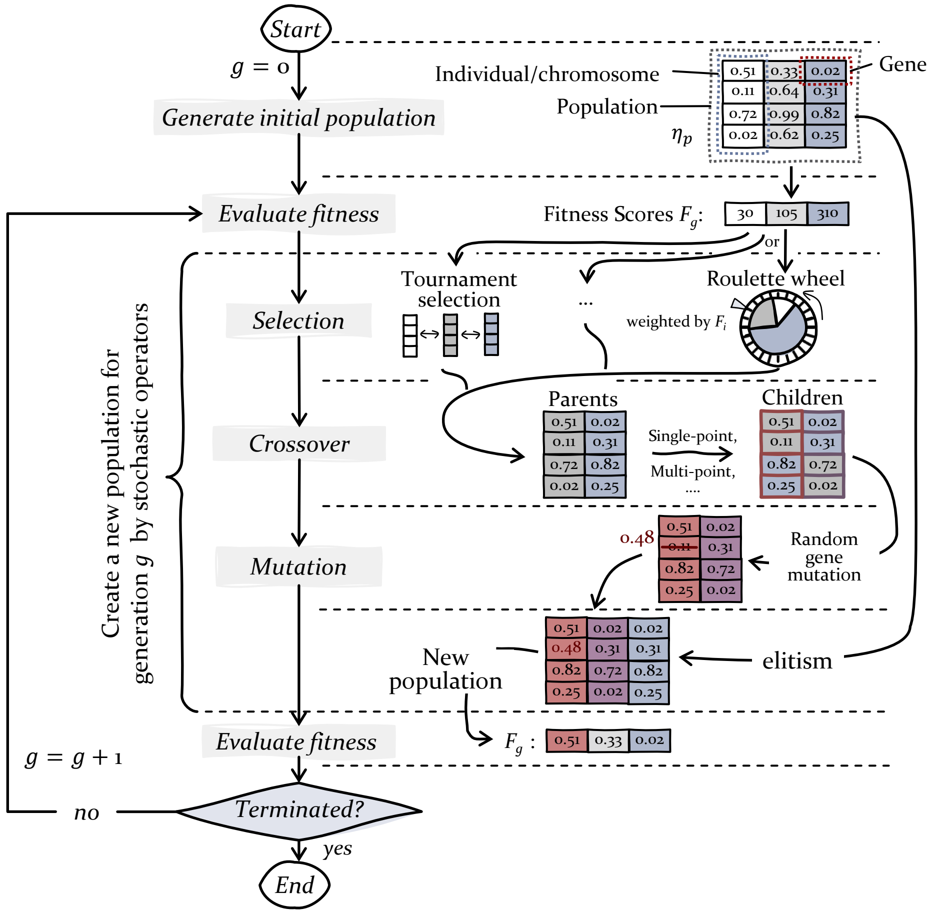

Figure 79: General workflow of GA with its stochastic operators of selection, reproduction, and mutation based on [744].

especially for highly constrained problems, to accept a portion of infeasible ones giving information to find the optimal solution [21, 735]. For this reason, the penalty approach acc. to Eq. (67) is often preferred.

The obtained fitness information serves as the basis to **select** the most promising parents for the subsequent reproduction steps [740] guiding the search into regions of optimality [21] (see Fig. 79). In contrast to crossover and mutation, the information on the individual fitness values is essential in the selection process [741]. Different techniques for parent selection were proposed in literature, e.g., ranking selection, random selection/pairing weighted random selection, well known under the term roulette wheel selection, tournament selection, $(\mu + \lambda)$-/(μ, λ)-selection, Boltzmann selection, or stochastic universal sampling [734, 740, 741, 743].

In the next step, **crossover** is used as a stochastic binary variation operator to recombine the genotypical information of the chosen parents to create at least one, mostly two, new individuals [740, 743] (see Fig. 79). Thus, genetic material is not newly generated, but valuable characteristics from the previous generation are inherited and passed to the offspring [21]. For GA, defining the crossover rate or probability, which determines the likelihood that crossover is performed or the number of applied crossover operations, is crucial [21, 740]. One-point (single-)crossover uses only one randomly chosen crossover site and exchanges the two segments of their parents, forming two new individuals [734, 740]. In contrast, two-point and N-point (multi-)crossover use a higher number of crossover points [734, 740]. Besides, further techniques exist, e.g., uniform, three parent crossover, or shuffle crossover [734].

After recombination, **mutation** is used to slightly and randomly modify some individual genes of the recombined chromosomes [740, 743] (see Fig. 79). It is a stochastic, unary variation step [740] incorporating new information [21] and, thus, avoids getting stuck in a local minimum [731, 734]. The mutation rate thereby defines the number of children to be modified [21] by, for instance, flipping single bits, randomly swapping two genes in the chromosome string [734], or scrambling a subset of values in the string [740]. The mutation probability controls the proportion of mutations within a chromosome, is typically set very low, and can be adaptive over the generations to balance exploitation and exploration [734, 742].

Since the population size has to stay constant but may increase by new individuals through recombination, **replacement selection** helps to shrink the population to its initial size [734, 740]. In contrast to stochastic parent selection, the selection of the survivors is typically deterministic, often based on their fitness, and, thus, along with other mechanisms, permits a certain amount of elitism [734, 740].

Although the success of GA mainly depends on the numerous parameters influencing the genetic operations, their choice is complex, and they cannot be globally defined for all optimization problems, but instead have to be adapted to the given optimization problem [735, 743]. Nonetheless, some basic guidelines and insights from prior studies can provide the user an initial starting point for finding a proper balance of the numerous settings, such as the population size or mutation and crossover rate, achieving an acceptable trade-off between efficiency and effectiveness.

A.3.2 Cuckoo Search algorithm (CS)

The Cuckoo Search (CS) algorithm, introduced in 2009 and evolved over the years into several variants and hybrid versions [745–747], has proven its applicability to a wide range of optimization problems, first and foremost to solve complex engineering problems [745, 746]. Applications of CS for sampling-based tolerance-cost optimization can, for example, be found in [P2, 294, 408]. CS is characterized by its efficiency [745], its comparative simplicity, as there is a low number of required algorithm steps and, thus, the code as well as setting parameters are manageable [748], and its good adaptability to new optimization problems [450, 748]. For this reason, CS is used in addition to GA in this thesis and briefly summarized in the following.

In line with GA, it is a metaheuristic, population-based optimization algorithm [748]. It is inspired by the breeding parasitism of certain species of cuckoos, viz. foisting their eggs in a host nest to be hatched by a host cuckoo [450, 748]. The workflow of CS in its original form is illustrated in Fig. 80.

It is assumed that cuckoos lay just one egg into one random of a fixed number of host nests [450]. Based on an initial population of host nests, a cuckoo i is randomly chosen, and its fitness F_i is evaluated and compared with a randomly chosen host nest j [450]. The exploration of the search space is based on a global random walk via Lévy flights getting from the current location $x_i^{(s)}$ to the new location $x_i^{(s+1)}$:

$$\boldsymbol{x}_i^{(s+1)} = \boldsymbol{x}_i^{(s)} + \alpha \oplus \text{Lévy}, \tag{75}$$

where the step size is $\alpha > 0$ and the step length is based on the Lévy distribution [747, 748]. If the new solution F_i, obtained by a suitable penalty function f_{P} considering both objective and constraints, is superior to the compared one F_j, it replaces the previous solution. In the next step, the worst nests are abandoned according to the predefined probability rate of discovery p_{a}. Lévy flights help to indicate new locations for new nests, while its fitness is used to rank the solutions and find the current best solution. This loop is iterated until the optimization algorithm reaches a predefined termination criterion. The step length α, the number of individuals η_p, and the discovery probability p_{a} are the three main algorithm-specific settings and must be chosen for the given optimization problem. [748] Besides, the total number of generations η_g and additional information are required to define the termination criteria.

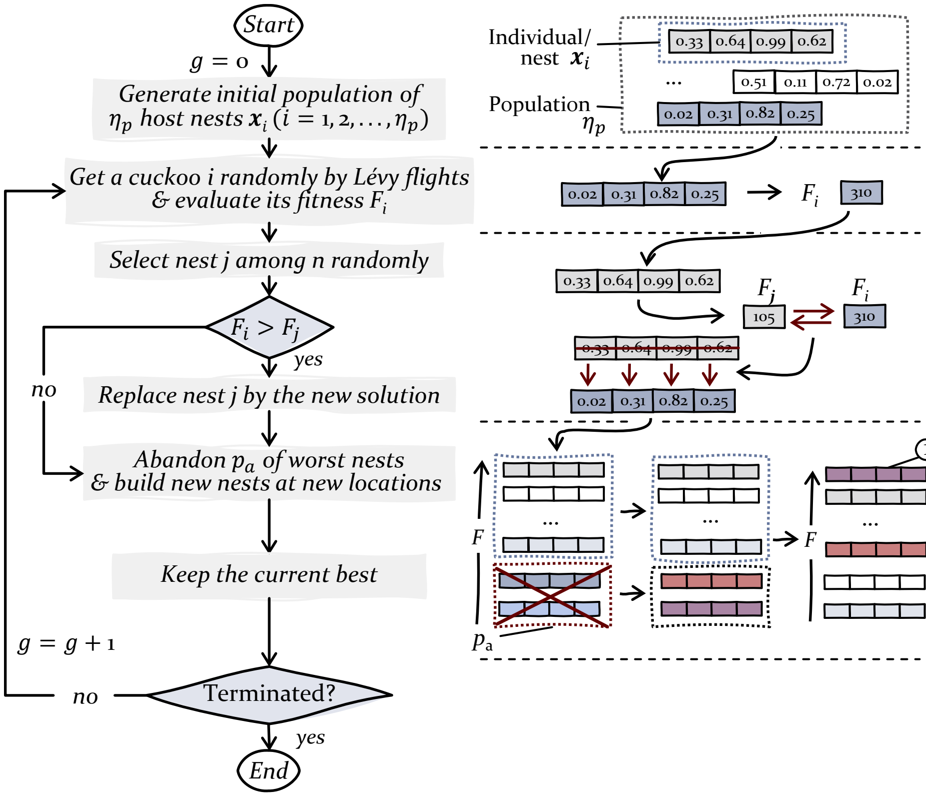

Figure 80: General workflow of CS based on the pseudo-code published in [748] and its illustration in [746].

A.4 Background information on statistics and sampling

The following paragraphs provide an overview of the statistical principles relevant to this work.

Pseudo-random number generation Sampling-based tolerance analysis attempts to infer the population of the resulting assembly response from a small number of n randomly selected samples. For the generation of the samples, different principles for the generation of the random variables $\boldsymbol{X}$ can be used, such as direct, composition, acceptance-rejection, or inverse transform methods [576, 749, 750]. This work applies the latter (see Sec. 4.1).

In the first step, n uniformly distributed random numbers $X_i' \sim \mathcal{U}(0; 1)$ are generated based on the principle of the chosen sampling technique and random number generators [576, 750]. The latter are often based on relatively simple algorithms used for practical reasons of repeatability, memory, and computing time [576, 750]. Though deterministic computer algorithms can generate a sequence of statistically random numbers, they are computer-generated and, thus, called *pseudo-random* [576].

In the second step, the generated variates X' are transformed using the inverse cumulative distribution function (icdf) Φ^{-1} as follows (see Fig. 17) [749]:

$$\Phi^{-1}(X_i') = \inf\{X_i \mid \Phi(X_i) \geq X_i'; \quad X_i' \in [0,1]\}. \tag{76}$$

Eq. (76) indicates that the icdf Φ^{-1} must explicitly be defined [751], but can also be approximated by similar and explicitly known functions or determined numerically, for example via the secant or the Newton Raphson Method [749]. For more information on the pseudo number and continuous random variate generation, please refer, for instance, to [576, 749–751].

Sampling techniques Statistical experimental designs are primarily used to reduce the effort of virtual and real experiments. In the context of tolerancing, they are primarily used for tolerance analysis to evaluate the assembly behavior under variations by means of the nc-rate using a small number of representative samples. As Sec. 2.2.2 emphasizes, Monte Carlo Sampling (MCS) is preferred for tolerance analysis.

In crude MCS, n random samples for each variable X_i are purely randomly generated using random number generators justified by the law of large numbers [752]. Hence, its implementation and application are comparatively simple, and its efficiency is determined by the used random number generators [392, 753]. However, Fig. 81 (left) exemplary illustrates that the pure random generation of the samples can lead to imbalanced sample spaces characterized by gaps and clusters of samples. If the design space is divided into a square grid, it will result in empty rows and columns and overcrowding. [392]

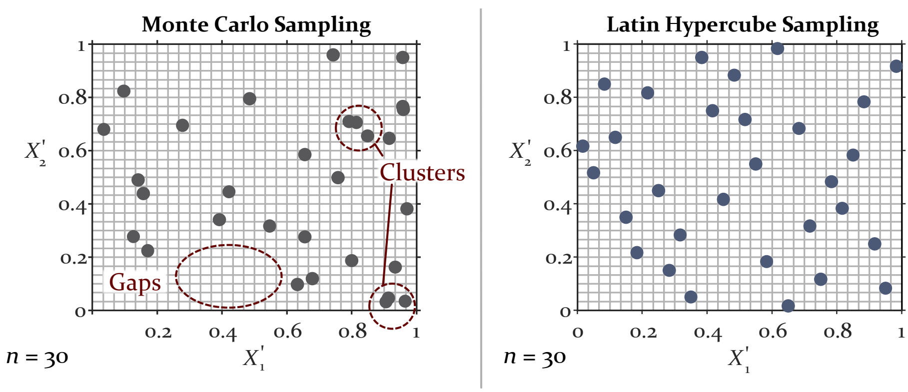

Figure 81: Two-dimensional MCS (left) vs. LHS (right) with a sample size $n = 30$.

A so-called Latin square results when the samples are arranged in such a way that only one sample point is included in each row and each column, thus providing better coverage of the design space (see Fig. 81 (right)) [392, 754]. The extension of the Latin square to multiple dimensions for each additional variable results in a hypercube, giving the *Latin Hypercube Sampling* (LHS), a stratified sampling technique, its name [755]. Thus, the design space is first divided into $1/n$ equally sized intervals according to the sample size n [756]. Subsequently, the samples are uniformly distributed and additionally optimized in such a way that, for instance, the correlation or the distance between the individual samples is minimum [757, 758]. The resulting hypercube contains n uniformly distributed sample points ranging between 0 and 1, which are then transformed into their final distributions using the inverse transform method [751, 754]. The order in which the samples are evaluated does not matter; it is purely random [754]. While a generated MCS can be extended arbitrarily and does not have to be evaluated completely, the validity of the LHS is only given if all of the generated n samples are evaluated. New sample points cannot be easily added post sampling [753]. Compared to MCS, the enhanced space filling results in a more accurate variance prediction for the same sample size n [752].

Besides LHS, *Quasi-MCS techniques* (QMCS) are used to lower the discrepancy, which is "a quantitative measure for the deviation of sampled points from the ideal (desired) uniform distribution" [753]. Consequently, low-discrepancy methods aim to generate the points as uniformly distributed as possible and are called quasi-random [392, 751, 753]. Sobol' sequences have proven their potential in general (and also for tolerance analysis in [392]) and show strengths over other lower discrepancy sampling methods [753].[4] Fig. 82 shows the difference of MCS and QMCS based on Sobol' sequences. Sobol' sequences are multidimensional sequences using the base 2 [759, 760], where operations such as scramble, leap, and skip can be used to decrease the correlations caused by the mechanism of sequence generation. Different scrambling methods, for example, described in [760, 761], can be used to shuffle and randomize the generated sequence. Skip is used to start the sequence only from $skip + 1$ and discard the first $skip$ points. Leap defines the number of points to be ignored between the chosen ones. [762] For more details on Sobol' sequences, the reader is referred to [760, 763, 764].

[4] Literature proposes further commonly used low-discrepancy methods for variance reduction, for example, the Halton or Hammersley sampling. This thesis focuses on crude MCS, QMCS based on Sobol' sequences, and LHS.

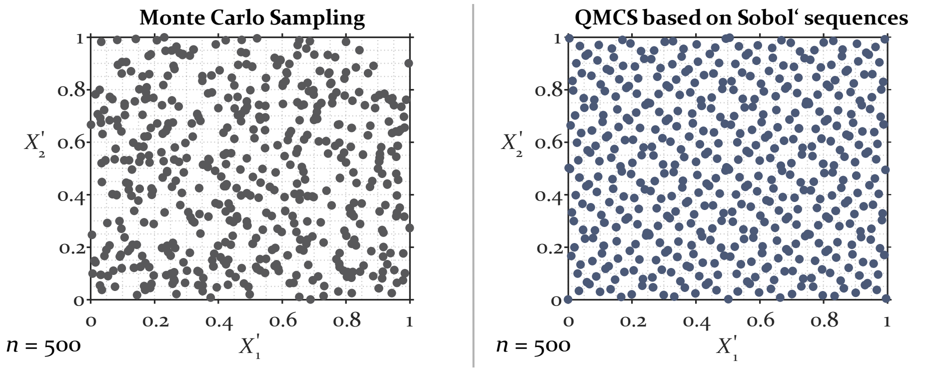

Figure 82: Two-dimensional Monte Carlo Sampling (left) vs. Quasi-MCS based on Sobol' sequences (right) with a sample size $n = 500$.

Distribution types The transformation of the uniform random numbers X_i' into the variates X_i following the machine-specific part tolerance distributions ρ_i as second step of inverse transform method (see Fig. 17) requires an analytical or numerical description of their probability density function (pdf) or inverse cumulative distribution function (icdf) [754]. Fig. 83 briefly summarizes common distribution types with their pdfs and characteristics used in tolerance analysis to represent the individual part variations.

The cumulative distribution function (cdf) Φ corresponds to the integral over the respective pdf, while the inverse cumulative distribution function (icdf) Φ^{-1} is the inverse of the cdf Φ [576]. The pdfs of the continuous distributions from Fig. 83 are given as follows:

- *Uniform distribution $\mathcal{U}_{[LL,UL]}$*: [576]

$$f(x) = \begin{cases} \frac{1}{UL-LL} & x \in [LL, UL], \\ 0 & \text{otherwise.} \end{cases} \tag{77}$$

- *Triangular distribution*: [765]

$$f(x) = \begin{cases} \frac{2}{UL-LL}\frac{x-LL}{H-LL} & \text{for } LL \leq x \leq H, \\ \frac{2}{UL-LL}\frac{UL-x}{UL-H} & \text{for } H \leq x \leq UL, \\ 0 & \text{otherwise.} \end{cases} \tag{78}$$

- *Normal distribution $\mathcal{N}(\mu, \sigma^2)$*: [576]

$$f(x) = \frac{1}{\sigma\sqrt{2\pi}} e^{\frac{-(x-\mu)^2}{2\sigma^2}} \qquad \text{for } x \in \mathbb{R}. \tag{79}$$

Type	PDF	μ	σ^2	γ_1	κ *
Uniform (UD)	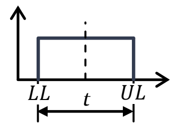	$\frac{LL+UL}{2}$	$\frac{t^2}{12}$	0	1.8
Triangular, symmetric (TD)	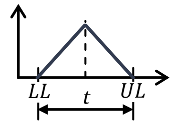	$\frac{LL+UL}{2}$	$\frac{t^2}{24}$	0	2.4
Triangular, skewed (TD)	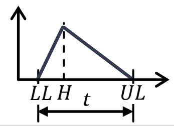	$\frac{LL+UL+H}{3}$	$\frac{1}{18}\cdot[(UL-LL)^2 - (UL-LL)\cdot(H-LL) + (H-LL)^2]$	**	2.4
Standard normal distribution (ND), $\pm 3\sigma$	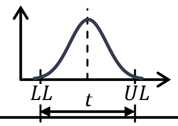	$\frac{LL+UL}{2}$	$\frac{t^2}{36}$	0	3
Pearson distribution (PD)	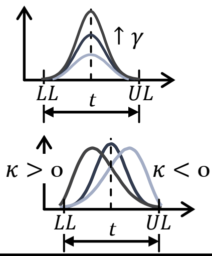	$\frac{LL+UL}{2}$	$\frac{t^2}{(2\cdot u)^2}$	*var*	*var*

* traditional kurtosis κ , excess kurtosis: $\gamma_2 = \kappa - 3$

** $\dfrac{\sqrt{2}\cdot(LL+UL-2\cdot H)(2\cdot LL-UL-H)(LL-2\cdot UL+H)}{5\cdot(LL^2+UL^2+H^2-LL\cdot UL-LL\cdot H-UL\cdot H)^{\frac{3}{2}}}$

Figure 83: Distributions commonly considered in the context of tolerancing acc. to [576, 765, 766].

The mean value μ corresponds to the nominal dimension $X_{i,0}$ and a potential mean shift $\Delta\mu$, the variance σ^2 results from the current tolerance t.

The Pearson distribution covers a family of distributions, which can be calculated as a function of the four standardized moments mean μ, variance σ^2, skewness γ_1 and excess kurtosis γ_2. The parameters $\beta_1 = \gamma_1^2$ and $\beta_2 = \gamma_2 + 3 = \kappa$ can be used to determine which of the six different Pearson distribution types applies. Thus, a wide range of continuous probability distributions can be represented, such as normal, Student's -t, beta, or gamma distribution. [767, 768]

Kernel density estimation Non-parametric, distribution-independent estimators are helpful if the density of the underlying distribution for a given set of random samples is unknown or cannot be statistically proven. Since they do not require any distribution type-specific parameters such as statistical moments, they can estimate the density and, thus, the cdf and icdf of any distribution. The *kernel density estimator* is a well-known non-parametric estimator that can be used for univariate [578, 769] as well as multivariate distributions [770].

Fig. 84 (left) illustrates the basic principle of kde for a univariate frequency distribution, where the kernels are shown in scaled form. A selected kernel K is evaluated n_K times along the frequency distributions approximating the unknown density function by a superposition of the individual kernel functions representing a weighting function [771]. The bandwidth h_K functions as a smoothing parameter defining the kernel's shape. Hence, the probability density function $\hat{f}_h(x)$ is the sum of all n_K kernels at given points x_i: [771]:

$$\hat{f}_h(x) = \frac{1}{n_\mathrm{K} \cdot h_\mathrm{K}} \sum_{i=1}^{n_\mathrm{K}} \mathrm{K}\left(\frac{x - x_i}{h_\mathrm{K}}\right). \tag{80}$$

Besides the Gaussian Kernel, exemplary used in Fig. 84, a small number of different kernel functions have established themselves for kde, in particular uniform, triangle, quartic, Cauchy, and Epanechnikov kernels [771]. Since the choice of bandwidth h_K, which controls the smoothing of $\hat{f}_h(x)$, (see Fig. 84 (right)) as well as the kernel function K is crucial, different rules of thumb and methods were proposed in literature to find a suitable trade-off [771].

A.5 Background information on surrogate modeling

Data mining, aiming to "mining [knowledge] from data" [772], comprises various ideas to transform raw data into useful information by using sophisticated algorithms [773]. The primary purpose is to analyze a given data set to identify patterns that can either be used for data explanation/description or prediction of unknown values [774, 775]. Therefore, it, among others, uses theoretical fundamentals and methods from statistics, pattern recognition, and machine learning [773]. Hence, algorithms are used to practically learn from given training (= learning) data, either supervised or unsupervised [772, 774]. Essentially, a distinction can be made between anomaly detection (= outlier analysis) [772]), clustering, learning of rules of association, visualization, classification, and regression [775, 776] (see Fig. 85).

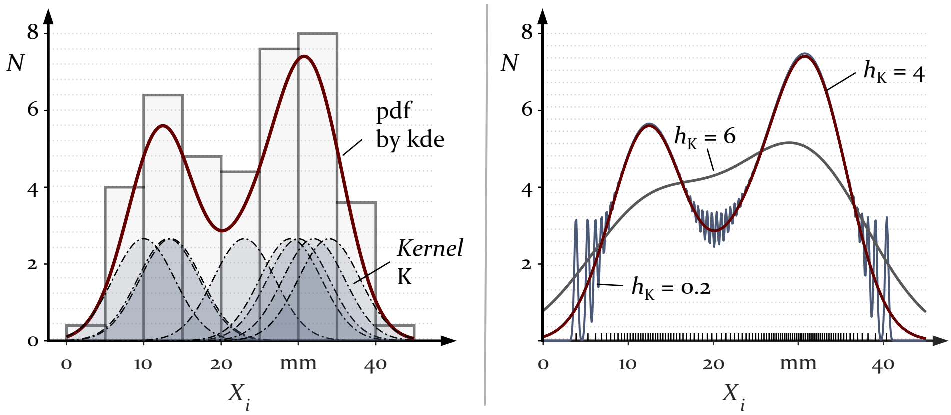

Figure 84: Principle of kernel density estimation (right) and the influence of the chosen bandwidth h_K (left).

Classification and regression are used to define a predictive model based on predefined training data sets consisting of independent input data (features) and output data (targets) using supervised learning techniques [773, 777]. Compared to classification for categorical/discrete output variables [773, 775], regression aims to learn a function that can predict continuous, real-valued numeric ones for new input values [772, 773, 775].

Regression Regression models, also called meta or surrogate models, are the approximated response function $\tilde{y} = \tilde{f}(x)$ of the real function $y = f(x)$ (see Eq. (65))[5], which is either unknown or (implicitly) known but too cost-intensive for an iterative evaluation [589].

Using statistical DOE, a set of input variables is determined in advance, either systematically (e.g., by grid search or (full)-factorial design of experiments) or randomly, by experiments, be it real trials or numerical simulations, for the response variables of interest y [589]. The resulting data set is divided into training, validation, and test data, whereby a validation data set is not always necessary [777]. Besides different data splitting methods, for instance, the p-fold cross-validation or the leave-k-out approach, differing recommendations on the ratio are proposed in literature [777], where their choice depends on the given data set and the interrelationships between input and output variables. These pre-processing steps are followed by the selection of a model type and fitting it to the previously obtained training data [589], where it is the challenge to find a balanced/good fit model with its parameters "that minimizes the error [e] between the predicted and true values of the target

[5] For this reason, regression techniques are also found in literature under the term response surface methodology [589].

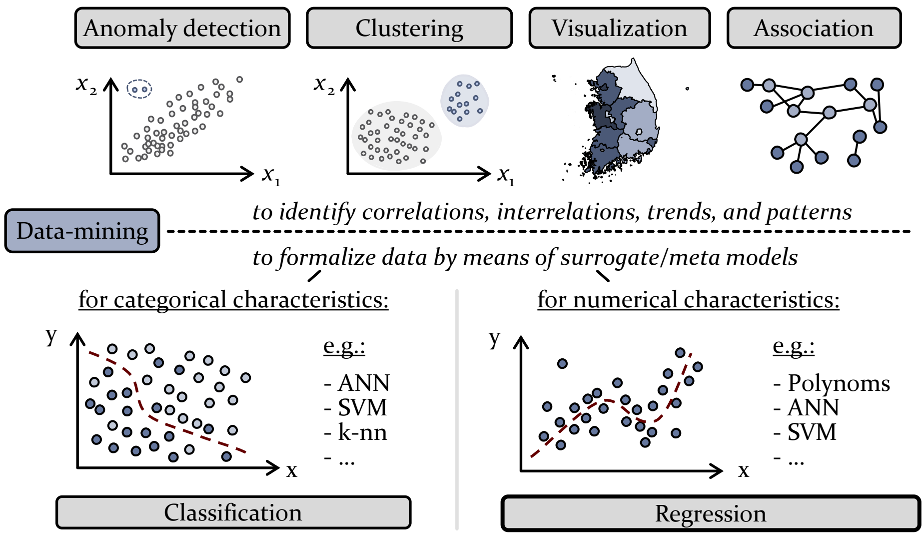

Figure 85: Classification of data mining methods based on illustrations given in [776].

variable“ [773]. Quantitative criteria for model evaluation thereby help to evaluate/validate the performance or quality [774, 775], thus help to indicate under- and overfitting (see Fig. 86) or to provide a basis for comparison of different models [778].

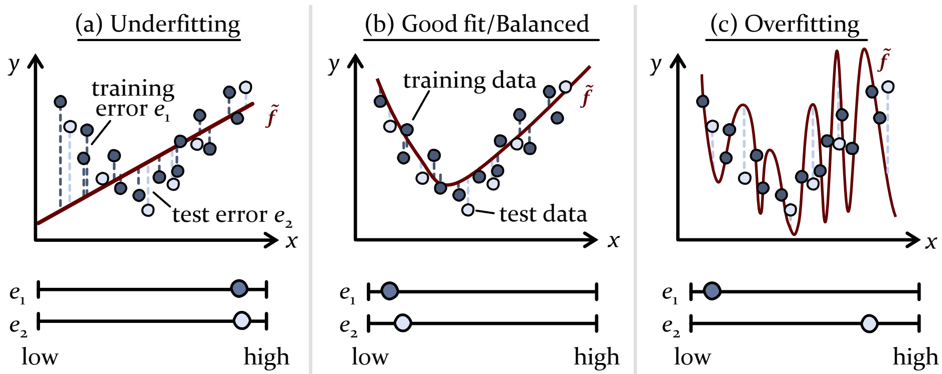

Figure 86: Underfitting (a), good fit (b), and overfitting (c) in surrogate modeling freely adopted from [779].

The *RMSE* is commonly used for the assessment of the model accuracy and is calculated by the root of the mean squared error as the absolute difference between the predicted values $\tilde{y}$ and the observed value y, taking m validation points into account:

$$RMSE = \sqrt{\frac{\sum_{i=1}^{m}(y_i - \tilde{y}_i)^2}{m}}. \tag{81}$$

Besides, the R^2-value:

$$R^2 = 1 - \frac{\sum_{i=1}^{m}(y_i - \tilde{y}_i)^2}{\sum_{i=1}^{m}(y_i - \mu_y)^2} \tag{82}$$

is often used to evaluate the model quality between $0 \leq R^2 \leq 1$ [589].

Artificial Neural Network (ANN) Among others, neural networks are powerful regression models mimicking the human nervous system, are adaptable to a wide range of problems, and, thus, used for both supervised and unsupervised learning [780, 781].

Following their biological analogy, ANNs are composed of a set of neurons, modeled as threshold logic units, interconnected and arranged in layers [781] (see Fig. 87). Neural networks are graphs where the neurons correspond to the vertices, and the edges are the connections, carrying a weight [781]. In feed-forward ANNs, the "successive layers feed into one another in the forward direction from input to output" [780]. So they do not include any cycles or loops compared to recurrent networks [781]. In single-layered networks, the inputs and outputs are directly mapped [780]. Adding multiple, so-called hidden layers leads to multilayered networks, the basis for deep learning approaches [780].

Each neuron is characterized by its network input function f_{net} and its activation function f_{act} [780, 781].[6] In each neuron, the f_{net} sums up all input variables x prioritized by individual weights w, while an additional constant bias b is useful to represent the invariant part of the prediction [780, 782]. Its scalar output serves as the input for the activation function f_{act}, which decides if the stimulus is larger than a threshold to be activated or not [781]. Choosing between different types of activation functions differing in their characteristics, such as sign-, sigmoid-, tanh-, or rectified linear unit functions, is decisive to assure a good fitness to the given data [780]. Moreover, an individual adaption of the structure of an ANN defined by the number of neurons and layers concerning the type of problem and amount of input data is decisive in holding the prediction errors low and avoiding overfitting.

The learning/training of an ANN is based on a stepwise adaption of the weight and bias values of the neurons as well as the thresholds [780, 781]. The

[6] Literature further introduces an additional output function [781]. Since it often corresponds to the identity function, this aspect is not further discussed here.

global aim is to gradually improve the prediction accuracy or minimize its corresponding error e of the ANN [780, 781] – the overall error e results from the accumulation of the individual errors of all layers. As the name indicates, error backpropagation methods propagate the effect of e backwards through the network, identifying the individual errors of each neuron and minimizing them with the aid of mostly gradient-based optimization algorithms [781].

Apart from the general disadvantage that ANNs are not directly interpretable, since they are encoded and not directly given in the form of mathematical equations [781], they have established themselves as valuable tools to represent complex, highly nonlinear interrelations without the need to define the model type in advance [783].

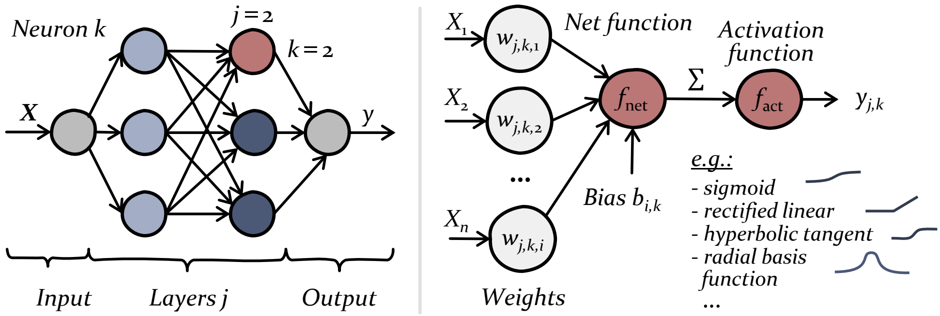

Figure 87: ANN's general structure and working principles freely adopted from [780, 782].

Surrogate models in and for optimization In the field of optimization, surrogate models are typically used, as the name indicates, as surrogates for expensive function evaluations in objective and constraints improving the overall optimization performance [587, 589]. Especially in the context of metaheuristic optimization, where the global optimum is found by learning from many trials and errors (see Appx. A.3), the time effort for a single evaluation is decisive [589]. The approximation of the response surface covering the entire design space helps to find the optimum with less computational effort and "(hopefully slight) loss of accuracy" [587, 589]. Thus, their integration fosters a fast design exploration considering the entire design space and enabling parallel computation [587, 588], facilitates the definition of the optimization problem by eliminating, combining, and modifying objectives or constraints, and decreasing the number and ranges of the design variables by giving insights into the problem [587, 592].

In literature, different approaches have been proposed under the name surrogate-assisted or surrogate/meta model-based optimization [587, 588, 784]. Traditionally, surrogate modeling and optimization are separated into two sequential, decoupled steps (see Fig. 88 (a)). Thus, no modifications on given optimization algorithm routines, but a typically large number of samples to generate a sufficiently large training data set are needed, while finding the best sample size is challenging [587, 588].

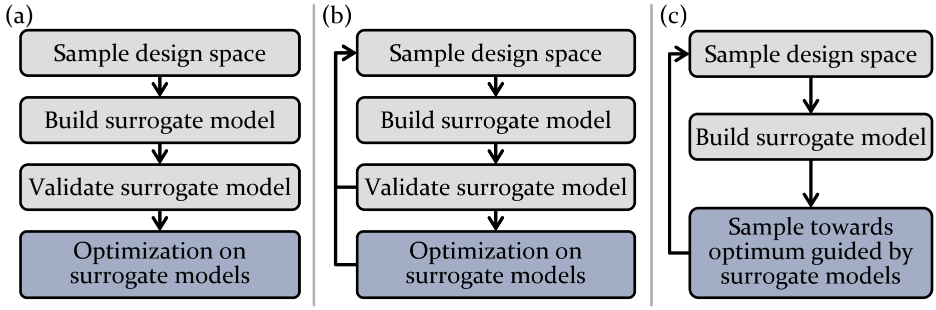

Figure 88: Three different strategies on surrogate model-based optimization: (a) sequential surrogate model-based optimization,(b) adaptive surrogate model-based optimization, (c) direct sampling approach according to [587].

To mitigate the initial DOE's impact and avoid finding actually infeasible optima, it is helpful to use both surrogate models and the real model together in optimization [784]. In metaheuristic optimization, a controlling and regularization of stochastic operations [588, 785] are achieved by performing the individual resampling at generation, population, or individual level [784]. Different strategies for selecting individuals to be reevaluated, such as a purely random selection or a selection of the best/fittest solutions, as well as the adaption of the reevaluation frequency, can be followed [778, 784, 786]. Adaptive surrogate modeling uses both resampling and remodeling to (re-)build the surrogate model within the optimization loop to systematically improve the accuracy in the regions of potential optima (see Fig. 88 (b)) [587, 592].

Another strategy is to replace the optimization process by combining adaptive sampling and surrogate modeling (see Fig. 88 (c)). In addition, other approaches exist, such as using multiple surrogates in different, significantly dissimilar regions of the design space [592, 784]. However, the choice of approach is always case-specific and mainly depends on the investment to (fully) evaluate the original and to build the surrogate model [588].

A.6 Embedding Teamcenter®Visualization Variation Analysis in tolerance-cost optimization

As shown in Sec. 2.2.2 and Sec. 3, it is helpful to integrate CAT-software for tolerance analysis as a black box model in the optimization framework. Although the usage of metaheuristic optimization algorithms principally enables the integration of any CAT-software, the software tool must have features and interfaces allowing the optimization algorithm to communicate in terms of relevant inputs, commands to perform the tolerance analysis, and processable outputs. The tolerance analysis software Variation Analysis (TCVisVA)[7] is an application of the product lifecycle management software Teamcenter®Visualization MockUp from Siemens PLM Inc. As TCVisVA is one of the most common CAT-tools used in the industry for statistical tolerance analysis, it was chosen for the evaluation studies in Chap. 8. MCS and HLM-contributor analysis and feature-based tolerance representation can analyze 3D assemblies while realistically considering function-relevant aspects, such as assembly sequences, gaps and floats, and overconstrained assembly conditions [S13].

In the following, the general working principle of sampling-based tolerance-cost optimization using TCVisVA, based on previous applications in literature [37, P19] and further used in [S14], is explained.

Fig. 89 illustrates replacing the tolerance analysis subroutine shown in Fig. 10. Based on current tolerance and machines/process information, represented by $\boldsymbol{t}_p^g$ and $\boldsymbol{x}_p^g$, tolerance analysis is performed to predict the probability distributions of the assembly responses Y_k. A comma-separated output text file is generated containing all virtually measured values for each sample, which is read in by the optimizer. These values are afterward used to estimate the nc-rate according to methods presented in Sec. 4.2. To run the tolerance analysis within the optimization loop in the background, TCVisVA is called per DOS command as follows:

```
"C:Program Files"\Siemens\Teamcenter14.2\Visualization \Products\
↪  Mockup\VPVsaBatchAutomation.exe -s <n> -import
↪  "<filepath><\filename>.txt"
```

The first argument indicates the executable to start the script for batch automation from the respective installation path, <n> defines the sample size, <filepath> the path, and <filename> the name of the input file, named process document (PDO), serving as the tolerance analysis information model.

[7] Further abbreviations of the CAT-software have been used in literature and practice due to official changes in tool names. Besides the current official term TCVisVA, it is also known under the terms VisVSA® [328, 787] or VSA® [280, 282, 788, 789].

The user must set up the latter in advance with the help of the graphical interface of TCVisVA, where a PMI-enriched CAD-model in JT™-data format can serve as the basis to facilitate the modeling process. This model is then exported in a comma-separated text file. The machine/supplier and tolerance information of the current individuals is indirectly considered in the tolerance analysis by modifying the initial tolerance analysis information model. In doing so, the text file, containing all information in a structured way, is searched using key-phrases[8] to find and replace the relevant sections by the currently chosen values. Although nearly any input can be overwritten in the text file, e.g., datums[9] or geometrical feature types and sizes (provided the structure and syntax of the process document is strictly adhered), only a limited scope is needed for tolerance-cost optimization for the specified context of use in this work. Tab. 5 summarizes the required information and their matching key-phrases/tags as defined in the text file.

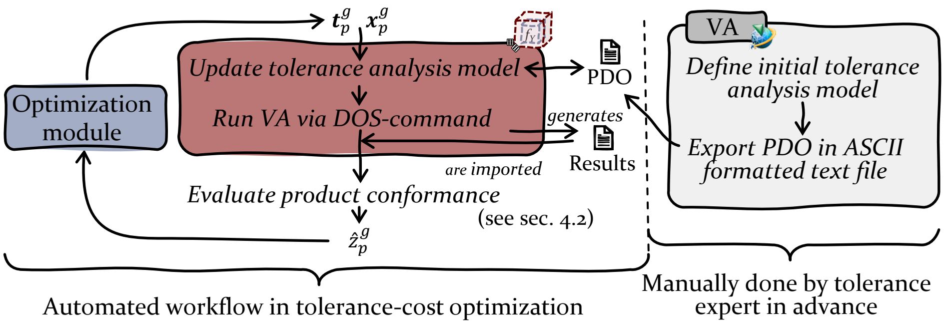

Figure 89: Using TCVisVA as sampling-based tolerance analysis subroutine in tolerance-cost optimization freely adopted from [37, P19].

[8] In this context, the term ”key-phrase” is used for phrases consisting of single or multiple keywords.

[9] A method for optimal datum selection using TCVisVA was studied in [S14], making it possible to reduce the nc-rates by an optimized datum system with rearranged sequences.

Table 5: Overview of information for tolerance-cost optimization using TCVisVA and its key-phrases used in software-specific input file PDO.

<table>
<tr><th colspan="2">Category</th><th colspan="2">Information</th><th>Key-phrases</th></tr>
<tr><td rowspan="16">Tolerance value t_i</td><td rowspan="5">Dim.</td><td rowspan="2">Unilateral</td><td>$LL = X_i - t_i; UL = X_i; \mu_i = X_{i,0} - t_i/2$</td><td>Unilateral 0,000000 -<t_i> Min: -<t_i> Max: 0,000</td></tr>
<tr><td>$LL = X_i; UL = X_i + t_i; \mu_i = X_{i,0} + t_i/2$</td><td>Unilateral <t_i> 0,000000 Min: 0,000 Max: <t_i></td></tr>
<tr><td>Equal bilateral</td><td>$LL = X_{i,0} - t_i/2; UL = X_{i,0} + t_i/2; \mu_i = X_{i,0}$</td><td>Equal Bilateral <t_i> Min: <t_i/2> Max: <t_i/2></td></tr>
<tr><td>Linear plus minus</td><td>$LL = X_{i,0} - t_i/2; UL = X_{i,0} + t_i/2; \mu_i = X_{i,0}$</td><td>| LPM | ± <t_i/2> |</td></tr>
<tr><td>Unequal bilateral</td><td>$LL = \mu_i - t_i/2; UL = \mu_i + t_i/2;$
$\mu_i = X_{i,0} + t_i^{ub} - (\lvert t_i^{ub} - t_i^{lb} \rvert)/2$</td><td>Unequal Bilateral <t_i_ub> <t_i_lb>
Min: <t_i_lb> Max: <t_i_ub></td></tr>
<tr><td rowspan="11">Geom.</td><td colspan="2">Straightness</td><td>| STR | <Tolerance zone> <t_i> |</td></tr>
<tr><td colspan="2">Flatness</td><td>| FLT | <t_i></td></tr>
<tr><td colspan="2">Cylindricity</td><td>| CYL | <t_i> |</td></tr>
<tr><td colspan="2">Profile</td><td>| SPF | <t_i> |</td></tr>
<tr><td colspan="2">Angularity</td><td>| ANG | <Tolerance zone> <t_i> <Modifier>|</td></tr>
<tr><td colspan="2">Perpendicularity</td><td>| PER | <Tolerance zone> <t_i> <Modifier>|</td></tr>
<tr><td colspan="2">Parallelism</td><td>| PAR | <Tolerance zone> <t_i> <Modifier>|</td></tr>
<tr><td colspan="2">Position</td><td>| POS | <Tolerance zone> <t_i> <Modifier>|</td></tr>
<tr><td colspan="2">Total run out</td><td>| TOR | <t_i></td></tr>
<tr><td colspan="2">Concentricity</td><td>| CON | <Tolerance zone> <t_i> |</td></tr>
<tr><td colspan="2">Symmetry</td><td>| SYM | <t_i> |</td></tr>
<tr><td colspan="2" rowspan="4">Tolerance distribution</td><td colspan="2">Uniform</td><td>Uniform</td></tr>
<tr><td colspan="2">Normal</td><td>Normal</td></tr>
<tr><td colspan="2">Extreme</td><td>Extreme</td></tr>
<tr><td colspan="2">Pearson</td><td>Pearson <Skewness> <Kurtosis></td></tr>
<tr><td colspan="2"></td><td colspan="2">Trapezoid</td><td>Trapezoid <Shift> <Width></td></tr>
</table>

`<Modifier>` and `<Tolerance zone>` are optional, fixed arguments based on the specifications in the initial TCVisVA-model considering feature-dependent restrictions. `<Tolerance zone>`: `Dia` – Ø; `S Dia` – S Ø; `<Modifier>`: `(L)` – Ⓛ, `(M)`: – Ⓜ. Tolerance distributions can be assigned to each of the three main groups of size, location/orientation, and form tolerances per feature individually. The tolerance sigma range is a global setting.

A.7 Comparability of probabilistic simulation and optimization

On the one hand, randomness is a key mechanism of sampling-based tolerance-cost optimization and its submethods (see Sec. 3.2). On the other hand, however, it must be specifically controlled and aligned to the objective of the respective comparative study to avoid drawing false conclusions from the obtained results. This is particularly important when combining multiple probabilistic approaches, such as sampling-based tolerance analysis and metaheuristic optimization algorithms. Otherwise, the randomnesses superimpose. For this purpose, Tbl. 6 overviews different strategies for *dealing with random numbers in the context of sampling-based tolerance-cost optimization* and serves as the basis for the studies from Chap. 4–6 & Chap. 8. A differentiation is made between random numbers for optimization (O) and for sampling-based tolerance analysis (S) with three strategies each, where $r_{o/s}$ is used as the index for the $r_{o/s}$-th repetition of the $c_{o/s}$-th optimization or sampling case. These cases differ in the studies in the variables to be investigated, such as optimization settings (O) or sample sizes and different sampling techniques (S):

- **O-1/S-1**: For each studied case $c_{o/s}$ and repetition $r_{o/s}$ new random numbers are used. However, this requires a sufficiently large number of repetitions $\eta_{r_{o/s}}$ for statistically valid statements. Otherwise, especially in optimization, this can lead to wrong conclusions regarding the variables under investigation based on non-optimal results and merely random optimization phenomena.
- **O-2/S-2**: Using the same sequence of random numbers for different study cases $c_{o/s}$ enables a direct pairwise comparison of the $r_{o/s}$-th repetitions. Similar to O-1/S-1, however, a sufficiently large total number of repetitions $\eta_{r_{o/s}}$ is required.
- **O-3/S-3**: By using the same random numbers for all cases and repetitions, the influence of randomness is eliminated. Hence, the results of the cases are deterministic and directly comparable. However, this excludes making statements about their behavior under repetition.

Table 6: Overview of different strategies for handling random numbers in the context of sampling-based tolerance-cost optimization.

Random numbers (rn) used in metaheuristic optimization operations Optimization repetition/run: $r_o = [1; \eta_{r_o}]$, Optimization case: $c_o = [1; \eta_{c_o}]$		
(O-1) Random–Random:	**(O-2) Equal–Random:**	**(O-3) Equal–Equal:**
Purely random for all optimization repetitions r_o and cases c_o	Same random number sequences of all repetitions for all optimization case c_o	Same random numbers for all optimization repetitions r_o and cases c_o
$rn_{r_o}^{c_o} \neq rn_{R_o}^{C_o}$	$rn_{r_o}^{c_o} = rn_{r_o}^{C_o}; rn_{r_o}^{c_o} \neq rn_{R_o}^{c_o}$	$rn_{r_o}^{c_o} = rn_{R_o}^{C_o}$
$\forall \quad r_o, R_o = 1, \dots, \eta_{r_o}\ ; \ \forall \quad c_o, C_o = 1, \dots, \eta_{c_o}; c_o \neq C_o\ r_o \neq R_o$		

Random numbers (rn) used in sampling-based tolerance analysis		
Resampling: $r_s = [1; \eta_{r_s}]$: Sampling case: $c_s = [1; \eta_{c_s}]$		
(S-1) Random–Random:	**(S-2) Equal–Random:**	**(S-3) Equal–Equal:**
Purely random for each sampling repetition r_s, and each c_s	Same random number sequences of all sampling repetitions r_s for all sampling cases c_s	Same random numbers for each sampling repetition r_s and c_s
$rn_{r_s}^{c_s} \neq rn_{R_s}^{C_s}$	$rn_{r_s}^{c_s} = rn_{r_s}^{C_s}\ ; \ rn_{r_s}^{c_s} \neq rn_{R_s}^{c_s}$	$rn_{r_s}^{c_s} = rn_{R_s}^{C_s}$
$\forall \quad r_s, R_s = 1, \dots, \eta_{r_s}\ ; \ \forall \quad c_s, C_s = 1, \dots, \eta_{c_s}; c_s \neq C_s\ r_s \neq R_s$		

A.8 Case studies

The case studies are presented in a general form below to serve as a basis for the optimization studies. All simplifications, extensions, or modifications necessary to address aspects that are the main subject of the individual studies are noted in their descriptions in the respective sections. The results are summarized in Appx. A.9. All examples follow the GD&T rules acc. to ASME Y.14.5-2009, setting the envelope principle concerning rule#1 as default [50]. All dimensions are in mm units.

A.8.1 Case Study 1: Wheel mounting assembly

The commonly used wheel mounting assembly example, initially presented as tolerance allocation problem in [5], serves as the basis for the individual studies on the accuracy, completeness, and efficiency in Chap. 4–6. While sampling-based machine selection and allocation for single dimensional tolerances are introduced in Sec. 5.1–Sec. 5.2 using a 1D vector loop model, a 3D TCVisVA-model is defined for Sec. 5.3 and Chap. 6 to extend the methods to geometrical and multiple tolerances per part.

1D vector loop model

In the given case study (see Fig. 90), the two interrelated gaps Y_1 and Y_2 are considered as critical [307]:

$$Y_1 = f_{Y_1}(\boldsymbol{X}) = X_2 - X_4, \tag{83}$$

$$Y_2 = f_{Y_2}(\boldsymbol{X}) = -X_1 - X_2 - X_3 + X_5. \tag{84}$$

The specification limits LSL, USL, the maximum nc-rate $z_{\max}$, and the tolerance-cost curve parameters and part tolerance distributions are defined individually to establish suitable use cases and scenarios. The tolerance-cost functions follow an exponential approach while the parameters are adopted from [307]. All information is given in the description of the respective optimization studies in Appx. A.9.

3D feature-based TCVisVA model

The wheel mounting example from literature is extended to a 3D example with multiple dimensional and geometrical tolerances, serving as the case study for Sec. 5.3 and Sec. 6.1–6.3. The distance between the wheel and the support 2 Y_1, as well as the tilting of the wheel Y_2, function as assembly responses and are represented by virtual measurements in TCVisVA. Fig. 91 gives an overview of the assembly with Y_1, Y_2 and the specified part tolerances

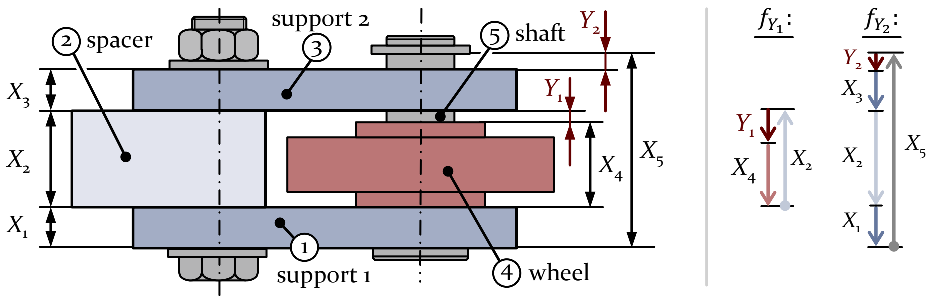

Figure 90: Overview of the wheel mounting assembly example with its part characteristics X_i (left) and two assembly response functions f_{Y_k} (right) acc. to [5, 307].

following the introduced feature notation in Sec. 5.3. The corresponding assembly and tolerance graph is given in Fig. 47.

As shown in Fig. 91 (top), the assembly consists of two identical supports $l = 1$, $l = 3$. Following Eq. (56):

$$\boldsymbol{B}_{\text{eq}} = \begin{array}{c} \begin{bmatrix} 1 & 0 & 1 & 0 & 0 \\ 0 & 1 & 0 & 0 & 0 \\ 1 & 0 & 1 & 0 & 0 \\ 0 & 0 & 0 & 1 & 0 \\ 0 & 0 & 0 & 0 & 1 \end{bmatrix} \end{array} \begin{array}{l} \leftarrow \text{support 1} \\ \leftarrow \text{spacer} \\ \leftarrow \text{support 2} \\ \leftarrow \text{wheel} \\ \leftarrow \text{shaft} \end{array} \tag{85}$$

Although the bottom and top planar features $u = 1$ and $u = 2$ of the wheel $l = 4$ are geometrically identical, they are considered independent in this example since they contribute differently to the KCs due to the defined assembly conditions.

The subsequent set of constraints is set here to comply with the general GD&T rules as well as the rule #1 acc. to Eq. (50)–(51), the default envelope principle, acc. to ASME Y14.5-2009 [50] within optimization:

$$\begin{array}{cccccccc} t_{1,2,2} < t_{1,2,1} & ; & t_{3,2,2} < t_{3,2,1} & ; & t_{4,2,2} < t_{4,2,1} & ; & t_{5,3,2} < t_{5,3,1} \\ t_{2,2,2} < t_{2,2,1} & ; & t_{4,1,2} < t_{4,1,1} & ; & t_{5,2,2} < t_{5,2,1} & ; & t_{5,3,2} < \frac{t_{5,3,3}}{2} \end{array} \tag{86}$$

Besides further information on the geometrical dimensions, the part tolerance specifications and the assembly graph (see Fig. 47 and Fig. 91) are used for the part feature and assembly operation definition in TCVisVA. The clearance fits of the shafts and holes are considered fixed. The tolerance-cost data for the studies are summarized in Chap. A.9.

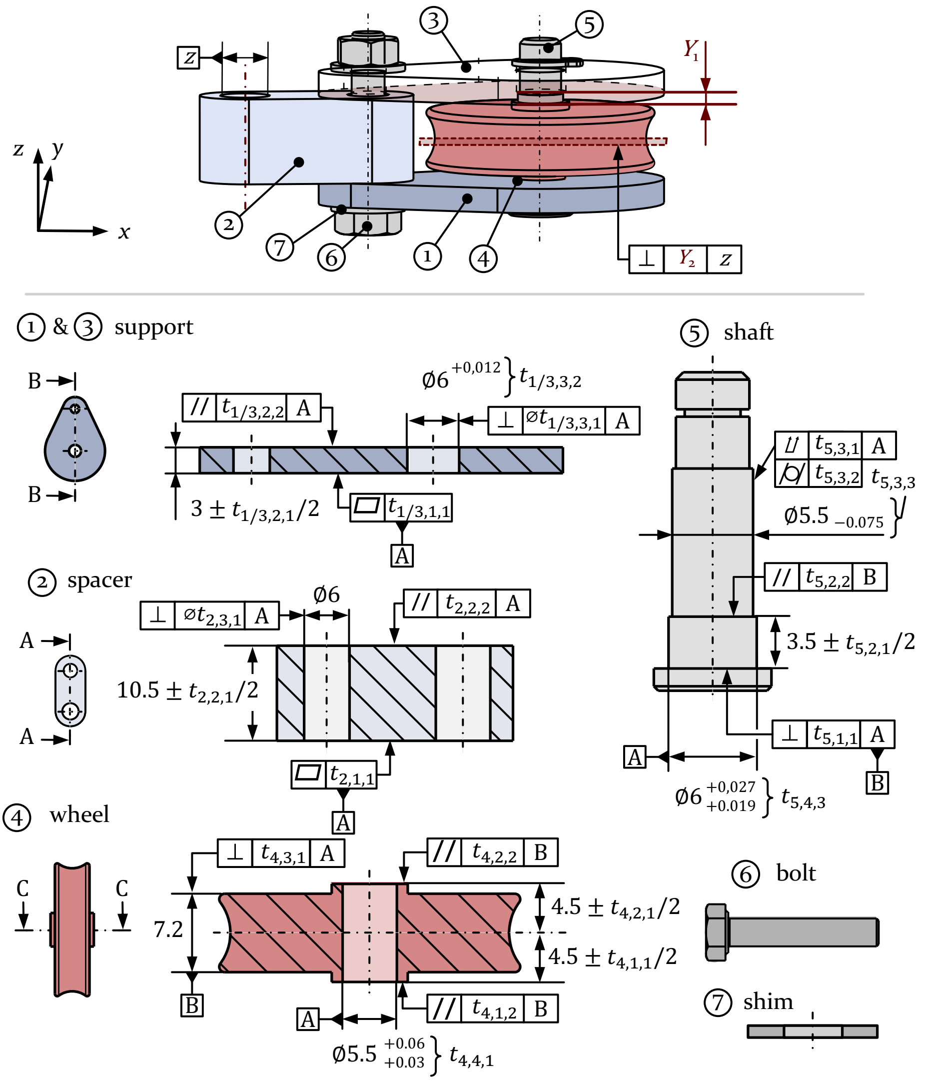

Figure 91: Overview of the wheel mounting assembly considered as a case study in Sec. 5.3 and Chap. 6 (top). Part tolerance specifications following the ASME Y14.5-2009 [50] (bottom).

A.8.2 Case Study 2: Electrified cross skate

To verify the findings and finally apply and evaluate the comprehensive framework with its single methods presented in Chap. 7, a more complex assembly of an electrified cross skate is used in Chap. 8.

The e-cross skate was developed at the Institute of Engineering Design at the Friedrich-Alexander-Universität Erlangen-Nürnberg as a micro-mobility solution for the last mile problem in personal transportation. It is based on the general idea of cross-skating. Like inline skates, cross skates are single-row roller skates. However, only two, usually pneumatic tire wheels are arranged in front of and behind the shoe (see Fig. 92). The skates are driven electrically via the rear wheel axle and the skating speed is controlled via inclination sensors by the rider's weight shifting. The steerable front axle, with the wheel pivoted on a fixed axle pin, leads to a shortening of the curve radius and enables cornering without lifting and replacing the skates, as it is typical, for example, in cross-country skiing. [599] More information on its fundamental principle, the different driving modes, and the technical details are given in [599, 790].

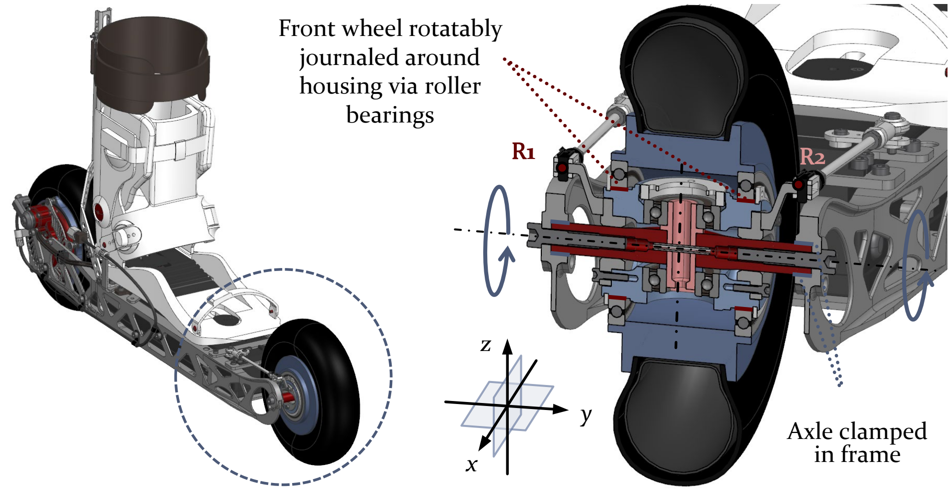

Figure 92: Overview of one electrified cross skate with its subassembly of the front tire.

In this thesis, *the front wheel assembly* is considered as a tolerance allocation problem (see Fig. 65, Fig. 92). Based on the overview of all relevant parts with their features given in Fig. 93, Fig. 67–68, given in Sec. 8.1, show the part tolerance specifications. A TCVisVA-model is set up following the assembly and tolerance graph of Fig. 94–95, while its notation is further explained in Fig. 96. The camber of the front wheel Y_1 is directly represented as a virtual measurement of the angle between the center plane of the rim and the frame. In contrast, the inclination and eccentricity of the steering are defined by and calculated using the point measurement information of the reference points R1 and R2 (see Fig. 66).

As it can be seen in Fig. 65, there are several identical parts. The equality matrix $\boldsymbol{B}_{\text{eq}}$ from Sec. 5.3 is useful to describe the interrelations within the entire assembly and to define the tolerance allocation problem. Only the relevant, non-zero entries $b_{l,\bar{l}} = 1$ are listed below for clarity. For completeness, all parts are considered, including those that do not contribute to the KCs.

$$\begin{aligned}
&b_{1,27} = b_{27,1} = 1, \qquad && b_{3,28} = b_{28,3} = 1, \qquad && b_{6,8} = b_{8,6} = 1\\
&b_{12,13} = b_{13,12} = 1, && b_{14,15} = b_{15,14} = 1, && b_{17,18} = b_{18,17} = 1,\\
&b_{19,20} = b_{20,19} = 1, && b_{21,22} = b_{22,21} = 1,
\end{aligned}$$

$$\begin{aligned}
b_{23,24} &= b_{23,25} = b_{23,26} = b_{24,23} = b_{24,25} = b_{24,26} = b_{25,23} = b_{25,24} = b_{25,26} =\\
&= b_{26,23} = b_{26,24} = b_{26,25}.
\end{aligned}$$

The feature equality matrices $\boldsymbol{A}_{\text{eq},l}$ of the relevant e-cross skate parts used for design dimension reduction for optimization are shown in the following:

$\boldsymbol{A}_{\text{eq},l=2} =$

u \ $\bar{u}$	1	2	3	4	5	6	7	
1			1					$\rightarrow t_{2,1,1} = t_{2,3,2}$
2				1				$\rightarrow t_{2,2,1/2} = t_{2,4,1/2}$
3	1							
4		1						
5							1	$\rightarrow t_{2,5,1} = t_{2,7,1}$
6								
7					1			

$\boldsymbol{A}_{\text{eq},l=4} =$

u \ $\bar{u}$	1	2	3	4	
1					
2			1		$\rightarrow t_{4,2,1} = t_{4,3,1}$
3		1			
4					

$\boldsymbol{A}_{\mathrm{eq},l=9} =$

u \ $\bar{u}$	1	2	3	4	5	6	7	8	9	10	11	12	
1													
2													
3													
4					1								$\rightarrow t_{9,4,2/3} = t_{9,5,2/3}$
5				1									
6								1					$\rightarrow t_{9,6,1/2/3} = t_{9,8,1/2/3}$
7									1				$\rightarrow t_{9,7,1} = t_{9,9,1}$
8						1							
9							1						
10													
11												1	$\rightarrow t_{9,11,1/2} = t_{9,12,1/2}$
12											1		

$\boldsymbol{A}_{\mathrm{eq},l=11} =$

u \ $\bar{u}$	1	2	3	4	5	
1			1			$\rightarrow t_{11,1,2} = t_{11,3,1}, t_{11,1,3} = t_{11,3,2}$
2				1		$\rightarrow t_{11,2,1} = t_{11,4,1}$
3	1					
4		1				
5						

As introduced for the wheel mounting assembly example, a set of nonlinear inequality constraints is applied for the e-cross skate example to assure the GD&T rules, including the envelope principle for the features with multiple tolerances acc. to Eq. (50)–(51):

$$
\begin{array}{llll}
t_{9,4,2} < t_{9,4,1}; & t_{9,4,2} < \frac{t_{9,4,3}}{2}; & t_{9,5,2} < t_{9,5,1}; & t_{9,5,2} < \frac{t_{9,5,3}}{2}; \\
t_{9,6,2} < t_{9,6,1}; & t_{9,6,2} < \frac{t_{9,6,3}}{2}; & t_{9,8,2} < t_{9,8,1}; & t_{9,8,2} < \frac{t_{9,8,3}}{2}; \\
t_{11,1,2} < t_{11,1,1}; & t_{11,1,2} < \frac{t_{11,1,3}}{2}; & t_{11,3,1} < t_{11,3,2} &
\end{array}
\tag{87}
$$

All information on the tolerance-cost data used is summarized in Tbl. 52.

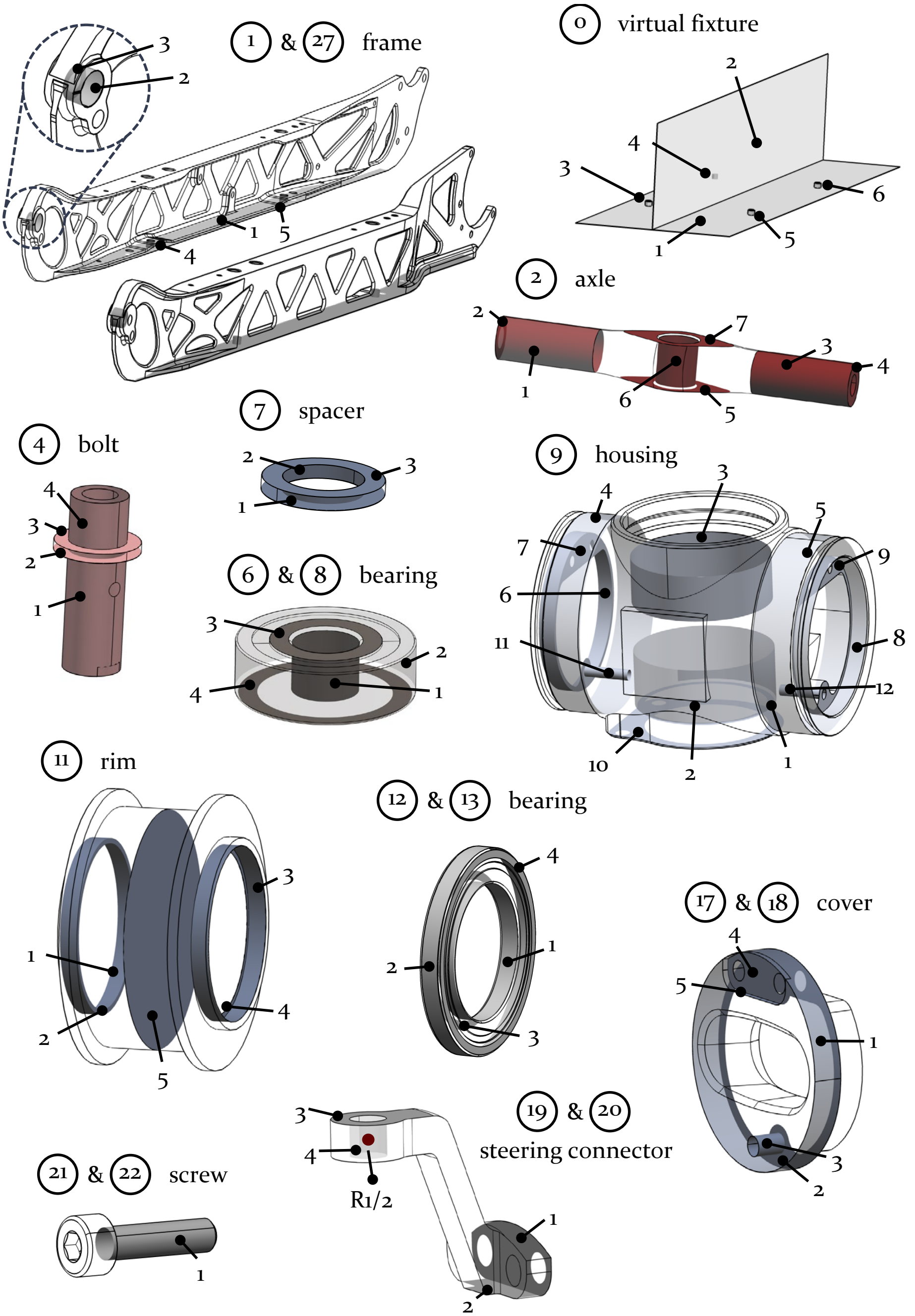

Figure 93: Overview of the parts of the e-cross skate assembly with its features and indices contributing to the focused KCs given in Fig. 65.

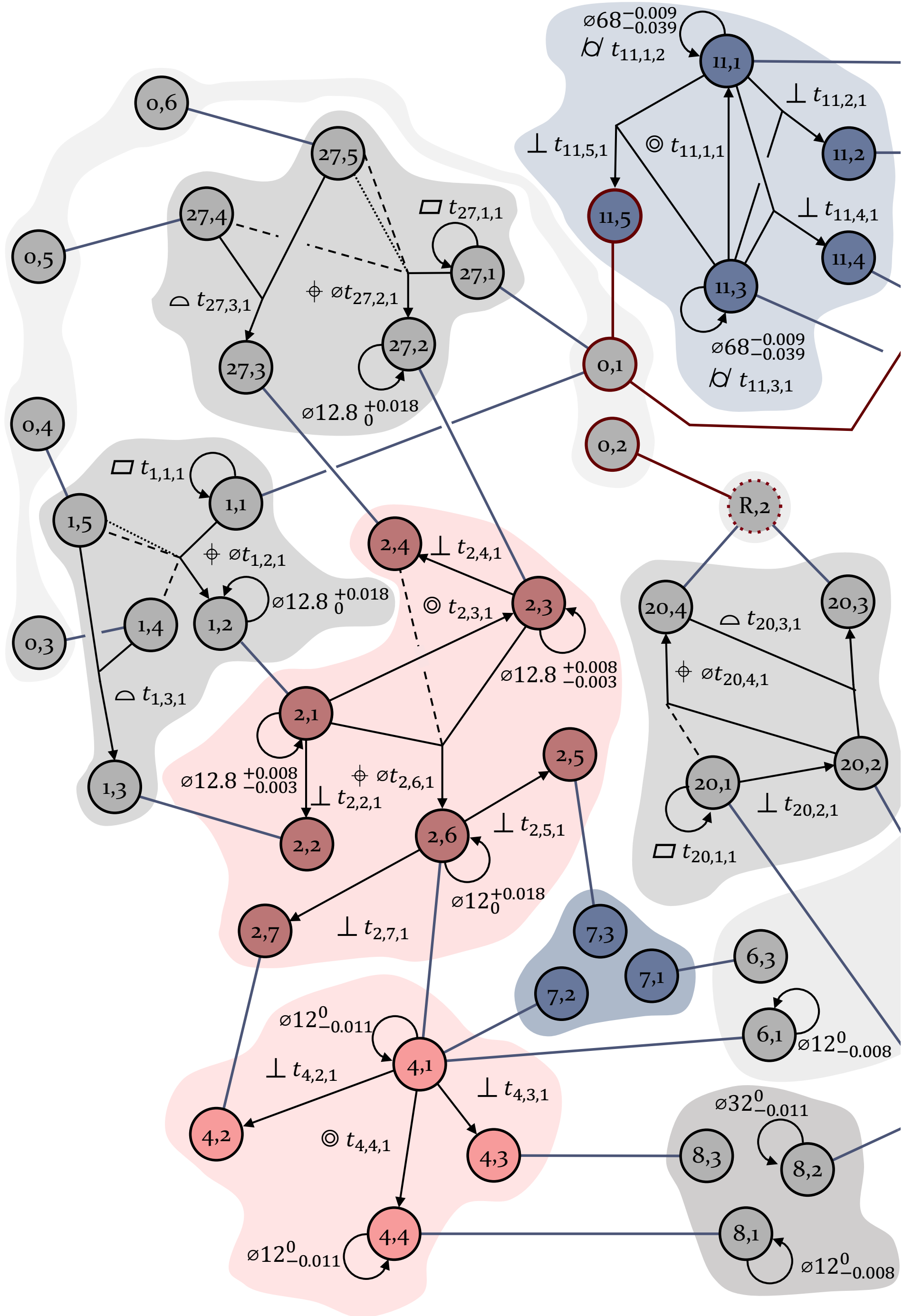

Figure 94: Overview of the part tolerance specifications of the e-cross skate example – I.

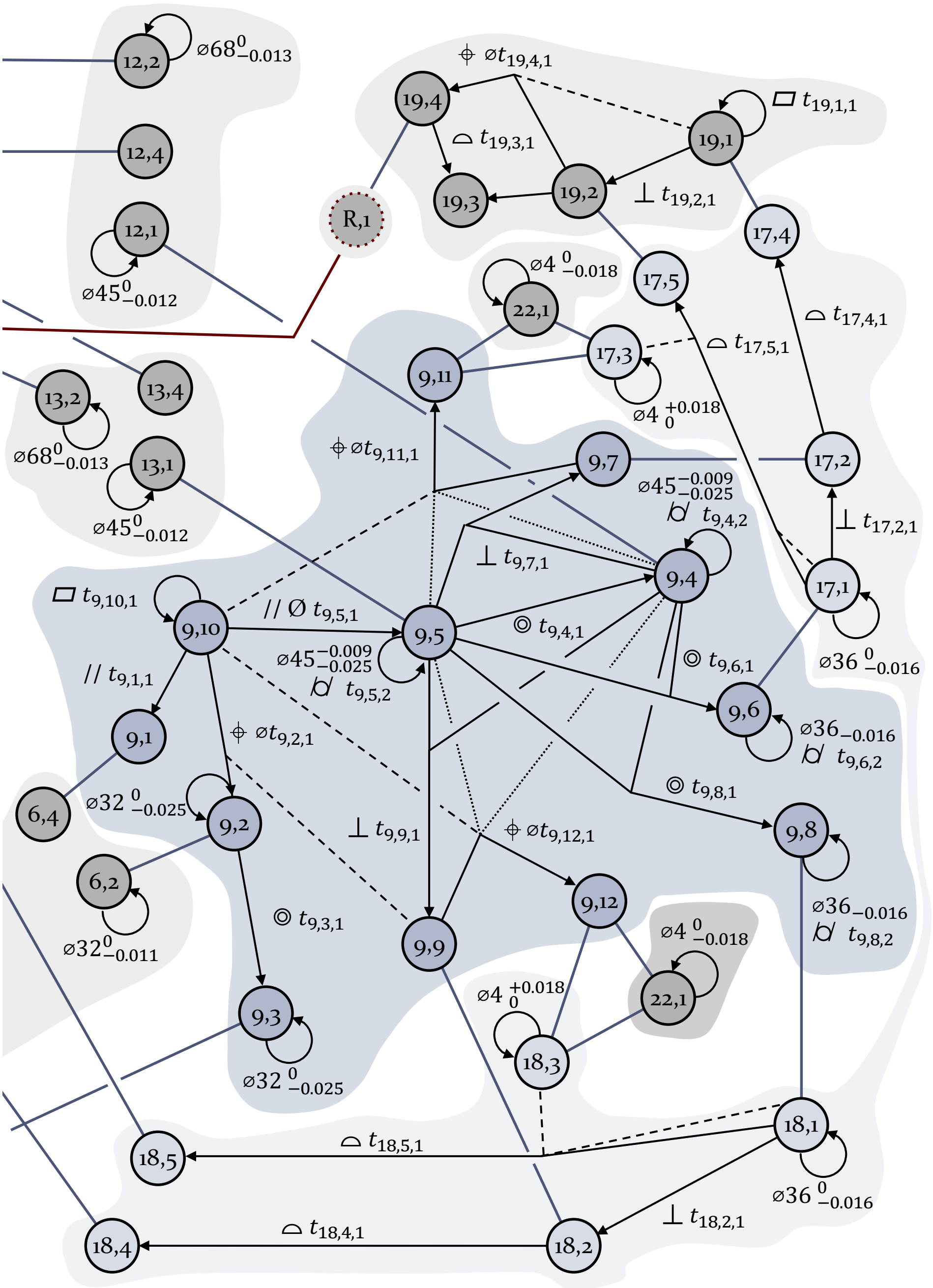

Figure 95: Overview of the part tolerance specifications of the e-cross skate example – II.

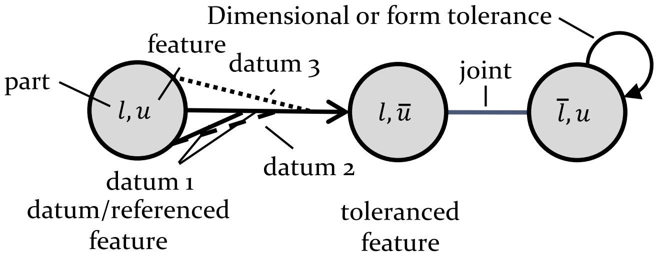

Figure 96: Notation of the assembly graph representation given in Fig. 47 and Fig. 94–95.

A.9 Details on optimization studies and results

The subsequent sections summarize the relevant settings and the main optimization results obtained in this thesis. While Tbl. 7 presents the main information of the different studies at a glance, further information on the studies and results are given in detail in the respective paragraphs.

In Chap. 4, a reference value to evaluate the results obtained by sampling with respect to their accuracy is needed. Under the assumption that all characteristics X_i follow a normal distribution, the general statistical equation can be used to estimate the resulting tolerance T_{Stat} of the yield with the aid of all single variances σ_i^2 [766, 791]:

$$T_{\text{Stat}} = 2 \cdot u \cdot \sqrt{\sum_{i=1}^{I} \left(\frac{\partial f_Y}{\partial X_i}\right)^2 \cdot \sigma_{\mathrm{i}}^2} \leq T_{\max}, \tag{88}$$

making use of the linearization of the assembly response function f_Y.

If $t_i = \pm 3\sigma_i$ and $u = 3$, Eq. (88) leads to the well-known RSS formula [40]:

$$T_{\text{RSS}} = \sqrt{\sum_{i=1}^{I} \left(\frac{\partial f_Y}{\partial X_i}\right)^2 t_i^2} \leq T_{\text{RSS,max}}. \tag{89}$$

Hence, for linear assembly response functions, Eq. (88) can suitably be used to calculate T_{Stat} and to define the specification limits $LSL = Y_0 - 0.5 \cdot T_{\text{Stat}}$ and $USL = Y_0 + 0.5 \cdot T_{\text{Stat}}$, where the assembly response $Y_0 = f_Y(\boldsymbol{X}_0)$ at its nominal and the sigma level u define the width of the conformance region. For the cases studied, where all tolerances do have the same contribution on f_Y with $\left| (\partial f_Y / \partial X_i) \right| = 1$, it can be used to define the specification limits for a multiple of u, so it will lead to the nc-rate $z_{\max} = f(u)$, where u and $z_{\max}$ are directly related over the standard normal distribution and can either be derived with the aid of its cumulative distribution or be found in tables for all standard values [571]. In contrast to pure analysis studies, where t_i are defined and fixed, the optimally allocated tolerance values depend on their sensitivity to cost and quality [287]. By defining the cost curves equally for all tolerances $f_{C_i} = f_C$, the optimum values are predefined at $t_i = t^{\text{opt}}\ \forall i = 1, \dots, I$ and can be used to define the specification limits inversely. In doing so, it helps to shape the optimum problem in advance, so the reference optimum is given at t^{opt} when the real value of $z_{\max} = f(u)$ is met.

Table 7: Summary of the simulation studies performed in this thesis.

Study	Objective	Case study	Study design	Optim.#1	Strategy#2	Ref.
Sec. 4.1: Estimation of the margin of error	Confidence intervals to predict the rate of sampling-induced under- and overestimation	Wheel mounting assembly; 1 KC	n = [10; 25; 50; 100; 250; 500; 1,000] $\cdot 10^3$; MCS $u = 3$ | z_{max} = 2,700 ppm nc-est.= ecdf	–	S-1	Fig. 16
Sec. 4.1: Variance reduction in sampling I	Effect of variance reduction of Latin Hypercube Sampling and Quasi-Monte Carlo Sampling based on Sobol' sequences on the accuracy of analysis results	Wheel mounting assembly; 1 KC	Samp.= [MCS; LHS; QMCS] n = [10; 25; 50; 100; 250] $\cdot 10^3$ u = [2; 3; 4] | z_{max} = [63.3; 2,700; 45,500] ppm nc-est.= ecdf	–	S-1	Fig. 18, Fig. 19
Sec. 4.1: Variance reduction in sampling II	Effect of variance reduction by Latin Hypercube Sampling and Quasi-Monte Carlo Sampling based on Sobol' sequences on the accuracy of optimization results	Wheel mounting assembly; 1 KC	Samp.= [MCS; LHS; QMCS] n = 10, 000 $u = 3$ | z_{max} = 2,700 ppm nc-est.= ecdf	CS	O-2/S-1	Fig. 20
Sec. 4.1: Scattering and discontinuity elimination I	Effect of scattering effects through repeated evaluation of elitist solutions from previous generations on the accuracy of optimization results	Wheel mounting assembly; 1 KC	Repeat evaluation of elitist solutions=[1; 0] n = 10,000 $u = 3$ | z_{max} = 2,700 ppm nc-est.= ecdf	CS, CS*	O-2/S-1	Fig. 21
Sec. 4.1: Scattering and discontinuity elimination II	Effect of random number generation strategy on the accuracy of optimization results	Wheel mounting assembly; 1 KC	n = [10; 50; 100] $\cdot 10^3$; MCS $u = 3$ | z_{max} = 2,700 ppm nc-est.= ecdf	CS	O-2/S-1 O-2/S-2	Fig. 23, Fig. 24
Sec. 4.2: Estimation of product (non-) conformance I	Effect of nc-rate estimation technique on the accuracy of constraint evaluation	Wheel mounting assembly; 1 KC	nc-est.=[ncdf; kde-cdf; ecdf] n = [10; 25; 50; 100; 250] $\cdot 10^3$ Samp.= [MCS; LHS; QMCS] u = [2; 3; 4] | z_{max} = [63.3; 2,700; 45,500] ppm	–	S-1	Fig. 26, Fig. 27, Fig. 97

Study	Objective	Case study	Study design	Optim.[#1]	Strategy[#2]	Ref.
Sec. 4.2: Estimation of product (non-)conformance II	Effect of nc-rate estimation technique on the accuracy of constraint evaluation in optimization	Wheel mounting assembly; 1 KC	nc-est.=[ncdf; kde-cdf; ecdf] n = [10; 50; 100] · 10^3 Samp.= MCS $u = 3 \mid z_{\max} = 2{,}700$ ppm	CS	O-2/S-2	Fig. 28
Sec. 4.3: Nc-rate estimation for multiple assembly responses	Dealing with multiple assembly response functions in optimization	Wheel mounting assembly; 2 KCs	Correlation of KCs=[0; 1] n = 100,000, MCS $u = 3 \mid$ $z_{\max} = 2{,}700$ ppm	CS	O-2/S-3	Fig. 31, Fig. 32
Sec. 5.1: Alternative machine and supplier selection I	Comparison of minimum-cost curve vs. mixed-integer approach for equal part tolerance distributions	Wheel mounting assembly; standard normal distributions for all part tolerances	Alt. sel.=[Min. cost; MIP.] η_p = [50; 100] n-est.=ecdf n = 100,000; MCS $u = 3 \mid z_{\max} = 2{,}700$ ppm	GA	O-2/S-3	Fig. 35
Sec. 5.1: Alternative machine and supplier selection II	Comparison of minimum-cost curve vs. mixed-integer approach for different part tolerance distributions	Wheel mounting assembly; varying part tolerance distributions	Alt.sel.=[Min. cost; MIP.] η_p = [50; 100] n = 100,000; MCS nc-est.= ecdf $z_{\max} = 2{,}700$ ppm	GA	O-2/S-3	Fig. 36, Fig. 37
Sec. 5.2.1: Multiple machine/supplier selection – Random assembly	Dealing with multiple machine selection with individual batch sizes and random assembly	Wheel mounting assembly; varying part tolerance distributions	OptimalBatch=[eq; diff] n = 100,000, MCS nc-rate=ecdf $z_{\max} = 2{,}700$ ppm	GA	O-2/S-3	Fig. 40, Fig. 41
Sec. 5.2.2: Multiple machine/supplier selection – Selective assembly	Dealing with multiple machine selection with individual batch sizes and selective assembly	Wheel mounting assembly; varying part tolerance distributions	Asm. strat.=[random; selective] assembly] Prefixed weights= [0; 1] n = 10,000; MCS nc-est.= ecdf $t_{i,j} = var$	GA	O-2/S-3	Fig. 44

Study	Objective	Case study	Study design	Optim.#1	Strategy#2	Ref.
Sec. 5.3: Multiple part tolerances in optimization	Dealing with multiple tolerances on feature, part, and assembly level using dimension reduction and additional constraints	Wheel mounting assembly; varying part tolerance distributions; TCVisVA-model	n = 10,000; MCS nc-est.= ecdf $z_{\max}$ = 2,700 ppm	GA	O-2/S-3	Fig. 48, Fig. 49
Chap. 6: Efficiency of sampling-based tolerance-cost optimization	Main contributors to the computation time for sampling-based tolerance-cost optimization	Wheel mounting assembly; 1 KC	n = [10; 25; 50; 75; 100] $\cdot 10^3$; MCS η_g = [50; 100; 200] nc-est.= ecdf $z_{\max}$ = 2,700 ppm	CS	O-1/S-1	Fig. 50
Sec. 6.1: Adaptive sample sizes	Effect of adaptive sample sizes on the efficiency and reliability of the optimization results	Wheel mounting assembly; standard normal distributions for all part tolerances; TCVisVA-model	$n_{\min}$ = 5,000 (1) n = 10,000; MCS $n_{\min}$ = 10,000 (2) n = 100,000; MCS $\xi_1 = 7$ ξ_2 = [0.3; 0.5; 0.7] r_p = [0; 0.2]	CS, CS**	O-3/S-3	Fig. 53, Fig. 54, Fig. 55
Sec. 6.2: Surrogate modeling	Effect of surrogate modeling on the efficiency and reliability of the optimization results	Wheel mounting assembly; standard normal distributions for all part tolerances; TCVisVA-model	n = 10,000; MCS nc-est.= ecdf nc-eval.=[TCVisVA; ANN]	CS	O-2/S-3	Fig. 58
Sec. 6.3: Adaptive surrogate model-based optimization	Effect of adaptive surrogate modeling on the efficiency and reliability of the optimization results	Wheel mounting assembly; standard normal distributions for all part tolerances; TCVisVA-model	n = 10,000; MCS nc-est.= ecdf $z_{\max}$ = 2,700 ppm nc-eval.=[TCVisVA; ANN; adapt. ANN]	CS, CS***	O-2/S-3	Fig. 60, Fig. 61, Fig. 62

Study	Objective	Case study	Study design	Optim.[#1]	Strategy[#2]	Ref.
Chap. 8: Application and evaluation of the developed optimal tolerance allocation framework	Application and evaluation of the developed approach on optimal tolerance allocation based on sampling-based tolerance-cost optimization	E-cross skate; standard normal distributions for all part tolerances TCVisVA-model	n = 10,000, MCS nc-est.= ecdf z_{max} = 2,700 ppm nc-evaluation=[TCVisVA; adapt. sample sizes; ANN; adapt. ANN]	CS CS**, CS***	O-2/S-3	Fig. 69, Fig. 70, Fig. 71, Fig. 72

[#1] Information on optimization algorithms used. GA: Genetic algorithm; CS Cuckoo Search algorithm; CS*: modified Cuckoo Search algorithm to illustrate the benefits of discarding a reevaluation of elitist solutions; CS**: extended Cuckoo Search algorithm for adaptive sample sizes; CS***: extended Cuckoo Search algorithm for (adaptive) surrogate model-based tolerance-cost optimization. The optimization settings are summarized in the respective descriptions of the individual studies in the main part and the following sections.

[#2] Strategy used to deal with random numbers within optimization and sampling operations (see Tbl. 6).

A.9.1 Accuracy studies

The tolerance-cost data is adopted from the data given in [307] and adapted to define suitable scenarios in the different studies. An exponential tolerance-cost function $C_i = f_{C_i}(t_i) = a_i + b_i \cdot e^{-c_i \cdot t_i}$ is applied for all tolerances (see Tbl. 1).

Table 8: Tolerance-cost data of wheel mounting assembly example used in the studies in Chap. 4.

i	$X_{i,0}$	Costs			Limits		Characteristics of ρ_i		
		a_i	b_i	c_i	t_i^{lb}	t_i^{ub}	*Type*	Δ_{μ_i}	σ_i
1, 2, 3, 4, 5	*	28.2	241	55.8	0.01	0.11	*ND*	0	$t_i/6$

* $X_{1,0} = 10$, $X_{2,0} = 25$, $X_{3,0} = 10$, $X_{4,0} = 23$, $X_{5,0} = 48$.
- $X_{i,0}$, t_i^{lb}, t_i^{ub} in mm.
- *Type* of ρ_i: *ND*, standard normal distribution with mean $\mu_i = X_{i,0} + \Delta_{\mu_i}$, and standard deviation σ_i.

Sec. 4.1: Estimation of the margin of error

- *Specification limits*:
  - f_{Y_2}, Eq. (84):

$$LSL_2 = Y_0 - \frac{u}{3 \cdot 2} * \sqrt{4 \cdot 0.05^2}, \tag{90}$$

$$USL_2 = Y_0 + \frac{u}{3 \cdot 2} * \sqrt{4 \cdot 0.05^2}, \tag{91}$$

with $u = 3$: $LSL = LSL_2 = 2.950$ mm; $USL = USL_2 = 3.050$ mm
- *Number of repetitions*: $\eta_r = 250$

Table 9: Summary of the results from Sec. 4.1: Estimation of margin of error.

	Sample size ($\times 10^3$)						
	10	**25**	**50**	**100**	**250**	**500**	**1,000**
$q_{Z,97.5\%}$	3,717.07	3,343.25	3,154.85	3,021.63	2,903.41	2,843.84	2,801.71
$q_{\hat{Z},97.5\%}$	3,800	3,410	3,205	3,055	2,903	2,833.50	2,797
$q_{Z,2.5\%}$	1,682.93	2,056.75	2,245.15	2,378.37	2,496.590	2,556.16	2,598.29
$q_{\hat{Z},2.5\%}$	1,700	2,120	2,255	2,357	2,492	2,566	2,579

Sec. 4.1: Variance reduction methods
(1) Analysis study:

- *Specification limits*: for f_{Y_2}, see Eq. (90)–(91)
  - with $u = 4$: $LSL = LSL_2 = 2.933$ mm; $USL = USL_2 = 3.067$ mm
  - with $u = 3$: $LSL = LSL_2 = 2.950$ mm; $USL = USL_2 = 3.050$ mm
  - with $u = 2$: $LSL = LSL_2 = 2.967$ mm; $USL = USL_2 = 3.033$ mm
- *Sampling*:
  - *QMCS*: *skip* = 0, *leap* = 0, scramble method: linear scramble combined with random digital shift acc. to [762, 792]
  - *LHS*: 5-fold repetition of each sampling finding the best design under the criterion of the maximum of minimum distance between the sample points (see Chap. A.4)
- *Number of repetitions*: $\eta_r = 100$

Table 10: Summary of the analysis study (1) in Sec. 4.1: Variance reduction methods.

u	Sampling	Measure	Sample size ($\times 10^3$)				
			10	**25**	**50**	**100**	**250**
$\pm 4\sigma$	MCS	$\widetilde{m}_{\hat{z}}$	0	40	60	60	64
		$qr_{\hat{z},95\%}$	200	160	120	110	68
		$\delta_{\hat{z},95\%}$	215.96	152.76	100.00	84.20	53.71
	LHS	$\widetilde{m}_{\hat{z}}$	50	40	60	60	64
		$qr_{\hat{z},95\%}$	300	200	160	100	56
		$\delta_{\hat{z},95\%}$	215.96	152.76	121.17	73.78	47.39
	QMCS	$\widetilde{m}_{\hat{z}}$	0	80	60	70	64
		$qr_{\hat{z},95\%}$	200	160	80	70	40
		$\delta_{\hat{z},95\%}$	215.96	152.76	68.40	57.98	32.70
$\pm 3\sigma$	MCS	$\widetilde{m}_{\hat{z}}$	2,800	2,680	2,690	2735	2,696
		$qr_{\hat{z},95\%}$	2,000	1,440	820	610	456
		$\delta_{\hat{z},95\%}$	37.04	26.67	15.19	12.04	8.59
	LHS	$\widetilde{m}_{\hat{z}}$	2,750	2,640	2,680	2,690	2,700
		$qr_{\hat{z},95\%}$	1,900	1,320	760	630	408
		$\delta_{\hat{z},95\%}$	37.04	24.44	14.44	11.67	7.56
	QMCS	$\widetilde{m}_{\hat{z}}$	2,650	2,720	2,720	2,685	2,708
		$qr_{\hat{z},95\%}$	1,100	920	480	420	204
		$\delta_{\hat{z},95\%}$	20.37	16.30	8.89	7.78	4.07
$\pm 2\sigma$	MCS	$\widetilde{m}_{\hat{z}}$	45,300	45,560	45,550	45,560	45,440
		$qr_{\hat{z},95\%}$	8,200	5,960	4,080	2,480	1,400
		$\delta_{\hat{z},95\%}$	8.35	6.15	4.42	2.73	1.53
	LHS	$\widetilde{m}_{\hat{z}}$	45,450	45,400	45,440	45,560	45,442
		$qr_{\hat{z},95\%}$	6,800	4,440	3,280	2,350	1,720
		$\delta_{\hat{z},95\%}$	8.24	5.05	3.60	2.58	1.89
	QMCS	$\widetilde{m}_{\hat{z}}$	45,600	45,400	45,460	45,475	45,534
		$qr_{\hat{z},95\%}$	4,300	2,240	1,480	920	592
		$\delta_{\hat{z},95\%}$	4.73	2.51	1.76	1.02	0.63

- $\widetilde{m}_{\hat{z}}, qr_{\hat{z},95\%}$ in ppm, $\delta_{\hat{z},95\%} = qr_{95\%}(|\hat{z} - z_{\text{ref}}|)/z_{\text{ref}}$ in %.

(2) Optimization study:

- *Tolerance-cost information* acc. to Tbl. 8
- *Specification limits*: see Eq. (90)–(91) with $u = 3$
- *Optimization settings*: $\eta_p = 25$, $\eta_g = 500$, $\eta_{g,\text{stall}} = \text{inf}$ with a fitness tolerance of 1e-04 (decimals to be relevant for fitness improvement evaluation), $p_\text{a} = 0.25$
- *Sampling information*: see analysis study (1) in Sec. 4.1: Variance reduction methods
- *Number of repetitions*: $\eta_r = 50$

Table 11: Summary of the results of the optimization study (2) in Sec. 4.1: Variance reduction methods.

Sampling	$\overline{m}_C$	$qr_{C,95\%}$	$\overline{m}_{\hat{z}}$	$qr_{\hat{z},95\%}$	FR	$\overline{\tau}_{\text{feas}}$
MCS	164.74	3.12	4,325.20	2,700	1.0	57.52
LHS	164.72	3.27	4,312.04	2,600	1.0	2,509.34
QMCS	166.94	2.37	3,749.30	1,700	1.0	97.08

- $qr_{C,95\%}$, $\overline{m}_C$ in MU; $qr_{\hat{z},95\%}$, $\overline{m}_{\hat{z}}$ in ppm; $\overline{\tau}_{\text{feas}}$ in s.
- *Flag* = 0 for all runs, i.e., the maximum number of generations η_g is reached.

Sec. 4.1: Reevaluation of elitist solutions

- *Tolerance-cost information*: see Tbl. 8
- *Specification limits*: see Eq. (90)–(91) with $u = 3$
- *Optimization settings*: $\eta_p = 25$, $\eta_g = 200$, $\eta_{g,\text{stall}} = \text{inf}$ with a fitness tolerance of 1e-04 (decimals to be relevant for fitness improvement evaluation), $p_{\text{a}} = 0.25$
- *Number of repetitions*: $\eta_r = 10$
- *Studied cases*:

  (a) Elitist individuals are reevaluated in the next generation with new random numbers in sampling-based tolerance analysis
  (b) Reevaluation is discarded, and tolerance analysis results from the previous run are used

Table 12: Summary of obtained optimal solutions for the optimization study presented in Sec. 4.1: Reevaluation of elitist solution.

r	(a)					(b)				
	$C_{\text{sum}}^{\text{opt}}$	$\hat{z}^{\text{opt}}$	C_{relation}	q_{feas}	$Flag^*$	$C_{\text{sum}}^{\text{opt}}$	$\hat{z}^{\text{opt}}$	C_{relation}	q_{feas}	$Flag^*$
1	170.87	2,700	0.21	1	0	166.75	2,600	0.37	1	0
2	171.08	2,500	0.25	1	0	167.27	2,600	0.35	1	0
3	170.32	2,700	0.04	1	0	167.43	2,500	0.18	1	0
4	171.53	2,700	0.31	1	0	165.07	2,500	0.23	1	0
5	170.70	2,700	0.27	1	0	164.91	2,700	0.39	1	0
6	170.57	2,700	0.20	1	0	165.70	2,400	0.19	1	0
7	169.84	2,700	0.26	1	0	166.73	2,500	0.34	1	0
8	170.83	2,600	0.33	1	0	166.72	2,700	0.34	1	0
9	170.97	1,900	0.14	1	0	165.75	2,400	0.43	1	0
10	172.11	2,600	0.17	1	0	165.95	2,700	0.22	1	0

* *Flag* = 0: Maximum number of generations η_g is reached.
- $C_{\text{sum}}^{\text{opt}}$ in MU, $\hat{z}^{\text{opt}}$ in ppm.

Sec. 4.1: Equal random numbers

- *Tolerance-cost information*: see Tbl. 8
- *Specification limits*: see Eq. (90)–(91) with $u = 3$
- *Optimization settings*: $\eta_p = 25$, $\eta_g = 500$, $\eta_{g,\text{stall}} = \text{inf}$ with a fitness tolerance of 1e-04 (decimals to be relevant for fitness improvement evaluation), $p_\text{a} = 0.25$
- *Sampling information*: see analysis study (1) in 4.1: Variance reduction methods
- *Number of repetitions*: $\eta_r = 50$
- *Studied cases*:
    (a) Iterative resampling with a newly generated set of random numbers for each individual
    (b) Reuse of the same, initially generated random numbers for repetitive tolerance analysis

Table 13: Summary of the results of the optimization study in Sec. 4.1: Equal random numbers.

Case	n	$\overline{m}_C$	$qr_{C,95\%}$	$\overline{m}_{\hat{z}}$	$qr_{\hat{z},95\%}$	FR	$\overline{\tau}_\text{feas}$
(a)	10,000	164.73	2.95	4,340.66	2,700	1	49.25
	50,000	168.63	1.55	3,364.72	1,080	1.0	185.11
	100,000	169.64	0.99	3,148	725	1.0	352.30
(b)	10,000	170.05	13.57	3,219.80	3,500	1	51.26
	50,000	171.19	4.69	2,887.99	1,240	1.0	168.88
	100,000	171.60	3.64	2,798.20	920	1.0	312.84

- $qr_{C,95\%}$, $\overline{m}_C$ in MU; $qr_{\hat{z},95\%}$, $\overline{m}_{\hat{z}}$ in ppm; $\overline{\tau}_\text{feas}$ in s.
- *Flag* = 0 for all runs, i.e., the maximum number of generations η_g is reached.

Sec. 4.2: Nc-rate estimation
(1) Analysis:

- *Tolerance-cost information*: see Tbl. 8
- *Specification limits*: see Eq. (90)–(91) with $u = 2, 3, 4$
- *Sampling information*: see analysis study (1) in Sec. 4.1: Variance reduction methods
- *Kernel density estimation*: kernel type K: Gaussian kernel, bandwidth h_K: optimal settings for estimating normal density acc. to [579] (see Chap. A.4)
- *Number of repetitions*: $\eta_r = 100$

- *Studied cases*:
  (a) empirically estimated cdf (ecdf)
  (b) cdf based on kernel density estimation (kde-cdf)
  (c) cdf for normal distribution $\mathcal{N}(\mu, \sigma^2)$ (ncdf)

Table 14: Summary of the results of the analysis study in Sec. 4.2, $u = 4$.

Samp-ling	**Nc-rate technique**	**Measure**	**Sample size** ($\times 10^3$)				
			10	**25**	**50**	**100**	**250**
MCS	(a) ecdf	$\widetilde{m}_{\hat{z}}$	0.00	40.00	60.00	60.00	56.00
		$qr_{\hat{z},95\%}$	300.00	160.00	140.00	90.00	52.00
		$\delta_{\hat{z},95\%}$	215.96	100.00	110.58	65.88	43.13
	(b) kde-cdf	$\widetilde{m}_{\hat{z}}$	57.38	74.77	71.59	65.36	64.58
		$qr_{\hat{z},95\%}$	207.80	159.22	126.46	82.18	50.48
		$\delta_{\hat{z},95\%}$	176.83	151.95	103.63	76.17	40.81
	(c) ncdf	$\widetilde{m}_{\hat{z}}$	64.43	63.42	63.02	62.75	63.27
		$qr_{\hat{z},95\%}$	27.65	16.89	14.15	8.43	5.88
		$\delta_{\hat{z},95\%}$	22.09	14.60	11.18	7.46	4.64
LHS	(a) ecdf	$\widetilde{m}_{\hat{z}}$	0.00	40.00	60.00	60.00	64.00
		$qr_{\hat{z},95\%}$	300.00	160.00	100.00	110.00	60.00
		$\delta_{\hat{z},95\%}$	215.96	152.76	89.57	78.99	47.39
	(b) kde-cdf	$\widetilde{m}_{\hat{z}}$	58.55	71.13	63.40	66.59	67.95
		$qr_{\hat{z},95\%}$	185.40	181.25	118.42	88.00	47.48
		$\delta_{\hat{z},95\%}$	162.48	145.44	111.01	69.09	40.69
	(c) ncdf	$\widetilde{m}_{\hat{z}}$	62.71	63.04	63.63	63.50	63.27
		$qr_{\hat{z},95\%}$	28.35	20.37	12.05	7.99	5.36
		$\delta_{\hat{z},95\%}$	21.60	14.19	9.24	6.58	4.38
QMCS	(a) ecdf	$\widetilde{m}_{\hat{z}}$	0.00	40.00	60.00	60.00	64.00
		$qr_{\hat{z},95\%}$	200.00	200.00	80.00	70.00	44.00
		$\delta_{\hat{z},95\%}$	215.96	184.36	68.40	52.61	32.70
	(b) kde-cdf	$\widetilde{m}_{\hat{z}}$	71.03	76.99	70.48	71.41	68.37
		$qr_{\hat{z},95\%}$	185.58	129.43	74.52	48.23	44.00
		$\delta_{\hat{z},95\%}$	186.21	110.83	60.67	46.61	29.72
	(c) ncdf	$\widetilde{m}_{\hat{z}}$	63.35	63.38	63.35	63.35	63.34
		$qr_{\hat{z},95\%}$	1.06	0.52	0.30	0.15	0.04
		$\delta_{\hat{z},95\%}$	0.83	0.49	0.29	0.17	0.10

- $\widetilde{m}_{\hat{z}}, q_{\hat{z},95\%}$ in ppm, $\delta_{\hat{z},95\%}$ in %.

Table 15: Summary of the results of the analysis study in Sec. 4.2, $u = 3$.

Sampling	Nc-rate technique	Measure	Sample size ($\times 10^3$) 10	25	50	100	250
MCS	(a) ecdf	$\widetilde{m}_{\hat{z}}$	2,600.00	2,640.00	2,680.00	2,700.00	2,698.00
		$qr_{\hat{z},95\%}$	2,200.00	1,520.00	1,020.00	600.00	404.00
		$\delta_{\hat{z},95\%}$	40.74	28.15	17.41	11.30	7.19
	(b) kde-cdf	$\widetilde{m}_{\hat{z}}$	2,967.53	2,982.75	2,865.09	2,838.93	2,809.90
		$qr_{\hat{z},95\%}$	1,858.44	1,093.61	892.78	509.58	398.65
		$\delta_{\hat{z},95\%}$	40.62	32.04	22.01	14.74	9.51
	(c) ncdf	$\widetilde{m}_{\hat{z}}$	2,687.72	2,690.79	2,687.96	2,697.07	2,698.25
		$qr_{\hat{z},95\%}$	681.94	487.10	348.20	234.79	127.98
		$\delta_{\hat{z},95\%}$	12.63	9.02	6.76	4.49	2.37
LHS	(a) ecdf	$\widetilde{m}_{\hat{z}}$	2,650.00	2,720.00	2,680.00	2,685.00	2,712.00
		$qr_{\hat{z},95\%}$	1,900.00	1,320.00	1,020.00	590.00	424.00
		$\delta_{\hat{z},95\%}$	35.19	25.19	17.04	10.93	7.78
	(b) kde-cdf	$\widetilde{m}_{\hat{z}}$	3,119.72	2,972.68	2,903.83	2,852.47	2,813.41
		$qr_{\hat{z},95\%}$	1,604.04	1,204.54	747.83	535.43	374.67
		$\delta_{\hat{z},95\%}$	38.78	29.31	21.03	13.75	10.48
	(c) ncdf	$\widetilde{m}_{\hat{z}}$	2,707.24	2,698.13	2,701.43	2,698.26	2,699.73
		$qr_{\hat{z},95\%}$	602.38	455.27	315.46	180.64	136.41
		$\delta_{\hat{z},95\%}$	11.16	8.43	5.57	3.45	2.48
QMCS	(a) ecdf	$\widetilde{m}_{\hat{z}}$	2,650.00	2,720.00	2,680.00	2,685.00	2,712.00
		$qr_{\hat{z},95\%}$	1,900.00	1,320.00	1,020.00	590.00	424.00
		$\delta_{\hat{z},95\%}$	35.19	25.19	17.04	10.93	7.78
	(b) kde-cdf	$\widetilde{m}_{\hat{z}}$	3,119.72	2,972.68	2,903.83	2,852.47	2,813.41
		$qr_{\hat{z},95\%}$	1,604.04	1,204.54	747.83	535.43	374.67
		$\delta_{\hat{z},95\%}$	38.78	29.31	21.03	13.75	10.48
	(c) ncdf	$\widetilde{m}_{\hat{z}}$	2,707.24	2,698.13	2,701.43	2,698.26	2,699.73
		$qr_{\hat{z},95\%}$	602.38	455.27	315.46	180.64	136.41
		$\delta_{\hat{z},95\%}$	11.16	8.43	5.57	3.45	2.48

- $\widetilde{m}_{\hat{z}}$, $qr_{\hat{z},95\%}$ in ppm, $\delta_{\hat{z},95\%}$ in %.

Table 16: Summary of the results of the analysis study in Sec. 4.2, $u = 2$.

Sampling	Nc-rate technique	Measure	Sample size ($\times 10^3$) 10	25	50	100	250
MCS	(a) ecdf	$\widetilde{m}_{\hat{z}}$	45,250.00	45,440.00	45,340.00	45,515.00	45,562.00
		$qr_{\hat{z},95\%}$	8,000.00	5,000.00	3,660.00	2,650.00	1,632.00
		$\delta_{\hat{z},95\%}$	9.23	5.45	4.07	2.88	1.78
	(b) kde-cdf	$\widetilde{m}_{\hat{z}}$	48,418.84	47,576.36	47,281.98	46,632.34	46,361.88
		$qr_{\hat{z},95\%}$	6,907.32	4,978.29	3,379.80	2,135.13	1,380.82
		$\delta_{\hat{z},95\%}$	13.87	9.46	6.92	4.88	3.14
	(c) ncdf	$\widetilde{m}_{\hat{z}}$	45,451.79	45,604.85	45,468.58	45,637.04	45,481.45
		$qr_{\hat{z},95\%}$	5,739.09	3,565.72	2,580.54	1,684.00	1,230.43
		$\delta_{\hat{z},95\%}$	6.91	3.82	2.72	2.02	1.37
LHS	(a) ecdf	$\widetilde{m}_{\hat{z}}$	45,650.00	45,380.00	45,560.00	45,460.00	45,538.00
		$qr_{\hat{z},95\%}$	8,300.00	5,000.00	2,940.00	2,560.00	1,468.00
		$\delta_{\hat{z},95\%}$	9.01	5.49	3.30	2.79	1.61
	(b) kde-cdf	$\widetilde{m}_{\hat{z}}$	48,900.29	47,521.32	47,014.45	46,727.74	46,378.83
		$qr_{\hat{z},95\%}$	6,478.73	4,205.85	2,907.30	2,264.28	1,505.68
		$\delta_{\hat{z},95\%}$	12.73	8.78	6.06	4.29	3.07
	(c) ncdf	$\widetilde{m}_{\hat{z}}$	45,191.47	45,510.66	45,535.29	45,515.20	45,517.66
		$qr_{\hat{z},95\%}$	6,081.21	3,132.44	2,484.57	1,618.03	999.78
		$\delta_{\hat{z},95\%}$	7.05	3.71	2.70	1.75	1.15
QMCS	(a) ecdf	$\widetilde{m}_{\hat{z}}$	45,400.00	45,480.00	45,480.00	45,460.00	45,496.00
		$qr_{\hat{z},95\%}$	3,900.00	2,120.00	1,860.00	1,090.00	484.00
		$\delta_{\hat{z},95\%}$	4.73	2.37	2.04	1.20	0.53
	(b) kde-cdf	$\widetilde{m}_{\hat{z}}$	48,540.69	47,612.12	47,129.81	46,730.98	46,326.01
		$qr_{\hat{z},95\%}$	2,064.86	1,333.28	882.30	607.06	338.48
		$\delta_{\hat{z},95\%}$	8.76	5.81	4.36	3.28	2.19
	(c) ncdf	$\widetilde{m}_{\hat{z}}$	45,508.63	45,508.37	45,501.54	45,502.04	45,500.14
		$qr_{\hat{z},95\%}$	234.43	115.87	49.50	28.34	8.39
		$\delta_{\hat{z},95\%}$	0.26	0.13	0.06	0.03	0.01

- $\widetilde{m}_{\hat{z}}$, $qr_{\hat{z},95\%}$ in ppm, $\delta_{\hat{z},95\%}$ in %.

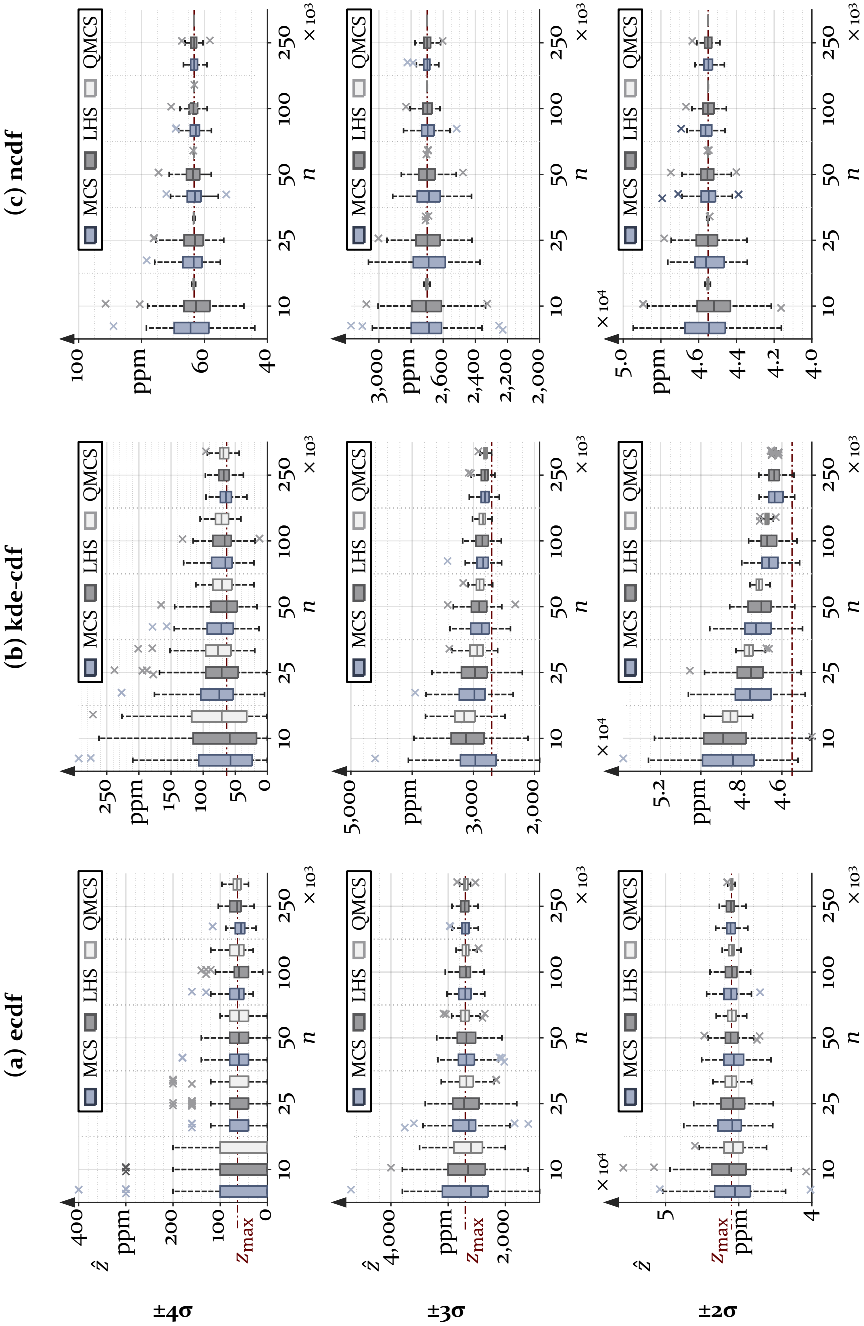

Figure 97: Summary of results for study (1) presented in Sec. 4.2, investigating the influence of the nc-rate estimation technique on the nc-rates $\hat{z}$ taking three different sampling strategies MCS, LHS and QMCS, different sample sizes, and sigma levels into account.

(2) Optimization study:

- *Tolerance-cost information*: see Tbl. 8
- *Specification limits*: see Eq. (90)–(91) with $u = 3$
- *Optimization settings*: $\eta_p = 25$, $\eta_g = 500$, $\eta_{g,\text{stall}} = \text{inf}$ with a fitness tolerance of 1e-04 (decimals to be relevant for fitness improvement evaluation), $p_\text{a} = 0.25$
- *Sampling* and *kernel density estimation* are identical to the settings defined in study (1) performed in Sec. 4.2: Nc-rate estimation
- *Number of repetitions*: $\eta_r = 50$
- *Studied cases*:
    - (a) empirically estimated cdf (ecdf)
    - (b) cdf based on kernel density estimation (kde-cdf)
    - (c) cdf for normal distribution $\mathcal{N}(\mu, \sigma^2)$ (ncdf)

Table 17: Summary of the results of the optimization study in Sec. 4.2.

Nc-tech.	n	$\overline{m}_C$	$qr_{C,95\%}$	$\overline{m}_{\hat{z}}$	$qr_{\hat{z},95\%}$	FR	$\overline{\tau}_\text{feas}$
(a)	10,000	170.20	13.53	3,205.08	3,400.00	1.0	123.91
	50,000	171.44	5.21	2,861.48	1,290.00	1.0	406.13
	100,000	171.39	3.38	2,826.32	880.00	1.0	526.93
(b)	10,000	174.37	11.75	2,756.81	2,576.11	1.0	130.11
	50,000	173.26	5.50	2,713.08	1,148.71	1.0	623.79
	100,000	172.79	3.20	2,728.98	793.89	1.0	995.65
(c)	10,000	171.75	5.20	2,758.37	1,179.64	1.0	44.72
	50,000	172.01	2.15	2,701.48	478.41	1.0	193.63
	100,000	171.93	1.63	2,712.82	356.45	1.0	359.93

- $\overline{m}_C$, $q_{C,95\%}$ in MU; $qr_{\hat{z},95\%}$, $\overline{m}_{\hat{z}}$ in ppm. $\overline{\tau}_\text{feas}$ in s.
- *Flag* = 0 for all runs, i.e., maximum number of generations η_g is reached.

Sec. 4.3: Multiple assembly responses

- *Tolerance-cost data*, *nominal dimensions*, *tolerance limits*, and *part tolerance probability distribution information* follow the information given in Tbl. 8
- *Specification limits*:
  - f_{Y_1}, Eq. (83) : $LSL_1 = Y_0 - 0.5 \cdot \sqrt{2 \cdot 0.05^2}$ mm $= 1.965$ mm
  - f_{Y_1}, Eq. (83): $USL_1 = Y_0 + 0.5 \cdot \sqrt{2 \cdot 0.05^2}$ mm $= 2.035$ mm
  - f_{Y_2}, Eq. (84): $LSL_2 = Y_0 - 0.5 \cdot \sqrt{4 \cdot 0.05^2}$ mm $= 2.950$ mm
  - f_{Y_2}, Eq. (84): $USL_2 = Y_0 + 0.5 \cdot \sqrt{4 \cdot 0.05^2}$ mm $= 3.050$ mm
- *Optimization settings*: $\eta_p = 25$, $\eta_g = 200$, $\eta_{g,\text{stall}} = 50$ with a fitness tolerance of 1e-04 (decimals to be relevant for fitness improvement evaluation), $p_\text{a} = 0.25$
- *Number of repetitions*: $\eta_r = 10$
- *Studied cases*:
  (a) Non-conformance requirement represented by K nc-constraints
  (b) Non-conformance requirement represented by one overall nc-constraint

Table 18: Summary of obtained optimal solutions for the optimization study presented in Sec. 4.3.

r	(a)					(b)				
	$C_{\text{sum}}^{\text{opt}}$	$\hat{z}_{\text{asm}}^{\text{opt}}$	$\hat{z}_1^{\text{opt}}$	$\hat{z}_2^{\text{opt}}$	$Flag^*$	$C_{\text{sum}}^{\text{opt}}$	$\hat{z}_{\text{asm}}^{\text{opt}}$	$\hat{z}_1^{\text{opt}}$	$\hat{z}_2^{\text{opt}}$	$Flag^*$
1	212.58	5,340	2,690	2,650	0	224.23	2,680	1,040	1,640	0
2	212.62	5,400	2,700	2,700	0	223.54	2,700	920	1,780	0
3	212.42	5,360	2,680	2,680	0	224.20	2,700	1,060	1,640	0
4	212.58	5,210	2,530	2,680	0	223.85	2,660	990	1,670	0
5	212.65	5,270	2,580	2,690	0	225.34	2,690	1,280	1,410	1
6	213.22	5,360	2,690	2,690	0	223.95	2,660	930	1,730	0
7	214.59	5,310	2,620	2,690	1	224.02	2,690	1,020	1,670	0
8	213.69	4,900	2,210	2,690	0	223.82	2,700	950	1,750	0
9	212.74	5,320	2,700	2,620	0	223.74	2,700	930	1,770	0
10	212.43	5,370	2,680	2,690	0	224.05	2,700	1,150	1,550	0

* *Flag* = 0: Maximum number of generations η_g is reached.

\- $C_{\text{sum}}^{\text{opt}}$ in MU; $\hat{z}_1, \hat{z}_2, \hat{z}_{\text{asm}}^{\text{opt}}$ in ppm.

Table 19: Performance measures for the optimization study presented in Sec. 4.3.

Case	$\boldsymbol{FR}^{*}$	$\boldsymbol{SR}^{**}$	$\overline{\boldsymbol{C}}_{\mathbf{relation}}$	$\boldsymbol{AFESO}^{**}$	$\overline{\boldsymbol{\tau}}^{*}_{\mathbf{feas}}$ **in s**
(a)	1.0	0.8	0.74	10,000	150.50
(b)	1.0	0.9	0.60	10,000	153.90

* with δ_{feas} acc. to the defined constraint tolerance.
** with $\delta_{\text{success}} = 0.005 \cdot C_{\text{sum}}\left(\boldsymbol{t}_{\text{opt}}\right)$, where $\boldsymbol{t}_{\text{opt}}$ are the solutions obtained for the best runs (see Tbl. 20).

Table 20: Least-cost tolerances obtained in the best runs presented in Sec. 4.3.

Case	$\boldsymbol{r}$	$\boldsymbol{v}^{*}$	$\boldsymbol{i}$				
			1	**2**	**3**	**4**	**5**
(a)	3	t_i	0.0515	0.0441	0.0518	0.0544	0.0534
(b)	2	t_i	0.0500	0.0420	0.0505	0.0486	0.0508

* t_i part tolerances in mm.

A.9.2 Completeness studies

All additional information and results are given below. In Sec. 5.1–5.2, an exponential tolerance-cost function $C_{i,j} = f_{C_{i,j}}(t_{i,j}) = a_{i,j} + b_{i,j} \cdot e^{-c_{i,j} \cdot t_{i,j}}$ is applied for all tolerances $t_{i,j}$ (see Tbl. 1).

Sec. 5.1: Machine/supplier selection Study (1):

- *Tolerance-cost information*: see Tbl. 21
- *Specification limits*:
  - f_{Y_1}, Eq. (83): $LSL_1 = 1.96$ mm; $USL_1 = 2.04$ mm
  - f_{Y_2}, Eq. (84): $LSL_2 = 2.95$ mm; $USL_2 = 3.05$ mm
- *Optimization settings*: $\eta_p = var$, $\eta_g = 500$, η_g, stall $= 50$ with a fitness tolerance of 1e-03 (decimals to be relevant for fitness improvement evaluation), penalty approach for constraint handling. Further GA optimization parameters and settings, such as elite count, crossover and migration fraction, and crossover and selection strategy, are set to the proposed default values in MATLAB®. For more information, see [793].
- *Number of repetitions*: $\eta_r = 10$
- *Studied cases*:
  - (a) minimum-cost curve approach
  - (b) mixed-integer optimization

Table 21: Tolerance-cost data of wheel mounting assembly example used in study (1) in Sec. 5.1.

i	$X_{i,0}$	j	Costs			Limits		Characteristics of $\rho_{i,j}$		
			$a_{i,j}$	$b_{i,j}$	$c_{i,j}$	$t_{i,j}^{lb}$	$t_{i,j}^{ub}$	*Type*	$\Delta_{\mu_{i,j}}$	$\sigma_{i,j}$
1, 2, 3	*	1	28.2	241	55.8	0.006	0.08	*ND*	0	$t_i/6$
		2	29.80	260	52	0.008	0.08	*ND*	0	$t_i/6$
		3	25.82	286.4	59.5	0.006	0.09	*ND*	0	$t_i/6$
		4	23	271.5	57.64	0.008	0.1	*ND*	0	$t_i/6$
4	23	1	42.2	312.84	105.66	0.002	0.08	*ND*	0	$t_i/6$
		2	35.	352.43	92.7	0.002	0.1	*ND*	0	$t_i/6$
5	48	1	22.5	208.25	62.45	0.01	0.1	*ND*	0	$t_i/6$
		2	20.2	240.43	66.7	0.01	0.12	*ND*	0	$t_i/6$
		3	25.05	211.42	40.05	0.02	0.11	*ND*	0	$t_i/6$
		4	27	214.16	58.82	0.03	0.12	*ND*	0	$t_i/6$

* $X_{1,0} = X_{3,0} = 10$, $X_{2,0} = 25$.
- $X_{i,0}$, $t_{i,j}^{lb}$, $t_{i,j}^{ub}$ in mm.
- *Type* of $\rho_{i,j}$: *ND*, standard normal distribution with mean $\mu_{i,j} = X_{i,0} + \Delta_{\mu_{i,j}}$, and standard deviation $\sigma_{i,j}$ (see Fig. 83).

Table 22: Summary of obtained optimal solutions for optimization study (1) in Sec. 5.1.

r	(a), $\eta_p = 50$					(a), $\eta_p = 100$				
	$C_{\mathrm{sum}}^{\mathrm{opt}}$	$\hat{z}_1^{\mathrm{opt}}$	$\hat{z}_2^{\mathrm{opt}}$	$\hat{z}_{\mathrm{asm}}^{\mathrm{opt}}$	$Flag^*$	$C_{\mathrm{sum}}^{\mathrm{opt}}$	$\hat{z}_1^{\mathrm{opt}}$	$\hat{z}_2^{\mathrm{opt}}$	$\hat{z}_{\mathrm{asm}}^{\mathrm{opt}}$	$Flag^*$
1	185.69	670	2,020	2,680	1	182.75	300	2,400	2,690	1
2	182.42	360	2,360	2,700	1	182.35	430	2,290	2,700	1
3	186.06	400	2,310	2,700	1	182.9	330	2,370	2,690	1
4	184.29	250	2,460	2,700	1	183.2	420	2,300	2,700	1
5	183.58	500	2,230	2,700	1	182.64	370	2,340	2,700	1
6	182.27	430	2,290	2,700	1	182.23	390	2,320	2,700	1
7	188.09	440	2,270	2,700	1	182.32	390	2,310	2,690	1
8	182.95	440	2,280	2,700	1	182.34	480	2,240	2,700	1
9	183.06	700	2,030	2,700	1	183.09	420	2,290	2,700	1
10	182.92	330	2,380	2,700	1	182.16	440	2,280	2,700	1

r	(b), $\eta_p = 50$					(b), $\eta_p = 100$				
	$C_{\mathrm{sum}}^{\mathrm{opt}}$	$\hat{z}_1^{\mathrm{opt}}$	$\hat{z}_2^{\mathrm{opt}}$	$\hat{z}_{\mathrm{asm}}^{\mathrm{opt}}$	$Flag^*$	$C_{\mathrm{sum}}^{\mathrm{opt}}$	$\hat{z}_1^{\mathrm{opt}}$	$\hat{z}_2^{\mathrm{opt}}$	$\hat{z}_{\mathrm{asm}}^{\mathrm{opt}}$	$Flag^*$
1	183.66	270	2,440	2,700	1	182.26	390	2,320	2,700	1
2	183.25	400	2,320	2,700	1	182.08	390	2,320	2,700	1
3	184.47	490	2,220	2,700	1	182.25	440	2,280	2,700	1
4	182.39	430	2,290	2,700	1	182.39	390	2,320	2,700	1
5	182.92	300	2,410	2,700	1	182.79	400	2,310	2,700	1
6	184.12	230	2,480	2,700	1	182.45	430	2,290	2,700	1
7	184.13	390	2,320	2,700	1	182.52	410	2,300	2,700	1
8	183.37	340	2,370	2,700	1	182.52	410	2,300	2,700	1
9	184.86	530	2,180	2,700	1	182.57	340	2,370	2,700	1
10	183.81	430	2,290	2,700	1	182.39	440	2,280	2,700	1

* *Flag* = 1: Average change in the penalty fitness value is less than the fitness tolerance and constraint violation is less than constraint tolerance.
\- $C_{\mathrm{sum}}^{\mathrm{opt}}$ in MU, $\hat{z}_1^{\mathrm{opt}}, \hat{z}_2^{\mathrm{opt}}, \hat{z}_{\mathrm{asm}}^{\mathrm{opt}}$ in ppm.

Table 23: Performance measures for the optimization study (1) in Sec. 5.1.

Case	FR^*	SR^{**}	$\overline{C}_{\mathrm{relation}}$	$AFESO^{**}$	$\overline{\tau}_{\mathrm{feas}}^*$ in s
(a), $\eta_p = 50$	1.0	0.5	0.78	3,155	69.72
(a), $\eta_p = 100$	1.0	0.8	0.58	5,829	132.48
(b), $\eta_p = 50$	1.0	0.3	0.90	2,890	49.40
(b), $\eta_p = 100$	1.0	1.0	0.54	6,242	96.36

* with δ_{feas} acc. to the defined constraint tolerance.
** with $\delta_{\mathrm{success}} = 0.005 \cdot C_{\mathrm{sum}}\left(\boldsymbol{t}_{\mathrm{opt}}\right)$, where $\boldsymbol{t}_{\mathrm{opt}}$ are the solutions obtained for the best runs (see Tbl. 24).

Table 24: Least-cost tolerances obtained in the best runs for optimization study (1) in Sec. 5.1.

Case	r	v^*	i				
			1	**2**	**3**	**4**	**5**
(a), η_p = 50	6	t_i	0.0503	0.0500	0.0521	0.0482	0.0470
		j for $x_{i,j} = 1$	4	4	4	2	2
(a), η_p = 100	10	t_i	0.0516	0.0488	0.0534	0.0498	0.0453
		j for $x_{i,j} = 1$	4	4	4	2	2
(b), η_p = 50	4	t_i	0.0519	0.0501	0.0495	0.0480	0.0482
		j for $x_{i,j} = 1$	4	4	4	2	2
(b), η_p = 100	2	t_i	0.0529	0.0477	0.0529	0.0501	0.0457
		j for $x_{i,j} = 1$	4	4	4	2	2

* t_i part tolerances in mm.

Study (2):

- *Tolerance-cost information*: see Tbl. 25
- *Specification limits*:
  - f_{Y_1}, Eq. (83): $LSL_1 = 1.94$ mm; $USL_1 = 2.06$ mm
  - f_{Y_2}, Eq. (84): $LSL_2 = 2.90$ mm; $USL_2 = 3.10$ mm
- *Optimization settings*: see study (1)
- *Number of repetitions*: $\eta_r = 10$
- *Studied cases*:
  - (a) minimum-cost curve approach
  - (b) mixed-integer optimization

Table 25: Tolerance-cost data of wheel mounting assembly example used in study (2) in Sec. 5.1.

i	$X_{i,0}$	j	Costs			Limits		Characteristics of $\rho_{i,j}$			
			$a_{i,j}$	$b_{i,j}$	$c_{i,j}$	$t_{i,j}^{\mathrm{lb}}$	$t_{i,j}^{\mathrm{ub}}$	*Type*	$\sigma_{i,j}$	$\gamma_{i,j}$	$\kappa_{i,j}$
1, 3	*	1	28.20	241	55.80	0.006	0.1	*PD*	$t_i/6$	0.5	3.05
		2	29.80	260	52	0.008	0.13	*PD*	$t_i/6$	−0.2	2.9
		3	25.82	286.4	59.5	0.006	0.14	*PD*	$t_i/6$	0.1	2.8
		4	23.00	271.5	57.64	0.008	0.15	*ND*	$t_i/6$	–	–
2	25	1	*Fixed:* $C_{i,j} = 42.2$			0.02	0.02	*ND*	$t_i/6$	0.5	3.05
		2	*Fixed*: $C_{i,j} = 35.80$			0.05	0.05	*PD*	$t_i/6$	−0.2	2.9
		3	*Fixed*: $C_{i,j} = 23.00$			0.06	0.06	*ND*	$t_i/6$	–	–
		4	*Fixed*: $C_{i,j} = 22.00$			0.1	0.1	*UD*	$t_i/6$	–	–
4	23	1	42.2	312.84	105.66	0.002	0.08	*ND*	$t_i/6$	–	–
		2	35.00	352.43	92.7	0.002	0.1	*PD*	$t_i/6$	0.3	3.1
5	48	1	22.50	208.25	62.45	0.01	0.1	*PD*	$t_i/6$	−0.2	2.9
		2	20.20	240.43	66.7	0.02	0.12	*ND*	$t_i/6$	–	–
		3	25.05	211.42	40.05	0.02	0.11	*PD*	$t_i/6$	−0.1	3
		4	300.00	214.16	58.82	0.03	0.12	*ND*	$t_i/6$	–	–

* $X_{1,0} = X_{3,0} = 10$.

- $X_{i,0}$ $t_{i,j}^{\mathrm{lb}}$, $t_{i,j}^{\mathrm{ub}}$ in mm.
- *Type* of $\rho_{i,j}$: *UD*, Uniform Distribution with $\mu_{i,j} =_{i,0} + \Delta_{\mu_{i,j}}$ *ND*, standard normal distribution with mean $\mu_{i,j} = X_{i,0} + \Delta_{\mu_{i,j}}$, $\Delta_{\mu_{i,j}} = 0\ \forall i = 1, \dots, I; j = 1, \dots, J_i$, standard deviation $\sigma_{i,j}$.; *PD*: Pearson distribution with mean $\mu_{i,j} =_{i,0} + \Delta_{\mu_{i,j}}$, standard deviation σ_{ij}, skewness $\tau_{i,j}$, and kurtosis $\gamma_{i,j}$ (see Fig. 83).

Table 26: Summary of obtained optimal solutions for optimization study (2) in Sec. 5.1.

r	(a), $\eta_p = 50$					(a), $\eta_p = 100$				
	$C_{\text{sum}}^{\text{opt}}$	$\hat{z}_1^{\text{opt}}$	$\hat{z}_2^{\text{opt}}$	$\hat{z}_{\text{asm}}^{\text{opt}}$	$Flag^*$	$C_{\text{sum}}^{\text{opt}}$	$\hat{z}_1^{\text{opt}}$	$\hat{z}_2^{\text{opt}}$	$\hat{z}_{\text{asm}}^{\text{opt}}$	$Flag^*$
1	149.78	1,520	1,180	2,700	1	150.01	1,420	1,280	2,700	1
2	149.6441	1,860	840	2,700	1	150.10	1,380	1,320	2,700	1
3	150.10	1,830	870	2,700	1	149.85	1,520	1,180	2,700	1
4	150.14	1,650	1,050	2,700	1	152.22	2,240	460	2,700	1
5	150.60	1,030	1,670	2,700	1	149.71	1,480	1,220	2,700	1
6	150.61	1,290	1,410	2,700	1	149.71	1,930	770	2,700	1
7	151.92	2,210	490	2,700	1	149.65	1,860	840	2,700	1
8	154.6	2,360	340	2,700	1	150.57	1,030	1,670	2,700	1
9	151.04	960	1,740	2,700	1	150.18	1,180	1,520	2,700	1
10	153.06	1,910	780	2,690	1	149.47	1,860	840	2,700	1

r	(b), $\eta_p = 50$					(b), $\eta_p = 100$				
	$C_{\text{sum}}^{\text{opt}}$	$\hat{z}_1^{\text{opt}}$	$\hat{z}_2^{\text{opt}}$	$\hat{z}_{\text{asm}}^{\text{opt}}$	$Flag^*$	$C_{\text{sum}}^{\text{opt}}$	$\hat{z}_1^{\text{opt}}$	$\hat{z}_2^{\text{opt}}$	$\hat{z}_{\text{asm}}^{\text{opt}}$	$Flag^*$
1	129.77	1,700	1,050	2,700	1	137.95	280	2,420	2,700	1
2	129.68	1,660	1,090	2,700	1	130.06	1,850	880	2,700	1
3	129.88	1,620	1,130	2,700	1	129.78	1,850	890	2,700	1
4	129.68	1,660	1,090	2,700	1	129.85	1,710	1,020	2,680	1
5	129.71	1,710	1,040	2,700	1	130.06	1,880	850	2,690	1
6	129.72	1,670	1,080	2,700	1	129.76	1,670	1,070	2,690	1
7	129.78	1,840	910	2,700	1	129.94	1,850	890	2,700	1
8	130.05	1,670	1,080	2,700	1	129.72	1,660	1,080	2,700	1
9	138.04	310	2,390	2,700	1	129.77	1,830	910	2,700	1
10	129.78	1,710	1,040	2,700	1	129.76	1,700	1,050	2,700	1

* *Flag* = 1: Average change in the penalty fitness value is less than the fitness tolerance and constraint violation is less than constraint tolerance.

\- $C_{\text{sum}}^{\text{opt}}$ in MU, $\hat{z}_1^{\text{opt}}, \hat{z}_2^{\text{opt}}, \hat{z}_{\text{asm}}^{\text{opt}}$ in ppm.

Table 27: Performance measures for the optimization study (2) in Sec. 5.1.

Case	FR^*	SR^{**}	$\overline{C}_{\text{relation}}$	$AFESO^{**}$	$\overline{\tau}_{\text{feas}}^{*}$ in s
(a), $\eta_p = 50$	1.0	0.4	0.72	2,650	579.00
(a), $\eta_p = 100$	1.0	0.8	0.47	5,211	1,019.90
(b), $\eta_p = 50$	1.0	0.9	0.13	2,790	1,121.24
(b), $\eta_p = 100$	1.0	0.9	0.50	5,858	2,738.33

* with δ_{feas} acc. to the defined constraint tolerance.

** with $\delta_{\text{success}} = 0.005 \cdot C_{\text{sum}}(\boldsymbol{t}_{\text{opt}})$, where $\boldsymbol{t}_{\text{opt}}$ are the solutions obtained for the best runs (see Tbl. 28).

Table 28: Least-cost tolerances obtained in the best runs for optimization study (2) in Sec. 5.1.

Case	r	v^*	i				
			1	**2**	**3**	**4**	**5**
(a), η_p = 50	2	t_i	0.06984	0.1000	0.0737	0.0335	0.0722
		j for $x_{i,j}$	4	4	4	2	2
(a), η_p = 100	10	t_i	0.0726	0.1000	0.0721	0.0335	0.0708
		j for $x_{i,j}$	4	4	4	2	2
(b), η_p = 50	4	t_i	0.0948	0.0600	0.0978	0.0543	0.0812
		j for $x_{i,j}$	4	3	4	2	2
(b), η_p = 100	8	t_i	0.0929	0.0600	0.0964	0.0542	0.0841
		j for $x_{i,j}$	4	3	4	2	2

* t_i part tolerances in mm.

Sec. 5.2.1: Machine/supplier allocation with random assembly

- *Tolerance-cost information*: see Tbl. 29
- *Specification limits*:
  - f_{Y_1}, Eq. (83): $LSL_1 = 1.94$ mm; $USL_1 = 2.06$ mm
  - f_{Y_2}, Eq. (84): $LSL_2 = 2.90$ mm; $USL_2 = 3.10$ mm
- *Optimization settings*: $\eta_p = 250$, $\eta_g = 1{,}000$, $\eta_{g,\text{stall}} = 1{,}000$ with a fitness tolerance of 1e-03 (decimals to be relevant for fitness improvement evaluation), penalty approach for constraint handling. Further settings are set to the proposed default values.
- *Number of repetitions*: $\eta_r = 10$
- *Studied cases*:

  (a) $t_{i,j} = t_i$

  (b) $t_{i,j} = var$

Table 29: Tolerance-cost data of wheel mounting assembly example for optimization study in Sec. 5.2.1.

i	$X_{i,0}$	j	Costs			Limits		Characteristics of $\rho_{i,j}$			$w_{i,j}^{\mathrm{ub}}$
			$a_{i,j}$	$b_{i,j}$	$c_{i,j}$	$t_{i,j}^{\mathrm{lb}}$	$t_{i,j}^{\mathrm{ub}}$	*Type*	$\gamma_{i,j}$	$\kappa_{i,j}$	
1,		1	28.2	241	55.8	0.006	0.1	*PD*	0.5	3.05	0.50
2,	*	2	29.8	260	52	0.008	0.13	*PD*	−0.2	2.9	0.05
3		3	25.82	286.4	59.5	0.006	0.14	*PD*	0.1	2.8	0.20
		4	23	271.5	57.64	0.008	0.15	*ND*	–	–	0.70
4	23	1	42.2	312.84	105.66	0.002	0.08	*ND*	–	–	0.8
		2	35	352.43	92.7	0.002	0.1	*PD*	0.3	3.1	0.50
5	48	1	22.5	208.25	62.45	0.01	0.1	*PD*	−0.2	2.9	0.4
		2	20.2	240.43	66.7	0.02	0.12	*ND*	–	–	0.35
		3	25.05	211.42	40.05	0.02	0.11	*PD*	−0.1	3	0.40
		4	300	214.16	58.82	0.03	0.12	*ND*	–	–	0.80

* $X_{1,0} = X_{3,0} = 10$, $X_{2,0} = 25$.
- $X_{i,0}$, $t_{i,j}^{\mathrm{lb}}$, $t_{i,j}^{\mathrm{ub}}$ in mm.
- *Type* of $\rho_{i,j}$: *ND*, standard normal distribution with mean $\Delta_{\mu_{i,j}} = X_{i,0}, \forall i = 1, \ldots, I; j = 1, \ldots, J_i$, standard deviation $\sigma_{i,j} = t_{i,j}/6$.
- *PD*: Pearson distribution with mean $\Delta_{\mu_{i,j}} = X_{i,0}, , \forall i = 1, \ldots, I; j = 1, \ldots, J_i$, standard deviation $\sigma_{i,j} = t_{i,j}/6$, skewness $\tau_{i,j}$ and kurtosis $\gamma_{i,j}$ (see Fig. 83).
- $w_{i,j}^{\mathrm{ub}}$: Maximum weight of machine j to realize tolerance $t_{i,j}$, $w_{i,j}^{\mathrm{lb}} = 0, \forall i = 1, \ldots, I; j = 1, \ldots, J_i$.

Table 30: Summary of obtained optimal solutions for optimization study in Sec. 5.2.1.

r	(a)					(b)				
	$C_{\mathrm{sum}}^{\mathrm{opt}}$	$\hat{z}_1^{\mathrm{opt}}$	$\hat{z}_2^{\mathrm{opt}}$	$\hat{z}_{\mathrm{asm}}^{\mathrm{opt}}$	*Flag**	$C_{\mathrm{sum}}^{\mathrm{opt}}$	$\hat{z}_1^{\mathrm{opt}}$	$\hat{z}_2^{\mathrm{opt}}$	$\hat{z}_{\mathrm{asm}}^{\mathrm{opt}}$	*Flag**
1	143.15	2,190	520	2,700	1	142.13	1,070	1,640	2,700	1
2	142.56	1,880	490	2,360	1	142.71	1,660	880	2,510	1
3	142.63	1,950	700	2,610	1	140.91	1,630	1,060	2,670	1
4	141.99	2,210	430	2,630	1	140.35	1,200	1,480	2,680	1
5	142.07	2,030	550	2,580	1	141.73	520	2,120	2,640	1
6	143.34	2,050	520	2,560	1	140.13	700	2,010	2,690	1
7	141.91	2,050	560	2,600	1	141.58	1,410	1,170	2,560	1
8	142.09	1,820	560	2,380	1	141.31	1,300	1,290	2,590	1
9	143.00	1,990	640	2,620	1	142.86	880	1,450	2,300	1
10	142.86	2,110	580	2,680	1	142.14	930	1,610	2,530	1

* *Flag* = 1: Average change in the penalty fitness value is less than the fitness tolerance and constraint violation is less than constraint tolerance.
- $C_{\mathrm{sum}}^{\mathrm{opt}}$ in MU, $\hat{z}_1^{\mathrm{opt}}, \hat{z}_2^{\mathrm{opt}}, \hat{z}_{\mathrm{asm}}^{\mathrm{opt}}$ in ppm.

Table 31: Performance measures for the optimization study in Sec. 5.2.1.

Case	FR^*	SR^{**}	$\overline{C}_{\text{relation}}$	$AFESO^{**}$	$\overline{\tau}^*_{\text{feas}}$ **in s**
(a)	1.0	0.5	0.65	91,003	13,417.72
(b)	1.0	0.2	0.72	148,725	13,843.93

* with δ_{feas} acc. to the defined constraint tolerance.
** with $\delta_{\text{success}} = 0.005 \cdot C_{\text{sum}}\left(\boldsymbol{t}_{\text{opt}}\right)$, where $\boldsymbol{t}_{\text{opt}}$ are the solutions obtained for the best runs (see Tbl. 32).

Table 32: Least-cost tolerances obtained in the best runs for optimization study in Sec. 5.2.1.

i	j	**Case**			
		(a), $r = 7$		**(b),** $r = 6$	
		$t_{i,j}$	$w_{i,j}$	$t_{i,j}$	$w_{i,j}$
1	1	0.0933	0.2707	0.0901	0.1049
	2	0.0933	0.0075	0.0780	0.0000
	3	0.0933	0.0226	0.1266	0.1958
	4	0.0933	0.6992	0.1044	0.6993
2	1	0.0851	0.1000	0.0791	0.0839
	2	0.0851	0.0000	0.0749	0.0210
	3	0.0851	0.2000	0.0865	0.1958
	4	0.0851	0.7000	0.0834	0.6993
3	1	0.0847	0.2657	0.0911	0.3007
	2	0.0847	0.0280	0.1023	0.0000
	3	0.0847	0.0070	0.1148	0.0000
	4	0.0847	0.6993	0.1128	0.6993
4	1	0.0681	0.5026	0.0604	0.5000
	2	0.0681	0.4974	0.0680	0.5000
5	1	0.0973	0.3333	0.0798	0.3333
	2	0.0973	0.3333	0.0878	0.3333
	3	0.0973	0.3333	0.1009	0.3333
	4	0.0973	0.0000	0.1021	0.0000

* $t_{i,j}$ part tolerances in mm.

Sec. 5.2.2: Machine/supplier allocation with selective assembly

- *Tolerance-cost information*: see Tbl. 33
- *Specification limits*:
  - f_{Y_1}, Eq. (83): $LSL_1 = 1.94$ mm; $USL_1 = 2.06$ mm
  - f_{Y_2}, Eq. (84): $LSL_2 = 2.90$ mm; $USL_2 = 3.10$ mm
- $N_C = \left(\frac{3!}{(3-2)!}\right)^4 * (2!/(2-2)!) \cdot \frac{1}{2!} = 1296$ acc. to Eq. (47) with $J_{\min} = 2$ for $j = 4$ and $J_i = 3$ for $i = 1, 2, 3, 5$ (see Tbl. 33)
- *Optimization settings*: $\eta_p = 250$, $\eta_g = 2{,}000$, η_g, stall $= 200$ with a fitness tolerance of 1e-03 (decimals to be relevant for fitness improvement evaluation), penalty approach for constraint handling. Further settings are set to the proposed default values.
- *Number of repetitions*: $\eta_r = 10$
- *Studied cases*:
  (a) random assembly
  (b) selective assembly

Table 33: Tolerance-cost data of wheel mounting assembly example used in Sec. 5.2.2.

i	j	Costs			Limits		Characteristics of $\rho_{i,j}$				$w^{ub}_{i,j}$
		$a_{i,j}$	$b_{i,j}$	$c_{i,j}$	$t^{lb}_{i,j}$	$t^{ub}_{i,j}$	*Type*	$\Delta_{\mu_{i,j}}$	$\sigma_{i,j}$	$p_{i,j}$	
1, 2, 3	1	100.00	271.506	57.64	0.02	0.10	*TD*	0	–	0.3	0.75
	2	29.80	260.00	52.00	0.03	0.06	*TD*	0	–	0.7	0.75
	3	28.20	241.00	55.80	0.03	0.06	*TD*	0	–	0.3	0.75
4	1	42.20	312.84	105.66	0.01	0.06	*UD*	0.1	–	–	0.75
	2	35.00	352.43	92.70	0.01	0.08	*ND*	−0.1	$t_{i,j}/6$	–	0.75
5	1	100.00	208.25	62.45	0.01	0.08	*UD*	0	–	–	0.75
	2	20.20	240.43	66.70	0.01	0.08	*UD*	0	–	–	0.75
	3	25.05	211.42	40.05	0.01	0.10	*ND*	0	$t_{i,j}/6$	–	0.75

* $X_{1,0} = 10$, $X_{2,0} = 25$, $X_{3,0} = 10$, $X_{4,0} = 23$, $X_{5,0} = 48$.
- $X_{i,0}$, $t^{lb}_{i,j}$, $t^{ub}_{i,j}$ in mm.
- *Type* of $\rho_{i,j}$: *UD*, Uniform Distribution with $\mu_{i,j} =_{i,0} +\Delta_{\mu_{i,j}}$ *ND*, standard normal distribution with mean $\mu_{i,j} = X_{i,0} + \Delta_{\mu_{i,j}}$, standard deviation $\sigma_{i,j}$.; TD: where peak location $H_{i,j}$ is defined by $X_{i,0} + (p_{i,j} - 0.5) \cdot t_{i,j}/2$ (see Tbl. 83).
- $w^{ub}_{i,j}$: Maximum weight of machine j to realize tolerance $t_{i,j}$, $w^{lb}_{i,j} = 0, \forall i = 1, \dots, I; j = 1, \dots, J_i$) for study (2).

Table 34: Summary of obtained optimal solutions for optimization study (1) in Sec. 5.2.2.

r	(a)					(b)					(b*)
	$C_{\text{sum}}^{\text{opt}}$	$\hat{z}_{\text{asm}}^{\text{opt}}$	$\hat{z}_1^{\text{opt}}$	$\hat{z}_2^{\text{opt}}$	$Flag^*$	$C_{\text{sum}}^{\text{opt}}$	$\hat{z}_{\text{asm}}^{\text{opt}}$	$\hat{z}_1^{\text{opt}}$	$\hat{z}_2^{\text{opt}}$	$Flag^*$	$\hat{z}_{\text{asm}}^{\text{opt}}$
1	315.19	2,700	0	2,700	1	302.09	2,700	0	2,700	1	17,100
2	314.45	2,700	0	2,700	1	303.15	2,600	100	2,700	1	17,400
3	314.21	2,700	0	2,700	1	301.39	2,700	0	2,700	1	26,000
4	313.37	2,700	0	2,700	1	301.15	2,700	0	2,700	1	17,500
5	315.16	2,700	0	2,700	1	300.74	2,700	0	2,700	1	19,100
6	315.51	2,700	0	2,700	1	302.65	2,700	0	2,700	1	17,400
7	316.48	2,700	0	2,700	1	302.51	2,700	0	2,700	1	17,600
8	314.85	2,700	0	2,700	1	305.45	2,700	0	2,700	1	12,600
9	315.56	2,700	0	2,700	1	302.56	2,600	100	2,700	1	17,200
10	314.61	2,700	0	2,700	1	302.15	2,700	0	2,700	1	17,900

* *Flag* = 1: Average change in the penalty fitness value is less than the fitness tolerance and constraint violation is less than constraint tolerance.

- $C_{\text{sum}}^{\text{opt}}$ in MU, $\hat{z}_1^{\text{opt}}, \hat{z}_2^{\text{opt}}, \hat{z}_{\text{asm}}^{\text{opt}}$ in ppm.
- (b*): $\hat{z}_{\text{asm}}^{\text{opt}}$ results when tolerance values obtained for selective assembly (b) are used for random assembly illustrating the effect of selective assembly on reducing the total non-conformance rate without tightening the tolerances.

Table 35: Performance measures for optimization study (1) in Sec. 5.2.2.

Case	FR^*	SR^{**}	$\overline{C}_{\text{relation}}$	$AFESO^{**}$	$\overline{\tau}_{\text{feas}}^*$ in s
(a)	1.0	0.5	1.0	244,667	2,558.84
(b)	1.0	0.5	0.25	103,841	1,305.12

* with δ_{feas} acc. to the defined constraint tolerance.

** with $\delta_{\text{success}} = 0.005 \cdot C_{\text{sum}}\left(\boldsymbol{t}_{\text{opt}}\right)$, where $\boldsymbol{t}_{\text{opt}}$ are the solutions obtained for the best runs (see Tbl. 36).

Table 36: Least-cost tolerances obtained in the best runs for optimization study (1) in Sec. 5.2.2.

i	j	Case (a), $r = 4$		Case (b), $r = 5$		
		$t_{i,j}$	$w_{i,j}$	$p_{i,j}$	$t_{i,j}$	$w_{i,j}$
1	1	0.0997	0.3333	3	0.0942	0.3333
	2	0.0599	0.3333	2	0.0598	0.3333
	3	0.0599	0.3333	1	0.0595	0.3333
2	1	0.0365	0.3333	2	0.0307	0.3333
	2	0.0356	0.3333	1	0.0594	0.3333
	3	0.0370	0.3333	3	0.0415	0.3333
3	1	0.0996	0.3333	1	0.0963	0.3333
	2	0.0599	0.3333	2	0.0599	0.3333
	3	0.0599	0.3333	3	0.0591	0.3333
4	1	0.0598	0.5000	1	0.0552	0.5000
	2	0.0251	0.5000	2	0.0298	0.5000
5	1	0.0797	0.3333	3	0.0737	0.3333
	2	0.0797	0.3333	2	0.0787	0.3333
	3	0.0999	0.3333	1	0.0988	0.3333

* $t_{i,j}$ part tolerances in mm.

Table 37: Summary of obtained optimal solutions for optimization study (2) in Sec. 5.2.2.

r	(a)					(b)					(b*)
	C_{sum}^{opt}	$\hat{z}_{asm}^{opt}$	$\hat{z}_1^{opt}$	$\hat{z}_2^{opt}$	$Flag^*$	C_{sum}^{opt}	$\hat{z}_{asm}^{opt}$	$\hat{z}_1^{opt}$	$\hat{z}_2^{opt}$	$Flag^*$	$\hat{z}_{asm}^{opt}$
1	205.76	2,700	0	2,700	1	198.14	2,700	0	2,700	1	10,600
2	206.93	2,700	0	2,700	0	197.32	2,600	0	2,600	1	9,600
3	219.68	2,700	0	2,700	0	207.11	2,700	0	2,700	1	6,900
4	204.16	2,700	0	2,700	0	199.51	2,700	0	2,700	1	7,900
5	206.97	2,700	0	2,700	1	199.27	2,700	0	2,700	1	10,300
6	206.29	2,700	0	2,700	1	210.39	2,700	0	2,700	1	8,000
7	204.2	2,700	0	2,700	0	199.3	2,700	0	2,700	1	8,700
8	215.99	2,700	0	2,700	0	203.03	1,700	0	1,700	0	13,900
9	216.55	2,700	0	2,700	0	203.76	2,700	0	2,700	1	12,800
10	205.75	2,700	0	2,700	1	203.85	2,700	0	2,700	1	8,700

* *Flag* = 0: Maximum number of generations is reached; *Flag* = 1: Average change in the penalty fitness value is less than the fitness tolerance and constraint violation is less than constraint tolerance.
- C_{sum}^{opt} in MU, $\hat{z}_1^{opt}, \hat{z}_2^{opt}, \hat{z}_{asm}^{opt}$ in ppm.
- (b*): $\hat{z}_{asm}^{opt}$ results when tolerance values obtained for selective assembly (b) are used for random assembly illustrating the effect of selective assembly on reducing the total non-conformance rate without tightening the tolerances.

Table 38: Performance measures for optimization study (2) in Sec. 5.2.2.

Case	$\boldsymbol{FR}^{*}$	$\boldsymbol{SR}^{**}$	$\overline{\boldsymbol{C}}_{\mathbf{relation}}$	$\boldsymbol{AFESO}^{**}$	$\overline{\tau}^{*}_{\mathbf{feas}}$ **in s**
(a)	1.0	0.2	0.845	487,257	4,791.30
(b)	1.0	0.2	0.003	355,125	4,614.26

* with δ_{feas} acc. to the defined constraint tolerance.
** with $\delta_{\text{success}} = 0.005 \cdot C_{\text{sum}}\left(\boldsymbol{t}_{\text{opt}}\right)$, where $\boldsymbol{t}_{\text{opt}}$ are the solutions obtained for the best runs (see Tbl. 39).

Table 39: Least-cost tolerances obtained in the best runs for optimization study (2) in Sec. 5.2.2.

$\boldsymbol{i}$	$\boldsymbol{j}$	**Case**				
		(a), $\boldsymbol{r} = 4$		**(b),** $\boldsymbol{r} = 2$		
		$\boldsymbol{t_{i,j}}$	$\boldsymbol{w_{i,j}}$	$\boldsymbol{p_{i,j}}$	$\boldsymbol{t_{i,j}}$	$\boldsymbol{w_{i,j}}$
	1	0.0761	0.0000	3	0.0330	0.0000
1	2	0.0600	0.2500	2	0.0596	0.2562
	3	0.0600	0.7500	1	0.0568	0.7438
	1	0.0765	0.0000	1	0.0201	0.0000
2	2	0.0404	0.2500	2	0.0305	0.2500
	3	0.0402	0.7500	3	0.0549	0.7500
	1	0.0832	0.0000	3	0.0754	0.0000
3	2	0.0600	0.2500	2	0.0583	0.2500
	3	0.0600	0.7500	1	0.0575	0.7500
4	1	0.0600	0.7500	1	0.0498	0.7500
	2	0.0250	0.2500	2	0.0349	0.2500
	1	0.0625	0.0000	1	0.0561	0.0000
5	2	0.0800	0.7500	2	0.0750	0.7477
	3	0.1000	0.2500	3	0.0987	0.2523

* $t_{i,j}$ part tolerances in mm.

Sec. 5.3: Multiple part tolerances

- *Tolerance-cost information*: summarized in Tbl. 40, following a reciprocal tolerance-cost function approach (see Tbl. 1) presented in [203, 600] and adapted to the given use case:

$$C_{l,u,i} = a_{l,u,i} + \frac{b_{l,u,i}}{t_{l,u,i}^{k}} = a_{l,u,i} + \frac{f_{\mathrm{M}_{l,u,i,j}} \cdot f_{\mathrm{F}_{l,u,i,j}} \cdot f_{\mathrm{A}_{l,u,i,j}} \cdot \beta \cdot X_{l,u,i}^{k/3}}{t_{l,u,i}^{k}}, \tag{92}$$

  where $a_{l,u,i}$ indicate the fixed costs, $f_{\mathrm{M}_{l,u,i,j}}, f_{\mathrm{F}_{l,u,i,j}}, f_{\mathrm{A}_{l,u,i,j}}, k$ and β are feature- and material-dependent cost coefficients, $X_{l,u,i}$ is the nominal value of the relevant feature dimension.

- *Specification limits*:
  - f_{Y_1}: $LSL_1 = 0$ mm, $USL_1 = 2.0$ mm
  - f_{Y_2}: $LSL_2 = 86.5°$, $USL_2 = 93.5°$
- *Optimization settings*: $\eta_p = 50$, $\eta_g = 1{,}000$, $\eta_{g,\text{stall}} = 50$ with a fitness tolerance of 1e-06 (decimals to be relevant for fitness improvement evaluation), penalty approach for constraint handling. Further settings are set to the proposed default values.
- *Number of repetitions*: $\eta_r = 10$

Table 40: Tolerance-cost data of wheel mounting assembly example used in Sec. 5.3.

Part	**Feat.**	**Tol.**	**Alt.**	**Coefficients of f_C**				**Boundaries**		**$\rho_{l,u,i,j}$**	
l	u	i	j	$f_{\mathrm{F}_{l,u,i,j}}$	$f_{\mathrm{A}_{l,u,i,j}}$	$f_{\mathrm{M}_{l,u,i,j}}$	$X_{l,u,i,j}$	$t^{\mathrm{lb}}_{l,u,i,j}$	$t^{\mathrm{ub}}_{l,u,i,j}$	$\gamma_{l,u,i,j}$	$\kappa_{l,u,i,j}$
1	1	1	1	850	1.5	1	42	0.005	0.200	0.1	3.1
			2	850	1.5	1.5	42	0.005	0.200	0	3
	2	1	1	850	1.5	1	3	0.004	0.200	−0.1	2.9
			2	850	1.5	1.5	3	0.004	0.200	0	3
		2	1	850	1.5	1	42	0.010	0.200	−0.1	3
			2	850	1.5	1.5	42	0.010	0.200	0	3
	3	2	1	57	11.4	1	6	0.012	0.012	0.2	3.1
			2	57	11.4	1.5	6	0.012	0.012	0	3
		1	1	57	11.4	1	3	0.024	0.400	−0.1	2.8
			2	57	11.4	1.5	3	0.024	0.400	0	3
2	1	1	1	212	1.5	1	26.9	0.005	0.200	0	3
	2	1	1	212	1.5	1	10.5	0.008	0.400	0	3
		2	1	212	1.5	1	26.9	0.010	0.200	0	3
	3	1	1	198	11.4	1	10	0.050	0.400	0	3
3	1	1	1	850	1.5	1	42	0.005	0.200	0.1	3.1
			2	850	1.5	1.5	42	0.005	0.200	0	3
	2	1	1	850	1.5	1	3	0.004	0.200	−0.1	2.9
			2	850	1.5	1.5	3	0.004	0.200	0	3
		2	1	850	1.5	1	42	0.010	0.200	−0.1	3
			2	850	1.5	1.5	42	0.010	0.200	0	3
	3	2	1	57	11.4	1	6	0.012	0.012	0.2	3.1
			2	57	11.4	1.5	6	0.012	0.012	0	3
		1	1	57	11.4	1	3	0.024	0.400	−0.1	2.8
			2	57	11.4	1.5	3	0.024	0.400	0	3
4	1	1	1	522	1	1	4.5	0.005	0.200	0	3
		2	1	19	1	1	22	0.010	0.200	0	3
	2	1	1	522	1	1	4.5	0.005	0.200	0	3
		2	1	19	1	1	22	0.010	0.200	0	3
	3	1	1	522	1	1	9	0.050	0.400	0	3

l	u	i	j	$f_{\mathrm{F}_{l,u,i,j}}$	$f_{\mathrm{A}_{l,u,i,j}}$	$f_{\mathrm{M}_{l,u,i,j}}$	$X_{l,u,i,j}$	$t^{\mathrm{lb}}_{l,u,i,j}$	$t^{\mathrm{ub}}_{l,u,i,j}$	$\gamma_{l,u,i,j}$	$\kappa_{l,u,i,j}$
	4	1	1	142	12.3	1	5.5	0.030	0.030	0	3
5	1	1	1	22	1	1	3.5	0.050	0.400	−0.1	3.1
			2	22	1	1.5	3.5	0.050	0.400	0	3
	2	1	1	5	1	1	3.5	0.004	0.200	0.1	3
			2	5	1	1.5	3.5	0.004	0.200	0	3
		2	1	5	1	1	6	0.010	0.100	−0.1	3.1
			2	5	1	1.5	6	0.010	0.100	0	3
		3	1	173	1	1	5.5	0.075	0.075	0	3.1
			2	173	1	1.5	5.5	0.075	0.075	0	3
	3	1	1	173	1	1	10	0.005	0.200	0.1	2.8
			2	173	1	1.5	10	0.005	0.200	0	3
		2	1	173	1	1	10	0.003	0.100	−0.1	3.1
			2	173	1	1.5	10	0.003	0.100	0	3
	4	1	1	66	1	1	6	0.008	0.008	−0.1	2.9
			2	66	1	1.5	6	0.008	0.008	0	3

- $X_{l,u,i}$, $t^{\mathrm{lb/ub}}_{l,u,i,j}$ in mm.
- $f_{\mathrm{Al,u,i,j}}$: coefficient related to the surface area of feature u in mm².
- $f_{\mathrm{F}_{l,u,i,j}}$: coefficient related to the feature type of feature u.
- $f_{\mathrm{M}_{l,u,i,j}}$: coefficient related to the material used and its machining difficulty. This thesis interprets it as a general difficulty factor to differ between different process alternatives.
- $a_{l,u,i} = 0$, $k = 0.55$, $\beta = 1.0 \cdot 10^{-3}$ for all tolerances.
- *Type* of $\rho_{l,u,i,j}$: all tolerances follow a Pearson distribution with $\Delta_{\mu_{l,u,i,j}} = 0$, standard deviation $\sigma_{l,u,i,j} = t_{l,u,i,j}/6$, skewness $\tau_{l,u,i,j}$, and kurtosis $\gamma_{l,u,i,j}$ (see Tbl. 83).

Table 41: Summary of obtained optimal solutions for the optimization study presented in Sec. 5.3.

r	$C^{\mathrm{opt}}_{\mathrm{sum}}$	$\hat{z}^{\mathrm{opt}}_{\mathrm{asm}}$	$\hat{z}^{\mathrm{opt}}_{1}$	$\hat{z}^{\mathrm{opt}}_{2}$	*Flag**
1	124.18	1,200	1,500	2,700	1
2	123.78	600	2,100	2,700	1
3	125.22	1,000	1,700	2,700	1
4	123.37	1,000	1,700	2,700	1
5	155.81	0	7,800	7,800	−2
6	125.23	700	2,000	2,700	1
7	156.45	0	18,500	18,500	−2
8	190.50	0	3,500	3,500	−2
9	123.40	300	2,400	2,700	1
10	123.19	700	2,000	2,700	1

* *Flag* = 1: Average change in the penalty fitness value is less than the fitness tolerance and constraint violation is less than constraint tolerance. *Flag* = −2: No feasible point found.
- $C^{\mathrm{opt}}_{\mathrm{sum}}$ in MU, $\hat{z}^{\mathrm{opt}}_{1}$, $\hat{z}^{\mathrm{opt}}_{2}$, $\hat{z}^{\mathrm{opt}}_{\mathrm{asm}}$ in ppm.

Table 42: Performance measures for the optimization study presented in Sec. 5.3.

FR***	***SR********	$\overline{C}_{\text{relation}}$	***AFESO********	$\overline{\tau}^{*}_{\text{feas}}$ **in s**
0.7	0.4	0.66	9,718	59,507.60

* with δ_{feas} acc. to the defined constraint tolerance.
** with $\delta_{\text{success}} = 0.005 \cdot C_{\text{sum}}\left(\boldsymbol{t}_{\text{opt}}\right)$, where $\boldsymbol{t}_{\text{opt}}$ are the solutions obtained for the best runs (see Tbl. 43).

Table 43: Least-cost tolerances obtained in the best runs for the optimization study presented in Sec. 5.3.

r	l	u	i	$t_{l,u,i}$	j for $x_{l,u,i} = 1$
10	1	1	1	0.200	2
		2	1	0.198	2
			2	0.197	2
		3	2	0.012	2
			1	0.127	2
	2	1	1	0.133	1
		2	1	0.360	1
			2	0.132	1
		3	1	0.368	1
	3	1	1	0.200	2
		2	1	0.198	2
			2	0.197	2
		3	2	0.012	2
			1	0.127	2
	4	1	1	0.200	1
			2	0.027	1
		2	1	0.190	1
			2	0.190	1
		3	1	0.339	1
		4	1	0.030	1
	5	1	1	0.360	1
		2	1	0.168	1
			2	0.036	1
		3	3	0.075	1
			1	0.180	1
			2	0.037	1
		4	1	0.008	1

* $t_{l,u,i}$ part tolerance i for feature u of part l in mm.

A.9.3 Efficiency studies

Initial study on the main contributors to the efficiency

- *Tolerance-cost data*, *nominal dimensions*, *tolerance limits*, and *part tolerance probability distribution information* follow the information given in Tbl. 8.
- *Specification limits*: Study considers only $f_Y = f_{Y_2}$ as functional relevant.
  - $f_Y = f_{Y_2}$, Eq. (84): $LSL = LSL_2 = Y_0 - 0.5 \cdot \sqrt{4 \cdot 0.05^2}$ mm $= 2.950$ mm
  - $f_Y = f_{Y_2}$, Eq. (84): $USL = USL_2 = Y_0 + 0.5 \cdot \sqrt{4 \cdot 0.05^2}$ mm $= 3.050$ mm
- *Optimization settings*: $\eta_p = 50$, $\eta_g = var$, $\eta_{g,\text{stall}} = \text{inf}$ with a fitness tolerance of 1e-04 (decimals to be relevant for fitness improvement evaluation), $p_\text{a} = 0.25$
- *Number of repetitions*: $\eta_r = 100$

Table 44: Summary of results for Chap. 6: Main contributors to the efficiency.

	$qr_{C,95\%}$ in MU				
	Sample size ($\times 10^3$)				
	$n = 10$	$n = 25$	$n = 50$	$n = 100$	$n = 250$
$\eta_g = 50$	8.8341	6.5196	6.4819	5.4710	4.6412
$\eta_g = 100$	4.7033	3.2156	2.9348	2.6655	2.2456
$\eta_g = 150$	3.4507	2.4478	1.7995	1.5540	1.5963
	$\bar{\tau}_{\text{feas}}$ in s				
$\eta_g = 50$	9.2796	18.1310	36.4013	53.8687	71.3512
$\eta_g = 100$	23.9998	43.7850	87.5755	134.4843	175.2458
$\eta_g = 150$	98.3651	140.7616	245.3145	392.9127	499.8576

- *Flag* = 0 for all runs, i.e., maximum number of generations η_g is reached.

Table 45: Tolerance-cost data of wheel mounting assembly example used in Sec. 6.1–6.3.

Part	Feat.	Tol.	Coefficients of f_C				Boundaries	
l	u	i	$f_{\mathrm{F}_{l,u,i}}$	$f_{\mathrm{A}_{l,u,i}}$	$f_{\mathrm{M}_{l,u,i}}$	$X_{l,u,i}$	$t^{\mathrm{lb}}_{l,u,i}$	$t^{\mathrm{ub}}_{l,u,i}$
1	1	1	850	1.5	1	42	0.005	0.200
	2	1	850	1.5	1	3	0.100	0.100
		2	850	1.5	1	42	0.010	0.100
	3	2	57	11.4	1	6	0.012	0.012
		1	57	11.4	1	3	0.024	0.400
2	1	1	212	1.5	1	26.9	0.005	0.200
	2	1	212	1.5	1	10.5	0.200	0.200
		2	212	1.5	1	26.9	0.010	0.200
	3	1	198	11.4	1	10	0.050	0.400
3	1	1	850	1.5	1	42	0.005	0.200
	2	1	850	1.5	1	3	0.100	0.100
		2	850	1.5	1	42	0.010	0.100
	3	2	57	11.4	1	6	0.012	0.012
		1	57	11.4	1	3	0.024	0.400
4	1	1	522	1	1	4.5	0.100	0.100
		2	19	1	1	22	0.010	0.100
	2	1	522	1	1	4.5	0.100	0.100
		2	19	1	1	22	0.010	0.100
	3	1	522	1	1	9	0.050	0.400
	4	1	142	12.3	1	5.5	0.030	0.030
5	1	1	22	1	1	3.5	0.050	0.400
	2	1	5	1	1	3.5	0.100	0.100
		2	5	1	1	6	0.010	0.100
	3	3	173	1	1	5.5	0.075	0.075
		1	173	1	1	10	0.005	0.200
		2	173	1	1	10	0.003	0.100
	4	1	66	1	1	6	0.008	0.008

- $X_{l,u,i}$, $t^{\mathrm{lb/ub}}_{l,u,i}$ in mm.
- $f_{\mathrm{A}_{l,u,i}}$: coefficient related to the surface area of feature u in mm².
- $f_{\mathrm{F}_{l,u,i}}$: coefficient related to the feature type of feature u.
- $f_{\mathrm{M}_{l,u,i}}$: coefficient related to the material used and its machining difficulty.
- $a_{l,u,i} = 0$, $k = 0.55$, $\beta = 1.0 \cdot 10^{-3}$ for all tolerances.
- *Type* of $\rho_{l,u,i}$: all tolerances follow a standard normal distribution with $\Delta_{\mu_{l,u,i}} = 0$, standard deviation $\sigma_{l,u,i} = t_{l,u,i}/6$.

Sec. 6.1: Adaptive sample sizes

- *Tolerance-cost information*: see Tbl. 45.
- *Specification limits*:
  - f_{Y_1}: $LSL_1 = 0$ mm, $USL_1 = 1.5$ mm
  - f_{Y_2}: $LSL_2 = 87.5°$, $USL_2 = 92.5°$
- *Optimization settings*: $\eta_p = 25$, $\eta_g = 250$, $\eta_{g,\text{stall}} = 200$ with a fitness tolerance of 1e-06 (decimals to be relevant for fitness improvement evaluation), $p_\text{a} = 0.25$
- *Number of repetitions*: $\eta_r = 5$ for $n = 10{,}000$ (1); $\eta_r = 1$ for $n = 100{,}000$ (2)

Table 46: Overview of obtained optimal solutions for the optimization study (1) presented in Sec. 6.1.

			$r \rightarrow$				
r_p	ξ_2		1	2	3	4	5
0	0.7	$C_\text{sum}^{g=200}$	109.85	110.72	110.13	110.22	110.09
		C_sum^opt	109.75	110.21	109.93	109.64	109.90
		$\hat{z}_\text{asm}^\text{opt}$	2,700	2,700	2,700	2,600	2,500
	0.5	$C_\text{sum}^{g=200}$	109.88	110.57	110.23	110.02	110.38
		C_sum^opt	109.54	109.92	109.61	109.80	109.90
		$\hat{z}_\text{asm}^\text{opt}$	2,700	2,700	2,600	2,600	2,700
	0.3	$C_\text{sum}^{g=200}$	109.95	110.10	109.98	110.09	110.01
		C_sum^opt	109.65	109.92	109.66	109.76	109.70
		$\hat{z}_\text{asm}^\text{opt}$	2,700	2,600	2,700	2,700	2,700
0.2	0.7	$C_\text{sum}^{g=200}$	109.86	110.18	110.71	109.93	110.08
		C_sum^opt	109.64	110.06	110.31	109.68	109.85
		$\hat{z}_\text{asm}^\text{opt}$	2,700	2,600	2,700	2,700	2,600
	0.5	$C_\text{sum}^{g=200}$	109.94	110.59	110.29	109.59	110.14
		C_sum^opt	109.62	110.21	109.92	109.49	109.73
		$\hat{z}_\text{asm}^\text{opt}$	2,500	2,600	2,700	2,600	2,600
	0.3	$C_\text{sum}^{g=200}$	109.71	110.31	109.97	110.03	110.26
		C_sum^opt	109.67	110.01	109.78	109.91	110.13
		$\hat{z}_\text{asm}^\text{opt}$	2,700	2,600	2,700	2,700	2,700
n = const	--	$C_\text{sum}^{g=200}$	110.05	110.38	110.17	110.35	110.21
		C_sum^opt	109.84	110.15	110.03	109.92	109.88
		$\hat{z}_\text{asm}^\text{opt}$	2,500	2,700	2,600	2,700	2,600

- C_sum^opt, $C_\text{sum}^{g=200}$ in MU, $\hat{z}_\text{asm}^\text{opt}$ in ppm.

Table 47: Summary of the optimization study (1) presented in Sec. 6.1.

	$r_p = 0$			$r_p = 0.2$			$n = \text{const}$
$\xi_2 =$	**0.7**	**0.5**	**0.3**	**0.7**	**0.5**	**0.3**	
$\widetilde{m}_{C_{\text{sum}}^{g=200}}$	110.13	110.23	110.01	110.08	110.14	110.03	110.21
$\widetilde{m}_{C_{\text{sum}}^{\text{opt}}}$	110	109.80	109.70	109.854	109.73	109.91	109.92
$\widetilde{m}_{\hat{z}_{\text{asm}}}$	2,700	2,700	2,700	2,700	2,600	2,700	2,600
FR^*	1.0	1.0	1.0	1.0	1.0	1.0	1.0
$\overline{\tau}_{\text{feas}}^*$	14.25	16	17.08	17.51	18.90	20.33	19.66

* with δ_{feas} acc. to the defined constraint tolerance.
- *Flag* = 0: maximum number of generations η_g in all runs is reached.
- $\widetilde{m}_{C_{\text{sum}}^{\text{opt}}}$, $\widetilde{m}_{C_{\text{sum}}^{g=200}}$ in MU, $\widetilde{m}_{\hat{z}_{\text{asm}}}$ in ppm, $\overline{\tau}_{\text{feas}}$ in h.

Table 48: Summary of the optimization study (2) presented in Sec. 6.1.

	$r_p = 0$			$r_p = 0.2$			$n = \text{const}$
$\xi_2 =$	**0.7**	**0.5**	**0.3**	**0.7**	**0.5**	**0.3**	
$C_{\text{sum}}^{g=200}$	110.61	110.81	110.53	110.48	110.54	110.18	110.64
$C_{\text{sum}}^{\text{opt}}$	110.40	110.53	110.29	110.41	110.40	110.07	110.49
$\hat{z}_{\text{asm}}^{\text{opt}}$	2660	2680	2620	2630	2670	2650	2650
q_{feas}^*	1.0	1.0	1.0	1.0	1.0	1.0	1.0
$Flag^{**}$	0	0	0	0	0	0	0
τ_{feas}^*	92.51	118.39	144.52	121.71	147.33	174.80	186.01

* with δ_{feas} acc. to the defined constraint tolerance.
** *Flag* = 0: maximum number of generations η_g is reached.
- $C_{\text{sum}}^{\text{opt}}$, $C_{\text{sum}}^{g=200}$ in MU, $\hat{z}_{\text{asm}}^{\text{opt}}$ in ppm, τ_{feas} in h.

Sec. 6.2: Surrogate modeling

- *Tolerance-cost information*: summarized in Tbl. 45
- *Specification limits*: see A.9.3, Sec. 6.1
- *Optimization settings*: $\eta_p = 25$, $\eta_g = 250$, $\eta_{g,\text{stall}} = 200$ with a fitness tolerance of 1e-06 (decimals to be relevant for fitness improvement evaluation), $p_\text{a} = 0.25$
- *Number of repetitions*: $\eta_r = 50$
- *ANN training settings*: Wide, single-layered feed-forward ANN, f_{act}: rectified linear unit function; layer size: 100

Table 49: Summary of obtained optimal solutions for the optimization study presented in Sec. 6.2.

	D				
	300	**1,500**	**3,000**	**7,500**	**15,000**
	D'				
	96	**487**	**988**	**2,460**	**4,943**
$RMSE$	3,091.91	2,596.89	1,829.95	1,465.65	1,365.81
$\overline{m}_C$	107.873617	108.916254	109.085649	109.891632	109.940416
$qr_{C,95\%}$	0.903	1.083	0.677	0.561	0.908
$\overline{m}_{\hat{z}_{\text{asm}}}$	10,358	5,526	4,446	3,066	2,984
$qr_{\hat{z},95\%}$	4,875	2,500	2,025	1,100	1,425
$\overline{m}_e$	7,850	3,034	1893.88268	425.09162	370.087729
$qr_{e,95\%}$	4,678	2,738	1,965	1,124	1,317
FR^*	1	1	1	1	1
$\overline{\tau}_{\text{PreOpt}}$	524.13	2,639.80	5,328.92	13,230.83	26,481.89
τ_{feas}	571.91	2,688.01	5,419.06	13,321.34	26,573.09

* with δ_{feas} acc. to the defined constraint tolerance.
- *Flag* = 0 for all runs, i.e., maximum number of generations η_g is reached.
- $\overline{m}_C, qr_{C,95\%}$ in MU, $RMSE, \overline{m}_{\hat{z}_{\text{asm}}}, qr_{\hat{z},95\%}, \overline{m}_e, qr_{e,95\%}$ in ppm, $\overline{\tau}_{\text{feas}}, \tau_{\text{PreOpt}}$ in s.

Sec. 6.3: Adaptive surrogate model-based optimization

- *Tolerance-cost information*: summarized in Tbl. 45
- *Optimization settings*: $\eta_p = 25$, $\eta_g = 250$, $\eta_{g,\text{stall}} = 200$ with a fitness tolerance of 1e-06 (decimals to be relevant for fitness improvement evaluation), $p_{\text{a}} = 0.25$
- *Number of repetitions*: $\eta_r = 5$
- *Surrogate modeling*: ANN layout and settings are identical to study of Sec. 6.2
- *Studied cases*:
    (a) direct embedding of TCVisVA
    (b) surrogate model-based optimization
    (c) surrogate model-based optimization with resampling
    (d) adaptive surrogate model-based optimization

Table 50: Summary of computation times for the study presented in Sec. 6.3.

	FR^*	D	$\overline{\tau}_{\text{feas}}^{**}$	τ_{train}^{**}	$\overline{\tau}_{\text{resamp}}^{**}$	$\overline{\tau}_{\text{retrain}}^{**}$
(a)	1		70,773	0	0	0
(b)	1		558		0	0
(c)	1	300	14,347	524	13,789	0
(d)	1		14,392		13,780	55
(b)	1		1,348		0	0
(c)	1	500	14,838	1,314	13,491	0
(d)	1		14,912		13,502	62
(b)	1		2,674		0	0
(c)	1	1,500	16,571	2,640	13,898	0
(d)	1		16,604		13,858	72

* with δ_{feas} acc. to the defined constraint tolerance.
** $\overline{\tau}_{\text{feas}}, \tau_{\text{train}}, \overline{\tau}_{\text{resamp}}, \overline{\tau}_{\text{retrain}}$ in s.

Table 51: Performance measures for the optimization study presented in Sec. 6.3.

			$r \rightarrow$				
Case	D		**1**	**2**	**3**	**4**	**5**
(a)	/	$C_{\text{sum}}^{\text{opt}}$	109.84	110.15	110.03	109.92	109.88
		$\hat{z}_{\text{asm}}^{\text{opt}}$	2,500	2,700	2,600	2,700	2,600
		τ_{feas}	69,783	70,532	73,839	69,687	70,026
(b)	300	$C_{\text{sum}}^{\text{opt}}$	107.79	108.03	108.06	107.46	108.00
		$\hat{z}_{\tilde{f}_{\hat{z}}}^{\text{opt}}$	2,587	2,541	2,670	2,550	2,595
		$\hat{z}_{\text{asm}}^{\text{opt}}$	10,700	8,900	10,900	11,500	9,300
		e	8,113	6,359	8,230	8,950	6,705
		τ_{feas}	562	558	557	558	558
	750	$C_{\text{sum}}^{\text{opt}}$	108.81	108.93	108.83	108.73	108.68
		$\hat{z}_{\tilde{f}_{\hat{z}}}^{\text{opt}}$	2,412	2,218	2,623	2,559	2,654
		$\hat{z}_{\text{asm}}^{\text{opt}}$	7,400	5,300	4,600	4,600	6,500
		e	4,988	3,082	1,977	2,041	3,846
		τ_{feas}	1,349	1,347	1,347	1,347	1,347
	1,500	$C_{\text{sum}}^{\text{opt}}$	109.47	109.41	108.95	108.82	109.08
		$\hat{z}_{\tilde{f}_{\hat{z}}}^{\text{opt}}$	2,646	2,570	2,693	2,440	2,691
		$\hat{z}_{\text{asm}}^{\text{opt}}$	4,900	6,400	7,000	8,100	5,100
		e	2,254	3,830	4,307	5,660	2,409
		τ_{feas}	2,676	2,673	2,673	2,673	2,673
(c)	300	$C_{\text{sum}}^{\text{opt}}$	110.93	110.24	110.47	110.31	110.52
		$\hat{z}_{\tilde{f}_{\hat{z}}}^{\text{opt}}$	3,086	3,081	2,239	1,731	3,086
		$\hat{z}_{\text{asm}}^{\text{opt}}$	2,000	2,600	2,500	2,400	2,700
		e	−1,086	−481	261	669	−386
		τ_{feas}	14,321	14,351	14,358	14,358	14,348

Case	D		$r \rightarrow$ 1	2	3	4	5
(c)	750	$C_{\mathrm{sum}}^{\mathrm{opt}}$	110.49	110.31	109.87	110.19	110.06
		$\hat{z}_{\tilde{f}_{\hat{z}}}^{\mathrm{opt}}$	2,527	3,035	2,411	2,351	2,451
		$\hat{z}_{\mathrm{asm}}^{\mathrm{opt}}$	2,700	2,700	2700	2,700	2,600
		e	173	−335	289	349	149
		τ_{feas}	14,834	14,855	14,835	14,842	14,826
	1,500	$C_{\mathrm{sum}}^{\mathrm{opt}}$	109.82	110.75	110.02	110.58	110.12
		$\hat{z}_{\tilde{f}_{\hat{z}}}^{\mathrm{opt}}$	2,623	1,942	2,795	2,217	3,217
		$\hat{z}_{\mathrm{asm}}^{\mathrm{opt}}$	2,700	2,400	2,700	2,400	2,600
		e	77	458	−95	183	−617
		τ_{feas}	16,552	16,569	16,554	16,590	16,589
(d)	300	$C_{\mathrm{sum}}^{\mathrm{opt}}$	109.72	109.91	110.11	110.10	109.91
		$\hat{z}_{\tilde{f}_{\hat{z}}}^{\mathrm{opt}}$	2,712	2,607	3,000	2,514	2,703
		$\hat{z}_{\mathrm{asm}}^{\mathrm{opt}}$	2,700	2,700	2,600	2,600	2,600
		e	−12	93	−400	86	−103
		τ_{feas}	14,435	14,385	14,371	14,383	14,385
	750	$C_{\mathrm{sum}}^{\mathrm{opt}}$	109.88	109.98	109.78	109.62	109.62
		$\hat{z}_{\tilde{f}_{\hat{z}}}^{\mathrm{opt}}$	2,846	2,796	2,742	2,674	2,669
		$\hat{z}_{\mathrm{asm}}^{\mathrm{opt}}$	2,600	2,700	2,600	2,600	2,500
		e	−246	−96	−142	−74	−169
		τ_{feas}	14,909	14,910	14,914	14,903	14,925
	1,500	$C_{\mathrm{sum}}^{\mathrm{opt}}$	109.78	109.66	110.02	109.81	109.80
		$\hat{z}_{\tilde{f}_{\hat{z}}}^{\mathrm{opt}}$	2,868	2,731	2,624	2,662	2,720
		$\hat{z}_{\mathrm{asm}}^{\mathrm{opt}}$	2,700	2,600	2,700	2,600	2,500
		e	−168	−131	76	−62	−220
		τ_{feas}	16,670	16,640	16,578	16,572	16,561

- Prediction error $e = \hat{z}_{\mathrm{asm}}^{\mathrm{opt}} - \hat{z}_{\tilde{f}_{\hat{z}}}^{\mathrm{opt}}$.
- $C_{\mathrm{sum}}^{\mathrm{opt}}$ in MU, $\hat{z}_{\mathrm{asm}}^{\mathrm{opt}}$, $\hat{z}_{\tilde{f}_{\hat{z}}}^{\mathrm{opt}}$ in ppm, τ_{feas} in s.
- *Flag* = 0: maximum number of generations η_g is reached for all optimization iterations.

A.9.4 Evaluation studies

- *Tolerance-cost information*: see Tbl. 52, reciprocal tolerance-cost approach acc. to Eq. (92)
- *Specification limits*:
  - f_{Y_1}: $LSL_1 = 88.5°$, $USL_1 = 91.5°$
  - f_{Y_2}: $LSL_2 = -1.5°$, $USL_2 = 1.5°$
  - f_{Y_3}: $LSL_3 = -1.0$ mm, $USL_3 = 1.0$ mm
- *Optimization settings*: $\eta_p = 25$, $\eta_g = 250$, $\eta_{g,\text{stall}} = 200$ with a fitness tolerance of 1e-06 (decimals to be relevant for fitness improvement evaluation), $p_\text{a} = 0.25$
- *Number of repetitions*: $\eta_r = 5$
- *Studied cases*:
  - (a) direct embedding of TCVisVA
  - (b) adaptive sample sizes including resampling, $\xi_1 = 7$, $\xi_2 = 0.5$, $n_\text{min} = 5{,}000$
  - (c) surrogate model-based optimization inclusive resampling
- *ANN training settings for (c)*: Wide, single-layered feed-forward ANN, f_act: rectified linear unit function; layer size: 100

Table 52: Tolerance-cost data for the e-cross skate example studied in Sec. 8.2.

Part	**Feat.**	**Tol.**	**Coefficients of f_C**				**Boundaries**	
l	u	i	$f_{\text{F}_{l,u,i,j}}$	$f_{\text{A}_{l,u,i,j}}$	$f_{\text{M}_{l,u,i,j}}$	$X_{l,u,i,j}$	$t^\text{lb}_{l,u,i,j}$	$t^\text{ub}_{l,u,i,j}$
1	1	1	0	0	0	530	0.300	0.300
	2	2	0	0	0	12.8	0.018	0.018
		1	0	0	0	45	0.300	0.300
	3	1	0	0	0	4.5	0.100	0.100
2	1	1	1,218	1	1	12.8	0.011	0.011
	2	1	95	1	1	12.8	0.010	0.400
	3	2	1,218	1	1	12.8	0.011	0.011
		1	1,218	1	1	30	0.006	0.200
	4	1	95	1	1	12.8	0.010	0.400
	5	1	250	1	1	14	0.010	0.400
	6	2	476	12	1	12	0.018	0.018
		1	476	12	1	14	0.008	0.600

	7	1	250	1	1	14	0.010	0.400
4	1	1	920	1	1	12	0.011	0.011
	2	1	142	1	1	18	0.010	0.200
	3	1	142	1	1	18	0.010	0.200
	4	2	378	1	1	12	0.011	0.011
		1	378	1	1	10	0.006	0.100
6	1	1	0	0	0	12	0.008	0.008
	2	1	0	0	0	32	0.011	0.011
8	1	1	0	0	0	12	0.008	0.008
	2	1	0	0	0	32	0.011	0.011
9	1	1	139	1.25	1	32	0.010	0.200
	2	2	1,030	1.25	1	32	0.025	0.025
		1	1,030	1.25	1	10	0.011	0.400
	3	2	828	1.25	1	32	0.025	0.025
		1	828	1.25	1	7.5	0.025	0.200
	4	3	1,287	1	1	45	0.016	0.016
		1	1,287	1	1	11.9	0.008	0.200
		2	1,287	1	1	11.9	0.003	0.008
	5	3	1,287	1	1	45	0.016	0.016
		1	1,287	1	1	9.2	0.020	0.200
		2	1,287	1	1	11.9	0.003	0.008
	6	3	399	1.25	1	36	0.016	0.016
		1	399	1.25	1	4	0.008	0.200
		2	399	1.25	1	4	0.003	0.008
	7	1	367	1.25	1	36	0.010	0.400
	8	3	399	1.5	1	36	0.016	0.016
		1	399	1.25	1	4	0.008	0.200
		2	399	1.25	1	4	0.003	0.008
	9	1	267	1.25	1	36	0.010	0.400
	10	1	449	1.5	1	37.5	0.005	0.200
	11	2	84	18	1	4	0.200	0.200
		1	84	18	1	10.5	0.006	0.400
	12	2	84	18	1	4	0.200	0.200
		1	84	18	1	10.5	0.006	0.400
11	1	3	1,496	1.25	1	68	0.030	0.030
		1	1,496	1.25	1	7	0.008	0.200
		2	1,496	1.25	1	7	0.003	0.015
	2	1	415	1.25	1	60	0.010	0.200
	3	2	1,496	1.25	1	68	0.030	0.030
		1	1,496	1.25	1	7	0.003	0.015
	4	1	415	1.25	1	60	0.010	0.400
	5	1	10,741	1	1	60	0.010	0.400

12	1	1	0	0	0	45	0.012	0.012
	2	1	0	0	0	68	0.013	0.013
13	1	1	0	0	0	45	0.012	0.012
	2	1	0	0	0	68	0.013	0.013
17	1	1	526	1	1	36	0.016	0.016
	2	1	299	1	1	10.5	0.010	0.400
	3	1	27	26	1	4	0.018	0.018
	4	1	99	1.5	1	18.5	0.011	0.200
	5	1	13	1.5	1	12.6	0.008	0.400
18	1	1	526	1	1	36	0.016	0.016
	2	1	299	1	1	10.5	0.010	0.400
	3	1	27	26	1	4	0.018	0.018
	4	1	99	1.5	1	18.5	0.011	0.200
	5	1	26	1.5	1	12.6	0.008	0.400
19	1	1	89	1.5	1	18	0.005	0.100
	2	1	44	1.5	1	4.5	0.010	0.400
	3	1	54	1.5	1	10.8	0.009	0.200
	4	1	51	32	1	4	0.005	0.400
20	1	1	89	1.5	1	18	0.005	0.100
	2	1	44	1.5	1	4.5	0.010	0.400
	3	1	54	1.5	1	10.8	0.009	0.200
	4	1	51	32	1	4	0.005	0.400
27	1	1	0	0	0	530	0.300	0.300
	2	2	0	0	0	12.8	0.018	0.018
		1	0	0	0	45	0.300	0.300
	3	1	0	0	0	4.5	0.100	0.100

- $X_{l,u,i}$, $t_{l,u,i}^{\mathrm{lb/ub}}$ in mm.
- $f_{\mathrm{A}_{l,u,i}}$: coefficient related to the surface area of feature u in mm².
- $f_{\mathrm{F}_{l,u,i}}$: coefficient related to the feature type of feature u.
- $f_{\mathrm{M}_{l,u,i}}$: coefficient related to the material used and its machining difficulty.
- $a_{l,u,i} = 0$, $k = 0.55$, $\beta = 1.0 \cdot 10^{-3}$ for all tolerances.
- *Type* of $\rho_{l,u,i}$: all tolerances follow a standard normal distribution with $\Delta_{\mu_{l,u,i}} = 0$, standard deviation $\sigma_{l,u,i} = t_{l,u,i}/6$.

Table 53: Summary of optimal solutions for the optimization study presented in Sec. 8.2.

Case	*RMSE*		$r \rightarrow$ 1	2	3	4	5
(a)	/	$C_{\text{sum}}^{\text{opt}}$	624.18	623.67	623.23	622.66	622.63
		$\hat{z}_{\text{asm}}^{\text{opt}}$	2,400	2,600	2,400	2,700	2,700
		τ_{feas}	170,878	170,864	169,014	169,773	170,558
(b)	/	$C_{\text{sum}}^{\text{opt}}$	626.03	627.86	624.84	626.03	626.03
		$\hat{z}_{\text{asm}}^{\text{opt}}$	2,500	2,700	2,600	2,500	2,500
		τ_{feas}	156,490	155,864	152,442	155,256	155,189
(c1), $D = 500$	5,341	$C_{\text{sum}}^{\text{opt}}$	625.82	624.21	625.50	624.46	623.44
		$\hat{z}_{\tilde{f}_{\hat{z}}}^{\text{opt}}$	2,500	2,600	2,600	2,300	2,600
		$\hat{z}_{\text{asm}}^{\text{opt}}$	2,553	2,820	2,647	2,768	2,622
		e	53	220	47	468	22
		τ_{feas}	41,403	41,722	41,400	42,215	42,221
(c2), $D = 1{,}000$	3,900	$C_{\text{sum}}^{\text{opt}}$	623.79	626.62	623.15	625.76	622.67
		$\hat{z}_{\tilde{f}_{\hat{z}}}^{\text{opt}}$	2,600	2,500	2,600	2,400	2,700
		$\hat{z}_{\text{asm}}^{\text{opt}}$	2,649	2,692	2,725	2,596	2,847
		e	49	192	125	196	147
		τ_{feas}	48,141	48,134	48,159	47,192	47,140

- *Flag* = 0 for all runs, i.e., maximum number of generations η_g is reached.
- $C_{\text{sum}}^{\text{opt}}$ in MU, *RMSE*, $\hat{z}_{\text{asm}}^{\text{opt}}$, $\hat{z}_{\tilde{f}_{\hat{z}}}^{\text{opt}}$, e in ppm, τ_{feas} in s.

Table 54: Performance measures for the optimization study presented in Sec. 8.2.

Case	***FR*****	***SR******	$\overline{\boldsymbol{C}}_{\textbf{relation}}$	$\overline{\boldsymbol{\tau}}^{*}_{\textbf{feas}}$ **in h**
(a)	1	1	0.996	47.28
(b)	1	0.20	1.000	43.07
(c1)	1	0.80	1.000	11.61
(c2)	1	0.60	1.000	13.26

* with δ_{feas} acc. to the defined constraint tolerance.
** with $\delta_{\text{success}} = 0.005 \cdot C_{\text{sum}}\left(\boldsymbol{t}_{\text{opt}}\right)$, where $\boldsymbol{t}_{\text{opt}}$ are the solutions obtained for the best runs (see Tbl. 55).

Table 55: Comparison of costs and nc-rates for initially and optimally allocated tolerances for the optimization study presented in Sec. 8.2 .

	$\boldsymbol{C}_{\textbf{sum}}$	$\hat{\boldsymbol{z}}_{\textbf{asm}}$	$\hat{\boldsymbol{z}}_{1}$	$\hat{\boldsymbol{z}}_{2}$	$\hat{\boldsymbol{z}}_{3}$
Initial	683.73	8,000	3,900	3,400	4,700
Optimal, $(a)\ r = 5$	622.63	2,700	1,500	600	1,100

- $C_{\text{sum}}^{\text{opt}}$ in MU, $\hat{z}_1, \hat{z}_2, \hat{z}_3, \hat{z}_{\text{asm}}$ in ppm.

Table 56: Least-cost tolerances obtained in the best runs for the study in Sec. 8.2.

l	u	i	$t^{\text{init}}_{l,u,i}$	$t^{\text{opt}}_{l,u,i}$
1	1	1	0.300	0.300
	2	2	0.018	0.018
		1	0.300	0.300
	3	1	0.100	0.100
2	1	1	0.018	0.018
	2	1	0.300	0.240
	3	2	0.011	0.011
		1	0.103	0.200
	4	1	0.205	0.240
	5	1	0.205	0.078
	6	2	0.018	0.018
		1	0.304	0.226
	7	1	0.205	0.078
4	1	1	0.011	0.011
	2	1	0.105	0.200
	3	1	0.105	0.200
	4	2	0.011	0.011
		1	0.053	0.096
6	1	1	0.008	0.008
	2	1	0.011	0.011
8	1	1	0.008	0.008
	2	1	0.011	0.011
9	1	1	0.105	0.200
	2	2	0.025	0.025
		1	0.206	0.096
	3	2	0.025	0.025
		1	0.113	0.200
	4	3	0.016	0.016
		1	0.104	0.200
		2	0.006	0.008
	5	3	0.016	0.016
		1	0.110	0.114
		2	0.006	0.008
	6	3	0.016	0.016
		1	0.104	0.090
		2	0.006	0.008
	7	1	0.205	0.314
	8	3	0.016	0.016
		1	0.104	0.090
		2	0.006	0.008
	9	1	0.205	0.314
	10	1	0.103	0.194
	11	2	0.200	0.200
		1	0.203	0.393
	12	2	0.200	0.200
		1	0.203	0.393

11	1	3 1 2	0.030 0.104 0.009	0.030 0.163 0.015
	2	1	0.105	0.186
	3	2 1	0.030 0.009	0.030 0.015
	4	1	0.105	0.186
	5	1	0.205	0.400
12	1	1	0.012	0.012
	2	1	0.013	0.013
13	1	1	0.012	0.012
	2	1	0.013	0.013
17	1	1	0.016	0.016
	2	1	0.205	0.400
	3	1	0.018	0.018
	4	1	0.106	0.170
	5	1	0.204	0.218
18	1	1	0.016	0.016
	2	1	0.205	0.400
	3	1	0.018	0.018
	4	1	0.106	0.170
	5	1	0.204	0.218
19	1	1	0.053	0.073
	2	1	0.205	0.027
	3	1	0.105	0.200
	4	1	0.203	0.389
20	1	1	0.053	0.073
	2	1	0.205	0.027
	3	1	0.105	0.200
	4	1	0.203	0.389
27	1	1	0.300	0.300
	2	2 1	0.018 0.300	0.018 0.300
	3	1	0.100	0.100

- $t_{l,u,i}^{\text{init/opt}}$: initial/optimal part tolerance i for feature u of part l in mm.

A.10 Information on used software and working systems

Software:

- MathWorks®MATrix LABoratory (MATLAB®) R2022b: Programming language and computing environment used for the analysis and optimization studies and implementation and application of the total framework
- Siemens Teamcenter®Visualization MockUp Version 14.2 including Variation Analysis (TCVisVA) application: MCS-based tolerance analysis software
- Siemens NX™ Version 2008: CAD/CAM/CAE-system used to create part and assembly models using PMI and export it in JT™-data format serving as an input for TCVisVA

Optimization algorithms:

- Genetic algorithm (GA): Global Optimization Toolbox
- Cuckoo Search algorithm (CS): Modified implementation of code published in [450]

Workstations:

OS:	Windows 10 Enterprise 21H2, 64-Bit
CPU:	Intel®Core ™i5-9400 CPU @ 2.90GHz
RAM:	16 GB
Graphics card:	Nividia® Quadro P400

A.11 Image credits

- Cover figure: The DNA-helix is inspired by a picture freely shared by *PublicDomainPictures* on *Pixabay*: https://pixabay.com/de/illustrations/dna-biologie-wissenschaft-dna-helix-163710/. Accessed on: 30.09.2022.
- Fig. 29: Knuckle joint assembly adopted from [203], racing seat mounting assembly adopted from [183].
- Fig. 45(b): Tolerance specification of shaft adopted from [794].
- Fig. 45(c): Example of slurry pump inspired by [795].
  Accessed on: 05.12.2022.

Bibliography

[1] Ulrich, K. T. and Eppinger, S. D., *Product Design and Development*, 5th ed. New York: McGraw-Hill/Irwin, 2012.

[2] Isaksson, O. and Eckert, C., "Product Development 2040: Technologies are just as good as the designer's ability to integrate them," The Design Society, Tech. Rep. DS107, 2020. DOI: 10.35199/report.pd2040.

[3] Ehrlenspiel, K.; Kiewert, A., and Lindemann, U., *Cost-Efficient Design*, Hundal, M. S., Ed. Berlin: Springer, 2007.

[4] Huang, G. Q., "Introduction," *Design for X*, Huang, G. Q., Ed., Dordrecht: Springer, 1996.

[5] Jeang, A. and Chang, C.-L., "Combined Robust Parameter and Tolerance Design Using Orthogonal Arrays," *The International Journal of Advanced Manufacturing Technology*, vol. 19, no. 6, pp. 442–447, 2002. DOI: 10.1007/s001700200046.

[6] Whitney, D. E., *Mechanical Assemblies: Their Design, Manufacture, and Role in Product Development*. New York: Oxford University Press, 2004.

[7] Johannesson, H. and Söderberg, R., "Structure and Matrix Models for Tolerance Analysis from Configuration to Detail Design," *Research in Engineering Design*, vol. 12, no. 2, pp. 112–125, 2000. DOI: 10.1007/s001630050027.

[8] Will, P. M., "Simulation and modeling in early concept design: An industrial perspective," *Research in Engineering Design*, vol. 3, no. 1, pp. 1–13, 1991. DOI: 10.1007/BF01580064.

[9] Xue, D.; Rousseau, J. H., and Dong, Z., "Joint Optimization of Functional Performance and Production Costs Based Upon Mechanical Features and Tolerances," *Proceedings of the ASME 1995 Design Engineering Technical Conferences Collocated with the ASME 1995 15th International Computers in Engineering Conference and the ASME 1995 9th Annual Engineering Database Symposium.Volume 2: 11th Biennial Conference on Reliability, Stress Analysis, and Failure Prevention; 7th International Conference on Design Theory and Methodology; JSME Symposium on Design and Production; Mechanical Design Education and History; Computer-Integrated Concurrent Design Conference*, Boston, Massachusetts, USA: ASME, 1995-09-17-20, pp. 1013–1028. DOI: 10.1115/DETC1995-0240.

[10] Meerkamm, H., "Design for X—A Core Area of Design Methodology," *Journal of Engineering Design*, vol. 5, no. 2, pp. 165–181, 1994. DOI: 10.1080/09544829408907881.

[11] Smith, R. P., "The historical roots of concurrent engineering fundamentals," *IEEE Transactions on Engineering Management*, vol. 44, no. 1, pp. 67–78, 1997. DOI: 10.1109/17.552809.

[12] Ledoux, Y.; Teissandier, D., and Sebastian, P., "Global optimisation of functional requirements and tolerance allocations based on designer preference modelling," *Journal of Engineering Design*, vol. 27, no. 9, pp. 591–612, 2016. DOI: 10.1080/09544828.2016.1191625.

[13] Jiang, H.; Zeng, Q., and Xiong, G., "Methodology and Technology for Design To Cost," *Tsinghua Science and Technology*, vol. 6, no. 1, pp. 29–33, 2001.

[14] Siva Kumar, M.; Lenin, N., and Rajamani, D., "Selection of Components and Their Optimum Manufacturing Tolerance for Selective Assembly Technique Using Intelligent Water Drops Algorithm to Minimize Manufacturing Cost," *Nature-Inspired Optimization in Advanced Manufacturing Processes and Systems*, Kakandikar, G. M. and Thakur, D. G., Eds., 1st ed., Boca Raton: CRC Press, 2020, pp. 211–227. DOI: 10.1201/9781003081166-13.

[15] Schleich, B.; Anwer, N.; Mathieu, L., and Wartzack, S., "Shaping the digital twin for design and production engineering," *CIRP Annals*, vol. 66, no. 1, pp. 141–144, 2017. DOI: 10.1016/j.cirp.2017.04.040.

[16] Hong, Y. S. and Chang, T. C., "A comprehensive review of tolerancing research," *International Journal of Production Research*, vol. 40, no. 11, pp. 2425–2459, 2002. DOI: 10.1080/00207540210128242.

[17] Lee, C. L. and Tang, G. R., "Tolerance design for products with correlated characteristics," *Mechanism and Machine Theory*, vol. 35, no. 12, pp. 1675–1687, 2000. DOI: 10.1016/S0094-114X(00)00022-7.

[18] Chase, K. W. and Parkinson, A. R., "A survey of research in the application of tolerance analysis to the design of mechanical assemblies," *Research in Engineering Design*, vol. 3, no. 1, pp. 23–37, 1991. DOI: 10.1007/BF01580066.

[19] Söderberg, R.; Lindkvist, L.; Wärmefjord, K., and Carlson, J. S., "Virtual Geometry Assurance Process and Toolbox," *Procedia CIRP*, vol. 43, pp. 3–12, 2016. DOI: 10.1016/j.procir.2016.02.043.

[20] Dantan, J.-Y.; Ballu, A., and Mathieu, L., "Geometrical product specifications — model for product life cycle," *Computer-Aided Design*, vol. 40, no. 4, pp. 493–501, 2008. DOI: 10.1016/j.cad.2008.01.004.

[21] Shan, A.; Roth, R. N., and Wilson, R. J., "Genetic algorithms in statistical tolerancing," *Mathematical and Computer Modelling*, vol. 38, no. 11-13, pp. 1427–1436, 2003. DOI: 10.1016/S0895-7177(03)90146-4.

[22] Mirdamadi, S.; Etienne, A.; Hassan, A.; Dantan, J. Y., and Siadat, A., "Cost Estimation Method for Variation Management," *Procedia CIRP*, vol. 10, pp. 44–53, 2013. DOI: 10.1016/j.procir.2013.08.011.

[23] Morse, E.; Dantan, J.-Y.; Anwer, N.; Söderberg, R.; Moroni, G.; Qureshi, A.; Jiang, X., and Mathieu, L., "Tolerancing: Managing uncertainty from conceptual design to final product," *CIRP Annals*, vol. 67, no. 2, pp. 695–717, 2018. DOI: 10.1016/j.cirp.2018.05.009.

[24] Söderberg, R.; Lindkvist, L., and Dahlström, S., "Computer-aided robustness analysis for compliant assemblies," *Journal of Engineering Design*, vol. 17, no. 5, pp. 411–428, 2006. DOI: 10.1080/09544820500275800.

[25] Roy, U.; Liu, C. R., and Woo, T. C., "Review of dimensioning and tolerancing: representation and processing," *Computer-Aided Design*, vol. 23, no. 7, pp. 466–483, 1991. DOI: 10.1016/0010-4485(91)90045-X.

[26] Jeang, A., "Economic tolerance design for quality," *Quality and Reliability Engineering International*, vol. 11, no. 2, pp. 113–121, 1995. DOI: 10.1002/qre.4680110207.

[27] Lee, J. and Johnson, G. E., "Optimal tolerance allotment using a genetic algorithm and truncated Monte Carlo simulation," *Computer-Aided Design*, vol. 25, no. 9, pp. 601–611, 1993. DOI: 10.1016/0010-4485(93)90075-Y.

[28] Zhang, H. C. and Huq, M. E., "Tolerancing techniques: The state-of-the-art," *International Journal of Production Research*, vol. 30, no. 9, pp. 2111–2135, 1992. DOI: 10.1080/00207549208948140.

[29] Martinsen, K.; Assuad, C. S. A.; Kito, T.; Matsumoto, M.; Reddy, V., and Guldbrandsen-Dahl, S., "Closed Loop Tolerance Engineering Modelling and Maturity Assessment in a Circular Economy Perspective," *EcoDesign and Sustainability I*, Kishita, Y.; Matsumoto, M.; Inoue, M., and Fukushige, S., Eds., Singapore: Springer, 2021, pp. 297–308. DOI: 10.1007/978-981-15-6779-7_21.

[30] Huq, M. E. and Zhang, H.-C., "Computerized tolerance techniques," *Computers & Industrial Engineering*, vol. 21, no. 1-4, pp. 165–172, 1991. DOI: 10.1016/0360-8352(91)90082-H.

[31] Otsuka, A. and Nagata, F., "Optimal allocation of statistical tolerance indices by genetic algorithms," *Artificial Life and Robotics*, vol. 19, no. 3, pp. 227–232, 2014. DOI: 10.1007/s10015-014-0157-x.

[32] Zhang, G., "Simultaneous tolerancing for design and manufacturing," *International Journal of Production Research*, vol. 34, no. 12, pp. 3361–3382, 1996. DOI: 10.1080/00207549608905095.

[33] Rao, Y. S.; Rao, C. S. P.; Janardhana, G. R., and Vundavilli, P. R., "Simultaneous Tolerance Synthesis for Manufacturing and Quality using Evolutionary Algorithms:" *International Journal of Applied Evolutionary Computation*, vol. 2, no. 2, pp. 1–20, 2011. DOI: 10.4018/jaec.2011040101.

[34] Graves, S. and Bisgaard, S., "Integrated Tolerance Management," *Global Consistency of Tolerances*, van Houten, F. and Kals, H., Eds., Dordrecht: Springer, 1999, pp. 385–394. DOI: 10.1007/978-94-017-1705-2_39.

[35] Grossman, D. D., "Monte Carlo simulation of tolerancing in discrete parts manufacturing and assembly," Stanford Artificial Intelligence Laboratory, Stanford, Technical Report STAN-CS-76-555, 1976, pp. 1–25.

[36] Lee, W.-J.; Woo, T. C., and Chou, S.-Y., "Tolerance synthesis for nonlinear systems based on nonlinear programming," *IIE Transactions*, vol. 25, no. 1, pp. 51–61, 1993. DOI: 10.1080/07408179308964265.

[37] Kanai, S.; Onozuka, M., and Takahashi, H., "Optimal Tolerance Synthesis by Genetic Algorithm under the Machining and Assembling Constraints," *Computer-Aided Tolerancing*, Kimura, F., Ed., Dordrecht: Springer, 1996, pp. 235–250. DOI: 10.1007/978-94-009-1529-9_16.

[38] Ostwald, P. F. and Huang, J., "A Method for Optimal Tolerance Selection," *Journal of Engineering for Industry*, vol. 99, no. 3, pp. 558–565, 1977. DOI: 10.1115/1.3439279.

[39] Karmakar, S. and Maiti, J., "A review on dimensional tolerance synthesis: Paradigm shift from product to process," *Assembly Automation*, vol. 32, no. 4, pp. 373–388, 2012. DOI: 10.1108/01445151211262438.

[40] Chase, K. W. and Greenwood, W. H., "Design Issues in Mechanical Tolerance Analysis," *Manufacturing Review*, vol. 1, no. 1, pp. 50–59, 1988.

[41] Singh, P. K.; Jain, P. K., and Jain, S. C., "Important issues in tolerance design of mechanical assemblies. Part 2: Tolerance synthesis," *Proceedings of the Institution of Mechanical Engineers, Part B: Journal of Engineering Manufacture*, vol. 223, no. 10, pp. 1249–1287, 2009. DOI: 10.1243/09544054JEM1304B.

[42] Wilde, D. J., "Product Quality in Optimization Models," *Concurrent Engineering*, vol. 1, no. 3, pp. 153–157, 1993. DOI: 10.1177/1063293X9300100303.

[43] Creveling, C. M., *Tolerance Design: A Handbook for Developing Optimal Specifications*. New Jersey: Addison-Wesley, 1997.

[44] Zhang, C.; Wang, H. P., and Li, J. K., "Simultaneous Optimization of Design and Manufacturing — Tolerances with Process (Machine) Selection," *CIRP Annals*, vol. 41, no. 1, pp. 569–572, 1992. DOI: 10.1016/S0007-8506(07)61270-0.

[45] Huang, Y. M. and Shiau, C.-S., "Optimal Tolerance Allocation for a Sliding Vane Compressor," *Journal of Mechanical Design*, vol. 128, no. 1, pp. 98–107, 2006. DOI: 10.1115/1.2114893.

[46] Iannuzzi, M. P. and Sandgren, E., "Tolerance Optimization Using Genetic Algorithms: Benchmarking with Manual Analysis," *Computer-Aided Tolerancing*, Kimura, F., Ed., Dordrecht: Springer, 1996, pp. 219–234. DOI: 10.1007/978-94-009-1529-9_15.

[47] Dong, Z., "Tolerance synthesis by manufacturing cost modeling and design optimization," *Advanced Tolerancing Techniques*, Zhang, H.-C., Ed., New York: Wiley, 1997, pp. 233–260.

[48] Walter, M. S. J.; Klein, C.; Heling, B., and Wartzack, S., "Statistical Tolerance Analysis—A Survey on Awareness, Use and Need in German Industry," *Applied Sciences*, vol. 11, no. 6, p. 2622, 2021. DOI: 10.3390/app11062622.

[49] Fortini, E. T., *Dimensioning for Interchangeable Manufacture*. New York: Industrial Press Inc, 1967.

[50] American Society of Mechanical Engineers, *ASME Y14.5-2018: Dimensioning and Tolerancing*, 2018.

[51] ISO/TC 213, "ISO 1101:2017: Geometrical product specifications (GPS) — Geometrical tolerancing — Tolerances of form, orientation, location and run-out," Standard, 2017.

[52] Srinivasan, V., "Computational Metrology for the Design and Manufacture of Product Geometry: A Classification and Synthesis," *Journal of Computing and Information Science in Engineering*, vol. 7, no. 1, pp. 3–9, 2007. DOI: 10.1115/1.2424246.

[53] Snee, R. D., "Statistical Thinking and Its Contribution to Total Quality," *The American Statistician*, vol. 44, no. 2, pp. 116–121, 1990. DOI: 10.2307/2684144.

[54] Forouraghi, B., "Worst-Case Tolerance Design and Quality Assurance via Genetic Algorithms," *Journal of Optimization Theory and Applications*, vol. 113, no. 2, pp. 251–268, 2002. DOI: 10.1023/A:1014826824323.

[55] Wärmefjord, K.; Carlson, J. S., and Söderberg, R., "Controlling Geometrical Variation Caused by Assembly Fixtures," *Journal of Computing and Information Science in Engineering*, vol. 16, no. 1, p. 011 007, 2016. DOI: 10.1115/1.4032625.

[56] Robles, N. and Roy, U., "Optimal tolerance allocation and process-sequence selection incorporating manufacturing capacities and quality issues," *Journal of Manufacturing Systems*, vol. 23, no. 2, pp. 127–133, 2004. DOI: 10.1016/S0278-6125(05)00002-6.

[57] Evans, D. H., "Statistical Tolerancing: The State of the Art: Part I. Background," *Journal of Quality Technology*, vol. 6, no. 4, pp. 188–195, 1974. DOI: 10.1080/00224065.1974.11980646.

[58] Parkinson, D. B., "Tolerancing of component dimensions in CAD," *Computer-Aided Design*, vol. 16, no. 1, pp. 25–32, 1984. DOI: 10.1016/S0010-4485(84)80005-6.

[59] Cheng, K. M. and Tsai, J. C., "A Closed-Form Approach for Optimum Tolerance Allocation of Assemblies with General Tolerance-Cost Function," *Advanced Materials Research*, vol. 201–203, pp. 1272–1278, 2011. DOI: 10.4028/www.scientific.net/AMR.201-203.1272.

[60] Craig, M., "Dimensional management versus tolerance assignment," *Assembly Automation*, vol. 16, no. 2, pp. 12–16, 1996. DOI: 10.1108/01445159610117645.

[61] Parkinson, A., "Robust Mechanical Design Using Engineering Models," *Journal of Vibration and Acoustics*, vol. 117, no. B, pp. 48–54, 1995. DOI: 10.1115/1.2838676.

[62] Reeves, C. A. and Bednar, D. A., "Defining Quality: Alternatives and Implications," *The Academy of Management Review*, vol. 19, no. 3, pp. 419–445, 1994. DOI: 10.5465/amr.1994.9412271805.

[63] Crosby, P. B., *Quality Is Free: The Art of Making Quality Certain*. New York: McGraw-Hill, 1979.

[64] Garvin, D. A., *Managing Quality: The Strategic and Competitive Edge*. New York: Free Press, 1988.

[65] INCOSE, *INCOSE Systems Engineering Handbook Version 2.0*. 2000.

[66] Thornton, A. C., "A Mathematical Framework for the Key Characteristic Process," *Research in Engineering Design*, vol. 11, no. 3, pp. 145–157, 1999. DOI: 10.1007/s001630050011.

[67] Thornton, A. C.; Donnelly, S., and Ertan, B., "More than Just Robust Design: Why Product Development Organizations Still Contend with Variation and its Impact on Quality," *Research in Engineering Design*, vol. 12, no. 3, pp. 127–143, 2000. DOI: 10.1007/s001630050028.

[68] Arvidsson, M.; Gremyr, I., and Johansson, P., "Use and knowledge of robust design methodology: A survey of Swedish industry," *Journal of Engineering Design*, vol. 14, no. 2, pp. 129–143, 2003. DOI: 10.1080/0954482031000138192.

[69] Yang, K.; Xie, W., and He, Y., "Parameter and tolerance design in the engineering modelling stage," *International Journal of Production Research*, vol. 32, no. 12, pp. 2803–2816, 1994. DOI: 10.1080/00207549408957101.

[70] Hasenkamp, T.; Arvidsson, M., and Gremyr, I., "A review of practices for robust design methodology," *Journal of Engineering Design*, vol. 20, no. 6, pp. 645–657, 2009. DOI: 10.1080/09544820802275557.

[71] Eifler, T.; Ebro, M., and Howard, T. J., "A classification of the industrial relevance of robust design methods," *DS 75-9: Proceedings of the 19th International Conference on Engineering Design (ICED13): Design For Harmonies*, Seoul, Korea, 19.08.-22.08.2013, pp. 427–436.

[72] Söderberg, R.; Lindkvist, L., and Carlson, J. S., "Managing physical dependencies through location system design," *Journal of Engineering Design*, vol. 17, no. 4, pp. 325–346, 2006. DOI: 10.1080/09544820500275685.

[73] Söderberg, R.; Lindkvist, L., and Carlson, J., "Virtual geometry assurance for effective product realization," *1st Nordic Conference on Product Lifecycle Management - NordPLM'06*, Gothenburg, Sweden, 25.01.-26.01.2006, pp. 75–88.

[74] Rosenqvist, M.; Falck, A.-C.; Lindkvist, L., and Söderberg, R., "Variation Analysis Considering Manual Assembly Complexity in a CAT Tool," *Procedia CIRP*, vol. 43, pp. 94–99, 2016. DOI: 10.1016/j.procir.2016.02.020.

[75] Voelcker, H. B., "The current state of affairs in dimensional tolerancing: 1997," *Integrated Manufacturing Systems*, vol. 9, no. 4, pp. 205–217, 1998. DOI: 10.1108/09576069810217793.

[76] Wittmann, M. and Scheer, A.-W., "Integrated Tolerance Information System," *Global Consistency of Tolerances*, van Houten, F. and Kals, H., Eds., Dordrecht: Springer, 1999, pp. 375–383. DOI: 10.1007/978-94-017-1705-2_38.

[77] ISO/TC 213, "ISO 17450-1:2011: Geometrical product specifications (GPS) — General concepts — Part 1: Model for geometrical specification and verification," Standard, 2011.

[78] Schleich, B. and Wartzack, S., "Motion Tolerancing Based on Skin Model Shapes by Form Deviation Parametrization and Meta-Modelling," *Proceedings of the ASME 2017 International Design Engineering Technical Conferences and Computers and Information in Engineering Conference. Volume 1: 37th Computers and Information in Engineering Conference*, Cleveland, Ohio, USA: ASME, 2017, V001T02A007. DOI: 10.1115/DETC2017-67227.

[79] Anwer, N.; Cid, G., and Mathieu, L., "XML based tolerance management for integrated design," *International CIRP design seminar*, no. 785, pp. 1–12, 2003.

[80] Müller, R.; Vette-Steinkamp, M.; Scholer, M.; Schirmer, L., and Blum, A., "Upgrading and Ensuring a Fully-Automated Assembly Process Using Tolerance Management Methods," *Procedia CIRP*, vol. 81, pp. 174–179, 2019. DOI: 10.1016/j.procir.2019.03.031.

[81] Franz, M.; Schleich, B., and Wartzack, S., "Tolerance management during the design of composite structures considering variations in design parameters," *The International Journal of Advanced Manufacturing Technology*, vol. 113, no. 5-6, pp. 1753–1770, 2021. DOI: 10.1007/s00170-020-06555-5.

[82] Nickolaisen, R. H., "Dimensional Management," *Dimensioning and Tolerancing Handbook*, Drake, P. J., Ed., New York: McGraw-Hill, 1999, pp. 2-1–2-11.

[83] Bacharoudis, K. C.; Bainbridge, D.; Turner, A.; Popov, A. A., and Ratchev, S. M., "Implementation of dimensional management methodology and optimisation algorithms for pre-drilled hinge line interfaces of critical aero assemblies – A case study," *Proceedings of the Institution of Mechanical Engineers, Part B: Journal of Engineering Manufacture*, vol. 235, no. 6-7, pp. 1074–1083, 2021. DOI: 10.1177/0954405420978101.

[84] Oberleiter, T.; Heling, B.; Schleich, B.; Willner, K., and Wartzack, S., "Fuzzy Sensitivity Analysis in the Context of Dimensional Management," *ASCE-ASME Journal of Risk and Uncertainty in Engineering Systems, Part B: Mechanical Engineering*, vol. 5, no. 1, p. 011 008, 2019. DOI: 10.1115/1.4040919.

[85] Forslund, K. and Söderberg, R., "Effects of Geometric Variation on Perceived Quality," *Product Lifecycle Management*, Giordano, M.; Mathieu, L., and Villeneuve, F., Eds., Hoboken, New Jersey: Wiley, 2010, pp. 503–519. DOI: 10.1002/9781118557921.ch29.

[86] Falk, B.; Stylidis, K.; Wickman, C.; Söderberg, R., and Schmitt, R., "Shifting paradigm: Towards a comprehensive understanding of quality," *DS 87-9 Proceedings of the 21st International Conference on Engineering Design (ICED 17)*, Vancouver, Canada, 21.08.-25.08.2017, pp. 255–264.

[87] Stylidis, K.; Wickman, C., and Söderberg, R., "Perceived quality of products: A framework and attributes ranking method," *Journal of Engineering Design*, vol. 31, no. 1, pp. 37–67, 2020. DOI: 10.1080/09544828.2019.1669769.

[88] Walter, M.; Storch, M., and Wartzack, S., "On uncertainties in simulations in engineering design: A statistical tolerance analysis application," *SIMULATION*, vol. 90, no. 5, pp. 547–559, 2014. DOI: 10.1177/0037549714529834.

[89] Thunnissen, D. P., "Uncertainty Classification for the Design and Development of Complex Systems," *3rd annual predictive methods conference*, vol. 16, 2003.

[90] Dantan, J. Y.; Gayton, N.; Qureshi, A. J.; Lemaire, M., and Etienne, A., "Tolerance Analysis Approach Based on the Classification of Uncertainty (Aleatory/Epistemic)," *Procedia CIRP*, vol. 10, pp. 287–293, 2013. DOI: 10.1016/j.procir.2013.08.044.

[91] Weill, R.; Clément, A.; Hocken, R.; Farmer, L. E.; Gladman, C. A.; Wirtz, A.; Bourdet, P.; Freckleton, J. E.; Kunzmann, H.; Ham, I.; Trumpold, H., and Matthias, E., "Tolerancing for Function," *CIRP Annals*, vol. 37, no. 2, pp. 603–610, 1988. DOI: 10.1016/S0007-8506(07)60757-4.

[92] Wartzack, S.; Meerkamm, H.; Stockinger, A.; Stoll, T.; Stuppy, J.; Voß, R.; Walter, M., and Wittmann, S., "Lifecycle-Oriented Tolerance Simulation," *Konstruktion*, vol. 6, pp. 63–67+74, 2011.

[93] Zhang, C. and Wang, H.-P., "Integrated tolerance optimisation with simulated annealing," *The International Journal of Advanced Manufacturing Technology*, vol. 8, no. 3, pp. 167–174, 1993. DOI: 10.1007/BF01749907.

[94] Schleich, B., *Skin Model Shapes: A New Paradigm for the Tolerance Analysis and the Geometrical Variations Modelling in Mechanical Engineering*, Ph.D. dissertation, Friedrich-Alexander-Universität Erlangen-Nürnberg, ser. Fortschritt-Berichte VDI Reihe 1, Konstruktionstechnik, Maschinenelemente Nr. 438. Düsseldorf: VDI-Verlag, 2017.

[95] Taguchi, G.; Chowdhury, S., and Wu, Y., *Taguchi's Quality Engineering Handbook*. Hoboken, New Jersey: Wiley, 2005.

[96] Singh, P. K.; Jain, S. C., and Jain, P. K., "A genetic algorithm based solution to optimum tolerance synthesis of mechanical assemblies with alternate manufacturing processes—benchmarking with the exhaustive search method using the Lagrange multiplier," *Proceedings of the Institution of Mechanical Engineers, Part B: Journal of Engineering Manufacture*, vol. 218, no. 7, pp. 765–778, 2004. DOI: 10.1177/095440540421800709.

[97] Cagan, J. and Kurfess, T. R., "Optimal design for tolerance and manufacturing allocation," Carnegie Mellon University Pittsburgh, Technical Report EDRC 24-67-91, 1991, pp. 1–22.

[98] Dantan, J.-Y.; Anwer, N., and Mathieu, L., "Integrated Tolerancing Process for conceptual design," *CIRP Annals*, vol. 52, no. 1, pp. 135–138, 2003. DOI: 10.1016/S0007-8506(07)60549-6.

[99] Krogstie, L. and Martinsen, K., "Closed Loop Tolerance Engineering – A Relational Model Connecting Activities of Product Development," *Procedia CIRP*, vol. 3, pp. 519–524, 2012. DOI: 10.1016/j.procir.2012.07.089.

[100] Sahani, A. K.; Jain, P. K., and Sharma Satish, C., "Geometrical Tolerance Stack Up Techniques," *DAAAM International Scientific Book*, Katalinic, B. and Tekic, Z., Eds., DAAAM International Vienna, 2013, pp. 857–872. DOI: 10.2507/daaam.scibook.2013.52.

[101] Kackar, R. N., "Off-Line Quality Control, Parameter Design, and the Taguchi Method," *Journal of Quality Technology*, vol. 17, no. 4, pp. 176–188, 1985. DOI: 10.1080/00224065.1985.11978964.

[102] Goetz, S.; Schleich, B., and Wartzack, S., "Integration of robust and tolerance design in early stages of the product development process," *Research in Engineering Design*, vol. 31, no. 2, pp. 157–173, 2020. DOI: 10.1007/s00163-019-00328-2.

[103] Dantan, J.-Y.; Bruyere, J.; Baudouin, R., and Bigot, R., "Allocation of Bevel Gear Tolerances modelling by a vectorial tolerancing," *Proceedings of the 10th CIRP International Seminar on Computer Aided Tolerancing*, Erlangen, Germany, 21.03.-23.03.2007.

[104] Armillotta, A., "A method for computer-aided specification of geometric tolerances," *Computer-Aided Design*, vol. 45, no. 12, pp. 1604–1616, 2013. DOI: 10.1016/j.cad.2013.08.007.

[105] Sampath Kumar, R.; Soundararajan, V., and Alagumurthi, N., "Review of Tolerance Analysis, Allocation and Constraints in Manufacturing," *Journal for Manufacturing Science and Production*, vol. 10, no. 1, pp. 1–16, 2009. DOI: 10.1515/IJMSP.2009.10.1.1.

[106] Gust, P.; Sersch, A., and Kuhlmeier, M., "Influence of specifications according to the system of geometrical product specifications (gps) on scrap in technical products," *Proceedings of the Design Society*, vol. 1, pp. 1847–1856, 2021. DOI: 10.1017/pds.2021.446.

[107] Hochmuth, R.; Meerkamm, H., and Schweiger, W., "An approach to a general view on tolerances in mechanical engineering," *IPD 98*, pp. 65–76, 1998.

[108] Mathieu, L. and Ballu, A., "A Model for a Coherent and Complete Tolerancing Process," *Models for Computer Aided Tolerancing in Design and Manufacturing*, Davidson, J. K., Ed., Dordrecht: Springer, 2007, pp. 35–44. DOI: 10.1007/1-4020-5438-6_5.

[109] Dantan, J.-Y., "Tolerancing," *CIRP Encyclopedia of Production Engineering*, Laperrière, L. and Reinhart, G., Eds., Berlin: Springer, 2014, pp. 1230–1237. DOI: 10.1007/978-3-642-20617-7_16688.

[110] Humienny, Z., "Can ISO GPS and ASME Tolerancing Systems Define the Same Functional Requirements?" *Applied Sciences*, vol. 11, no. 17, p. 8269, 2021. DOI: 10.3390/app11178269.

[111] ISO/TC 213, "ISO 14638:2015: Geometrical product specifications (GPS) — Matrix model," Standard, 2015.

[112] Salomons, O. W.; Poerink, H. J. J.; van Slooten, F.; van Houten, F. J. A. M., and Kals, H. J. J., "A Tolerancing Tool Based on Kinematic Analogies," *Computer-Aided Tolerancing*, Kimura, F., Ed., Dordrecht: Springer, 1996, pp. 47–70. DOI: 10.1007/978-94-009-1529-9_4.

[113] Anselmetti, B.; Chavanne, R.; Yang, J.-X., and Anwer, N., "Quick GPS: A new CAT system for single-part tolerancing," *Computer-Aided Design*, vol. 42, no. 9, pp. 768–780, 2010. DOI: 10.1016/j.cad.2010.04.006.

[114] Haghighi, P.; Mohan, P.; Kalish, N.; Vemulapalli, P.; Shah, J. J., and Davidson, J. K., "Toward Automatic Tolerancing of Mechanical Assemblies: First-Order GD&T Schema Development and Tolerance Allocation," *Journal of Computing and Information Science in Engineering*, vol. 15, no. 4, p. 041 003, 2015. DOI: 10.1115/1.4030939.

[115] Desrochers, A. and Clément, A., "A dimensioning and tolerancing assistance model for CAD/CAM systems," *The International Journal of Advanced Manufacturing Technology*, vol. 9, no. 6, pp. 352–361, 1994. DOI: 10.1007/BF01748479.

[116] Zhao, Q.; Li, T.; Cao, Y.; Yang, J., and Jiang, X., "A rule-based exclusion method for tolerance specification of revolving components," *Proceedings of the Institution of Mechanical Engineers, Part B: Journal of Engineering Manufacture*, vol. 234, no. 3, pp. 527–537, 2020. DOI: 10.1177/0954405419871137.

[117] Schleich, B. and Anwer, N., "Tolerancing Informatics: Towards Automatic Tolerancing Information Processing in Geometrical Variations Management," *Applied Sciences*, vol. 11, no. 1, p. 198, 2021. DOI: 10.3390/app11010198.

[118] Zhong, Y.; Qin, Y.; Huang, M.; Lu, W.; Gao, W., and Du, Y., "Automatically generating assembly tolerance types with an ontology-based approach," *Computer-Aided Design*, vol. 45, no. 11, pp. 1253–1275, 2013. DOI: 10.1016/j.cad.2013.06.006.

[119] Qie, Y.; Qiao, L.; Cui, Y., and Anwer, N., "A Domain Ontology for Assembly Tolerance Design," *Proceedings of the ASME 2017 International Mechanical Engineering Congress and Exposition. Volume 2: Advanced Manufacturing*, Tampa, Florida, USA: ASME, 2017, V002T02A112. DOI: 10.1115/IMECE2017-72526.

[120] Goetz, S. and Schleich, B., "Ontology-based representation of tolerancing and design knowledge for an automated tolerance specification of product concepts," *Procedia CIRP*, vol. 92, pp. 194–199, 2020. DOI: 10.1016/j.procir.2020.03.128.

[121] Cui, L.-j.; Sun, M.-y.; Cao, Y.-l.; Zhao, Q.-j.; Zeng, W.-h., and Guo, S.-r., "A novel tolerance geometric method based on machine learning," *Journal of Intelligent Manufacturing*, vol. 32, no. 3, pp. 799–821, 2021. DOI: 10.1007/s10845-020-01706-7.

[122] Zhong, Y.; Qin, Y.; Huang, M.; Lu, W., and Chang, L., "Constructing a meta-model for assembly tolerance types with a description logic based approach," *Computer-Aided Design*, vol. 48, pp. 1–16, 2014. DOI: 10.1016/j.cad.2013.10.009.

[123] Sfantsikopoulos, M. M., "A cost-tolerance analytical approach for design and manufacturing," *The International Journal of Advanced Manufacturing Technology*, vol. 5, no. 2, pp. 126–134, 1990. DOI: 10.1007/BF02601602.

[124] Latta, L. W., "Least-cost tolerancing," *Product Engineering*, vol. 16, pp. 111–113, 1963.

[125] Pike, E. W. and Silverberg, T. R., "Assigning tolerances for maximum economy," *Machine design*, vol. 25, no. 9, pp. 139–146, 1953.

[126] Peters, J., "Tolerancing the Components of an Assembly for Minimum Cost," *Journal of Engineering for Industry*, vol. 92, no. 3, pp. 677–682, 1970. DOI: 10.1115/1.3427830.

[127] Bjørke, Ø., *Computer-aided Tolerancing*. New York: Tapir, 1978.

[128] Zhang, C. and Wang, H.-P., "Robust design of assembly and machining tolerance allocations," *IIE Transactions*, vol. 30, no. 1, pp. 17–29, 1998. DOI: 10.1080/07408179808966434.

[129] Chase, K. W., "Tolerance Allocation Methods for Designers," ADCATS Report No. 99-6, 1999.

[130] Grohmann, P. and Walter, M. S. J., "Speeding up Statistical Tolerance Analysis to Real Time," *Applied Sciences*, vol. 11, no. 9, p. 4207, 2021. DOI: 10.3390/app11094207.

[131] Sigurdarson, N.; Eifler, T., and Ebro, M., "The Applicability of CAT tools in industry – boundaries and challenges in tolerance engineering practice observed in a medical device company," *Procedia CIRP*, vol. 75, pp. 261–266, 2018. DOI: 10.1016/j.procir.2018.04.066.

[132] Marziale, M. and Polini, W., "A review of two models for tolerance analysis of an assembly: vector loop and matrix," *The International Journal of Advanced Manufacturing Technology*, vol. 43, no. 11-12, pp. 1106–1123, 2009. DOI: 10.1007/s00170-008-1790-0.

[133] Ciarallo, F. W. and Yang, C. C., "Optimization of propagation in interval constraint networks for tolerance design," *1997 IEEE International Conference on Systems, Man, and Cybernetics. Computational Cybernetics and Simulation*, vol. 2, Orlando, FL, USA: IEEE, 12.10.-15.10.1997, pp. 1924–1929. DOI: 10.1109/ICSMC.1997.638348.

[134] Wu, F.; Dantan, J.-Y.; Etienne, A.; Siadat, A., and Martin, P., "Improved algorithm for tolerance allocation based on Monte Carlo simulation and discrete optimization," *Computers & Industrial Engineering*, vol. 56, no. 4, pp. 1402–1413, 2009. DOI: 10.1016/j.cie.2008.09.005.

[135] Lin, C.-Y.; Huang, W.-H.; Jeng, M.-C., and Doong, J.-L., "Study of an assembly tolerance allocation model based on Monte Carlo simulation," *Journal of Materials Processing Technology*, vol. 70, no. 1-3, pp. 9–16, 1997. DOI: 10.1016/S0924-0136(97)00034-4.

[136] Kusiak, A. and Feng, C.-X., "Deterministic tolerance synthesis: a comparative study," *Computer-Aided Design*, vol. 27, no. 10, pp. 759–768, 1995. DOI: 10.1016/0010-4485(94)00028-C.

[137] Yeo, S. H.; Ngoi, B. K. A., and Chen, H., "A cost-tolerance model for process sequence optimisation," *The International Journal of Advanced Manufacturing Technology*, vol. 12, no. 6, pp. 423–431, 1996. DOI: 10.1007/BF01186931.

[138] Irani, S. A.; Mittal, R. O., and Lehtihet, E. A., "Tolerance chart optimization," *International Journal of Production Research*, vol. 27, no. 9, pp. 1531–1552, 1989. DOI: 10.1080/00207548908942638.

[139] Uttam, S., "Optimal tolerance synthesis for process planning with machine selection," Regional Engineering College, Calicut, India, Master's Thesis, 2001.

[140] Wei, C.-C. and Lee, Y.-C., "Designing Process Tolerances with Concurrent Minimization of Production Loss," *Concurrent Engineering*, vol. 5, no. 4, pp. 301–305, 1997. DOI: 10.1177/1063293X9700500402.

[141] Ngoi, B. K. A. and Seow, M. S., "Tolerance control for dimensional and geometrical specifications," *The International Journal of Advanced Manufacturing Technology*, vol. 11, no. 1, pp. 34–42, 1996. DOI: 10.1007/BF01177182.

[142] Ngoi, B. K. A. and Ong, C. T., "Product and process dimensioning and tolerancing techniques. A state-of-the-art review," *The International Journal of Advanced Manufacturing Technology*, vol. 14, no. 12, pp. 910–917, 1998. DOI: 10.1007/BF01179081.

[143] Ming, X. G. and Mak, K. L., "Intelligent approaches to tolerance allocation and manufacturing operations selection in process planning," *Journal of Materials Processing Technology*, vol. 117, no. 1-2, pp. 75–83, 2001. DOI: 10.1016/S0924-0136(01)01154-2.

[144] Dong, Z. and Wang, G. G., "Automated Tolerance Optimization Using Feature-driven, Production Operation-based Cost Models," 2001.

[145] Wheeler, D. L.; Cavalier, T. M., and Lehtihet, E. A., "An implicit enumeration approach to probabilistic tolerance allocation under conventional tolerance control," *International Journal of Production Research*, vol. 37, no. 16, pp. 3773–3789, 1999. DOI: 10.1080/002075499190040.

[146] Li, W.; Bai, G.; Zhang, C., and Wang, B., "Optimization of machining datum selection and machining tolerance allocation with genetic algorithms," *International Journal of Production Research*, vol. 38, no. 6, pp. 1407–1424, 2000. DOI: 10.1080/002075400188924.

[147] Whybrew, K.; Britton, G. A.; Robinson, D. F., and Sermsuti-anuwat, Y., "A graph-theoretic approach to tolerance charting," *The International Journal of Advanced Manufacturing Technology*, vol. 5, no. 2, pp. 175–183, 1990. DOI: 10.1007/BF02601605.

[148] Ngoi, B. K. A., "Applying linear programming to tolerance chart balancing," *The International Journal of Advanced Manufacturing Technology*, vol. 7, no. 4, pp. 187–192, 1992. DOI: 10.1007/BF02601622.

[149] Ahluwalia, R. S. and Karolin, A. V., "CATC — A Computer Aided Tolerance Control system," *Journal of Manufacturing Systems*, vol. 3, no. 2, pp. 153–160, 1984. DOI: 10.1016/0278-6125(84)90006-2.

[150] Ji, P., "A linear programming model for tolerance assignment in a tolerance chart," *International Journal of Production Research*, vol. 31, no. 3, pp. 739–751, 1993. DOI: 10.1080/00207549308956754.

[151] Morse, E.; Heysiattalab, S.; Barnard-Feeney, A., and Hedberg, T., "Interoperability: Linking Design and Tolerancing with Metrology," *Procedia CIRP*, vol. 43, pp. 13–16, 2016. DOI: 10.1016/j.procir.2016.04.106.

[152] Xue, D. and Dong, Z., "Developing a quantitative intelligent system for implementing concurrent engineering design," *Journal of Intelligent Manufacturing*, vol. 5, no. 4, pp. 251–267, 1994. DOI: 10.1007/BF00123697.

[153] Sohlenius, G., "Concurrent Engineering," *CIRP Annals*, vol. 41, no. 2, pp. 645–655, 1992. DOI: 10.1016/S0007-8506(07)63251-X.

[154] Al-Ansary, M. D. and Deiab, I. M., "Concurrent optimization of design and machining tolerances using the genetic algorithms method," *International Journal of Machine Tools and Manufacture*, vol. 37, no. 12, pp. 1721–1731, 1997. DOI: 10.1016/S0890-6955(97)00033-3.

[155] Islam, M., "Functional dimensioning and tolerancing software for concurrent engineering applications," *Computers in Industry*, vol. 54, no. 2, pp. 169–190, 2004. DOI: 10.1016/j.compind.2003.09.006.

[156] Salomons, O. W.; van Houten, F. J. A. M., and Kals, H. J. J., "Current Status of CAT Systems," *Geometric Design Tolerancing: Theories, Standards and Applications*, ElMaraghy, H. A., Ed., Boston: Springer, 1998, pp. 438–452. DOI: 10.1007/978-1-4615-5797-5_35.

[157] Söderberg, R.; Wärmefjord, K.; Carlson, J. S., and Lindkvist, L., "Toward a Digital Twin for real-time geometry assurance in individualized production," *CIRP Annals*, vol. 66, no. 1, pp. 137–140, 2017. DOI: 10.1016/j.cirp.2017.04.038.

[158] Schleich, B.; Wärmefjord, K.; Söderberg, R., and Wartzack, S., "Geometrical Variations Management 4.0: Towards next Generation Geometry Assurance," *Procedia CIRP*, vol. 75, pp. 3–10, 2018. DOI: 10.1016/j.procir.2018.04.078.

[159] Camba, J.; Contero, M.; Johnson, M., and Company, P., "Extended 3D annotations as a new mechanism to explicitly communicate geometric design intent and increase CAD model reusability," *Computer-Aided Design*, vol. 57, pp. 61–73, 2014. DOI: 10.1016/j.cad.2014.07.001.

[160] Lipman, R. and Lubell, J., "Conformance checking of PMI representation in CAD model STEP data exchange files," *Computer-Aided Design*, vol. 66, pp. 14–23, 2015. DOI: 10.1016/j.cad.2015.04.002.

[161] Fang, F. Z.; Li, Z.; Arokiam, A., and Gorman, T., "Closed Loop PMI Driven Dimensional Quality Lifecycle Management Approach for Smart Manufacturing System," *Procedia CIRP*, vol. 56, pp. 614–619, 2016. DOI: 10.1016/j.procir.2016.10.121.

[162] Aderiani, A. R.; Wärmefjord, K., and Söderberg, R., "Model-based definition in computer aided tolerance analyses," *Procedia CIRP*, vol. 114, pp. 112–116, 2022. DOI: 10.1016/j.procir.2022.10.016.

[163] ISO/TC 184/SC 4, "ISO 10303-242:2020: Industrial automation systems and integration — Product data representation and exchange — Part 242: Application protocol: Managed model-based 3D engineering," Standard, 2020.

[164] ISO/TC 184/SC 4, "ISO 14306:2017: Industrial automation systems and integration — JT file format specification for 3D visualization," Standard, 2017.

[165] ISO/TC 184/SC 4, "ISO 23952:2020: Automation systems and integration — Quality information framework (QIF) — An integrated model for manufacturing quality information," Standard, 2020.

[166] Hedberg, T.; Feeney, A. B.; Helu, M., and Camelio, J. A., "Toward a Lifecycle Information Framework and Technology in Manufacturing," *Journal of Computing and Information Science in Engineering*, vol. 17, no. 2, p. 021 010, 2017. DOI: 10.1115/1.4034132.

[167] Rachuri, S.; Subrahmanian, E.; Bouras, A.; Fenves, S. J.; Foufou, S., and Sriram, R. D., "Information sharing and exchange in the context of product lifecycle management: Role of standards," *Computer-Aided Design*, vol. 40, no. 7, pp. 789–800, 2008. DOI: 10.1016/j.cad.2007.06.012.

[168] Barbau, R.; Krima, S.; Rachuri, S.; Narayanan, A.; Fiorentini, X.; Foufou, S., and Sriram, R. D., "OntoSTEP: Enriching product model data using ontologies," *Computer-Aided Design*, vol. 44, no. 6, pp. 575–590, 2012. DOI: 10.1016/j.cad.2012.01.008.

[169] Kwon, S.; Monnier, L. V.; Barbau, R., and Bernstein, W. Z., "Enriching standards-based digital thread by fusing as-designed and as-inspected data using knowledge graphs," *Advanced Engineering Informatics*, vol. 46, p. 101 102, 2020. DOI: 10.1016/j.aei.2020.101102.

[170] Sarigecili, M. I.; Roy, U., and Rachuri, S., "Interpreting the semantics of GD&T specifications of a product for tolerance analysis," *Computer-Aided Design*, vol. 47, pp. 72–84, 2014. DOI: 10.1016/j.cad.2013.09.002.

[171] Lenne, D.; Thouvenin, I., and Aubry, S., "Supporting design with 3D-annotations in a collaborative virtual environment," *Research in Engineering Design*, vol. 20, no. 3, pp. 149–155, 2009. DOI: 10.1007/s00163-009-0071-8.

[172] Quintana, V.; Rivest, L.; Pellerin, R.; Venne, F., and Kheddouci, F., "Will Model-based Definition replace engineering drawings throughout the product lifecycle? A global perspective from aerospace industry," *Computers in Industry*, vol. 61, no. 5, pp. 497–508, 2010. DOI: 10.1016/j.compind.2010.01.005.

[173] Qin, Y.; Qi, Q.; Lu, W.; Liu, X.; Scott, P. J., and Jiang, X., "A review of representation models of tolerance information," *The International Journal of Advanced Manufacturing Technology*, vol. 95, no. 5-8, pp. 2193–2206, 2018. DOI: 10.1007/s00170-017-1352-4.

[174] Glancy, C.; Stoddard, J., and Law, M., "Automating the Tolerancing Process," *Dimensioning and Tolerancing Handbook*, Drake, P. J., Ed., New York: McGraw-Hill, 1999, pp. 15-1–15-15.

[175] Mohan, P.; Haghighi, P.; Vemulapalli, P.; Kalish, N.; Shah, J. J., and Davidson, J. K., "Toward Automatic Tolerancing of Mechanical Assemblies: Assembly Analyses," *Journal of Computing and Information Science in Engineering*, vol. 14, no. 4, p. 041 009, 2014. DOI: 10.1115/1.4028592.

[176] Balling, R. J.; Free, J. C., and Parkinson, A. R., "Consideration of Worst-Case Manufacturing Tolerances in Design Optimization," *Journal of Mechanisms, Transmissions, and Automation in Design*, vol. 108, no. 4, pp. 438–441, 1986. DOI: 10.1115/1.3258751.

[177] Zhang, C. and Wang, H.-P., "The Discrete Tolerance Optimization Problem," *Manufacturing Review*, vol. 6, no. 1, pp. 60–71, 1993.

[178] Cheikh, A. and McGoldrick, P. F., "The Influence of Cost, Function and Process Capability on Tolerance," *International Journal of Quality & Reliability Management*, vol. 5, no. 3, pp. 15–28, 1988. DOI: 10.1108/eb002904.

[179] Wu, Z.; ElMaraghy, W. H., and ElMaraghy, H. A., "Evaluation of Cost-Tolerance Algorithms for Design Tolerance Analysis and Synthesis," *Manufacturing Review*, vol. 1, no. 3, pp. 168–179, 1988.

[180] Andersen, C. B., "General System for Least Cost Tolerance Allcoation in Mechanical Assemblies," ADCATS Report No. 90-2, 1990.

[181] Söderberg, R. and Lindkvist, L., "Geometrical Coupling Analysis in Assembly Design," *Proceedings of ICAD2002 Second International Conference on Axiomatic Design*, Cambridge, Massachusetts, USA, 10.06.-11.06.2002.

[182] Ziegler, P. and Wartzack, S., "Sensitivity Analysis of Tolerances which Restrict Mutliple Similar Features," *Proceedings of the International Symposium on Robust Design - ISoRD14*, Copenhagen, Denmark, 14.08.-15.08.2014, pp. 91–101.

[183] Heling, B.; Oberleiter, T.; Schleich, B.; Willner, K., and Wartzack, S., "On the Selection of Sensitivity Analysis Methods in the Context of Tolerance Management," *Journal of Verification, Validation and Uncertainty Quantification*, vol. 4, no. 1, p. 011 001, 2019. DOI: 10.1115/1.4043912.

[184] Lee, W.-J. and Woo, T. C., "Optimum selection of discrete tolerances," The University of Michigan, Technical Report No. 87-34, 1987.

[185] Ngoi, B. K. A. and Min, O. J., "Optimum Tolerance Allocation in Assembly," *The International Journal of Advanced Manufacturing Technology*, vol. 15, no. 9, pp. 660–665, 1999. DOI: 10.1007/s001700050116.

[186] Lee, W.-J. and Woo, T. C., "Optimum Selection of Discrete Tolerances," *Journal of Mechanisms, Transmissions, and Automation in Design*, vol. 111, no. 2, pp. 243–251, 1989. DOI: 10.1115/1.3258990.

[187] Youngworth, R. N. and Stone, B. D., "Elements of Cost-Based Tolerancing," *Optical Review*, vol. 8, no. 4, pp. 276–280, 2001. DOI: 10.1007/s10043-001-0276-1.

[188] Sayed, S. E. Y. and Kheir, N. A., "An efficient technique for minimum-cost tolerance assignment," *SIMULATION*, vol. 44, no. 4, pp. 189–195, 1985. DOI: 10.1177/003754978504400404.

[189] Prabhaharan, G.; Asokan, P.; Ramesh, P., and Rajendran, S., "Genetic-algorithm-based optimal tolerance allocation using a least-cost model," *The International Journal of Advanced Manufacturing Technology*, vol. 24, no. 9-10, pp. 647–660, 2004. DOI: 10.1007/s00170-003-1606-1.

[190] Dong, Z.; Hu, W., and Xue, D., "New Production Cost-Tolerance Models for Tolerance Synthesis," *Journal of Engineering for Industry*, vol. 116, no. 2, pp. 199–206, 1994. DOI: 10.1115/1.2901931.

[191] Kumar, V., "Optimization of tolerance for minimum manufacturing cost of satisfactory journal bearings," *Wear*, vol. 86, no. 1, pp. 21–27, 1983. DOI: 10.1016/0043-1648(83)90085-6.

[192] Nassef, A. O., "Optimal allocation of types and magnitudes of geometric tolerances," Ph.D. dissertation, McMaster University, Hamilton, Canada, 1996.

[193] Governi, L.; Furferi, R., and Volpe, Y., "A Genetic Algorithms-based Procedure for Automatic Tolerance Allocation Integrated in a Commercial Variation Analysis Software," *Journal of Artificial Intelligence*, vol. 5, no. 3, pp. 99–112, 2012. DOI: 10.3923/jai.2012.99.112.

[194] Wang, Y.; Calhoun, S.; Bosman, L., and Sutherland, J. W., "Tolerance Allocations on Products: A Life Cycle Engineering Perspective," *Procedia CIRP*, vol. 80, pp. 174–179, 2019. DOI: 10.1016/j.procir.2019.01.089.

[195] Hoffenson, S.; Dagman, A., and Söderberg, R., "Visual quality and sustainability considerations in tolerance optimization: A market-based approach," *International Journal of Production Economics*, vol. 168, pp. 167–180, 2015. DOI: 10.1016/j.ijpe.2015.06.023.

[196] Li, Z.; Kokkolaras, M.; Papalambros, P., and Hu, S. J., "Product and Process Tolerance Allocation in Multistation Compliant Assembly Using Analytical Target Cascading," *Journal of Mechanical Design*, vol. 130, no. 9, p. 091 701, 2008. DOI: 10.1115/1.2943296.

[197] Abdel-Malek, L. and Asadathorn, N., "Process and design tolerance in relation to manufacturing cost: A review & extension," *The Engineering Economist*, vol. 40, no. 1, pp. 73–100, 1994. DOI: 10.1080/00137919408903139.

[198] Sanz-Lobera, A.; Gómez, E.; Pérez, J., and Sevilla, L., "A proposal of cost-tolerance models directly collected from the manufacturing process," *International Journal of Production Research*, vol. 54, no. 15, pp. 4584–4598, 2016. DOI: 10.1080/00207543.2015.1086036.

[199] Rajasekera, J. R. and Fang, S. C., "A new approach to tolerance allocation in design cost analysis," *Engineering Optimization*, vol. 24, no. 4, pp. 283–291, 1995. DOI: 10.1080/03052159508941194.

[200] Söderberg, R., "Tolerance Allocation Considering Customer and Manufacturer Objectives," *Proceedings of the ASME 1993 Design Technical Conferences. 19th Design Automation Conference: Volume 2 — Design Optimization; Geometric Modeling and Tolerance Analysis; Mechanism Synthesis and Analysis; Decomposition and Design Optimization*, Albuquerque, New Mexico, USA: ASME, 1993, pp. 149–157. DOI: 10.1115/DETC1993-0387.

[201] Ye, B. and Salustri, F. A., "Simultaneous tolerance synthesis for manufacturing and quality," *Research in Engineering Design*, vol. 14, no. 2, pp. 98–106, 2003. DOI: 10.1007/s00163-003-0029-1.

[202] Sanz Lobera, A.; Villeta López, M.; Sebastían Pérez, M. A., and Segui, V. J., "Comparative Research among Cost-Tolerance Models Used in Mechanical Manufacturing," *AIP Conference Proceedings*, vol. 1181, no. 1, pp. 254–265, 2009. DOI: 10.1063/1.3273638.

[203] Armillotta, A., "Selection of parameters in cost-tolerance functions: review and approach," *The International Journal of Advanced Manufacturing Technology*, vol. 108, no. 1-2, pp. 167–182, 2020. DOI: 10.1007/s00170-020-05400-z.

[204] Chase, K. W., "Minimum-Cost Tolerance Allocation," ADCATS Report No. 99-5, 1999.

[205] Evans, D. H., "Optimum Tolerance Assignment to Yield Minimum Manufacturing Cost," *Bell System Technical Journal*, vol. 37, no. 2, pp. 461–484, 1958. DOI: 10.1002/j.1538-7305.1958.tb01529.x.

[206] Sanz-Lobera, A.; Sebastián, M. A., and Pérez, J. M., "New cost–tolerance model for mechanical part design," *The International Journal of Advanced Manufacturing Technology*, vol. 51, no. 5-8, pp. 421–430, 2010. DOI: 10.1007/s00170-010-2661-z.

[207] Ghie, W., "Functional Requirement Cost for product using Jacobian-Torsor model," *Proceedings of the 11th CIRP International Conference on Computer Aided Tolerancing*, Annecy, France, 26.03.– 27.03.2009.

[208] Yeo, S. H.; Ngoi, B. K. A.; Poh, L. S., and Hang, C., "Cost-tolerance relationships for non-traditional machining processes," *The International Journal of Advanced Manufacturing Technology*, vol. 13, no. 1, pp. 35–41, 1997. DOI: 10.1007/BF01179228.

[209] Evans, D. H., "An Application of Numerical Integration Techniques to Statistical Tolerancing," *Technometrics*, vol. 9, no. 3, pp. 441–456, 1967. DOI: 10.2307/1266512.

[210] He, J., "Tolerancing for manufacturing via cost minimization," *International Journal of Machine Tools and Manufacture*, vol. 31, no. 4, pp. 455–470, 1991. DOI: 10.1016/0890-6955(91)90029-3.

[211] Janakiraman, V. and Saravanan, R., "Concurrent optimization of machining process parameters and tolerance allocation," *The International Journal of Advanced Manufacturing Technology*, vol. 51, no. 1-4, pp. 357–369, 2010. DOI: 10.1007/s00170-010-2602-x.

[212] Chen, Y.; Ding, Y.; Jin, J., and Ceglarek, D., "Integration of Process-Oriented Tolerancing and Maintenance Planning in Design of Multistation Manufacturing Processes," *IEEE Transactions on Automation Science and Engineering*, vol. 3, no. 4, pp. 440–453, 2006. DOI: 10.1109/TASE.2006.872105.

[213] Roy, U.; Pramanik, N.; Wang, H.; Sudarsan, R.; Sriram, R. D., and Lyons, K. W., "Tolerance Synthesis Scheme," National Institute of Standards and Technology (NIST), Gaithersburg, USA, Tech. Rep. NIST IR 6836, 2003. DOI: 10.6028/NIST.IR.6836.

[214] Dantan, J.-Y.; Etienne, A.; Mohammadi, M.; Khezri, A.; Homri, L.; Tavakkoli-Moghaddam, R., and Siadat, A., "Modular cost model for Tolerance allocation, Process selection and Inspection planning," *Procedia CIRP*, vol. 114, pp. 1–6, 2022. DOI: 10.1016/j.procir.2022.10.001.

[215] Khezri, A.; Homri, L.; Etienne, A.; Dantan, J.-Y., and Lanza, G., "A Framework for Integration of Resource Allocation and Reworking Concept into Design Optimisation Problem," *IFAC-PapersOnLine*, vol. 55, no. 10, pp. 1037–1042, 2022. DOI: 10.1016/j.ifacol.2022.09.524.

[216] Tsutsumi, D.; Gyulai, D.; Kovács, A.; Tipary, B.; Ueno, Y.; Nonaka, Y., and Fujita, K., "Joint optimization of product tolerance design, process plan, and production plan in high-precision multi-product assembly," *Journal of Manufacturing Systems*, vol. 54, pp. 336–347, 2020. DOI: 10.1016/j.jmsy.2020.01.004.

[217] Hoffenson, S.; Dagman, A., and Söderberg, R., "A Multi-objective Tolerance Optimization Approach for Economic, Ecological, and Social Sustainability," *Re-Engineering Manufacturing for Sustainability*, Nee, A. Y. C.; Song, B., and Ong, S.-K., Eds., Singapore: Springer, 2013, pp. 729–734. DOI: 10.1007/978-981-4451-48-2_119.

[218] Liu, S.; Wang, P., and Jin, Q., "Optimal tolerance design for green manufacturing," *International Technology and Innovation Conference 2009 (ITIC 2009)*, Xi'an, China: IET, 12.10.-14.10.2009, pp. 1–3. DOI: 10.1049/cp.2009.1466.

[219] Gerth, R. J. and Pfeifer, T., "Minimum cost tolerancing under uncertain cost estimates," *IIE Transactions*, vol. 32, no. 6, pp. 493–503, 2000. DOI: 10.1080/07408170008963926.

[220] Sanz-Lobera, A. and Garcia, J. P., "Economic considerations in the assignment of manufacturing tolerances," *International Journal of Production Research*, vol. 44, no. 15, pp. 3131–3145, 2006. DOI: 10.1080/00207540500244344.

[221] Lin, S.-S.; Wang, H.-P., and Zhang, C., "Optimal tolerance design for integrated design, manufacturing and inspection with genetic algorithms," *Advanced Tolerancing Techniques*, Zhang, H.-C., Ed., New York: Wiley, 1997, pp. 261–281.

[222] Dong, Z. and Wang, G. G., "Integrated Concurrent Design of Tolerance Using Empirical Manufacturing Cost Models," pp. 1–18, 1998.

[223] Shehabi, M. K., "Cost tolerance optimization for piecewise continuous cost tolerance functions," Ohio University, Master's Thesis, 2002.

[224] Dong, Z. and Hu, W., "Optimal process sequence identification and optimal process tolerance assignment in computer-aided process planning," *Computers in Industry*, vol. 17, no. 1, pp. 19–32, 1991. DOI: 10.1016/0166-3615(91)90100-N.

[225] Yeo, S. H.; Ngoi, B. K. A., and Chen, H., "Process sequence optimization based on a new cost-tolerance model," *Journal of Intelligent Manufacturing*, vol. 9, no. 1, pp. 29–37, 1998. DOI: 10.1023/A:1008895224256.

[226] Cao, Y.; Zhang, H.; Mao, J., and Yang, J., "Novel cost–tolerance model based on fuzzy neural networks," *Proceedings of the Institution of Mechanical Engineers, Part B: Journal of Engineering Manufacture*, vol. 224, no. 11, pp. 1757–1765, 2010. DOI: 10.1243/09544054JEM1789.

[227] Jayaprakash, G.; Sivakumar, K., and Thilak, M., "Parametric Tolerance Analysis of Mechanical Assembly by Developing Direct Constraint Model in CAD and Cost Competent Tolerance Synthesis," *Intelligent Control and Automation*, vol. 1, no. 1, pp. 1–14, 2010. DOI: 10.4236/ica.2010.11001.

[228] Wang, Q.; Stockton, D. J., and Baguley, P., "Process cost modelling using neural networks," *International Journal of Production Research*, vol. 38, no. 16, pp. 3811–3821, 2000. DOI: 10.1080/00207540050176021.

[229] Saravanan, A.; Jerald, J., and Carolina Rani, A. D., "An explicit methodology for manufacturing cost–tolerance modeling and optimization using the neural network integrated with the genetic algorithm," *Artificial Intelligence for Engineering Design, Analysis and Manufacturing*, vol. 34, no. 3, pp. 430–443, 2020. DOI: 10.1017/S0890060420000219.

[230] Lin, Z.-C. and Chang, D.-Y., "Cost-tolerance analysis model based on a neural networks method," *International Journal of Production Research*, vol. 40, no. 6, pp. 1429–1452, 2002. DOI: 10.1080/00207540110116282.

[231] Chen, M.-C., "Tolerance synthesis by neural learning and nonlinear programming," *International Journal of Production Economics*, vol. 70, no. 1, pp. 55–65, 2001. DOI: 10.1016/S0925-5273(00)00044-X.

[232] Vasseur, H.; Kurfess, T. R., and Cagan, J., "Use of a Quality Loss Function to Select Statistical Tolerances," *Journal of Manufacturing Science and Engineering*, vol. 119, no. 3, pp. 410–416, 1997. DOI: 10.1115/1.2831121.

[233] Hsieh, K.-L., "The study of cost-tolerance model by incorporating process capability index into product lifecycle cost," *The International Journal of Advanced Manufacturing Technology*, vol. 28, no. 5-6, pp. 638–642, 2006. DOI: 10.1007/s00170-004-2385-z.

[234] Peat, A. P., *Cost Reduction Charts for Designers and Production Engineers*. London: The Machinery Publishing Company, 1968.

[235] Trucks, H. E. and Lewis, G., *Designing for Economical Production*, 2nd ed. Dearborn, Michigan, USA: Society of Manufacturing Engineers, 1987.

[236] Dieter, G. E., *Engineering Design: A Materials and Processing Approach*. New York: McGraw-Hill, 1983.

[237] Johnson, R. C., "The cost of finishes and tolerances," *Journal of the American Society for Naval Engineers*, vol. 70, no. 4, pp. 607–614, 1958. DOI: 10.1111/j.1559-3584.1958.tb01777.x.

[238] Freek Huele, A. and Engel, J., "A response surface approach to tolerance design," *Statistica Neerlandica*, vol. 60, no. 3, pp. 379–395, 2006. DOI: 10.1111/j.1467-9574.2006.00332.x.

[239] Haghighi, A. and Li, L., "Joint Asymmetric Tolerance Design and Manufacturing Decision-Making for Additive Manufacturing Processes," *IEEE Transactions on Automation Science and Engineering*, vol. 16, no. 3, pp. 1259–1270, 2019. DOI: 10.1109/TASE.2018.2879719.

[240] Franz, M. and Wartzack, S., "Tolerance Optimization of Patch Parameters for Locally Reinforced Composite Structures," *Applied Composite Materials*, 2022. DOI: 10.1007/s10443-022-10072-x.

[241] Haghighi, A. and Li, L., "Study of the relationship between dimensional performance and manufacturing cost in fused deposition modeling," *Rapid Prototyping Journal*, vol. 24, no. 2, pp. 395–408, 2018. DOI: 10.1108/RPJ-11-2016-0177.

[242] Etienne, A.; Dantan, J.-Y.; Siadat, A., and Martin, P., "Cost estimation for tolerance allocation," *Proceedings of the 10th CIRP Conference on Computer-Aided Tolerancing*, Erlangen, Germany, 21.03.-23.03.2007.

[243] Etienne, A.; Mirdamadi, S.; Mohammadi, M.; Babaeizadeh Malmiry, R.; Antoine, J.-F.; Siadat, A.; Dantan, J.-Y.; Tavakkoli, R., and Martin, P., "Cost engineering for variation management during the product and process development," *International Journal on Interactive Design and Manufacturing (IJIDeM)*, vol. 11, no. 2, pp. 289–300, 2017. DOI: 10.1007/s12008-016-0318-3.

[244] Bennett, G. and Gupta, L. C., "Least-cost tolerances—I," *International Journal of Production Research*, vol. 8, no. 1, pp. 65–74, 1970. DOI: 10.1080/00207547008929830.

[245] Singh, P. K.; Jain, P. K., and Jain, S. C., "Optimal tolerance design of mechanical assemblies for economical manufacturing in the presence of alternative machines — a genetic algorithm-based hybrid methodology," *Proceedings of the Institution of Mechanical Engineers, Part B: Journal of Engineering Manufacture*, vol. 222, no. 5, pp. 591–604, 2008. DOI: 10.1243/09544054JEM967.

[246] Terán, A.; Pratt, D. B., and Case, K. E., "Present worth of external quality losses for symmetric nominal-is-better quality characteristics," *The Engineering Economist*, vol. 42, no. 1, pp. 39–52, 1996. DOI: 10.1080/00137919608903168.

[247] Chou, C.-Y. and Chang, C.-L., "Minimum-Loss Assembly Tolerance Allocation by Considering Product Degradation and Time Value of Money," *The International Journal of Advanced Manufacturing Technology*, vol. 17, no. 2, pp. 139–146, 2001. DOI: 10.1007/s001700170202.

[248] Feng, Q. and Kapur, K. C., "Quality Engineering: Control, Design and Optimization," *Handbook of Performability Engineering*, Misra, K. B., Ed., London: Springer, 2008, pp. 171–186. DOI: 10.1007/978-1-84800-131-2_13.

[249] Kapur, K. C.; Raman, S., and Simin Pulat, P., "Methodology for tolerance design using quality loss function," *Computers & Industrial Engineering*, vol. 19, no. 1-4, pp. 254–257, 1990. DOI: 10.1016/0360-8352(90)90116-4.

[250] Cheng, B.-W. and Maghsoodloo, S., "Optimization of mechanical assembly tolerances by incorporating Taguchi's quality loss function," *Journal of Manufacturing Systems*, vol. 14, no. 4, pp. 264–276, 1995. DOI: 10.1016/0278-6125(95)98879-B.

[251] Feng, C.-X. and Kusiak, A., "Robust Tolerance Design With the Integer Programming Approach," *Journal of Manufacturing Science and Engineering*, vol. 119, no. 4A, pp. 603–610, 1997. DOI: 10.1115/1.2831193.

[252] Li, M.-H. C., "Unbalanced Tolerance Design and Manufacturing Setting with Asymmetrical Linear Loss Function," *The International Journal of Advanced Manufacturing Technology*, vol. 20, no. 5, pp. 334–340, 2002. DOI: 10.1007/s001700200160.

[253] Li, M.-H. C., "Quality Loss Function Based Manufacturing Process Setting Models for Unbalanced Tolerance Design," *International Journal of Advanced Manufacturing Technology*, vol. 16, no. 1, pp. 39–45, 2000. DOI: 10.1007/PL00013130.

[254] Jin, Q.; Liu, S., and Wang, P., "Optimal tolerance design for products with non-normal distribution based on asymmetric quadratic quality loss," *The International Journal of Advanced Manufacturing Technology*, vol. 78, no. 1-4, pp. 667–675, 2015. DOI: 10.1007/s00170-014-6681-y.

[255] Wang, M.-L.; Liu, X.-T.; Wang, Y.-S.; Wang, X.-L.; Guo, H., and Xing, Y.-F., "Research on assembly tolerance allocation and quality control based on fuzzy reliability," *Proceedings of the Institution of Mechanical Engineers, Part C: Journal of Mechanical Engineering Science*, vol. 230, no. 20, pp. 3755–3766, 2016. DOI: 10.1177/0954406215615909.

[256] Liao, M.-Y., "Economic tolerance design for folded normal data," *International Journal of Production Research*, vol. 48, no. 14, pp. 4123–4137, 2010. DOI: 10.1080/00207540902960307.

[257] Mao Huang, Y. and Shiau, C.-S., "An optimal tolerance allocation model for assemblies with consideration of manufacturing cost, quality loss and reliability index," *Assembly Automation*, vol. 29, no. 3, pp. 220–229, 2009. DOI: 10.1108/01445150910972903.

[258] Jeang, A., "An approach of tolerance design for quality improvement and cost reduction," *International Journal of Production Research*, vol. 35, no. 5, pp. 1193–1211, 1997. DOI: 10.1080/002075497195272.

[259] Wu, C. C. and Tang, G., "Tolerance design for products with asymmetric quality losses," *International Journal of Production Research*, vol. 36, no. 9, pp. 2529–2541, 1998. DOI: 10.1080/002075498192670.

[260] Feng, C.-X.; Wang, J., and Wang, J.-S., "An optimization model for concurrent selection of tolerances and suppliers," *Computers & Industrial Engineering*, vol. 40, no. 1-2, pp. 15–33, 2001. DOI: 10.1016/S0360-8352(00)00047-4.

[261] Peng, H. P.; Jiang, X. Q., and Liu, X. J., "Concurrent optimal allocation of design and process tolerances for mechanical assemblies with interrelated dimension chains," *International Journal of Production Research*, vol. 46, no. 24, pp. 6963–6979, 2008. DOI: 10.1080/00207540701427037.

[262] Mustajib, M. I., "Concurrent Engineering of Tolerance Synthesis and Process Selection for Products with Multiple Quality Characteristcs Considering Process Capability," *Makara of Technology Series*, vol. 16, no. 1, pp. 7–14, 2012. DOI: 10.7454/mst.v16i1.1040.

[263] Huang, M. F.; Zhong, Y. R., and Xu, Z. G., "Concurrent process tolerance design based on minimum product manufacturing cost and quality loss," *The International Journal of Advanced Manufacturing Technology*, vol. 25, no. 7-8, pp. 714–722, 2005. DOI: 10.1007/s00170-003-1911-8.

[264] Gerth, R. J., "A spreadsheet approach to minimum cost tolerancing for rocket engines," *Computers & Industrial Engineering*, vol. 27, no. 1-4, pp. 549–552, 1994. DOI: 10.1016/0360-8352(94)90356-5.

[265] Gerth, R. J.; Klonaris, P., and Pfeiffer, T., "Cost Tolerance Sensitivity Analysis for Concurrent Engineering Design Support," *Global Consistency of Tolerances*, van Houten, F. and Kals, H., Eds., Dordrecht: Springer, 1999, pp. 313–324. DOI: 10.1007/978-94-017-1705-2_32.

[266] Gerth, R. J., "A minimum cost tolerance allocation method for rocket engines and robust rocket engine design," The Ohio University, Technical Report N94-24419, 1993.

[267] Janakiram, D.; Prasad, L. V., and Rao, U. R. K., "Tolerancing of parts using an expert system," *The International Journal of Advanced Manufacturing Technology*, vol. 4, no. 2, pp. 157–167, 1989. DOI: 10.1007/BF02601517.

[268] Ghie, W.; Laperrière, L.; Nadeau, D., and Desrochers, A., "Allocation tolerance by Jacobian-torsor model," *Proceedings of the 18th IASTED International Conference MODELLING AND SIMULATION*, Montreal, Quebec, Canada, 30.05.-01.06.2007, pp. 191–196.

[269] Ghali, M.; Tlija, M.; Aifaoui, N., and Pairel, E., "A CAD method for tolerance allocation considering manufacturing difficulty based on FMECA tool," *The International Journal of Advanced Manufacturing Technology*, vol. 91, no. 5-8, pp. 2435–2446, 2017. DOI: 10.1007/s00170-016-9961-x.

[270] Kumar, A.; Choi, S.-K., and Goksel, L., "Tolerance allocation of assemblies using fuzzy comprehensive evaluation and decision support process," *The International Journal of Advanced Manufacturing Technology*, vol. 55, no. 1-4, pp. 379–391, 2011. DOI: 10.1007/s00170-010-3047-y.

[271] Dupinet, É.; Balazinski, M., and Czogala, E., "Tolerance allocation based on fuzzy logic and simulated annealing," *Journal of Intelligent Manufacturing*, vol. 7, no. 6, pp. 487–497, 1996. DOI: 10.1007/BF00122838.

[272] Zhijie, Z.; Yuan, L.; Jianfeng, J., and Shuilong, T., "Optimal assembly tolerance design based on fuzzy information entropy and seeker optimization algorithm," *2010 3rd International Conference on Advanced Computer Theory and Engineering(ICACTE)*, Chengdu, China: IEEE, 20.08.-22.08.2010, pp. V5-610-V5–613. DOI: 10.1109/ICACTE.2010.5579339.

[273] Zhao, Y. M.; Liu, D. S., and Wen, Z. J., "Optimal tolerance design of product based on service quality loss," *The International Journal of Advanced Manufacturing Technology*, vol. 82, no. 9-12, pp. 1715–1724, 2016. DOI: 10.1007/s00170-015-7480-9.

[274] Yang, B.; Yang, T., and Ze, X., "Functional tolerance theory in incremental growth design," *Frontiers of Mechanical Engineering in China*, vol. 2, no. 3, pp. 336–343, 2007. DOI: 10.1007/s11465-007-0059-x.

[275] Wang, Y.; Zhai, W.-j.; Yang, L.-p.; Wu, W.-g.; Ji, S.-p., and Ma, Y.-l., "Study on the tolerance allocation optimization by fuzzy-set weight-center evaluation method," *The International Journal of Advanced Manufacturing Technology*, vol. 33, no. 3-4, pp. 317–322, 2007. DOI: 10.1007/s00170-006-0471-0.

[276] Wang, Y.; Zhai, W.-j.; Yang, L.-p.; Wu, W.-g.; Ji, S.-p., and Ma, Y.-l., "Objective function of cost in optimal tolerance allocation," *Journal of Harbin Institute of Technology*, vol. 14, no. 6, pp. 741–746, 2007.

[277] Ji, S. and Li, X., "Tolerance synthesis using second-order fuzzy comprehensive evaluation and genetic algorithm," *International Journal of Production Research*, vol. 38, no. 15, pp. 3471–3483, 2000. DOI: 10.1080/002075400422752.

[278] Lee, W.-J. and Woo, T. C., "Tolerancing: Its distribution, analysis, and synthesis," The University of Michigan, Technical Report No. 86–30, 1986.

[279] Bruyere, J.; Dantan, J.-Y.; Wu, F., and Bigot, R., "Optimization of Gear Tolerances by Statistical Analysis and Genetic Algorithm," *Advances in Integrated Design and Manufacturing in Mechanical Engineering II*, Tichkiewitch, S.; Tollenaere, M., and Ray, P., Eds., Dordrecht: Springer, 2007, pp. 401–415. DOI: 10.1007/978-1-4020-6761-7_27.

[280] Singh, P. K.; Jain, P. K., and Jain, S. C., "Important issues in tolerance design of mechanical assemblies. Part 1: Tolerance analysis," *Proceedings of the Institution of Mechanical Engineers, Part B: Journal of Engineering Manufacture*, vol. 223, no. 10, pp. 1225–1247, 2009. DOI: 10.1243/09544054JEM1304A.

[281] Singh, P. K.; Jain, P. K., and Jain, S. C., "Simultaneous optimal selection of design and manufacturing tolerances with different stack-up conditions using genetic algorithms," *International Journal of Production Research*, vol. 41, no. 11, pp. 2411–2429, 2003. DOI: 10.1080/0020754031000087328.

[282] Shah, J. J.; Ameta, G.; Shen, Z., and Davidson, J., "Navigating the Tolerance Analysis Maze," *Computer-Aided Design and Applications*, vol. 4, no. 5, pp. 705–718, 2007. DOI: 10.1080/16864360.2007.10738504.

[283] Hu, J. and Xiong, G., "Concurrent design of a geometric parameter and tolerance for assembly and cost," *International Journal of Production Research*, vol. 43, no. 2, pp. 267–293, 2005. DOI: 10.1080/00207540412331282051.

[284] Hu, J. and Peng, Y., "Tolerance modelling and robust design for concurrent engineering," *Proceedings of the Institution of Mechanical Engineers, Part C: Journal of Mechanical Engineering Science*, vol. 221, no. 4, pp. 455–465, 2007. DOI: 10.1243/0954406JMES438.

[285] Park, G.-J.; Lee, T.-H.; Lee, K. H., and Hwang, K.-H., "Robust Design: An Overview," *AIAA Journal*, vol. 44, no. 1, pp. 181–191, 2006. DOI: 10.2514/1.13639.

[286] Walter, M.; Spruegel, T., and Wartzack, S., "Least Cost Tolerance Allocation for Systems with Time-variant Deviations," *Procedia CIRP*, vol. 27, pp. 1–9, 2015. DOI: 10.1016/j.procir.2015.04.035.

[287] Walter, M. S. J., *Toleranzanalyse und Toleranzsynthese abweichungsbehafteter Mechanismen*, Ph.D. dissertation, Friedrich-Alexander-Universität Erlangen-Nürnberg, ser. Fortschritt-Berichte VDI Reihe 1, Konstruktionstechnik, Maschinenelemente Nr. 437. Düsseldorf: VDI-Verlag, 2016.

[288] Jeang, A.; Hwan, C.-L., and Chen, T.-K., "A Statistical Dimension and Tolerance Design for Mechanical Assembly Under Thermal Impact," *The International Journal of Advanced Manufacturing Technology*, vol. 20, no. 12, pp. 907–915, 2002. DOI: 10.1007/s001700200214.

[289] Spruegel, T. C.; Walter, M., and Wartzack, S., "Robust tolerance design of systems with varying ambient temperature influence due to worldwide manufacturing and operation," *DS 77: Proceedings of the DESIGN 2014 13th International Design Conference*, Dubrovnik, Croatia, 19.05.-22.05.2014, pp. 1189–1198.

[290] Jayaprakash, G.; Sivakumar, K., and Thilak, M., "Integration of thermo mechanical strains into optimal tolerance design of mechanical assembly using NSGA II and FE simulation," *Journal of Mechanical Engineering Research*, vol. 3, no. 6, pp. 168–180, 2011. DOI: 10.5897/JMER.9000028.

[291] Jayaprakash, G. and Sivakumar, K., "Parametric Tolerance Analysis of Mechanical Assembly Using FEA and Cost Competent Tolerance Synthesis Using Neural Network," *Journal of Software Engineering and Applications*, vol. 3, no. 12, pp. 1148–1154, 2010. DOI: 10.4236/jsea.2010.312134.

[292] Mazur, M., "Tolerance analysis and synthesis of assemblies subject to loading with process integration and design optimization tools," Ph.D. dissertation, RMIT University, Melbourne, Australia, 2013.

[293] Mazur, M.; Leary, M., and Subic, A., “A case study of efficient tolerance synthesis in product assemblies under loading,” *DS 81: Proceedings of NordDesign 2014*, Espoo, Finland, 27.08.-29.08.2014, pp. 855–864.

[294] Zeng, W.; Yi, J.; Lin, R., and Lu, W., “Statistical tolerance–cost–service life optimization of blade bearing of controllable pitch propeller considering the marine environment conditions through meta-heuristic algorithm,” *Journal of Computational Design and Engineering*, vol. 9, no. 2, pp. 689–705, 2022. DOI: 10.1093/jcde/qwac023.

[295] Michael, W. and Siddall, J. N., “The Optimization Problem With Optimal Tolerance Assignment and Full Acceptance,” *Journal of Mechanical Design*, vol. 103, no. 4, pp. 842–848, 1981. DOI: 10.1115/1.3254996.

[296] Michael, W. and Siddall, J. N., “The Optimal Tolerance Assignment With Less Than Full Acceptance,” *Journal of Mechanical Design*, vol. 104, no. 4, pp. 855–860, 1982. DOI: 10.1115/1.3256448.

[297] Lee, W.-J. and Woo, T. C., “Tolerances: Their Analysis and Synthesis,” *Journal of Engineering for Industry*, vol. 112, no. 2, pp. 113–121, 1990. DOI: 10.1115/1.2899553.

[298] Jordaan, J. P. and Ungerer, C. P., “Optimization of Design Tolerances Through Response Surface Approximations,” *Journal of Manufacturing Science and Engineering*, vol. 124, no. 3, pp. 762–767, 2002. DOI: 10.1115/1.1381400.

[299] Kao, C.; Li, C.-C., and Chen, S.-P., “Tolerance allocation via simulation embedded sequential quadratic programming,” *International Journal of Production Research*, vol. 38, no. 17, pp. 4345–4355, 2000. DOI: 10.1080/002075400050205136.

[300] Andolfatto, L.; Thiébaut, F.; Lartigue, C., and Douilly, M., “Assisted Decision-Making for Assembly Technique Selection and Geometrical Tolerance Allocation,” *Smart Product Engineering*, Abramovici, M. and Stark, R., Eds., Berlin: Springer, 2013, pp. 315–324. DOI: 10.1007/978-3-642-30817-8_31.

[301] Dantan, J.-Y. and Eifler, T., “Tolerance allocation under behavioural simulation uncertainty of a multiphysical system,” *CIRP Annals*, vol. 70, no. 1, pp. 127–130, 2021. DOI: 10.1016/j.cirp.2021.04.054.

[302] ISO/TC 69, “ISO 22514-1:2014: Statistical methods in process management - Capability and performance - Part 1: General principles and concepts (I),” Standard, 2014.

[303] Andolfatto, L.; Thiébaut, F.; Lartigue, C., and Douilly, M., "Quality- and cost-driven assembly technique selection and geometrical tolerance allocation for mechanical structure assembly," *Journal of Manufacturing Systems*, vol. 33, no. 1, pp. 103–115, 2014. DOI: 10.1016/j.jmsy.2013.03.003.

[304] Kane, V. E., "Process Capability Indices," *Journal of Quality Technology*, vol. 18, no. 1, pp. 41–52, 1986. DOI: 10.1080/00224065.1986.11978984.

[305] ISO/TC 69, "ISO 22514-2:2017: Statistical methods in process management — Capability and performance — Part 2: Process capability and performance of time-dependent process models," Standard, 2017.

[306] Speckhart, F. H., "Calculation of Tolerance Based on a Minimum Cost Approach," *Journal of Engineering for Industry*, vol. 94, no. 2, pp. 447–453, 1972. DOI: 10.1115/1.3428175.

[307] Singh, P. K.; Jain, P. K., and Jain, S. C., "A genetic algorithm-based solution to optimal tolerance synthesis of mechanical assemblies with alternative manufacturing processes: focus on complex tolerancing problems," *International Journal of Production Research*, vol. 42, no. 24, pp. 5185–5215, 2004. DOI: 10.1080/00207540410001733931.

[308] Balakrishnan, N., "A multiple-choice knapsack model for tolerance allocation in mechanical assemblies," *IIE Transactions*, vol. 25, no. 4, pp. 13–14, 1993. DOI: 10.1080/07408179308964300.

[309] Litwa, F.; Gottwald, M.; Forstmeier, J., and Vielhaber, M., "Determination of functional intersections between multiple tolerance-chains by the use of the assembly-graph," *NAFEMS World Congress 2015. The 2nd International SPDM Conference*, San Diego, California, USA, 21.06.-24.06.2015, pp. 189–203.

[310] Aschenbrenner, A.; Schleich, B., and Wartzack, S., "An Overview and Classification of Tolerance Compensation Methods," *Proceedings of the Design Society: International Conference on Engineering Design*, vol. 1, no. 1, pp. 3471–3480, 2019. DOI: 10.1017/dsi.2019.354.

[311] Huang, W.; Phoomboplab, T., and Ceglarek, D., "Process capability surrogate model-based tolerance synthesis for multi-station manufacturing systems," *IIE Transactions*, vol. 41, no. 4, pp. 309–322, 2009. DOI: 10.1080/07408170802510408.

[312] Chase, K. W.; Greenwood, W. H.; Loosli, B. G., and Hauglund, L. F., "Least Cost Tolerance Allocation for Mechanical Assemblies with Automated Process Selection," *Manufacturing Review*, vol. 3, no. 1, pp. 49–59, 1990.

[313] Singh, P. K.; Jain, S. C., and Jain, P. K., "Advanced optimal tolerance design of mechanical assemblies with interrelated dimension chains and process precision limits," *Computers in Industry*, vol. 56, no. 2, pp. 179–194, 2005. DOI: 10.1016/j.compind.2004.06.008.

[314] Dantan, J.-Y.; Gayton, N.; Etienne, A., and Qureshi, A. J., "Mathematical issues in mechanical tolerance analysis," *13e Colloque National AIP PRIMECA*, Mont-Dore, France, 27.03.-30.03.2012, pp. 1–12.

[315] Schleich, B.; Anwer, N.; Mathieu, L., and Wartzack, S., "Skin Model Shapes: A new paradigm shift for geometric variations modelling in mechanical engineering," *Computer-Aided Design*, vol. 50, pp. 1–15, 2014. DOI: 10.1016/j.cad.2014.01.001.

[316] Dumas, A.; Dantan, J.-Y., and Gayton, N., "Impact of a behavior model linearization strategy on the tolerance analysis of over-constrained mechanisms," *Computer-Aided Design*, vol. 62, pp. 152–163, 2015. DOI: 10.1016/j.cad.2014.11.002.

[317] Requicha, A. G., "Representations for Rigid Solids: Theory, Methods, and Systems," *ACM Computing Surveys*, vol. 12, no. 4, pp. 437–464, 1980. DOI: 10.1145/356827.356833.

[318] Turner, J., "New methods for tolerance analysis in solid modeling," *[Proceedings] 1988 International Conference on Computer Integrated Manufacturing*, Troy, NY, USA: IEEE, 23.05.1988, pp. 306–314. DOI: 10.1109/CIM.1988.5423.

[319] Ostrovsky-Berman, Y. and Joskowicz, L., "Tolerance envelopes of planar mechanical parts with parametric tolerances," *Computer-Aided Design*, vol. 37, no. 5, pp. 531–544, 2005. DOI: 10.1016/j.cad.2004.07.005.

[320] Gao, J.; Chase, K. W., and Magleby, S. P., "Comparison of Assembly Tolerance Analysis by the Direct Linearization and Modified Monte Carlo Simulation Methods," *Proceedings of the ASME 1995 Design Engineering Technical Conferences Collocated with the ASME 1995 15th International Computers in Engineering Conference and the ASME 1995 9th Annual Engineering Database Symposium. Volume 1: 21st Design Automation Conference*, Boston, Massachusetts, USA: ASME, 1995, pp. 353–360. DOI: 10.1115/DETC1995-0047.

[321] Bourdet, P. and Clement, A., "Controlling a Complex Surface with a 3 Axis Measuring Machine," *CIRP Annals - Manufacturing Technology*, vol. 25, no. 1, pp. 359–361, 1976.

[322] Bourdet, P.; Mathieu, L.; Lartigue, C., and Ballu, A., "The concept of small displacement torsor in metrology," *Series on Advances in Mathematics for Applied Sciences*, vol. 40, pp. 100–122, 1996.

[323] Anwer, N.; Schleich, B.; Mathieu, L., and Wartzack, S., "From solid modelling to skin model shapes: Shifting paradigms in computer-aided tolerancing," *CIRP Annals*, vol. 63, no. 1, pp. 137–140, 2014. DOI: 10.1016/j.cirp.2014.03.103.

[324] Scholz, F., "Tolerance Stack Analysis Methods," *Boeing Information & Support Services*, 1995.

[325] Gao, J.; Chase, K. W., and Magleby, S. P., "Generalized 3-D tolerance analysis of mechanical assemblies with small kinematic adjustments," *IIE Transactions*, vol. 30, no. 4, pp. 367–377, 1998. DOI: 10.1080/07408179808966476.

[326] Whitney, D. E.; Gilbert, O. L., and Jastrzebski, M., "Representation of geometric variations using matrix transforms for statistical tolerance analysis in assemblies," *Research in Engineering Design*, vol. 6, no. 4, pp. 191–210, 1994. DOI: 10.1007/BF01608399.

[327] Ameta, G.; Serge, S., and Giordano, M., "Comparison of Spatial Math Models for Tolerance Analysis: Tolerance-Maps, Deviation Domain, and TTRS," *Journal of Computing and Information Science in Engineering*, vol. 11, no. 2, p. 021 004, 2011. DOI: 10.1115/1.3593413.

[328] Shen, Z.; Ameta, G.; Shah, J. J., and Davidson, J. K., "A Comparative Study Of Tolerance Analysis Methods," *Journal of Computing and Information Science in Engineering*, vol. 5, no. 3, pp. 247–256, 2005. DOI: 10.1115/1.1979509.

[329] Teissandier, D.; Couetard, Y., and Delos, V., "Operations on polytopes: application to tolerance analysis," *Global Consistency of Tolerances*, van Houten, F. and Kals, H., Eds., Dordrecht: Springer, 1999, pp. 425–434. DOI: 10.1007/978-94-017-1705-2_43.

[330] Mansuy, M.; Giordano, M., and Hernandez, P., "A new calculation method for the worst case tolerance analysis and synthesis in stack-type assemblies," *Computer-Aided Design*, vol. 43, no. 9, pp. 1118–1125, 2011. DOI: 10.1016/j.cad.2011.04.010.

[331] Giordano, M.; Samper, S., and Petit, J. P., "Tolerance Analysis and Synthesis by Means of Deviation Domains, Axi-Symmetric Cases," *Models for Computer Aided Tolerancing in Design and Manufacturing*, Davidson, J. K., Ed., Dordrecht: Springer, 2007, pp. 85–94. DOI: 10.1007/1-4020-5438-6_10.

[332] Bo, C.; Yang, Z.; Wang, L., and Chen, H., "A comparison of tolerance analysis models for assembly," *The International Journal of Advanced Manufacturing Technology*, vol. 68, no. 1-4, pp. 739–754, 2013. DOI: 10.1007/s00170-013-4795-2.

[333] Cao, Y.; Liu, T., and Yang, J., "A comprehensive review of tolerance analysis models," *The International Journal of Advanced Manufacturing Technology*, vol. 97, no. 5-8, pp. 3055–3085, 2018. DOI: 10.1007/s00170-018-1920-2.

[334] DeFelice, J. D., "Economic partitioning of tolerances," *Quality Engineering*, vol. 13, no. 2, pp. 219–228, 2000. DOI: 10 . 1080 / 08982110108918644.

[335] Jefferson, T. R. and Scott, C. H., "Quality Tolerancing and Conjugate Duality," *Annals of Operations Research*, vol. 105, no. 1/4, pp. 185–200, 2001. DOI: 10.1023/A:1013309716875.

[336] Shan, A.; Roth, R. N., and Wilson, R. J., "A New Approach to Statistical Geometrical Tolerance Analysis," *The International Journal of Advanced Manufacturing Technology*, vol. 15, no. 3, pp. 222–230, 1999. DOI: 10.1007/s001700050060.

[337] Gladman, C. A., "Applying Probability in Tolerance Technology," *Mechanical Engineering Transactions*, vol. 5, no. 2, pp. 82–88, 1980.

[338] Greenwood, W. H. and Chase, K. W., "A New Tolerance Analysis Method for Designers and Manufacturers," *Journal of Engineering for Industry*, vol. 109, no. 2, pp. 112–116, 1987. DOI: 10.1115/1.3187099.

[339] Nigam, S. D. and Turner, J. U., "Review of statistical approaches to tolerance analysis," *Computer-Aided Design*, vol. 27, no. 1, pp. 6–15, 1995. DOI: 10.1016/0010-4485(95)90748-5.

[340] D'Errico, J. R. and Zaino, N. A., "Statistical Tolerancing Using a Modification of Taguchi's Method," *Technometrics*, vol. 30, no. 4, pp. 397–405, 1988. DOI: 10.1080/00401706.1988.10488434.

[341] Evans, D. H., "Statistical Tolerancing: The State of the Art: Part II. Methods for Estimating Moments," *Journal of Quality Technology*, vol. 7, no. 1, pp. 1–12, 1975. DOI: 10.1080/00224065.1975.11980657.

[342] Di Stefano, P., "Tolerance analysis and synthesis using the mean shift model," *Proceedings of the Institution of Mechanical Engineers, Part C: Journal of Mechanical Engineering Science*, vol. 217, no. 2, pp. 149–159, 2003. DOI: 10.1243/095440603762826477.

[343] Scholz, F., "Tolerance Stack Analysis Methods – A Critical Review," *Boeing Information & Support Services*, 1995.

[344] Deng, J. and Deng, S., "The Adaptive Branch and Bound Method of Tolerance Synthesis Based on the Reliability Index," *The International Journal of Advanced Manufacturing Technology*, vol. 20, no. 3, pp. 190–200, 2002. DOI: 10.1007/s001700200142.

[345] Xu, L.; Cheng, G., and Yi, P., "Tolerance synthesis by a new method for system reliability-based optimization," *Engineering Optimization*, vol. 37, no. 7, pp. 717–732, 2005. DOI: 10.1080/03052150500229467.

[346] Di Stefano, P., "Tolerances analysis and cost evaluation for product life cycle," *International Journal of Production Research*, vol. 44, no. 10, pp. 1943–1961, 2006. DOI: 10.1080/00207540500465832.

[347] Glancy, C. G. and Chase, K. W., "A Second-Order Method for Assembly Tolerance Analysis," *Proceedings of the ASME 1999 Design Engineering Technical Conferences. Volume 1: 25th Design Automation Conference*, Las Vegas, Nevada, USA: ASME, 1999, pp. 977–984. DOI: 10.1115/DETC99/DAC-8707.

[348] Cvetko, R.; Chase, K. W., and Magleby, S. P., "New Metrics for Evaluating Monte Carlo Tolerance Analysis of Assemblies," *Proceedings of the ASME 1998 International Mechanical Engineering Congress and Exposition. Manufacturing Science and Engineering*, Anaheim, California, USA: ASME, 1998, pp. 379–386. DOI: 10.1115/IMECE1998-1050.

[349] Dantan, J.-Y.; Eifler, T., and Homri, L., "Multiphysical tolerance analysis – Assessment technique of the impact of the model parameter imprecision," *Procedia CIRP*, vol. 92, pp. 206–211, 2020. DOI: 10.1016/j.procir.2020.05.192.

[350] Weiss, P., "A Discussion of Scientific Methods for Setting Manufacturing Tolerances," University of Wisconsin, Report Series in Quality and Productivity Report No. 98, 1993.

[351] Dige, N. and Diwekar, U., "Efficient sampling algorithm for large-scale optimization under uncertainty problems," *Computers & Chemical Engineering*, vol. 115, pp. 431–454, 2018. DOI: 10.1016/j.compchemeng.2018.05.007.

[352] Skowronski, V. J. and Turner, J. U., "Using Monte-Carlo variance reduction in statistical tolerance synthesis," *Computer-Aided Design*, vol. 29, no. 1, pp. 63–69, 1997. DOI: 10.1016/S0010-4485(96)00050-4.

[353] Charpentier, F.; Ballu, A., and Pailhes, J., "A scientific point of view of a simple industrial tolerancing process," *Procedia Engineering*, 2011.

[354] Mantripragada, R. and Whitney, D. E., "Modeling and controlling variation propagation in mechanical assemblies using state transition models," *IEEE Transactions on Robotics and Automation*, vol. 15, no. 1, pp. 124–140, 1999. DOI: 10.1109/70.744608.

[355] Ballu, A.; Plantec, J.-Y., and Mathieu, L., "Geometrical reliability of overconstrained mechanisms with gaps," *CIRP Annals*, vol. 57, no. 1, pp. 159–162, 2008. DOI: 10.1016/j.cirp.2008.03.038.

[356] Myszka, D. H., *Machines and Mechanisms: Applied Kinematic Analysis*, 4th ed. Boston: Prentice Hall, 2012.

[357] Sutherland, G. H. and Roth, B., "Mechanism Design: Accounting for Manufacturing Tolerances and Costs in Function Generating Problems," *Journal of Engineering for Industry*, vol. 97, no. 1, pp. 283–286, 1975. DOI: 10.1115/1.3438551.

[358] Rao, S. S. and Hati, S. K., "Game Theory Approach in Multicriteria Optimization of Function Generating Mechanisms," *Journal of Mechanical Design*, vol. 101, no. 3, pp. 398–406, 1979. DOI: 10.1115/1.3454072.

[359] Rhyu, J. H. and Kwak, B. M., "Optimal Stochastic Design of Four-Bar Mechanisms for Tolerance and Clearance," *Journal of Mechanisms, Transmissions, and Automation in Design*, vol. 110, no. 3, pp. 255–262, 1988. DOI: 10.1115/1.3267455.

[360] Sharfi, O. M. A., "A study of the optimal allocation of tolerances and clearances in planar linkage mechanisms," Ph.D. dissertation, University of Newcastle upon Tyne, 1982.

[361] Rao, S. S. and Wu, W., "Optimum tolerance allocation in mechanical assemblies using an interval method," *Engineering Optimization*, vol. 37, no. 3, pp. 237–257, 2005. DOI: 10.1080/03052150512331328240.

[362] Chun, H.; Kwon, S. J., and Tak, T., "Multibody approach for tolerance analysis and optimization of mechanical systems," *Journal of Mechanical Science and Technology*, vol. 22, no. 2, pp. 276–286, 2008. DOI: 10.1007/s12206-007-1024-7.

[363] Choi, J.-H.; Lee, S. J., and Choi, D.-H., "Tolerance Optimization for Mechanisms with Lubricated Joints," *Multibody System Dynamics*, vol. 2, no. 2, pp. 145–168, 1998. DOI: 10.1023/A:1009785211763.

[364] Zhang, C. and Ben Wang, H.-P., "Tolerance analysis and synthesis for cam mechanisms," *International Journal of Production Research*, vol. 31, no. 5, pp. 1229–1245, 1993. DOI: 10.1080/00207549308956785.

[365] Cheng, H. Y., "Optimum Tolerances Synthesis for Globoidal Cam Mechanisms.," *JSME International Journal Series C*, vol. 45, no. 2, pp. 519–526, 2002. DOI: 10.1299/jsmec.45.519.

[366] Xu, R.; Huang, K.; Guo, J.; Yang, L.; Qiu, M., and Ru, Y., "Gear-tolerance optimization based on a response surface method," *Transactions of the Canadian Society for Mechanical Engineering*, vol. 42, no. 3, pp. 309–322, 2018. DOI: 10.1139/tcsme-2018-0006.

[367] Lin, K.-S.; Chan, K.-Y., and Lee, J.-J., "Kinematic error analysis and tolerance allocation of cycloidal gear reducers," *Mechanism and Machine Theory*, vol. 124, pp. 73–91, 2018. DOI: 10.1016/j.mechmachtheory.2017.12.028.

[368] Dantan, J.-Y.; Bruyere, J.; Vincent, J.-P., and Bigot, R., "Vectorial tolerance allocation of bevel gear by discrete optimization," *Mechanism and Machine Theory*, vol. 43, no. 11, pp. 1478–1494, 2008. DOI: 10.1016/j.mechmachtheory.2007.11.002.

[369] Ding, Y.; Jin, J.; Ceglarek, D., and Shi, J., "Process-oriented tolerancing for multi-station assembly systems," *IIE Transactions*, vol. 37, no. 6, pp. 493–508, 2005. DOI: 10.1080/07408170490507774.

[370] Huang, W.; Kong, Z., and Chennamaraju, A., "Robust Design for Fixture Layout in Multistation Assembly Systems Using Sequential Space Filling Methods," *Journal of Computing and Information Science in Engineering*, vol. 10, no. 4, p. 041 001, 2010. DOI: 10.1115/1.3503880.

[371] Izquierdo, L. E.; Hu, S. J.; Du, H.; Jin, R.; Jee, H., and Shi, J., "Robust Fixture Layout Design for a Product Family Assembled in a Multistage Reconfigurable Line," *Journal of Manufacturing Science and Engineering*, vol. 131, no. 4, p. 041 008, 2009. DOI: 10.1115/1.3123320.

[372] Wärmefjord, K.; Söderberg, R., and Lindkvist, L., "Strategies for Optimization of Spot Welding Sequence With Respect to Geometrical Variation in Sheet Metal Assemblies," *Proceedings of the ASME 2010 International Mechanical Engineering Congress and Exposition. Volume 3: Design and Manufacturing, Parts A and B*, Vancouver, British Columbia, Canada: ASME, 2010, pp. 569–577. DOI: 10.1115/IMECE2010-38471.

[373] Sadeghi Tabar, R.; Lorin, S.; Cromvik, C.; Lindkvist, L.; Wärmefjord, K., and Söderberg, R., "Efficient Spot Welding Sequence Simulation in Compliant Variation Simulation," *Journal of Manufacturing Science and Engineering*, vol. 143, no. 7, p. 071 009, 2021. DOI: 10.1115/1.4049654.

[374] Polini, W. and Corrado, A., "Uncertainty in manufacturing of lightweight products in composite laminate: Part 1—numerical approach," *The International Journal of Advanced Manufacturing Technology*, vol. 101, no. 5-8, pp. 1423–1434, 2019. DOI: 10.1007/s00170-018-3024-4.

[375] Shahi, V. J.; Masoumi, A.; Franciosa, P., and Ceglarek, D., "Quality-driven Optimization of Assembly Line Configuration for Multi-Station Assembly Systems with Compliant Non-ideal Sheet Metal Parts," *Procedia CIRP*, vol. 75, pp. 45–50, 2018. DOI: 10.1016/j.procir.2018.02.022.

[376] Shiu, B. W.; Li, B.; Fu, X. Y., and Liu, Y., "Tolerance Allocation of Sheet Metal Assembly Using a Finite Element Model," *JSME International Journal Series C Mechanical Systems, Machine Elements and Manufacturing*, vol. 45, no. 1, pp. 258–266, 2002. DOI: 10.1299/jsmec.45.258.

[377] Ding, Y.; Ceglarek, D., and Shi, J., "Modeling and diagnosis of multistage manufacturing processes: Part I – state space model," *Proceedings of the 2000 Japan/USA Symposium on Flexible Automation*, pp. 23–26, 2000.

[378] Jin, J. and Shi, J., "State Space Modeling of Sheet Metal Assembly for Dimensional Control," *Journal of Manufacturing Science and Engineering*, vol. 121, no. 4, pp. 756–762, 1999. DOI: 10.1115/1.2833137.

[379] Ceglarek, D.; Huang, W.; Zhou, S.; Ding, Y.; Kumar, R., and Zhou, Y., "Time-Based Competition in Multistage Manufacturing: Stream-of-Variation Analysis (SOVA) Methodology—Review," *International Journal of Flexible Manufacturing Systems*, vol. 16, no. 1, pp. 11–44, 2004. DOI: 10.1023/B:FLEX.0000039171.25141.a4.

[380] Huang, W.; Lin, J.; Kong, Z., and Ceglarek, D., "Stream-of-Variation (SOVA) Modeling II: A Generic 3D Variation Model for Rigid Body Assembly in Multistation Assembly Processes," *Journal of Manufacturing Science and Engineering*, vol. 129, no. 4, pp. 832–842, 2007. DOI: 10.1115/1.2738953.

[381] Li, Z.; Yue, J.; Kokkolaras, M.; Camelio, J.; Papalambros, P. Y., and Hu, S. J., "Product Tolerance Allocation in Compliant Multistation Assembly Through Variation Propagation and Analytical Target Cascading," *Proceedings of the ASME 2004 International Mechanical Engineering Congress and Exposition. Design Engineering*, Anaheim, California, USA: ASME, 2004, pp. 813–820. DOI: 10.1115/IMECE2004-60521.

[382] Jayaprakash, G.; Thilak, M., and SivaKumar, K., "Optimal tolerance design for mechanical assembly considering thermal impact," *The International Journal of Advanced Manufacturing Technology*, vol. 73, no. 5-8, pp. 859–873, 2014. DOI: 10.1007/s00170-014-5845-0.

[383] Goka, E.; Homri, L.; Beaurepaire, P., and Dantan, J.-Y., "Statistical Tolerance Analysis of Over-Constrained Mechanical Assemblies With Form Defects Considering Contact Types," *Journal of Computing and Information Science in Engineering*, vol. 19, no. 2, p. 021 010, 2019. DOI: 10.1115/1.4042018.

[384] Schleich, B.; Anwer, N.; Mathieu, L., and Wartzack, S., "Contact and Mobility Simulation for Mechanical Assemblies Based on Skin Model Shapes," *Journal of Computing and Information Science in Engineering*, vol. 15, no. 2, p. 021 009, 2015. DOI: 10.1115/1.4029051.

[385] Qureshi, A. J.; Dantan, J.-Y.; Sabri, V.; Beaucaire, P., and Gayton, N., "A statistical tolerance analysis approach for over-constrained mechanism based on optimization and Monte Carlo simulation," *Computer-Aided Design*, vol. 44, no. 2, pp. 132–142, 2012. DOI: 10.1016/j.cad.2011.10.004.

[386] Jeang, A., "Optimal tolerance design by response surface methodology," *International Journal of Production Research*, vol. 37, no. 14, pp. 3275–3288, 1999. DOI: 10.1080/002075499190284.

[387] Jeang, A. and Leu, E., "Robust tolerance design by computer experiment," *International Journal of Production Research*, vol. 37, no. 9, pp. 1949–1961, 1999. DOI: 10.1080/002075499190851.

[388] Jeang, A., "Combined parameter and tolerance design optimization with quality and cost," *International Journal of Production Research*, vol. 39, no. 5, pp. 923–952, 2001. DOI: 10.1080/00207540010006717.

[389] Cao, S. K.; Li, Z. Q.; Gao, Q., and Xu, J., "Tolerance Optimal Design System Development and Application Based on UG Quick Stack Module," *Applied Mechanics and Materials*, vol. 10–12, pp. 801–805, 2007. DOI: 10.4028/www.scientific.net/AMM.10-12.801.

[390] Lööf, J.; Hermansson, T., and Söderberg, R., "An Efficient Solution to the Discrete Least-Cost Tolerance Allocation Problem with General Loss Functions," *Models for Computer Aided Tolerancing in Design and Manufacturing*, Davidson, J. K., Ed., Dordrecht: Springer, 2007, pp. 115–124. DOI: 10.1007/1-4020-5438-6_13.

[391] Litwa, F.; Gottwald, M.; Spudeiko, S.; Paetzold, K., and Vielhaber, M., "Optimization Coupling Approach for/with Non-Static Point Based CAT-models," *Procedia CIRP*, vol. 43, pp. 166–171, 2016. DOI: 10.1016/j.procir.2016.02.034.

[392] Bacharoudis, K.; Popov, A., and Ratchev, S., "Application of Advanced Simulation Methods for the Tolerance Analysis of Mechanical Assemblies," *Smart Technologies for Precision Assembly. IPAS 2020. IFIP Advances in Information and Communication Technology*, Ratchev, S., Ed., vol. 620, Cham: Springer International Publishing, 2021, pp. 153–167. DOI: 10.1007/978-3-030-72632-4_11.

[393] Zheng, H.; Litwa, F., and Paetzold, K., "Improvement of Tolerance Simulation Model in Body in White Product Realization Loop by Integrating Manufacturing Joining Simulation," *ASME 2021 International Mechanical Engineering Congress and Exposition. Volume 2B: Advanced Manufacturing*, Virtual, Online: ASME, 2021, V02BT02A068. DOI: 10.1115/IMECE2021-66534.

[394] Petruccioli, A.; Pini, F., and Leali, F., "Model-Based Approach for Optimal Allocation of GD&T," *Design Tools and Methods in Industrial Engineering II*, Rizzi, C.; Campana, F.; Bici, M.; Gherardini, F.; Ingrassia, T., and Cicconi, P., Eds., Cham: Springer International Publishing, 2022, pp. 277–284. DOI: 10.1007/978-3-030-91234-5_28.

[395] Petruccioli, A.; Fabio, P., and Francesco, L., "Development of a Computer-Aided integrated method for the tolerance-cost multidisciplinary optimization of an automotive engine," *International Journal on Interactive Design and Manufacturing (IJIDeM)*, vol. 16, no. 4, pp. 1457–1469, 2022. DOI: 10.1007/s12008-022-00941-x.

[396] Ramos Barbero, B.; Pérez Azcona, J., and González Pérez, J., "A tolerance analysis and optimization methodology. The combined use of 3D CAT, a dimensional hierarchization matrix and an optimization algorithm," *The International Journal of Advanced Manufacturing Technology*, vol. 81, no. 1-4, pp. 371–385, 2015. DOI: 10.1007/s00170-015-7068-4.

[397] Jayaprakash, G.; Sivakumar, K., and Thilak, M., "A numerical study on effect of temperature and inertia on tolerance design of mechanical assembly," *Engineering Computations*, vol. 29, no. 7, pp. 722–742, 2012. DOI: 10.1108/02644401211257236.

[398] Lyu, N.; Shimura, A., and Saitou, K., "Optimal Tolerance Allocation of Automotive Pneumatic Control Valves Based on Product and Process Simulations," *Proceedings of the ASME 2006 International Design Engineering Technical Conferences and Computers and Information in Engineering Conference. Volume 1: 32nd Design Automation Conference, Parts A and B*, Philadelphia, Pennsylvania, USA: ASME, 2006, pp. 301–308. DOI: 10.1115/DETC2006-99592.

[399] Zheng, H.; Litwa, F.; Bohn, M., and Paetzold, K., "Tolerance optimization for sheet metal parts based on joining simulation," *Procedia CIRP*, vol. 100, pp. 583–588, 2021. DOI: 10.1016/j.procir.2021.05.127.

[400] Zhou, Z.; Huang, W., and Zhang, L., "Sequential Algorithm Based on Number Theoretic Method for Statistical Tolerance Analysis and Synthesis," *Journal of Manufacturing Science and Engineering*, vol. 123, no. 3, pp. 490–493, 2001. DOI: 10.1115/1.1378795.

[401] Singhal, K. and Pinel, J., "Statistical design centering and tolerancing using parametric sampling," *IEEE Transactions on Circuits and Systems*, vol. 28, no. 7, pp. 692–702, 1981. DOI: 10.1109/TCS.1981.1085029.

[402] Han, M. and Tan, M. H. Y., "Optimal robust and tolerance design for computer experiments with mixture proportion inputs," *Quality and Reliability Engineering International*, vol. 33, no. 8, pp. 2255–2267, 2017. DOI: 10.1002/qre.2188.

[403] Skowronski, V. J. and Turner, J. U., "Estimating gradients for statistical tolerance synthesis," *Computer-Aided Design*, vol. 28, no. 12, pp. 933–941, 1996. DOI: 10.1016/0010-4485(96)00032-2.

[404] Jung, S.; Choi, D.-H.; Choi, B.-L., and Kim, J. H., "Tolerance optimization of a mobile phone camera lens system," *Applied Optics*, vol. 50, no. 23, pp. 4688–4700, 2011. DOI: 10.1364/AO.50.004688.

[405] Nassef, A. O. and ElMaraghy, H. A., "Allocation of Geometric Tolerances: New Criterion and Methodology," *CIRP Annals*, vol. 46, no. 1, pp. 101–106, 1997. DOI: 10.1016/S0007-8506(07)60785-9.

[406] Bernardo, F. P. and Saraiva, P. M., "Robust optimization framework for process parameter and tolerance design," *AIChE Journal*, vol. 44, no. 9, pp. 2007–2017, 1998. DOI: 10.1002/aic.690440908.

[407] Skowronski, V. J., "Calculating derivatives in statistical tolerance analysis," *Computer-Aided Design*, vol. 30, no. 5, pp. 367–375, 1998. DOI: 10.1016/S0010-4485(97)00100-0.

[408] Zeng, W.; Rao, Y., and Wang, P., "An effective strategy for improving the precision and computational efficiency of statistical tolerance optimization," *The International Journal of Advanced Manufacturing Technology*, vol. 92, no. 5-8, pp. 1933–1944, 2017. DOI: 10.1007/s00170-017-0256-7.

[409] Jin, R.; Chen, W., and Sudjianto, A., "Analytical Metamodel-Based Global Sensitivity Analysis and Uncertainty Propagation for Robust Design," *SAE Transactions*, vol. 113, pp. 121–128, 2004. DOI: 10.4271/2004-01-0429.

[410] Kleijnen, J. P. C., *Statistical Tools for Simulation Practitioners*, Owen, D. B., Ed., ser. Statistics: Textbooks and Monographs vol. 76. New York: Marcel Dekker, 1987.

[411] Jeusfeld, M. A., "Metamodel," *Encyclopedia of Database Systems*, LIU, L. and ÖZSU, M. T., Eds., Boston, Massachusetts: Springer, 2009, pp. 1727–1730. DOI: 10.1007/978-0-387-39940-9_898.

[412] Jeang, A., "Computer-aided tolerance synthesis with statistical method and optimization techniques," *Quality and Reliability Engineering International*, vol. 17, no. 2, pp. 131–139, 2001. DOI: 10.1002/qre.387.

[413] Bayram, U. and Acar, E., "Tolerance Analysis with Multiple Surrogate Models," *Acta Physica Polonica A*, vol. 128, no. 2B, B-447-B–450, 2015. DOI: 10.12693/APhysPolA.128.B-447.

[414] Khodaygan, S., "Meta-model based multi-objective optimisation method for computer-aided tolerance design of compliant assemblies," *International Journal of Computer Integrated Manufacturing*, vol. 32, no. 1, pp. 27–42, 2019. DOI: 10.1080/0951192X.2018.1543953.

[415] Ma, B.; Lei, G.; Liu, C.; Zhu, J., and Guo, Y., "Robust Tolerance Design Optimization of a PM Claw Pole Motor With Soft Magnetic Composite Cores," *IEEE Transactions on Magnetics*, vol. 54, no. 3, pp. 1–4, 2018. DOI: 10.1109/TMAG.2017.2756262.

[416] Han, M. and Yong Tan, M. H., "Integrated parameter and tolerance design with computer experiments," *IIE Transactions*, vol. 48, no. 11, pp. 1004–1015, 2016. DOI: 10.1080/0740817X.2016.1167289.

[417] Ghaderi, A.; Hassani, H., and Khodaygan, S., "A Bayesian-reliability based multi-objective optimization for tolerance design of mechanical assemblies," *Reliability Engineering & System Safety*, vol. 213, p. 107 748, 2021. DOI: 10.1016/j.ress.2021.107748.

[418] Han, M.; Liu, X.; Huang, M., and Tan, M. H. Y., "Integrated parameter and tolerance optimization of a centrifugal compressor based on a complex simulator," *Journal of Quality Technology*, vol. 52, no. 4, pp. 404–421, 2020. DOI: 10.1080/00224065.2019.1611358.

[419] Rao, S. S., *Engineering Optimization: Theory and Practice*, 4th ed. Hoboken, New Jersey: Wiley, 2009.

[420] Dean, E. and Unal, R., "Designing For Cost," *Transactions of the American Association of Cost Engineer. 35th Annual Meeting*, Seattle, Washington, USA, 23.06.-26.06.1991, pp. D.4.1–D4.6.

[421] Dean, E. and Unal, R., "Elements of designing for cost," *Aerospace Design Conference*, Irvine, California, USA: American Institute of Aeronautics and Astronautics, 3.02.-06.02.1992, pp. 1–6. DOI: 10.2514/6.1992-1057.

[422] Bandler, J. W., "Optimization of design tolerances using nonlinear programming," *Journal of Optimization Theory and Applications*, vol. 14, no. 1, pp. 99–114, 1974. DOI: 10.1007/BF00933176.

[423] Liu, S.; Jin, Q.; Dong, Y., and Wang, Y., "A closed-form method for statistical tolerance allocation considering quality loss and different kinds of manufacturing cost functions," *The International Journal of Advanced Manufacturing Technology*, vol. 93, no. 5-8, pp. 2801–2811, 2017. DOI: 10.1007/s00170-017-0681-7.

[424] Barraja, M., "Tolerance allocation for kinematic systems," University of Kentucky, Master's Thesis, 2004.

[425] Lööf, J. and Söderberg, R., "Top-Down Decomposition of Multi-Product Requirements Onto Locator Tolerances," *Proceedings of the ASME 2007 International Mechanical Engineering Congress and Exposition. Volume 3: Design and Manufacturing*, Seattle, Washington, USA: ASME, 2007, pp. 247–255. DOI: 10.1115/IMECE2007-43453.

[426] Takematsu, R.; Satonaka, N.; Thasana, W.; Iwamura, K., and Sugimura, N., "A study on tolerances design of parallel link robots based on mathematical models," *Journal of Advanced Mechanical Design, Systems, and Manufacturing*, vol. 12, no. 1, pp. 1–14, 2018. DOI: 10.1299/jamdsm.2018jamdsm0015.

[427] González, I. and Sánchez, I., "Optimal centering and tolerance design for correlated variables," *The International Journal of Advanced Manufacturing Technology*, vol. 66, no. 9-12, pp. 1499–1510, 2013. DOI: 10.1007/s00170-012-4434-3.

[428] Chen, M.-S., "Optimising tolerance allocation for mechanical components correlated by selective assembly," *The International Journal of Advanced Manufacturing Technology*, vol. 12, no. 5, pp. 349–355, 1996. DOI: 10.1007/BF01179810.

[429] Islam, M. N., "A Practical Approach to Tolerance Allocation," *International Review of Mechanical Engineering*, vol. 2, no. 4, pp. 614–623, 2008.

[430] Balamurugan, C.; Saravanan, A.; Dinesh Babu, P.; Jagan, S., and Ranga Narasimman, S., "Concurrent optimal allocation of geometric and process tolerances based on the present worth of quality loss using evolutionary optimisation techniques," *Research in Engineering Design*, vol. 28, no. 2, pp. 185–202, 2017. DOI: 10.1007/s00163-016-0230-7.

[431] Sivakumar, K.; Balamurugan, C., and Ramabalan, S., "Evolutionary multi-objective concurrent maximisation of process tolerances," *International Journal of Production Research*, vol. 50, no. 12, pp. 3172–3191, 2012. DOI: 10.1080/00207543.2010.550637.

[432] Sivakumar, K.; Balamurugan, C.; Ramabalan, S., and Venkata raman, S., "Optimal concurrent dimensional and geometrical tolerancing based on evolutionary algorithms," *2009 World Congress on Nature & Biologically Inspired Computing (NaBIC)*, Coimbatore, India: IEEE, 9.12.-11.12.2009, pp. 300–305. DOI: 10.1109/NABIC.2009.5393725.

[433] Sivakumar, K.; Balamurugan, C., and Ramabalan, S., "Concurrent multi-objective tolerance allocation of mechanical assemblies considering alternative manufacturing process selection," *The International Journal of Advanced Manufacturing Technology*, vol. 53, no. 5-8, pp. 711–732, 2011. DOI: 10.1007/s00170-010-2871-4.

[434] Sivakumar, K.; Balamurugan, C., and Ramabalan, S., "Evolutionary Advanced Multi Objective Concurrent Tolerance Design of Mechanical Assemblies," *Journal of Manufacturing Technology Research*, vol. 3, no. 1/2, pp. 29–53, 2011.

[435] Sivakumar, K.; Balamurugan, C., and Ramabalan, S., "Simultaneous optimal selection of design and manufacturing tolerances with alternative manufacturing process selection," *Computer-Aided Design*, vol. 43, no. 2, pp. 207–218, 2011. DOI: 10.1016/j.cad.2010.10.001.

[436] Jeang, A., "Optimal tolerance design for product life cycle," *International Journal of Production Research*, vol. 34, no. 8, pp. 2187–2209, 1996. DOI: 10.1080/00207549608905020.

[437] Bowman, R. A., "Efficient Gradient-Based Tolerance Optimization Using Monte Carlo Simulation," *Journal of Manufacturing Science and Engineering*, vol. 131, no. 3, p. 031 005, 2009. DOI: 10.1115/1.3123328.

[438] Lee, J., "Tolerance optimization using genetic algorithm and approximated simulation," Ph.D. dissertation, University of Michigan, 1992.

[439] Aragon, L.; Puente, J., and Cho, B. R., "Integrating the Lambert W Function into Optimal Tolerance Design," *Proceedings of the 2009 Industrial Engineering Research Conference*, pp. 2206–2211, 2009.

[440] Shin, S.; Kongsuwon, P., and Cho, B. R., "Development of the parametric tolerance modeling and optimization schemes and cost-effective solutions," *European Journal of Operational Research*, vol. 207, no. 3, pp. 1728–1741, 2010. DOI: 10.1016/j.ejor.2010.07.009.

[441] Liu, S.-G.; Jin, Q.; Liu, C., and Xie, R.-J., "Analytical method for optimal component tolerances based on manufacturing cost and quality loss," *Proceedings of the Institution of Mechanical Engineers, Part B: Journal of Engineering Manufacture*, vol. 227, no. 10, pp. 1484–1491, 2013. DOI: 10.1177/0954405413488769.

[442] Wang, B.; Huang, X., and Chang, M., "Reliability-based tolerance redesign of mechanical assemblies using Jacobian-Torsor model," *Science Progress*, vol. 104, no. 2, 2021. DOI: 10.1177/00368504211013227.

[443] Shin, S.; Govindaluri, M. S., and Cho, B. R., "Integrating the Lambert W Function to a Tolerance Optimization Problem," *Quality and Reliability Engineering International*, vol. 21, no. 8, pp. 795–808, 2005. DOI: 10.1002/qre.687.

[444] Nesmachnow, S., "An overview of metaheuristics: accurate and efficient methods for optimisation," *International Journal of Metaheuristics*, vol. 3, no. 4, pp. 320–347, 2014. DOI: 10.1504/IJMHEUR.2014.068914.

[445] Gandomi, A. H.; Yang, X.-S.; Talatahari, S., and Alavi, A. H., "Metaheuristic Algorithms in Modeling and Optimization," *Metaheuristic Applications in Structures and Infrastructures*, Elsevier, 2013, pp. 1–24. DOI: 10.1016/B978-0-12-398364-0.00001-2.

[446] Siddique, N. and Adeli, H., "Nature Inspired Computing: An Overview and Some Future Directions," *Cognitive Computation*, vol. 7, no. 6, pp. 706–714, 2015. DOI: 10.1007/s12559-015-9370-8.

[447] Chen, T.-C. and Fischer, G. W., "A GA-based search method for the tolerance allocation problem," *Artificial Intelligence in Engineering*, vol. 14, no. 2, pp. 133–141, 2000. DOI: 10.1016/S0954-1810(00)00006-6.

[448] Wolpert, D. H. and Macready, W. G., "No free lunch theorems for optimization," *IEEE Transactions on Evolutionary Computation*, vol. 1, no. 1, pp. 67–82, 1997. DOI: 10.1109/4235.585893.

[449] Chopard, B. and Tomassini, M., *An Introduction to Metaheuristics for Optimization*, ser. Natural Computing Series. Cham: Springer International Publishing, 2018. DOI: 10.1007/978-3-319-93073-2.

[450] Yang, X.-S., *Nature-Inspired Metaheuristic Algorithms*, 2nd ed. Frome: Luniver Press, 2010.

[451] Vasseur, H.; Kurfess, T., and Cagan, J., "Optimal Tolerance Allocation for Improved Productivity," *IFAC Proceedings Volumes*, vol. 25, no. 8, pp. 211–218, 1992. DOI: 10.1016/S1474-6670(17)54066-5.

[452] Ashiagbor, A.; Liu, H.-C., and Nnaji, B. O., "Tolerance control and propagation for the product assembly modeller," *International Journal of Production Research*, vol. 36, no. 1, pp. 75–94, 1998. DOI: 10.1080/002075498193949.

[453] Haq, A. N.; Sivakumar, K.; Saravanan, R., and Muthiah, V., "Tolerance design optimization of machine elements using genetic algorithm," *The International Journal of Advanced Manufacturing Technology*, vol. 25, no. 3-4, pp. 385–391, 2005. DOI: 10.1007/s00170-003-1855-z.

[454] Li, F. Z.; Lu, C., and Jiang, W. R., "A Robust Approach for Concurrent Tolerances Allocation Using Immune Genetic Algorithm," *Advanced Materials Research*, vol. 308–310, pp. 776–779, 2011. DOI: 10.4028/www.scientific.net/AMR.308-310.776.

[455] Sivakumar, K.; Balamurugan, C., and Ramabalan, S., "Evolutionary sensitivity-based conceptual design and tolerance allocation for mechanical assemblies," *The International Journal of Advanced Manufacturing Technology*, vol. 48, no. 1-4, pp. 307–324, 2010. DOI: 10.1007/s00170-009-2256-8.

[456] Noorul Haq, A.; Karthikeyan, K.; Sivakumar, K., and Saravanan, R., "Particle swarm optimization (PSO) algorithm for optimal machining allocation of clutch assembly," *The International Journal of Advanced Manufacturing Technology*, vol. 27, no. 9-10, pp. 865–869, 2006. DOI: 10.1007/s00170-004-2274-5.

[457] Zhou, C.; Gao, L.; Gao, H.-B., and Zan, K., "Particle Swarm Optimization for Simultaneous Optimization of Design and Machining Tolerances," *Simulated Evolution and Learning*, Wang, T.-D.; Li, X.; Chen, S.-H.; Wang, X.; Abbass, H.; Iba, H.; Chen, G.-L., and Yao, X., Eds., vol. 4247, Berlin: Springer, 2006, pp. 873–880. DOI: 10.1007/11903697_110.

[458] Muthu, P.; Dhanalakshmi, V., and Sankaranarayanasamy, K., "Optimal tolerance design of assembly for minimum quality loss and manufacturing cost using metaheuristic algorithms," *The International Journal of Advanced Manufacturing Technology*, vol. 44, no. 11-12, pp. 1154–1164, 2009. DOI: 10.1007/s00170-009-1930-1.

[459] Heling, B.; Aschenbrenner, A.; Walter, M. S. J., and Wartzack, S., "On Connected Tolerances in Statistical Tolerance-Cost-Optimization of Assemblies with Interrelated Dimension Chains," *Procedia CIRP*, vol. 43, pp. 262–267, 2016. DOI: 10.1016/j.procir.2016.02.031.

[460] Khodaygan, S., "A framework for tolerance design considering systematic and random uncertainties due to operating conditions," *Assembly Automation*, vol. 39, no. 5, pp. 854–871, 2019. DOI: 10.1108/AA-10-2018-0160.

[461] Forouraghi, B., "Optimal tolerance allocation using a multiobjective particle swarm optimizer," *The International Journal of Advanced Manufacturing Technology*, vol. 44, no. 7-8, pp. 710–724, 2009. DOI: 10.1007/s00170-008-1892-8.

[462] Qiu, H. B.; Dong, Y. Y.; Wang, Y., and Gao, L., "Tolerance Optimization Design Based on Physical Programming Methods and PSO Algorithm," *Advanced Materials Research*, vol. 346, pp. 584–592, 2011. DOI: 10.4028/www.scientific.net/AMR.346.584.

[463] Rout, B. K. and Mittal, R. K., "Simultaneous selection of optimal parameters and tolerance of manipulator using evolutionary optimization technique," *Structural and Multidisciplinary Optimization*, vol. 40, no. 1-6, pp. 513–528, 2010. DOI: 10.1007/s00158-009-0368-2.

[464] Krishna, A. G. and Rao, K. M., "Simultaneous optimal selection of design and manufacturing tolerances with different stack-up conditions using scatter search," *The International Journal of Advanced Manufacturing Technology*, vol. 30, no. 3-4, pp. 328–333, 2006. DOI: 10.1007/s00170-005-0059-0.

[465] Prabhaharan, G.; Ramesh, R., and Asokan, P., "Concurrent optimization of assembly tolerances for quality with position control using scatter search approach," *International Journal of Production Research*, vol. 45, no. 21, pp. 4959–4988, 2007. DOI: 10.1080/00207540600596866.

[466] Kumar, M. S.; Kannan, S. M., and Jayabalan, V., "A new algorithm for optimum tolerance allocation of complex assemblies with alternative processes selection," *The International Journal of Advanced Manufacturing Technology*, vol. 40, no. 7-8, pp. 819–836, 2009. DOI: 10.1007/s00170-008-1389-5.

[467] Sampath Kumar, R.; Alagumurthi, N., and Ramesh, R., "Optimization of design tolerance and asymmetric quality loss cost using pattern search algorithm," *International Journal of Physical Sciences*, vol. 4, no. 11, pp. 629–637, 2009.

[468] Sampath Kumar, R.; Alagumurthi, N., and Ramesh, R., "Integrated optimization of machining tolerance and Asymmetric quality loss cost for Rotor key base assembly," *International Conference on Recent Advances in Mechanical Engineering (ICRAME2010)*, Noorul Islam University, Kanyakumar, India, 2010.

[469] Prabhaharan, G.; Asokan, P., and Rajendran, S., "Sensitivity-based conceptual design and tolerance allocation using the continuous ants colony algorithm (CACO)," *The International Journal of Advanced Manufacturing Technology*, vol. 25, no. 5-6, pp. 516–526, 2005. DOI: 10.1007/s00170-003-1846-0.

[470] Sivakumar, M.; Lenin, N.; Jayakrishna, K., and Prasath, N. E., "Minimizing Cost of Assembly of an Interrelated Dimensional Chain Product Using ABC Algorithm," *Mathematical Problems in Engineering*, vol. 2021, p. 9 811 204, 2021. DOI: 10.1155/2021/9811204.

[471] Vignesh Kumar, D.; Ravindran, D.; Lenin, N., and Siva Kumar, M., "Tolerance allocation of complex assembly with nominal dimension selection using Artificial Bee Colony algorithm," *Proceedings of the Institution of Mechanical Engineers, Part C: Journal of Mechanical Engineering Science*, vol. 233, no. 1, pp. 18–38, 2019. DOI: 10.1177/0954406218756439.

[472] Kumar, L. R.; Padmanaban, K. P.; Kumar, S. G., and Balamurugan, C., "Design and optimization of concurrent tolerance in mechanical assemblies using bat algorithm," *Journal of Mechanical Science and Technology*, vol. 30, no. 6, pp. 2601–2614, 2016. DOI: 10.1007/s12206-016-0521-y.

[473] Nagarajan, L.; Mahalingam, S. K.; Salunkhe, S.; Nasr, E. A.; Davim, J. P., and Hussein, H. M. A., "A Novel Methodology for Simultaneous Minimization of Manufacturing Objectives in Tolerance Allocation of Complex Assembly," *Applied Sciences*, vol. 11, no. 19, p. 9164, 2021. DOI: 10.3390/app11199164.

[474] dos Santos Coelho, L., "Self-organizing migration algorithm applied to machining allocation of clutch assembly," *Mathematics and Computers in Simulation*, vol. 80, no. 2, pp. 427–435, 2009. DOI: 10.1016/j.matcom.2009.08.003.

[475] Jin, S.; Zheng, C.; Yu, K., and Lai, X., "Tolerance design optimization on cost–quality trade-off using the Shapley value method," *Journal of Manufacturing Systems*, vol. 29, no. 4, pp. 142–150, 2010. DOI: 10.1016/j.jmsy.2011.01.003.

[476] Li, L.-l.; Chen, K.; Gao, J.-m.; Liu, J.-k.; Gao, Z.-y., and Wang, M.-x., "Multiobjective Optimization Method and Application of Tolerance Allocation for the Steam Turbine Based on Cooperative Game Theory," *Shock and Vibration*, vol. 2021, p. 9 244 389, 2021. DOI: 10.1155/2021/9244389.

[477] Lu, C.; Zhao, W.-H., and Yu, S.-J., "Concurrent tolerance design for manufacture and assembly with a game theoretic approach," *The International Journal of Advanced Manufacturing Technology*, vol. 62, no. 1-4, pp. 303–316, 2012. DOI: 10.1007/s00170-011-3783-7.

[478] Towsyfyan, H.; Adnani-Salehi, S. A.; Ghayyem, M., and Mosaedi, F., "The Comparison of Imperialist Competitive Algorithm Applied and Genetic Algorithm for Machining Allocation of Clutch Assembly," *International Journal of Engineering, Transactions C: Aspects*, vol. 26, no. 12, 2013. DOI: 10.5829/idosi.ije.2013.26.12c.09.

[479] Rao, R. V. and More, K. C., "Simultaneous Optimal Selection of Design and Manufacturing Tolerances with Different Stack- up Conditions using TLBO Algorithm," *International Conference on Innovations in Engineering and Technology (ICIET'2013)*, Bangkok, Thailand, 25.12.-26.12.2013, pp. 158–162. DOI: 10.15242/IIE.E1213621.

[480] Rao, R. V. and More, K. C., "Advanced optimal tolerance design of machine elements using teaching-learning-based optimization algorithm," *Production & Manufacturing Research*, vol. 2, no. 1, pp. 71–94, 2014. DOI: 10.1080/21693277.2014.892845.

[481] Ying, H. and Wang, L., "The genetic polygon algorithm and its application in concurrent tolerance optimization design," *International Technology and Innovation Conference 2006 (ITIC 2006)*, vol. 2006, Hangzhou, China: IEE, 6.11.-07.11.2006, pp. 542–545. DOI: 10.1049/cp:20060821.

[482] Shringi, D. and Purohit, K., "Simultaneous Optimization of Tolerances for Prismatic Part Assembly in Different Stack up Conditions," *International Journal of Mining, Metallurgy and Mechanical Engineering*, vol. 1, no. 2, pp. 183–186, 2013.

[483] Zahara, E. and Kao, Y.-T., "A hybridized approach to optimal tolerance synthesis of clutch assembly," *The International Journal of Advanced Manufacturing Technology*, vol. 40, no. 11-12, pp. 1118–1124, 2009. DOI: 10.1007/s00170-008-1418-4.

[484] Ezugwu, A. E.; Adeleke, O. J.; Akinyelu, A. A., and Viriri, S., "A conceptual comparison of several metaheuristic algorithms on continuous optimisation problems," *Neural Computing and Applications*, vol. 32, no. 10, pp. 6207–6251, 2020. DOI: 10.1007/s00521-019-04132-w.

[485] Wang, Y.; Huang, A.; Quigley, C. A.; Li, L., and Sutherland, J. W., "Tolerance allocation: Balancing quality, cost, and waste through production rate optimization," *Journal of Cleaner Production*, vol. 285, p. 124 837, 2021. DOI: 10.1016/j.jclepro.2020.124837.

[486] Deiab, I. and Al-Ansary, M., "Concurrent optimization of manufacturing cycle cost by genetic algorithms," *Proceedings of the Institution of Mechanical Engineers, Part B: Journal of Engineering Manufacture*, vol. 221, no. 5, pp. 821–834, 2007. DOI: 10.1243/09544054JEM752.

[487] Gerth, R. J. and Islam, Z., "Towards A Designed Experiments Approach to Tolerance Design," *Geometric Design Tolerancing: Theories, Standards and Applications*, ElMaraghy, H. A., Ed., Boston, Massachusetts: Springer, 1998, pp. 337–345. DOI: 10.1007/978-1-4615-5797-5_26.

[488] Jeang, A., "Robust Tolerance Design by Response Surface Methodology," *The International Journal of Advanced Manufacturing Technology*, vol. 15, no. 6, pp. 399–403, 1999. DOI: 10.1007/s001700050082.

[489] Jeang, A. and Chang, C.-L., "Concurrent Optimisation of Parameter and Tolerance Design via Computer Simulation and Statistical Method," *The International Journal of Advanced Manufacturing Technology*, vol. 19, no. 6, pp. 432–441, 2002. DOI: 10.1007/s001700200045.

[490] Şehirlioğlu, A. K. and Özler, C., "The use of mixture experiments in tolerance allocation problems," *The International Journal of Advanced Manufacturing Technology*, vol. 35, no. 7-8, pp. 769–777, 2008. DOI: 10.1007/s00170-006-0754-5.

[491] Piepel, G. F.; Özler, C., and Şehirlioğlu, A. K., "Optimum tolerance design using component-amount and mixture-amount experiments," *The International Journal of Advanced Manufacturing Technology*, vol. 68, no. 9-12, pp. 2359–2369, 2013. DOI: 10.1007/s00170-013-4844-x.

[492] Martin, A. J.; Karthikeyan, S.; Ramesh Kumar, P. L., and Karthikeyan, V. S., "Manufacturing tolerance design using monte carlo method," *TAGA JOURNAL*, vol. 14, pp. 2214–2221, 2018.

[493] Li, Z.; Kokkolaras, M.; Izquierdo, L. E.; Hu, S. J., and Papalambros, P. Y., "Multiobjective Optimization for Integrated Tolerance Allocation and Fixture Layout Design in Multistation Assembly," *Proceedings of the ASME 2006 International Design Engineering Technical Conferences and Computers and Information in Engineering Conference. Volume*

1: 32nd Design Automation Conference, Parts A and B, Philadelphia, Pennsylvania, USA: ASME, 2006, pp. 199–206. DOI: 10.1115/DETC2006-99467.

[494] Rosyidi, C. N. and Pratama, M. A., "Two-stage optimization model for process/supplier selection, component allocation, and quality improvement," *Cogent Engineering*, vol. 5, no. 1, p. 1 557 504, 2018. DOI: 10.1080/23311916.2018.1557504.

[495] Singh, P. K.; Jain, S. C., and Jain, P. K., "Concurrent optimal adjustment of nominal dimensions and selection of tolerances considering alternative machines," *Computer-Aided Design*, vol. 38, no. 10, pp. 1074–1087, 2006. DOI: 10.1016/j.cad.2006.05.006.

[496] Huang, M. and Zhong, Y., "Dimensional and geometrical tolerance balancing in concurrent design," *The International Journal of Advanced Manufacturing Technology*, vol. 35, no. 7-8, pp. 723–735, 2008. DOI: 10.1007/s00170-006-0749-2.

[497] Wang, P. and Liang, M., "An integrated approach to tolerance synthesis, process selection and machining parameter optimization problems," *International Journal of Production Research*, vol. 43, no. 11, pp. 2237–2262, 2005. DOI: 10.1080/00207540500050063.

[498] Nagarwala, M. Y.; Simin Pulat, P., and Raman, S., "A Slope-Based Method for Least Cost Tolerance Allocation," *Concurrent Engineering*, vol. 3, no. 4, pp. 319–328, 1995. DOI: 10.1177/1063293X9500300407.

[499] Rosyidi, C. N.; Akbar, R. R., and Jauhari, W. A., "Make or Buy Analysis Model Based on Tolerance Design to Minimize Manufacturing Cost and Quality Loss," *Makara Journal of Technology*, vol. 18, no. 2, 2014. DOI: 10.7454/mst.v18i2.2947.

[500] Sabatini, N.; Jauhari, W. A., and Rosyidi, C. N., "Supplier Selection Model Based On Tolerance Allocation To Minimize Purchasing Cost And Quality Loss," *Proceeding of Industrial Engineering and Service Science*, 20.09.-21.09.2011.

[501] Loosli, B. G., "Manufacturing Tolerance Cost Minimization. Using Discrete Optimization For Alternate Process Selection," ADCATS Report No. 87-4, 1987.

[502] Siva Kumar, M. and Stalin, B., "Optimum tolerance synthesis for complex assembly with alternative process selection using Lagrange multiplier method," *The International Journal of Advanced Manufacturing Technology*, vol. 44, no. 3-4, pp. 405–411, 2009. DOI: 10.1007/s00170-008-1866-x.

[503] Siva Kumar, M.; Islam, M. N.; Lenin, N., and Vignesh Kumar, D., "Optimum Tolerance Synthesis for Complex Assembly with Alternative Process Selection Using Bottom Curve Follower Approach," *International Journal of Engineering (IJE)*, vol. 3, no. 4, pp. 380–402, 2009.

[504] Kim, S. H. and Knott, K., "A pseudo-boolean approach to determining least cost tolerances," *International Journal of Production Research*, vol. 26, no. 1, pp. 157–167, 1988. DOI: 10.1080/00207548808947848.

[505] Choi, H.-G. R.; Park, M.-H., and Salisbury, E., "Optimal Tolerance Allocation With Loss Functions," *Journal of Manufacturing Science and Engineering*, vol. 122, no. 3, pp. 529–535, 2000. DOI: 10.1115/1.1285918.

[506] Tseng, Y.-J. and Huang, F.-Y., "A multi-plant tolerance allocation model for products manufactured in a multi-plant collaborative manufacturing environment," *International Journal of Production Research*, vol. 47, no. 3, pp. 733–749, 2009. DOI: 10.1080/00207540701528792.

[507] Geetha, K.; Ravindran, D.; Kumar, M. S., and Islam, M. N., "Multi-objective optimization for optimum tolerance synthesis with process and machine selection using a genetic algorithm," *The International Journal of Advanced Manufacturing Technology*, vol. 67, no. 9-12, pp. 2439–2457, 2013. DOI: 10.1007/s00170-012-4662-6.

[508] Khezri, A.; Homri, L.; Etienne, A., and Dantan, J.-Y., "An integrated resource allocation and tolerance allocation optimization: A statistical-based dimensional tolerancing," *Procedia CIRP*, vol. 114, pp. 88–93, 2022. DOI: 10.1016/j.procir.2022.10.012.

[509] Mustajib, M. I. and Irianto, D., "An integrated model for process selection and quality improvement in multi-stage processes," *Journal of Advanced Manufacturing Systems*, vol. 9, no. 1, pp. 31–48, 2010. DOI: 10.1142/S0219686710001788.

[510] Tabar, R. S.; Wärmefjord, K., and Söderberg, R., "Evaluating evolutionary algorithms on spot welding sequence optimization with respect to geometrical variation," *Procedia CIRP*, vol. 75, pp. 421–426, 2018. DOI: 10.1016/j.procir.2018.04.061.

[511] Aderiani, A. R.; Wärmefjord, K., and Söderberg, R., "A Multistage Approach to the Selective Assembly of Components Without Dimensional Distribution Assumptions," *Journal of Manufacturing Science and Engineering*, vol. 140, no. 7, p. 071 015, 2018. DOI: 10.1115/1.4039767.

[512] Mease, D.; Nair, V. N., and Sudjianto, A., "Selective Assembly in Manufacturing: Statistical Issues and Optimal Binning Strategies," *Technometrics*, vol. 46, no. 2, pp. 165–175, 2004. DOI: 10 . 1198 / 004017004000000185.

[513] Mansoor, E. M., "SELECTIVE ASSEMBLY — ITS ANALYSIS AND APPLICATIONS," *International Journal of Production Research*, vol. 1, no. 1, pp. 13–24, 1961. DOI: 10.1080/00207546108943070.

[514] Lanza, G.; Haefner, B., and Kraemer, A., "Optimization of selective assembly and adaptive manufacturing by means of cyber-physical system based matching," *CIRP Annals*, vol. 64, no. 1, pp. 399–402, 2015. DOI: 10.1016/j.cirp.2015.04.123.

[515] Fang, X. D. and Zhang, Y., "A new algorithm for minimising the surplus parts in selective assembly," *Computers & Industrial Engineering*, vol. 28, no. 2, pp. 341–350, 1995. DOI: 10.1016/0360-8352(94)00183-N.

[516] Malaichamy, T.; Sivasubramanian, R., and Sivakumar, M., "Selective Assembly - A software approach," *International Journal of Advanced Engineering Technology*, vol. 7, no. 1, pp. 729–735, 2016.

[517] Wärmefjord, K.; Söderberg, R.; Schleich, B., and Wang, H., "Digital Twin for Variation Management: A General Framework and Identification of Industrial Challenges Related to the Implementation," *Applied Sciences*, vol. 10, no. 10, p. 3342, 2020. DOI: 10.3390/app10103342.

[518] Wagner, R.; Haefner, B., and Lanza, G., "Function-Oriented Quality Control Strategies for High Precision Products," *Procedia CIRP*, vol. 75, pp. 57–62, 2018. DOI: 10.1016/j.procir.2018.04.069.

[519] Rezaei Aderiani, A.; Wärmefjord, K., and Söderberg, R., "Combining selective assembly and individualized locator adjustments techniques in a smart assembly line," *Procedia CIRP*, vol. 97, pp. 429–434, 2021. DOI: 10.1016/j.procir.2020.05.263.

[520] Sadeghi Tabar, R.; Lindkvist, L.; Wärmefjord, K., and Söderberg, R., "Efficient Joining Sequence Variation Analysis of Stochastic Batch Assemblies," *Proceedings of the ASME 2021 International Mechanical Engineering Congress and Exposition. Volume 2B: Advanced Manufacturing*, Virtual, Online: ASME, 2021, V02BT02A077. DOI: 10.1115/IMECE2021-70288.

[521] Victor Raj, M.; Saravana Sankar, S., and Ponnambalam, S. G., "Genetic algorithm to optimize manufacturing system efficiency in batch selective assembly," *The International Journal of Advanced Manufacturing Technology*, vol. 57, no. 5-8, pp. 795–810, 2011. DOI: 10.1007/s00170-011-3326-2.

[522] Victor Raj, M.; Saravana Sankar, S., and Ponnambalam, S. G., "Optimization of assembly tolerance variation and manufacturing system efficiency by using genetic algorithm in batch selective assembly," *The International Journal of Advanced Manufacturing Technology*, vol. 55, no. 9-12, pp. 1193–1208, 2011. DOI: 10.1007/s00170-010-3124-2.

[523] Lu, C. and Fei, J.-F., "An approach to minimizing surplus parts in selective assembly with genetic algorithm," *Proceedings of the Institution of Mechanical Engineers, Part B: Journal of Engineering Manufacture*, vol. 229, no. 3, pp. 508–520, 2015. DOI: 10.1177/0954405414530896.

[524] Kannan, S. M.; Sivasubramanian, R., and Jayabalan, V., "Particle swarm optimization for minimizing assembly variation in selective assembly," *The International Journal of Advanced Manufacturing Technology*, vol. 42, no. 7-8, pp. 793–803, 2009. DOI: 10.1007/s00170-008-1638-7.

[525] Chen, J.; Dai, K. S., and Xu, S. L., "Selective Assembly for Components with Multiple Characteristics," *Advanced Materials Research*, vol. 542–543, pp. 79–86, 2012. DOI: 10.4028/www.scientific.net/AMR.542-543.79.

[526] Siva Kumar, M.; Kannan, S. M., and Jayabalan, V., "A new algorithm for minimizing surplus parts in selective assembly by using genetic algorithm," *International Journal of Production Research*, vol. 45, no. 20, pp. 4793–4822, 2007. DOI: 10.1080/00207540600810085.

[527] Kumar, M. S. and Kannan, S. M., "Optimum manufacturing tolerance to selective assembly technique for different assembly specifications by using genetic algorithm," *The International Journal of Advanced Manufacturing Technology*, vol. 32, no. 5-6, pp. 591–598, 2007. DOI: 10.1007/s00170-005-0337-x.

[528] Dantan, J.-Y.; Etienne, A.; Petronijevic, J., and Siadat, A., "Tolerance & Time margin," *Procedia CIRP*, vol. 92, pp. 51–56, 2020. DOI: 10.1016/j.procir.2020.04.139.

[529] Parkinson, D. B., "The Application of a Robust Design Method to Tolerancing," *Journal of Mechanical Design*, vol. 122, no. 2, pp. 149–154, 2000. DOI: 10.1115/1.533564.

[530] Jeang, A.; Chung, C.-P., and Hsieh, C.-K., "Simultaneous process mean and process tolerance determination with asymmetrical loss function," *The International Journal of Advanced Manufacturing Technology*, vol. 31, no. 7-8, pp. 694–704, 2007. DOI: 10.1007/s00170-005-0250-3.

[531] Jeang, A.; Chen, T.; Li, H.-C., and Liang, F., "Simultaneous process mean and process tolerance determination with adjustment and compensation for precision manufacturing process," *The International Journal of Advanced Manufacturing Technology*, vol. 33, no. 11-12, pp. 1159–1172, 2007. DOI: 10.1007/s00170-006-0542-2.

[532] Li, C.-C.; Kao, C., and Chen, S.-P., "Robust tolerance allocation using stochastic programming," *Engineering Optimization*, vol. 30, no. 3-4, pp. 333–350, 1998. DOI: 10.1080/03052159808941250.

[533] Swift, K. G.; Raines, M., and Booker, J. D., "Tolerance optimization in assembly stacks based on capable design," *Proceedings of the Institution of Mechanical Engineers, Part B: Journal of Engineering Manufacture*, vol. 213, no. 7, pp. 677–693, 1999. DOI: 10.1243/0954405991517119.

[534] Schmitt, R. and Behrens, C., "A Statistical Method for Analyses of Cost- and Riskoptimal Tolerance Allocations Based on Assured Input Data," *Proceedings of the 10th CIRP Conference on Computer-Aided Tolerancing*, Erlangen, Germany, 21.03.-23.03.2007.

[535] Parkinson, D. B., "Assessment and optimization of dimensional tolerances," *Computer-Aided Design*, vol. 17, no. 4, pp. 191–199, 1985. DOI: 10.1016/0010-4485(85)90216-7.

[536] Behrens, C. and Schmitt, R., "Automated Tolerance Web Generation from CAD Data and Life Cycle oriented Optimisation," *Proceedings of the 11th CIRP International Conference on Computer Aided Tolerancing*, Annecy, France, 26.03.–27.03.2009.

[537] Landschoof, W.-R., *Kostenoptimale Tolerierung unter Berücksichtigung von Fertigungsgesichtspunkten*, Ph.D. dissertation, Bergische Universität Wuppertal, ser. Fortschritt-Berichte VDI Reihe 1, Konstruktionstechnik, Maschinenelemente Nr. 453. Düsseldorf: VDI Verlag, 2022.

[538] McGhee, R. B. and Levine, A., "Determination of optimum production tolerances by analog simulation," *Proceedings of the eastern joint computer conference*, Boston, Massachusetts, USA: ACM Press, 1.12.-03.12.1959, pp. 249–254. DOI: 10.1145/1460299.1460330.

[539] McGhee, R. and Levine, A., "Determination of Optimum Production Tolerances by Combined Analog-Digital Computation," *SIMULATION*, vol. 3, no. 5, pp. 24–31, 1964. DOI: 10.1177/003754976400300508.

[540] Iyer, R. and Downs, T., "A variance minimization approach to tolerance design," *IEEE Transactions on Circuits and Systems*, vol. 27, no. 9, pp. 737–747, 1980. DOI: 10.1109/TCS.1980.1084887.

[541] Pinel, J. and Roberts, K., “Tolerance assignment in linear networks using nonlinear programming,” *IEEE Transactions on Circuit Theory*, vol. 19, no. 5, pp. 475–479, 1972. DOI: 10.1109/TCT.1972.1083506.

[542] Schjaer-Jacobsen, H., “Worst-case tolerance optimization of antenna systems,” *IEEE Transactions on Antennas and Propagation*, vol. 28, no. 2, pp. 247–250, 1980. DOI: 10.1109/TAP.1980.1142296.

[543] Walter, M. S. J., “Dimensional and Geometrical Tolerances in Mechanical Engineering – a Historical Review,” *Machine Design*, vol. 11, no. 3, pp. 67–74, 2019. DOI: 10.24867/MD.11.2019.3.67-74.

[544] Maghsoodloo, S. and Li, M.-H. C., “Optimal asymmetric tolerance design,” *IIE Transactions*, vol. 32, no. 12, pp. 1127–1137, 2000. DOI: 10.1080/07408170008967467.

[545] Hennessy, J. L. and Patterson, D. A., *Computer Architecture: A Quantitative Approach*, 6th ed. Cambridge, MA: Morgan Kaufmann Publishers, 2019.

[546] Shiu, B.; Apley, D.; Ceglarek, D., and Shi, J., “Tolerance allocation for compliant beam structure assemblies,” *IIE Transactions*, vol. 35, no. 4, pp. 329–342, 2003. DOI: 10.1080/07408170304376.

[547] Holland, J. H., *Adaptation in Natural and Artificial Systems: An Introductory Analysis with Applications to Biology, Control, and Artificial Intelligence*. Michigan: University of Michigan Press, 1975.

[548] Glover, F., “Heuristics for integer programming using surrogate constraints,” *Decision Sciences*, vol. 8, no. 1, pp. 156–166, 1977. DOI: 10.1111/j.1540-5915.1977.tb01074.x.

[549] Kirkpatrick, S.; Gelatt, C. D., and Vecchi, M. P., “Optimization by Simulated Annealing,” *Science*, vol. 220, no. 4598, pp. 671–680, 1983. DOI: 10.1126/science.220.4598.671.

[550] Eberhart, R. and Kennedy, J., “A new optimizer using particle swarm theory,” *MHS’95. Proceedings of the Sixth International Symposium on Micro Machine and Human Science*, Nagoya, Japan: IEEE, 4.10.-06.10.1995, pp. 39–43. DOI: 10.1109/MHS.1995.494215.

[551] Dong, Z. and Wang, G. G., “Automated Cost Modeling for Tolerance Synthesis Using Manufacturing Process Data, Knowledge Reasoning and Optimization,” *Geometric Design Tolerancing: Theories, Standards and Applications*, ElMaraghy, H. A., Ed., Dordrecht: Springer, 1998, pp. 282–293. DOI: 10.1007/978-1-4615-5797-5_22.

[552] Ramani, B.; Cheraghi, S. H., and Twomey, J. M., "CAD-based integrated tolerancing system," *International Journal of Production Research*, vol. 36, no. 10, pp. 2891–2910, 1998. DOI: 10 . 1080 / 002075498192535.

[553] Domazet, D. S.; Lu, S. C.-Y., and Kalajdzic, M., "Concurrent Design and Process Planning of Rotational Parts," *CIRP Annals*, vol. 41, no. 1, pp. 181–184, 1992. DOI: 10.1016/S0007-8506(07)61180-9.

[554] Manivannan, S.; Lehtihet, A., and Egbelu, P. J., "A knowledge based system for the specification of manufacturing tolerances," *Journal of Manufacturing Systems*, vol. 8, no. 2, pp. 153–160, 1989. DOI: 10.1016/0278-6125(89)90033-2.

[555] Lu, S. C.-Y. and Wilhelm, R. G., "Automating tolerance synthesis: A framework and tools," *Journal of Manufacturing Systems*, vol. 10, no. 4, pp. 279–296, 1991. DOI: 10.1016/0278-6125(91)90023-U.

[556] Willhelm, R. G. and Lu, S. C.-Y., "Tolerance Synthesis to Support Concurrent Engineering," *CIRP Annals*, vol. 41, no. 1, pp. 197–200, 1992. DOI: 10.1016/S0007-8506(07)61184-6.

[557] Sauer, C.; Heling, B.; Schmutzler, S., and Schleich, B., "A Knowledge-Based Engineering Workbench for Automated Tolerance Specification," *Proceedings of the ASME 2019 International Mechanical Engineering Congress and Exposition. Volume 2B: Advanced Manufacturing*, Salt Lake City, Utah, USA: ASME, 2019, V02BT02A062. DOI: 10.1115/IMECE2019-11225.

[558] Söderberg, R., "Tolerance Allocation in a CAD Environment Considering Quality and Manufacturing Cost," *Lean Production: From Concept to Product*, vol. 11, pp. 789–800, 1994.

[559] Tlija, M.; Ghali, M., and Aifaoui, N., "Integrated CAD tolerancing model based on difficulty coefficient evaluation and Lagrange multiplier," *The International Journal of Advanced Manufacturing Technology*, vol. 101, no. 9-12, pp. 2519–2532, 2019. DOI: 10.1007/s00170-018-3140-1.

[560] Gavankar, P. and Bedworth, D., "Stacked tolerance analysis and allocation using assembly models," *Journal of Intelligent Manufacturing*, vol. 2, no. 6, pp. 365–377, 1991. DOI: 10.1007/BF01471939.

[561] Jourdan, F. A., "Computerunterstützte Toleranzfestlegung zur Qualitätssicherung und Optimierung der Fertigungskosten," Ph.D. dissertation, ETH Zürich, 2003. DOI: 10.3929/ETHZ-A-004550613.

[562] Li, H.; Zhu, H.; Zhou, X.; Li, P., and Yu, Z., "A new computer-aided tolerance analysis and optimization framework for assembling processes using DP-SDT theory," *The International Journal of Advanced Manufacturing Technology*, vol. 86, no. 5-8, pp. 1299–1310, 2016. DOI: 10.1007/s00170-015-8266-9.

[563] Dimitrellou, S. C.; Diplaris, S. C., and Sfantsikopoulos, M. M., "A Systematic Approach for Cost Optimal Tolerance Design," *DS 42: Proceedings of ICED 2007, the 16th International Conference on Engineering Design*, Paris, France, 28.07.-31.07.2007.

[564] Bligh, A., "Understanding the Manufacturing Cost Drivers of Tolerances," *2020 NAFEMS UK Conference "Inspiring Innovation through Engineering Simulation*, Milton Keynes, United Kingdom, 9.11.-10.11.2020.

[565] ISO/TC 159/SC 4, "ISO 9241-11: Ergonomics of human-system interaction — Part 11: Usability: Definitions and concepts," Standard, 2018.

[566] ISO/IEC JTC 1/SC 7, "ISO/IEC 25010:2011: Systems and software engineering — Systems and software Quality Requirements and Evaluation (SQuaRE) — System and software quality models," Tech. Rep., 2011.

[567] Moro, T.; Askri, R.; Rance, P.-A.; Clozel, P.; Martin, J.; Veen, S. V. D.; Canderatz, F., and Judic, J.-M., "New flexible tolerancing strategy and development for complex structural aeronautical assemblies analysis in MECAmaster® software environment," *Procedia CIRP*, vol. 114, pp. 171–176, 2022. DOI: 10.1016/j.procir.2022.10.023.

[568] Singh, P. K. and Gulati, V., "Tolerance analysis and yield estimation using Monte Carlo simulation – case study on linear and nonlinear mechanical systems," *Sādhanā*, vol. 46, no. 1, p. 34, 2021. DOI: 10.1007/s12046-020-01545-5.

[569] Doydum, C. and Duke Perreira, N., "Use of Monte Carlo simulation to select dimensions, tolerances, and precision for automated assembly," *Journal of Manufacturing Systems*, vol. 10, no. 3, pp. 209–222, 1991. DOI: 10.1016/0278-6125(91)90034-Y.

[570] Bluman, A. G., *Elementary Statistics: A Step by Step Approach*, 8th ed. New York: McGraw-Hill, 2012.

[571] Kubiak, T. M., *The Certified Six Sigma Master Black Belt Handbook*. Milwaukee, Wisconsin: ASQ Quality Press, 2012.

[572] Pettitt, A. N., "Testing the Normality of Several Independent Samples Using the Anderson-Darling Statistic," *Applied Statistics*, vol. 26, no. 2, pp. 156–161, 1977. DOI: 10.2307/2347023.

[573] Marsaglia, G.; Tsang, W. W., and Wang, J., "Evaluating Kolmogorov's Distribution," *Journal of Statistical Software*, vol. 8, no. 18, pp. 1–4, 2003. DOI: 10.18637/jss.v008.i18.

[574] Randall, R., "Statistical Background and Concepts," *Dimensioning and Tolerancing Handbook*, Drake, P. J., Ed., New York: McGraw-Hill, 1999, pp. 10-1–10-18.

[575] Forbes, C. S.; Evans, M.; Hastings, N., and Peacock, B., *Statistical Distributions*, 4th ed. Hoboken, New Jersey: Wiley, 2011.

[576] Zwillinger, D., *Standard Mathematical Tables and Formulae*, 31st ed. Boca Raton: Chapman & Hall/CRC Press, 2003.

[577] Silverman, B. W., *Density Estimation for Statistics and Data Analysis*, ser. Monographs on Statistics and Applied Probability 26. Boca Raton: Chapman & Hall/CRC, 1998.

[578] Parzen, E., "On Estimation of a Probability Density Function and Mode," *The Annals of Mathematical Statistics*, vol. 33, no. 3, pp. 1065–1076, 1962. DOI: 10.1214/aoms/1177704472.

[579] Bowman, A. W. and Azzalini, A., *Applied Smoothing Techniques for Data Analysis: The Kernel Approach with S-Plus Illustrations*, ser. Oxford Statistical Science Series 18. Oxford, New York, USA: Clarendon Press, 1997.

[580] Whitney, D. E.; Mantripragada, R.; Adams, J., and Cunningham, T., "Use of Screw Theory to Detect Multiple Conflicting Key Characteristics in Complex Mechanical Products," *Proceedings of the ASME 1999 Design Engineering Technical Conferences .Volume 4: 4th Design for Manufacturing Conference*, Las Vegas, Nevada, USA: ASME, 1999, pp. 295–302. DOI: 10.1115/DETC99/DFM-8974.

[581] Heling, B.; Schleich, B., and Wartzack, S., "Robust-Design-Optimization of mechanisms based on kinematic requirements considering uncertainties," *Procedia CIRP*, vol. 75, pp. 27–32, 2018. DOI: 10.1016/j.procir.2018.04.048.

[582] Rezaei Aderiani, A.; Wärmefjord, K., and Söderberg, R., "An Improved Phenotype-Genotype Mapping for Solving Selective Assembly Problem Using Evolutionary Optimization Algorithms," *Journal of Computing and Information Science in Engineering*, vol. 20, no. 6, p. 061 010, 2020. DOI: 10.1115/1.4047241.

[583] ISO/TC 213, "ISO 8015:2011: Geometrical product specifications (GPS) - Fundamentals - Concepts, principles and rules," Standard, 2011.

[584] Lehtihet, E. A.; Ranade, S., and Dewan, P., "Comparative evaluation of tolerance control chart models," *International Journal of Production Research*, vol. 38, no. 7, pp. 1539–1556, 2000. DOI: 10.1080/002075400188717.

[585] Song, H.; Yang, Y. D.; Zhou, Y., and Rong, Y. K., "Tolerance Assignment Using Genetic Algorithm for Production Planning," *Models for Computer Aided Tolerancing in Design and Manufacturing*, Davidson, J. K., Ed., Dordrecht: Springer, 2007, pp. 213–224. DOI: 10.1007/1-4020-5438-6_22.

[586] Halim, A. H.; Ismail, I., and Das, S., "Performance assessment of the metaheuristic optimization algorithms: an exhaustive review," *Artificial Intelligence Review*, vol. 54, no. 3, pp. 2323–2409, 2021. DOI: 10.1007/s10462-020-09906-6.

[587] Wang, G. G. and Shan, S., "Review of Metamodeling Techniques in Support of Engineering Design Optimization," *Journal of Mechanical Design*, vol. 129, no. 4, pp. 370–380, 2007. DOI: 10.1115/1.2429697.

[588] Palar, P. S.; Liem, R. P.; Zuhal, L. R., and Shimoyama, K., "On the use of surrogate models in engineering design optimization and exploration: the key issues," *Proceedings of the Genetic and Evolutionary Computation Conference Companion*, Prague, Czech Republic: ACM, 13.07–17.07.2019, pp. 1592–1602. DOI: 10.1145/3319619.3326813.

[589] Simpson, T. W.; Poplinski, J. D.; Koch, P. N., and Allen, J. K., "Metamodels for Computer-based Engineering Design: Survey and recommendations," *Engineering with Computers*, vol. 17, no. 2, pp. 129–150, 2001. DOI: 10.1007/PL00007198.

[590] Eason, J. and Cremaschi, S., "Adaptive sequential sampling for surrogate model generation with artificial neural networks," *Computers & Chemical Engineering*, vol. 68, pp. 220–232, 2014. DOI: 10.1016/j.compchemeng.2014.05.021.

[591] Barton, R. R., "Simulation optimization using metamodels," *Proceedings of the 2009 Winter Simulation Conference (WSC)*, Austin, Texas, USA: IEEE, 13.12–16.12.2009, pp. 230–238. DOI: 10.1109/WSC.2009.5429328.

[592] Viana, F. A. C.; Gogu, C., and Haftka, R. T., "Making the Most Out of Surrogate Models: Tricks of the Trade," *Proceedings of the ASME 2010 International Design Engineering Technical Conferences and Computers and Information in Engineering Conference. Volume 1: 36th Design Automation Conference, Parts A and B*, Montreal, Quebec, Canada: ASME, 2010, pp. 587–598. DOI: 10.1115/DETC2010-28813.

[593] Bramerdorfer, G. and Zăvoianu, A.-C., "Surrogate-Based Multi-Objective Optimization of Electrical Machine Designs Facilitating Tolerance Analysis," *IEEE Transactions on Magnetics*, vol. 53, no. 8, pp. 1–11, 2017. DOI: 10.1109/TMAG.2017.2694802.

[594] Han, Z.-H. and Zhang, K.-S., "Surrogate-Based Optimization," *Real-World Applications of Genetic Algorithms*, Roeva, O., Ed., InTech, 2012, pp. 343–362. DOI: 10.5772/36125.

[595] Horber, D.; Goetz, S.; Schleich, B., and Wartzack, S., "A Model-Based Approach for Integrated Variation Management," *Proceedings of the ASME 2022 International Mechanical Engineering Congress and Exposition: Volume 2B: Advanced Manufacturing*, Columbus, Ohio, USA: ASME, 2022, V02BT02A067. DOI: 10.1115/IMECE2022-90956.

[596] Suh, N. P., *The Principles of Design*, ser. Oxford Series on Advanced Manufacturing 6. New York: Oxford University Press, 1990.

[597] Plischke, E.; Borgonovo, E., and Smith, C. L., "Global sensitivity measures from given data," *European Journal of Operational Research*, vol. 226, no. 3, pp. 536–550, 2013. DOI: 10.1016/j.ejor.2012.11.047.

[598] Madrid, J.; Vallhagen, J.; Söderberg, R., and Wärmefjord, K., "Enabling Reuse of Inspection Data to Support Robust Design: A Case in the Aerospace Industry," *Procedia CIRP*, vol. 43, pp. 41–46, 2016. DOI: 10.1016/j.procir.2016.02.137.

[599] Kramer, V.; Wirsching, S.; Wartzack, S., and Miehling, J., "Electrified cross skate as a micromobility solution," *Konstruktion*, vol. 75, no. 9, pp. 59–66, 2023. DOI: 10.37544/0720-5953-2023-09-59.

[600] Armillotta, A., "Allocation of geometric tolerances in one-dimensional stackup problems," *The International Journal of Advanced Manufacturing Technology*, vol. 122, no. 3-4, pp. 1957–1973, 2022. DOI: 10.1007/s00170-022-09918-2.

[601] Gille, M.; Beaurepaire, P.; Dumas, A.; Taghon, F.; Yalamas, T., and Gayton, N., "On the identification of the probability density function of a dimension from data with measurement errors," *Procedia CIRP*, vol. 114, pp. 60–66, 2022. DOI: 10.1016/j.procir.2022.10.009.

[602] Cheng, K.-M. and Tsai, J.-C., "An Investigation on Optimal Tolerance Allocation by Lagrange Multipliers," 2014.

[603] Dong, J. and Shi, Y., "Tolerance Analysis and Synthesis in Variational Design," *Advanced Tolerancing Techniques*, Zhang, H.-C., Ed., New York: Wiley, 1997, pp. 303–325.

[604] Etienne, A.; Dantan, J.-Y.; Qureshi, J., and Siadat, A., "Variation management by functional tolerance allocation and manufacturing process selection," *International Journal on Interactive Design and Manufacturing (IJIDeM)*, vol. 2, no. 4, pp. 207–218, 2008. DOI: 10.1007/s12008-008-0055-3.

[605] González, I. and Sánchez, I., "Statistical tolerance synthesis with correlated variables," *Mechanism and Machine Theory*, vol. 44, no. 6, pp. 1097–1107, 2009. DOI: 10.1016/j.mechmachtheory.2008.10.006.

[606] Chou, C.-Y. and Chang, C.-L., "Bivariate tolerance design for lock wheels by considering quality loss," *Quality and Reliability Engineering International*, vol. 16, no. 2, pp. 129–138, 2000. DOI: 10.1002/(SICI)1099-1638(200003/04)16:2%3C129::AID-QRE310%3E3.0.CO;2-J.

[607] Blessing, L. T. M. and Chakrabarti, A., *DRM, a Design Research Methodology*. London: Springer, 2009. DOI: 10.1007/978-1-84882-587-1.

[608] Bennett, G. and Gupta, L. C., "Least-cost tolerances—II," *International Journal of Production Research*, vol. 8, no. 2, pp. 169–182, 1970. DOI: 10.1080/00207547008929838.

[609] Spotts, M. F., "Allocation of Tolerances to Minimize Cost of Assembly," *Journal of Engineering for Industry*, vol. 95, no. 3, pp. 762–764, 1973. DOI: 10.1115/1.3438222.

[610] Thorbjornsen, A. and Director, S., "Computer-aided tolerance assignment for linear circuits with correlated elements," *IEEE Transactions on Circuit Theory*, vol. 20, no. 5, pp. 518–524, 1973. DOI: 10.1109/TCT.1973.1083737.

[611] Wilde, D. and Prentice, E., "Minimum Exponential Cost Allocation of Sure-Fit Tolerances," *Journal of Engineering for Industry*, vol. 97, no. 4, pp. 1395–1398, 1975. DOI: 10.1115/1.3438796.

[612] Bloebaum, C. L.; Mulubagal, G. S., and Rosner, A., "Multidisciplinary design with tolerance allocation for maximum quality," *35th Structures, Structural Dynamics, and Materials Conference*, Hilton Head, South Carolina, USA: American Institute of Aeronautics and Astronautics, 18.04.-20.04.1994. DOI: 10.2514/6.1994-1417.

[613] Gadallah, M. H. and El Maraghy, H. A., "A new algorithm for discrete tolerance optimization," *Proceedings of the Fourth International Conference on Computer Integrated Manufacturing and Automation Technology*, Troy, New York, USA: IEEE, 10.10.-12.10.1994, pp. 292–297. DOI: 10.1109/CIMAT.1994.389058.

[614] Jeang, A., "Tolerance design: Choosing optimal tolerance specifications in the design of machined parts," *Quality and Reliability Engineering International*, vol. 10, no. 1, pp. 27–35, 1994. DOI: 10.1002/qre.4680100107.

[615] Söderberg, R., "Robust Design by Tolerance Allocation Considering Quality and Manufacturing Cost," *Proceedings of the ASME 1994 Design Technical Conferences Collocated with the ASME 1994 International Computers in Engineering Conference and Exhibition and the ASME 1994 8th Annual Database Symposium. 20th Design Automation Conference: Volume 1 — Dynamic Mechanical Systems; Geometric Modeling and Features; Concurrent Engineering*, Minneapolis, Minnesota, USA: ASME, 1994, pp. 219–226. DOI: 10.1115/DETC1994-0064.

[616] Kopardekar, P. and Anand, S., "Tolerance allocation using neural networks," *The International Journal of Advanced Manufacturing Technology*, vol. 10, no. 4, pp. 269–276, 1995. DOI: 10.1007/BF01186878.

[617] Söderberg, R., "Optimal Tolerance Band and Manufacturing Target for Monotonic Loss Functions With Functional Limits," *Proceedings of the ASME 1995 Design Engineering Technical Conferences Collocated with the ASME 1995 15th International Computers in Engineering Conference and the ASME 1995 9th Annual Engineering Database Symposium. Volume 1: 21st Design Automation Conference*, Boston, Massachusetts, USA: ASME, 1995, pp. 345–352. DOI: 10.1115/DETC1995-0046.

[618] Kusiak, A. and Feng, C.-X., "Robust Tolerance Design for Quality," *Journal of Engineering for Industry*, vol. 118, no. 1, pp. 166–169, 1996. DOI: 10.1115/1.2803639.

[619] Ngoi, B. K. A. and Teck, O. C. A., "A tolerancing optimisation method for product design," *The International Journal of Advanced Manufacturing Technology*, vol. 13, no. 4, pp. 290–299, 1997. DOI: 10.1007/BF01179611.

[620] Roy, U. and Fang, Y.-C., "Optimal tolerance re-allocation for the generative process sequence," *IIE Transactions*, vol. 29, no. 1, pp. 37–44, 1997. DOI: 10.1080/07408179708966310.

[621] Wei, C.-C., "Allocating tolerances to minimize cost of nonconforming assembly," *Assembly Automation*, vol. 17, no. 4, pp. 303–306, 1997. DOI: 10.1108/01445159710191589.

[622] Gadallah, M. H. and ElMaraghy, H. A., "A New Algorithm for Combinatorial Optimization: Application to Tolerance Synthesis with Optimum Process Selection," *Geometric Design Tolerancing: Theories, Standards and Applications*, ElMaraghy, H. A., Ed., Boston, Massachusetts: Springer, 1998, pp. 265–281. DOI: 10.1007/978-1-4615-5797-5_21.

[623] Wu, C.-C.; Chen, Z., and Tang, G.-R., "Component tolerance design for minimum quality loss and manufacturing cost," *Computers in Industry*, vol. 35, no. 3, pp. 223–232, 1998. DOI: 10.1016/S0166-3615(97)00087-0.

[624] Chen, M.-S. and Young, K. W., "Optimising Tolerance Allocation for Mechanical Assemblies Considering Geometric Tolerances Based on a Simplified Algorithm," *Global Consistency of Tolerances*, van Houten, F. and Kals, H., Eds., Dordrecht: Springer, 1999, pp. 27–36. DOI: 10.1007/978-94-017-1705-2_2.

[625] Kim, C.-B.; Pulat, P. S.; Foote, B. L., and Lee, D. H., "Least cost tolerance allocation and bicriteria extension," *International Journal of Computer Integrated Manufacturing*, vol. 12, no. 5, pp. 418–426, 1999. DOI: 10.1080/095119299130155.

[626] Li, W. and Wu, C. F. J., "An integrated method of parameter design and tolerance design," *Quality Engineering*, vol. 11, no. 3, pp. 417–425, 1999. DOI: 10.1080/08982119908919258.

[627] Zhang, C.; Luo, J., and Wang, B., "Statistical tolerance synthesis using distribution function zones," *International Journal of Production Research*, vol. 37, no. 17, pp. 3995–4006, 1999. DOI: 10.1080/002075499189880.

[628] Cho, B.-R.; Kim, Y. J.; Kimbler, D. L., and Phillips, M. D., "An integrated joint optimization procedure for robust and tolerance design," *International Journal of Production Research*, vol. 38, no. 10, pp. 2309–2325, 2000. DOI: 10.1080/00207540050028115.

[629] Diplaris, S. C. and Sfantsikopoulos, M. M., "Cost–Tolerance Function. A New Approach for Cost Optimum Machining Accuracy," *International Journal of Advanced Manufacturing Technology*, vol. 16, no. 1, pp. 32–38, 2000. DOI: 10.1007/PL00013129.

[630] Feng, C.-X. and Kusiak, A., "Robust Tolerance Synthesis With the Design of Experiments Approach," *Journal of Manufacturing Science and Engineering*, vol. 122, no. 3, pp. 520–528, 2000. DOI: 10.1115/1.1285860.

[631] Gadallah, M. H., "The Tolerance Optimization Problem Using a Near-to-Global Optimum," *Proceedings of the ASME 2000 International Design Engineering Technical Conferences and Computers and Information in Engineering Conference. Volume 2: 26th Design Automation Conference*, Baltimore, Maryland, USA: ASME, 2000, pp. 981–990. DOI: 10.1115/DETC2000/DAC-14294.

[632] Gerth, R. J.; Pfeifer, T., and Oehme, O., "Early cost tolerance sensitivity analysis for inspection planning," *Human Factors and Ergonomics in Manufacturing & Service Industries*, vol. 10, no. 3, pp. 309–329, 2000. DOI: 10.1002/1520-6564(200022)10:3<309::AID-HFM6>3.0.CO;2-W.

[633] Gerth, R. J. and Hancock, W. M., "Computer aided tolerance analysis for improved process control," *Computers & Industrial Engineering*, vol. 38, no. 1, pp. 1–19, 2000. DOI: 10.1016/S0360-8352(00)00007-3.

[634] Ji, S.; Li, X.; Ma, Y., and Cai, H., "Optimal Tolerance Allocation Based on Fuzzy Comprehensive Evaluation and Genetic Algorithm," *The International Journal of Advanced Manufacturing Technology*, vol. 16, no. 7, pp. 461–468, 2000. DOI: 10.1007/s001700070053.

[635] Gadallah, M. H., "Tolerance Optimization: A Decomposition Scheme, Variance Reduction and Fractional Approximation," *Proceedings of the ASME 2001 International Design Engineering Technical Conferences and Computers and Information in Engineering Conference. Volume 5: 15th Reliability, Stress Analysis, and Failure Prevention Conference; International Issues in Engineering Design*, Pittsburgh, Pennsylvania, USA: ASME, 2001, pp. 183–192. DOI: 10.1115/DETC2001/IED-21222.

[636] Kim, Y. J. and Cho, B. R., "The use of response surface designs in the selection of optimum tolerance allocation," *Quality Engineering*, vol. 13, no. 1, pp. 35–42, 2001. DOI: 10.1080/08982110108918622.

[637] Teeravaraprug, J., "Deterministic Tolerance Synthesis with a Consideration of Nominal Values," *Thammasat International Journal of Science and Technology*, vol. 7, no. 1, pp. 50–55, 2002.

[638] Pramanik, N., "A generic framework for design evolution: From function-to-form mapping to synthesis of tolerances," Ph.D. dissertation, Syracuse University, New York, USA, 2003.

[639] Steiner, G. and Watzenig, D., "Particle swarm optimization for worst case tolerance design," *IEEE International Conference on Industrial Technology, 2003*, Maribor, Slovenia: IEEE, 10.12.-12.12.2003, pp. 78–82. DOI: 10.1109/ICIT.2003.1290245.

[640] Yang, C. C. and Achutha Naikan, V., "Optimum tolerance design for complex assemblies using hierarchical interval constraint networks," *Computers & Industrial Engineering*, vol. 45, no. 3, pp. 511–543, 2003. DOI: 10.1016/S0360-8352(03)00072-X.

[641] Yang, C. C. and Achutha Naikan, V. N., "Optimum tolerance design using constraint networks and relative sensitivity ratio algorithm," *Applied Artificial Intelligence*, vol. 17, no. 7, pp. 631–660, 2003. DOI: 10.1080/713827209.

[642] Singh, P. K.; Jain, S. C., and Jain, P. K., "Optimal tolerance allocation of mechanical assemblies with alternative manufacturing processes (machines)," *Proceedings of the 3rd International Conference "Business Systems Management"*, Mostar, Bosnia and Herzegovina, 23.09-24.09.2004, pp. 211–213.

[643] Yoo, H.; Kang, D.-K.; Lee, S.; Lee, J., and Gweon, D.-G., "Error analysis and tolerance allocation for confocal scanning microscopy using the Monte Carlo method," *Proceedings Volume 5324, Three-Dimensional and Multidimensional Microscopy: Image Acquisition and Processing XI. Biomedical Optics 2004*, Conchello, J.-A.; Cogswell, C. J., and Wilson, T., Eds., vol. 5325, San Jose, California, USA, 24.01.-29.01.2004, pp. 242–249. DOI: 10.1117/12.529942.

[644] Hu, J. and Xiong, G., "Dimensional and geometric tolerance design based on constraints," *The International Journal of Advanced Manufacturing Technology*, vol. 26, no. 9-10, pp. 1099–1108, 2005. DOI: 10.1007/s00170-004-2086-7.

[645] Kim, Y. J.; Cho, B. R.; Lee, M. K., and Kwon, H. M., "Design Optimization Modeling for Customer-Driven Concurrent Tolerance Allocation," *Computational Science and Its Applications – ICCSA 2005*, Gervasi, O.; Gavrilova, M. L.; Kumar, V.; Laganá, A.; Lee, H. P.; Mun, Y.; Taniar, D., and Tan, C. J. K., Eds., vol. 3483, Berlin: Springer, 2005, pp. 212–221. DOI: 10.1007/11424925_24.

[646] Pramanik, N.; Roy, U.; Sudarsan, R.; Sriram, R. D., and Lyons, K. W., "A Generic Deviation-Based Approach for Synthesis of Tolerances," *IEEE Transactions on Automation Science and Engineering*, vol. 2, no. 4, pp. 358–368, 2005. DOI: 10.1109/TASE.2005.853584.

[647] Singh, P. K.; Jain, S. C., and Jain, P. K., "Comparative study of genetic algorithm and simulated annealing for optimal tolerance design formulated with discrete and continuous variables," *Proceedings of the Institution of Mechanical Engineers, Part B: Journal of Engineering Manufacture*, vol. 219, no. 10, pp. 735–758, 2005. DOI: 10.1243/095440505X32643.

[648] Cao, Y.-l.; Mao, J.; Yang, J.-x.; Wu, Z.-t., and Wu, L.-q., "A Robust Tolerance Design Method Based on Fuzzy Quality Loss," *Frontiers of Mechanical Engineering in China*, vol. 1, no. 1, pp. 101–105, 2006. DOI: 10.1007/s11465-005-0010-y.

[649] Chen, T. C. and Hsu, T.-C., "An Immune Algorithm for Least Cost Advanced Tolerance Design Problem," *Materials Science Forum*, vol. 505–507, pp. 511–516, 2006. DOI: 10.4028/www.scientific.net/MSF.505-507.511.

[650] Savage, G. J.; Tong, D., and Carr, S. M., "Optimal Mean and Tolerance Allocation Using Conformance-based Design," *Quality and Reliability Engineering International*, vol. 22, no. 4, pp. 445–472, 2006. DOI: 10.1002/qre.721.

[651] Siva Kumar, M.; Kannan, S. M., and Jayabalan, V., "Construction of closed-form equations and graphical representation for optimal tolerance allocation," *International Journal of Production Research*, vol. 45, no. 6, pp. 1449–1468, 2007. DOI: 10.1080/00207540600547422.

[652] Wu, W. and Rao, S. S., "Uncertainty analysis and allocation of joint tolerances in robot manipulators based on interval analysis," *Reliability Engineering & System Safety*, vol. 92, no. 1, pp. 54–64, 2007. DOI: 10.1016/j.ress.2005.11.009.

[653] Jeang, A. and Chung, C.-P., "Process mean, process tolerance, and use time determination for product life application under deteriorating process," *The International Journal of Advanced Manufacturing Technology*, vol. 36, no. 1-2, pp. 97–113, 2008. DOI: 10.1007/s00170-006-0814-x.

[654] Peng, H. P.; Jiang, X. Q.; Xu, Z. G., and Liu, X. J., "Optimal tolerance design for products with correlated characteristics by considering the present worth of quality loss," *The International Journal of Advanced Manufacturing Technology*, vol. 39, no. 1-2, pp. 1–8, 2008. DOI: 10.1007/s00170-007-1205-7.

[655] Cao, Y.; Mao, J.; Ching, H., and Yang, J., "A robust tolerance optimization method based on fuzzy quality loss," *Proceedings of the Institution of Mechanical Engineers, Part C: Journal of Mechanical Engineering Science*, vol. 223, no. 11, pp. 2647–2653, 2009. DOI: 10.1243/09544062JMES1451.

[656] Dimitrellou, S. C.; Kaisarlis, G.; Diplaris, S. C., and Sfantsikopoulos, M. M., "A Cost Optimal Tolerance Synthesis Methodology for Design

and Manufacturing Integration," *Proceedings of the 11th CIRP International Conference on Computer Aided Tolerancing*, Annecy, France, 26.03.–27.03.2009.

[657] Kumar, R. S.; Alagumurthi, N., and Ramesh, R., "Calculation of Total Cost, Tolerance Based on Taguchi's, Asymmetric Quality Loss Function Approach," *American Journal of Engineering and Applied Sciences*, vol. 2, no. 4, pp. 628–634, 2009. DOI: 10.3844/ajeassp.2009.628.634.

[658] Kumar, R. S.; Alagumurthy, N., and Ramesh, R., "Simultaneous Optimization of Design Tolerance and Total Cost for a Piston and Cylinder Assembly," *2009 International Conference on Advances in Recent Technologies in Communication and Computing*, Kottayam, Kerala, India: IEEE, 27.10.-28.10.2009, pp. 783–789. DOI: 10.1109/ARTCom.2009.179.

[659] Mao, J.; Cao, Y. L.; Liu, S. Q., and Yang, J. X., "Manufacturing environment-oriented robust tolerance optimization method," *The International Journal of Advanced Manufacturing Technology*, vol. 41, no. 1-2, pp. 57–65, 2009. DOI: 10.1007/s00170-008-1460-2.

[660] Cui, A. and Zhang, H. P., "Tolerance Allocation and Maintenance Optimal Design for Fixture in Multi-Station Panel Assembly Process," *Applied Mechanics and Materials*, vol. 34–35, pp. 1039–1045, 2010. DOI: 10.4028/www.scientific.net/AMM.34-35.1039.

[661] Edholm, P.; Lööf, J.; Trangärd, A., and Söderberg, R., "Robust Tolerance Design Applied on Robot Concept Development," *DS 61: Proceedings of NordDesign 2010*, Gothenburg, Sweden, 25.08.-27.08.2010, pp. 21–30.

[662] Sampath Kumar, R.; Alagumurthi, N., and Ramesh, R., "Integrated total cost and Tolerance Optimization with Genetic Algorithm," *International Journal of Computational Intelligence Systems*, vol. 3, no. 3, pp. 325–333, 2010. DOI: 10.1080/18756891.2010.9727703.

[663] Zhang, J.; Li, S.; Bao, N. S.; Zhang, G. J.; Xue, D. Y., and Gu, P. H., "A robust design approach to determination of tolerances of mechanical products," *CIRP Annals*, vol. 59, no. 1, pp. 195–198, 2010. DOI: 10.1016/j.cirp.2010.03.099.

[664] Campatelli, G., "Tolerance synthesis using axiomatic design," *Proceedings of the 6th International Conference on Axiomatic Design*, Kaist, Korea, 30.03.-31.03.2011, pp. 152–157.

[665] Cheng, K. M. and Tsai, J. C., "Optimal Statistical Tolerance Allocation of Assemblies for Minimum Manufacturing Cost," *Applied Mechanics and Materials*, vol. 52–54, pp. 1818–1823, 2011. DOI: 10.4028/www.scientific.net/AMM.52-54.1818.

[666] Zhong, B., "Fuzzy-Robust Design Optimization of Dimension Tolerance Using the Improved Genetic Algorithm," *Applied Mechanics and Materials*, vol. 55–57, pp. 1502–1505, 2011. DOI: 10.4028/www.scientific.net/AMM.55-57.1502.

[667] Ai, Y. T.; Tian, J.; Zhang, F. L.; Zhai, X., and Bai, S. S., "Study on Technique of Tolerance Optimal Allocation Based on Adaptive Genetic Algorithm," *Advanced Materials Research*, vol. 490–495, pp. 1436–1440, 2012. DOI: 10.4028/www.scientific.net/AMR.490-495.1436.

[668] Kaisarlis, G. J., "A Systematic Approach for Geometrical and Dimensional Tolerancing in Reverse Engineering," *Reverse Engineering - Recent Advances and Applications*, Telea, A. C., Ed., InTech, 2012, pp. 133–160. DOI: 10.5772/32001.

[669] Lin, C.-W., "Simultaneous optimal design of parameters and tolerance of bearing locations for high-speed machine tools using a genetic algorithm and Monte Carlo simulation method," *International Journal of Precision Engineering and Manufacturing*, vol. 13, no. 11, pp. 1983–1988, 2012. DOI: 10.1007/s12541-012-0261-6.

[670] Lööf, J. and Söderberg, R., "Discrete tolerance allocation for product families," *Engineering Optimization*, vol. 44, no. 1, pp. 75–85, 2012. DOI: 10.1080/0305215X.2011.569545.

[671] Sanz, A.; Guimeráns, M.; González, I., and Pérez, J., "Comparative analysis of tolerance allocation in mechanical assemblies based on cost-tolerance curves," *AIP Conference Proceedings*, vol. 1431, no. 1, pp. 197–206, 2012. DOI: 10.1063/1.4707566.

[672] Peng, H., "Concurrent tolerancing for design and manufacturing based on the present worth of quality loss," *The International Journal of Advanced Manufacturing Technology*, vol. 59, no. 9-12, pp. 929–937, 2012. DOI: 10.1007/s00170-011-3542-9.

[673] Cheng, K.-M. and Tsai, J.-C., "Optimal statistical tolerance allocation for reciprocal exponential cost–tolerance function," *Proceedings of the Institution of Mechanical Engineers, Part B: Journal of Engineering Manufacture*, vol. 227, no. 5, pp. 650–656, 2013. DOI: 10.1177/0954405412473720.

[674] Guo, H. X., "Design Optimization for the Robustness of Dimensional Tolerance by Using Evidence Theory," *Applied Mechanics and Materials*, vol. 483, pp. 434–437, 2013. DOI: 10.4028/www.scientific.net/AMM.483.434.

[675] Hoffenson, S.; Dagman, A.; Söderberg, R., and Steen, B., "Tolerance Optimization for Economic and Ecological Sustainability Using RD&T," *The 6th International Conference on Life Cycle Management*, Gothenburg, Sweden, 25.08.-28.08.2013, pp. 856–859.

[676] Hoffenson, S.; Dagman, A., and Söderberg, R., "Tolerance Specification Optimization for Economic and Ecological Sustainability," *Smart Product Engineering*, Abramovici, M. and Stark, R., Eds., Berlin: Springer, 2013, pp. 865–874. DOI: 10.1007/978-3-642-30817-8_85.

[677] Hoffenson, S. and Söderberg, R., "Comparing Standards and Policies for Sustainability in Tolerance Optimization," *Proceedings of the ASME 2013 International Design Engineering Technical Conferences and Computers and Information in Engineering Conference. Volume 4: 18th Design for Manufacturing and the Life Cycle Conference; 2013 ASME/IEEE International Conference on Mechatronic and Embedded Systems and Applications*, Portland, Oregon, USA: ASME, 2013, V004T05A034. DOI: 10.1115/DETC2013-12104.

[678] Liu, S. G. and Jin, Q., "Closed-Form Optimal Tolerance for Minimum Manufacturing Cost and Quality Loss Cost," *Advanced Materials Research*, vol. 655–657, pp. 2084–2087, 2013. DOI: 10.4028/www.scientific.net/AMR.655-657.2084.

[679] Shen, L.; Yang, J., and Zhao, Y., "Simultaneous Optimization of Robust Parameter and Tolerance Design Based on Generalized Linear Models," *Quality and Reliability Engineering International*, vol. 29, no. 8, pp. 1107–1115, 2013. DOI: 10.1002/qre.1462.

[680] Walter, M. and Wartzack, S., "Statistical Tolerance-Cost-Optimization of Systems in Motion Taking into Account Different Kinds of Deviations," *Smart Product Engineering*, Abramovici, M. and Stark, R., Eds., Berlin: Springer, 2013, pp. 705–714. DOI: 10.1007/978-3-642-30817-8_69.

[681] Hoffenson, S.; Dagman, A., and Söderberg, R., "Tolerance optimisation considering economic and environmental sustainability," *Journal of Engineering Design*, vol. 25, no. 10-12, pp. 367–390, 2014. DOI: 10.1080/09544828.2014.994481.

[682] Liu, S.-G.; Jin, Q.; Wang, P., and Xie, R.-J., "Closed-form solutions for multi-objective tolerance optimization," *The International Journal of Advanced Manufacturing Technology*, vol. 70, no. 9-12, pp. 1859–1866, 2014. DOI: 10.1007/s00170-013-5437-4.

[683] Sahani, A. K.; Jain, P. K.; Sharma, S. C., and Bajpai, J. K., "Design Verification through Tolerance Stack up Analysis of Mechanical Assembly and Least Cost Tolerance Allocation," *Procedia Materials Science*, vol. 6, pp. 284–295, 2014. DOI: 10.1016/j.mspro.2014.07.036.

[684] Saravanan, A.; Balamurugan, C.; Sivakumar, K., and Ramabalan, S., "Optimal geometric tolerance design framework for rigid parts with assembly function requirements using evolutionary algorithms," *The International Journal of Advanced Manufacturing Technology*, vol. 73, no. 9-12, pp. 1219–1236, 2014. DOI: 10.1007/s00170-014-5908-2.

[685] Zhao, Y. M.; Liu, D. S., and Wen, Z. J., "Optimization design method of product general tolerance system," *The International Journal of Advanced Manufacturing Technology*, vol. 70, no. 1-4, pp. 363–374, 2014. DOI: 10.1007/s00170-013-5193-5.

[686] Chattinnawat, W., "Statistical tolerance design to minimize dual-responses of APFA height deviations with tolerance cost-quality loss model," *International Journal of Quality & Reliability Management*, vol. 32, no. 5, pp. 434–455, 2015. DOI: 10.1108/IJQRM-06-2013-0096.

[687] Geetha, K.; Ravindran, D.; Kumar, M. S., and Islam, M. N., "Concurrent tolerance allocation and scheduling for complex assemblies," *Robotics and Computer-Integrated Manufacturing*, vol. 35, pp. 84–95, 2015. DOI: 10.1016/j.rcim.2015.03.001.

[688] Kumar, L. R. and Padmanaban, K., "Optimal Manufacturing Cost and Quality Loss by Reciprocal Exponential Cost-Tolerance Function," *Applied Mechanics and Materials*, vol. 766–767, pp. 1097–1102, 2015. DOI: 10.4028/www.scientific.net/AMM.766-767.1097.

[689] Mazur, M.; Leary, M., and Subic, A., "Application of Polynomial Chaos Expansion to Tolerance Analysis and Synthesis in Compliant Assemblies Subject to Loading," *Journal of Mechanical Design*, vol. 137, no. 3, p. 031 701, 2015. DOI: 10.1115/1.4029283.

[690] Wu, Z.; Gao, Z.; Cao, Y.; Ye, X., and Yang, J., "Tolerance Design and Adjustment of Complex Customized Product Based on Cloud Manufacturing," *Procedia CIRP*, vol. 27, pp. 169–175, 2015. DOI: 10.1016/j.procir.2015.04.061.

[691] Zong, Y. and Mao, J., "Tolerance Optimization Design Based on the Manufacturing-costs of Assembly Quality," *Procedia CIRP*, vol. 27, pp. 324–329, 2015. DOI: 10.1016/j.procir.2015.04.087.

[692] Ramesh Kumar, L.; Padmanaban, K., and Balamurugan, C., "Least cost–tolerance allocation based on Lagrange multiplier," *Concurrent Engineering*, vol. 24, no. 2, pp. 164–177, 2016. DOI: 10.1177/1063293X15625722.

[693] Ramesh Kumar, L.; Padmanaban, K. P., and Balamurugan, C., "Optimal Tolerance Allocation in a Complex Assembly Using Evolutionary Algorithms," *International Journal of Simulation Modelling*, vol. 15, no. 1, pp. 121–132, 2016. DOI: 10.2507/IJSIMM15(1)10.331.

[694] Shoukr, D. S. L.; Gadallah, M. H., and Metwalli, S. M., "The Reduced Tolerance Allocation Problem," *Proceedings of the ASME 2016 International Mechanical Engineering Congress and Exposition. Volume 11: Systems, Design, and Complexity*, Phoenix, Arizona, USA: ASME, 2016, V011T15A023. DOI: 10.1115/IMECE2016-65848.

[695] Vignesh Kumar, D.; Ravindran, D.; Siva Kumar, M., and Islam, M., "Optimum tolerance synthesis of simple assemblies with nominal dimension selection using genetic algorithm," *Proceedings of the Institution of Mechanical Engineers, Part C: Journal of Mechanical Engineering Science*, vol. 230, no. 19, pp. 3488–3508, 2016. DOI: 10.1177/0954406215613366.

[696] Ghali, M.; Tlija, M., and Aifaoui, N., "An approach to unique transfer and allocation of tolerances considering manufacturing difficulty," *CFM 2017-23ème Congrès Français de Mécanique*, Lille, France, 28.08.-01.09.2017.

[697] Guo, Y.; Luo, Y.; Zhao, Y.; He, H., and Tan, H., "Constraint Tolerance Optimization Design Based on Performance Deviation," *China Mechanical Engineering*, vol. 28, no. 17, pp. 2069–2074, 2017.

[698] Hazrati-Marangaloo, H. and Shahriari, H., "A Novel Approach to Simultaneous Robust Design of Product Parameters and Tolerances Using Quality Loss and Multivariate ANOVA Concepts: Robust Design of High Quality Products," *Quality and Reliability Engineering International*, vol. 33, no. 1, pp. 71–85, 2017. DOI: 10.1002/qre.1991.

[699] Jawahar, N.; Sivasankaran, R., and Ramesh, M., "Optimal Pareto front for manufacturing tolerance allocation model," *Proceedings of the Institution of Mechanical Engineers, Part B: Journal of Engineering Manufacture*, vol. 231, no. 7, pp. 1190–1203, 2017. DOI: 10.1177/0954405415586548.

[700] Kaisarlis, G. and Stathakis, G., "A Novel Tolerance Design Approach to Manufacturing and Quality Loss Cost Optimization in Mechanical Assemblies," *International Review of Mechanical Engineering (IREME)*, vol. 11, no. 9, pp. 651–660, 2017. DOI: 10.15866/ireme.v11i9.11794.

[701] Panari, D.; Renzi, C.; Vergnano, A.; Bonazzi, E., and Leali, F., "Integrated design method for optimal tolerance stack evaluation for top class automotive chassis," *Advances on Mechanics, Design Engineering and Manufacturing*, Eynard, B.; Nigrelli, V.; Oliveri, S. M.; Peris-Fajarnes, G., and Rizzuti, S., Eds., Cham: Springer International Publishing, 2017, pp. 1013–1022. DOI: 10.1007/978-3-319-45781-9_101.

[702] Rosyidi, C. N.; Murtisari, R., and Jauhari, W., "A concurrent optimization model for supplier selection with fuzzy quality loss," *Journal of Industrial Engineering and Management*, vol. 10, no. 1, pp. 98–110, 2017. DOI: 10.3926/jiem.800.

[703] Xu, S.; Xing, Y., and Chen, W., "Multi-objective optimization based on improved non-dominated sorting genetic algorithm II for tolerance allocation of auto-body parts," *Advances in Mechanical Engineering*, vol. 9, no. 9, pp. 1–9, 2017. DOI: 10.1177/1687814017718123.

[704] Ghali, M.; Tlija, M., and Aifaoui, N., "Optimal tolerance allocation based on Difficulty matrix using FMECA tool," *Procedia CIRP*, vol. 70, pp. 132–137, 2018. DOI: 10.1016/j.procir.2018.03.005.

[705] Natarajan, J.; Sivasankaran, R., and Kanagaraj, G., "Bi-objective optimization for tolerance allocation in an interchangeable assembly under diverse manufacturing environment," *The International Journal of Advanced Manufacturing Technology*, vol. 95, no. 5-8, pp. 1571–1595, 2018. DOI: 10.1007/s00170-017-1232-y.

[706] Sun, W.; Mu, X.; Sun, Q.; Sun, Z., and Wang, X., "Analysis and optimization of assembly precision-cost model based on 3D tolerance expression," *Assembly Automation*, vol. 38, no. 4, pp. 497–510, 2018. DOI: 10.1108/AA-10-2017-137.

[707] Khodaygan, S., "An interactive method for computer-aided optimal process tolerance design based on automated decision making," *International Journal on Interactive Design and Manufacturing (IJIDeM)*, vol. 13, no. 1, pp. 349–364, 2019. DOI: 10.1007/s12008-018-0462-z.

[708] Saravanan, A. and Jerald, J., "Ontological model-based optimal determination of geometric tolerances in an assembly using the hybridised neural network and Genetic algorithm," *Journal of Engineering Design*, vol. 30, no. 4-5, pp. 180–198, 2019. DOI: 10.1080/09544828.2019.1605585.

[709] Wang, Y.; Li, L.; Hartman, N. W., and Sutherland, J. W., "Allocation of assembly tolerances to minimize costs," *CIRP Annals*, vol. 68, no. 1, pp. 13–16, 2019. DOI: 10.1016/j.cirp.2019.04.027.

[710] Armillotta, A., "Concurrent optimization of dimensions and tolerances on structures and mechanisms," *The International Journal of Advanced Manufacturing Technology*, vol. 111, no. 11-12, pp. 3141–3157, 2020. DOI: 10.1007/s00170-020-06322-6.

[711] Bacharoudis, K.; Popov, A., and Ratchev, S., "Tolerance allocation: A reliability based optimisation approach," *Procedia Manufacturing*, vol. 51, pp. 1038–1045, 2020. DOI: 10.1016/j.promfg.2020.10.146.

[712] He, C.; Zhang, S.; Qiu, L.; Wang, Z.; Wang, Y., and Liu, X., "Statistical tolerance allocation design considering form errors based on rigid assembly simulation and deep Q-network," *The International Journal of Advanced Manufacturing Technology*, vol. 111, no. 11-12, pp. 3029–3045, 2020. DOI: 10.1007/s00170-020-06283-w.

[713] Jing, T.; Tian, X.; Liu, X.; Hu, H.; Zhang, M., and Li, B., "A multiple alternative processes-based cost-tolerance optimal model for aircraft assembly," *The International Journal of Advanced Manufacturing Technology*, vol. 107, no. 1-2, pp. 667–677, 2020. DOI: 10.1007/s00170-020-05020-7.

[714] Velmurugan, S. and Sivakumar, K., "Minimization of Performance Error for A Planar Robot By Tolerance Optimization using an Evolutionary Algorithm," *IOP Conference Series: Materials Science and Engineering*, vol. 1059, no. 1, p. 012 067, 2021. DOI: 10.1088/1757-899X/1059/1/012067.

[715] Wang, J.; Mao, T., and Tu, Y., "Simultaneous multi-response optimisation for parameter and tolerance design using Bayesian modelling method," *International Journal of Production Research*, vol. 59, no. 8, pp. 2269–2293, 2021. DOI: 10.1080/00207543.2020.1730011.

[716] Armillotta, A., "An extended form of the reciprocal-power function for tolerance allocation," *The International Journal of Advanced Manufacturing Technology*, vol. 119, no. 11-12, pp. 8091–8104, 2022. DOI: 10.1007/s00170-021-08579-x.

[717] Kumar Dharmaraj, V.; Durairaj, R.; Lenin, N.; Siva Kumar, M., and Marcel Moshi Antony Joseph Decruz, A., "Minimization of total manufacturing cost of a knuckle joint assembly by means of optimal tolerance allocation using various optimization algorithms," *Proceedings of the Institution of Mechanical Engineers, Part D: Journal*

of Automobile Engineering, vol. 237, no. 4, pp. 816–838, 2022. DOI: 10.1177/09544070221078657.

[718] Miah, M. H.; Zhang, J., and Singh Chand, D., "Knowledge creation and application of optimal tolerance distribution method for aircraft product assembly," *Aircraft Engineering and Aerospace Technology*, vol. 94, no. 3, pp. 431–436, 2022. DOI: 10.1108/AEAT-07-2021-0193.

[719] Brahmia, A.; Kelaiaia, R.; Chemori, A., and Company, O., "On Robust Mechanical Design of a PAR2 Delta-Like Parallel Kinematic Manipulator," *Journal of Mechanisms and Robotics*, vol. 14, no. 1, p. 011 001, 2022. DOI: 10.1115/1.4051360.

[720] Li, Z.; Feng, C.; Li, C.; Zhong, Z., and Sun, Y., "Multi-objective optimization design of assembly tolerance based on improved NSGA-II algorithm," *Proc. SPIE 12344. International Conference on Intelligent and Human-Computer Interaction Technology (IHCIT 2022)*, vol. 12344, Wei, W., Ed., 2022. DOI: 10.1117/12.2655688.

[721] Thilak, M.; Jayaprakash, G.; Paulraj, G.; Bejaxhin, A. B. H.; Nagaprasad, N.; Buddhi, D.; Gupta, M.; Jule, L. T., and Ramaswamy, K., "Non-traditional tolerance design techniques for low machining cost," *International Journal on Interactive Design and Manufacturing (IJIDeM)*, 2022. DOI: 10.1007/s12008-022-00992-0.

[722] Madhavi Reddy, G. V. and Reddy Sreenivasulu, A., "Assembly Gap Tolerance Calculation Using ANFIS and Cost Function Optimization," *International Journal for Research in Applied Science and Engineering Technology*, vol. 10, no. 2, pp. 1111–1117, 2022. DOI: 10.22214/ijraset.2022.40460.

[723] Chen, S. and Su, W., "Tolerance optimization design of RV reducer's cycloid-pin gear pair considering multiple targets," *Proc. of SPIE Vol. 12589. International Conference on Optical Technology, Semiconductor Materials, and Devices (OTSMD 2022)*, vol. 12589, pp. 130–135, 2023. DOI: 10.1117/12.2668420.

[724] Homri, L.; Mirafzal, M. R., and Dantan, J.-Y., "A new tolerance allocation approach based on decision tree and Monte Carlo simulation," *CIRP Annals*, vol. 72, no. 1, pp. 105–108, 2023. DOI: 10.1016/j.cirp.2023.03.017.

[725] Ghali, M.; Elghali, S., and Aifaoui, N., "Genetic algorithm optimization based on manufacturing prediction for an efficient tolerance allocation approach," *Journal of Intelligent Manufacturing*, 2023. DOI: 10.1007/s10845-023-02132-1.

[726] Khezri, A.; Homri, L.; Etienne, A., and Dantan, J.-Y., "Hybrid Cost-Tolerance Allocation and Production Strategy Selection for Complex Mechanisms: Simulation and Surrogate Built-In Optimization Models," *Journal of Computing and Information Science in Engineering*, vol. 23, no. 5, p. 051 003, 2023. DOI: 10.1115/1.4056687.

[727] Khezri, A.; Schiller, V.; Goka, E.; Homri, L.; Etienne, A.; Stamer, F.; Dantan, J.-Y., and Lanza, G., "Evolutionary cost-tolerance optimization for complex assembly mechanisms via simulation and surrogate modeling approaches: Application on micro gears," *The International Journal of Advanced Manufacturing Technology*, vol. 126, no. 9, pp. 4101–4117, 2023. DOI: 10.1007/s00170-023-11360-x.

[728] Liu, X.; Zheng, L.; Wang, Y.; Yang, W.; Wang, B., and Liu, B., "Assembly Error Modeling and Tolerance Dynamic Allocation of Large-Scale Space Deployable Mechanism toward Service Performance," *Applied Sciences*, vol. 13, no. 8, p. 4999, 2023. DOI: 10.3390/app13084999.

[729] Petruccioli, A.; Pini, F., and Leali, F., "Interoperability Framework for a Computer-Aided Approach of Tolerance-Cost Optimization," *Advances on Mechanics, Design Engineering and Manufacturing IV*, Gerbino, S.; Lanzotti, A.; Martorelli, M.; Mirálbes Buil, R.; Rizzi, C., and Roucoules, L., Eds., Cham: Springer International Publishing, 2023, pp. 839–850. DOI: 10.1007/978-3-031-15928-2_73.

[730] Yang, K.; Gan, Y.; Cao, Y.; Yang, J., and Wu, Z., "Optimization of 3D Tolerance Design Based on Cost–Quality–Sensitivity Analysis to the Deviation Domain," *Automation*, vol. 4, no. 2, pp. 123–150, 2023. DOI: 10.3390/automation4020009.

[731] Abdel-Basset, M.; Abdel-Fatah, L., and Sangaiah, A. K., "Metaheuristic Algorithms: A Comprehensive Review," *Computational Intelligence for Multimedia Big Data on the Cloud with Engineering Applications*, Sangaiah, A. K.; Sheng, M., and Zhang, Z., Eds., Academic Press, 2018, pp. 185–231. DOI: 10.1016/B978-0-12-813314-9.00010-4.

[732] Rajabi Moshtaghi, H.; Toloie Eshlaghy, A., and Motadel, M. R., "A comprehensive review on meta-heuristic algorithms and their classification with novel approach," *Journal of Applied Research on Industrial Engineering*, vol. 8, no. 1, pp. 63–89, 2021. DOI: 10.22105/jarie.2021.238926.1180.

[733] Sörensen, K.; Sevaux, M., and Glover, F., "A History of Metaheuristics," *Handbook of Heuristics*, Martí, R.; Pardalos, P. M., and Resende, M. G. C., Eds., Cham: Springer International Publishing, 2018, pp. 791–808. DOI: 10.1007/978-3-319-07124-4_4.

[734] Sivanandam, S. N. and Deepa, S. N., *Introduction to Genetic Algorithms*. Berlin: Springer, 2008.

[735] Gen, M. and Cheng, R., *Genetic Algorithms and Engineering Optimization*, 1st ed. New York: Wiley-Interscience, 2010.

[736] Liang, J. J.; Runarsson, T. P.; Mezura-Montes, E.; Clerc, M.; Suganthan, P. N.; Coello, C. A. C., and Deb, K., "Problem Definitions and Evaluation Criteria for the CEC 2006 Special Session on Constrained Real-Parameter Optimization," *Journal of Applied Mechanics*, vol. 41, no. 8, pp. 8–31, 2006.

[737] Suganthan, P. N.; Hansen, N.; Liang, J. J.; Deb, K.; Chen, Y.-P.; Auger, A., and Tiwari, S., "Problem Definitions and Evaluation Criteria for the CEC 2005 Special Session on Real-Parameter Optimization," Nanyang Technological University Singapore, Tech. Rep. KanGAL report No. 2005005, 2005.

[738] Zhou, A.-H.; Zhu, L.-P.; Hu, B.; Deng, S.; Song, Y.; Qiu, H., and Pan, S., "Traveling-Salesman-Problem Algorithm Based on Simulated Annealing and Gene-Expression Programming," *Information*, vol. 10, no. 1, p. 7, 2018. DOI: 10.3390/info10010007.

[739] Das, S.; Abraham, A.; Chakraborty, U. K., and Konar, A., "Differential Evolution Using a Neighborhood-Based Mutation Operator," *IEEE Transactions on Evolutionary Computation*, vol. 13, no. 3, pp. 526–553, 2009. DOI: 10.1109/TEVC.2008.2009457.

[740] Eiben, A. E. and Smith, J. E., *Introduction to Evolutionary Computing*, 2nd ed., ser. Natural Computing Series. Berlin: Springer, 2015. DOI: 10.1007/978-3-662-44874-8.

[741] Bäck, T., *Evolutionary Algorithms in Theory and Practice: Evolution Strategies, Evolutionary Programming, Genetic Algorithms*. New York: Oxford University Press, 1996.

[742] Goldberg, D. E., *Genetic Algorithms in Search, Optimization, and Machine Learning*. Reading, Massachusetts: Addison-Wesley, 1989.

[743] Haupt, R. L. and Haupt, S. E., *Practical Genetic Algorithms*, 1st ed. Hoboken, New Jersey: Wiley, 2003. DOI: 10.1002/0471671746.

[744] Woodward, R. I. and Kelleher, E. J. R., "Towards 'smart lasers': Self-optimisation of an ultrafast pulse source using a genetic algorithm," *Scientific Reports*, vol. 6, no. 1, p. 37 616, 2016. DOI: 10.1038/srep37616.

[745] Fister, I.; Yang, X.-S.; Fister, D., and Fister, I., "Cuckoo Search: A Brief Literature Review," *Cuckoo Search and Firefly Algorithm*, Yang, X.-S., Ed., vol. 516, Cham: Springer International Publishing, 2014, pp. 49–62. DOI: 10.1007/978-3-319-02141-6_3.

[746] Shehab, M.; Khader, A. T., and Al-Betar, M. A., "A survey on applications and variants of the cuckoo search algorithm," *Applied Soft Computing*, vol. 61, pp. 1041–1059, 2017. DOI: 10.1016/j.asoc.2017.02.034.

[747] Yang, X.-S. and Deb, S., "Cuckoo search: recent advances and applications," *Neural Computing and Applications*, vol. 24, no. 1, pp. 169–174, 2014. DOI: 10.1007/s00521-013-1367-1.

[748] Yang, X.-S. and Deb, S., "Cuckoo Search via Lévy Flights," *2009 World Congress on Nature & Biologically Inspired Computing (NaBIC)*, Coimbatore, India: IEEE, 9.12.-11.12.2009, pp. 210–214. DOI: 10.1109/NABIC.2009.5393690.

[749] Devroye, L., *Non-Uniform Random Variate Generation*. New York: Springer, 1986.

[750] Rubinstein, R. Y. and Kroese, D. P., *Simulation and the Monte Carlo Method*, 3rd ed., ser. Wiley Series in Probability and Statistics. Hoboken, New Jersey: Wiley, 2017.

[751] Lemieux, C., *Monte Carlo and Quasi-Monte Carlo Sampling*, ser. Springer Series in Statistics. New York: Springer, 2009. DOI: 10.1007/978-0-387-78165-5.

[752] Owen, A. B., "Quasi-Monte Carlo Sampling," *Monte Carlo Ray Tracing: Siggraph*, vol. 1, pp. 69–88, 2003.

[753] Kucherenko, S.; Albrecht, D., and Saltelli, A., *Exploring multi-dimensional spaces: A Comparison of Latin Hypercube and Quasi Monte Carlo Sampling Techniques*, 2015. arXiv: 1505.02350. http://arxiv.org/abs/1505.02350.

[754] Keramat, M. and Kielbasa, R., "Modfied Latin Hypercube Sampling Monte Carlo (MLHSMC) Estimation for Average Quality Index," *Analog Integrated Circuits and Signal Processing*, vol. 19, no. 1, pp. 87–98, 1999. DOI: 10.1023/A:1008386501079.

[755] Raj, D., *Sampling Theory*, ser. McGraw-Hill Series in Probability and Statistics. New York: McGraw-Hill, 1968.

[756] McKay, M. D.; Beckman, R. J., and Conover, W. J., "A Comparison of Three Methods for Selecting Values of Input Variables in the Analysis of Output from a Computer Code," *Technometrics*, vol. 21, no. 2, pp. 239–245, 1979. DOI: 10.2307/1268522.

[757] Jin, R.; Chen, W., and Sudjianto, A., "An efficient algorithm for constructing optimal design of computer experiments," *Journal of Statistical Planning and Inference*, vol. 134, no. 1, pp. 268–287, 2005. DOI: 10.1016/j.jspi.2004.02.014.

[758] Morris, M. D. and Mitchell, T. J., "Exploratory designs for computational experiments," *Journal of Statistical Planning and Inference*, vol. 43, no. 3, pp. 381–402, 1995. DOI: 10.1016/0378-3758(94)00035-T.

[759] Sobol', I. M., "On the distribution of points in a cube and the approximate evaluation of integrals," *USSR Computational Mathematics and Mathematical Physics*, vol. 7, no. 4, pp. 86–112, 1967. DOI: 10.1016/0041-5553(67)90144-9.

[760] Kocis, L. and Whiten, W. J., "Computational investigations of low-discrepancy sequences," *ACM Transactions on Mathematical Software*, vol. 23, no. 2, pp. 266–294, 1997. DOI: 10.1145/264029.264064.

[761] Hong, H. S. and Hickernell, F. J., "Algorithm 823: Implementing scrambled digital sequences," *ACM Transactions on Mathematical Software*, vol. 29, no. 2, pp. 95–109, 2003. DOI: 10.1145/779359.779360.

[762] MathWorks, *Generating Quasi-Random Numbers*, 2023. https://de.mathworks.com/help/stats/generating-quasi-random-numbers.html (visited on 03/24/2023).

[763] Joe, S. and Kuo, F. Y., "Remark on algorithm 659: Implementing Sobol's quasirandom sequence generator," *ACM Transactions on Mathematical Software*, vol. 29, no. 1, pp. 49–57, 2003. DOI: 10.1145/641876.641879.

[764] Bratley, P. and Fox, B. L., "Algorithm 659: Implementing Sobol's quasirandom sequence generator," *ACM Transactions on Mathematical Software*, vol. 14, no. 1, pp. 88–100, 1988. DOI: 10.1145/42288.214372.

[765] Kotz, S. and Dorp, J. R. van, *Beyond Beta: Other Continuous Families of Distributions with Bounded Support and Applications*. Singapore: World Scientific, 2004.

[766] Mannewitz, F., *Prozeßfähige Tolerierung von Bauteilen und Baugruppen: ein Lösungsansatz zur Optimierung der Werkstattfertigung im Informationsverbund zwischen CAD und CAQ*, Ph.D. dissertation, Universität Gesamthochschule Kassel, ser. Fortschritt-Berichte / VDI Reihe 20, Rechnerunterstützte Verfahren 256. Düsseldorf: VDI-Verlag, 1997.

[767] Ord, J. K., *Families of Frequency Distributions*, ser. Griffin's Statistical Monographs and Courses no. 30. London: Griffin, 1972.

[768] Rhind, A., "Tables to facilitate the computation of the probable errors of the chief constants of skew frequency distributions," *Biometrika*, vol. 7, no. 1-2, pp. 127–147, 1909. DOI: 10.1093/biomet/7.1-2.127.

[769] Rosenblatt, M., "Remarks on Some Nonparametric Estimates of a Density Function," *The Annals of Mathematical Statistics*, vol. 27, no. 3, pp. 832–837, 1956. DOI: 10.1214/aoms/1177728190.

[770] Epanechnikov, V. A., "Non-Parametric Estimation of a Multivariate Probability Density," *Theory of Probability & Its Applications*, vol. 14, no. 1, pp. 153–158, 1969. DOI: 10.1137/1114019.

[771] Härdle, W.; Werwatz, A.; Müller, M., and Sperlich, S., *Nonparametric and Semiparametric Models*, ser. Springer Series in Statistics. Berlin: Springer, 2004. DOI: 10.1007/978-3-642-17146-8.

[772] Han, J.; Kamber, M., and Pei, J., *Data Mining: Concepts and Techniques*, 3rd ed, ser. The Morgan Kaufmann Series in Data Management Systems. Burlington, MA: Elsevier, 2012.

[773] Tan, P.-N.; Steinbach, M., and Kumar, V., *Introduction to Data Mining*, Pearson international ed., ser. Pearson International Edition. Boston: Pearson Addison-Wesley, 2006.

[774] Witten, I. H.; Frank, E., and Hall, M. A., *Data Mining: Practical Machine Learning Tools and Techniques*, 3rd ed, ser. The Morgan Kaufmann Series in Data Management Systems. Burlington, MA: Morgan Kaufmann, 2011.

[775] Fayyad, U.; Piatetsky-Shapiro, G., and Smyth, P., "From Data Mining to Knowledge Discovery in Databases," *AI Magazine*, vol. 17, no. 3, pp. 37–54, 1996. DOI: 10.1609/aimag.v17i3.1230.

[776] Küstner, C., *Assistenzsystem zur Unterstützung der datengetriebenen Produktentwicklung*, Ph.D. dissertation, Friedrich-Alexander-Universität Erlangen-Nürnberg, ser. FAU Studien aus dem Maschinenbau 353. Erlangen: FAU University Press, 2020. https://doi.org/10.25593/978-3-96147-349-6.

[777] Sprügel, T., *Sphärische Detektorflächen als Unterstützung der Produktentwicklung zur Datenanalyse im Rahmen des Digital Engineering*, Ph.D. dissertation, Friedrich-Alexander-Universität Erlangen-Nürnberg, ser. FAU Studien aus dem Maschinenbau 379. Erlangen: FAU University Press, 2021. https://doi.org/10.25593/978-3-96147-476-9.

[778] Jin, R.; Chen, W., and Simpson, T., "Comparative studies of metamodelling techniques under multiple modelling criteria," *Structural and Multidisciplinary Optimization*, vol. 23, no. 1, pp. 1–13, 2001. DOI: 10.1007/s00158-001-0160-4.

[779] Kiourt, C.; Pavlidis, G., and Markantonatou, S., "Deep Learning Approaches in Food Recognition," *Machine Learning Paradigms.Learning and Analytics in Intelligent Systems*, Tsihrintzis, G. A. and Jain, L. C., Eds., vol. 18, Cham: Springer, 2020, pp. 83–108. DOI: 10.1007/978-3-030-49724-8_4.

[780] Aggarwal, C. C., *Neural Networks and Deep Learning: A Textbook*. Cham: Springer International Publishing, 2018. DOI: 10.1007/978-3-319-94463-0.

[781] Kruse, R.; Borgelt, C.; Klawonn, F.; Moewes, C.; Steinbrecher, M., and Held, P., *Computational Intelligence: A Methodological Introduction*, ser. Texts in Computer Science. London: Springer, 2013. DOI: 10.1007/978-1-4471-5013-8.

[782] Beale, M. H.; Hagan, M. T., and Demuth, H. B., *Neural Network Toolbox™. User's Guide*. 2012.

[783] Livingstone, D.; Manallack, D., and Tetko, I., "Data modelling with neural networks: Advantages and limitations," *Journal of Computer-Aided Molecular Design*, vol. 11, no. 2, pp. 135–142, 1997. DOI: 10.1023/A:1008074223811.

[784] Jin, Y., "Surrogate-assisted evolutionary computation: Recent advances and future challenges," *Swarm and Evolutionary Computation*, vol. 1, no. 2, pp. 61–70, 2011. DOI: 10.1016/j.swevo.2011.05.001.

[785] Jin, Y.; Olhofer, M., and Sendhoff, B., "On Evolutionary Optimization with Approximate Fitness Functions," *Proceedings of the Genetic and Evolutionary Computation Conference GECCO*, pp. 786–793, 2000.

[786] Jin, Y.; Hüsken, M., and Sendhoff, B., "Quality Measures for Approximate Models in Evolutionary Computation," *GECCO 2003: Proceedings of the Bird of a Feather Workshop, Genetic and Evolutionary Computation Conference*, 2003, pp. 170–173.

[787] Syrjälä, T., "Tolerance Design and Coordinate Measurement in Product Development," Helsinki University of Technology, Helsinki, Finland, Master's Thesis, 2004.

[788] Craig, M., "Managing Variation by design using simulation methods," *Failure Prevention and Reliability-1989*, vol. 16, pp. 153–163, 1989.

[789] Wisniewski, D. M. and Gomer, P., "Tolerance Analysis Using VSA-3D® for Engine Applications," *Geometric Design Tolerancing: Theories, Standards and Applications*, ElMaraghy, H. A., Ed., Boston, Massachusetts: Springer, 1998, pp. 453–464. DOI: 10.1007/978-1-4615-5797-5_36.

[790] Rathert, T. A.; Miehling, J.; Wartzack, S.; Biehler, M.; Kramer, V.; Duschl, S., and Kuhn, D., "Verfahren zum Betrieb eines Paares Skates und Skatingsystem," DE102019212389B4, 2022.

[791] Drake, P. J., "Traditional Approaches to Analyzing Mechanical Tolerance Stacks," *Dimensioning and Tolerancing Handbook*, Drake, P. J., Ed., New York: McGraw-Hill, 1999, pp. 9-1–9-39.

[792] Matoušek, J., "On the L2-Discrepancy for Anchored Boxes," *Journal of Complexity*, vol. 14, no. 4, pp. 527–556, 1998. DOI: 10.1006/jcom.1998.0489.

[793] MathWorks, *Ga. Find minimum of function using genetic algorithm*, 2023. https://de.mathworks.com/help/gads/ga.html (visited on 12/04/2022).

[794] Schaeffler Technologies GmbH & Co.KG, *Wälzlager. Technische Grundlagen und Produktdaten zur Gestaltung von Wälzlagerungen*. 2017.

[795] Sunbo Pump, *Slurry Pump Bearing Assembly*, 2022. http://www.sunbopump.com/Pump-Parts/Bearing-Assembly/Slurry-Pump-Bearing-Assembly-143.html (visited on 11/28/2022).

Own publications referring to this work

[P1] Hallmann, M.; Schleich, B., and Wartzack, S., “From tolerance allocation to tolerance-cost optimization: a comprehensive literature review,” *The International Journal of Advanced Manufacturing Technology*, vol. 107, no. 3-4, pp. 4859–4912, 2020. DOI: 10.1007/s00170-020-05254-5.

[P2] Hallmann, M.; Schleich, B., and Wartzack, S., “Sampling-based tolerance analysis: the key to establish tolerance-cost optimization in the product development process,” *Procedia CIRP*, vol. 100, pp. 560–565, 2021. DOI: 10.1016/j.procir.2021.05.123.

[P3] Goetz, S.; Roth, M., and Schleich, B., “Early Robust Design—Its Effect on Parameter and Tolerance Optimization,” *Applied Sciences*, vol. 11, no. 20, p. 9407, 2021. DOI: 10.3390/app11209407.

[P4] Hallmann, M.; Goetz, S., and Schleich, B., “Mapping of GD&T information and PMI between 3D product models in the STEP and STL format,” *Computer-Aided Design*, vol. 115, pp. 293–306, 2019. DOI: 10.1016/j.cad.2019.06.006.

[P5] Hallmann, M.; Schleich, B.; Heling, B.; Aschenbrenner, A., and Wartzack, S., “Comparison of different methods for scrap rate estimation in sampling-based tolerance-cost-optimization,” *Procedia CIRP*, vol. 75, pp. 51–56, 2018. DOI: 10.1016/j.procir.2018.01.005.

[P6] Roth, M.; Schaechtl, P.; Giesert, A.; Schleich, B., and Wartzack, S., “Toward cost-efficient tolerancing of 3D-printed parts: a novel methodology for the development of tolerance-cost models for fused layer modeling,” *The International Journal of Advanced Manufacturing Technology*, vol. 119, no. 11-12, pp. 2461–2478, 2022. DOI: 10.1007/s00170-021-08488-z.

[P7] Brückner, K.; Storch, M.; Hallmann, M.; Heling, B.; Schleich, B., and Wartzack, S., “Ansatz zur Ermittlung von Toleranz-Kosten-Kurven in der Serienfertigung,” *Konstruktion*, vol. 71, no. 11–12, pp. 84–90, 2019. DOI: 10.37544/0720-5953-2019-11-12-84.

[P8] Hallmann, M.; Schleich, B., and Wartzack, S., “Sampling-based Tolerance-Cost Optimization of Systems with Interrelated Key Characteristics,” *Procedia CIRP*, vol. 91, pp. 87–92, 2020. DOI: 10.1016/j.procir.2020.02.153.

[P9] Hallmann, M.; Schleich, B., and Wartzack, S., "Process and machine selection in sampling-based tolerance-cost optimisation for dimensional tolerancing," *International Journal of Production Research*, vol. 60, no. 17, pp. 5201–5216, 2021. DOI: 10.1080/00207543.2021.1951867.

[P10] Hallmann, M.; Schleich, B., and Wartzack, S., "How to consider Overconstrained Assemblies in Tolerance-Cost Optimization," *Procedia CIRP*, vol. 92, pp. 88–93, 2020. DOI: 10.1016/j.procir.2020.05.168.

[P11] Rezaei Aderiani, A.; Hallmann, M.; Wärmefjord, K.; Schleich, B.; Söderberg, R., and Wartzack, S., "Integrated Tolerance and Fixture Layout Design for Compliant Sheet Metal Assemblies," *Applied Sciences*, vol. 11, no. 4, p. 1646, 2021. DOI: 10.3390/app11041646.

[P12] Roth, M.; Seitz, M. J.; Schleich, B., and Wartzack, S., "Coupling Sampling-based Tolerance-Cost Optimization and Selective Assembly – An Integrated Approach for Optimal Tolerance Allocation," *ASME 2022 International Mechanical Engineering Congress and Exposition. Volume 2A: Advanced Manufacturing*, Columbus, Ohio, USA: ASME, 2022, V02AT02A008. DOI: 10.1115/IMECE2022-88775.

[P13] Hallmann, M.; Schleich, B., and Wartzack, S., "Sampling-basierte Toleranz-Kosten-Optimierung - Eine optimierungsbasierte Methode zur Vergabe kostenminimaler Toleranzen," *WiGeP News, Ausgabe 2*, pp. 24–26, 2020.

[P14] Roth, M.; Schleich, B., and Wartzack, S., "Handling Sampling-induced Uncertainties in Tolerance-Cost Optimization," *Procedia CIRP*, vol. 114, pp. 209–214, 2022. DOI: 10.1016/j.procir.2022.10.029.

[P15] Roth, M.; Schleich, B., and Wartzack, S., "Concurrent Machine and Batch Size Selection in Sampling-based Tolerance-Cost Optimization," *Procedia CIRP*, vol. 109, pp. 13–18, 2022. DOI: 10.1016/j.procir.2022.05.207.

[P16] Roth, M.; Freitag, S.; Franz, M.; Goetz, S., and Wartzack, S., "Accelerating Sampling-based Tolerance-Cost Optimisation by Surrogate Modelling," *Engineering Optimization – accepted*, 2024.

[P17] Hallmann, M., "Statistische Toleranz-Kosten-Optimierung mit diskreten Toleranzwerten und mehrstufigem Kostenmodell," *Summer School Toleranzmanagement – Beiträge zur 3. Summer School – September 2017*, (Erlangen), Wartzack, S., Ed., Stamsried: Druck+Verlag Ernst Vögel GmbH, 2017, pp. 17–24.

[P18] Schaechtl, P.; Roth, M.; Goetz, S.; Schleich, B., and Wartzack, S., "Effiziente, prozessorientierte Konformitätsbewertung bei Toleranzsimulationen auf Basis von Klassifikationsmodellen," *Tagungsband der 5. Summer School Toleranzmanagement 2023*, Wartzack, S., Ed., FAU University Press, 2023, pp. 25–32. DOI: 10.25593/978-3-96147-665-7.

[P19] Haigis, N. and Hallmann, M., "Integration kommerzieller Toleranzanalysesoftware in die Toleranz-Kosten-Optimierung," *Summer School Toleranzmanagement – Beiträge zur 4. Summer School – September 2020*, (Erlangen), Wartzack, S., Ed., Stamsried: Druck+Verlag Ernst Vögel GmbH, 2020, pp. 29–36.

Students' theses referring to this work

[S1] Zhan, Y., "Untersuchung der Eignung deterministischer Optimierungsalgorithmen für die Toleranz-Kosten-Optimierung," Projektarbeit, Friedrich-Alexander-Universität Erlangen-Nürnberg, 2019.

[S2] Düngfelder, A., "Systematische Untersuchung varianzreduzierender Samplingverfahren im Kontext der Toleranz-Kosten-Optimierung," Masterarbeit, Friedrich-Alexander-Universität Erlangen-Nürnberg, 2022.

[S3] Giesert, A., "Repräsentation von Form- und Lagetoleranzen in der samplingbasierten Toleranz-Kosten-Optimierung," Projektarbeit, Friedrich-Alexander-Universität Erlangen-Nürnberg, 2021.

[S4] Seitz, M. J., "Integration selektiver Montagemethoden in die Sampling-basierte Toleranz-Kosten-Optimierung," Projektarbeit, Friedrich-Alexander-Universität Erlangen-Nürnberg, 2022.

[S5] Kohl, L., "Entwicklung einer Methode zur Maschinen- und Prozessselektion für die Sampling-basierte Toleranz-Kosten-Optimierung," Projektarbeit, Friedrich-Alexander-Universität Erlangen-Nürnberg, 2020.

[S6] Weisser, G., "Einsatz adaptiver Samplingverfahren in der Toleranz-Kosten-Optimierung," Bachelorarbeit, Friedrich-Alexander-Universität Erlangen-Nürnberg, 2021.

[S7] Kelber, V., "Einsatz von Data Mining und Machine Learning im Kontext der Toleranz-Kosten-Optimierung," Masterarbeit, Friedrich-Alexander-Universität Erlangen-Nürnberg, 2020.

[S8] Freitag, S., "Potentiale und Grenzen des Einsatzes von Surrogate Optimization in der Toleranz-Kosten-Optimierung," Masterarbeit, Friedrich-Alexander-Universität Erlangen-Nürnberg, 2022.

[S9] Zhan, Y., "Untersuchung der Eignung ausgewählter Toleranzanalyseverfahren für die Toleranz-Kosten-Optimierung unterbestimmter Systeme," Masterarbeit, Friedrich-Alexander-Universität Erlangen-Nürnberg, 2019.

[S10] Einwag, J.-M., "Digitale Repräsentation semantischer Informationen für die Toleranz-Kosten-Optimierung," Bachelorarbeit, Friedrich-Alexander-Universität Erlangen-Nürnberg, 2021.

[S11] Christ, S., "Konzeption und Implementierung einer Toleranz-Kosten-Datenbank für die samplingbasierte Toleranz- Kosten-Optimierung," Bachelorarbeit, Friedrich-Alexander-Universität Erlangen-Nürnberg, 2022.

[S12] Giesert, A., "Erhebung von Toleranz-Kosten-Kurven für die Additive Fertigung am Beispiel des Fused-Deposition-Modelings," Bachelorarbeit, Friedrich-Alexander-Universität Erlangen-Nürnberg, 2020.

[S13] Haigis, N., "Grenzen und Potentiale kommerzieller Softwaresysteme für die Toleranzanalyse und -optimierung statisch nicht bestimmter Systeme," Projektarbeit, Friedrich-Alexander-Universität Erlangen-Nürnberg, 2020.

[S14] Haigis, N., "Entwicklung einer Vorgehensweise zur Berücksichtigung von Montagereihenfolgen in der Toleranz-Kosten-Optimierung," Bachelorarbeit, Friedrich-Alexander-Universität Erlangen-Nürnberg, 2019.

Reihenübersicht

Koordination der Reihe (Stand 2024):
Geschäftsstelle Maschinenbau, Dr.-Ing. Oliver Kreis, www.mb.fau.de/diss/

Im Rahmen der Reihe sind bisher die nachfolgenden Bände erschienen.

Band 1 – 52
Fertigungstechnik – Erlangen
ISSN 1431-6226
Carl Hanser Verlag, München

Band 53 – 307
Fertigungstechnik – Erlangen
ISSN 1431-6226
Meisenbach Verlag, Bamberg

ab Band 308
FAU Studien aus dem Maschinenbau
ISSN 2625-9974
FAU University Press, Erlangen

Die Zugehörigkeit zu den jeweiligen Lehrstühlen ist wie folgt gekennzeichnet:

Lehrstühle:

FAPS	Lehrstuhl für Fertigungsautomatisierung und Produktionssystematik
FMT	Lehrstuhl für Fertigungsmesstechnik
KTmfk	Lehrstuhl für Konstruktionstechnik
LFT	Lehrstuhl für Fertigungstechnologie
LGT	Lehrstuhl für Gießereitechnik
LPT	Lehrstuhl für Photonische Technologien
REP	Lehrstuhl für Ressourcen- und Energieeffiziente Produktionsmaschinen

Band 1: Andreas Hemberger
Innovationspotentiale in der rechnerintegrierten Produktion durch wissensbasierte Systeme
FAPS, 208 Seiten, 107 Bilder. 1988.
ISBN 3-446-15234-2.

Band 2: Detlef Classe
Beitrag zur Steigerung der Flexibilität automatisierter Montagesysteme durch Sensorintegration und erweiterte Steuerungskonzepte
FAPS, 194 Seiten, 70 Bilder. 1988.
ISBN 3-446-15529-5.

Band 3: Friedrich-Wilhelm Nolting
Projektierung von Montagesystemen
FAPS, 201 Seiten, 107 Bilder, 1 Tab. 1989.ISBN 3-446-15541-4.

Band 4: Karsten Schlüter
Nutzungsgradsteigerung von Montagesystemen durch den Einsatz der Simulationstechnik
FAPS, 177 Seiten, 97 Bilder. 1989.
ISBN 3-446-15542-2.

Band 5: Shir-Kuan Lin
Aufbau von Modellen zur Lageregelung von Industrierobotern
FAPS, 168 Seiten, 46 Bilder. 1989.
ISBN 3-446-15546-5.

Band 6: Rudolf Nuss
Untersuchungen zur Bearbeitungsqualität im Fertigungssystem Laserstrahlschneiden
LFT, 206 Seiten, 115 Bilder, 6 Tab. 1989. ISBN 3-446-15783-2.

Band 7: Wolfgang Scholz
Modell zur datenbankgestützten Planung automatisierter Montageanlagen
FAPS, 194 Seiten, 89 Bilder. 1989.
ISBN 3-446-15825-1.

Band 8: Hans-Jürgen Wißmeier
Beitrag zur Beurteilung des Bruchverhaltens von Hartmetall-Fließpreßmatrizen
LFT, 179 Seiten, 99 Bilder, 9 Tab. 1989. ISBN 3-446-15921-5.

Band 9: Rainer Eisele
Konzeption und Wirtschaftlichkeit von Planungssystemen in der Produktion
FAPS, 183 Seiten, 86 Bilder. 1990.
ISBN 3-446-16107-4.

Band 10: Rolf Pfeiffer
Technologisch orientierte Montageplanung am Beispiel der Schraubtechnik
FAPS, 216 Seiten, 102 Bilder, 16 Tab. 1990. ISBN 3-446-16161-9.

Band 11: Herbert Fischer
Verteilte Planungssysteme zur Flexibilitätssteigerung der rechnerintegrierten Teilefertigung
FAPS, 201 Seiten, 82 Bilder. 1990.
ISBN 3-446-16105-8.

Band 12: Gerhard Kleineidam
CAD/CAP: Rechnergestützte Montagefeinplanung
FAPS, 203 Seiten, 107 Bilder. 1990.
ISBN 3-446-16112-0.

Band 13: Frank Vollertsen
Pulvermetallurgische Verarbeitung eines übereutektoiden verschleißfesten Stahls
LFT, XIII u. 217 Seiten, 67 Bilder, 34 Tab. 1990.
ISBN 3-446-16133-3.

Band 14: Stephan Biermann
Untersuchungen zur Anlagen- und Prozeßdiagnostik für das Schneiden mit CO2-Hochleistungslasern
LFT, VIII u. 170 Seiten, 93 Bilder, 4 Tab. 1991. ISBN 3-446-16269-0.

Band 15: Uwe Geißler
Material- und Datenfluß in einer flexiblen Blechbearbeitungszelle
LFT, 124 Seiten, 41 Bilder, 7 Tab. 1991. ISBN 3-446-16358-1.

Band 16: Frank Oswald Hake
Entwicklung eines rechnergestützten Diagnosesystems für automatisierte Montagezellen
FAPS, XIV u. 166 Seiten, 77 Bilder. 1991. ISBN 3-446-16428-6.

Band 17: Herbert Reichel
Optimierung der Werkzeugbereitstellung durch rechnergestützte Arbeitsfolgenbestimmung
FAPS, 198 Seiten, 73 Bilder, 2 Tab. 1991. ISBN 3-446-16453-7.

Band 18: Josef Scheller
Modellierung und Einsatz von Softwaresystemen für rechnergeführte Montagezellen
FAPS, 198 Seiten, 65 Bilder. 1991.
ISBN 3-446-16454-5.

Band 19: Arnold vom Ende
Untersuchungen zum Biegeumforme mit elastischer Matrize
LFT, 166 Seiten, 55 Bilder, 13 Tab. 1991. ISBN 3-446-16493-6.

Band 20: Joachim Schmid
Beitrag zum automatisierten Bearbeiten von Keramikguß mit Industrierobotern
FAPS, XIV u. 176 Seiten, 111 Bilder, 6 Tab. 1991.
ISBN 3-446-16560-6.

Band 21: Egon Sommer
Multiprozessorsteuerung für kooperierende Industrieroboter in Montagezellen
FAPS, 188 Seiten, 102 Bilder. 1991.
ISBN 3-446-17062-6.

Band 22: Georg Geyer
Entwicklung problemspezifischer Verfahrensketten in der Montage
FAPS, 192 Seiten, 112 Bilder. 1991.
ISBN 3-446-16552-5.

Band 23: Rainer Flohr
Beitrag zur optimalen Verbindungstechnik in der Oberflächenmontage (SMT)
FAPS, 186 Seiten, 79 Bilder. 1991.
ISBN 3-446-16568-1.

Band 24: Alfons Rief
Untersuchungen zur Verfahrensfolge Laserstrahlschneiden und -schweißen in der Rohkarosseriefertigung
LFT, VI u. 145 Seiten, 58 Bilder, 5 Tab. 1991. ISBN 3-446-16593-2.

Band 25: Christoph Thim
Rechnerunterstützte Optimierung von Materialflußstrukturen in der Elektronikmontage durch Simulation
FAPS, 188 Seiten, 74 Bilder. 1992.
ISBN 3-446-17118-5.

Band 26: Roland Müller
CO2 -Laserstrahlschneiden von kurzglasverstärkten Verbundwerkstoffen
LFT, 141 Seiten, 107 Bilder, 4 Tab. 1992. ISBN 3-446-17104-5.

Band 27: Günther Schäfer
Integrierte Informationsverarbeitung bei der Montageplanung
FAPS, 195 Seiten, 76 Bilder. 1992.
ISBN 3-446-17117-7.

Band 28: Martin Hoffmann
Entwicklung einerCAD/CAM-Prozeßkette für die Herstellung von Blechbiegeteilen
LFT, 149 Seiten, 89 Bilder. 1992.
ISBN 3-446-17154-1.

Band 29: Peter Hoffmann
Verfahrensfolge Laserstrahlschneiden und –schweißen: Prozeßführung und Systemtechnik in der 3D-Laserstrahlbearbeitung von Blechformteilen
LFT, 186 Seiten, 92 Bilder, 10 Tab.
1992. ISBN 3-446-17153-3.

Band 30: Olaf Schrödel
Flexible Werkstattsteuerung mit objektorientierten Softwarestrukturen
FAPS, 180 Seiten, 84 Bilder. 1992.
ISBN 3-446-17242-4.

Band 31: Hubert Reinisch
Planungs- und Steuerungswerkzeuge zur impliziten Geräteprogrammierung in Roboterzellen
FAPS, XI u. 212 Seiten, 112 Bilder.
1992. ISBN 3-446-17380-3.

Band 32: Brigitte Bärnreuther
Ein Beitrag zur Bewertung des Kommunikationsverhaltens von Automatisierungsgeräten in flexiblen Produktionszellen
FAPS, XI u. 179 Seiten, 71 Bilder.
1992. ISBN 3-446-17451-6.

Band 33: Joachim Hutfless
Laserstrahlregelung und Optikdiagnostik in der Strahlführung einer CO_2-Hochleistungslaseranlage
LFT, 175 Seiten, 70 Bilder, 17 Tab.
1993. ISBN 3-446-17532-6.

Band 34: Uwe Günzel
Entwicklung und Einsatz eines Simula-tionsverfahrens für operative undstrategische Probleme der Produktionsplanung und -steuerung
FAPS, XIV u. 170 Seiten, 66 Bilder, 5 Tab. 1993. ISBN 3-446-17604-7.

Band 35: Bertram Ehmann
Operatives Fertigungscontrolling durch Optimierung auftragsbezogener Bearbeitungsabläufe in der Elektronikfertigung
FAPS, XV u. 167 Seiten, 114 Bilder.
1993. ISBN 3-446-17658-6.

Band 36: Harald Kolléra
Entwicklung eines benutzerorientierten Werkstattprogrammiersystems für das Laserstrahlschneiden
LFT, 129 Seiten, 66 Bilder, 1 Tab.
1993. ISBN 3-446-17719-1.

Band 37: Stephanie Abels
Modellierung und Optimierung von Montageanlagen in einem integrierten Simulationssystem
FAPS, 188 Seiten, 88 Bilder. 1993.
ISBN 3-446-17731-0.

Band 38: Robert Schmidt-Hebbel
Laserstrahlbohren durchflußbestimmender Durchgangslöcher
LFT, 145 Seiten, 63 Bilder, 11 Tab.
1993. ISBN 3-446-17778-7.

Band 39: Norbert Lutz
Oberflächenfeinbearbeitung keramischer Werkstoffe mit XeCl-Excimerlaserstrahlung
LFT, 187 Seiten, 98 Bilder, 29 Tab.
1994. ISBN 3-446-17970-4.

Band 40: Konrad Grampp
Rechnerunterstützung bei Test und Schulung an Steuerungssoftware von SMD-Bestücklinien
FAPS, 178 Seiten, 88 Bilder. 1995.
ISBN 3-446-18173-3.

Band 41: Martin Koch
Wissensbasierte Unterstützung derAngebotsbearbeitung in der Investitionsgüterindustrie
FAPS, 169 Seiten, 68 Bilder. 1995.
ISBN 3-446-18174-1.

Band 42: Armin Gropp
Anlagen- und Prozeßdiagnostik beim Schneiden mit einem gepulsten Nd:YAG-Laser
LFT, 160 Seiten, 88 Bilder, 7 Tab.
1995. ISBN 3-446-18241-1.

Band 43: Werner Heckel
Optische 3D-Konturerfassung und on-line Biegewinkelmessung mit dem Lichtschnittverfahren
LFT, 149 Seiten, 43 Bilder, 11 Tab.
1995. ISBN 3-446-18243-8.

Band 44: Armin Rothhaupt
Modulares Planungssystem zur Optimierung der Elektronikfertigung
FAPS, 180 Seiten, 101 Bilder. 1995.
ISBN 3-446-18307-8.

Band 45: Bernd Zöllner
Adaptive Diagnose in der Elektronikproduktion
FAPS, 195 Seiten, 74 Bilder, 3 Tab.
1995. ISBN 3-446-18308-6.

Band 46: Bodo Vormann
Beitrag zur automatisierten Handhabungsplanung komplexer Blechbiegeteile
LFT, 126 Seiten, 89 Bilder, 3 Tab.
1995. ISBN 3-446-18345-0.

Band 47: Peter Schnepf
Zielkostenorientierte Montageplanung
FAPS, 144 Seiten, 75 Bilder. 1995.
ISBN 3-446-18397-3.

Band 48: Rainer Klotzbücher
Konzept zur rechnerintegrierten Materialversorgung in flexiblen Fertigungssystemen
FAPS, 156 Seiten, 62 Bilder. 1995.
ISBN 3-446-18412-0.

Band 49: Wolfgang Greska
Wissensbasierte Analyse undKlassifizierung von Blechteilen
LFT, 144 Seiten, 96 Bilder. 1995.
ISBN 3-446-18462-7.

Band 50: Jörg Franke
Integrierte Entwicklung neuer Produkt- und Produktionstechnologien für räumliche spritzgegossene Schaltungsträger (3-D MID)
FAPS, 196 Seiten, 86 Bilder, 4 Tab.
1995. ISBN 3-446-18448-1.

Band 51: Franz-Josef Zeller
Sensorplanung und schnelle Sensorregelung für Industrieroboter
FAPS, 190 Seiten, 102 Bilder, 9 Tab.
1995. ISBN 3-446-18601-8.

Band 52: Michael Solvie
Zeitbehandlung und Multimedia-Unterstützung in Feldkommunikationssystemen
FAPS, 200 Seiten, 87 Bilder, 35 Tab. 1996. ISBN 3-446-18607-7.

Band 53: Robert Hopperdietzel
Reengineering in der Elektro- und Elektronikindustrie
FAPS, 180 Seiten, 109 Bilder, 1 Tab.
1996. ISBN 3-87525-070-2.

Band 54: Thomas Rebhahn
Beitrag zur Mikromaterialbearbeitung mit Excimerlasern - Systemkomponenten und Verfahrensoptimierungen
LFT, 148 Seiten, 61 Bilder, 10 Tab.
1996. ISBN 3-87525-075-3.

Band 55: Henning Hanebuth
Laserstrahlhartlöten mit Zweistrahltechnik
LFT, 157 Seiten, 58 Bilder, 11 Tab.
1996. ISBN 3-87525-074-5.

Band 56: Uwe Schönherr
Steuerung und Sensordatenintegration für flexible Fertigungszellen mitkooperierenden Robotern
FAPS, 188 Seiten, 116 Bilder, 3 Tab.
1996. ISBN 3-87525-076-1.

Band 57: Stefan Holzer
Berührungslose Formgebung mit-Laserstrahlung
LFT, 162 Seiten, 69 Bilder, 11 Tab.
1996. ISBN 3-87525-079-6.

Band 58: Markus Schultz
Fertigungsqualität beim 3D-Laserstrahlschweißen vonBlechformteilen
LFT, 165 Seiten, 88 Bilder, 9 Tab.
1997. ISBN 3-87525-080-X.

Band 59: Thomas Krebs
Integration elektromechanischer CA-Anwendungen über einem STEP-Produktmodell
FAPS, 198 Seiten, 58 Bilder, 8 Tab.
1997. ISBN 3-87525-081-8.

Band 60: Jürgen Sturm
Prozeßintegrierte Qualitätssicherung in der Elektronikproduktion
FAPS, 167 Seiten, 112 Bilder, 5 Tab.
1997. ISBN 3-87525-082-6.

Band 61: Andreas Brand
Prozesse und Systeme zur Bestückung räumlicher elektronischer Baugruppen (3D-MID)
FAPS, 182 Seiten, 100 Bilder. 1997.
ISBN 3-87525-087-7.

Band 62: Michael Kauf
Regelung der Laserstrahlleistung und der Fokusparameter einer CO_2-Hochleistungslaseranlage
LFT, 140 Seiten, 70 Bilder, 5 Tab.
1997. ISBN 3-87525-083-4.

Band 63: Peter Steinwasser
Modulares Informationsmanagement in der integrierten Produkt- und Prozeßplanung
FAPS, 190 Seiten, 87 Bilder. 1997.
ISBN 3-87525-084-2.

Band 64: Georg Liedl
Integriertes Automatisierungskonzept für den flexiblen Materialfluß in der Elektronikproduktion
FAPS, 196 Seiten, 96 Bilder, 3 Tab.
1997. ISBN 3-87525-086-9.

Band 65: Andreas Otto
Transiente Prozesse beim Laserstrahlschweißen
LFT, 132 Seiten, 62 Bilder, 1 Tab.
1997. ISBN 3-87525-089-3.

Band 66: Wolfgang Blöchl
Erweiterte Informationsbereitstellung an offenen CNC-Steuerungen zur Prozeß- und Programmoptimierung
FAPS, 168 Seiten, 96 Bilder. 1997.
ISBN 3-87525-091-5.

Band 67: Klaus-Uwe Wolf
Verbesserte Prozeßführung und Prozeßplanung zur Leistungs- und Qualitätssteigerung beim Spulenwickeln
FAPS, 186 Seiten, 125 Bilder. 1997.
ISBN 3-87525-092-3.

Band 68: Frank Backes
Technologieorientierte Bahnplanung für die 3D-Laserstrahlbearbeitung
LFT, 138 Seiten, 71 Bilder, 2 Tab.
1997. ISBN 3-87525-093-1.

Band 69: Jürgen Kraus
Laserstrahlumformen von Profilen
LFT, 137 Seiten, 72 Bilder, 8 Tab.
1997. ISBN 3-87525-094-X.

Band 70: Norbert Neubauer
Adaptive Strahlführungen für CO_2-Laseranlagen
LFT, 120 Seiten, 50 Bilder, 3 Tab.
1997. ISBN 3-87525-095-8.

Band 71: Michael Steber
Prozeßoptimierter Betrieb flexibler Schraubstationen in der automatisierten Montage
FAPS, 168 Seiten, 78 Bilder, 3 Tab.
1997. ISBN 3-87525-096-6.

Band 72: Markus Pfestorf
Funktionale 3D-Oberflächenkenngrößen in der Umformtechnik
LFT, 162 Seiten, 84 Bilder, 15 Tab.
1997. ISBN 3-87525-097-4.

Band 73: Volker Franke
Integrierte Planung und Konstruktion von Werkzeugen für die Biegebearbeitung
LFT, 143 Seiten, 81 Bilder. 1998.
ISBN 3-87525-098-2.

Band 74: Herbert Scheller
Automatisierte Demontagesysteme und recyclinggerechte Produktgestaltung elektronischer Baugruppen
FAPS, 184 Seiten, 104 Bilder, 17 Tab. 1998. ISBN 3-87525-099-0.

Band 75: Arthur Meßner
Kaltmassivumformung metallischer Kleinstteile – Werkstoffverhalten, Wirkflächenreibung, Prozeßauslegung
LFT, 164 Seiten, 92 Bilder, 14 Tab.
1998. ISBN 3-87525-100-8.

Band 76: Mathias Glasmacher
Prozeß- und Systemtechnik zum Laserstrahl-Mikroschweißen
LFT, 184 Seiten, 104 Bilder, 12 Tab.
1998. ISBN 3-87525-101-6.

Band 77: Michael Schwind
Zerstörungsfreie Ermittlung mechanischer Eigenschaften von Feinblechen mit dem Wirbelstromverfahren
LFT, 124 Seiten, 68 Bilder, 8 Tab.
1998. ISBN 3-87525-102-4.

Band 78: Manfred Gerhard
Qualitätssteigerung in der Elektronikproduktion durch Optimierung der Prozeßführung beim Löten komplexer Baugruppen
FAPS, 179 Seiten, 113 Bilder, 7 Tab.
1998. ISBN 3-87525-103-2.

Band 79: Elke Rauh
Methodische Einbindung der Simulation in die betrieblichen Planungs- und Entscheidungsabläufe
FAPS, 192 Seiten, 114 Bilder, 4 Tab.
1998. ISBN 3-87525-104-0.

Band 80: Sorin Niederkorn
Meßeinrichtung zur Untersuchung der Wirkflächenreibung bei umformtechnischen Prozessen
LFT, 99 Seiten, 46 Bilder, 6 Tab. 1998. ISBN 3-87525-105-9.

Band 81: Stefan Schuberth
Regelung der Fokuslage beim Schweißen mit CO2-Hochleistungslasern unter Einsatz von adaptiven Optiken
LFT, 140 Seiten, 64 Bilder, 3 Tab. 1998. ISBN 3-87525-106-7.

Band 82: Armando Walter Colombo
Development and Implementation of Hierarchical Control Structures of Flexible Production Systems Using High Level Petri Nets
FAPS, 216 Seiten, 86 Bilder. 1998. ISBN 3-87525-109-1.

Band 83: Otto Meedt
Effizienzsteigerung bei Demontage und Recycling durch flexible Demontagetechnologien und optimierte Produktgestaltung
FAPS, 186 Seiten, 103 Bilder. 1998. ISBN 3-87525-108-3.

Band 84: Knuth Götz
Modelle und effiziente Modellbildung zur Qualitätssicherung in der Elektronikproduktion
FAPS, 212 Seiten, 129 Bilder, 24 Tab. 1998. ISBN 3-87525-112-1.

Band 85: Ralf Luchs
Einsatzmöglichkeiten leitender Klebstoffe zur zuverlässigen Kontaktierung elektronischer Bauelemente in der SMT
FAPS, 176 Seiten, 126 Bilder, 30 Tab. 1998. ISBN 3-87525-113-7.

Band 86: Frank Pöhlau
Entscheidungsgrundlagen zur Einführung räumlicher spritzgegossener Schaltungsträger (3-D MID)
FAPS, 144 Seiten, 99 Bilder. 1999. ISBN 3-87525-114-8.

Band 87: Roland T. A. Kals
Fundamentals on the miniaturization of sheet metal working processes
LFT, 128 Seiten, 58 Bilder, 11 Tab. 1999. ISBN 3-87525-115-6.

Band 88: Gerhard Luhn
Implizites Wissen und technisches Handeln am Beispiel der Elektronikproduktion
FAPS, 252 Seiten, 61 Bilder, 1 Tab. 1999. ISBN 3-87525-116-4.

Band 89: Axel Sprenger
Adaptives Streckbiegen von Aluminium-Strangpreßprofilen
LFT, 114 Seiten, 63 Bilder, 4 Tab. 1999. ISBN 3-87525-117-2.

Band 90: Hans-Jörg Pucher
Untersuchungen zur Prozeßfolge Umformen, Bestücken und Laserstrahllöten von Mikrokontakten
LFT, 158 Seiten, 69 Bilder, 9 Tab. 1999. ISBN 3-87525-119-9.

Band 91: Horst Arnet
Profilbiegen mit kinematischer Gestalterzeugung
LFT, 128 Seiten, 67 Bilder, 7 Tab. 1999. ISBN 3-87525-120-2.

Band 92: Doris Schubart
Prozeßmodellierung und Technologieentwicklung beim Abtragen mit CO2-Laserstrahlung
LFT, 133 Seiten, 57 Bilder, 13 Tab. 1999. ISBN 3-87525-122-9.

Band 93: Adrianus L. P. Coremans
Laserstrahlsintern von Metallpulver - Prozeßmodellierung, Systemtechnik, Eigenschaften laserstrahlgesinterter Metallkörper
LFT, 184 Seiten, 108 Bilder, 12 Tab. 1999. ISBN 3-87525-124-5.

Band 94: Hans-Martin Biehler
Optimierungskonzepte für Qualitätsdatenverarbeitung und Informationsbereitstellung in der Elektronikfertigung
FAPS, 194 Seiten, 105 Bilder. 1999. ISBN 3-87525-126-1.

Band 95: Wolfgang Becker
Oberflächenausbildung und tribologische Eigenschaften excimerlaserstrahlbearbeiteter Hochleistungskeramiken
LFT, 175 Seiten, 71 Bilder, 3 Tab. 1999. ISBN 3-87525-127-X.

Band 96: Philipp Hein
Innenhochdruck-Umformen von Blechpaaren: Modellierung, Prozeßauslegung und Prozeßführung
LFT, 129 Seiten, 57 Bilder, 7 Tab. 1999. ISBN 3-87525-128-8.

Band 97: Gunter Beitinger
Herstellungs- und Prüfverfahren für thermoplastische Schaltungsträger
FAPS, 169 Seiten, 92 Bilder, 20 Tab. 1999. ISBN 3-87525-129-6.

Band 98: Jürgen Knoblach
Beitrag zur rechnerunterstützten verursachungsgerechten Angebotskalkulation von Blechteilen mit Hilfe wissensbasierter Methoden
LFT, 155 Seiten, 53 Bilder, 26 Tab. 1999. ISBN 3-87525-130-X.

Band 99: Frank Breitenbach
Bildverarbeitungssystem zur Erfassung der Anschlußgeometrie elektronischer SMT-Bauelemente
LFT, 147 Seiten, 92 Bilder, 12 Tab. 2000. ISBN 3-87525-131-8.

Band 100: Bernd Falk
Simulationsbasierte Lebensdauervorhersage für Werkzeuge der Kaltmassivumformung
LFT, 134 Seiten, 44 Bilder, 15 Tab. 2000. ISBN 3-87525-136-9.

Band 101: Wolfgang Schlögl
Integriertes Simulationsdaten-Management für Maschinenentwicklung und Anlagenplanung
FAPS, 169 Seiten, 101 Bilder, 20 Tab. 2000. ISBN 3-87525-137-7.

Band 102: Christian Hinsel
Ermüdungsbruchversagen hartstoffbeschichteter Werkzeugstähle in der Kaltmassivumformung
LFT, 130 Seiten, 80 Bilder, 14 Tab. 2000. ISBN 3-87525-138-5.

Band 103: Stefan Bobbert
Simulationsgestützte Prozessauslegung für das Innenhochdruck-Umformen von Blechpaaren
LFT, 123 Seiten, 77 Bilder. 2000. ISBN 3-87525-145-8.

Band 104: Harald Rottbauer
Modulares Planungswerkzeug zum Produktionsmanagement in der Elektronikproduktion
FAPS, 166 Seiten, 106 Bilder. 2001.
ISBN 3-87525-139-3.

Band 105: Thomas Hennige
Flexible Formgebung von Blechen durch Laserstrahlumformen
LFT, 119 Seiten, 50 Bilder. 2001.
ISBN 3-87525-140-7.

Band 106: Thomas Menzel
Wissensbasierte Methoden für die rechnergestützte Charakterisierung und Bewertung innovativer Fertigungsprozesse
LFT, 152 Seiten, 71 Bilder. 2001.
ISBN 3-87525-142-3.

Band 107: Thomas Stöckel
Kommunikationstechnische Integration der Prozeßebene in Produktionssysteme durch Middleware-Frameworks
FAPS, 147 Seiten, 65 Bilder, 5 Tab.
2001. ISBN 3-87525-143-1.

Band 108: Frank Pitter
Verfügbarkeitssteigerung von Werkzeugmaschinen durch Einsatz mechatronischer Sensorlösungen
FAPS, 158 Seiten, 131 Bilder, 8 Tab.
2001. ISBN 3-87525-144-X.

Band 109: Markus Korneli
Integration lokaler CAP-Systeme in einen globalen Fertigungsdatenverbund
FAPS, 121 Seiten, 53 Bilder, 11 Tab.
2001. ISBN 3-87525-146-6.

Band 110: Burkhard Müller
Laserstrahljustieren mit Excimer-Lasern - Prozeßparameter und Modelle zur Aktorkonstruktion
LFT, 128 Seiten, 36 Bilder, 9 Tab.
2001. ISBN 3-87525-159-8.

Band 111: Jürgen Göhringer
Integrierte Telediagnose via Internet zum effizienten Service von Produktionssystemen
FAPS, 178 Seiten, 98 Bilder, 5 Tab.
2001. ISBN 3-87525-147-4.

Band 112: Robert Feuerstein
Qualitäts- und kosteneffiziente Integration neuer Bauelementetechnologien in die Flachbaugruppenfertigung
FAPS, 161 Seiten, 99 Bilder, 10 Tab.
2001. ISBN 3-87525-151-2.

Band 113: Marcus Reichenberger
Eigenschaften und Einsatzmöglichkeiten alternativer Elektroniklote in der Oberflächenmontage (SMT)
FAPS, 165 Seiten, 97 Bilder, 18 Tab.
2001. ISBN 3-87525-152-0.

Band 114: Alexander Huber
Justieren vormontierter Systeme mit dem Nd:YAG-Laser unter Einsatz von Aktoren
LFT, 122 Seiten, 58 Bilder, 5 Tab.
2001. ISBN 3-87525-153-9.

Band 115: Sami Krimi
Analyse und Optimierung von Montagesystemen in der Elektronikproduktion
FAPS, 155 Seiten, 88 Bilder, 3 Tab.
2001. ISBN 3-87525-157-1.

Band 116: Marion Merklein
Laserstrahlumformen von Aluminiumwerkstoffen - Beeinflussung der Mikrostruktur und der mechanischen Eigenschaften
LFT, 122 Seiten, 65 Bilder, 15 Tab.
2001. ISBN 3-87525-156-3.

Band 117: Thomas Collisi
Ein informationslogistisches Architekturkonzept zur Akquisition simulationsrelevanter Daten
FAPS, 181 Seiten, 105 Bilder, 7 Tab.
2002. ISBN 3-87525-164-4.

Band 118: Markus Koch
Rationalisierung und ergonomische Optimierung im Innenausbau durch den Einsatz moderner Automatisierungstechnik
FAPS, 176 Seiten, 98 Bilder, 9 Tab.
2002. ISBN 3-87525-165-2.

Band 119: Michael Schmidt
Prozeßregelung für das Laserstrahl-Punktschweißen in der Elektronikproduktion
LFT, 152 Seiten, 71 Bilder, 3 Tab.
2002. ISBN 3-87525-166-0.

Band 120: Nicolas Tiesler
Grundlegende Untersuchungen zum Fließpressen metallischer Kleinstteile
LFT, 126 Seiten, 78 Bilder, 12 Tab.
2002. ISBN 3-87525-175-X.

Band 121: Lars Pursche
Methoden zur technologieorientierten Programmierung für die 3D-Lasermikrobearbeitung
LFT, 111 Seiten, 39 Bilder, 0 Tab.
2002. ISBN 3-87525-183-0.

Band 122: Jan-Oliver Brassel
Prozeßkontrolle beim Laserstrahl-Mikroschweißen
LFT, 148 Seiten, 72 Bilder, 12 Tab.
2002. ISBN 3-87525-181-4.

Band 123: Mark Geisel
Prozeßkontrolle und -steuerung beim Laserstrahlschweißen mit den Methoden der nichtlinearen Dynamik
LFT, 135 Seiten, 46 Bilder, 2 Tab.
2002. ISBN 3-87525-180-6.

Band 124: Gerd Eßer
Laserstrahlunterstützte Erzeugung metallischer Leiterstrukturen auf Thermoplastsubstraten für die MID-Technik
LFT, 148 Seiten, 60 Bilder, 6 Tab.
2002. ISBN 3-87525-171-7.

Band 125: Marc Fleckenstein
Qualität laserstrahl-gefügter Mikroverbindungen elektronischer Kontakte
LFT, 159 Seiten, 77 Bilder, 7 Tab.
2002. ISBN 3-87525-170-9.

Band 126: Stefan Kaufmann
Grundlegende Untersuchungen zum Nd:YAG- Laserstrahlfügen von Silizium für Komponenten der Optoelektronik
LFT, 159 Seiten, 100 Bilder, 6 Tab.
2002. ISBN 3-87525-172-5.

Band 127: Thomas Fröhlich
Simultanes Löten von Anschlußkontakten elektronischer Bauelemente mit Diodenlaserstrahlung
LFT, 143 Seiten, 75 Bilder, 6 Tab.
2002. ISBN 3-87525-186-5.

Band 128: Achim Hofmann
Erweiterung der Formgebungsgrenzen beim Umformen von Aluminiumwerkstoffen durch den Einsatz prozessangepasster Platinen
LFT, 113 Seiten, 58 Bilder, 4 Tab. 2002. ISBN 3-87525-182-2.

Band 129: Ingo Kriebitzsch
3 - D MID Technologie in der Automobilelektronik
FAPS, 129 Seiten, 102 Bilder, 10 Tab. 2002. ISBN 3-87525-169-5.

Band 130: Thomas Pohl
Fertigungsqualität und Umformbarkeit laserstrahlgeschweißter Formplatinen aus Aluminiumlegierungen
LFT, 133 Seiten, 93 Bilder, 12 Tab. 2002. ISBN 3-87525-173-3.

Band 131: Matthias Wenk
Entwicklung eines konfigurierbaren Steuerungssystems für die flexible Sensorführung von Industrierobotern
FAPS, 167 Seiten, 85 Bilder, 1 Tab. 2002. ISBN 3-87525-174-1.

Band 132: Matthias Negendanck
Neue Sensorik und Aktorik für Bearbeitungsköpfe zum Laserstrahlschweißen
LFT, 116 Seiten, 60 Bilder, 14 Tab. 2002. ISBN 3-87525-184-9.

Band 133: Oliver Kreis
Integrierte Fertigung - Verfahrensintegration durch Innenhochdruck-Umformen, Trennen und Laserstrahlschweißen in einem Werkzeug sowie ihre tele- und multimediale Präsentation
LFT, 167 Seiten, 90 Bilder, 43 Tab. 2002. ISBN 3-87525-176-8.

Band 134: Stefan Trautner
Technische Umsetzung produktbezogener Instrumente der Umweltpolitik bei Elektro- und Elektronikgeräten
FAPS, 179 Seiten, 92 Bilder, 11 Tab. 2002. ISBN 3-87525-177-6.

Band 135: Roland Meier
Strategien für einen produktorientierten Einsatz räumlicher spritzgegossener Schaltungsträger (3-D MID)
FAPS, 155 Seiten, 88 Bilder, 14 Tab. 2002. ISBN 3-87525-178-4.

Band 136: Jürgen Wunderlich
Kostensimulation - Simulationsbasierte Wirtschaftlichkeitsregelung komplexer Produktionssysteme
FAPS, 202 Seiten, 119 Bilder, 17 Tab. 2002. ISBN 3-87525-179-2.

Band 137: Stefan Novotny
Innenhochdruck-Umformen von Blechen aus Aluminium- und Magnesiumlegierungen bei erhöhter Temperatur
LFT, 132 Seiten, 82 Bilder, 6 Tab. 2002. ISBN 3-87525-185-7.

Band 138: Andreas Licha
Flexible Montageautomatisierung zur Komplettmontage flächenhafter Produktstrukturen durch kooperierende Industrieroboter
FAPS, 158 Seiten, 87 Bilder, 8 Tab. 2003. ISBN 3-87525-189-X.

Band 139: Michael Eisenbarth
Beitrag zur Optimierung der Aufbau- und Verbindungstechnik für mechatronische Baugruppen
FAPS, 207 Seiten, 141 Bilder, 9 Tab. 2003. ISBN 3-87525-190-3.

Band 140: Frank Christoph
Durchgängige simulationsgestützte Planung von Fertigungseinrichtungen der Elektronikproduktion
FAPS, 187 Seiten, 107 Bilder, 9 Tab. 2003. ISBN 3-87525-191-1.

Band 141: Hinnerk Hagenah
Simulationsbasierte Bestimmung der zu erwartenden Maßhaltigkeit für das Blechbiegen
LFT, 131 Seiten, 36 Bilder, 26 Tab. 2003. ISBN 3-87525-192-X.

Band 142: Ralf Eckstein
Scherschneiden und Biegen metallischer Kleinstteile - Materialeinfluss und Materialverhalten
LFT, 148 Seiten, 71 Bilder, 19 Tab. 2003. ISBN 3-87525-193-8.

Band 143: Frank H. Meyer-Pittroff
Excimerlaserstrahlbiegen dünner metallischer Folien mit homogener Lichtlinie
LFT, 138 Seiten, 60 Bilder, 16 Tab. 2003. ISBN 3-87525-196-2.

Band 144: Andreas Kach
Rechnergestützte Anpassung von Laserstrahlschneidbahnen an Bauteilabweichungen
LFT, 139 Seiten, 69 Bilder, 11 Tab. 2004. ISBN 3-87525-197-0.

Band 145: Stefan Hierl
System- und Prozeßtechnik für das simultane Löten mit Diodenlaserstrahlung von elektronischen Bauelementen
LFT, 124 Seiten, 66 Bilder, 4 Tab. 2004. ISBN 3-87525-198-9.

Band 146: Thomas Neudecker
Tribologische Eigenschaften keramischer Blechumformwerkzeuge-Einfluss einer Oberflächenendbearbeitung mittels Excimerlaserstrahlung
LFT, 166 Seiten, 75 Bilder, 26 Tab. 2004. ISBN 3-87525-200-4.

Band 147: Ulrich Wenger
Prozessoptimierung in der Wickeltechnik durch innovative maschinenbauliche und regelungstechnische Ansätze
FAPS, 132 Seiten, 88 Bilder, 0 Tab. 2004. ISBN 3-87525-203-9.

Band 148: Stefan Slama
Effizienzsteigerung in der Montage durch marktorientierte Montagestrukturen und erweiterte Mitarbeiterkompetenz
FAPS, 188 Seiten, 125 Bilder, 0 Tab. 2004. ISBN 3-87525-204-7.

Band 149: Thomas Wurm
Laserstrahljustieren mittels Aktoren-Entwicklung von Konzepten und Methoden für die rechnerunterstützte Modellierung und Optimierung von komplexen Aktorsystemen in der Mikrotechnik
LFT, 122 Seiten, 51 Bilder, 9 Tab. 2004. ISBN 3-87525-206-3.

Band 150: Martino Celeghini
Wirkmedienbasierte Blechumformung: Grundlagenuntersuchungen zum Einfluss von Werkstoff und Bauteilgeometrie
LFT, 146 Seiten, 77 Bilder, 6 Tab.
2004. ISBN 3-87525-207-1.

Band 151: Ralph Hohenstein
Entwurf hochdynamischer Sensor- und Regelsysteme für die adaptiveLaserbearbeitung
LFT, 282 Seiten, 63 Bilder, 16 Tab.
2004. ISBN 3-87525-210-1.

Band 152: Angelika Hutterer
Entwicklung prozessüberwachender Regelkreise für flexible Formgebungsprozesse
LFT, 149 Seiten, 57 Bilder, 2 Tab.
2005. ISBN 3-87525-212-8.

Band 153: Emil Egerer
Massivumformen metallischer Kleinstteile bei erhöhter Prozesstemperatur
LFT, 158 Seiten, 87 Bilder, 10 Tab.
2005. ISBN 3-87525-213-6.

Band 154: Rüdiger Holzmann
Strategien zur nachhaltigen Optimierung von Qualität und Zuverlässigkeit in der Fertigung hochintegrierter Flachbaugruppen
FAPS, 186 Seiten, 99 Bilder, 19 Tab.
2005. ISBN 3-87525-217-9.

Band 155: Marco Nock
Biegeumformen mit Elastomerwerkzeugen Modellierung, Prozessauslegung und Abgrenzung des Verfahrens am Beispiel des Rohrbiegens
LFT, 164 Seiten, 85 Bilder, 13 Tab.
2005. ISBN 3-87525-218-7.

Band 156: Frank Niebling
Qualifizierung einer Prozesskette zum Laserstrahlsintern metallischer Bauteile
LFT, 148 Seiten, 89 Bilder, 3 Tab.
2005. ISBN 3-87525-219-5.

Band 157: Markus Meiler
Großserientauglichkeit trockenschmierstoffbeschichteter Aluminiumbleche im Presswerk Grundlegende Untersuchungen zur Tribologie, zum Umformverhalten und Bauteilversuche
LFT, 104 Seiten, 57 Bilder, 21 Tab.
2005. ISBN 3-87525-221-7.

Band 158: Agus Sutanto
Solution Approaches for Planning of Assembly Systems in Three-Dimensional Virtual Environments
FAPS, 169 Seiten, 98 Bilder, 3 Tab.
2005. ISBN 3-87525-220-9.

Band 159: Matthias Boiger
Hochleistungssysteme für die Fertigung elektronischer Baugruppen auf der Basis flexibler Schaltungsträger
FAPS, 175 Seiten, 111 Bilder, 8 Tab.
2005. ISBN 3-87525-222-5.

Band 160: Matthias Pitz
Laserunterstütztes Biegen höchstfester Mehrphasenstähle
LFT, 120 Seiten, 73 Bilder, 11 Tab.
2005. ISBN 3-87525-223-3.

Band 161: Meik Vahl
Beitrag zur gezielten Beeinflussung des Werkstoffflusses beim Innenhochdruck-Umformen von Blechen
LFT, 165 Seiten, 94 Bilder, 15 Tab.
2005. ISBN 3-87525-224-1.

Band 162: Peter K. Kraus
Plattformstrategien - Realisierung einer varianz- und kostenoptimierten Wertschöpfung
FAPS, 181 Seiten, 95 Bilder, 0 Tab.
2005. ISBN 3-87525-226-8.

Band 163: Adrienn Cser
Laserstrahlschmelzabtrag - Prozessanalyse und -modellierung
LFT, 146 Seiten, 79 Bilder, 3 Tab.
2005. ISBN 3-87525-227-6.

Band 164: Markus C. Hahn
Grundlegende Untersuchungen zur Herstellung von Leichtbauverbundstrukturen mit Aluminiumschaumkern
LFT, 143 Seiten, 60 Bilder, 16 Tab.
2005. ISBN 3-87525-228-4.

Band 165: Gordana Michos
Mechatronische Ansätze zur Optimierung von Vorschubachsen
FAPS, 146 Seiten, 87 Bilder, 17 Tab.
2005. ISBN 3-87525-230-6.

Band 166: Markus Stark
Auslegung und Fertigung hochpräziser Faser-Kollimator-Arrays
LFT, 158 Seiten, 115 Bilder, 11 Tab.
2005. ISBN 3-87525-231-4.

Band 167: Yurong Zhou
Kollaboratives Engineering Management in der integrierten virtuellen Entwicklung der Anlagen für die Elektronikproduktion
FAPS, 156 Seiten, 84 Bilder, 6 Tab.
2005. ISBN 3-87525-232-2.

Band 168: Werner Enser
Neue Formen permanenter und lösbarer elektrischer Kontaktierungen für mechatronische Baugruppen
FAPS, 190 Seiten, 112 Bilder, 5 Tab.
2005. ISBN 3-87525-233-0.

Band 169: Katrin Melzer
Integrierte Produktpolitik bei elektrischen und elektronischen Geräten zur Optimierung des Product-Life-Cycle
FAPS, 155 Seiten, 91 Bilder, 17 Tab.
2005. ISBN 3-87525-234-9.

Band 170: Alexander Putz
Grundlegende Untersuchungen zur Erfassung der realen Vorspannung von armierten Kaltfließpresswerkzeugen mittels Ultraschall
LFT, 137 Seiten, 71 Bilder, 15 Tab.
2006. ISBN 3-87525-237-3.

Band 171: Martin Prechtl
Automatisiertes Schichtverfahren für metallische Folien - System- und Prozesstechnik
LFT, 154 Seiten, 45 Bilder, 7 Tab.
2006. ISBN 3-87525-238-1.

Band 172: Markus Meidert
Beitrag zur deterministischen Lebensdauerabschätzung von Werkzeugen der Kaltmassivumformung
LFT, 131 Seiten, 78 Bilder, 9 Tab.
2006. ISBN 3-87525-239-X.

Band 173: Bernd Müller
Robuste, automatisierte Montagesysteme durch adaptive Prozessführung und montageübergreifende Fehlerprävention am Beispiel flächiger Leichtbauteile
FAPS, 147 Seiten, 77 Bilder, 0 Tab.
2006. ISBN 3-87525-240-3.

Band 174: Alexander Hofmann
Hybrides Laserdurchstrahlschweißen von Kunststoffen
LFT, 136 Seiten, 72 Bilder, 4 Tab.
2006. ISBN 978-3-87525-243-9.

Band 175: Peter Wölflick
Innovative Substrate und Prozesse mit feinsten Strukturen für bleifreie Mechatronik-Anwendungen
FAPS, 177 Seiten, 148 Bilder, 24 Tab. 2006.
ISBN 978-3-87525-246-0.

Band 176: Attila Komlodi
Detection and Prevention of Hot Cracks during Laser Welding of Aluminium Alloys Using Advanced Simulation Methods
LFT, 155 Seiten, 89 Bilder, 14 Tab. 2006. ISBN 978-3-87525-248-4.

Band 177: Uwe Popp
Grundlegende Untersuchungen zum Laserstrahlstrukturieren von Kaltmassivumformwerkzeugen
LFT, 140 Seiten, 67 Bilder, 16 Tab. 2006. ISBN 978-3-87525-249-1.

Band 178: Veit Rückel
Rechnergestützte Ablaufplanung und Bahngenerierung Für kooperierende Industrieroboter
FAPS, 148 Seiten, 75 Bilder, 7 Tab. 2006. ISBN 978-3-87525-250-7.

Band 179: Manfred Dirscherl
Nicht-thermische Mikrojustiertechnik mittels ultrakurzer Laserpulse
LFT, 154 Seiten, 69 Bilder, 10 Tab. 2007. ISBN 978-3-87525-251-4.

Band 180: Yong Zhuo
Entwurf eines rechnergestützten integrierten Systems für Konstruktion und Fertigungsplanung räumlicher spritzgegossener Schaltungsträger (3D-MID)
FAPS, 181 Seiten, 95 Bilder, 5 Tab. 2007. ISBN 978-3-87525-253-8.

Band 181: Stefan Lang
Durchgängige Mitarbeiterinformation zur Steigerung von Effizienz und Prozesssicherheit in der Produktion
FAPS, 172 Seiten, 93 Bilder. 2007.
ISBN 978-3-87525-257-6.

Band 182: Hans-Joachim Krauß
Laserstrahlinduzierte Pyrolyse präkeramischer Polymere
LFT, 171 Seiten, 100 Bilder. 2007.
ISBN 978-3-87525-258-3.

Band 183: Stefan Junker
Technologien und Systemlösungen für die flexibel automatisierte Bestückung permanent erregter Läufer mit oberflächenmontierten Dauermagneten
FAPS, 173 Seiten, 75 Bilder. 2007.
ISBN 978-3-87525-259-0.

Band 184: Rainer Kohlbauer
Wissensbasierte Methoden für die simulationsgestützte Auslegung wirkmedienbasierter Blechumformprozesse
LFT, 135 Seiten, 50 Bilder. 2007.
ISBN 978-3-87525-260-6.

Band 185: Klaus Lamprecht
Wirkmedienbasierte Umformung tiefgezogener Vorformen unter besonderer Berücksichtigung maßgeschneiderter Halbzeuge
LFT, 137 Seiten, 81 Bilder. 2007.
ISBN 978-3-87525-265-1.

Band 186: Bernd Zolleiß
Optimierte Prozesse und Systeme für die Bestückung mechatronischerBaugruppen
FAPS, 180 Seiten, 117 Bilder. 2007.
ISBN 978-3-87525-266-8.

Band 187: Michael Kerausch
Simulationsgestützte Prozessauslegung für das Umformen lokal wärmebehandelter Aluminiumplatinen
LFT, 146 Seiten, 76 Bilder, 7 Tab. 2007. ISBN 978-3-87525-267-5.

Band 188: Matthias Weber
Unterstützung der Wandlungsfähigkeit von Produktionsanlagen durch innovative Softwaresysteme
FAPS, 183 Seiten, 122 Bilder, 3 Tab. 2007. ISBN 978-3-87525-269-9.

Band 189: Thomas Frick
Untersuchung der prozessbestimmenden Strahl-Stoff-Wechselwirkungen beim Laserstrahlschweißen von Kunststoffen
LFT, 104 Seiten, 62 Bilder, 8 Tab. 2007. ISBN 978-3-87525-268-2.

Band 190: Joachim Hecht
Werkstoffcharakterisierung und Prozessauslegung für die wirkmedienbasierte Doppelblech-Umformung von Magnesiumlegierungen
LFT, 107 Seiten, 91 Bilder, 2 Tab. 2007. ISBN 978-3-87525-270-5.

Band 191: Ralf Völkl
Stochastische Simulation zur Werkzeuglebensdaueroptimierung und Präzisionsfertigung in der Kaltmassivumformung
LFT, 178 Seiten, 75 Bilder, 12 Tab. 2008. ISBN 978-3-87525-272-9.

Band 192: Massimo Tolazzi
Innenhochdruck-Umformen verstärkter Blech-Rahmenstrukturen
LFT, 164 Seiten, 85 Bilder, 7 Tab. 2008. ISBN 978-3-87525-273-6.

Band 193: Cornelia Hoff
Untersuchung der Prozesseinflussgrößen beim Presshärten des höchstfesten Vergütungsstahls 22MnB5
LFT, 133 Seiten, 92 Bilder, 5 Tab. 2008. ISBN 978-3-87525-275-0.

Band 194: Christian Alvarez
Simulationsgestützte Methoden zur effizienten Gestaltung von Lötprozessen in der Elektronikproduktion
FAPS, 149 Seiten, 86 Bilder, 8 Tab. 2008. ISBN 978-3-87525-277-4.

Band 195: Andreas Kunze
Automatisierte Montage von makromechatronischen Modulen zur flexiblen Integration in hybride Pkw-Bordnetzsysteme
FAPS, 160 Seiten, 90 Bilder, 14 Tab. 2008.
ISBN 978-3-87525-278-1.

Band 196: Wolfgang Hußnätter
Grundlegende Untersuchungen zur experimentellen Ermittlung und zur Modellierung von Fließortkurven bei erhöhten Temperaturen
LFT, 152 Seiten, 73 Bilder, 21 Tab. 2008. ISBN 978-3-87525-279-8.

Band 197: Thomas Bigl
Entwicklung, angepasste Herstellungsverfahren und erweiterte Qualitätssicherung von einsatzgerechten elektronischen Baugruppen
FAPS, 175 Seiten, 107 Bilder, 14 Tab. 2008.
ISBN 978-3-87525-280-4.

Band 198: Stephan Roth
Grundlegende Untersuchungen zum Excimerlaserstrahl-Abtragen unter Flüssigkeitsfilmen
LFT, 113 Seiten, 47 Bilder, 14 Tab. 2008. ISBN 978-3-87525-281-1.

Band 199: Artur Giera
Prozesstechnische Untersuchungen zum Rührreibschweißen metallischer Werkstoffe
LFT, 179 Seiten, 104 Bilder, 36 Tab. 2008. ISBN 978-3-87525-282-8.

Band 200: Jürgen Lechler
Beschreibung und Modellierung des Werkstoffverhaltens von presshärtbaren Bor-Manganstählen
LFT, 154 Seiten, 75 Bilder, 12 Tab. 2009. ISBN 978-3-87525-286-6.

Band 201: Andreas Blankl
Untersuchungen zur Erhöhung der Prozessrobustheit bei der Innenhochdruck-Umformung von flächigen Halbzeugen mit vor- bzw. nachgeschalteten Laserstrahlfügeoperationen
LFT, 120 Seiten, 68 Bilder, 9 Tab. 2009. ISBN 978-3-87525-287-3.

Band 202: Andreas Schaller
Modellierung eines nachfrageorientierten Produktionskonzeptes für mobile Telekommunikationsgeräte
FAPS, 120 Seiten, 79 Bilder, 0 Tab. 2009. ISBN 978-3-87525-289-7.

Band 203: Claudius Schimpf
Optimierung von Zuverlässigkeitsuntersuchungen, Prüfabläufen und Nacharbeitsprozessen in der Elektronikproduktion
FAPS, 162 Seiten, 90 Bilder, 14 Tab. 2009.
ISBN 978-3-87525-290-3.

Band 204: Simon Dietrich
Sensoriken zur Schwerpunktslagebestimmung der optischen Prozessemissionen beim Laserstrahltiefschweißen
LFT, 138 Seiten, 70 Bilder, 5 Tab. 2009. ISBN 978-3-87525-292-7.

Band 205: Wolfgang Wolf
Entwicklung eines agentenbasierten Steuerungssystems zur Materialflussorganisation im wandelbaren Produktionsumfeld
FAPS, 167 Seiten, 98 Bilder. 2009. ISBN 978-3-87525-293-4.

Band 206: Steffen Polster
Laserdurchstrahlschweißen transparenter Polymerbauteile
LFT, 160 Seiten, 92 Bilder, 13 Tab. 2009. ISBN 978-3-87525-294-1.

Band 207: Stephan Manuel Dörfler
Rührreibschweißen von walzplattiertem Halbzeug und Aluminiumblech zur Herstellung flächiger Aluminiumschaum-Sandwich-Verbundstrukturen
LFT, 190 Seiten, 98 Bilder, 5 Tab. 2009. ISBN 978-3-87525-295-8.

Band 208: Uwe Vogt
Seriennahe Auslegung von Aluminium Tailored Heat Treated Blanks
LFT, 151 Seiten, 68 Bilder, 26 Tab. 2009. ISBN 978-3-87525-296-5.

Band 209: Till Laumann
Qualitative und quantitative Bewertung der Crashtauglichkeit von höchstfesten Stählen
LFT, 117 Seiten, 69 Bilder, 7 Tab. 2009. ISBN 978-3-87525-299-6.

Band 210: Alexander Diehl
Größeneffekte bei Biegeprozessen-Entwicklung einer Methodik zur Identifikation und Quantifizierung
LFT, 180 Seiten, 92 Bilder, 12 Tab. 2010. ISBN 978-3-87525-302-3.

Band 211: Detlev Staud
Effiziente Prozesskettenauslegung für das Umformen lokal wärmebehandelter und geschweißter Aluminiumbleche
LFT, 164 Seiten, 72 Bilder, 12 Tab. 2010. ISBN 978-3-87525-303-0.

Band 212: Jens Ackermann
Prozesssicherung beim Laserdurchstrahlschweißen thermoplastischer Kunststoffe
LPT, 129 Seiten, 74 Bilder, 13 Tab. 2010. ISBN 978-3-87525-305-4.

Band 213: Stephan Weidel
Grundlegende Untersuchungen zum Kontaktzustand zwischen Werkstück und Werkzeug bei umformtechnischen Prozessen unter tribologischen Gesichtspunkten
LFT, 144 Seiten, 67 Bilder, 11 Tab. 2010. ISBN 978-3-87525-307-8.

Band 214: Stefan Geißdörfer
Entwicklung eines mesoskopischen Modells zur Abbildung von Größeneffekten in der Kaltmassivumformung mit Methoden der FE-Simulation
LFT, 133 Seiten, 83 Bilder, 11 Tab. 2010. ISBN 978-3-87525-308-5.

Band 215: Christian Matzner
Konzeption produktspezifischer Lösungen zur Robustheitssteigerung elektronischer Systeme gegen die Einwirkung von Betauung im Automobil
FAPS, 165 Seiten, 93 Bilder, 14 Tab. 2010. ISBN 978-3-87525-309-2.

Band 216: Florian Schüßler
Verbindungs- und Systemtechnik für thermisch hochbeanspruchte und miniaturisierte elektronische Baugruppen
FAPS, 184 Seiten, 93 Bilder, 18 Tab. 2010.
ISBN 978-3-87525-310-8.

Band 217: Massimo Cojutti
Strategien zur Erweiterung der Prozessgrenzen bei der Innhochdruck-Umformung von Rohren und Blechpaaren
LFT, 125 Seiten, 56 Bilder, 9 Tab. 2010. ISBN 978-3-87525-312-2.

Band 218: Raoul Plettke
Mehrkriterielle Optimierung komplexer Aktorsysteme für das Laserstrahljustieren
LFT, 152 Seiten, 25 Bilder, 3 Tab. 2010. ISBN 978-3-87525-315-3.

Band 219: Andreas Dobroschke
Flexible Automatisierungslösungen für die Fertigung wickeltechnischer Produkte
FAPS, 184 Seiten, 109 Bilder, 18 Tab. 2011.
ISBN 978-3-87525-317-7.

Band 220: Azhar Zam
Optical Tissue Differentiation for Sensor-Controlled Tissue-Specific Laser Surgery
LPT, 99 Seiten, 45 Bilder, 8 Tab. 2011. ISBN 978-3-87525-318-4.

Band 221: Michael Rösch
Potenziale und Strategien zur Optimierung des Schablonendruckprozesses in der Elektronikproduktion
FAPS, 192 Seiten, 127 Bilder, 19 Tab. 2011.
ISBN 978-3-87525-319-1.

Band 222: Thomas Rechtenwald
Quasi-isothermes Laserstrahlsintern von Hochtemperatur-Thermoplasten - Eine Betrachtung werkstoff-prozessspezifischer Aspekte am Beispiel PEEK
LPT, 150 Seiten, 62 Bilder, 8 Tab. 2011. ISBN 978-3-87525-320-7.

Band 223: Daniel Craiovan
Prozesse und Systemlösungen für die SMT-Montage optischer Bauelemente auf Substrate mit integrierten Lichtwellenleitern
FAPS, 165 Seiten, 85 Bilder, 8 Tab. 2011. ISBN 978-3-87525-324-5.

Band 224: Kay Wagner
Beanspruchungsangepasste Kaltmassivumformwerkzeuge durch lokal optimierte Werkzeugoberflächen
LFT, 147 Seiten, 103 Bilder, 17 Tab. 2011. ISBN 978-3-87525-325-2.

Band 225: Martin Brandhuber
Verbesserung der Prognosegüte des Versagens von Punktschweißverbindungen bei höchstfesten Stahlgüten
LFT, 155 Seiten, 91 Bilder, 19 Tab. 2011. ISBN 978-3-87525-327-6.

Band 226: Peter Sebastian Feuser
Ein Ansatz zur Herstellung von pressgehärteten Karosseriekomponenten mit maßgeschneiderten mechanischen Eigenschaften: Temperierte Umformwerkzeuge. Prozessfenster, Prozesssimuation und funktionale Untersuchung
LFT, 195 Seiten, 97 Bilder, 60 Tab. 2012. ISBN 978-3-87525-328-3.

Band 227: Murat Arbak
Material Adapted Design of Cold Forging Tools Exemplified by Powder Metallurgical Tool Steels and Ceramics
LFT, 109 Seiten, 56 Bilder, 8 Tab. 2012. ISBN 978-3-87525-330-6.

Band 228: Indra Pitz
Beschleunigte Simulation des Laserstrahlumformens von Aluminiumblechen
LPT, 137 Seiten, 45 Bilder, 27 Tab. 2012. ISBN 978-3-87525-333-7.

Band 229: Alexander Grimm
Prozessanalyse und -überwachung des Laserstrahlhartlötens mittels optischer Sensorik
LPT, 125 Seiten, 61 Bilder, 5 Tab. 2012. ISBN 978-3-87525-334-4.

Band 230: Markus Kaupper
Biegen von höhenfesten Stahlblechwerkstoffen - Umformverhalten und Grenzen der Biegbarkeit
LFT, 160 Seiten, 57 Bilder, 10 Tab. 2012. ISBN 978-3-87525-339-9.

Band 231: Thomas Kroiß
Modellbasierte Prozessauslegung für die Kaltmassivumformung unter Brücksichtigung der Werkzeug- und Pressenauffederung
LFT, 169 Seiten, 50 Bilder, 19 Tab. 2012. ISBN 978-3-87525-341-2.

Band 232: Christian Goth
Analyse und Optimierung der Entwicklung und Zuverlässigkeit räumlicher Schaltungsträger (3D-MID)
FAPS, 176 Seiten, 102 Bilder, 22 Tab. 2012.
ISBN 978-3-87525-340-5.

Band 233: Christian Ziegler
Ganzheitliche Automatisierung mechatronischer Systeme in der Medizin am Beispiel Strahlentherapie
FAPS, 170 Seiten, 71 Bilder, 19 Tab. 2012. ISBN 978-3-87525-342-9.

Band 234: Florian Albert
Automatisiertes Laserstrahllöten und -reparaturlöten elektronischer Baugruppen
LPT, 127 Seiten, 78 Bilder, 11 Tab. 2012. ISBN 978-3-87525-344-3.

Band 235: Thomas Stöhr
Analyse und Beschreibung des mechanischen Werkstoffverhaltens von presshärtbaren Bor-Manganstählen
LFT, 118 Seiten, 74 Bilder, 18 Tab. 2013. ISBN 978-3-87525-346-7.

Band 236: Christian Kägeler
Prozessdynamik beim Laserstrahlschweißen verzinkter Stahlbleche im Überlappstoß
LPT, 145 Seiten, 80 Bilder, 3 Tab. 2013. ISBN 978-3-87525-347-4.

Band 237: Andreas Sulzberger
Seriennahe Auslegung der Prozesskette zur wärmeunterstützten Umformung von Aluminiumblechwerkstoffen
LFT, 153 Seiten, 87 Bilder, 17 Tab. 2013. ISBN 978-3-87525-349-8.

Band 238: Simon Opel
Herstellung prozessangepasster Halbzeuge mit variabler Blechdicke durch die Anwendung von Verfahren der Blechmassivumformung
LFT, 165 Seiten, 108 Bilder, 27 Tab. 2013. ISBN 978-3-87525-350-4.

Band 239: Rajesh Kanawade
In-vivo Monitoring of Epithelium Vessel and Capillary Density for the Application of Detection of Clinical Shock and Early Signs of Cancer Development
LPT, 124 Seiten, 58 Bilder, 15 Tab. 2013. ISBN 978-3-87525-351-1.

Band 240: Stephan Busse
Entwicklung und Qualifizierung eines Schneidclinchverfahrens
LFT, 119 Seiten, 86 Bilder, 20 Tab. 2013. ISBN 978-3-87525-352-8.

Band 241: Karl-Heinz Leitz
Mikro- und Nanostrukturierung mit kurz und ultrakurz gepulster Laserstrahlung
LPT, 154 Seiten, 71 Bilder, 9 Tab. 2013. ISBN 978-3-87525-355-9.

Band 242: Markus Michl
Webbasierte Ansätze zur ganzheitlichen technischen Diagnose
FAPS, 182 Seiten, 62 Bilder, 20 Tab. 2013.
ISBN 978-3-87525-356-6.

Band 243: Vera Sturm
Einfluss von Chargenschwankungen auf die Verarbeitungsgrenzen von Stahlwerkstoffen
LFT, 113 Seiten, 58 Bilder, 9 Tab. 2013. ISBN 978-3-87525-357-3.

Band 244: Christian Neudel
Mikrostrukturelle und mechanisch-technologische Eigenschaften widerstandspunktgeschweißter Aluminium-Stahl-Verbindungen für den Fahrzeugbau
LFT, 178 Seiten, 171 Bilder, 31 Tab. 2014. ISBN 978-3-87525-358-0.

Band 245: Anja Neumann
Konzept zur Beherrschung der Prozessschwankungen im Presswerk
LFT, 162 Seiten, 68 Bilder, 15 Tab. 2014. ISBN 978-3-87525-360-3.

Band 246: Ulf-Hermann Quentin
Laserbasierte Nanostrukturierung mit optisch positionierten Mikrolinsen
LPT, 137 Seiten, 89 Bilder, 6 Tab. 2014. ISBN 978-3-87525-361-0.

Band 247: Erik Lamprecht
Der Einfluss der Fertigungsverfahren auf die Wirbelstromverluste von Stator-Einzelzahnblechpaketen für den Einsatz in Hybrid- und Elektrofahrzeugen
FAPS, 148 Seiten, 138 Bilder, 4 Tab. 2014. ISBN 978-3-87525-362-7.

Band 248: Sebastian Rösel
Wirkmedienbasierte Umformung von Blechhalbzeugen unter Anwendung magnetorheologischer Flüssigkeiten als kombiniertes Wirk- und Dichtmedium
LFT, 148 Seiten, 61 Bilder, 12 Tab. 2014. ISBN 978-3-87525-363-4.

Band 249: Paul Hippchen
Simulative Prognose der Geometrie indirekt pressgehärteter Karosseriebauteile für die industrielle Anwendung
LFT, 163 Seiten, 89 Bilder, 12 Tab. 2014. ISBN 978-3-87525-364-1.

Band 250: Martin Zubeil
Versagensprognose bei der Prozesssimulation von Biegeumform- und Falzverfahren
LFT, 171 Seiten, 90 Bilder, 5 Tab. 2014. ISBN 978-3-87525-365-8.

Band 251: Alexander Kühl
Flexible Automatisierung der Statorenmontage mit Hilfe einer universellen ambidexteren Kinematik
FAPS, 142 Seiten, 60 Bilder, 26 Tab. 2014.
ISBN 978-3-87525-367-2.

Band 252: Thomas Albrecht
Optimierte Fertigungstechnologien für Rotoren getriebeintegrierter PM-Synchronmotoren von Hybridfahrzeugen
FAPS, 198 Seiten, 130 Bilder, 38 Tab. 2014.
ISBN 978-3-87525-368-9.

Band 253: Florian Risch
Planning and Production Concepts for Contactless Power Transfer Systems for Electric Vehicles
FAPS, 185 Seiten, 125 Bilder, 13 Tab. 2014.
ISBN 978-3-87525-369-6.

Band 254: Markus Weigl
Laserstrahlschweißen von Mischverbindungen aus austenitischen und ferritischen korrosionsbeständigen Stahlwerkstoffen
LPT, 184 Seiten, 110 Bilder, 6 Tab. 2014. ISBN 978-3-87525-370-2.

Band 255: Johannes Noneder
Beanspruchungserfassung für die Validierung von FE-Modellen zur Auslegung von Massivumformwerkzeugen
LFT, 161 Seiten, 65 Bilder, 14 Tab. 2014. ISBN 978-3-87525-371-9.

Band 256: Andreas Reinhardt
Ressourceneffiziente Prozess- und Produktionstechnologie für flexible Schaltungsträger
FAPS, 123 Seiten, 69 Bilder, 19 Tab. 2014. ISBN 978-3-87525-373-3.

Band 257: Tobias Schmuck
Ein Beitrag zur effizienten Gestaltung globaler Produktions- und Logistiknetzwerke mittels Simulation
FAPS, 151 Seiten, 74 Bilder. 2014.
ISBN 978-3-87525-374-0.

Band 258: Bernd Eichenhüller
Untersuchungen der Effekte und Wechselwirkungen charakteristischer Einflussgrößen auf das Umformverhalten bei Mikroumformprozessen
LFT, 127 Seiten, 29 Bilder, 9 Tab. 2014. ISBN 978-3-87525-375-7.

Band 259: Felix Lütteke
Vielseitiges autonomes Transportsystem basierend auf Weltmodellerstellung mittels Datenfusion von Deckenkameras und Fahrzeugsensoren
FAPS, 152 Seiten, 54 Bilder, 20 Tab. 2014.
ISBN 978-3-87525-376-4.

Band 260: Martin Grüner
Hochdruck-Blechumformung mit formlos festen Stoffen als Wirkmedium
LFT, 144 Seiten, 66 Bilder, 29 Tab. 2014. ISBN 978-3-87525-379-5.

Band 261: Christian Brock
Analyse und Regelung des Laserstrahltiefschweißprozesses durch Detektion der Metalldampffackelposition
LPT, 126 Seiten, 65 Bilder, 3 Tab. 2015. ISBN 978-3-87525-380-1.

Band 262: Peter Vatter
Sensitivitätsanalyse des 3-Rollen-Schubbiegens auf Basis der Finite Elemente Methode
LFT, 145 Seiten, 57 Bilder, 26 Tab. 2015. ISBN 978-3-87525-381-8.

Band 263: Florian Klämpfl
Planung von Laserbestrahlungen durch simulationsbasierte Optimierung
LPT, 169 Seiten, 78 Bilder, 32 Tab. 2015. ISBN 978-3-87525-384-9.

Band 264: Matthias Domke
Transiente physikalische Mechanismen bei der Laserablation von dünnen Metallschichten
LPT, 133 Seiten, 43 Bilder, 3 Tab. 2015. ISBN 978-3-87525-385-6.

Band 265: Johannes Götz
Community-basierte Optimierung des Anlagenengineerings
FAPS, 177 Seiten, 80 Bilder, 30 Tab. 2015.
ISBN 978-3-87525-386-3.

Band 266: Hung Nguyen
Qualifizierung des Potentials von Verfestigungseffekten zur Erweiterung des Umformvermögens aushärtbarer Aluminiumlegierungen
LFT, 137 Seiten, 57 Bilder, 16 Tab. 2015. ISBN 978-3-87525-387-0.

Band 267: Andreas Kuppert
Erweiterung und Verbesserung von Versuchs- und Auswertetechniken für die Bestimmung von Grenzformänderungskurven
LFT, 138 Seiten, 82 Bilder, 2 Tab. 2015. ISBN 978-3-87525-388-7.

Band 268: Kathleen Klaus
Erstellung eines Werkstofforientierten Fertigungsprozessfensters zur Steigerung des Formgebungsvermögens von Alumi-niumlegierungen unter Anwendung einer zwischengeschalteten Wärmebehandlung
LFT, 154 Seiten, 70 Bilder, 8 Tab. 2015. ISBN 978-3-87525-391-7.

Band 269: Thomas Svec
Untersuchungen zur Herstellung von funktionsoptimierten Bauteilen im partiellen Presshärtprozess mittels lokal unterschiedlich temperierter Werkzeuge
LFT, 166 Seiten, 87 Bilder, 15 Tab. 2015. ISBN 978-3-87525-392-4.

Band 270: Tobias Schrader
Grundlegende Untersuchungen zur Verschleißcharakterisierung beschichteter Kaltmassivumformwerkzeuge
LFT, 164 Seiten, 55 Bilder, 11 Tab. 2015. ISBN 978-3-87525-393-1.

Band 271: Matthäus Brela
Untersuchung von Magnetfeld-Messmethoden zur ganzheitlichen Wertschöpfungsoptimierung und Fehlerdetektion an magnetischen Aktoren
FAPS, 170 Seiten, 97 Bilder, 4 Tab. 2015. ISBN 978-3-87525-394-8.

Band 272: Michael Wieland
Entwicklung einer Methode zur Prognose adhäsiven Verschleißes an Werkzeugen für das direkte Presshärten
LFT, 156 Seiten, 84 Bilder, 9 Tab. 2015. ISBN 978-3-87525-395-5.

Band 273: René Schramm
Strukturierte additive Metallisierung durch kaltaktives Atmosphärendruckplasma
FAPS, 136 Seiten, 62 Bilder, 15 Tab. 2015. ISBN 978-3-87525-396-2.

Band 274: Michael Lechner
Herstellung beanspruchungsangepasster Aluminiumblechhalbzeuge durch eine maßgeschneiderte Variation der Abkühlgeschwindigkeit nach Lösungsglühen
LFT, 136 Seiten, 62 Bilder, 15 Tab. 2015. ISBN 978-3-87525-397-9.

Band 275: Kolja Andreas
Einfluss der Oberflächenbeschaffenheit auf das Werkzeugeinsatzverhalten beim Kaltfließpressen
LFT, 169 Seiten, 76 Bilder, 4 Tab. 2015. ISBN 978-3-87525-398-6.

Band 276: Marcus Baum
Laser Consolidation of ITO Nanoparticles for the Generation of Thin Conductive Layers on Transparent Substrates
LPT, 158 Seiten, 75 Bilder, 3 Tab. 2015. ISBN 978-3-87525-399-3.

Band 277: Thomas Schneider
Umformtechnische Herstellung dünnwandiger Funktionsbauteile aus Feinblech durch Verfahren der Blechmassivumformung
LFT, 188 Seiten, 95 Bilder, 7 Tab. 2015. ISBN 978-3-87525-401-3.

Band 278: Jochen Merhof
Sematische Modellierung automatisierter Produktionssysteme zur Verbesserung der IT-Integration zwischen Anlagen-Engineering und Steuerungsebene
FAPS, 157 Seiten, 88 Bilder, 8 Tab. 2015. ISBN 978-3-87525-402-0.

Band 279: Fabian Zöller
Erarbeitung von Grundlagen zur Abbildung des tribologischen Systems in der Umformsimulation
LFT, 126 Seiten, 51 Bilder, 3 Tab. 2016. ISBN 978-3-87525-403-7.

Band 280: Christian Hezler
Einsatz technologischer Versuche zur Erweiterung der Versagensvorhersage bei Karosseriebauteilen aus höchstfesten Stählen
LFT, 147 Seiten, 63 Bilder, 44 Tab. 2016. ISBN 978-3-87525-404-4.

Band 281: Jochen Bönig
Integration des Systemverhaltens von Automobil-Hochvoltleitungen in die virtuelle Absicherung durch strukturmechanische Simulation
FAPS, 177 Seiten, 107 Bilder, 17 Tab. 2016.
ISBN 978-3-87525-405-1.

Band 282: Johannes Kohl
Automatisierte Datenerfassung für diskret ereignisorientierte Simulationen in der energieflexibelen Fabrik
FAPS, 160 Seiten, 80 Bilder, 27 Tab. 2016.
ISBN 978-3-87525-406-8.

Band 283: Peter Bechtold
Mikroschockwellenumformung mittels ultrakurzer Laserpulse
LPT, 155 Seiten, 59 Bilder, 10 Tab. 2016. ISBN 978-3-87525-407-5.

Band 284: Stefan Berger
Laserstrahlschweißen thermoplastischer Kohlenstofffaserverbundwerkstoffe mit spezifischem Zusatzdraht
LPT, 118 Seiten, 68 Bilder, 9 Tab. 2016. ISBN 978-3-87525-408-2.

Band 285: Martin Bornschlegl
Methods-Energy Measurement - Eine Methode zur Energieplanung für Fügeverfahren im Karosseriebau
FAPS, 136 Seiten, 72 Bilder, 46 Tab. 2016.
ISBN 978-3-87525-409-9.

Band 286: Tobias Rackow
Erweiterung des Unternehmenscontrollings um die Dimension Energie
FAPS, 164 Seiten, 82 Bilder, 29 Tab. 2016.
ISBN 978-3-87525-410-5.

Band 287: Johannes Koch
Grundlegende Untersuchungen zur Herstellung zyklisch-symmetrischer Bauteile mit Nebenformelementen durch Blechmassivumformung
LFT, 125 Seiten, 49 Bilder, 17 Tab. 2016. ISBN 978-3-87525-411-2.

Band 288: Hans Ulrich Vierzigmann
Beitrag zur Untersuchung der tribologischen Bedingungen in der Blechmassivumformung - Bereitstellung von tribologischen Modellversuchen und Realisierung von Tailored Surfaces
LFT, 174 Seiten, 102 Bilder, 34 Tab. 2016. ISBN 978-3-87525-412-9.

Band 289: Thomas Senner
Methodik zur virtuellen Absicherung der formgebenden Operation des Nasspressprozesses von Gelege-Mehrschichtverbunden
LFT, 156 Seiten, 96 Bilder, 21 Tab. 2016. ISBN 978-3-87525-414-3.

Band 290: Sven Kreitlein
Der grundoperationsspezifische Mindestenergiebedarf als Referenzwert zur Bewertung der Energieeffizienz in der Produktion
FAPS, 185 Seiten, 64 Bilder, 30 Tab. 2016.
ISBN 978-3-87525-415-0.

Band 291: Christian Roos
Remote-Laserstrahlschweißen verzinkter Stahlbleche in Kehlnahtgeometrie
LPT, 123 Seiten, 52 Bilder, 0 Tab. 2016. ISBN 978-3-87525-416-7.

Band 292: Alexander Kahrimanidis
Thermisch unterstützte Umformung von Aluminiumblechen
LFT, 165 Seiten, 103 Bilder, 18 Tab. 2016. ISBN 978-3-87525-417-4.

Band 293: Jan Tremel
Flexible Systems for Permanent Magnet Assembly and Magnetic Rotor Measurement / Flexible Systeme zur Montage von Permanentmagneten und zur Messung magnetischer Rotoren
FAPS, 152 Seiten, 91 Bilder, 12 Tab. 2016. ISBN 978-3-87525-419-8.

Band 294: Ioannis Tsoupis
Schädigungs- und Versagensverhalten hochfester Leichtbauwerkstoffe unter Biegebeanspruchung
LFT, 176 Seiten, 51 Bilder, 6 Tab. 2017. ISBN 978-3-87525-420-4.

Band 295: Sven Hildering
Grundlegende Untersuchungen zum Prozessverhalten von Silizium als Werkzeugwerkstoff für das Mikroscherschneiden metallischer Folien
LFT, 177 Seiten, 74 Bilder, 17 Tab. 2017. ISBN 978-3-87525-422-8.

Band 296: Sasia Mareike Hertweck
Zeitliche Pulsformung in der Lasermikromaterialbearbeitung – Grundlegende Untersuchungen und Anwendungen
LPT, 146 Seiten, 67 Bilder, 5 Tab. 2017. ISBN 978-3-87525-423-5.

Band 297: Paryanto
Mechatronic Simulation Approach for the Process Planning of Energy-Efficient Handling Systems
FAPS, 162 Seiten, 86 Bilder, 13 Tab. 2017. ISBN 978-3-87525-424-2.

Band 298: Peer Stenzel
Großserientaugliche Nadelwickeltechnik für verteilte Wicklungen im Anwendungsfall der E-Traktionsantriebe
FAPS, 239 Seiten, 147 Bilder, 20 Tab. 2017.
ISBN 978-3-87525-425-9.

Band 299: Mario Lušić
Ein Vorgehensmodell zur Erstellung montageführender Werkerinformationssysteme simultan zum Produktentstehungsprozess
FAPS, 174 Seiten, 79 Bilder, 22 Tab. 2017.
ISBN 978-3-87525-426-6.

Band 300: Arnd Buschhaus
Hochpräzise adaptive Steuerung und Regelung robotergeführter Prozesse
FAPS, 202 Seiten, 96 Bilder, 4 Tab. 2017. ISBN 978-3-87525-427-3.

Band 301: Tobias Laumer
Erzeugung von thermoplastischen Werkstoffverbunden mittels simultanem, intensitätsselektivem Laserstrahlschmelzen
LPT, 140 Seiten, 82 Bilder, 0 Tab. 2017. ISBN 978-3-87525-428-0.

Band 302: Nora Unger
Untersuchung einer thermisch unterstützten Fertigungskette zur Herstellung umgeformter Bauteile aus der höherfesten Aluminiumlegierung EN AW-7020
LFT, 142 Seiten, 53 Bilder, 8 Tab. 2017. ISBN 978-3-87525-429-7.

Band 303: Tommaso Stellin
Design of Manufacturing Processes for the Cold Bulk Forming of Small Metal Components from Metal Strip
LFT, 146 Seiten, 67 Bilder, 7 Tab. 2017. ISBN 978-3-87525-430-3.

Band 304: Bassim Bachy
Experimental Investigation, Modeling, Simulation and Optimization of Molded Interconnect Devices (MID) Based on Laser Direct Structuring (LDS) / Experimentelle Untersuchung, Modellierung, Simulation und Optimierung von Molded Interconnect Devices (MID) basierend auf Laser Direktstrukturierung (LDS)
FAPS, 168 Seiten, 120 Bilder, 26 Tab. 2017.
ISBN 978-3-87525-431-0.

Band 305: Michael Spahr
Automatisierte Kontaktierungsverfahren für flachleiterbasierte Pkw-Bordnetzsysteme
FAPS, 197 Seiten, 98 Bilder, 17 Tab. 2017. ISBN 978-3-87525-432-7.

Band 306: Sebastian Suttner
Charakterisierung und Modellierung des spannungszustandsabhängigen Werkstoffverhaltens der Magnesiumlegierung AZ31B für die numerische Prozessauslegung
LFT, 150 Seiten, 84 Bilder, 19 Tab. 2017. ISBN 978-3-87525-433-4.

Band 307: Bhargav Potdar
A reliable methodology to deduce thermo-mechanical flow behaviour of hot stamping steels
LFT, 203 Seiten, 98 Bilder, 27 Tab. 2017. ISBN 978-3-87525-436-5.

Band 308: Maria Löffler
Steuerung von Blechmassivumformprozessen durch maßgeschneiderte tribologische Systeme
LFT, viii u. 166 Seiten, 90 Bilder, 5 Tab. 2018. ISBN 978-3-96147-133-1.

Band 309: Martin Müller
Untersuchung des kombinierten Trenn- und Umformprozesses beim Fügen artungleicher Werkstoffe mittels Schneidclinchverfahren
LFT, xi u. 149 Seiten, 89 Bilder, 6 Tab. 2018.
ISBN: 978-3-96147-135-5.

Band 310: Christopher Kästle
Qualifizierung der Kupfer-Drahtbondtechnologie für integrierte Leistungsmodule in harschen Umgebungsbedingungen
FAPS, xii u. 167 Seiten, 70 Bilder, 18 Tab. 2018.
ISBN 978-3-96147-145-4.

Band 311: Daniel Vipavc
Eine Simulationsmethode für das 3-Rollen-Schubbiegen
LFT, xiii u. 121 Seiten, 56 Bilder, 17 Tab. 2018. ISBN 978-3-96147-147-8.

Band 312: Christina Ramer
Arbeitsraumüberwachung und autonome Bahnplanung für ein sicheres und flexibles Roboter-Assistenzsystem in der Fertigung
FAPS, xiv u. 188 Seiten, 57 Bilder, 9 Tab. 2018.
ISBN 978-3-96147-153-9.

Band 313: Miriam Rauer
Der Einfluss von Poren auf die Zuverlässigkeit der Lötverbindungen von Hochleistungs-Leuchtdioden
FAPS, xii u. 209 Seiten, 108 Bilder, 21 Tab. 2018.
ISBN 978-3-96147-157-7.

Band 314: Felix Tenner
Kamerabasierte Untersuchungen der Schmelze und Gasströmungen beim Laserstrahlschweißen verzinkter Stahlbleche
LPT, xxiii u. 184 Seiten, 94 Bilder, 7 Tab. 2018.
ISBN 978-3-96147-160-7.

Band 315: Aarief Syed-Khaja
Diffusion Soldering for High-temperature Packaging of Power Electronics
FAPS, x u. 202 Seiten, 144 Bilder, 32 Tab. 2018.
ISBN 978-3-87525-162-1.

Band 316: Adam Schaub
Grundlagenwissenschaftliche Untersuchung der kombinierten Prozesskette aus Umformen und Additive Fertigung
LFT, xi u. 192 Seiten, 72 Bilder, 27 Tab. 2019.
ISBN 978-3-96147-166-9.

Band 317: Daniel Gröbel
Herstellung von Nebenformelementen unterschiedlicher Geometrie an Blechen mittels Fließpressverfahren der Blechmassivumformung
LFT, x u. 165 Seiten, 96 Bilder, 13 Tab. 2019. ISBN 978-3-96147-168-3.

Band 318: Philipp Hildenbrand
Entwicklung einer Methodik zur Herstellung von Tailored Blanks mit definierten Halbzeugeigenschaften durch einen Taumelprozess
LFT, ix u. 153 Seiten, 77 Bilder, 4 Tab. 2019. ISBN 978-3-96147-174-4.

Band 319: Tobias Konrad
Simulative Auslegung der Spann- und Fixierkonzepte im Karosserierohbau: Bewertung der Baugruppenmaßhaltigkeit unter Berücksichtigung schwankender Einflussgrößen
LFT, x u. 203 Seiten, 134 Bilder, 32 Tab. 2019.
ISBN 978-3-96147-176-8.

Band 320: David Meinel
Architektur applikationsspezifischer Multi-Physics-Simulationskonfiguratoren am Beispiel modularer Triebzüge
FAPS, xii u. 166 Seiten, 82 Bilder, 25 Tab. 2019.
ISBN 978-3-96147-184-3.

Band 321: Andrea Zimmermann
Grundlegende Untersuchungen zum Einfluss fertigungsbedingter Eigenschaften auf die Ermüdungsfestigkeit kaltmassivumgeformter Bauteile
LFT, ix u. 160 Seiten, 66 Bilder, 5 Tab. 2019.
ISBN 978-3-96147-190-4.

Band 322: Christoph Amann
Simulative Prognose der Geometrie nassgepresster Karosseriebauteile aus Gelege-Mehrschichtverbunden
LFT, xvi u. 169 Seiten, 80 Bilder, 13 Tab. 2019.
ISBN 978-3-96147-194-2.

Band 323: Jennifer Tenner
Realisierung schmierstofffreier Tiefziehprozesse durch maßgeschneiderte Werkzeugoberflächen
LFT, x u. 187 Seiten, 68 Bilder, 13 Tab. 2019.
ISBN 978-3-96147-196-6.

Band 324: Susan Zöller
Mapping Individual Subjective Values to Product Design
KTmfk, xi u. 223 Seiten, 81 Bilder, 25 Tab. 2019.
ISBN 978-3-96147-202-4.

Band 325: Stefan Lutz
Erarbeitung einer Methodik zur semiempirischen Ermittlung der Umwandlungskinetik durchhärtender Wälzlagerstähle für die Wärmebehandlungssimulation
LFT, xiv u. 189 Seiten, 75 Bilder, 32 Tab. 2019.
ISBN 978-3-96147-209-3.

Band 326: Tobias Gnibl
Modellbasierte Prozesskettenabbildung rührreibgeschweißter Aluminiumhalbzeuge zur umformtechnischen Herstellung höchstfester Leichtbau-strukturteile
LFT, xii u. 167 Seiten, 68 Bilder, 17 Tab. 2019.
ISBN 978-3-96147-217-8.

Band 327: Johannes Bürner
Technisch-wirtschaftliche Optionen zur Lastflexibilisierung durch intelligente elektrische Wärmespeicher
FAPS, xiv u. 233 Seiten, 89 Bilder, 27 Tab. 2019.
ISBN 978-3-96147-219-2.

Band 328: Wolfgang Böhm
Verbesserung des Umformverhaltens von mehrlagigen Aluminiumblechwerkstoffen mit ultrafeinkörnigem Gefüge
LFT, ix u. 160 Seiten, 88 Bilder, 14 Tab. 2019.
ISBN 978-3-96147-227-7.

Band 329: Stefan Landkammer
Grundsatzuntersuchungen, mathematische Modellierung und Ableitung einer Auslegungsmethodik für Gelenkantriebe nach dem Spinnenbeinprinzip
LFT, xii u. 200 Seiten, 83 Bilder, 13 Tab. 2019.
ISBN 978-3-96147-229-1.

Band 330: Stephan Rapp
Pump-Probe-Ellipsometrie zur Messung transienter optischer Materialeigen-schaften bei der Ultrakurzpuls-Lasermaterialbearbeitung
LPT, xi u. 143 Seiten, 49 Bilder, 2 Tab. 2019.
ISBN 978-3-96147-235-2.

Band 331: Michael Scholz
Intralogistics Execution System mit integrierten autonomen, servicebasierten Transportentitäten
FAPS, xi u. 195 Seiten, 55 Bilder, 11 Tab. 2019.
ISBN 978-3-96147-237-6.

Band 332: Eva Bogner
Strategien der Produktindividualisierung in der produzierenden Industrie im Kontext der Digitalisierung
FAPS, ix u. 201 Seiten, 55 Bilder, 28 Tab. 2019.
ISBN 978-3-96147-246-8.

Band 333: Daniel Benjamin Krüger
Ein Ansatz zur CAD-integrierten muskuloskelettalen Analyse der Mensch-Maschine-Interaktion
KTmfk, x u. 217 Seiten, 102 Bilder, 7 Tab. 2019.
ISBN 978-3-96147-250-5.

Band 334: Thomas Kuhn
Qualität und Zuverlässigkeit laserdirektstrukturierter mechatronisch integrierter Baugruppen (LDS-MID)
FAPS, ix u. 152 Seiten, 69 Bilder, 12 Tab. 2019.
ISBN: 978-3-96147-252-9.

Band 335: Hans Fleischmann
Modellbasierte Zustands- und Prozessüberwachung auf Basis soziocyber-physischer Systeme
FAPS, xi u. 214 Seiten, 111 Bilder, 18 Tab. 2019.
ISBN: 978-3-96147-256-7.

Band 336: Markus Michalski
Grundlegende Untersuchungen zum Prozess- und Werkstoffverhalten bei schwingungsüberlagerter Umformung
LFT, xii u. 197 Seiten, 93 Bilder, 11 Tab. 2019.
ISBN: 978-3-96147-270-3.

Band 337: Markus Brandmeier
Ganzheitliches ontologiebasiertes Wissensmanagement im Umfeld der industriellen Produktion
FAPS, xi u. 255 Seiten, 77 Bilder, 33 Tab. 2020.
ISBN: 978-3-96147-275-8.

Band 338: Stephan Purr
Datenerfassung für die Anwendung lernender Algorithmen bei der Herstellung von Blechformteilen
LFT, ix u. 165 Seiten, 48 Bilder, 4 Tab. 2020.
ISBN: 978-3-96147-281-9.

Band 339: Christoph Kiener
Kaltfließpressen von gerad- und schrägverzahnten Zahnrädern
LFT, viii u. 151 Seiten, 81 Bilder, 3 Tab. 2020.
ISBN 978-3-96147-287-1.

Band 340: Simon Spreng
Numerische, analytische und empirische Modellierung des Heißcrimpprozesses
FAPS, xix u. 204 Seiten, 91 Bilder, 27 Tab. 2020.
ISBN 978-3-96147-293-2.

Band 341: Patrik Schwingenschlögl
Erarbeitung eines Prozessverständnisses zur Verbesserung der tribologischen Bedingungen beim Presshärten
LFT, x u. 177 Seiten, 81 Bilder, 8 Tab. 2020.
ISBN 978-3-96147-297-0.

Band 342: Emanuela Affronti
Evaluation of failure behaviour of sheet metals
LFT, ix u. 136 Seiten, 57 Bilder, 20 Tab. 2020.
ISBN 978-3-96147-303-8.

Band 343: Julia Degner
Grundlegende Untersuchungen zur Herstellung hochfester Aluminiumblechbauteile in einem kombinierten Umform- und Abschreckprozess
LFT, x u. 172 Seiten, 61 Bilder, 9 Tab. 2020.
ISBN 978-3-96147-307-6.

Band 344: Maximilian Wagner
Automatische Bahnplanung für die Aufteilung von Prozessbewegungen in synchrone Werkstück- und Werkzeugbewegungen mittels Multi-Roboter-Systemen
FAPS, xxi u. 181 Seiten, 111 Bilder, 15 Tab. 2020.
ISBN 978-3-96147-309-0.

Band 345: Stefan Härter
Qualifizierung des Montageprozesses hochminiaturisierter elektronischer Bauelemente
FAPS, ix u. 194 Seiten, 97 Bilder, 28 Tab. 2020.
ISBN 978-3-96147-314-4.

Band 346: Toni Donhauser
Ressourcenorientierte Auftragsregelung in einer hybriden Produktion mittels betriebsbegleitender Simulation
FAPS, xix u. 242 Seiten, 97 Bilder, 17 Tab. 2020.
ISBN 978-3-96147-316-8.

Band 347: Philipp Amend
Laserbasiertes Schmelzkleben von Thermoplasten mit Metallen
LPT, xv u. 154 Seiten, 67 Bilder. 2020. ISBN 978-3-96147-326-7.

Band 348: Matthias Ehlert
Simulationsunterstützte funktionale Grenzlagenabsicherung
KTmfk, xvi u. 300 Seiten, 101 Bilder, 73 Tab. 2020.
ISBN 978-3-96147-328-1.

Band 349: Thomas Sander
Ein Beitrag zur Charakterisierung und Auslegung des Verbundes von Kunststoffsubstraten mit harten Dünnschichten
KTmfk, xiv u. 178 Seiten, 88 Bilder, 21 Tab. 2020.
ISBN 978-3-96147-330-4.

Band 350: Florian Pilz
Fließpressen von Verzahnungselementen an Blechen
LFT, x u. 170 Seiten, 103Bilder, 4 Tab. 2020.
ISBN 978-3-96147-332-8.

Band 351: Sebastian Josef Katona
Evaluation und Aufbereitung von Produktsimulationen mittels abweichungsbehafteter Geometriemodelle
KTmfk, ix u. 147 Seiten, 73 Bilder, 11 Tab. 2020.
ISBN 978-3-96147-336-6.

Band 352: Jürgen Herrmann
Kumulatives Walzplattieren. Bewertung der Umformeigenschaften mehrlagiger Blechwerkstoffe der ausscheidungshärtbaren Legierung AA6014
LFT, x u. 157 Seiten, 64 Bilder, 5 Tab. 2020.
ISBN 978-3-96147-344-1.

Band 353: Christof Küstner
Assistenzsystem zur Unterstützung der datengetriebenen Produktentwicklung
KTmfk, xii u. 219 Seiten, 63 Bilder, 14 Tab. 2020.
ISBN 978-3-96147-348-9.

Band 354: Tobias Gläßel
Prozessketten zum Laserstrahlschweißen von flachleiterbasierten Formspulenwicklungen für automobile Traktionsantriebe
FAPS, xiv u. 206 Seiten, 89 Bilder, 11 Tab. 2020.
ISBN 978-3-96147-356-4.

Band 355: Andreas Meinel
Experimentelle Untersuchung der Auswirkungen von Axialschwingungen auf Reibung und Verschleiß in Zylinderrol-lenlagern
KTmfk, xii u. 162 Seiten, 56 Bilder, 7 Tab. 2020.
ISBN 978-3-96147-358-8.

Band 356: Hannah Riedle
Haptische, generische Modelle weicher anatomischer Strukturen für die chirurgische Simulation
FAPS, xxx u. 179 Seiten, 82 Bilder, 35 Tab. 2020.
ISBN 978-3-96147-367-0.

Band 357: Maximilian Landgraf
Leistungselektronik für den Einsatz dielektrischer Elastomere in aktorischen, sensorischen und integrierten sensomotorischen Systemen
FAPS, xxiii u. 166 Seiten, 71 Bilder, 10 Tab. 2020.
ISBN 978-3-96147-380-9.

Band 358: Alireza Esfandyari
Multi-Objective Process Optimization for Overpressure Reflow Soldering in Electronics Production
FAPS, xviii u. 175 Seiten, 57 Bilder, 23 Tab. 2020.
ISBN 978-3-96147-382-3.

Band 359: Christian Sand
Prozessübergreifende Analyse komplexer Montageprozessketten mittels Data Mining
FAPS, XV u. 168 Seiten, 61 Bilder, 12 Tab. 2021.
ISBN 978-3-96147-398-4.

Band 360: Ralf Merkl
Closed-Loop Control of a Storage-Supported Hybrid Compensation System for Improving the Power Quality in Medium Voltage Networks
FAPS, xxvii u. 200 Seiten, 102 Bilder, 2 Tab. 2021.
ISBN 978-3-96147-402-8.

Band 361: Thomas Reitberger
Additive Fertigung polymerer optischer Wellenleiter im Aerosol-Jet-Verfahren
FAPS, xix u. 141 Seiten, 65 Bilder, 11 Tab. 2021.
ISBN 978-3-96147-400-4.

Band 362: Marius Christian Fechter
Modellierung von Vorentwürfen in der virtuellen Realität mit natürlicher Fingerinteraktion
KTmfk, x u. 188 Seiten, 67 Bilder, 19 Tab. 2021.
ISBN 978-3-96147-404-2.

Band 363: Franziska Neubauer
Oberflächenmodifizierung und Entwicklung einer Auswertemethodik zur Verschleißcharakterisierung im Presshärteprozess
LFT, ix u. 177 Seiten, 42 Bilder, 6 Tab. 2021.
ISBN 978-3-96147-406-6.

Band 364: Eike Wolfram Schäffer
Web- und wissensbasierter Engineering-Konfigurator für roboterzentrierte Automatisierungslösungen
FAPS, xxiv u. 195 Seiten, 108 Bilder, 25 Tab. 2021.
ISBN 978-3-96147-410-3.

Band 365: Daniel Gross
Untersuchungen zur kohlenstoffdioxidbasierten kryogenen Minimalmengenschmierung
REP, xii u. 184 Seiten, 56 Bilder, 18 Tab. 2021.
ISBN 978-3-96147-412-7.

Band 366: Daniel Junker
Qualifizierung laser-additiv gefertigter Komponenten für den Einsatz im Werkzeugbau der Massivumformung
LFT, vii u. 142 Seiten, 62 Bilder, 5 Tab. 2021.
ISBN 978-3-96147-416-5.

Band 367: Tallal Javied
Totally Integrated Ecology Management for Resource Efficient and Eco-Friendly Production
FAPS, xv u. 160 Seiten, 60 Bilder, 13 Tab. 2021.
ISBN 978-3-96147-418-9.

Band 368: David Marco Hochrein
Wälzlager im Beschleunigungsfeld – Eine Analysestrategie zur Bestimmung des Reibungs-, Axialschub- und Temperaturverhaltens von Nadelkränzen –
KTmfk, xiii u. 279 Seiten, 108 Bilder, 39 Tab. 2021.
ISBN 978-3-96147-420-2.

Band 369: Daniel Gräf
Funktionalisierung technischer Oberflächen mittels prozessüberwachter aerosolbasierter Drucktechnologie
FAPS, xxii u. 175 Seiten, 97 Bilder, 6 Tab. 2021.
ISBN 978-3-96147-433-2.

Band 370: Andreas Gröschl
Hochfrequent fokusabstandsmodulierte Konfokalsensoren für die Nanokoordinatenmesstechnik
FMT, x u. 144 Seiten, 98 Bilder, 6 Tab. 2021.
ISBN 978-3-96147-435-6.

Band 371: Johann Tüchsen
Konzeption, Entwicklung und Einführung des Assistenzsystems D-DAS für die Produktentwicklung elektrischer Motoren
KTmfk, xii u. 178 Seiten, 92 Bilder, 12 Tab. 2021.
ISBN 978-3-96147-437-0.

Band 372: Max Marian
Numerische Auslegung von Oberflächenmikrotexturen für geschmierte tribologische Kontakte
KTmfk, xviii u. 276 Seiten, 85 Bilder, 45 Tab. 2021.
ISBN 978-3-96147-439-4.

Band 373: Johannes Strauß
Die akustooptische Strahlformung in der Lasermaterialbearbeitung
LPT, xvi u. 113 Seiten, 48 Bilder. 2021. ISBN 978-3-96147-441-7.

Band 374: Martin Hohmann
Machine learning and hyper spectral imaging: Multi Spectral Endoscopy in the Gastro Intestinal Tract towards Hyper Spectral Endoscopy
LPT, x u. 137 Seiten, 62 Bilder, 29 Tab. 2021.
ISBN 978-3-96147-445-5.

Band 375: Timo Kordaß
Lasergestütztes Verfahren zur selektiven Metallisierung von epoxidharzbasierten Duromeren zur Steigerung der Integrationsdichte für dreidimensionale mechatronische Package-Baugruppen
FAPS, xviii u. 198 Seiten, 92 Bilder, 24 Tab. 2021.
ISBN 978-3-96147-443-1.

Band 376: Philipp Kestel
Assistenzsystem für den wissensbasierten Aufbau konstruktionsbegleitender Finite-Elemente-Analysen
KTmfk, xviii u. 209 Seiten, 57 Bilder, 17 Tab. 2021.
ISBN 978-3-96147-457-8.

Band 377: Martin Lerchen
Messverfahren für die pulverbettbasierte additive Fertigung zur Sicherstellung der Konformität mit geometrischen Produktspezifikationen
FMT, x u. 150 Seiten, 60 Bilder, 9 Tab. 2021.
ISBN 978-3- 96147-463-9.

Band 378: Michael Schneider
Inline-Prüfung der Permeabilität in weichmagnetischen Komponenten
FAPS, xxii u. 189 Seiten, 79 Bilder, 14 Tab. 2021.
ISBN 978-3-96147-465-3.

Band 379: Tobias Sprügel
Sphärische Detektorflächen als Unterstützung der Produktentwicklung zur Datenanalyse im Rahmen des Digital Engineering
KTmfk, xiii u. 213 Seiten, 84 Bilder, 33 Tab. 2021.
ISBN 978-3-96147-475-2.

Band 380: Tom Häfner
Multipulseffekte beim Mikro-Materialabtrag von Stahllegierungen mit Pikosekunden-Laserpulsen
LPT, xxviii u. 159 Seiten, 57 Bilder, 13 Tab. 2021.
ISBN 978-3-96147-479-0.

Band 381: Björn Heling
Einsatz und Validierung virtueller Absicherungsmethoden für abweichungs-behaftete Mechanismen im Kontext des Robust Design
KTmfk, xi u. 169 Seiten, 63 Bilder, 27 Tab. 2021.
ISBN 978-3-96147-487-5.

Band 382: Tobias Kolb
Laserstrahl-Schmelzen von Metallen mit einer Serienanlage – Prozesscharakterisierung und Erweiterung eines Überwachungssystems
LPT, xv u. 170 Seiten, 128 Bilder, 16 Tab. 2021.
ISBN 978-3-96147-491-2.

Band 383: Mario Meinhardt
Widerstandselementschweißen mit gestauchten Hilfsfügeelementen - Umformtechnische Wirkzusammenhänge zur Beeinflussung der Verbindungsfestigkeit
LFT, xii u. 189 Seiten, 87 Bilder, 4 Tab. 2022.
ISBN 978-3-96147-473-8.

Band 384: Felix Bauer
Ein Beitrag zur digitalen Auslegung von Fügeprozessen im Karosseriebau mit Fokus auf das Remote-Laserstrahlschweißen unter Einsatz flexibler Spanntechnik
LFT, xi u. 185 Seiten, 74 Bilder, 12 Tab. 2022.
ISBN 978-3-96147-498-1.

Band 385: Jochen Zeitler
Konzeption eines rechnergestützten Konstruktionssystems für optomechatronische Baugruppen
FAPS, xix u. 172 Seiten, 88 Bilder, 11 Tab. 2022.
ISBN 978-3-96147-499-8.

Band 386: Vincent Mann
Einfluss von Strahloszillation auf das Laserstrahlschweißen hochfester Stähle
LPT, xiii u. 172 Seiten, 103 Bilder, 18 Tab. 2022.
ISBN 978-3-96147-503-2.

Band 387: Chen Chen
Skin-equivalent opto-/elastofluidic in-vitro microphysiological vascular models for translational studies of optical biopsies
LPT, xx u. 126 Seiten, 60 Bilder, 10 Tab. 2022.
ISBN 978-3-96147-505-6.

Band 388: Stefan Stein
Laser drop on demand joining as bonding method for electronics assembly and packaging with high thermal requirements
LPT, x u. 112 Seiten, 54 Bilder, 10 Tab. 2022.
ISBN 978-3-96147-507-0

Band 389: Nikolaus Urban
Untersuchung des Laserstrahlschmelzens von Neodym-Eisen-Bor zur additiven Herstellung von Permanentmagneten
FAPS, x u. 174 Seiten, 88 Bilder, 18 Tab. 2022.
ISBN 978-3-96147-501-8.

Band 390: Yiting Wu
Großflächige Topographiemessungen mit einem Weißlichtinterferenzmikroskop und einem metrologischen Rasterkraftmikroskop
FMT, xii u. 142 Seiten, 68 Bilder, 11 Tab. 2022.
ISBN: 978-3-96147-513-1.

Band 391: Thomas Papke
Untersuchungen zur Umformbarkeit hybrider Bauteile aus Blechgrundkörper und additiv gefertigter Struktur
LFT, xii u. 194 Seiten, 71 Bilder, 16 Tab. 2022.
ISBN 978-3-96147-515-5.

Band 392: Bastian Zimmermann
Einfluss des Vormaterials auf die mehrstufige Kaltumformung vom Draht
LFT, xi u. 182 Seiten, 36 Bilder, 6 Tab. 2022.
ISBN 978-3-96147-519-3.

Band 393: Harald Völkl
Ein simulationsbasierter Ansatz zur Auslegung additiv gefertigter FLM-Faserverbundstrukturen
KTmfk, xx u. 204 Seiten, 95 Bilder, 22 Tab. 2022.
ISBN 978-3-96147-523-0.

Band 394: Robert Schulte
Auslegung und Anwendung prozessangepasster Halbzeuge für Verfahren der Blechmassivumformung
LFT, x u. 163 Seiten, 93 Bilder, 5 Tab. 2022.
ISBN 978-3-96147-525-4.

Band 395: Philipp Frey
Umformtechnische Strukturierung metallischer Einleger im Folgeverbund für mediendichte Kunststoff-Metall-Hybridbauteile
LFT, ix u. 180 Seiten, 83 Bilder, 7 Tab. 2022.
ISBN 978-3-96147-534-6.

Band 396: Thomas Johann Luft
Komplexitätsmanagement in der Produktentwicklung - Holistische Modellierung, Analyse, Visualisierung und Bewertung komplexer Systeme
KTmfk, xiii u. 510 Seiten, 166 Bilder, 16 Tab. 2022.
ISBN 978-3-96147-540-7.

Band 397: Li Wang
Evaluierung der Einsetzbarkeit des lasergestützten Verfahrens zur selektiven Metallisierung für die Verbesserung passiver Intermodulation in Hochfrequenzanwendungen
FAPS, xxii u.151 Seiten, 72 Bilder, 22 Tab. 2022.
ISBN 978-3-96147-542-1.

Band 398: Sebastian Reitelshöfer
Der Aerosol-Jet-Druck Dielektrischer Elastomere als additives Fertigungsverfahren für elastische mechatronische Komponenten
FAPS, xxv u. 206 Seiten, 87 Bilder, 13 Tab. 2022.
ISBN 978-3-96147-547-6.

Band 399: Alexander Meyer
Selektive Magnetmontage zur Verringerung des Rastmomentes permanenterregter Synchronmotoren
FAPS, xv u. 164 Seiten, 90 Bilder, 18 Tab. 2022.
ISBN 978-3-96147-555-1.

Band 400: Rong Zhao
Design verschleißreduzierender amorpher Kohlenstoffschichtsysteme für trockene tribologische Gleitkontakte
KTmfk, x u. 148 Seiten, 69 Bilder, 14 Tab. 2022.
ISBN 978-3-96147-557-5.

Band 401: Christian P. J. Schwarzer
Kupfersintern als Fügetechnologie für Leistungselektronik
FAPS, xxvii u. 234 Seiten, 125 Bilder, 24 Tab. 2022.
ISBN 978-3-96147-566-7.

Band 402: Alexander Horn
Grundlegende Untersuchungen zur Gradierung der mechanischen Eigenschaften pressgehärteter Bauteile durch eine örtlich begrenzte Aufkohlung
LFT, xii u. 204 Seiten, 58 Bilder, 6 Tab. 2022.
ISBN 978-3-96147-568-1.

Band 403: Artur Klos
Werkstoff- und umformtechnische Bewertung von hochfesten Aluminiumblechwerkstoffen für den Karosseriebau
LFT, x u. 192 Seiten, 73 Bilder, 12 Tab. 2022.
ISBN 978-3-96147-572-8.

Band 404: Harald Schmid
Ganzheitliche Erarbeitung eines Prozessverständnisses von Tiefziehprozessen mit Ziehsicken auf Basis mechanischer und tribologischer Analysen
LFT, xiii u. 211 Seiten, 78 Bilder, 5 Tab. 2022.
ISBN 978-3-96147-577-3.

Band 405: Johannes Henneberg
Blechmassivumformung von Funktionsbauteilen aus Bandmaterial
LFT, viii u. 176 Seiten, 101 Bilder, 2 Tab. 2022.
ISBN 978-3-96147-579-7.

Band 406: Anton Schmailzl
Festigkeits- und zeitoptimierte Prozessführung beim quasi-simultanen Laser-Durchstrahlschweißen
LPT, xiii u. 157 Seiten, 84 Bilder, 7 Tab. 2022.
ISBN 978-3-96147-583-4.

Band 407: Alexander Wolf
Modellierung und Vorhersage menschlichen Interaktionsverhaltens zur Analyse der Mensch-Produkt Interaktion
KTmfk, x u. 207 Seiten, 69 Bilder, 10 Tab. 2022.
ISBN 978-3-96147-585-8.

Band 408: Tim Weikert
Modifikationen amorpher Kohlenstoffschichten zur Anpassung der Reibungsbedingungen und zur Erhöhung des Verschleißschutzes
KTmfk, xvii u. 258 Seiten, 91 Bilder, 9 Tab. 2022.
ISBN 978-3-96147-589-6.

Band 409: Stefan Götz
Frühzeitiges konstruktionsbegleitendes Toleranzmanagement
KTmfk, ix u. 276 Seiten, 127 Bilder, 13 Tab. 2022.
ISBN 978-3-96147-593-3.

Band 410: Markus Hubert
Einsatzpotenziale der Rotationsschneidtechnologie in der Verarbeitung von metallischen Funktionsfolien für mechatronische Produkte
FAPS, xviii u. 139 Seiten, 86 Bilder, 7 Tab. 2022.
ISBN 978-3-96147-603-9.

Band 411: Manfred Vogel
Grundlagenuntersuchungen und Erarbeitung einer Methodik zur Herstellung maßgeschneiderter Halbzeuge auf Basis eines neuartigen flexiblen Walzprozesses
LFT, ix u. 176 Seiten, 61 Bilder, 11 Tab. 2022.
ISBN 978-3-96147-605-3.

Band 412: Michael Weigelt
Multidimensionale Optionenanalyse alternativer Antriebskonzepte für die individuelle Langstreckenmobilität
FAPS, xv u. 222 Seiten, 89 Bilder, 38 Tab. 2022.
ISBN 978-3-96147-607-7.

Band 413: Frank Bodendorf
Machine Learning im Cost Engineering des Supply Managements
FAPS, xiii u. 165 Seiten, 75 Bilder, 13 Tab. 2023.
ISBN 978-3-96147-609-1.

Band 414: Maximilian Metzner
Planung und Simulation taktiler, intelligenter und kollaborativer Roboterfähigkeiten in der Montage
FAPS, xix u. 174 Seiten, 72 Bilder, 3 Tab. 2023.
ISBN 978-3-96147-611-4.

Band 415: Tina Buker
Ein Ansatz zur Reduktion produktinduzierter Nutzerstigmatisierung durch Förderung einer gleichermaßen gebrauchstauglichen wie emotionalen Produktgestalt
KTmfk, x u. 236 Seiten, 54 Bilder, 44 Tab. 2022.
ISBN 978-3-96147-613-8.

Band 416: Marlene Kuhn
Model-based Traceability System Development for Complex Manufacturing Applying Blockchain and Graphs
FAPS, xv u. 167 Seiten, 63 Bilder, 10 Tab. 2022.
ISBN 978-3-96147-615-2.

Band 417: Benjamin Lengenfelder
Remote photoacoustic sensing using speckle-analysis for biomedical imaging
LPT, xv u. 124 Seiten, 86 Bilder, 10 Tab. 2023.
ISBN 978-3-96147-617-6.

Band 418: Benjamin Pohrer
Analyse des Zusammenhangs zwischen dem tribochemischen Aufbau von Grenzschichten und der Ausbildung von White Etching Crack-Schäden
KTmfk, xv u. 258 Seiten, 103 Bilder, 10 Tab. 2023.
ISBN 978-3-96147- 621-3.

Band 419: Matthias Friedlein
Zuverlässigkeitsmethoden zur Beschleunigung von Qualifizierungsuntersuchungen für Steckkontakte
FAPS, xxv u. 162 Seiten, 98 Bilder, 7 Tab. 2023.
ISBN 978-3-96147-625-1.

Band 420: Thomas Stoll
Laser Powder Bed Fusion von Kupfer auf Aluminiumoxid-Keramiken
FAPS, xxvii u. 236 Seiten, 103 Bilder, 11 Tab. 2023.
ISBN 978-3-96147-631-2.

Band 421: Eric Eschner
Relation of Particle Motion and Process Zone Formation as a Basis for Sensing Approaches within PBF-LB/M
LPT, xiv u. 143 Seiten, 87 Bilder, 0 Tab. 2023.
ISBN 978-3-96147-633-6.

Band 422: Fanuel Mehari
Laser-induced Breakdown Spectroscopy (LIBS) as a diagnostics tool for biological tissue analysis.
LPT, xv u. 145 Seiten, 68 Bilder, 12 Tab. 2023.
ISBN 978-3-96147-641-1.

Band 423: Uwe Leicht
Ultraschallüberlagertes Umformen und Verstemmen von Stahlwerkstoffen
LFT, xi u. 165 Seiten, 65 Bilder, 6 Tab. 2023.
ISBN 978-3-96147-643-5.

Band 424: Thomas Braun
Potenzialanalyse der plasmabasierten, strukturierten Metallisierung thermoaktiver Oberflächen im industriellen Hausbau
FAPS, xvii u. 152 Seiten, 72 Bilder, 11 Tab. 2023.
ISBN 978-3-96147-653-4.

Band 425: Reinhardt Seidel
Modellbasierte Optimierung des Selektivwellenlötprozesses
FAPS, xxii u. 167 Seiten, 73 Bilder, 23 Tab. 2023.
ISBN: 978-3-96147-651-0.

Band 426: Matthias Lenzen
Maßgeschneiderte Werkstoffcharakterisierung für die numerische Auslegung von Blechumformprozessen
LFT, xi u. 187 Seiten, 77 Bilder, 13 Tab. 2023.
ISBN: 978-3-96147-663-3.

Band 427: Matthias Graser
Analyse lokaler Kurzzeitwärmebehandlungsmethoden zur Verbesserung des Umformverhaltens und der Bauteileigenschaften von Aluminiumstrangpresshohlprofilen
LFT, xi u. 169 Seiten, 81 Bilder, 1 Tab. 2023.
ISBN: 978-3-96147-666-4.

Band 428: Markus Lieret
Sicheres autonomes Flugrobotersystem für den Einsatz im Produktions- und Logistikumfeld
FAPS, xix u. 198 Seiten, 54 Bilder, 7 Tab. 2023.
ISBN 978-3-96147-668-8.

Band 429: Petar Vukovic
Simulation komplexer Kommunikationssysteme in der Fertigungsautomatisierung
FAPS, xiv u. 163 Seiten, 57 Bilder, 21 Tab. 2023.
ISBN 978-3-96147-673-2.

Band 430: Fabian Knieps
Finite Elemente Simulation dünnster Verpackungsstähle: Entwicklung einer geeigneten Charakterisierungs- und Validierungsstrategie
LFT, xix, 189 Seiten, 122 Bilder, 17 Tab. 2023
ISBN 978-3-96147-689-3

Band 431: Julian Seßner
Multimodale Bildsegmentierung gering strukturierter Umgebungen für die Navigation am Beispiel eines Assistenzsystems für sehbeeinträchtigte Personen
FAPS, xxv, 203 Seiten, 57 Bilder, 25 Tab. 2023
ISBN 978-3-96147-697-8

Band 432: Benjamin Samuel Lutz
Smart Manufacturing System for Process Optimization Regarding Deviations among Material Batches
FAPS, xix, 208 Seiten, 77 Bilder, 14 Tab. 2023
ISBN 978-3-96147-703-6

Band 433: Michael Jüttner
Bewertung von Kantenpressungen auf Basis von Simulationen mehrfach überrollter elasto-plastischer Kontakte
KTmfk, xii, 162 Seiten, 59 Bilder, 7 Tab. 2024
ISBN 978-3-96147-713-5

Band 434: Sebastian Wiesenmayer
Untersuchungen zur Stoffflusssteuerung beim Fügen durch Umformen von hochfesten Aluminiumlegierungen mittels lokaler Kurzzeitwärmebehandlung
LFT, xii u. 197 Seiten, 81 Bilder, 19 Tab. 2024.
ISBN 978-3-96147-715-9.

Band 435: Clara-Maria Kuball
Grundlegende Untersuchungen zur umformtechnischen Herstellung von Halbhohlstanznieten aus hochverfestigenden Werkstoffen
LFT, viii u. 180 Seiten, 64 Bilder, 13 Tab. 2024.
ISBN 978-3-96147-717-3.

Band 436: Martin Roth
Sampling-based Tolerance-Cost Optimization: The Key to Optimal Tolerance Allocation
KTmfk, xxxvii u. 337 Seiten, 97 Bilder, 56 Tab. 2024.
ISBN 978-3-96147-719-7.

Kurzfassung

Die Einschränkung fertigungsbedingter Einzelteilabweichungen mithilfe von Maß-, Form- und Lagetoleranzen hat primär die Sicherstellung der Baugruppenqualität zum Ziel. Zugleich werden dadurch jedoch bereits in der Produktentwicklung die Randbedingungen für die Fertigung und somit implizit die Herstellungskosten festgelegt. Die Methode der samplingbasierten Toleranz-Kosten-Optimierung, eine Kombination aus statistischer Toleranzanalyse auf Basis von Samplingverfahren und metaheuristischen Optimierungsalgorithmen, ermöglicht hierbei eine optimale Festlegung der Toleranzwerte und löst so automatisiert den Zielkonflikt zwischen Kosten und Qualität. Allerdings stehen Einschränkungen in Effektivität und Effizienz einem gewinnbringenden Einsatz zur Lösung komplexer, praxisrelevanter Problemstellungen und somit einer Ausschöpfung verborgener Kostenpotentiale bislang noch im Wege.

Um die aktuellen Forschungslücken zu schließen, werden in dieser Arbeit die beteiligten Einzelmethoden, insbesondere das Sampling, die Ausschussratenschätzung und die Optimierung auf Basis von Ersatzmodellen, gezielt (weiter-)entwickelt und in einem Gesamtansatz aufeinander abgestimmt, sodass verlässliche Optimierungsergebnisse in adäquaten Rechenzeiten erzielt werden können. Dessen Erweiterung zur simultanen Maschinenselektion und –allokation mit unterschiedlichen Losgrößen und selektiver Montage unter Berücksichtigung von maschinenspezifischen Fertigungsverteilungen und geometrischen, sich gegenseitig bedingenden Toleranzen trägt hierbei wesentlich zur Ausweitung des Anwendungskontextes um praxisrelevante Aspekte bei. Eine abschließende Evaluation des entwickelten Gesamtrahmenwerks stellt dessen Potential für eine produktive Anwendung an praxisnahen Problemstellungen unter Beweis und dient der Identifikation weiterer Forschungspotentiale.

Limiting manufacturing-caused part variations by size, location, orientation, and form tolerances primarily aims to assure the total assembly quality. At the same time, however, the manufacturing conditions and, thus, the manufacturing costs are already predefined in the product development phase. The method of sampling-based tolerance-cost optimization, a combination of statistical tolerance analysis based on sampling techniques and metaheuristic optimization algorithms, enables an automated and optimal allocation of tolerance values and, thus, solves the conflict of objectives between costs and quality. However, limitations in effectiveness and efficiency still prevent its profitable application for solving complex, industry-relevant problems and exploiting hidden cost potentials.

To close the current research gaps, the individual methods involved, in particular the sampling, non-conformance rate estimation and surrogate model-based optimization, are (further) developed and harmonized in one common approach, ensuring that reliable optimization results can be obtained in adequate computing times. Its extension to simultaneous machine selection and allocation with different batch sizes and selective assembly, considering machine-specific part tolerance distributions and geometrical, mutually dependent tolerances, significantly expands the context of use to practical aspects. A final evaluation of the developed framework proves its potential for a profitable application to practical problems and serves to identify further research potentials.

ISBN 978-3-96147-719-7

9 783961 477197

FAU UNIVERSITY PRESS 2024